The morphology of the knee joint in Homo sapiens : a morphometric study of form variation in the distal femur and proximal tibia.

Stevens, Sally Diane

The morphology of the knee joint in *Homo sapiens*:

A morphometric study of form variation in the distal femur and proximal tibia

Sally Diane Stevens

Department of Anthropology

September 2005

Thesis submitted to the University of Durham for the degree of Doctor of Philosophy

Abstract

The morphology of the knee joint in *Homo sapiens*: a morphometric study of form variation in the distal femur and proximal tibia

This thesis explores form variation in the knee joint of thirteen geographically and economically distinct populations of modern *Homo sapiens* from different ancestral backgrounds. Shape differences are interpreted within the context of the size of the knee joint and against size differences in the femur and tibia. Three dimensional coordinate data are taken from the distal femur and proximal tibia and statistical shape analysis is conducted using geometric morphometric techniques. Results from initial intra-population analyses using a restricted number of samples determine the data that are submitted for inter-population analyses using the full dataset.

Three series of intra-population analyses test for asymmetry, sexual dimorphism and age. Significant shape asymmetry exists in all samples examined. Results therefore preclude the use of both right- and left-sided specimens within any single sample in subsequent analyses. Results indicate the existence of a significant degree of sexual dimorphism in all sample, but that the nature and degree of variation is population specific. Significant differences also exist with ageing, although again, variation in nature and degree is population specific. For both sexual dimorphism and shape variation with ageing, differences are of lesser significance relative to inter-population variation.

Using the full dataset, results indicate the existence of size and (particularly) shape differences between samples at a high level of statistical significance. Morphological variation between populations arises from a number of influential factors, including climate and more specifically, cold temperature. The powerful influence of additional factors, including working practices, disease and nutrition is examined in greater depth in relation to the Spitalfields sample from London, which shows a distinctive pattern of form variation relative to the other population samples.

Acknowledgements

Firstly, I would like to thank my two supervisors, Una Strand Viðarsdóttir and Alan Bilsborough for all their help and guidance throughout my period of study. They have continually inspired me in a fascinating subject.

Thanks are also due to the curators and assistants in the museums where I gathered data. I would like to thank Robert Kruszynski and Louise Humphrey of the Natural History Museum, London for their considerable help and friendship, together with David Hunt of the National Museum of Natural History, Smithsonian Institution, Washington DC. David made valuable and much needed extra time available to me during my stays in Washington by allowing me access to the collections at weekends and Bank Holidays, at no small cost to himself.

I would also like to thank my friends and colleagues of the Evolutionary Anthropology Research Group at Durham University for their helpful comments, especially Trudi Buck, whose friendship, help and great good sense have been invaluable.

Finally, I would like to thank my family, especially my son, Chris and daughter, Alexandra for their encouragement throughout. I reserve my greatest, heartfelt thanks, however, for my husband John, whose help, encouragement, support and good humour has been and continues to be, inestimable. Thank you, John.

CONTENTS

Chapter 3 Asymmetry in the form of the knee joint in *Homo sapiens*

List of Tables

All large tables and figures are included in the text on the page subsequent to referral in the text, unless directed by page reference.

List of Figures

Chapter 5 Changes with ageing of the knee joint

Chapter 1

Introduction and Background Material.

1.1 Introduction

The knee joint is the largest and arguably the most loaded and stressed joint in the human skeleton (Palastanga et al., 1998). It is unquestionably complicated in its movement being neither a simple hinge joint with one degree of freedom like the elbow, nor a ball-and-socket joint with three degrees of freedom like the hip. The knee joint represents a compromise; it is a hinge joint with an accessory, i.e., a second degree of freedom. From a mechanical point of view, this compromise attempts to reconcile the two mutually exclusive requirements to provide great stability with great mobility and in so doing, presents both its inherent strength and potential weakness. The knee resolves this dilemma by providing great mobility at the expense of a relatively poor interlocking mechanism between three articular surfaces (Kapandji, 2001).

Because of this great complexity and its high load-bearing function during locomotion, the knee joint is exposed to considerable internal and external stresses and strains throughout the lifetime of each individual. In addition, each individual uses his or her body in a unique way, regardless of sex, height, weight, environmental or climatic factors. Being subject to compressive and shear forces which can reach up to 24 times body weight under normal physical activities (see section 1.7.2), different individuals will inevitably load this part of the skeleton in manifestly variable ways (Palastanga et al., 1998).

Therefore, with the expectation in mind of finding considerable variation in the morphology of the knee joint in *Homo sapiens*, this study will first explore whether any underlying similarities of shape exist between groups within the same population, i.e., between specimens of the same side, of the same sex or of the same age group. Subsequently, this study will explore whether fundamental differences in knee joint

shape are present between different populations. Supplementary analyses are also conducted on the size of the knee joint together with the size of the long bones, to aid the interpretation of knee joint shape and to place the joint within the overall context of the lower limbs.

Until the advent of three-dimensional geometric morphometric techniques, it was difficult to compare complex three-dimensional shapes such as bones by using one or two-dimensional measurements. Many previous studies have been restricted to analysing the fundamental features of bones by using simple measurements between major landmarks. Inevitably, much of the essential information relating to the shape in its entirety has been lost. The ability to analyse sets of landmark data and to visualise the complete three-dimensional configuration, makes the challenge of comparing and contrasting complex anatomical structures more realistic.

This study makes use of these geometric morphometric techniques to compare and contrast the shapes of each bone, both within and between samples of modern humans. In addition, by analysing the distal femur alongside the proximal tibia, it also proposes to explore characteristics of each bone relative to the other and by so doing, to analyse the knee joint as an integrated unit.

1.2 Overview of Chapter 1

The bones of the knee joint examined here are the distal femur and proximal tibia. The patella, the third bone of the joint, is omitted from the study for two reasons: firstly, because relatively few patellae are available within archaeological collections, particularly in conjunction with long bones from the same individuals and, being easily damaged and eroded, few collections include specimens in good condition. Also, it is a relatively small and smooth bone with few anatomical landmarks of Types I or II (see Chapter 2 section 2.2.1 for landmark types).

Chapter 1, sections 1.3 and 1.4 provide an overview of the composition of both trabecular bone (primarily relating to the epiphyses) and cortical bone (primarily relating

to the diaphyses) and of the processes of bone modelling and remodelling. Section 1.5 provides a brief summary of the anatomy of the femur and tibia and section 1.6 provides a more detailed description of the anatomy of the knee joint. Section 1.7 provides an overview of the biomechanics of movement within the lower limbs, followed by a detailed exposition of the biomechanics of movement within the knee joint itself. Section 1.8 outlines the biomechanics of gait and the process of human walking and section 1.9, the effects of footwear on gait. Finally, section 1.10 outlines the structure of the analyses examined within the study. Each analysis chapter examines a set of hypotheses relating to a specific subject: Chapter 3 explores the nature of asymmetry in the form of the knee joint; Chapter 4 explores sexual dimorphism in the form of the knee joint; Chapter 5 examines changes in shape with ageing at the knee joint and Chapter 6 analyses differences in the form of the knee joint between populations and of the possible reasons for those differences. Therefore as each chapter explores a specific subject, the literature relating to that particular field will be reviewed in the introduction to the chapter. In addition, each analysis chapter will be accompanied by a discussion examining those results and placing them within the context of the research reviewed in the introduction to the chapter.

1.3 The composition and ossification of bone

The skeletal system provides support and protection to the viscera, allows movement of the body, is the site of blood cell production and is the storage site of some fats and minerals, of which the most important is calcium. In times of stress when calcium cannot be absorbed in sufficient quantities from the diet, for example in pregnancy, additional supplies are drawn from the skeleton (Gallagher, 1991).

Bones exist in the skeleton as both tissue and organs. Mesenchymal tissue is the fundamental embryonic tissue from which all other connective tissue in the body is ultimately formed, including cartilage. Osteoprogenitor cells, the stem cells of bone that are formed from the primitive mesenchymal tissue, migrate to sites of future osteogenesis where they condense, either as a result of increased cellular activity or by an aggregation of similar cells clustering together. Ultimately they form either

precartilage blastema leading to the development of endochondrial bone or predominantly fibrous condensations that lead to the development of intramembraneous bone, which is ossified directly from the connective tissue membranes. In the development of endochondrial bone, increasing cellular activity with varying levels of different mineral secretions permits the formation of cellular aggregations that, in turn, initiate the transition from the precartilage, mesenchymal tissue into hyaline cartilage. Endochondrial ossification is more closely associated with the development of long bones and intramembraneous ossification tends to occur in most of the plate-like bones of the skull, the facial bones, the mandible and clavicle (Seeley et al., 1998; Scheuer and Black, 2000).

Osteoprogenitor cells then differentiate into the more specialised bone-forming osteoblast cells. Osteoblasts line both the inner (endosteal) and outer (periosteal) surfaces of all bone, whilst depositing bony matrix. As a form of connective tissue, bone is made up of specialised cells (i.e., secondary stage osteoblast cells), which secrete an extracellular matrix and, subsequently osteocyte cells, which are the more mature bone cells for which osteoblasts are the developmental precursors. Osteocytes can be differentiated from the former by being completely encased in bone within small cavities (lacunae). Adjacent osteocytes are linked to each other by means of cytoplasmic material within the cell lying along narrow channels known as canaliculi. By means of these channels, osteocytes (and indeed, osteoblasts) remain in communication with all other cells and by so doing, allow the processes of bone development, growth, repair and regeneration to be signalled and maintained. Through these interconnecting channels, osteocytes receive sufficient nutrients to survive and may also resorb formed bone matrix in order to release calcium (Seeley et al., 1998; Stevens and Lowe, 1998).

In addition, the bone tissue includes the retained mineralised extracellular matrix that is formed by the osteoblast cells. Its distinguishing characteristic of extreme hardness is derived from this composite mineral substance, formed largely from calcium, phosphate and carbonate, within a relatively soft matrix. By weight, 35% of the matrix is an organic material primarily consisting of collagen and proteoglycans. The remaining 65%

inorganic mineral component consists almost entirely of hydroxyapatite crystals. Whilst collagen provides flexibility and tensile strength to bone, the inorganic component provides additional strength and the ability to withstand compression (Hall, 1988; Seeley et al., 1998; White, 2000).

Because bone is unable to increase in size through interstitial growth, i.e., growth from within, it must do so by apposition, i.e., addition from the surface. During the rapid development of foetal life and in childhood, osteoblast activity alone is not sufficient to provide the longitudinal growth necessary. Because of this, most of the postcranial bones of the skeleton are pre-formed in cartilage (which *is* capable of interstitial growth), and which is then replaced through the modelling process into bone. In addition to the ossification of new bone, the shape of bones change as the infant grows by means of remodelling, i.e., the resorption of old bone and the replacement of new, both at the same site and in areas of additional loading (Seeley et al., 1998).

Woven bone is the most immature type of developing bone and present in both intramembranous and enchondrial bone. It tends to be poorly organised, interspersed with large vascular spaces, is relatively weak and easily fractured. Osteoblast activity, producing concentric lamellae on the vascular walls creates primary osteons, which for most practical purposes are known as Haversian systems. These primary osteons, together with their Haversian canals and associated neurovascular contents, eventually reduce the vascular spaces within the bone. On the periosteal surface, activity surrounding the lamellar structure forms primary osteons at the location eventually forming the more mature, well-organised and stronger lamellar bone. Primary bone, which is formed by these early Haversian systems, is short-lived and quickly remodelled and replaced by the stronger lamellar bone (Steele and Bramblett, 1988; Seeley et al., 1998; Scheuer and Black, 2000)

Other non-Haversian system primary osteons and several varieties of secondary osteons also exist in cortical bone and these have proved useful as indicators for predicting age-of-death in forensic contexts. The numbers of secondary osteons and also this type of primary osteons increase with age; the cortex becoming crowded with secondary

osteons, many of which become fragmented (Robling and Stout, 2000). The estimation of non-Haversian system primary and secondary intact and fragmented osteons, shows not only age-related variation but is also thought to be sex-related and population specific (Erikson, 1991), although not all research has proved conclusive (Pfeiffer, 1998).

In summary, the majority of mature bones within the skeleton have a basic architecture, comprised of an outer cortical shell of compact bone with a 'spongy' trabecular inner area. The outer shell resists compression through hardness and rigidity whilst the inner zone containing a trabecular meshwork absorbs force even in the face of changing physiological stress. The fine particles or struts (trabeculae) surround cavities containing both red and fatty marrow and blood vessels whilst the trabeculae themselves consist of several lamellae with osteocytes interspersed. The trabeculae provide internal strength and absorb stress by aligning themselves to the direction of external forces to which they are subjected. Long bone diaphyses are predominantly constructed of cortical bone with a thinner trabecular zone, which together surround a central medullary core. The epiphyses are primarily constructed of trabecular bone.

The density of cortical bone varies both within the lifetime of an individual and within even a small area of the same bone. As a general rule, density peaks during young adulthood and declines into old age, although this is variable between populations (Eriksen, 1976; Gregg and Gregg, 1987; Rogueka et al., 2000). During remodelling, rapid mineralisation occurs within the resorption Haversian cavities, with about 70% mineralisation completed within a matter of days. The remaining mineralisation is completed more slowly and may take up to six weeks or longer (Vaughan, 1981).

1.4 Bone modelling and remodelling

Bone modelling and remodelling are the processes mobilised during the initial growth of the skeleton during foetal and childhood development and for the maintenance of healthy bone. This latter process is achieved by means of routine replacement of tissue

throughout maturity and during periods of stress caused by fracture, injury or insufficiency of mineral requirements. 'Modelling' refers to the process by which bone achieves and maintains its shape; 'repair' is a response to fracture and injury; and 'remodelling' is a continuous cycle of resorbtion and renewal of bone that occurs throughout life (Marcus, 1987).

The osteocyte cells within the bone matrix may be distinguished from each other during three functional states: quiescent cells, found in sites not currently undergoing resorption, most frequently in adult bone; formative cells that shows evidence of matrix formation similar to osteoblasts; and resorptive cells showing evidence of removal of matrix (Ross et al., 1998). There is a fourth type of bone cells (i.e., osteoclasts) that are large cells with multiple nuclei and are thought to originate from blood monocytes. They are therefore of a distinct derivation to the other three types of cells. When active, these osteoclasts rest on the surface of the bone about to undergo resorption where enzyme activity produces a localised acidic environment to break down the calcium salts of the bone. Healthy osteoclast cells are highly mobile and will sweep away bone from as wide an area as requires resorption (Marcus, 1987; Seeley et al., 1998).

In normal healthy bone, once resorption is complete, osteoblast activity will start to deposit new bone, which then becomes mineralised. Following remodelling the bone returns to the quiescent state. The remodelling process, however, may not be completely efficient and a small deficit in bone mass may remain after the cycle is complete, particularly in post-menopausal women. This has a profound effect over the individual's lifetime with the inevitable age-related loss of bone substance that may be exacerbated by dietary or hormonal deficiency (Marcus, 1987). However, it is also widely recognised that weight-bearing exercise can slow the rate of bone substance loss and that cultural expectation and encouragement of exercise in more elderly age groups affect differential rates of loss between populations (Snow et al., 2000; Kai et al., 2003).

There are two primary functions of remodelling. The first is to replace bone that suffers from microfractures throughout the inevitable wear and tear of daily life. Despite the

risk of loss of bone mass outlined above, the benefit of being supplied with newly replaced bone still outweighs the penalties imposed by the replacement process itself. Strictly speaking, the response to microfractures (i.e., stress within bone) is known as 'adaptive remodelling'. In this process, osteocytes continually exchange calcium with the matrix as part of the process of calcium homeostasis. This balancing of calcium levels is not strictly part of the mechanism of either modelling or remodelling (Thomason, 1995).

The second function is to enable bone to orient itself to best withstand the direction of force to which it is being subjected. This will change throughout the individual's lifetime; both throughout childhood as the bones are growing and throughout life as activity patterns change and existing bone becomes exposed to new forces. New bone will become deposited in the direction of force whilst old bone will be resorbed. If the old bone were allowed to remain, the new direction of force would still be absorbed and catered for. This would result, however, in a heavy block of bone, which, if repeated throughout the body would result in a bulky mass, restricting movement and impeding locomotor efficiency (Stevens and Lowe, 1998).

To summarise, the process of remodelling is illustrated by Marcus (1987) as follows:

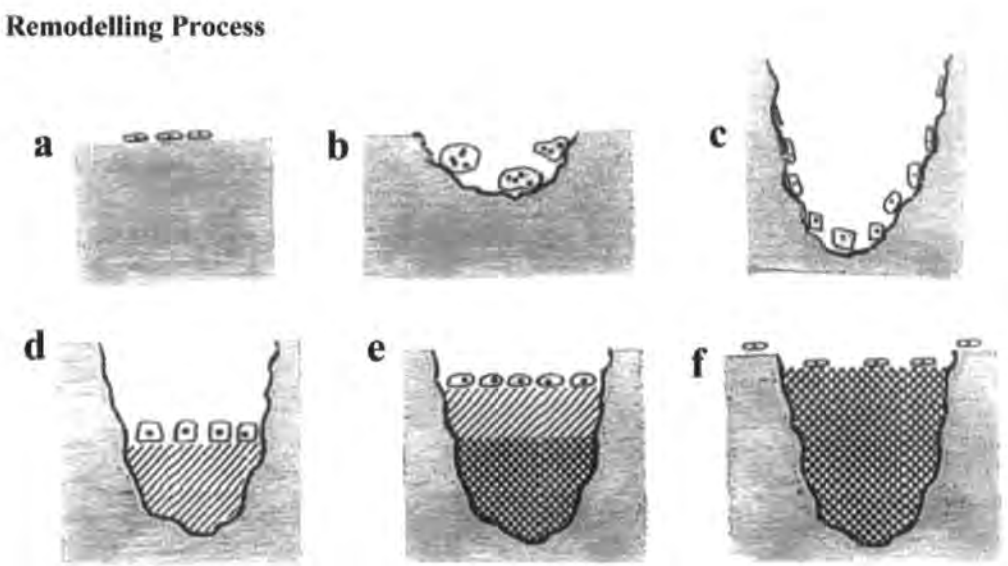

Figure 1.1: The remodelling process

Reproduced from Marcus, 1987

Key:

a Osteoclasts lying in the quiescent state on the bone surface

b Osteoclasts dig a cavity into the bone surface

c Osteoblast precursors are signalled to the base of the resorption cavity

d Secretion of new matrix by osteoblasts

e Continued secretion of matrix whilst commencement of calcification

f Completion of mineralisation of new matrix

1.5 The anatomy of the femur and tibia:

1.5.1 The femur

The femur (see Figure 1.2) is the longest, strongest and most robust bone of the skeleton as it supports the body's weight during standing, walking and running (White, 2000). Even the weakest section of the bone, the femoral neck, is able to withstand loading of between 12 and 15 times body weight prior to fracture (Saudek, 1985). Because of this strength and density, it is frequently recovered in forensic, archaeological and paleontological contexts where it offers valuable information with regard to the lifestyle and activity patterns of individuals and therefore, given sufficient data, of populations. Lower long bone length, primarily of the femur, also provides the best source of information for calculating the height and body build of individuals and populations within archaeological contexts (White, 2000).

Proximally, the femur articulates with the pelvis through the acetabulum. The femoral head forms approximately two-thirds of a sphere and connects to the acetabular notch through the ligamentum teres at the fovea capitis, the small depression at the centre of the head. The head connects with the shaft through the neck; the neck extending inferio-laterally to meet the shaft at an angle of about 125°. The importance of this angle lies in its relationship with the lower leg through the femoral neck to the shaft, creating the weight-bearing mechanical axis which passes through the middle of the knee joint to the middle of the calcaneus in the foot (Palastanga et.al., 1998; Platzer, 2004).

Because the femoral neck overhangs the shaft, the anatomical axis of the femur is not the same as the mechanical axis. This is in contrast to the tibia, where the mechanical and anatomical axes coincide. However, the mechanical axis, which centres on the mid-points of the hip, knee and ankle, in turn does not equate to the vertical because the hip joint is spread wider than the ankle joint. The difference in angle between the mechanical axis and the vertical is approximately 3°, although higher in females because of the increased width of the pelvis. The bicondylar angle of the femur lies at approximately 9° from the horizontal plane and is made by the femur in relation to the

vertical plane when both condyles of the distal femur are resting on the horizontal plane and intersecting with the angle of inclination at the base of the femoral neck (Palastanga et al., 1998). See Figure 1.3.

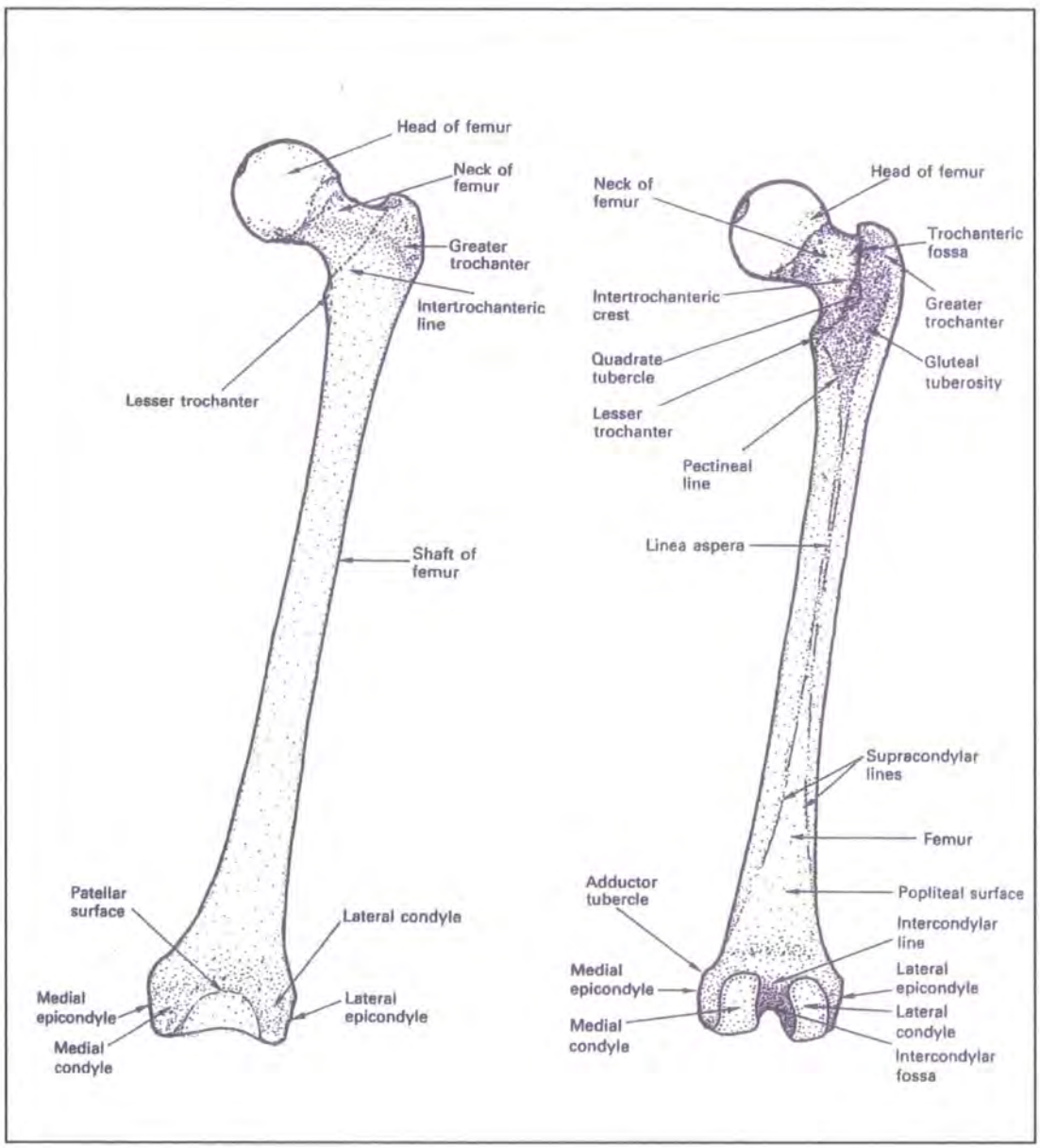

Figure 1.2 Views of the femur (anterior view and posterior view) together with major features of bone. Reproduced from Palastanga et al. (1998).

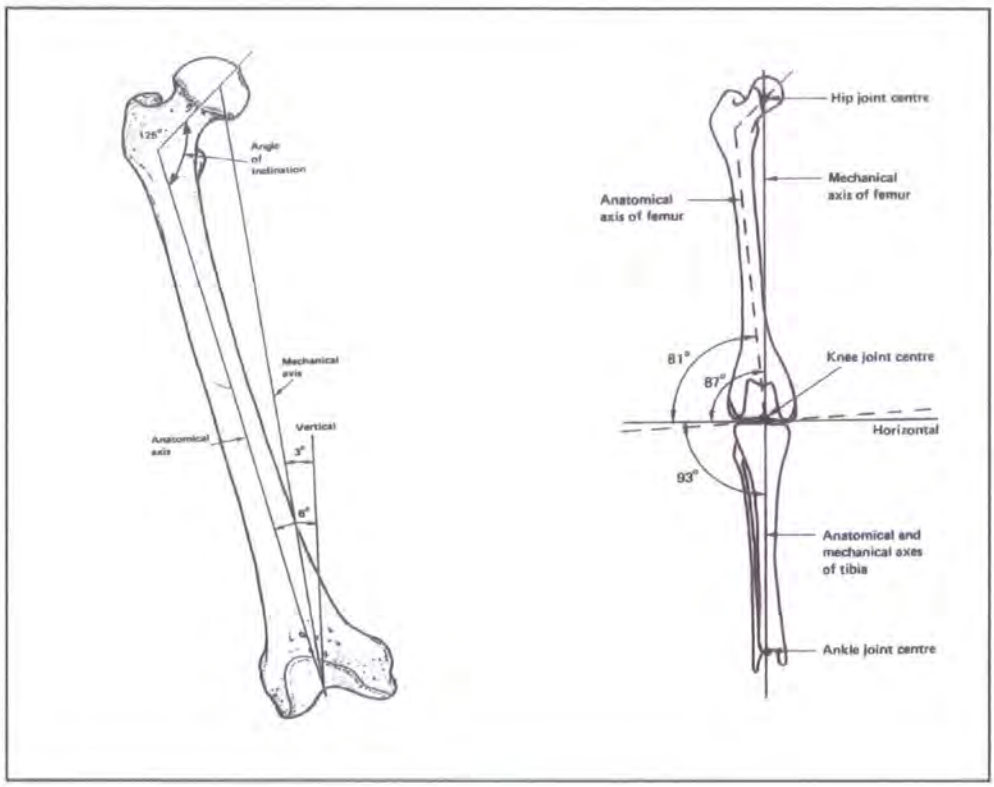

Figure 1.3 Anatomical and mechanical axes of femur and femur with tibia relative to the vertical axis. Reproduced from Palastanga et al. (1998).

The shaft comprises three main surfaces; the anterior, medial and lateral, of which the medial and lateral surfaces are separated by the linea aspera, a double crest running lengthways down the shaft. A nutrient foramen is found towards the central region of the shaft close to the linea aspera. Each crest diverges proximally and distally; at the distal end these supracondylar ridges terminate on the medial side at the adductor tubercle and in a corresponding position on the lateral side, forming a triangle with the intercondylar line; the popliteal surface (Palastanga et al., 1998; Platzer, 2004).

Major muscles, which adduct the thigh at the hip, include the powerful gluteus muscles that insert on the proximal femur. Some of those muscles however, require the full

length of the femur to function efficiently by extending the moment arm, i.e., the distance from the point of force to the fulcrum and measured to the line of action of the force. Such muscles include sartorius, the longest muscle in the body which crosses from the lateral side of the hip to the medial side of the tibial tuberosity (Palastanga et al., 1998; Stone and Stone, 2000).

The patella surface of the distal femur forms a smooth, articular area on the anterior surface, over which the patella moves during flexion of the knee. Both medial and lateral condyles become united on the anterior patella surface (White, 2000).

1.5.2 The tibia

The tibia is the major weight-bearing bone of the lower leg (see Figure 1.4). It articulates with the distal femur at the proximal end, with the fibula on the lateral side both proximally and distally and distally with the talus. The fibula articulates only with the tibia and talus. The angle of articulation between the femur and the tibia is known as the quadriceps or femorotibial angle and is formed between the shafts of the two long bones, creating the valgus position of the knee. It is governed by the width of the pelvis and normal values will therefore differ between males and females at c.13° and c.18° respectively (White, 2000; Kingston, 2001).

The tibial shaft is roughly triangular in cross-section, with a sharp anterior lip separating the medial and lateral surfaces. At the proximal end, this border culminates in the tibial tuberosity and becomes flattened at the distal end. On the proximal end, on the posterior side of the shaft, the roughened solteal line extends obliquely from the distomedial side to the proximolateral side, passing a nutrient foramen on the lateral side (Platzer, 2004).

All major muscle groupings which originate in the proximal tibia largely insert on the ankle and foot, including the primary tibial muscle, the tibialis anterior. The short popliteus muscle, one of the primary muscles responsible for rotating the knee and

which originates on the lateral surface of the lateral femoral condyle, inserts on the upper posterior surface of the tibia (see also section 1.7.2) (Stone and Stone, 2000).

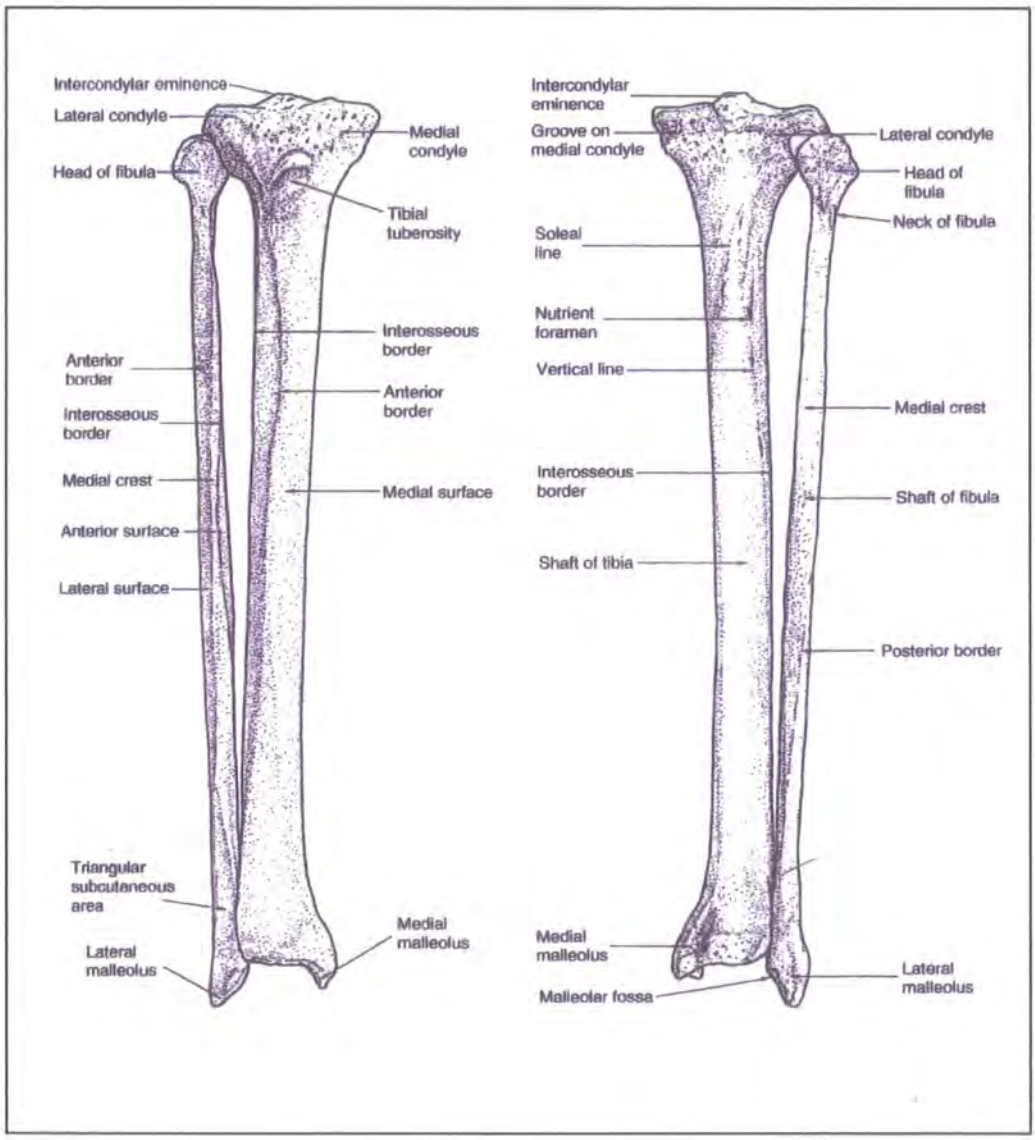

Figure 1.4 Tibia and fibula anterior view and posterior view, together with major features of bone. Reproduced from Palastanga et.al. (1998)

1.6 The anatomy of the knee joint

The knee joint has a dual function: the transmission of weight-bearing load and to allow the necessary degree of movement in the lower limbs for efficient locomotion. It is a synovial bicondylar hinge joint, i.e., a joint in which the articulating bone is covered with hyaline cartilage within a ligamentous 'sleeve'. The knee joint comprises articulations between the condyles of the femur and tibia and between the femur and patella. It therefore provides weight-bearing strength in supporting the opposing ends of the two largest bones in the skeleton, together with the flexibility to allow a relatively complex range of movement in the leg.

On the distal femur, the lateral condyle forms a large protrusion on the lateral side together with the lateral epicondyle, a convexity on the lateral side of the lateral condyle (see Figure 1.5). The medial condyle together with the medial epicondyle extends more distally than the lateral condyle and forms the second large protrusion on the distal femur. The condyles differ both in size and shape; the lateral condyle is wider at the front than at the back, while the medial condyle is of uniform width (Figure 1.1 and section 1.6 below) (Palastanga et al., 1998; Platzer, 2004).

From the distal view, both femoral condyles are seen to be slightly curved in a lateral direction although the medial condyle curves to a greater degree. In the sagittal plane, the condyles form a considerable curvature that increases posteriorly such that the radius of curvature decreases posteriorly. In so doing, the condyles pass through different midpoints in a series of curves; permitting a greater range of movement and allowing the knee joint to both roll and glide over the tibial plateau during flexion (Kapandji, 2001).

The proximal tibial is expanded in all directions relative to the shaft but particularly over the lateral posterior section, underneath which is the proximal tibiofibula articulation (see Figure 1.6). This expanded platform creates a 'shelf' that overhangs the tibial shaft and forms a narrow and relatively straight side posteriorly, laterally and medially. Anteriorly, the roughened area at the front of the plateau descends down the shaft to a

raised and roughly triangular section culminating in the tibial tuberosity. This region forms the insertion site for the patella ligament of the quadriceps femoris muscle.

The tibial plateau consists of two condyles that articulate with the femoral condyles; the medial condyle being longer anteroposteriorly relative to the lateral condyle to accommodate the movement of the curved, wheel-like medial femoral condyle. The smaller and rounder lateral condyle reflects the smaller degree of contact made by the lateral femoral condyle. The two smooth surfaces are divided by the intercondylar eminence a double raised border running antioposteriorly and formed from the margins of the condyles and by the medial and lateral intercondylar tubercles; two raised and easily located landmarks. The intercondylar eminence anchors the anterior and posterior cruciate ligaments and the anterior and posterior extremities of the lateral and medial menisci. The condyles are flattened on their lateral edges to accommodate the menisci. In mature adults, the proximal end of the tibia is inclined slightly backwards forming an angle of retroversion. This angle forms between the superior articular surfaces of the tibial plateau and the horizontal and averages approximately 4° to 6° in adults, although this angle will have decreased considerably from about 30° at birth (Palastanga et al., 1998; Stone and Stone, 2000; Platzer, 2004).

The conformation between the femoral and tibial surfaces is imprecise and in healthy joints there should be little area of contact between them. The articular surfaces are covered by a synovial membrane that is well supplied by blood vessels and nerves and that secretes a highly viscose liquid, the synovial fluid that fills the remaining space between the two surfaces, the menisci and ligaments. The synovial membrane also extends into bursae, fluid-filled pockets that provide both additional protection and aid lubrication. The joint space is additionally cushioned by a wide fatty pad, the infrapatella fat pad, which sits inside the joint capsule on the lower margin of the patella (Palastanga et al., 1998; McGowan, 1999; Platzer, 2004).

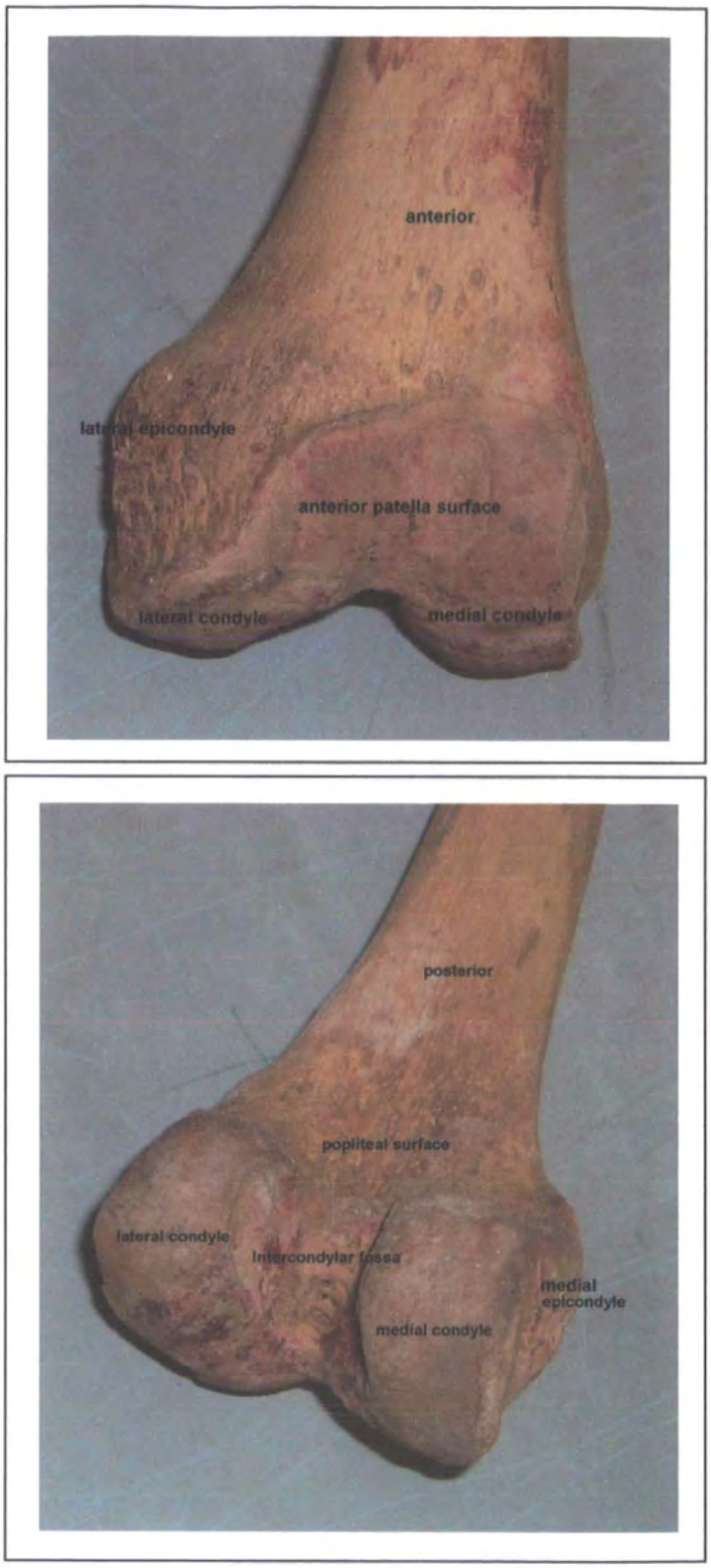

Figure 1.5 Distal femur anterior view and posterior view, together with major features of bone.

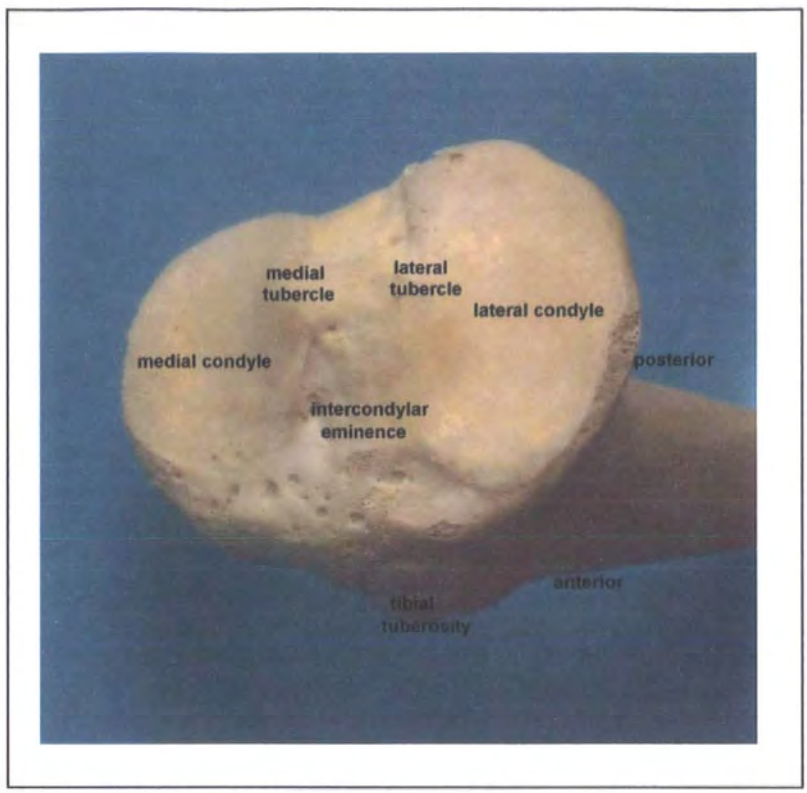

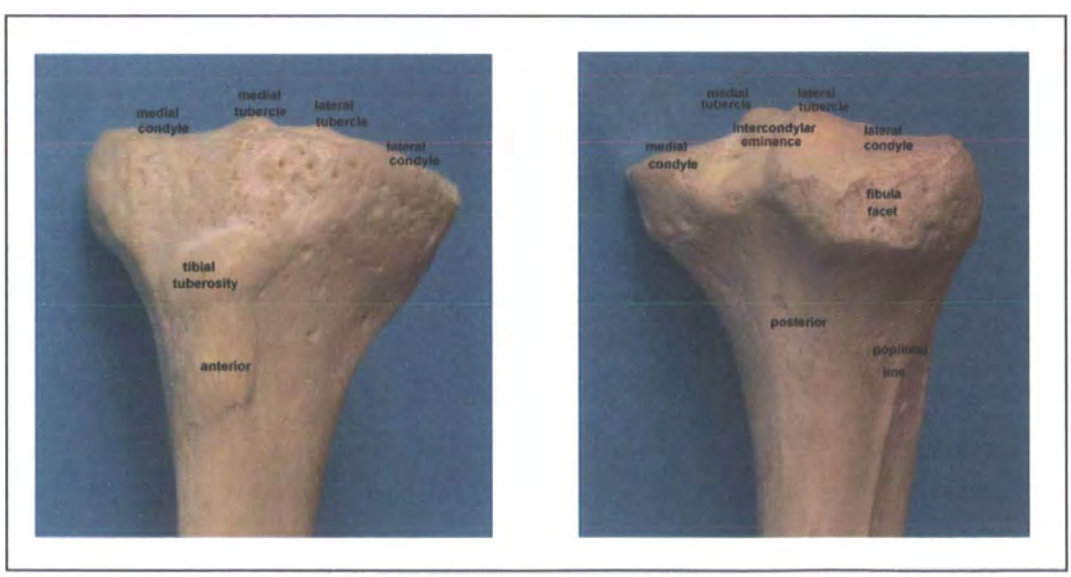

Figure 1.6 Tibial plateau with proximal tibial anterior and posterior, together with major features of bone.

The barrel-shaped sleeve of ligamentous fibres which encapsulates the knee joint is attached at one end to the femur and at the other to the tibia. This articular capsule is open on the anterior side where it is replaced by the quadriceps tendon and the retinacular and the patella ligaments. This ligamentous sleeve is thicker in various parts depending on the functional demands being made on each area (Palastanga, 1998).

Internally, the anterior and posterior cruciate ligaments are fundamental in preserving the stability of the joint (see Figures 1.7 and 1.8). The anterior ligament runs from the anterior intercondylar area of the tibia to the inner surface on the lateral side of the intercondylar fossa of the femur. The femoral attachment is less strong than the tibial attachment with the fibres becoming more widespread as they undergo a medial spiral. The posterior ligament is almost twice as strong as the anterior ligament, passing from the medial intercondylar surface of the femur to the posterior depression of the intercondylar area of the tibia. Being centered around the pivotal rotational mechanism of the knee joint, it forms the joint's principal stabiliser (Palastanga et al., 1998; Kapandji, 2001; Platzer, 2004).

Together with the cruciate ligaments, the medial and lateral menisci form an essential part of the locking mechanism of the joint by restraining the femur from gliding too far forward on the tibia. They also take the principal role in shock-absorbing the two opposing bone ends, thus decreasing the incongruence between them. Constructed of articular cartilage, the hardest of the soft tissues, the menisci are capable of maintaining shape and configuration under moderate stress for short periods. They are also able to withstand the considerable impact loading and wear at the joint by helping to spread the load across the width of the condyles (see section 1.7.2). Being supplied with blood, they provide the synovial membrane with the fluid necessary to lubricate the joint, some of which appears to seep from the cartilage itself and some of which is contained within the bursae, the mobile, fluid-filled sacs lined with this membrane (Al-Turaiki, 1986; Nordin and Frankel, 2001).

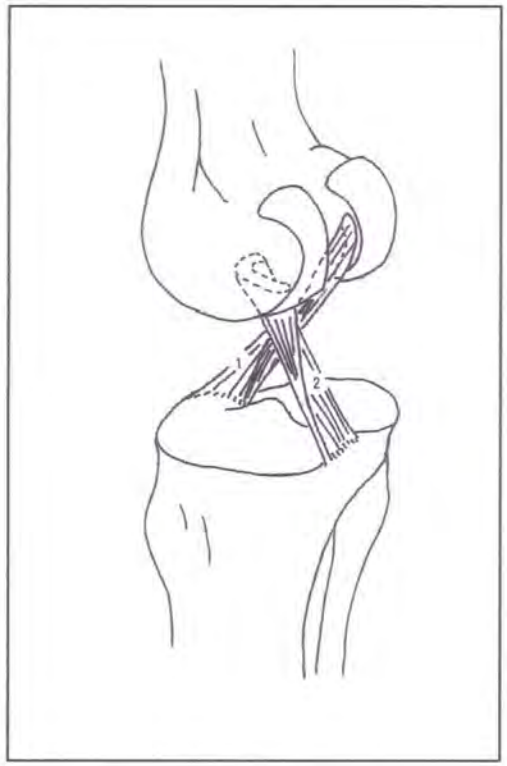

Figure 1.7 (a) Knee joint
Key:

1 Anterior cruciate ligament
2 Posterior cruciate ligament

Reproduced from Kingston, 2001

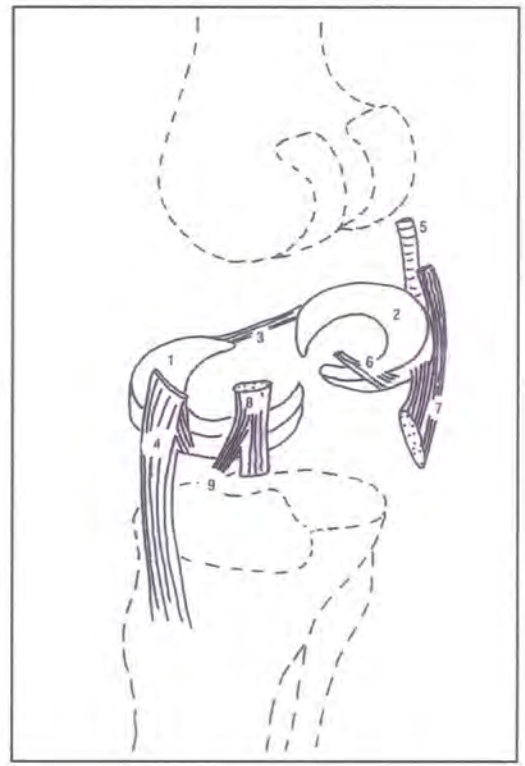

Figure 1.7 (b) Knee joint
Key:

1 Medial menisci 2 Lateral menisci 3 Transverse ligament
4 Medial collateral ligament (with deep fibres attached to meniscus
5 Lateral collateral ligament 6 Posterior meniscofemoral ligament
7 Popliteus tendon 8 Semimembranosus tendon
9 Semimembranosus expansion (the attachment to medial collateral ligament)

The medial meniscus is semicircular in shape with widely separated attachment areas on the anterior and posterior sides of the medial condyle. It also attaches to the collateral ligament on the outside edge of the medial condyle. The lateral meniscus forms four-fifths of a circle and lies more within the confines of the lateral condyle. With no outside attachment sites, the lateral meniscus is considerably more mobile than its medial counterpart (Palastanga et al., 1998).

1.7 Biomechanics of the knee joint

1.7.1 Overview

The study of biomechanics is the application of mechanical principles to the analysis of biological systems. Thus, biomechanics involves the use of the tools of mechanics (i.e., the analysis of the action of forces) in the study of anatomical and functional aspects of living organisms. Unlike the mechanical analysis of inert building materials, however, the biomechanical analysis of living tissue deals with material that is continually modifying itself to differing loading pressures through changing activity patterns (i.e., by remodelling) (Hall, 1995; Larsen, 2000).

The broad spectrum of biomechanics includes the fundamental aspects of kinematics, which is the description of motion incorporating the pattern and speed of movements and kinetics, the study of forces associated with motion. Both provide an understanding of the appearance and sequencing of motion, together with the amount of force required by muscle action to produce optimal efficiency for the intended motion of the movement (Hall, 1995; McNeill Alexander, 2002).

In relation to the analysis of lower limb anatomy and the efficiency of human locomotion, the study of biomechanics indicates that the gait selected for operates at a stride length and rate that optimises metabolic energy consumption at a given speed (Perry et al., 1988). Perry et al. believe that as speed increases in humans and other vertebrates, the transition from walking to running may occur before reaching energetic optimality and that comfort and the ease of motion may not strictly parallel efficiency.

They also suggest that muscle stresses at the preferred speed indicate an optimal safety factor to injury.

All movements of the human body are dependent on the interaction of forces moving loads, by means of levers, around a pivotal fulcrum. In the human body, the arrangement of the positions of the fulcra, the points of force and the points of load create three types of levers with the fulcra usually situated at the joints; the loads being body weight or external resistance and the forces being that supplied by muscular tension. Mechanical advantage is measured as the ratio of force applied to the load compared to that applied by the force (Palastanga et al., 1998).

Lower limb bones are responsible for human locomotion and as such are subjected to considerable weight. The levers in the human body are therefore constructed in such a manner as to enable them to incorporate loading from various forces, either throughout the entire bone or within sections of bone (Larsen, 1999). Humans, like most terrestrial vertebrates, rely upon the ability to move relatively quickly whilst supporting the body's weight. In this respect they and other cursorial animals differ from animals such as elephants whose legs are primarily required to support a considerable bulk at no great speed. Whilst the legs of graviportal animals are held vertical to the ground like upright columns to maximise weight bearing, the long bones of cursorial animals are angled to maximise locomotor efficiency (see also section 1.5.1 above relating to the bicondylar angle of the femur and section 1.8 below relating to the biomechanics of gait) (McGowan, 1999).

Locomotor efficiency and the ability to move fluidly and quickly, demands that the body's centre of gravity lies as close to the midline as is feasible. The angled bones, however, then become subjected to one or more of the various forces of compression, tension, bending, shear and torsion. In relation to the ends of the bones, some of these forces are attributed to gravity, whilst others are from tension. Gravity tends to load the dorsal surfaces of the bones in compression whilst the proximal surfaces of the bones are subject to forces attributed to tensions generated by muscular action. In addition,

because of the curved shape of long bones, muscular forces tend to be applied off-centre to the bone's axis. As axial loading from either compression or tension is rarely equal, the diaphyses of long bones are usually subjected to eccentrically applied pressures. To enable such angled bones to cope with the multidirectional stresses generated, they are tubular in construction with the shafts being constructed of relatively thin-walled compact bone; tubes being stronger than solid rods of the same mass (McGowan, 1999).

In contrast to the shafts, the dorsal and proximal ends of the bones are constructed from honeycombed trabecular bone due to their requirement to transmit stresses from the joint surfaces to the shaft. Within these ends, trabeculae act both as bony strengtheners in their own right and as a material made up of small beams and columns that are free to move and bend slightly within the bony matrix, so providing maximum ability to cope with the demands of habitual strain. The adaptive advantage of trabecular systems lies in their resilience and ability to absorb the considerable forces to which the lower limb bones are particularly subjected (McGowan, 1999).

1.7.2 Movements of the knee joint

The knee is arguably the most mechanically vulnerable joint in the body, both in terms of the forces and leverage acting directly upon it and because any dysfunction in the hip and ankle joints will also strongly impact upon it (Kingston, 2001). Two sets of forces act over the knee joint, those acting upon the femorotibial joint connecting the femur to tibia, controlling the lengthening and shortening of the lower limb and those acting upon the femoropatella joint, allowing the patella to act as a pulley for the quadriceps tendon relative to the femur. The femorotibial joint is loaded with both compressive and shear forces; weight-bearing and tension in the muscles that cross the joint contribute to the applied forces, with compression dominating when the knee is fully extended (Hall, 1995; Palastanga et al., 1998).

During level walking, the forces acting upon the femorotibial joint can reach five times body weight, although for most of the gait cycle it is usually between two and four times

body weight (Palastanga et al. (1998). In similar circumstances of level walking, forces acting upon the femoropatella constitute approximately half body weight. In the tibia, the medial condyle is roughly 60% greater in area than the lateral condyle and bears most of the load during the heavier-weighted stance phase of walking. The lesser degree of stress during the swing phase is taken by the lateral condyle (see section 1.7.3 below). The force is cushioned by the menisci, which normally accept up to 45% of the total loading. However, at high levels of loading this can account for 70% of total contact area, providing elastic stability to the joint and having both weight-bearing and load-spreading functions. During flexion, the loading pressure becomes shear and this force is accommodated by the ligaments, which if shear is applied excessively can stretch and rupture (Palastanga et al., 1998; Nordin and Frankel, 2001).

The principal movement of the knee joint relates to the extension and flexion of the lower limbs; limited rotation of the joint is also possible when the knee is fully flexed (Al-Turaiki, 1986). Few muscles act exclusively upon the knee joint, with the majority also acting upon the ankle and subtalar joints. Extension is almost exclusively controlled by the quadriceps femoris group, originating on the ischial tuberosity and inserting on and around the patella and ligaments attached to the tubercles of the tibia. Flexion is governed by a wider series of muscles, including the posterior thigh muscles of the hamstring group and three medial thigh muscles including sartorius. Rotation is largely controlled by these flexor muscles together with the short popliteus, which also serves to stabilise the knee by preventing lateral rotation of the tibia during medial rotation of the thigh while the foot is planted (Palastanga et.al., 1998; Stone and Stone, 2000).

The range of flexion depends both on the position of the hip and whether the movement is active or passive; active movements being those relying solely upon the action of the joint itself and which cannot reach the same degree of magnitude as passive movements that rely upon additional pressure placed upon them. Active flexion can reach approximately 140° if the hip is fully flexed and 120° if the hip is fully extended; passive flexion can reach up to 160° with the hip fully flexed. The extent of knee flexion is largely dependent upon the ability of the hamstring muscles to stretch sufficiently

relative to the hip as these muscles not only act as knee flexors but also as hip extensors. If the hip is fully extended, the distance between their origin on the ischial tuberosity and the insertion points on the proximal tibia becomes relatively shortened, reducing the extent of knee flexion. In contrast, a fully flexed hip allows the hamstrings greater efficiency in knee flexion. The ability of the hamstrings to operate at maximum efficiency is also governed by the action of the quadriceps muscles and the capsular ligaments, which can also be brought into play in certain stages of flexion (Kapandji, 2001).

A combination of sliding and rolling movements is permitted in the knee joint by the asymmetric curvature of the femoral condyles, which create a "screwing" action from the combined movements of the narrower wheel-like medial condyle and broader lateral condyle on the asymmetric surfaces of the larger medial and smaller lateral tibial condyles. Although the basic shapes of the articular surfaces only allow movement in one plane (i.e., for flexion and extension) axial rotation is also permitted by the interconnection of the intercondylar tubercles of the tibia seating within the intercondylar fossa of the femur. The tubercles of the tibia act as a pivot and are constrained from excess movement by the inside borders of the medial and lateral femoral condyles. The range of movement within the knee joint depends upon this hard-tissue structure, with the soft-tissue constraints surrounding the bony framework (Kingston, 2001; Platzer, 2004).

Full extension movement in the joint is finalised by a 'screw-home' or locking mechanism that confers a greater degree of stability on weight-bearing and is aided by the menisci and the cruciate ligaments. The cruciate ligaments tighten in extension and provide an end point, which not only prevents further extension but also provides a final twist to take the tibia into lateral rotation and the femur into medial rotation. The knee unlocks from full extension by contracting the popliteus muscle, which pulls the tibia back into a slight medial rotation and the femur into a slight lateral rotation (Kingston, 2001).

The knee can only be properly rotated with the joint in the flexed position. In medial rotation, the medial femoral condyle moves forward over the medial tibial condyle while the lateral femoral condyle moves backwards over the lateral tibial condyle. In lateral rotation the movements are reversed. The range of rotation is governed largely by the degree of flexion of the knee at the start of rotation and by the direction of rotation. Medial rotation is always less than lateral rotation due to the position of the cruciate ligaments. In medial rotation the cruciate ligaments become twisted around each other which prevent further movement. In lateral rotation, the cruciate ligaments become unwound but are prevented from rotating too far by the action of collateral ligaments. Active rotation is limited to 30° for medial rotation and 40° for lateral rotation but can be increased to 35-45° and 50-60°, respectively with passive rotation. In addition, because of the asymmetry in size and shape of the two sets of condyles, the extent of the anteroposterior movement varies for each side with the lateral femoral condyle moving considerably further than the medial condyle, being unimpeded by the lateral tubercle on the tibial plateau. There are two sets of forces producing rotation; from the popliteus and from the flexor and medial rotator muscles (gracilis, sartorius and the hamstring semitendinosus) (Kapandji, 2001).

Different activities will have varying consequences for the two forces of compression and shear acting upon the knee joint, depending upon external factors such as the speed of walking and environmental conditions. For instance, those forces acting upon the femoropatella increase to between one-and-half and two times body weight when ascending stairs or ramps and between two-and-half and three times when descending. In contrast, ascending or descending stairs or ramps appears to have little effect upon the femorotibial joint. The degree of forces across the joint is dependent upon the acceptance of full body weight onto the supporting limb, together with the level of muscle activity upon the joint (Palastanga et al., 1998).

The high contact forces from both above and below and from side-to-side are reflected in the patterns of trabeculae around the knee joint. The distal end of the femur shows trabecular arrangements running both lengthways down the shaft and crossways uniting

both condyles. The proximal end of the tibia displays a similar arrangement (Palastanga et al., 1998; Kapandji, 2001).

Any alterations in the normal biomechanics of the joint surfaces (including those of the patella) may initiate degenerative changes. If continuously repeated, abnormal loads or changes in activity patterns cause loading to alter across the joint, together with an increase in the number of microfractures within the trabeculae. If the resultant stiffening of trabeculae under remodelling creates too great an incongruity in the fit between the articular surfaces, damage to the joint is likely to occur. Loss of congruence and excessive loading in the wrong areas (i.e., onto thinner articular cartilage), frequently leads to osteoarthrosis (Palastanga et al., 1998; Kingston, 2001).

1.8 The biomechanics of gait and the process of human walking

Human bipedal walking is essentially a learned operation and not an inborn reflex. Unlike quadrupedal locomotion, where three of the four limbs and feet are constantly in contact with the ground surface, bipedal locomotion requires a higher degree of neural control. Children normally teach themselves the skill by the process of observation and trial and error until stability is achieved but congenitally blind children need to be carefully taught by others before the skill is acquired. The process of walking as a basic method of locomotion conforms to a general pattern. As a learned skill, however, individuals superimpose their own characteristic peculiarities onto the basic pattern (Inman and Ralston, 1981).

The basic pattern requires that the moving body is supported firstly by one leg then the other. As the moving body passes over the supporting leg (the stance phase), the other leg is swinging forward in preparation for its own support phase (the swing phase). Whilst one leg is transferring support from the leading to the trailing leg, both feet will be on the ground for a brief moment (the double-support phase). With increasing speed the double-support phase decreases until, for a brief moment, neither foot will be on the ground at the same time (the float phase). The stance phase comprises approximately

60% of the gait cycle, with the swing phase comprising approximately 40%, although the proportion of swing to stance increases with increasing speed (Inman and Ralston, 1981; Pribut, 2003).

The stance phase is subdivided into three stages: contact, when the heel strikes the ground; midstance, when the entire foot is on the ground; and propulsion, from 'heel-off' to 'toe-off'. The swing phase begins immediately after the toe-off subphase when the second leg is carrying the foot forward; the knee is flexed and the foot is dorsiflexed. The second half of the swing phase occurs when the foot is descending, ready to bear the body's weight with the muscles preparing to absorb the shock of heel contact. At heel contact, the swing phase ends and the gait cycle is complete (Pribut, 2003).

Gait can be defined by several variables:

Step length; the distance between the point of initial contact of one foot and the point of initial contact of the second foot. In normal gait right and left step lengths are similar.

Stride length; the distance between successive points of initial contact of the same foot. Right and left stride lengths are normally equal.

Cadence; the walking rate calculated in steps per minute.

Velocity; the product of cadence and step length. This is an variable measurement that depends on each individual's comfortable rate and circumstance.

Walking base or 'base of support'; the sum of the perpendicular distances from the points of initial contact of the right and left feet to the line of forward progression.

Foot angle; the 'toe-out' angle between the line of progression and the midpoints of the calcaneous and second metatarsal head (Cech and Martin, 2002).

The significance of these variables lies in the differences seen between individual gait patterns, between the typical gait patterns of the two sexes and, importantly, variation in gait throughout the lifespan (Cech and Martin, 2002; Thompson, 2002a; Thompson, 2002b; Pribut, 2003).

The seminal work by Inman and Ralston (1981) outline the two basic requirements for locomotion: first, that there are continuing ground forces that support the body and second, that there is a periodic movement of each foot from one position of support to the next in the direction of progression. During progression the body undertakes movements in all three planes in space; it speeds up and slows down, it rises and falls and it sways slightly from side to side.

Therefore to maximise energy efficiency, human walking should incorporate the following elements:

i) The pelvis should rotate within a horizontal plane. By so doing, it prevents the centre of mass of the body from falling too far during the double-support phase when both feet are at maximum distance apart.

ii) The pelvis should list downwards to approximately 5° on the side opposite to the weight bearing limb. This movement means that the centre of mass need not be raised so far, thus conserving energy efficiency. The pelvic list also contributes to the efficiency of the abductor muscles of the hip.

iii) The knee should flex to enable the swinging limb to be elevated off the ground in compensation for the pelvic list, which serves to lower the arc of the swing. At the same time as the knee on the swinging limb is flexing to allow clearance, the other knee begins its own cycle of flexion. The knee joint is therefore at full extension as the supporting limb enters the stance phase at heel strike. It then begins to flex and continues to do so to a maximum of approximately 15°. Just before midstance the knee joint once again becomes extended, then immediately starts to flex at heel-rise when the swing-phase begins. Thus, the cycle takes the knee joint through extension, flexion, extension and finally flexion again.

Thus the three elements of pelvic rotation, pelvic list and knee extension all serve to lessen the vertical displacement of the body. Pelvic rotation serves to prevent any undue movement at the end of each phase of the cycle and pelvic list and knee flexion prevent excessive rise at the midpoint of the cycle. In addition, other mechanisms at the knee,

ankle and foot serve to smooth the process by once again minimising the vertical displacement of the body in allowing the pathway of displacement of the knee to remain relatively horizontal. In its turn, the hip operates more efficiently because of the smoother pathway of the knee.

The actions that allow this greater bipedal efficiency involve the proper phasing of extensor and flexor muscles of both the leg and foot. In addition, rotation of both the leg and foot cause shortening of the leg by a crucial few millimetres when appropriate. Transverse rotations in the ankle and subtalar joints of the foot, together with rotation in the leg, are also instrumental in preventing the foot from slipping sideways. Thus, when the leg rotates internally, the foot pronates; when the leg externally rotates, the foot supinates. Whilst the ankle is effecting the motions of plantarflexion and dorsiflexion between heel-strike and toe-off, rotatory actions of both the leg and the foot create a pattern of normal, more energy efficient walking.

Transverse rotations of the pelvis, thigh and leg are co-ordinated to the stride cycle such that internal rotation begins towards the weight bearing leg at the beginning of the swing phase, continuing during the double-support phase and into midstance. At this point external rotation takes over and continues to the beginning of the next swing phase. An increase in rotation occurs from hip to leg, with the leg rotating as much as three times more than the pelvis. The degree of rotation as a whole varies from individual to individual, however, and it is this attribute that tends to mark out each person's characteristic manner of walking (Inman and Ralston, 1981).

Whilst the pelvis needs to tilt over the supporting limb, this lateral displacement can be minimised by keeping the feet more closely together and therefore closer to the body's midline. Efficient bipedalism, therefore demands that the pelvis should be as narrow as possible. The female pelvis however, presents a compromise between efficient locomotion and a channel for the delivery of large-brained offspring. Because of this compromise women, with wider hips than men, can rarely run as fast as men and female athletes are normally masculine in body shape with relatively narrow hips. Obesity also

forces the feet wider apart and creates the characteristic exaggerated dip of the hips and rolling gait whilst walking in both males and females (Inman and Ralston, 1981).

Human gait is thus a complex process. All bones, joints and muscles of the lower limbs must work together in unity to produce a complete stride cycle operating at maximum efficiency. Although in evolutionary terms the attainment of efficient bipedalism freed the upper limbs for carrying food, tools, children and suchlike, the upper limbs are still necessary as an aid to efficient walking. Indeed, every part of the body including the musculature of the head and neck are vital for efficient coordination in walking (Platzer, 2000; Cech and Martin, 2002). Rotation of the thorax and shoulders, causing the arms to swing counter to the rotation of the pelvis, provides a balance that aids forward progression. Impeding this swing at higher speeds suppresses the ability to keep to a straight line and is thus counter to energetic efficiency.

1.9 The effects of footwear on gait

William Rossi (2005) defined human gait in terms of that which is 'normal' and that which is 'natural'; 'normal' gait being that which is expected in shoe-wearing cultures and being different to that which is 'natural' and found in bare-foot societies. All shoes alter natural gait in that they take the heel away from the natural position of 180° to the upright body and weight distributed equally between the heel and the ball of the foot. With a heeled shoe, the increased angle of the heel shifts body weight forward in such a way that weight becomes proportionately greater on the ball as it decreases over the heel. In low heeled shoes, the proportions will be c. 60% body weight on the ball and 40% on the heel, increasing to 90% and 10% respectively with high heels. Under these conditions the step sequence is altered and no longer goes through the same heel-to-ball-to-toe and push-off phase as seen in the bare foot but, depending on the height of the heel, is forced to rely on the ball of the foot to supply the required propulsion. In addition, because the soles of shoes create less flexibility over the ball, the toe area is built to raise the toes away from the horizontal (the 'toe-spring') in order to compensate. Whilst this design compensates for the decreased flexibility of the ball, it also angles the

toes upwards by as much as 20°, preventing them from performing their natural function of grasping the ground and providing additional propulsion. Because the hallux and other digits are largely immobilised by this design, step propulsion must come from the metatarsal heads, placing undue pressure on the heads and affecting the mechanics of the gait cycle. Additionally, not only is the natural step sequence changed and loading pressure placed on different sites in the foot altered but the Achilles tendon and calf muscles become shortened. This shortening places greater reliance for supplying adequate propulsion on other muscles in the knee, thigh, hip and trunk (Rossi, 2005).

Whilst acknowledging the necessity of having to wear shoes in less hospitable regions and climates for protection and warmth, Rossi (2005) also maintains that the "remarkable feat of bioengineering" of the natural human gait has been warped by footwear, obstructing its engineering efficiency. Rossi's (2005) conclusions are supported by Lanyon et al. (1975) who found that, during running, the lower limb strain measurements in any individual can vary by up to 40% depending whether he or she is shod or unshod. In the light of such research such as that by Lanyon et al. (1975) and Rossi (2005), Chapter 6 will examine whether the habitual wearing of footwear is a sufficiently influential variable to significantly contribute towards any differences in knee joint shape between populations.

1.10 Structure and summary of analysis chapters

The materials and methodology used in the study are outlined in **Chapter 2.**

Asymmetry between right and left knee joints is analysed in **Chapter 3** with results placed within the context of any asymmetries found in the lower limbs. Previous research has tended to concentrate on asymmetries within the upper limbs because of the preference for right-handedness in all human populations. In relation to the knee joint, previous studies (using a limited number of linear measurements between homologous landmarks of the distal femur and proximal tibia) have found no apparent differences between right and left sides (Craig, 1995; Gill, 2000). It has frequently been considered

feasible, therefore, to use either the right or left side to represent any individual for comparative purposes. Indeed, for simplicity, gait symmetry has frequently been assumed and with it, the underlying expectation of bone symmetry (Arsenault, 1986). Even when experiments using observations from both right and left limbs have looked for gait symmetry and have confirmed its presence (Chou et al., 1995), other researchers have found significant degrees of asymmetrically applied forces during normal walking (Sadeghi, 2000). By analysing the shape of both distal femur and proximal tibia, Chapter 3 seeks to determine whether knee joint shape can be regarded as symmetric and, if so, whether right and left limbs can be regarded as transposable for comparative purposes.

Sexual dimorphism in the form of the knee joint is examined in **Chapter 4** and, if present, places such differences within the context of sexual dimorphism in the lower limbs. Differences in size between the limbs of males and females are visually obvious and have been well researched in the past by, for example, Black (1978), Dittrick and Suchey (1986) and Iscan and co-workers (1984a, 1984b, 1986, 1994 and 1995). Although it is acknowledged that different patterns and levels of activity affect the shape of the diaphysis between men and women (Ruff and Hayes, 1983; Ruff, 1987; Brock and Ruff, 1988; Bridges, 1989; Hawkey and Merbs, 1995; Larsen, 1995; Larsen, 2000), and that men and women flex the knee joint to significantly different levels in normal walking (Murray et al., 1964, 1970), little previous work has been conducted on sexual dimorphism in the knee joint itself.

Changes in the shape of the knee joint during ageing are analysed in **Chapter 5.** It is well understood from previous research that bone alters in structure during the ageing process (Marcus, 1987; Parfitt, 1991; Seeman, 2002; Robling and Stout, 2000; Erikson, 1991 and Pfeiffer, 1998). Gait patterns are also known to change with ageing (Cech and Martin, 2002) and degenerative diseases are known to affect the knee joint more than any other joint (Felson, 1988).

Results of intra-population analyses will indicate whether, despite the expected variability in knee joint shape between individuals, patterns of similarities or differences are present between different groups within populations. **Chapter 6** proceeds to analyse whether differences in the form of the knee joint and lower limbs are also present between populations and explores possible reasons behind such differences.

Previous research designed to compare and contrast the morphology of different skeletal parts of different populations has found significant variation between samples (for example, Giles and Elliott, 1962; Howells, 1970, 1973, 1989, Krogman and Iscan, 1986; Bass, 1987; Relethford, 1994; Craig, 1995; Hanihara, 1996; Viðarsdóttir, 1999; Gill, 2000). In relation to the knee joint, research has found that different populations use their knees in different ways; for example, groups who habitually squat such as the Japanese can rotate the knee joint to a greater extent than others who do not, such as the majority of Caucasian groups (Freeman, 2001). Differing use between groups and therefore different loading pressures imply that bone shape will be strongly influenced if it shares a common functionality. If distinct patterns are apparent within population samples, Chapter 6 will compare the shapes of each population sample relative to those of other populations and assess which influences, for example climatic, cultural or economic are instrumental in governing shape.

Chapter 7 gives a summary of the discussions of results from the previous four chapters and an overall discussion of differences and reasons for those differences in the morphology of the knee joint in *Homo sapiens*.

Chapter 2

Materials and Methods

2.1 Materials

2.1.1 Introduction

This study is based on data from thirteen distinct samples of recent *Homo sapiens*. The total dataset includes adult specimens of right and left bones, males and females and those of unknown sex. Three population samples include reliably aged specimens; the rest are of unknown age. Adulthood is determined by full epiphyseal fusion of the articular surfaces to the diaphyses. Sex is taken from collection records and reliable estimation from accompanying pelves. Any ambiguity arising after examination resulted in specimens being designated as sex unknown.

Distal femora or proximal tibiae with post-mortem damage, pathologies or osteophytes on joint surfaces were not included. Bone ends in seemingly healthy condition but with broken shafts were, however included. Complete long bones with minor disfigurements of the articular surfaces (making them unsuitable for digitisation) but with undamaged shafts were included for measurements of maximum length and robusticity of the shafts. Therefore, although nearly all individuals used for both shape and size analyses of the knee joints and size analyses of the long bones were from the same individuals, the small discrepancy in numbers is to allow for the maximisation of data.

Tables 2.1 and 2.2 summarise the total number of specimens used in the following analyses, together with the history of the specimens and the museums where the collections are located. Only certain specimens were selected in each of the four sets of analyses, however and the numbers and type of bones used are specified at the beginning of each chapter.

2.1.2 The thirteen populations of *Homo sapiens*

The thirteen population samples are distinct, coming from geographically widespread regions over six continents and being economically diverse and from different ancestral backgrounds. For analysing postcranial material, which is subject to considerable local loading pressures, it would have been preferable use material from specified tribal or local groups in all cases. Due to lack of data in museum collections, however, this was not always possible.

In analysing reasons for differences in the form of the knee joint in Chapter 6, various environmental factors are taken into account. Therefore, the thirteen populations are described below in as full and accurate detail as possible. Abbreviations of samples are included that are used within the text and in tables.

Climatic data used in the following descriptions are taken from WorldClimate.com (2004).

2.1.2a The Aleut

Location: Aleutian Islands and Coastal Alaska, USA
Ancestry: Native North American Amerindian
Abbreviation used in study: At

The specimens:

The skeletons were mainly collected from sites at Shiprock, Alaska and the Unalaska Islands of Chernovski, Kagamil and Kashega of the Aleutian Island chain, having been excavated by Aleš Hrdlička, in the 1930s (Hrdlička, 1941, 1945). The dating of the collection is disputed, although it is likely to be from c. 1000 BP (Black, 1983). The postcranial material has been well catalogued and sexed by archaeologists from the NMNH Smithsonian Institution, using accompanying skeletal and cultural artifacts (personal communication with museum curators).

Population	Location of collection	Date of collection/ Age of specimens	Geographic Location/ subsistance	Bone	Total right used	Total left used	Total males	Total females	Sex unknown	Aged
Aleut	NMNH	1930s	Alaska, USA	Femur	26	0	15	11	0	0
		c.1000BP?	Marine HGs	Tibia	26	0	17	9	0	0
Pachacama	NMNH	1890	Peru	Femur	29	0	18	11	0	0
		400BC-1500AD	Trade/Agric?	Tibia	27	0	15	9	3	0
Arikara	NMNH	1957-62	S. Dakota, USA	Femur	34	19	24	10	0	0
		1600-1750AD	HGs/Farmers	Tibia	32	23	24	10	0	0
Chinese	NMNH	1930	Northern China	Femur	25	23	25	0	0	0
		late 19th century	Agric/Industrial?	Tibia	29	27	29	0	0	0
Australian	NMNH/NHM	19th century	Australia	Femur	32	0	5	7	20	0
		19th century	HGs	Tibia	28	0	5	10	13	0
African Americans	NMNH	early 20th century	Missouri, USA	Femur	122	47	63	59	0	121
		early 20th century	Industrial	Tibia	116	49	57	59	0	120
Ibo	NMNH/NHM	19th century	Nigeria	Femur	14	0	4	7	3	0
		19th century	HGs	Tibia	9	0	0	2	7	0
Andaman Islanders	NHM	1902-05	Andaman Isles, India	Femur	34	0	7	8	27	0
		1875-1900	HGs	Tibia	33	0	9	9	15	0
Sri Lankan	NMNH/NHM	1880s	Sri Lanka	Femur	18	0	5	13	0	0
		1880s	HGs	Tibia	13	0	4	8	1	0
Khoisan	NMNH/NHM	late 19th century	S. Africa/Namibia	Femur	22	0	10	11	1	0
		late 19th century	HGs	Tibia	23	0	14	8	1	0
Egyptians	NHM	1920s	Upper Egypt	Femur	33	0	17	10	6	0
		c.3,500BC	Trade/Admin?	Tibia	30	0	15	10	5	0
Spitalfields	NHM	1984-86	London, England	Femur	77	49	35	42	0	67
		mostly 1750-1850	Industrial/weavers	Tibia	81	51	36	45	0	71
Caucasian Americans	NMNH	early 20th century	Missouri, USA	Femur	58	31	30	28	0	58
		early 20th century	Industrial	Tibia	58	30	30	28	0	58
Femur Total					524	169	258	217	57	246
Tibia Total					505	180	255	207	42	249
All Specimens Total					1029	349	513	424	99	495

Table 2.1: Total numbers used for the analyses of form of the knee joint in 13 populations of modern humans. NMNH: National Museum of Natural History, Smithsonian Institution, Washington DC ; NHM: Natural History Museum, London

Population	Location of collection	Date of collection/ Age of specimens	Geographic Location/ subsistance	Bone	Total right used	Total left used	Total males	Total females	Sex unknown
Aleut	NMNH	1930s	Alaska, USA	Femur	30	0	18	12	0
		c.1000BP?	Marine HGs	Tibia	26	0	17	9	0
Pachacama	NMNH	1890	Peru	Femur	22	0	10	12	0
		400BC-1500AD	Trade/Agric?	Tibia	27	15	9	3	0
Arikara	NMNH	1957-62	S. Dakota, USA	Femur	36	22	24	12	0
		1600-1750AD	HGs/Farmers	Tibia	32	23	21	11	0
Chinese	NMNH	1930	Northern China	Femur	29	26	29	0	0
		late 19th century	Agric/Industrial?	Tibia	29	28	29	0	0
Australian	NMNH/NHM	19th century	Australia	Femur	32	0	5	9	18
		19th century	HGs	Tibia	28	0	5	10	13
African Americans	NMNH	early 20th century	Missouri, USA	Femur	121	50	63	58	0
		early 20th century	Industrial	Tibia	129	50	63	66	0
Ibo	NMNH/NHM	19th century	Nigeria	Femur	20	0	5	6	9
		19th century	HGs	Tibia	9	0	2	7	0
Andaman Islanders	NHM	1902-05	Andaman Isles, India	Femur	25	0	2	2	21
		1875-1900	HGs	Tibia	33	0	9	9	15
Sri Lankan	NMNH/NHM	1880s	Sri Lanka	Femur	22	0	5	12	5
		1880s	HGs	Tibia	13	0	4	8	1
Khoisan	NMNH/NHM	late 19th century	S. Africa/Namibia	Femur	25	0	7	10	8
		late 19th century	HGs	Tibia	23	0	14	8	1
Egyptians	NHM	1920s	Upper Egypt	Femur	36	0	12	10	14
		c.3,500BC	Trade/Admin?	Tibia	30	0	15	10	5
Spitalfields	NHM	1984-86	London, England	Femur	71	32	34	37	0
		mostly 1750-1850	Industrial/weavers	Tibia	69	44	32	37	0
Caucasian Americans	NMNH	early 20th century	Missouri, USA	Femur	59	32	30	29	0
		early 20th century	Industrial	Tibia	59	42	30	29	0
Femur Total					528	162	244	209	75
Tibia Total					507	202	250	207	35
All Specimens Total					1035	364	494	416	110

Table 2.2: Total numbers used to analyse maximum length and robusticity of the diaphyses in 13 populations of modern humans. NMNH: National Museum of Natural History, Smithsonian Institution, Washington DC ; NHM: Natural History Museum, London.

Although some limbs formed parts of complete skeletons, many are located in ossuaries. Of the total number of limbs in the collection, only a small proportion is in sufficiently good condition for accurate digitisation.

The Aleut people and the environmental background:

The Eskimo-Aleut populations are thought to have arrived in North America from the Asian mainland in one of the later waves of migration about 8-10,000 years ago, after the land bridge across the Bering Straits was severed. Alternative theories do, however, exist (Black, 1983). The Aleut and other Eskimo groups probably split from each other about 4,000 years ago with the Aleut becoming specialised maritime fishermen and hunters of seal, sea lion and otter. Physically, the Arctic populations have a more Asian appearance than other Amerindian groups and their languages have Siberian roots (Taylor, 2000). Within recent centuries, the Aleut have been under strong Russian influence with considerable intermarriage, resulting in a recognised 'creole' population (Taylor, 2000). It is likely, however, that this sample represents a population without significant admixture (Black, 1983).

The Aleut of recent centuries have been well fed, with starvation practically unknown. Although land-mammals are scarce in the region, the Aleutians have always been supplied with a good variety of plant, marine fauna and bird-life (Taylor, 2000).

Climate:

Two centres have been chosen to indicate temperature, rainfall and altitude for the region inhabited by the Aleut; Chinik, South Coast and Anchorage Elemendorf, Cook Inlet, Alaska. The climate is cold year-round with a mean annual temperature of 2°C, ranging from a mid-winter temperature of -7.9°C although this is exacerbated by bitter winds and a high wind-chill factor, to a mid-summer high of 12.8°C. Annual rainfall is relatively high with much of it falling as snow. Altitude is at, or just above, sea level.

Footwear:

Aleutian women were highly skilled at weaving with fine grasses, including waterproof hosiery for wearing inside heavy waterproof boots made of animal skins, sewn with sinew (Taylor, 2000). Hostile conditions would have ensured that substantial footwear would have been worn at all times, as a matter of course.

2.1.2b The Pachacama

Location: Pachacamac, Lurin Valley, Peru, South America
Ancestry: Native South American Amerindian
Abbreviation used in study: Pu

The specimens:

The limbs from the Pachacama collection were exhumed in 1890 from the important archaeological site of Pachacamac. This site, at the ruins of one of the foremost religious temples in South America (the 'Temple of the Sun') and the seat of one of the most influential Inca deities, has a deep history, dating from c. 400 BC to Spanish contact at c.1500 AD. The site lies in the Lurin Valley about 30 kilometres from the modern city of Lima. This coastal region consists of vast barren deserts, broken by small strips of extremely fertile valleys running alongside rivers draining from the Andean mountains into the ocean (Uhle, 1903).

All bones were from ossuaries, although all had been carefully catalogued and sexed at the time of excavation. There were many more male specimens in the collection than females and, inexplicably, many more left than right limbs.

The Pachacama people and the environmental background:

The specimens are from the pre-Spanish contact period, from a time when the valley was heavily populated. It is possible that the bones were from people who lived in the more mountainous region of the old province of Yauyos, lying to the southeast of Lima (Howells, 1989) although all bones used in this study were labelled 'Pachacama'. The

ancient city served as a sanctuary, a thriving trade centre and a place of pilgrimage for many people during the pre-contact period (Wilson, 1999). The arrival of the Spanish saw massive depopulation thereafter and, by the seventeenth century, few of the original Inca people survived.

The graves from which the specimens were obtained had been desecrated over many centuries, both by the Incas themselves, by later Spanish conquerors and by amateur archaeologists and travellers, many bones were found lying above ground at the time of Uhle's excavations and reports. None were found with grave goods, although the temple was known to have been adorned with a wealth of pottery, textiles and sound architecture and the city was recognised as an important centre for trade and craft production, indicating that the people belonged to a sophisticated and civilised society (Saloman and Schwarz, 1999).

Climate:

Pachacamac lies on the coastal strip only 550 metres from the ocean. The people buried there, however, may well have come from a wider region and at a distance of only 75 metres away, the surrounding land rises into the foothills of the Andes to a height of nearly 3000 metres. At Pachcamac itself the sun is intense, although a cooling breeze moderates the heat (Uhle, 1903). Temperature, rainfall and altitude in this study have been based upon modern Lima with a mean annual temperature of 18.2°C, mid-winter temperatures at 15.3°C and mid-summer temperatures at 21.4°C. Mean annual rainfall is very low at 25mm and altitude is relatively low at 140 metres above sea level. Unfortunately, it is not known whether these Pachacama specimens were local people or had originated from the surrounding much higher and much colder regions.

Footwear:

Pictures of the Incas and photographs of modern Amerindians of the region indicate that the Pachacama people were skilled textile workers and would have been used to making and wearing shoes. Artifacts from the Pachacama 'Cemetery for Sacrificed Women'

include sandals made from lightweight materials, having fabric soles and rope thongs and uppers (Uhle, 1903).

2.1.2c The Arikara

Location: South Dakota, USA
Ancestry: Native North American Amerindian
Abbreviation used in study: SD

The specimens:

The skeletons were mainly collected from the Fort Sully site on the eastern banks of the Missouri River with the majority excavated by William Bass between 1957 and 1962. They are believed to be protohistoric Arikara who lived from about 1600 to 1750 A.D. (Howells, 1989). This group was largely living prior to the period of acute population stress from the smallpox epidemic of 1781-1782, when 75% of the population were thought to have died. They are also thought to be relatively free of genetic admixture with Caucasians (Jantz, 1973).

Many limbs came from complete or semi-complete skeletons, although the majority of limbs in the collection were in poor condition and too eroded for reliable digitisation. All specimens were well catalogued and the majority could be sexed from accompanying pelves. In his documentation of accompanying cranial remains, Howells noted a disparity in numbers between male and female skulls with many more males being evident (Howells, 1989). A disparity between male and female postcranial skeletons was also noted during data collection.

The Arikara people and the environmental background:

The Arikara were village farmers (speaking a dialect of the Caddoan language) and closely related to the Skiri Pawnees with whom there may have been some admixture. They lived a semi-sedentary life and supplemented agricultural produce by hunting the plentiful supplies of bison and antelope that inhabited the region in vast herds (Taylor,

2002). They were some of the first agriculturalists in the region, growing a variety of crops (maize, squash, beans and pumpkins), traded for extra supplies of meat and hides with neighbouring tribes. Their homes were complex earth-covered wooden structures and their ornate and richly decorated deerskin clothing included leggings and moccasins.

Climate:

The Great Plains environment is a land of sun, wind and grassland with limited rainfall producing a semi-desert terrain. The Arikara homelands in the Missouri valley, however, have a higher level of annual rainfall than the surrounding regions, which often produces humid conditions and taller and more luxuriant vegetation. Modern-day Mobridge is used to provide the data for climate, annual rainfall and altitude and shows that there is a wide range between mid-winter temperatures at -10°C and mid-summer temperatures at 23.0°C, with a mean annual temperature of 6.8°C.

Footwear:

Hunting herbivores required silent stalking and the Arikara wore moccasins fabricated from animal skins to both protect their feet and to deaden noise. The majority of nineteenth century descendants are pictured wearing richly decorated moccasins of soft leather for ceremonial dress, whilst many are shown with bare feet on less formal occasions (Taylor, 2002). Given the low winter temperatures on the Plains, however, the wearing of footwear of at least moderate weight would have been necessary for much of the year. In the few available pictures of women, they are also seen wearing light leather moccasins similar to those of men.

2.1.2d The Chinese

Location: China
Ancestry: Northern Asian
Abbreviation used in study: Ch

The specimens:

The Chinese specimens were excavated from a cemetery in the Kodiak Islands, Alaska by Aleš Hrdlička in 1930. They had arrived in Alaska from northern China in the 1880s to 1890s as adult migrants, to work in the salmon canning factories. As such, this male-only group had arrived without families, living in work-towns and having been buried locally (personal communication, David Hunt, NMNH, Smithsonian Institution). As first generation adult migrants in Alaska, their skeletons would have retained the genetic and cultural influences of their Chinese backgrounds. Any modification to their skeletons as a result of new environmental circumstances would have been a very recent adaptation. The limbs formed parts of complete skeletons and were largely in good condition. It is not known whether this group of migrants was from agricultural stock or had been urban dwellers or a mixture of both in their Chinese homeland.

The Chinese people and the environmental background:

Various studies based on a comparison of genetic traits and confirmed by linguistic and surname conventions, have determined that the northern Chinese are significantly different to the southern Chinese and that the division is one which goes back possibly as far as the Palaeolithic (Cavelli-Sforza et al., 1994; Du et al., 1992). The boundary appears to correspond to the basins of the two major rivers, the Huang-Ho and the Yangtze; to the north the people conform more closely to a 'typical' north Asian type associated with the cold-adapted Siberian peoples, whilst to the south, the greater influence of south-east Asia has modified certain characteristics. The Chinese skeletons used in this study appear to conform to the northern type in being relatively tall and robust. Native American Amerindians are thought to be more closely related to the northern Chinese people, having migrated from Manchuria and Siberia through the Bering land bridge.

Climate:

Three modern Chinese cities of Harbin, Shenyang and Beijing have been used to provide an indication of the temperature and rainfall of the region where these people originated. All three cities are subject to high summer temperatures (mean 24.0°C), which are

significantly warmer than those reached in Alaska but with very cold winter temperatures, commensurate with, if not colder than, those experienced in Alaska (mean -12.2°C). Mean annual temperature is estimated at 7.6°C. Average annual rainfall at 634 mm per annum is under half the amount in northern China to that of Alaska. A mean altitude over the three cities is relatively low at less than 100 metres above sea level.

Footwear:

These Chinese workers would have been used to wearing heavy protective footwear in the Alaskan canning factories. They would also have been accustomed to wearing relatively substantial footwear in their homeland, either as agricultural or urban workers. Until the advent of Western footwear, Chinese peasants wore shoes and sandals made either of leather or of tightly woven layers of grasses, depending on their wealth (personal communication with native Chinese residents).

2.1.2e The Australian Aborigines

Location: Australia (all regions)
Ancestry: Australian Aborigine
Abbreviation used in the study: Au

The specimens:

Due to the demands of repatriation, too few specimens were available in museum collections to restrict the sample to one specific tribal group or even one region, although a high proportion in this sample appears to have come from Western Australia. The majority of limbs were originally collected during the nineteenth century from a variety of sources; many are now in ossuaries in the museums without accompanying information or other skeletal parts to help identify sex. Many limbs in the collections are too eroded for accurate digitisation.

The Australian people and the environmental background:

The Aboriginal people are thought to have arrived into the Australian mainland from South-eastern Asia, probably via New Guinea, possibly as far back as 50, 0000 years ago. By the time of the arrival of Europeans into Australia, the native people were living in numerous tribes, speaking over 600 different languages and dialects and using a multiplicity of belief systems and cultures. The vast majority of people were nomadic hunter-gatherers with only a few groups, mainly in the northern and Torres Islands region having developed a sedentary form of agriculture. By the end of the nineteenth century, under the influence of Western subjugation, the Aboriginal population had been reduced to a fraction of its former size, frequently living a marginal existence on the edge of the dominant Western culture (Fagan, 1998; The Colombia Electronic Encyclopaedia, 2004; Australian Aborigines: From Wikipedia, 2005)

Climate:

Five locations throughout Australia have been used to give an indication of temperature and rainfall: Alice Springs in the centre, Darwin in the north, Adelaide in the south, Perth in the west and Sydney in the east. Mid-summer temperatures tend to be relatively constant with a range of only 7°C between locations. Mid-winter temperatures are considerably more variable with a range of nearly 14°C between Darwin at 24.9°C and the other locations at c.11°C. Annual rainfall averages 896mm between the five centres but is again variable with Darwin averaging 1,757mm and Alice Springs only 281mm. Inevitably, such variability in climate will have dictated considerable variability in the subsistence patterns of the native people. Mean altitude is estimated at 280 metres above sea level.

Footwear:

Photographs of Australian people in native dress taken in the early part of the twentieth century indicate that footwear was never worn. Rock art paintings made over the centuries prior to this period also depict people with bare feet (Layton, 1992).

2.1.2f African Americans and Caucasian Americans

Location: St. Louis, Missouri, USA

Ancestry: African American: (primarily) of African derivation

Caucasian American: Caucasian

Abbreviations used in study: AA (African Americans)

CA (Caucasian Americans)

The specimens:

Robert J. Terry collected the skeletons during his tenure as head of the Anatomy Department at Washington University Medical School in St. Louis, Missouri from 1899 to 1941. Initially, the cadavers had been used for anatomy classes and were primarily from the local St Louis hospital and intuitional morgues. Many of the early skeletons were from the poorest sections of the population without relatives who could afford to bury them. Later on, more skeletons came from middle or upper middle-income families donating their bodies for scientific purposes, although bodies from this source contributed a small proportion to the whole. After Terry's retirement, his successor Mildred Trotter took over the collection and focused upon filling the gaps in the collection, notably younger Caucasian females. Despite the total of 1728 skeletons, the collection is still deficient in numbers in this particular group, something that became apparent when collecting data for analysis of ageing (Chapter 5).

The collection is well catalogued with documentation detailing sex, age of death, cause of death and any pathologies present, ancestral history, dental charts, plaster death masks and other valuable material. Many of the limbs were disease-free and in excellent condition.

The people and the environmental background:

African Americans:

The original slave populations of Missouri came from Africa via the Dominican Republic sugar plantations, having been brought to America in 1720 to work the local

lead mines and later on, in the rapidly expanding cotton plantations. Many of the ancestors of these slaves were originally taken from West Africa and more specifically, from the region of the Ibo peoples of Nigeria, a practice that continued for at least another one hundred years (see Ibo section 2.1.2g). Once established in America, there was considerable genetic admixture between the incoming slaves and the resident Caucasian European and Native American populations. An estimate made on the basis of one single gene (the Gm protein, found in blood) found that in the African American gene pool of today, 27% is derived from admixture with Caucasian Europeans (Weiss and Mann, 1989). Such a high figure, however, is not obtained when repeated with different gene loci. By the early twentieth century, the African American community of Missouri was largely living as poor urban workers in the lowest strata of society.

Caucasian Americans:

The Caucasian population of the USA originates from many countries worldwide. The current census defines 'white' as a person having origins in any of the original peoples of Europe, the Middle East or North Africa, although the majority of Caucasian Americans in the early years of the twentieth century would have come from Eastern and Western Europe.

As the earlier skeletons in the Terry Collection were those of poorer people, the majority would probably have been industrial urban dwellers living difficult and stressful lives.

Climate:

The mean annual temperature in St. Louis is 13.3°C but the range between mid-winter and mid-summer temperatures is wide, from –1.5°C to 26.5°C. Rainfall averages 940mm per annum and altitude is 175 metres above sea level.

Footwear:

Urban streets would have dictated the need for substantial shoes, which even the poorest people would have worn, particularly in the coldest months.

2.1.2g The Ibo

Location: South-Eastern Nigeria, West Africa.
Ancestry: West African
Abbreviation used in study: Ibo

The specimens:

Various collectors brought the few specimens of postcranial material to the UK from Nigeria during the middle to the late nineteenth century. They are stored in containers without associated skeletal parts and, for the most part, cannot be safely sexed. They are classified as members of the Ibo 'tribe' from the south-eastern region of Nigeria although, prior to the advent of Europeans, the people of this area gave themselves no common name and can be considered a single people only in so far as speaking a number of related dialects (Forde and Jones, 1950).

Although the number of specimens is small, this population was included in the present study as a comparison group to the African American population. The Ibo made up a large proportion of the slaves shipped out of West Africa during the latter years of the eighteenth century; estimated as comprising 16,000 of the 20,000 slaves sold annually (Forde and Jones, 1950). Many of these slaves were initially transported to the West Indies to work the sugar plantations but were subsequently taken to the southern United States to work in the cotton fields.

The Ibo people and the environmental background:

The Ibo were primarily subsistence farmers, although land available for cultivation was variable, with areas of heavy farming and dense population together with unpopulated swampland. The prevalence of tsetse fly infestation in the region restricted the use of animal husbandry. Because of tsetse flies, which carry the disease trypanosomiasis (or 'sleeping sickness') and mosquitoes, which carry the four species of the *Plasmodium* parasites causing malaria (primarily *P. falciparum*), the Ibo homelands suffer from endemic disease. In addition, because of the prevalence of malaria, the population is also

known to suffer from a high incidence of sickle-cell anaemia, a debilitating and frequently fatal blood disorder in the homozygous state. Although in the heterozygous state the disease is known to confer some protection against malaria, heterozygous carriers can suffer from severe anaemia (Forde and Jones, 1950; Weiss and Mann, 1989).

Climate:

Three modern cities have been used to estimate the temperature and rainfall of the region; Lagos, Ibadan and Benin City. The geography ranges from low-lying swampland in the Niger Delta to low gently inclined tableland further inland. The wet and dry seasons are well defined with the wet season lasting from March to November (Forde and Jones, 1950). Mean annual temperature for the region is estimated at 26.5°C with mid-winter temperatures at 24.6°C and mid-summer temperatures at 28.5°C. Average rainfall is a humid 1,866mm per annum and altitude is 393 metres above sea level.

Footwear:

Photographs of West African people in native dress taken in the early part of the twentieth century indicate that footwear was rarely, if ever, used (Landau and Kaspin, 2002).

2.1.2h The Andaman Islanders

Location: Andaman Islands, India
Ancestry: Southern Asian
Abbreviation used in this study: AI

The specimens:

The Andaman Islands specimens were collected between 1902 and 1905 on behalf of a Governor of the Andaman Islands and originally donated to the Royal College of Surgeons, London in 1945 by a descendant of the Governor. The people represented by these specimens were living in the last quarter of the nineteenth century, many of whom were from the Aka-Bea tribe of South Andaman. The Andaman people come from two

main groups that have been separated long enough for their languages to be no longer mutually intelligible, although both conform to the so-called Asian 'Negrito' type and are described as having short stature, black skin and peppercorn or frizzly hair (Weber, 2004).

The limbs used in the study formed parts of skeletons of which the majority were only partially complete. As pelves were rarely present, most limbs were classified of unknown sex. The majority of limbs appeared to be in good condition although many other parts of the skeletons show signs of syphilis.

Although the majority of the people originally came from South Andaman, a small number came from Middle Andaman. Very few, if any came from the more isolated northern Andaman Islands. Although the Andaman Islanders were said to be 'pure-bred' at this date, having no admixture with either Europeans or other immigrants, the prevalence of syphilis (introduced around the 1870s) points to some degree of interbreeding with incomers. The bodies were collected from the so-called 'Andaman Homes', which were shelters providing hospitality and free medicine; the presence of the disease amongst the Andamanese is probably reflected in this (Weber, 2004). In addition, although the majority of limbs in the sample were of small size (between approximately 370 to 380mm maximum male femur length), two male specimens were considerably taller, at 436 and 454mm. Such discrepancy in height between these two individuals and the others may also reflect a degree of admixture.

The Andaman Islanders and the environmental background:

The aboriginal people had been isolated in the Islands for many thousands of years prior to colonisation by Europeans and today probably represent one of (if not the most) genetically homogenous populations in the world. Their relative isolation has resulted in a unique suite of several characteristics, including short stature, steatopygia, intense blue-black skin colour and profuse sweating that is said to help repel insects. Some of these traits are reminiscent of some African populations, notably the Mbuti Pygmies,

although they have closer genetic links with other Asian populations of the region (Endicott et al., 2003)

Prior to contact, all Andamanese groups had a narrow economic basis in hunting and gathering in the deep-forest environment. The population was estimated to have been at the maximum sustainable for that type of economic base but was quickly reduced after the introduction of Western diseases (Weber, 2004).

Climate:

Port Blair lies in the middle of Aka-Bea territory and this city has been used to indicate the temperature and average rainfall for the Andaman Islands. Port Blair experiences almost constant temperatures year-round at 27.3°C (ranging from 26.6°C in mid-winter to 29.1°C in mid-summer), with high average rainfall at almost 3000mm per annum; the highest recorded for the thirteen populations used in this study. Altitude is 75 metres above sea level.

Footwear:

Until the latter part of the nineteenth century, the Andamanese wore the minimum of clothing. Footwear was never worn until the British authorities forced the groups under their direct control into western dress including shoes, although the climate caused rapid disintegration of such garments. The subjects in the Andaman Homes were probably forced into using footwear although this would have been a very recent development and the majority of people would probably have avoided their use if possible. This study therefore classifies the population as barefooted (Weber, 2004).

2.1.2i The Sri Lankans

Location: Sri Lanka

Ancestry: Indian Sub-Continent

Abbreviation used in study: SL

The specimens:

Specimens used in this study come from three of Sri Lanka's several communities; the Veddahs, Singhalese and Tamils. The specimens are few in number and mostly held in ossuaries without accompanying skeletal parts. Many are in poor condition and only a few were suitable for accurate digitisation. All specimens come from patients who died during the 1880s at the Government Civil Hospital in the Galle District of Colombo, Sri Lanka (catalogues held in the NHM).

As the number of bones available from each of the three Sri Lankan communities is small, they have been amalgamated into one population for inclusion in the study. Justification for this approach has been based on two criteria: cultural and biological.

Cultural justification for amalgamation

The Sri Lankans and the environmental background:

The Veddahs represent the original settlers of Sri Lanka. They have been living on the island for thousands of years and are believed to have originated from South India, sharing an ancestral history with the peoples of that region (Amirthalingam, 2003). In the late nineteenth century, their clans were divided into three groups; the Gam and Gal Veddahs and the Muhudu coastal Veddahs. By that time, although many were still living as hunter-gatherers (especially the Gam and Gal Veddahs), others, including many Muhudu Veddahs, had been absorbed into the wider communities for economic reasons and were living in close proximity to the bigger towns and cities on the coast, near to other Sri Lankan groups. This settled group was living by cultivation and had a long association with the neighbouring Singhalese. Some Veddahs had intermarried into these other groups, particularly with the Singhalese (from catalogues held in the NHM).

The Singhalese represent the largest ethnic group in Sri Lanka, which accounts for 74% of the population today. Despite a conviction by the Singhalese themselves of an Aryan past, current archaeological thinking suggests that this community also has ancestral connections with the peoples of southern India, having migrated from India around

500BC (Amirthalingam, 2003). They were agriculturalists with a flourishing tradition of pottery and iron use.

Two different groups of Singhalese were living at the beginning of the twentieth century; the Kandyan or 'Up-country' group who are descended from 'a blend of Veddahs with the ancient Gangetic [original] settlers, with some admixture of Tamil blood' (from catalogues held in the NHM), and 'Low-country' Singhalese. This second group which comes from the coastal region is likely to have included the people represented by these specimens; having a lower proportion of Veddah ancestry but a higher proportion of Tamil.

The Tamil community on the island has close links with the Tamil states of South India, sharing their culture, customs, fine arts, religion, dress and language. Sri Lanka was invaded by the Tamils of South India several times, until it became occupied and dominated by Europeans (Portuguese, Dutch and British) from the sixteenth century onwards. These invasions resulted in alternating Tamil and Singhalese governments 'until from the two elements a people was welded together having a distinct language and religion of its own and, at least for a time, a separate nationality' (from catalogues held in the NHM). Despite the Singhalese possessing considerable Tamil ancestry however, the distinction between the two communities was, and still is a real one.

Both Singhalese and Tamil societies belong to a caste system and the people represented by these specimens were likely to have been of the lowest castes. They were citizens of Colombo and surrounding districts and, together with the Veddah individuals, had died in hospital and were never claimed by relatives or friends for burial.

Biological justification for amalgamation:

Tests are carried out to determine whether it is biologically justifiable to amalgamate the three Sri Lankan groups into a single sample. Two methods have been used for these tests. The first method uses discriminant and cross-validation analyses on the three

groups; however because the sample sizes for the three groups are very small (sample sizes for the femur are eight Veddah, six Tamils and four Singhalese. For the tibia, sample sizes are four Veddah, five Tamils and four Singhalese), this method may give unreliable results and is used to give an indication only. The second method calculates the Procrustes distances between each specimen and, from these distances, the proximity of each specimen to all others in the dataset.

All methods used in the following analyses are described in Chapter 2, section 2.2. Only right sided specimens are used for the tests. See Chapter 3 for reasons for the use of only right-sided specimens.

Results and Discussion:

Femur:

To test the separation of the three Sri Lankan groups, the first method uses discriminant function analysis on the total 18 specimens. The data are analysed after GPA and by subjecting the Procrustes fitted co-ordinates to PCA. Table 2.3 gives the proportional and accumulated variance for PCs 1 to 16, which represent the total variance within the sample. The scores for each specimen on the PCs are then subjected to canonical discriminant analysis to establish the relationships between groups based on the Mahalanobis' squared distances between means.

PCs	Prop.	Cumul.	PCs	Prop.	Cumul.
PC1	21.30	21.3	PC10	3.46	89.5
PC2	16.50	37.9	PC11	2.68	92.2
PC3	10.60	48.4	PC12	2.32	94.5
PC4	10.20	58.6	PC13	1.87	96.4
PC5	7.27	65.8	PC14	1.57	97.9
PC6	6.58	72.4	PC15	1.13	99.1
PC7	5.70	78.1	PC16	0.94	100.0
PC8	4.26	82.4			
PC9	3.64	86.0			

Table 2.3 The proportion and accumulated variance for PCs 1-16 for the femur, which accounts for 100% of total variance.

For the femur, the best separation of groups is achieved using c.60% of total variance. This assessment was reached after separate discriminant and cross-validation analyses were carried out using PCs accounting for between c.50% to 100% of total variance. Results are summarised in Figure 2.1:

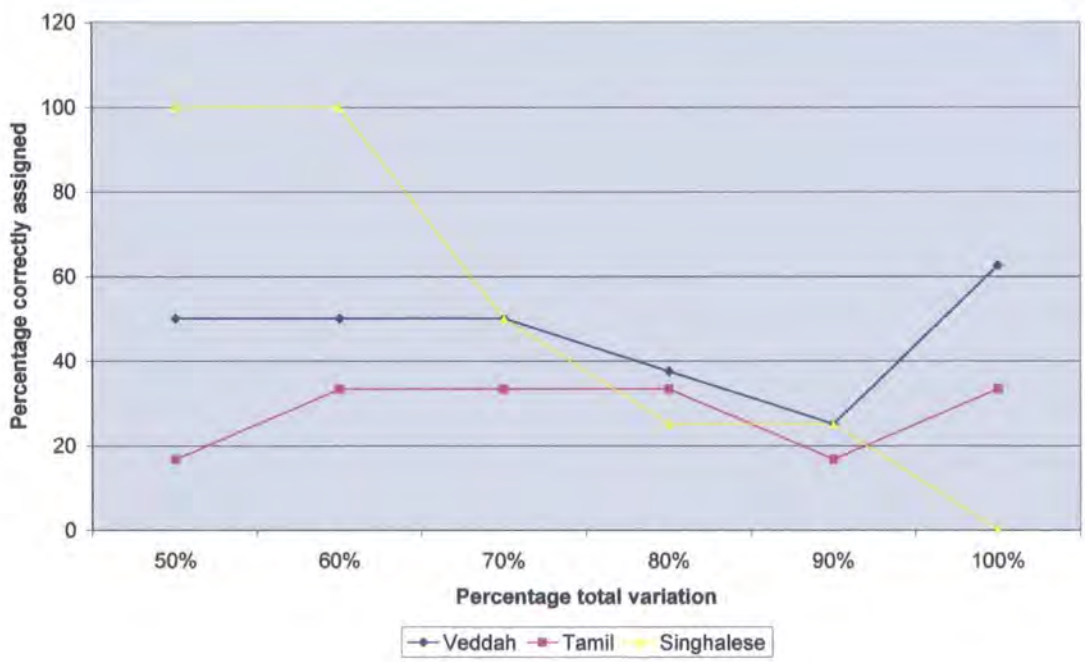

Figure 2.1 Summary of separate discriminant analyses and cross-validation analyses for the femur, using the PC scores accounting for c.50% of total variance PCs 1-3, c.60% PCs 1-4, c.70% PCs 1-6, c.80% PCs 1-7, c.90% PCs 1-10 and 100% PCs 1-16.

The Mahalanobis' squared distances between populations, generated by the discriminant analysis are shown in Table 2.4. Only one distance between Singhalese and Veddah reaches a level of statistical significance. Table 2.5 shows the results of cross-validation analysis with individuals assigned to the correct groups, ranging from 100% for the Singhalese to 33.33% for the Tamils.

Veddah	0		
	1.000		
Tamils	1.22	0	
	0.53	1.000	
Sing.	8.14	5.77	0
	0.02	0.08	1.000
	Veddah	Tamils	Sing.

Table 2.4 Results of canonical discriminant analysis of the 3 Sri Lankan samples for the femur, on the basis of c. 60% variance. The upper value in red gives the Mahalanobis' squared distance between groups, lower value in black gives the Hotelling's t^2 *p*-value.

Number of Observations and Percent Classified into Group				
From Group	Veddah	Tamils	Sing.	Total
Veddah	4 50	2 25	2 25	8 100
Tamils	2 33.33	2 33.33	2 33.33	6 100
Sing.	0 0	0 0	4 100	4 100
Total	6 33.33	4 22.22	8 44.44	18 100

Table 2.5 Separation of 3 Sri Lankan samples for the femur, using 60% total variation. Upper figure denotes number of individuals correctly assigned; lower figure denotes percentage. Red figures denote number and percentage of individuals placed into their correct group

Because of small sample sizes for each of the three constituent groups, the second method of analysis tests the separation between groups by analysing distances between the individual specimens.

The Procrustes distances between individuals are shown in Table 2.6 Table 2.7 illustrates the relationship of each individual to all others on the basis of the Procrustes distances by showing the distance of each primary individual to all others and ranking them accordingly from the closest at position 1 to the most distant at position 17.

Twelve individuals from the same community of the total 18 individuals occupy the closest position to the primary individual in position 1; with six from the same community in position 2. Placement appears to be relatively random after position 1 although there appears to be a tendency for the Singhalese to show a greater degree of discrimination.

The Procrustes distances cluster individuals into two groups of eight and ten specimens each. Distances between individuals clustering within each group are relatively close. Distances between the two groups are, however relatively large. With individuals from each of the three communities clustering within each group, this division within the total Sri Lankan sample is based on a more influential factor than community affiliation. This factor is unlikely to be based on sexual dimorphism as four males and four females comprise one group and, although nine females and only one male comprise the second group, this is probably due to the much higher proportion of females in the total sample. Lack of information associated with the sample prohibits further understanding of the causes of the relatively high distance between the two groups. This separation of the two sections of the total sample is discussed further in Chapter 6 section 6.5.6a.

Ved277	0																	
Ved274	131.23	0																
Ved39	3088.28	3128.40	0															
Ved278	3036.78	3077.72	105.47	0														
Ved341	2951.57	2999.16	259.41	188.29	0													
Ved342	2900.26	2943.20	242.42	155.11	128.03	0												
Ved273	3075.91	3119.32	216.03	199.26	252.91	275.62	0											
Ved270	3002.60	3044.46	166.06	92.95	174.50	144.10	193.51	0										
Tam182	3039.06	3091.14	342.91	289.78	148.68	269.46	311.85	286.27	0									
Tam188	192.30	292.09	2926.06	2872.26	2782.46	2733.81	2909.95	2866.96	2866.92	0								
Tam279	3309.66	3355.24	305.67	308.75	362.48	417.58	322.98	312.07	320.55	3141.13	0							
Tam189	3152.60	3196.54	166.06	143.65	220.75	256.38	216.41	146.70	241.64	2985.67	169.93	0						
Tam312	3090.94	3135.04	134.99	98.29	167.90	201.08	194.63	100.21	220.42	2924.44	232.66	68.61	0					
Tam39	340.79	432.09	2861.79	2803.52	2708.47	2662.09	2841.27	2798.02	2788.77	169.20	3066.56	2913.65	2853.63	0				
Sing181	147.64	195.37	2982.05	2928.94	2845.42	2791.89	2969.40	2923.73	2934.22	145.98	3202.00	3045.11	2984.16	272.91	0			
Sing720	172.09	260.12	2990.43	2935.67	2846.81	2796.59	2975.41	2930.30	2931.66	117.80	3204.42	3049.17	2988.45	215.37	101.78	0		
Sing183	220.14	300.94	2894.47	2840.10	2751.96	2701.74	2879.37	2834.81	2837.60	57.70	3110.00	2954.19	2893.21	154.84	145.13	133.91	0	
Sing715	144.59	50.34	3099.51	3049.46	2972.02	2915.44	3092.27	3044.47	3064.73	289.74	3327.95	3168.83	3107.16	432.13	192.91	264.26	294.46	0
	Ved277	**Ved274**	**Ved39**	**Ved278**	**Ved341**	**Ved342**	**Ved273**	**Ved270**	**Tam182**	**Tam188**	**Tam279**	**Tam189**	**Tam312**	**Tam39**	**Sing181**	**Sing720**	**Sing183**	**Sing715**

Table 2.6 Procrustes distances between the 18 Sri Lankan specimens for the femur.

	1	2	3	4	5	6	7	8	9	10	11	12	13	14	15	16	17
Ved277	Ved	Sing	Sing	Sing	Tam	Sing	Tam	Ved	Ved	Ved	Ved	Tam	Ved	Ved	Tam	Tam	Tam
Ved274	Sing	Ved	Sing	Sing	Tam	Sing	Tam	Ved	Ved	Ved	Ved	Tam	Ved	Ved	Tam	Tam	Tam
Ved39	Ved	Tam	Ved	Tam	Ved	Ved	Ved	Tam	Tam	Tam	Sing	Tam	Sing	Sing	Ved	Sing	Ved
Ved278	Ved	Tam	Ved	Tam	Ved	Ved	Ved	Tam	Tam	Tam	Sing	Tam	Sing	Sing	Ved	Sing	Ved
Ved341	Ved	Tam	Tam	Ved	Ved	Tam	Ved	Ved	Tam	Tam	Sing	Tam	Sing	Sing	Ved	Sing	Ved
Ved342	Ved	Ved	Ved	Tam	Ved	Tam	Tam	Ved	Tam	Tam	Sing	Tam	Sing	Sing	Ved	Sing	Ved
Ved273	Ved	Tam	Ved	Ved	Tam	Ved	Ved	Tam	Tam	Sing	Tam	Tam	Sing	Sing	Ved	Sing	Ved
Ved270	Ved	Tam	Ved	Tam	Ved	Ved	Ved	Tam	Tam	Tam	Sing	Tam	Sing	Sing	Ved	Ved	Sing
Tam182	Ved	Tam	Tam	Ved	Ved	Ved	Ved	Tam	Ved	Tam	Sing	Tam	Sing	Sing	Ved	Sing	Ved
Tam188	Sing	Sing	Sing	Tam	Ved	Sing	Ved	Ved	Ved	Tam	Ved	Ved	Tam	Ved	Ved	Tam	Tam
Tam279	Tam	Tam	Ved	Ved	Ved	Tam	Ved	Ved	Ved	Tam	Sing	Tam	Sing	Sing	Ved	Sing	Ved
Tam189	Tam	Ved	Ved	Ved	Tam	Ved	Ved	Tam	Ved	Tam	Sing	Tam	Sing	Sing	Ved	Sing	Ved
Tam312	Tam	Ved	Ved	Ved	Ved	Ved	Ved	Tam	Tam	Tam	Sing	Tam	Sing	Sing	Ved	Sing	Ved
Tam39	Sing	Tam	Sing	Sing	Ved	Ved	Sing	Ved	Ved	Tam	Ved	Ved	Ved	Tam	Ved	Tam	Tam
Sing181	Sing	Sing	Tam	Ved	Sing	Ved	Tam	Ved	Ved	Ved	Ved	Tam	Ved	Ved	Tam	Tam	Tam
Sing720	Sing	Tam	Sing	Ved	Tam	Ved	Sing	Ved	Ved	Tam	Ved	Ved	Tam	Ved	Ved	Tam	Tam
Sing183	Tam	Sing	Sing	Tam	Ved	Sing	Ved	Ved	Ved	Tam	Ved	Ved	Ved	Tam	Ved	Tam	Tam
Sing715	Ved	Ved	Sing	Sing	Tam	Sing	Tam	Ved	Ved	Ved	Ved	Tam	Ved	Ved	Tam	Tam	Tam

Table 2.7 The order of proximity in distance of each primary individual from the other individuals in the dataset for the femur, on the basis of the Procrustes distances between them. Veddah individuals are highlighted in black, Tamils in blue and Singhalese in red.

Tibia:

For the tibia, the first test for the separation of the three Sri Lankan groups uses discriminant function analysis on the total thirteen specimens. The data are analysed after GPA and by subjecting the Procrustes fitted co-ordinates to PCA. Table 2.8 gives the proportional and accumulated variance for PCs 1 to 12, which represent the total variance within the sample. The scores for each specimen on the PCs are then subjected to canonical discriminant analysis to establish the relationships between groups based on the Mahalanobis' squared distances between means.

PCs	Prop.	Cumul.	PCs	Prop.	Cumul.
PC1	21.80	21.8	PC8	4.36	89.6
PC2	17.70	39.4	PC9	3.56	93.2
PC3	14.80	54.3	PC10	3.35	96.5
PC4	9.90	64.2	PC11	1.92	98.4
PC5	7.76	71.9	PC12	1.56	100.0
PC6	7.23	79.2			
PC7	6.10	85.3			

Table 2.8 The proportion and accumulated variance for PCs 1-12 for the tibia, which accounts for 100% of total variance.

The best separation of groups is achieved using c.70% of total variance. This assessment was reached after separate discriminant and cross-validation analyses were carried out using PCs accounting for between c.50% to 100% of total variance. Results are summarised in Figure 2.2.

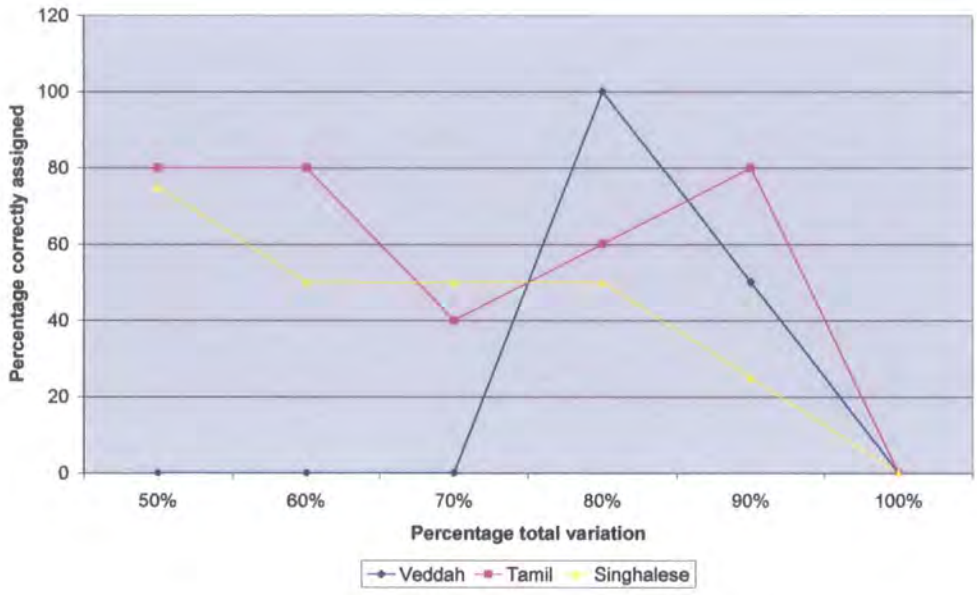

Figure 2.2 Summary of separate discriminant analyses and cross-validation analyses for the tibia, using the PC scores accounting for c.50% of total variance PCs 1-3, c.60% PCs 1-4, c.70% PCs 1-5, c.80% PCs 1-6, c.90% PCs 1-8 and 100% PCs 1-12.

The Mahalanobis' squared distances between populations, generated by the discriminant analysis, are shown in Table 2.9. No pairwise comparisons reach a level of statistical significance. Table 2.10 shows the results of cross-validation analysis with individuals assigned to the correct groups, ranging from 75% for the Singhalese to 60% for the Tamils.

Because of small sample numbers for each of the three constituent groups, the second method of analysis tests the separation between groups by analysing distances between the individual specimens.

Veddah	0		
	1.000		
Tamils	2.78	0	
	0.64	1.000	
Sing.	3.05	4.68	0
	0.52	0.54	1.000
	Veddah	Tamils	Sing.

Table 2.9 Results of canonical discriminant analysis of the 3 Sri Lankan samples fro the tibia, on the basis of c. 70% variance. The upper value in red gives the Mahalanobis' squared distance between groups, lower value in black gives the Hotelling's t^2 *p*-value.

Number of Observations and Percent Classified into Group				
From Group	Veddah	Tamils	Sing.	Total
Veddah	3 75	1 25	0 0	4 100
Tamils	0 0	3 60	2 40	5 100
Sing.	1 25	0 0	3 75	4 100
Total	4 30.77	4 30.77	5 38.46	13 100

Table 2.10 Separation of 3 Sri Lankan samples using 70% total variation for the tibia. Upper figure denotes number of individuals correctly assigned; lower figure denotes percentage. Red figures denote number and percentage of individuals placed into their correct group.

The Procrustes distances between individuals are shown in Table 2.11. Table 2.12 illustrates the relationship of each individual to all others on the basis of the Procrustes distances by showing the distance of each primary individual to all others and ranking them accordingly from the closest at position 1 to the most distant at position 12. Eight individuals from the same community out of

the total thirteen individuals occupy the closest position to the primary individual, with five from the same community in position 2. Placement appears to be relatively random after position 2, although, as with the femur there appears to be a slight tendency for the Singhalese to show a greater degree of discrimination. However, these results suggest that none of the three groups shows a markedly high degree of discrimination regarding the shape of the proximal tibia.

As with the femur, the Procrustes distances cluster individuals into two groups of five and eight specimens each. Distances between individuals clustering within each group are relatively close. Distances between the two groups are, however relatively large. With individuals from the three communities clustering within each group (with the exception of the Tamils in the group of five individuals), this division within the total Sri Lankan sample is unlikely to be based upon community affiliation. Again, this factor is unlikely to be based on sexual dimorphism as one male and three females plus one unknown comprise one group and three males and five females comprise the second group. Lack of information associated with the sample prohibits further understanding of the cause of the relatively high distance between the two branches.

Conclusion

These tests suggest that the Veddah, Singhalese and Tamils are relatively indistinct from each other in the shape of the distal femur and proximal tibia. Amalgamating the three groups into a single sample would introduce minimal errors.

Ved277	0												
Ved272	41.94	0											
Ved39	2663.00	2667.11	0										
Ved341	2547.45	2553.22	231.97	0									
Tam279	2744.02	2749.38	184.77	204.93	0								
Tam188	2622.09	2626.71	82.28	152.43	158.07	0							
Tam312	2645.95	2651.40	143.92	119.79	110.28	82.57	0						
Tam728	2535.36	2541.11	240.68	43.37	214.26	164.82	135.78	0					
Tam131	2554.79	2560.78	258.57	71.31	206.53	185.61	144.11	51.29	0				
Sing714	2639.36	2644.94	223.07	112.59	124.44	157.72	107.71	112.19	97.42	0			
Sing745	179.43	187.19	2502.12	2383.93	2580.53	2460.05	2483.60	2371.60	2390.34	2474.54	0		
Sing720	148.88	160.26	2535.89	2415.93	2613.14	2493.32	2516.01	2403.70	2422.33	2506.94	53.90	0	
Sing83	217.05	228.11	2516.89	2391.32	2589.30	2472.30	2493.36	2378.97	2396.71	2481.26	102.21	87.72	0
	Ved277	**Ved272**	**Ved39**	**Ved341**	**Tam279**	**Tam188**	**Tam312**	**Tam728**	**Tam131**	**Sing714**	**Sing745**	**Sing720**	**Sing83**

Table 2.11 Procrustes distances between the 13 Sri Lankan specimens for the tibia.

	1	2	3	4	5	6	7	8	9	10	11	12
Ved277	Ved	Sing	Sing	Sing	Tam	Ved	Tam	Tam	Sing	Ved	Tam	Tam
Ved272	Ved	Sing	Sing	Sing	Tam	Ved	Tam	Tam	Tam	Ved	Sing	Tam
Ved39	Tam	Tam	Tam	Sing	Ved	Tam	Tam	Sing	Sing	Sing	Ved	Ved
Ved341	Tam	Tam	Sing	Tam	Tam	Tam	Ved	Sing	Sing	Sing	Ved	Ved
Tam279	Tam	Sing	Tam	Ved	Ved	Tam	Tam	Sing	Sing	Sing	Ved	Ved
Tam188	Ved	Tam	Ved	Sing	Tam	Tam	Tam	Sing	Sing	Sing	Ved	Ved
Tam312	Tam	Sing	Tam	Ved	Tam	Ved	Tam	Sing	Sing	Sing	Ved	Ved
Tam728	Ved	Tam	Sing	Tam	Tam	Tam	Ved	Sing	Sing	Sing	Ved	Ved
Tam131	Tam	Ved	Sing	Tam	Tam	Tam	Ved	Sing	Sing	Sing	Ved	Ved
Sing714	Tam	Tam	Tam	Ved	Tam	Tam	Ved	Sing	Sing	Sing	Ved	Ved
Sing745	Sing	Sing	Ved	Ved	Tam	Ved	Tam	Tam	Sing	Tam	Ved	Tam
Sing720	Sing	Sing	Ved	Ved	Tam	Ved	Tam	Tam	Sing	Ved	Tam	Tam
Sing83	Sing	Sing	Ved	Ved	Tam	Ved	Sing	Tam	Sing	Tam	Tam	Ved

Table 2.10 The order of proximity in distance of each primary individual from the other individuals in the dataset for the tibia, on the basis of the Procrustes distances between them. Veddah individuals are highlighted in black, Tamils in blue and Singhalese in red.

Climate:
The three major centres of Colombo, Kandy and Jaffna have been used to indicate the temperature and average rainfall for Sri Lanka. The temperature between the three centres lies within a close range of approximately 3°C although rainfall and altitude is more variable. The average temperature for the island is therefore estimated at 25.0°C in mid-winter to 27.9°C in mid-summer, with a mean annual temperature of 26.5°C. Mean annual rainfall is 1,748mm per annum, with an mean altitude of nearly 250 metres above sea level.

Footwear:
The people represented by these specimens were probably very poor city dwellers or from the immediate coastal district and unlikely to have owned and worn substantial footwear, perhaps over several generations. Lacking information to contradict this assumption, this study has classed the Sri Lankan population as using no footwear.

2.1.2j The Khoisan

Location: South Africa, Namibia and Botswana
Ancestry: Southern African
Abbreviation used in study: Kh

The specimens:
The Khoisan specimens are located in the NHM in London and the NMNH, Smithsonian Institution, Washington DC. A few limbs are from complete skeletons, in good condition and can provide a reliable estimation of sex. Others are held in ossuaries without additional skeletal parts to indicate sex. Many specimens in the collections are in too poor a condition for accurate digitisation and were not included in this study. Little accompanying information is available to identify any of the bones although museum curators responsible for the collections believe them to be late nineteenth or early twentieth century specimens.

The Khoisan and their environmental background:

The Khoi and San form two closely related communities, speaking a similar dialect of the common Khoisan language. They are descendants of some of the most ancient people of Africa and until recent times, their cultures were widespread throughout central, eastern and southern Africa. By the twentieth century, the range of the hunter-gatherer groups had dwindled and in recent years the few remaining groups not absorbed into the wider community are confined largely to the Kalahari Desert of Namibia and Botswana.

The San were originally assumed by Europeans to have been purely hunters and gatherers, practicing no agriculture and keeping no domestic animals apart from dogs. This portrayal of all San communities, however, is probably a myth. Recent research indicates that the majority of hunter-gatherer groups throughout many centuries have augmented their resources by moving into cattle and sheep-owning in times of plenty (and when left in peace to do so by neighbouring tribes), then reverting back to hunting and gathering during times of persecution. Indeed, some San communities adopted pasturalism as a matter of course, including the Khoi. Like the San, the Khoi also practiced hunting and gathering, both as a supplement to their main pastoralist economy and as a fallback in times of natural hazard and persecution (Omer-Cooper, 1994).

Previous research shows that morphological and genetic differences between the Khoi and San are insignificant and that the Khoisan can be regarded as a distinct group in relation to surrounding populations (Rightmire, 1963).

Climate:

Four cities have been used to provide a range for calculating the average temperature, rainfall and altitude experienced by the Khoisan; Upington, Kimberley and Okiep in South Africa and Karasburg in Namibia. Altitude for the region is high at 1,034 metres above sea level, annual rainfall is low at 305mm and mean annual temperature is estimated at 18.5°C, with mid-winter temperature at 11.1°C, and mid-summer temperature at 25.1°C.

Footwear:

Photographs of the Khoisan in native dress indicate that footwear is never worn.

2.1.2k The Egyptians

Location: Egypt, North Africa

Ancestry: North African Caucasian

Abbreviation used in study: Eg

The specimens:

The Egyptian remains were mainly excavated from the two cemeteries of El Amrah and Abydos in Upper Egypt and are dated from the early part of the pre-Dynastic period (c. 3500 BC). Both sites were excavated in the first decade of the twentieth century. It is likely that the skeletons were from the higher strata of society, as the Abydos cemetery is known to have contained royal tombs. The grave goods found with the human remains indicate considerable wealth and include pottery, basketry, vases and pieces of jewellery containing semi-precious stones (catalogues from NHM, London).

Many limbs in the collection formed parts of semi-complete skeletons and some could be reasonably well sexed from accompanying pelves. The vast majority of limbs, however, were too eroded for accurate digitisation and great effort was made to select only those in sufficiently good condition.

The Egyptian people and the environmental background:

Upper Egypt extends from just above the modern city of Aswan southwards along the River Nile valley. The Nile River basin is a region of fertile alluvial soils, supporting both arable and pastoral agriculture with a wide range of plant crops, domestic and wild animal, bird and fish resources available to eat. It is unlikely that the wealthy would have been undernourished or have suffered from poor shelter, as Egyptian houses from this early period were comfortable and relatively sophisticated (Fagan, 1998).

Climate:

Two centres, Aswan and Cairo were chosen to estimate the temperature and rainfall of the region. Mean annual temperature is 24°C, with mid-winter temperatures at 14.5°C rising to high average mid-summer temperatures of 30.5°C. Average yearly rainfall is very low (only 27mm) and altitude is low at 68 metres above sea level.

Footwear:

The numerous depictions of ancient Egyptians show the majority wearing light thong sandals, sometimes strapped to the legs. Elaborate footwear would have been worn by the wealthy both as symbols of decoration and to protect the feet from hot surfaces. Even the numerous urban labourers and agricultural workers, however, are shown wearing sandals to protect the feet. Such footwear would have been made from lightweight materials of animal skin or tightly woven grasses.

2.1.2l The Spitalfields collection

Location: London, Great Britain
Ancestry: European Caucasian
Abbreviation used in study: Sp

The specimens:

The Spitalfields collection is extensive and for the most part, in good condition providing a reasonable choice of specimens for accurate digitisation. They comprise the remains of people who had lived in the Spitalfields area of East London who were buried in the crypt of St. Stephens' Church. Many of the limbs form parts of complete skeletons, which could therefore be sexed by reference to other skeletal parts. Of the total collection of skeletons, 40% come from named coffins (the 'named sample'), which can be traced back to accurate records of sex, occupation, family membership, age at death and causes of death, although some gaps exist in the sequence (for example in the number of named and aged younger men) (Molleson and Cox, 1993; Cox, 1996).

The Spitalfields people and the environmental background:

Only 3.4% of the named sample of the Spitalfields collection was born outside of Great Britain although 66.9% had French or European sounding names, the majority of these being French. Many of the people with French origins were the descendants of Protestant Huguenots who had left the Continent from the Middle Ages onwards until well into the nineteenth century. Although the sequence of named specimens begins in 1640 until approximately 1850, the majority of specimens date from the latter half of this period. Molleson and Cox (1993) use Daniel Defoe's description of the majority of the sample as 'the middling sort', divided between two groups; those who 'live well' and those who 'labour hard but feel no want'.

Many of the immigrant Huguenots were silk weavers and the Spitalfields area was recognised as the centre of the London silk industry. Of the named sample, the occupations of 61% are known. Of this known proportion, 40% were directly employed in the silk industry with 31.8% being described as 'master craftsman', of whom weavers formed a large number. The weaving was done on handlooms, which were powered by the legs. The foot-treadles raised and lowered alternate warp-threads, so allowing the passage of the shuttle. A proportion of handlooms had treadles designed for use by one leg only, whilst others required the use of both legs. Joints in both upper and lower limbs were in constant motion, particularly the knee, which was forced into continual flexion and extension (Bythell, 1969). Although powerlooms were developed and started to be used in the early nineteenth century, (mainly in the cotton weaving industry), they were too destructive of the fine silk threads in the early years and would not have been used by this Spitalfields sample (Timmins, 1993).

Once successful, the life of the master weaver was relatively easy he did little of the weaving himself, although he would have served the same seven to twelve year apprenticeship from his early teens until early twenties as journeymen (Cox, 1996; Porter, 1990). The lives of journeymen continued to be physically hard, over many long hours each day, for many years and starting at a young age. The lives of wives and children reflected those of their husbands and fathers, although a few women ran businesses or worked as journeymen in their own right. Families of the wealthy rarely

undertook paid employment but wages from the families of the poorer classes were a vital part of the family income. Children of journeymen were frequently employed in physically strenuous tasks from a very early age and such work would have affected normal growth in the postcranial skeleton. Molleson and Cox (1993) quote a woman weaver, born in c. 1844:

> "Sometimes I used to get fidgety and want to get up and move about. To prevent this my father used to tie me to the loom in the morning, before he went out, and dare me to leave it till he came back. I have often been tied in the loom all day and eaten my meals as I sat there."

Many of the bones show evidence of various diseases including infections, osteoarthritis, osteoporosis and other joint diseases. Although many members of the community lived well into old age, a large proportion died from tuberculosis, 'convulsions', 'dropsy' or various fevers. Even by the middle of the nineteenth century, by the time they reached the age of five, 35 out of every 45 children had had either smallpox, measles, scarlet fever, diphtheria, whooping cough, typhus, enteric fever (or a combination of them), any of which could kill, together with the lesser but still dangerous childhood illnesses such as chicken pox or mumps (Flanders, 2003).

The local water supply was heavily contaminated by raw sewage and food and milk supplies were heavily adulterated by various contaminants including chalk, lead, copper and sulphuric acid. Much of this adulteration was deliberate and often designed to enhance the colour, appearance and taste of foodstuffs. As such, it would have been sold to the wealthy and poor alike. Although one would expect to find abnormally high levels of lead within the bones of skeletons exhumed from lead coffins, Cox (1996) points out that lead is also found in high concentrations in those skeletons taken from wooden coffins. It was impossible to find out whether the uptake of lead into the skeleton had been gradual through life, or during adulthood or whether it had been ingested or inhaled. The highest number of deaths attributed to natural causes was the result of 'convulsions', which may reflect the heavy contamination of foodstuffs and water by heavy metals that are now known to attack the central nervous system.

Climate:

The climate of London today is temperate with an average mid-winter temperature of 5.5°C and an average mid-summer temperature of 18.9°C. Rainfall is moderate with an average yearly rate of 752mm. However, Molleson and Cox (1993) point out that at the time the Spitalfields people were living the climate was generally much colder than today and colder that at any time since the last Ice Age ended. Throughout northern and western Europe the coldest years of the 'Little Ice Age', were those of the 1690s, around the early 1740s and between 1816 and 1819, and resulted in years of bad harvests and severe food shortages,. The standard deviation of winter temperatures in England during these years was about 40% to 50% greater than during the early twentieth century (Fagan, 2000).

Footwear:

The named sample used in this study was sufficiently well off to wear strong and relatively decent footwear. Paintings of the period, including those by Hogarth, show even the 'English rabble' to be wearing shoes, while the Huguenots were well turned out and sporting elegant and fashionable footwear (Molleson and Cox, 1993).

2.2 Methods

2.2.1 Landmark data

Anatomical landmarks, (i.e., discrete features that can be recognised on each individual specimen) have been chosen to represent homologous points on the bone surface. Similar landmarks share the same position and have the same structure and evolutionary origins, although in other biological contexts, not necessarily the same analogous functions. Such points should be regarded as the best possible representation of equivalent bony features arising in individuals through the same morphogenetic processes (O'Higgins and Jones, 1998).

The homologous landmarks used for this study include 26 on the distal femur and 21 on the proximal tibia. The catagorisation of landmarks into three types has been devised to indicate the reliability of their homology and the stability of the co-ordinates (Bookstein, 1991; Marcus et al., 1996; Dryden and Mardia, 1998). The three types in descending order of reliability are:

1. Type I: An anatomical landmark with homology which is strongly supported by easily located local evidence such as a tubercle.
2. Type II: A mathematical landmark showing points on the object corresponding to some mathematical or geometrical property such as an extreme point of curvature on a facet.
3. Type III: A landmark in a relative position on an object without relating to a specific, identifiable point. Such landmarks include those around the outline of an object.

Tables 2.13 and 2.14 indicate the landmarks used for the distal femur and proximal tibia respectively. Figures 2.3 and 2.4 provide visualisation of the landmarks; together with the lines connecting landmarks which form interlocking triangles to aid visualisation (see section 2.2.3e below).

Table 2.13 Femur:

See also Figure 2.3

Distal femur: intercondylar fossa

Number	Type	Description
1	II	Central, deepest point of intercondylar fossa
2	II	Point on lateral corner of intercondylar line (posterior side)
3	III	Central point on intercondylar line (posterior side)
4	II	Point on medial corner of intercondylar line (posterior side)
5	II	Central, highest point on medial intercondylar facet
6	III	Centre of medial intercondylar facet
7	II	Point on medial corner with anterior patella surface
8	II	Point on lateral corner with anterior patella surface
9	II	Central, highest point on lateral intercondylar facet
10	III	Centre of lateral intercondylar facet

Distal femur: popliteal surface area

Number	Type	Description
11	III	Central point of popliteal surface
12	I	Adductor tubercle (medial side)
13	II	Corresponding point to adductor tubercle, lateral side

Distal femur: distal view, anterior side facing

Number	Type	Description
14	II	Deepest point on lateral epicondyle (indented feature)
15	II	Point of maximum height on lateral epicondylar edge
16	II	Central point of lateral condyle on epicondylar edge (indented feature)
17	II	Point of maximum width of lateral condyle
18	I	Point of intersection of anterior patella surface with shaft (medial side)
19	III	Point of maximum convexity of lateral epicondyle
20	II	Centre intersection of ant. patella surface with shaft (indented feature)
21	I	Point of intersection of anterior patella surface with shaft (lateral side)
22	II	Point of max. height on medial epicondylar edge (indented feature)
23	II	Point of maximum width of medial condyle
24	III	Point of maximum convexity of medial epicondyle
25	III	Point of maximum height on medial condyle
26	III	Point of maximum height on lateral condyle

(a)

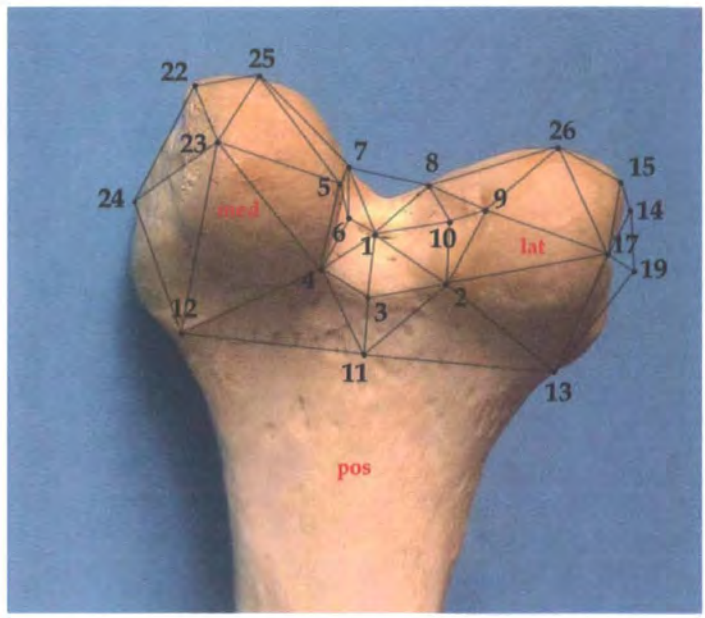

(b)

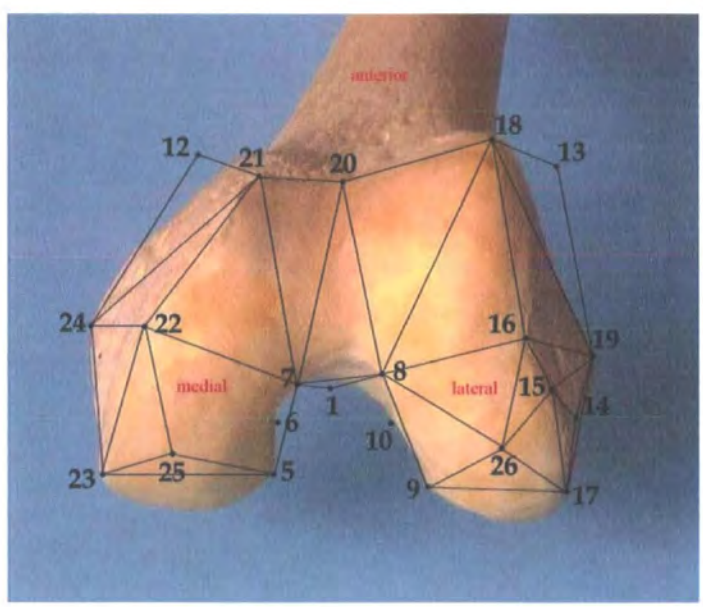

Figure 2.3: (a) posterior view and (b) anterior view of distal femur showing landmarks outlined in section 2.2.1. Landmarks are connected by lines forming interlocking triangles to aid visualisation (see section 2.2.3.5).

Table 2.14 Tibia:

See Figure 2.4

Proximal tibia: tibial plateau

Number	Type	Description
1	I	Medial intercondylar tubercle
2	II	Point of intersection of anterior side intercondylar and medial condyle
3	II	Maximum anterior point on medial condyle
4	II	Maximum posterior point on medial condyle
5	III	Maximum point of width of medial condyle (anterior side)
6	III	Maximum point of width of medial condyle (posterior side)
7	III	Deepest central point on medial condyle
8	I	Lateral intercondylar tubercle
9	II	Maximum anterior point on lateral condyle
10	II	Maximum posterior point on lateral condyle
11	III	Maximum point of width of lateral condyle (anterior side)
12	III	Maximum point of width of lateral condyle (posterior side)
13	III	Deepest central point on lateral condyle

Proximal tibia: tibial tuberosity

Number	Type	Description
14	I/II	Point of maximum convexity of tibial tuberosity
15	III	Point on anterior lateral edge of tibial shelf with tibial tuberosity
16	III	Point on anterior medial edge of tibial shelf with tibial tuberosity

Proximal tibia: posterior section

Number	Type	Description
17	II	Point of maximum width of articular fibular facet (medial side)
18	II	Deepest point of intersection of intercondylar eminence and shaft
19	III	Point of maximum width of fibula facet (medial side)
20	III	Head of interosseous crest at intersection with tibial shelf (medial side)
21	III	Head of popliteal crest at intersection with tibial shelf (lateral side)

(a)

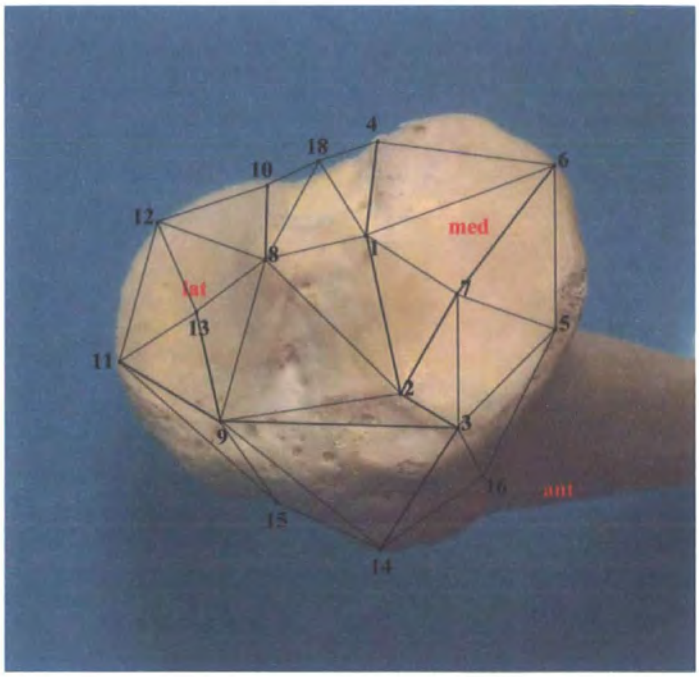

(b)

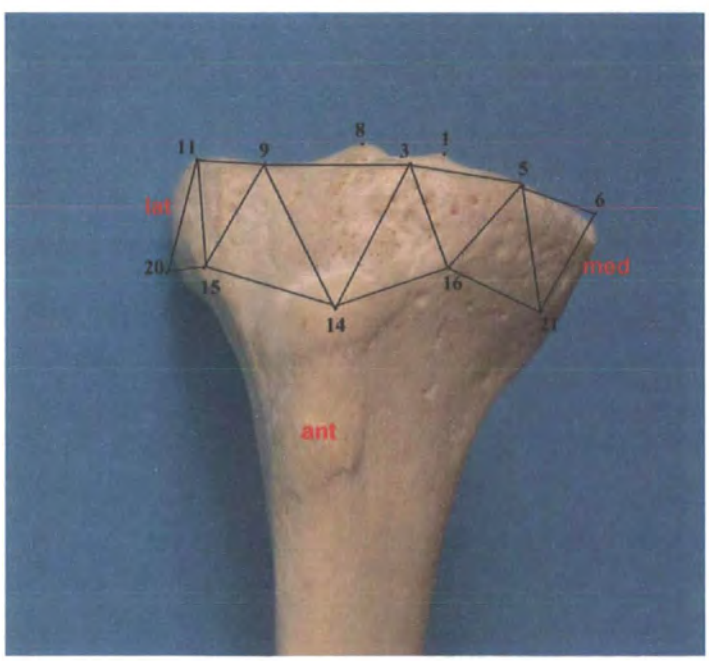

Figure 2.4: (a) Tibial plateau and (b) anterior view and of proximal tibia showing landmarks outlined in Table 2.4 section 2.2.1. Landmarks are connected by lines forming interlocking triangles to aid visualisation (see section 2.2.3.5).

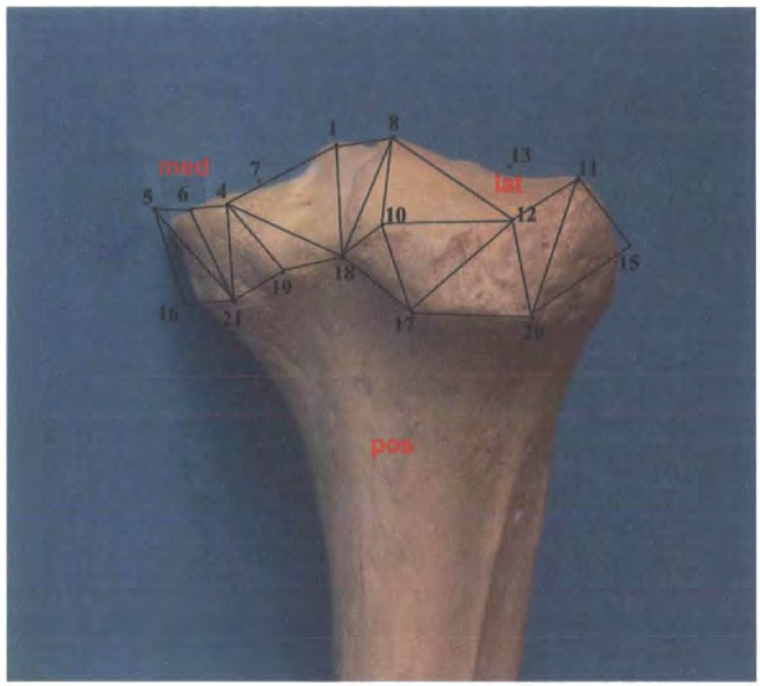

Figure 2.4: (c) Posterior view of proximal tibia showing landmarks outlined in Table 2.4 section 2.2.1. Landmarks are connected by lines forming interlocking triangles to aid visualisation (see section 2.2.3.5).

2.2.2 Collection of data

2.2.2a Digitising equipment

The three-dimensional coordinates of the 26 femoral and 21 tibial landmarks were collected using a Microscribe 3DX desktop digitising system (Immersion Corporation San Jose, C.A.). The bones were held securely in a portable desktop vice with padded clamps to enable all landmarks to be reached by the digital sensor from its stylus tip without removing or turning the specimens during digitisation. The three x,y,z coordinates were delivered by the digitiser to an Excel spreadsheet on a laptop computer, where the data were stored for later analysis (Microsoft Excel © Microsoft Corporation).

2.2.2b Equipment for measurements of the diaphyses

Measurement equipment used in the analyses of maximum length and robusticity indices of the diaphyses included the use of osteometric boards, loaned by the museum curators.

To optimise the standardisation of data, the same board at each museum location was used during all visits. Medial-lateral and anterior-posterior measurements of long bones were taken with a digital sliding caliper. The calipers are accurate to within 0.1 mm.

The three measurements for the femur and three for the tibia were taken according to the Definitions of Cranial and Postcranial Measurements (numbers 60, 66, 67, 69, 72 and 73) by Buikstra and Ubelaker (1994); derived from Martin (1957).

No	Measurement	Description of Measurement
60	Femur: Maximum Length	Distance from the most superior point on the head of the femur to the most inferior point on the condyles
66	Femur: Anterior-Posterior Midshaft Diameter	Distance between anterior and posterior surfaces measured approximately midpoint (of the diaphysis), at the highest elevation of linea aspera
67	Femur: Medial-Lateral Midshaft Diameter	Distances between the medial and lateral surfaces at the midshaft, measured perpendicular to the anterior-posterior diameter
69	Tibia: Length	Distance from the articular surface of the lateral condyle to the tip of the medial malleolus
72	Tibia: Maximum Diameter at the Nutrient Foramen	Distance between the anterior crest and the posterior surface at the level of the nutrient foramen
73	Tibia: Medial-Lateral Diameter at the Nutrient Foramen	Straight line distance of the medial margin from the interosseous crest at the level of the nutrient foramen

Table 2.15: Measurements of the diaphyses used in this study, according to the definitions of cranial and postcranial measurements by Buikstra and Ubelaker (1994).

Robusticity Indices for the diaphyses were calculated as the square root of the product of midshaft (femur) or nutrient foramen (tibia) anterior-posterior and medial-lateral breadths divided by length x 100 (Collier, 1989).

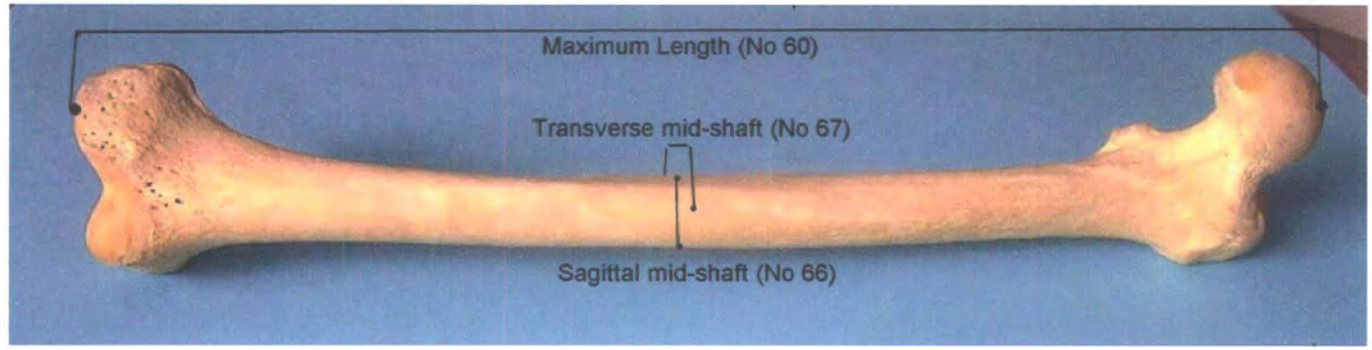

(a)

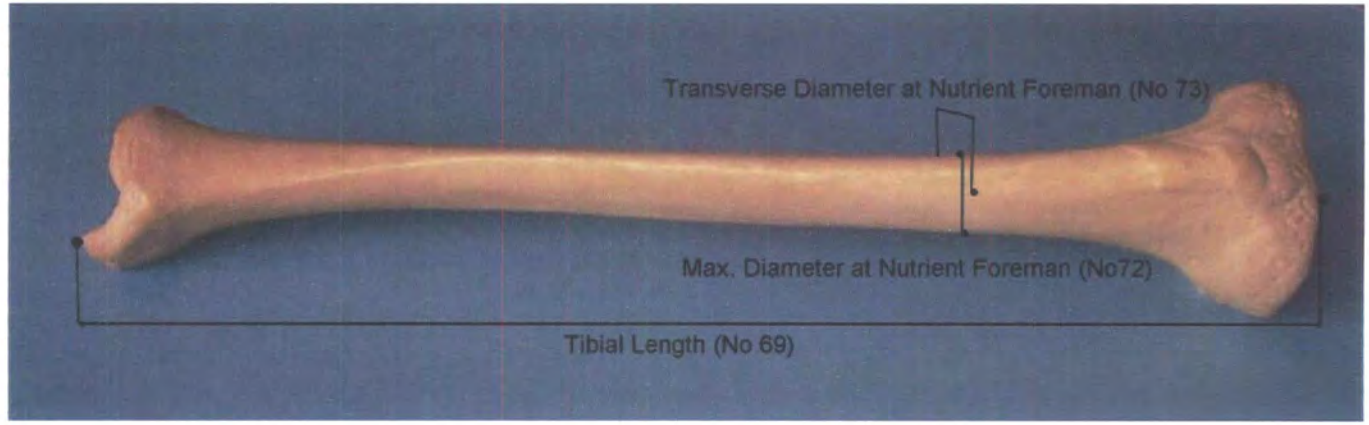

(b)

Figure 2.5: Long bone measurements for (a) femur and (b) tibia used in this study according to the definitions of cranial and postcranial measurements by Buikstra and Ubelaker (1994). See section 2.2.2.2. All measurements are in millimeters.

2.2.2c Tests for digitisation and operator error

Digitisation and operator error was investigated by taking 10 repeat measurements from 1 right-sided laboratory specimen together with 40 other random right-sided specimens from the total collection, in two separate analyses using distal femora and proximal tibiae. The data were submitted to Generalised Procrustes Analysis (GPA) and Principal Components Analysis (PCA) (see sections 2.2.3c and 2.2.3d below). Figure 2.6 shows the bivariate plots of PC1 with PC2, which cumulatively account for 31.5% and 22.5% of total variation respectively. For both femur and tibia, the 10 repeats form a very tight cluster on both PCs and this result remains true for all higher PCs. This test was repeated on two further occasions, producing similar results. Results indicate that precision errors are small with respect to sample variability and are unlikely to influence results.

2.2.3 Methods used for data analysis

2.2.3a Introduction

For the analyses of form of the knee joint, this study uses geometric morphometric techniques, a suite of morphometric analytical methods that preserves complete information about the relative spatial configuration of landmarks throughout an analysis (Slice et al., 1996). These shape spaces and the associated statistics are well understood, having been developed and used for over 20 years (Dryden and Mardia, 1998; O'Higgins and Jones, 1998; Viðarsdóttir et al., 2002). These techniques are concerned with analysing differences between objects based upon three fundamental concepts: 'form', the characteristic which remains after 'registration' i.e., translation (location in space), rotation and, possibly but not necessarily, 'reflection' of an object have been removed; 'size', the measure of scale of the form and 'shape', or form independent of size. The additional removal of reflection (mirror-imaging) is also preferable. Enabling reflection, however, allows the maximisation of scarce data and for many types of analysis where the object or organism is (supposedly) symmetrical (e.g., in cranio-facial

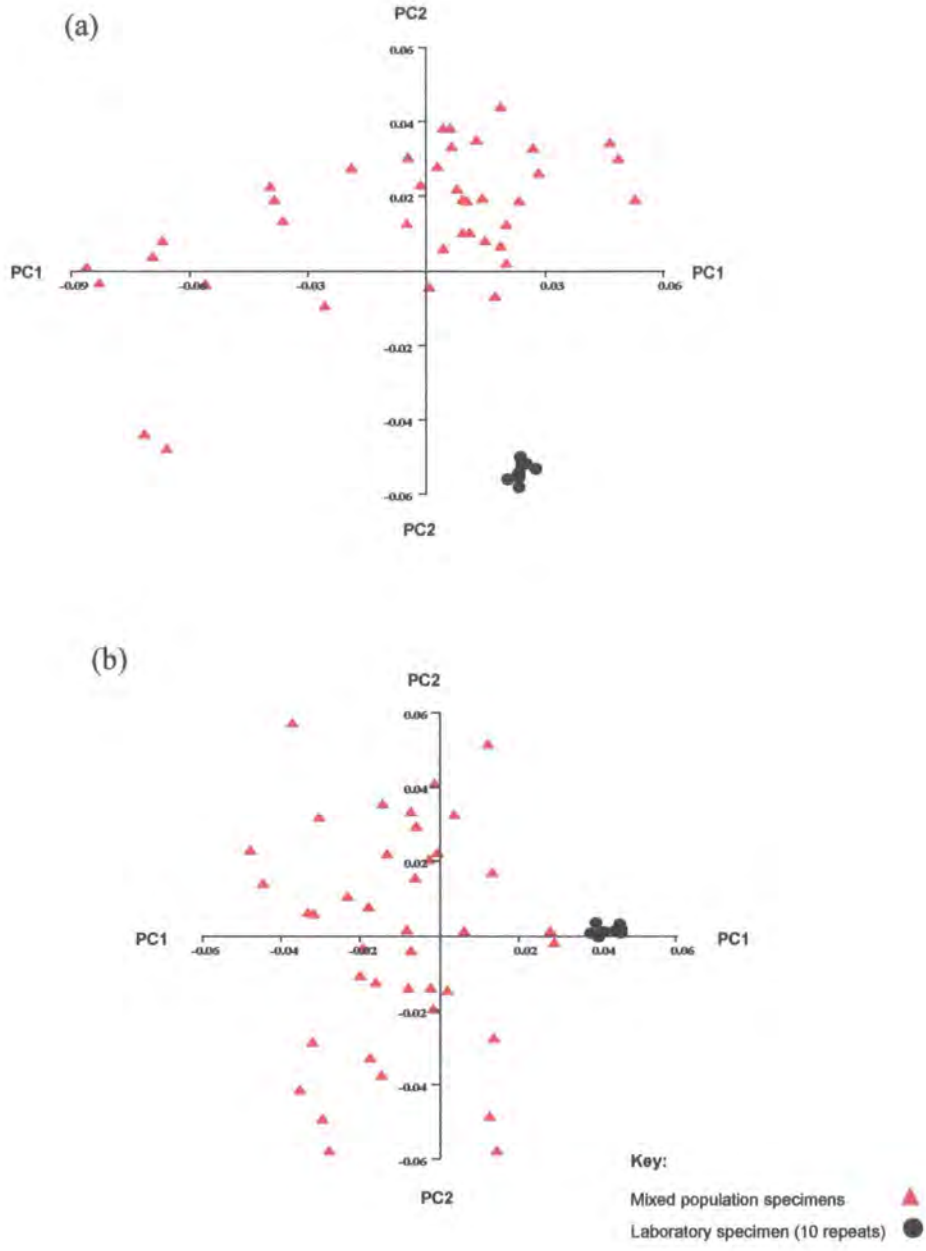

Figure 2.6:

40 randomly selected human specimens for (a) femur and (b) tibia, from 5 populations together with 1 laboratory specimen (10 repeats)

examinations using landmarks from either the right or left sides up to a mid-line or when using 'matched' postcranial bones), the inclusion of reflection should (hopefully) not confuse results (Goodall, 1991). If a mixed group of right and left sided objects is asymmetric, any asymmetries remain part of the residual shape difference. If an unacceptable degree of asymmetry is found, analyses should be restricted to one side only.

In this study size refers to the centroid size of the landmark configuration. It is computed from the landmark data, being the square root of the sum of the squared distances of the set of landmarks from their centroid (Slice, 1996). It is considered to be the only measure of size that is statistically independent of shape, taking the data directly into Kendall's shape space, which is the natural shape space for geometric morphometrics (see section 2.2.3c). It also takes account of the overall spread of landmarks and thus of the scale of the object (Dryden and Mardia, 1998; O'Higgins and Jones, 1998, O'Higgins and Viðarsdóttir, 2000) and, because it is calculated directly from the landmark configuration being analysed, it has an advantage over other methods of size calculation which may be more arbitrary (such as those based on body mass or single defining measurements, e.g., epicondylar breadth). Although other measurements of size can be used in geometric morphometric analyses and the use of different size measurements may affect results to some degree (Lele and Richtsmeier, 2001), if morphological variation between objects is fairly small with respect to size differences, the differences in results through using different size measurements will also be small (O'Higgins and Viðarsdóttir, 2000). Because centroid size is considered biologically sensible, this study uses centroid size throughout (O'Higgins and Viðarsdóttir, 2000).

There are two main approaches within the suite of three-dimensional morphometric techniques: those using distance-based techniques ('invariant approaches') such as Euclidean Distance Matrix Analysis (EDMA) and those using superimposition techniques, including those based upon Generalised Procrustes Analysis (GPA).

2.2.3b Euclidean Distance Matrix Analysis (EDMA)

EDMA is interlandmark distances (*ilds*) to describe the form of an object. It is described as invariant to the 'nuisance' parameters of translation, rotation and reflection, as registration is not intrinsic to this technique (Lele and Richtsmeier, 1991, 1992, 1993, 1995, 2001). EDMA works by calculating distances between all landmarks in a data set or a subset of those landmarks (Cole and Richtsmeier, 1998; Lele, 1991, 1993, 1999; Lele and McCulloch, 2002; Lele and Richtsmeier, 2001). EDMA calculates the set of distances into a form matrix from each of two groups in the data set; the form matrix can then be said to represent the three-dimensional shape of the whole or part of the object. A 'form difference matrix' is then computed from the form matrices by comparing the ratios of all corresponding pairs of landmarks from the two groups. Confidence levels are generated by a bootstrap method, which uses a random sampling procedure directly from the data (Lele and Richtsmeier, 1998, 2001). Comparisons between more than two groups are examined on a pairwise basis. The form difference matrix can be used to determine which *ilds* are more influential in determining form and shape differences by comparing each corresponding value for the two samples and observing which landmarks generate the highest variance between the denominator and numerator samples. Shape is calculated on the same principle, producing an equivalent shape difference matrix.

EDMA elicits criticism on several fronts: first, as form matrices are calculated from all possible distances between landmarks ((k (k - 1) / 2), where k = number of landmarks), the resultant matrices can be considered large and unwieldy; second, it can be difficult to interpret differences in form and shape from results of the form or shape difference matrices and third, it is difficult to visualise shape differences from this method. In addition, the supposed advantage over other statistical methods of being coordinate-free by operating purely on distance (thus making it invariant to the nuisance factors of translation, rotation and reflection), may not be unique as other methods such as Procrustes analyses can also operate independently from these parameters after

registration (Rohlf and Marcus, 1993). Proponents of EDMA, however, provide a spirited defense of all such criticisms (Lele and Richtsmeier, 2001).
EDMA is used as a supplementary method of analysis in the examination of asymmetry in Chapter 3, to provide an additional confirmation of the results obtained using GPA, the principal method chosen for all other analyses in this study (see section 2.2.3c below). An outline of EDMA is therefore provided to aid interpretation of Tables 3.12 and 3.14 (p161 and p169) for the femur and tibia, respectively. No attempt is made to provide visualisation of the results obtained through EDMA.

Interpretation of data using the form difference matrix relies upon examination of the degree and nature of where differences between distances lie between the two samples. The analysis of form (shape + size) provides a probability of difference between the two samples. The probability p value represents the probability of obtaining the bootstrapped T-value (where T = the maximal invariant statistic), if the two samples are identical in form; thus the p-value is generated from the observed T-value (T_{obs}). The analysis of shape uses two procedures: the estimate from the 'shape difference matrix' (form minus the scaling element) of minimum and maximum differences between all *ilds*, providing a maximum Z statistic and secondly, the generation of a confidence interval for the Z statistic using a parametric bootstrap procedure. An examination of the distribution of the bootstrapped Z statistics indicates whether the two samples are different. If a difference in form is indicated, analyses of shape will also indicate whether this difference is in size and/or in shape. Once sorted for easier inspection, an examination of the estimated shape difference matrix will indicate which distances are *sufficiently* different within the set confidence level; thus enabling the worker to highlight the regions of bone where maximum differences lie between the two samples.

2.2.3c Superimposition methods: Generalised Procrustes Analysis (GPA)

'Superimposition' methods involve the simultaneous placement in space of a series of specimens so that the corresponding homologous landmarks match as closely as possible

to produce the 'best fit', according to the approach used (see below). Differences in shape are recorded as residuals from a reference shape (Marcus et al., 1996).

Superimposition methods firstly require the removal of the nuisance factors of translation and rotation by registration. The partition of size also enables shape to be analysed independently of form. The additional removal of reflection is also preferable. It is frequently retained, however, as it enables the maximisation of scarce data (see section 2.2.3.1).

Registration can proceed by several methods, including Bookstein's 2-point or edge superimposition, which registers all shapes between two landmarks along one axis (Bookstein, 1984) and a 'robust' or 'resistant' superimposition, whereby the majority of landmarks is best fitted and those falling further from one another are removed (Siegel and Benson, 1982). An alternative method of registration is an 'optimal' superimposition by Generalised Procrustes Analysis (GPA), which registers landmark data by fixing one specimen, superimposing all others onto that one through the centroid and minimising the sum of the squared distances between the corresponding landmarks of all specimens (Rohlf and Slice, 1990; Goodall, 1991).

All registrations yield relatively similar results if variation is small (Kent, 1994), although GPA gives equal weight to all landmarks and thus introduces less bias towards specific regions of the object within the overall shape analysis (O'Higgins et al., 2001). All analyses in this study relating to the form of the knee joint use GPA for registration of landmarks.

Once registration has been carried out, each individual shape is represented by a point in a 'shape space' known as Kendall's shape space (Kendall, 1984). The dimensions of the shape space are $km - m - (m\,(m\text{-}1) / 2) - 1$; k being the number of landmarks and m the number of dimensions after registration i.e., translation = m dimensions; rotation = $(m(m\text{-}1)/2$ dimensions and scale = 1 dimension. Therefore, for analyses involving three dimensions = km-7 (O'Higgins and Jones, 1998). In analyses using more than the

minimum three landmarks, Kendall's shape space becomes complex, being both high dimensional and non-Euclidean (curved). It has been estimated, however, that if variation is relatively small (which is usually the case with biological specimens), the amount of space taken up within the total area is equally small and it is possible to project the data points from Kendall's shape space into a linear tangent plane to the shape space (Dryden and Mardia, 1998; O'Higgins and Jones, 1998). Once projected into a linear tangent plane, it then becomes possible to analyse the relationships between specimens by means of powerful statistical methods such as Principal Components Analysis or PCA (O'Higgins, 1998, 2000).

2.2.3d Principal Components Analysis (PCA)

PCA is a multivariate statistical tool that can be used to explore the relationships between specimens within the tangent space. It transforms a number of (possibly) correlated variables into a (smaller) number of uncorrelated variables called principal components. By so doing, it reduces the dimensionality of the dataset but retains most of the original variability in the data (Boersma and Weenik, 1999). PCA makes no prior assumption of dependence of one variable on another but describes the hyperdimensional 'cloud' of points, which represent each specimens in the sample, by calculating the principal axes of variation through it. There can be as many PCs as there are variables, to the point where the number of specimens exceeds the maximum number of variables (whichever is smaller). The maximum number of variables produced for the femur is 75, with 60 for the tibia, although degrees of variation after PCs 71 and 56 respectively are negligible. In the majority of analyses, most variation is explained by the first few components.

PC1 is the line that goes through the centroid, minimising the square of the distance of each individual point to that line and thus explaining the greatest degree of variation in the sample. PC2 explains the second greatest degree of variation within the sample, PC3, the third greatest degree of variation and so on. All PCs are orthogonal (at right angles) to each other and are therefore statistically independent of each other (Palmer, 2004).

For this study, both GPA and PCA are carried out using *morphologika*© (P. O'Higgins and N. Jones, University College London).

2.2.3e Visualisation of shapes

The *morphologika*© software also allows the visualisation of the mean configurations of landmarks with the choice of wireframe or flat or smooth shaded models, together with the landmark number display. The mean configurations are constructed from the landmarks through the connection of lines forming interlocking triangles (see Figures 2.3 and 2.4); thus producing a close approximation of the biological entity for visualisation purposes. These mean configurations can be 'morphed' or 'warped' to any point in PC space, allowing visualisation of each specimen or sample mean and therefore the range of variance represented by the PCs. This study uses the smooth surface-filled mean configurations to provide the best visualisation (O'Higgins and Jones, 1998).

2.2.3f Cartesian Transformation Grids using Thin Plate Splines (TPS)

The concept of using Cartesian transformation grids to highlight regions of biological difference in shape was the creation of Thompson (1917). His construct allowed the exploration of shape differences by superimposing a grid over a 'reference' shape and distorting this shape onto a second 'target' shape; so visualising where the regions of maximum difference lie. Thin Plate Splines are a version of Thompson's original concept. They are based upon the principle of bending an infinitely thin metal grid which is constrained at some combination of points whilst otherwise being free to adopt the underlying form, using minimal bending energy. This deformation is registration-free (Bookstein, 1989; Dryden and Mardia, 1998). In this study, the TPS function is performed by the *morphologika*© software where the bending of the TPS can be visualised against the mean configurations as they are morphed to any point in PC space from the reference to target shapes.

2.2.3g Calculation of distances

This study uses two methods of calculating distances between specimens and sample means; Mahalanobis' squared distances (Mahalanobis' D^2) and Procrustes distances.

The principal method of estimating distances between groups in this study is the statistical criterion of Mahalanobis' D^2, which is based upon the distance between pairs of group centroids, which is then generalised to distances over multiple pairs of groups. This calculation of Mahalanobis' D^2 is used for cross-validation discriminant function analysis (see section 2.2.3g) and stepwise discriminant function analysis (see section 2.2.3h) where it is used in evaluating the reliability of a set of predictors to predict group membership (Tabachnick and Fidell, 2001). The Mahalanobis' D^2 used in this study are calculated using SAS learning edition 1.0 (© SAS Institute Inc Carey, NC, USA).

The Procrustes distances measure the degree of fit between individuals or sample means and represents the square root of the sum of squared differences between the positions of the landmarks after GPA; thus it relates to the distance between specimens in Kendall's shape space. In this study the Procrustes distances are calculated using the executable Procrustes distances.exe (P. O'Higgins, University College London).

2.2.3h Discriminant function analysis and Cross-validation analysis

Discriminant function analysis is designed to predict group membership from a set of variables, by determining whether the group means differ. Cross-validation analysis (or jackknifed classification) is a linked procedure to discriminant function analysis and predicts the affiliation of individuals to the designated groups which indicate the closest fit. The distances between groups are the Mahalanobis' D^2 between the centroids of those groups. Each specimen is assigned to the group for which its Mahalanobis' D^2 is smallest. Thus, the smaller the Mahalanobis' D^2, the closer the individual is to the group centroid and the most likely it is to belong to that group. The significance of the

differences between the group means is derived from the Mahalanobis' D^2 and based on the F-test of Wilks's lambda (Tabachnick and Fidell, 2001).

Ideally, one would wish to predict group membership of individuals from samples other than those from which the group means was originally derived. When using a large sample, part of the original data to construct the group means (the calibration data) can be partitioned and 'hidden' in the program so that the accuracy of classification can be later used on the withheld cases (the test data). If the sample sizes are relatively small, cross-validation analysis will remove one arbitrary individual at a time during calibration and then assign it to a group. Over the course of the analysis each individual is therefore treated as unknown (Tabachnick and Fidell, 2001). Cross-validation in this study is carried out using SAS learning edition 1.0 (© SAS Institute Inc Carey, NC, USA).

2.2.3i Stepwise discriminant function analysis

Stepwise discriminant analysis is a variant of discriminant analysis. If a researcher has no reason for assigning some predictors higher priority than others, stepwise discriminant analysis can be used to determine an order of entry in a preliminary search, with the discriminant functions producing a subset of variables.

The progression of the stepwise selection of variables used in this study is by forward selection. The first variable chosen contributes most to the discriminatory criterion of the model; the second, the second greatest amount and so on. When all variables have been entered into the model, those that meet a suitable level of discriminatory contribution stay, whilst those that do not are removed. As stepwise discriminant function uses only a subset of variables, it does not discriminate groups to an equivalent level of significance to a discriminant function analysis which uses all variables. It is used therefore, to discriminate groups on specific criteria; in this study stepwise discriminant analysis is used to discriminate groups on the basis of sexual dimorphism (Chapter 4) and ageing

(Chapter 5). Stepwise discriminant analysis is carried out using SAS (SAS Institute Inc., Cary, NC, USA).

2.2.3j Clustering analysis

Dendograms provide a useful (if simplified) visual method of summarising the relationship between individuals or groups based upon the distances between them. They are a relatively crude representation, however, as they show two-dimensional relationships whilst attempting to explain multi-dimensional information. The dendograms used in this study are calculated using the UPGMA (unweighted pair-group method using arithmetic averages). Distances between individuals are based upon the Procrustes distances between individuals or Mahalanobis' D^2 between group means. By giving each individual in the dataset equal weighting, the procedure calculates the proximity of that individual or group to an existing cluster. It then calculates a new distance matrix, using the arithmetic average of the existing clusters as a basis for calculating the new distances. This is repeated until all clusters have been joined up. All the cluster analyses in this study are carried out on NT-SYSpc program (Rohlf et al., 1971; © F James Rohlf, Exeter Software, NY, USA).

2.2.3k Correlation analysis

Correlation analysis calculates the degree to which two sets of variables are associated, making no assumption about the dependence of each set to the other. It generates a linear association for the two sets of variables (the correlation coefficient or r) and ranges from a perfect positive correlation at 1 to a perfect negative correlation at -1. The statistical significance of the correlation is indicated by a probability *p* value based upon a t-test. In this study, all correlation analyses are carried out using Microsoft Excel (© Microsoft Corporation).

2.2.3l Student's t-test

The Student's t-test compares the means of two groups of univariate data to determine whether any difference between their means is due to random variation or is statistically significant. The level of statistical significance in t-tests used in this study is at the 95% level of confidence. Where the Student's t-test is used in the comparison of samples, it is assumed that the two samples have equal variance. All t-tests in this study are carried out using Microsoft Excel (© Microsoft Corporation).

Chapter 3

Asymmetry in the form of the knee joint in *Homo sapiens*

3.1 Introduction:

This chapter assesses the presence of asymmetric shape differences between left and right knee joint surfaces in *Homo sapiens*. One example population, African Americans, is analysed in detail and, if asymmetric shape differences at the knee joint are found in this population, the nature of this asymmetry will be described in order to provide a comparison against other population samples when analysed jointly. The African American population is chosen for examination in detail as it has more individuals with matching right and left sides in good condition than other population samples.

For analyses comparing asymmetric shape differences within and between several populations, the African American sample is examined in conjunction with the Caucasian Americans, Spitalfields, Arikara and Chinese collections. For analyses examining the presence of sexual dimorphism in asymmetry, three populations are examined; the African and Caucasian Americans and the Spitalfields collection. Supplementary analyses comparing the length and robusticity of the left and right femora and tibiae are included to provide additional insight into possible differences between left and right knee joints. Data from all five populations are used when comparing the length and robusticity of the long bones. Only those individuals with matching left and right limbs are used for all analyses.

3.2 The examination of issues relating to skeletal asymmetry in *Homo sapiens*

Asymmetry is expressed in organisms through three mechanisms; directional asymmetry, fluctuating asymmetry and antisymmetry. In non-pathological humans, the most influential type of asymmetry of skeletal form is bilateral directional asymmetry. Although this type of asymmetry has a strong genetic basis (Ruff and Jones, 1981; Annett, 1985; Hepper et al., 1998; Auffray et al., 1999; Steele, 2000; McManus, 2003; Faurie and Raymond, 2004) it is developed and accentuated as a response to differential mechanical loading on specific parts of one side of the

skeleton (Lowrance and Latimer, 1957; Mays et al., 1999). Mechanical loading stimulates the metabolism of chondrocytes, the cells in articular cartilage responsible for endochondral bone growth (Chapter 1, section 1.3); therefore greater loading on one side encourages more bone remodelling activity on that side, leading to additional growth and hence further skeletal asymmetry (Inglemark, 1974; Plochocki, 2004).

Variation in skeletal size and shape between individuals exhibiting directional asymmetrical traits can also be affected by fluctuating asymmetries. Fluctuating asymmetry is primarily caused by various environmental stresses on the developing organism. Whilst the gene complexes will remain constant for both sides of the bilaterally symmetric trait, in the process of development the organism is forced to adapt to numerous environmental pressures (such as food deprivation, changes in temperature, pollution), resulting in phenotypic variation between sides (Auffray et al., 1999; McManus, 2003). As such, fluctuating asymmetry is random with respect to side as the developmental processes in each individual are unique.

Antisymmetry is a genotypic adaptation to cope with a specific functional need. The classic example is the claws of the male fiddler crab, in which one front claw is demonstrably bigger than the other, although handedness and footedness in humans have also been described as examples of antisymmetry (Livshits and Smouse, 1993).

It is strongly suggested that all three asymmetries are closely interrelated and investigations into directional asymmetries and antisymmetries may be influenced by fluctuating asymmetry within the same trait. Equally, directional asymmetry may hide a slight but true antisymmetry (Auffray et al., 1999).

Until recently, research has been heavily biased towards examination of directional bilateral asymmetry in the upper limbs (e.g., Latimer and Lowrance, 1965; Coren and Porac, 1977; Plato et al, 1980, 1985; Ruff and Jones, 1981; Ruff and Hayes, 1983; Fresia et al., 1990; Stirland, 1993; Kannus et al., 1994; Roy et al., 1994; Trinkaus et al, 1994; Steele and Mays, 1995; Wilczak, 1998; Mays et al., 1999; Sakaue, 1998; Steele, 2000; Ruff, 2000; Dittmar, 2002). Such research has concentrated on comparisons of maximum length measurements and internal and

external differences in shape and robusticity of the shafts. Humeri have been especially subject to scrutiny, because of the greater load bearing in right relative to left arms, in response to the preference for right-handedness. The universal preference for right-handedness is estimated to have been part of the human condition for over five thousand years (Coren and Porac, 1977) and probably much longer (Steele, 2000). At least 90% of humans are estimated to be right handed (Plato et al, 1980; Roy et al., 1994), consequently upper limb dominance in muscle weight and mass is overwhelmingly right sided.

Footedness has been a less well studied phenomenon until recent years when the advent of interest in sports sciences and the effects of footedness on sportsmen has helped produce some (albeit limited) data. Such research has shown that right footedness (as well as right handedness) is strongly preferred in humans; 79% of world-class footballers, who are both trained to use and skilled at using both feet equally as the lead foot, consider themselves as preferentially right-footed. This percentage appears to be about average for the general population (Carey et al., 2001).

Asymmetry of the trunk has been the subject of some scientific interest, mainly in the medical context of back problems and illnesses faced by adults and largely caused by asymmetric posture in children (e.g., Marras and Mirka, 1989; Joskeliene et al, 1996; Nissensen, 2000). Relatively little research, however, has been conducted on the possibility and causes of asymmetry of the legs and feet. Any slight differences in size and shape between sides in individuals has frequently been regarded as largely idiosyncratic and caused by individual development, i.e., fluctuating asymmetry.

Until recently any research on asymmetry of the lower limbs has focused on the length, robusticity and shape of the diaphyses. Freed from the constraints of balance for locomotion (Chapter 1, section 1.6), it is possible for the human upper limbs to be relatively bilaterally asymmetric without detriment to functionality. Marsk (1958), however, suggests that handedness in the upper limbs forces a degree of natural dominance of one side in the lower limbs. His research analysed the length of lower limbs of individuals working in a stationery position at a factory bench. He suggests that such individuals, using one leg as the 'standing leg' and distributing more load

pressure over that leg whilst in a standing position, creates a dominance of the left side over the right. The concept of asymmetric standing was a theme derived from earlier research by Smith (1953), who observed the shifting distribution of weight by people queuing in line. Smith calculated that up to four times more of the body's weight was held over one side than the other.

Optimal balance is achieved if total load-pressure is transmitted to the ground equally through both feet, with the centre of gravity falling vertically over the supporting base. Using the arms whilst in a standing position, however, will cause the centre of gravity to shift from side to side, throwing the load pressure from one leg to the other. Using one dominant arm more than the other will put greater load pressure upon the leg that is attempting to uphold balance throughout the skeleton by distributing the weight of the body over its supporting base. The leg that is forced to take on the greater load bearing is defined by Marsk (1953) as the standing leg. Thus, for the majority of individuals who are right handed, the left leg will become the standing leg. His results for dominance of the right leg in left-handers were less conclusive, which he attributed to the greater degree of ambidexterity in such individuals coping with machinery and technology primarily designed for a right-handed world.

Conclusions of dominance based upon crossed asymmetry, however, are debateable. Huelster (1953) also found a marked degree of lower limb bilateral asymmetry of length and weight, again predominantly on the left side but she placed less emphasis on the response of the lower limbs to upper limb dominance and handedness. She suggests that greater body weight is supported on the dominant side in both standing *and* walking, creating hypertrophy on this side, thus defining its dominance. Her work was supported in later research by Chhibber and Singh (1970) who looked into the asymmetry of muscle and bone weight of the dominant lower limbs of ten cadavers and, although the difference in weight between dominant and non-dominant sides was highly significant ($p<0.001$) and occurred in seven of the ten bodies on the left side, again they found no specific correlation between dominance in the upper and lower limbs. An additional confounding variable highlighted by DeVita et al. (1998), is the effect of asymmetric load bearing on the biomechanics of normal walking, which they found to produce significant degrees of unbalanced trunk

muscle dominance between right and left limbs, together with asymmetric hip and knee movements. Asymmetric load-carrying *is*, naturally, related to upper-limb dominance and handedness. In relation to the results by Chhibber and Singh (1970), later work by other authors has shown them to be less conclusive, as it has been suggested that there is probably less than 1% difference in length and weight between the left and right femora when using a larger data set (Hayes et al., 1978). Inglemark (1943) also reported a slight (but not statistically significant) dominance in length in the left leg of right-handed adults (and *vice versa*); although, when the two component bones were analysed separately, she found left tibiae to be proportionately longer than right, with right and left femora equal in length.

As results from research are conflicting, this study will examine the lengths and robusticity of femoral and tibial shafts to determine whether one side shows a consistent directional asymmetry. The samples involved are small and results are therefore unlikely to offer indisputable conclusions [see above in relation to the research conducted on a small data set of only ten bodies by Chhibber and Singh (1970)]; data sets include individuals from five separate populations of modern humans, firstly with males and females pooled into population samples and secondly subdivided into sexed samples, where data are available.

Therefore the first hypothesis is erected:

H.3.1. There is no significant difference in the lengths and robusticity indices between right and left femora and tibiae in *Homo sapiens.*

Relatively little work has been done on estimating asymmetry of the distal and proximal ends of long bones in either the upper or lower limbs. Ruff (2000) reasons that asymmetry of these areas is unlikely to be as prominent as in the shafts, due to the joint ends being less sensitive to load bearing pressures than the diaphyses and less able to respond to such pressures after epiphyseal fusion. This assumption has been made elsewhere, as well as by Gill (2001) who, in assessing racial differences between African and Caucasian Americans, used one specific measurement (the maximum intercondylar notch height) on the distal femur for comparison. His samples were subdivided by known sex and race and the chosen measurement

proved relatively accurate at predicting group affiliation. The data included measurements from both right and left joints, as he found "no discernable morphological variation between right and left notch heights of the same individual and therefore obtained each individual's notch height value from the femur that best preserved the outline of the notch" (Gill, 2001: 792).

This research reflected earlier work by Craig (1995), who used the intercondylar shelf angle to determine race from the distal femur. Again, whilst neither Gill nor Craig specifically looked at asymmetry in this region of bone, they believed that there was none present. Like Gill, Craig also used both left and right bones, depending on the condition of the best of a pair.

Research has also determined, however, that in humans the lower limbs do *not* behave symmetrically in normal, able-bodied walking (Sadeghi, 2000). In relation to the knee, the ranges for different phases of gait produce different results for the means of degrees of movement for each knee. For example, in flexion-extension during swing and stance and abduction-adduction and rotation, the mean for right knees is 68.1°, and the mean for left knees is 66.7° (Kettlekamp et al., 1970; Nordin and Frankel, 2001). Thus, whilst in relation to one specific interlandmark measurement (e.g., intercondylar notch height or intercondylar shelf angle), there may be little apparent difference between right and left sides, it may not be safe to assume that the overall shape of the two sides of a joint is symmetric. In the research by Kettlekamp et al. (1970) and Nordin and Frankel (2001), no firm conclusions are drawn to explain such asymmetry which they thought was a reflection of a natural functional difference between the limbs.

In the light of the above research, this study seeks to determine whether the right and left knee joints are symmetric in overall shape and whether it is safe to assume that sides are interchangeable for statistical analysis of intra- and inter-sample variation.

Therefore the following hypothesis is erected:

H.3.2. There is no significant difference in asymmetry in the size and shape of the knee joint in *Homo sapiens.*

In relation to shape changes occurring with changing subsistence practices amongst North American native groups, researchers such as Ruff (1984, 1994, 2000), Bridges (1985, 1989), Freesia et al (1990) and Larsen (1997), among others, have examined the internal as well as external architecture of the diaphyses. All have emphasised that, not only is the length of the dominant limb proportionately greater on that side, but that the internal dimensions of the shaft also differ between right and left sides. In addition, they emphasise that there are substantial asymmetric differences in the shape of the diaphyses between males and females.

Given the findings of such previous research, that asymmetric differences are present in the shape of the diaphyses between males and females, if H.3.2 is falsified in relation to the knee joint, it is then proposed to separate males and females within the three populations to determine whether there is significant variation in the degree and nature of asymmetry between the sexes at the knee joint. Thus the following hypothesis is erected:

H.3.3. There is a no significant difference in asymmetry in the shape of the knee joint between males and females in *Homo sapiens.*

3.3 Materials and Methods

This chapter will examine the presence of asymmetry in the femur and tibia in relation to the maximum length and robusticity of the diaphyses. Subsequently, it will examine the presence of asymmetry in relation to the size and shape of the knee joint. Again, this will be examined in relation to the above five population samples, although a more detailed analysis of one of the samples (the African Americans) will precede the inter-population analysis. The nature and degree of asymmetry in relation to males and females will also be examined in relation to the African and Caucasian Americans and the Spitalfields collection.

The composition and original locations of the data sets are shown in Tables 3.1 and 3.2 and Tables 3.3 and 3.4. Nearly all individuals used for both size and shape

Population	Total individuals	Males	Females	Collection
African American	47	26	21	NMNH
Caucasian American	31	15	16	NMNH
Spitalfields	49	22	27	NHM
Arikara	19	13	6	NMNH
Chinese	23	23	0	NMNH
Total	169	99	70	

Table 3.1: The composition and original locations of the data sets used for the analyses of shape and centroid size of the femur.

Population	Total individuals	Males	Females	Collection
African American	49	26	23	NMNH
Caucasian American	30	15	15	NMNH
Spitalfields	51	18	33	NHM
Arikara	23	16	7	NMNH
Chinese	27	27	0	NMNH
Total	180	102	78	

Table 3.2: The composition and original locations of the data sets used for the analyses of shape and centroid size of the tibia.

Key: NMNH: National Museum of Natural History, Smithsonian Institution, Washington DC. NHM: Natural History Museum, London

Population	Total individuals	Males	Females	Collection
African American	50	25	25	NMNH
Caucasian American	32	15	17	NMNH
Spitalfields	44	20	24	NHM
Arikara	22	13	9	NMNH
Chinese	26	26	0	NMNH
Total	174	99	75	

Table 3.3: The composition and original locations of the data sets used for the analyses maximum length (M2) and robusticity indices (RI) of the femur.

Population	Total individuals	Males	Females	Collection
African American	50	25	25	NMNH
Caucasian American	32	15	17	NMNH
Spitalfields	42	21	21	NHM
Arikara	23	15	8	NMNH
Chinese	28	28	0	NMNH
Total	175	104	71	

Table 3.4: The composition and original locations of the data sets used for the analyses maximum length (M2) and robusticity indices (RI) of the tibia.

Key: NMNH: National Museum of Natural History, Smithsonian Institution, Washington DC. NHM: Natural History Museum, London

analyses are the same. The small discrepancy in numbers is to maximise data and to use any remaining individuals that may have knee joints in good condition but with damaged shafts or have shafts in good condition but with damaged knee joints.

All analyses of shape are conducted on all landmarks for both distal femora and proximal tibiae. The specimens are superimposed using Generalised Procrustes Analysis (GPA) and the Procrustes fitted data are subjected to Principal Components Analysis (PCA). These methods are described in Chapter 2 section 2.2.3c and 2.2.3d.

The centroid sizes of the knee joints are calculated in *morphologika*© as part of the GPA analysis. The correlation analyses of size are calculated using Microsoft Excel. These methods are described in Chapter 2 section 2.2.3j.

For the purpose of maximising scarce data, it is often expedient to assume that each side of a bilateral trait or each side of the craniofacial skeleton is largely a reflected image of the other side. A technique of reflecting the right onto the left side or left onto the right side can be carried out in the *morphologika*© programme, thus enabling the use of the best preserved side of a pair of specimens or either side if only one side of a specimen is available. When analysing asymmetry between two sides of the same bilateral trait, it could be argued that to do so by using a programme that *assumes* symmetry may introduce errors. Therefore a secondary method of Euclidean Distance Matrix Analysis (EDMA) is also used to analyse asymmetry in the African American sample.

Results generated by EDMA are tabulated and described in section 3.4.3. These results are compared with results calculated in *morphologika*©, which uses superimposition techniques as part of the GPA analysis. These two methods are described in Chapter 2 sections 2.2.3b and 2.2.3c.

3.4 Results

3.4.1 Asymmetry of size of the maximum length and robusticity indices of the diaphyses

3.4.1a Femur:

Tables 3.5 and 3.6 show the results of comparisons of maximum length measurements and robusticity indices of the left and right femora of the five populations. For both maximum length and robusticity, results do not reach a level of statistical significance in any comparison. For pooled-sex samples, the difference in millimeters between right and left sides ranges from 0.38mm (Chinese) to 3.19mm (Spitalfields). In every case, for both pooled-sex and male and female only samples, the slightly longer femur is on the left. This equates to a percentage difference, however, of less than 1% of total length in all cases. Sample size for some of the sexed groups is relatively small, particularly for the Arikara females, and this should be borne in mind when interpreting results. It is recognised that differences in sample sizes can often influence results (Harvati, 2003).

For robusticity of the femur, no result is statistically significant. The small percentage differences (at less than 1.30% in eleven results) reflect this failure to reach statistical significance, including the result for the Arikara females with a higher percentage difference at 2.82%. Small sample size may be unduly influencing results for this female group.

Population	Mean Right mm	Mean Left mm	Diff. Rt against Lt mm	% diff. Rt against Lt	t =	P =
African American Males	470.96	472.52	1.56	0.33	0.22	0.82
African American Females	435.84	436.60	0.76	0.17	0.09	0.93
African American Pooled	453.40	454.56	2.32	0.26	0.18	0.86
Caucasian Americans Males	454.80	455.93	1.13	0.25	0.11	0.92
Caucasian Americans Females	432.35	432.64	0.29	0.07	0.04	0.96
Caucasian Americans Pooled	443.58	444.29	1.42	0.16	0.10	0.92
Spitalfields Males	442.25	444.75	2.50	0.57	0.34	0.73
Spitalfields Females	414.91	418.79	3.88	0.94	0.53	0.60
Spitalfields Pooled	428.58	431.77	3.19	0.74	0.55	0.58
Arikara Males	445.92	448.38	2.46	0.55	0.28	0.79
Arikara Females	407.70	410.60	2.90	0.71	0.40	0.70
Arikara Pooled	426.81	429.49	5.36	0.63	0.33	0.74
Chinese Males	430.23	430.61	0.38	0.09	0.06	0.95

Table 3.5: Comparisons of maximum length (M2) between right and left femora in 5 populations. Figures in black denote sexed groups; figures in red denote pooled-sex populations.

Population	Mean Right mm	Mean Left mm	Diff. Rt against Lt mm	% diff. Rt against Lt	t =	*p* =
African American Males	6.095	6.082	0.020	0.33	0.13	0.90
African American Females	6.054	6.054	0.000	0.00	0.006	1.00
African American Pooled	6.075	6.068	0.007	0.11	0.08	0.94
Caucasian Americans Males	6.169	6.082	0.087	1.14	0.53	0.60
Caucasian Americans Females	5.870	5.892	0.022	0.37	0.14	0.90
Caucasian Americans Pooled	6.020	5.987	0.032	0.55	0.26	0.80
Spitalfields Males	6.383	6.384	0.001	0.00	0.007	1.00
Spitalfields Females	6.263	6.222	0.041	0.66	0.31	0.76
Spitalfields Pooled	6.323	6.303	0.020	0.32	0.25	0.80
Arikara Males	6.440	6.428	0.012	0.19	0.44	0.67
Arikara Females	6.165	6.339	0.174	2.82	1.60	0.13
Arikara Pooled	6.302	6.384	0.081	1.30	1.27	0.21
Chinese Males	6.172	6.096	0.076	1.25	0.70	0.49

Table 3.6: Comparisons of robusticity indices (RI) between right and left femora in 5 populations. Figures in black denote sexed groups; figures in red denote pooled-sex populations.

3.4.1b Tibia:

Tables 3.7 and 3.8 show the results of comparisons of maximum length measurements and robusticity indices of the left and right tibiae from the five populations. For both maximum length and robusticity, results do not reach a level of statistical significance in any comparison.

For the pooled-sex samples, the difference in millimeters between right and left sides ranges from 0.39mm (Chinese) to 2.01mm (Spitalfields). This equates to a percentage difference of considerably less than 1% of total length in all cases. In four of the five populations, the longer tibia is on the left for both males and females. The Arikara shows greater length on the right side for both males and females although for this sample the percentage difference is negligible (0.15%). Sample size for this group is low and may be unduly influencing results.

With respect to the robusticity of the tibial shaft, the comparison of measurements equate to percentage differences of less than 1%, with the one exception for the Arikara females at 2.39% where the sample size is low.

3.4.2 Asymmetry of centroid size of the knee joint

3.4.2a Femur:

Table 3.9 shows the results of comparisons of the centroid size of the left and right distal femora for the five populations. Results do not reach a level of statistical significance in any comparison.

For the pooled-sex samples, the difference in means ranges from 0.64mm for the Arikara to 1.81mm for the Spitalfields collection. This equates to a percentage difference of approximately 1% of total size (or less) in all cases. In all samples, the bigger side is on the right for both males and females.

Population	Mean Right mm	Mean Left mm	Diff. Rt against Lt mm	% diff. Rt against Lt	t =	*p* =
African American Males	401.80	403.88	2.08	0.52	0.06	0.95
African American Females	369.00	369.44	0.44	0.12	0.07	0.95
African American Pooled	385.40	386.66	1.26	0.33	0.0004	0.99
Caucasian Americans Males	376.33	377.93	1.60	0.33	0.25	0.80
Caucasian Americans Females	355.59	357.29	1.70	0.48	0.24	0.81
Caucasian Americans Pooled	365.96	367.61	1.65	0.45	0.25	0.80
Spitalfields Males	368.14	368.62	0.48	0.13	0.09	0.93
Spitalfields Females	338.90	342.43	3.53	1.04	0.31	0.76
Spitalfields Pooled	353.52	355.53	2.01	0.57	0.25	0.80
Arikara Males	385.13	384.93	0.20	0.05	0.08	0.98
Arikara Females	340.38	339.50	0.88	0.23	0.41	0.89
Arikara Pooled	362.76	362.22	0.54	0.15	0.26	0.96
Chinese Males	353.29	353.68	0.39	0.11	0.08	0.94

Table 3.7: Comparisons of maximum length (M2) between right and left tibiae in 5 populations. Figures in black denote sexed groups; figures in red denote pooled-sex populations.

Population	Mean Right mm	Mean Left mm	Diff. Rt against Lt mm	% diff. Rt against Lt	t =	*p* =
African American Males	7.714	7.719	0.005	0.65	0.03	0.98
African American Females	7.523	7.476	0.047	0.63	0.27	0.79
African American Pooled	7.619	7.598	0.021	0.27	0.18	0.85
Caucasian Americans Males	7.795	7.864	0.069	0.89	0.25	0.71
Caucasian Americans Females	7.250	7.300	0.050	0.69	0.40	0.70
Caucasian Americans Pooled	7.523	7.582	0.059	0.79	0.37	0.80
Spitalfields Males	7.965	7.953	0.012	0.15	0.08	0.94
Spitalfields Females	7.466	7.536	0.070	0.94	0.41	0.69
Spitalfields Pooled	7.716	7.745	0.029	0.38	0.26	0.80
Arikara Males	7.709	7.744	0.035	0.45	0.20	0.85
Arikara Females	7.630	7.812	0.182	2.39	0.64	0.53
Arikara Pooled	7.670	7.778	0.109	1.41	0.57	0.57
Chinese Males	7.814	7.789	0.025	0.32	0.19	0.85

Table 3.8: Comparisons of robusticity indices (RI) between right and left tibiae in 5 populations. Figures in black denote sexed groups; figures in red denote pooled-sex populations.

Population	Mean Right	Mean Left	Diff. Rt against Lt mm	% diff. Rt against Lt	t =	p =
African American Males	165.97	165.39	0.59	0.36	0.35	0.73
African American Females	147.21	146.10	1.13	0.77	0.55	0.59
African American Pooled	157.59	156.76	0.83	0.53	0.35	0.73
Caucasian Americans Males	161.37	160.00	1.38	0.86	0.29	0.77
Caucasian Americans Females	146.49	146.07	0.42	0.29	0.19	0.85
Caucasian Americans Pooled	153.69	152.81	0.88	0.58	0.31	0.76
Spitalfields Males	157.93	157.63	0.31	0.19	0.14	0.89
Spitalfields Females	144.14	141.11	3.03	2.15	1.41	0.16
Spitalfields Pooled	150.33	148.52	1.81	1.21	0.84	0.41
Arikara Males	161.05	160.61	0.45	0.28	0.20	0.84
Arikara Females	143.99	142.94	1.05	0.74	0.25	0.81
Arikara Pooled	155.66	155.03	0.64	0.41	0.19	0.85
Chinese Males	148.68	147.61	1.07	0.72	0.54	0.59

Table 3.9: Comparisons of centroid size of the knee joint between right and left femora in 5 populations. Figures in black denote sexed groups; figures in red denote pooled-sex populations.

3.4.2b Tibia:

Table 3.10 show the results of comparisons of the centroid size of the left and right proximal tibiae of the five populations. Results do not reach a level of statistical significance in any comparison.

For the pooled-sex samples, the difference in means between right and left sides ranges from 0.10mm for the Chinese to 1.56mm for the Arikara. This equates to a percentage difference of approximately 1% of total size (or less) in all cases.

3.4.3 Asymmetry of shape of the knee joint: African Americans

3.4.3a(i) Femur: African Americans using the total sample

Differences in shape of the left and right distal femora from 47 individuals are analysed using the Procrustes fitted co-ordinates and by subjecting the data to PCA. Table 3.11 gives the proportional and accumulated variance for PCs 1 to 71, which represents the total variance within the sample. The scores for each specimen on the resultant PCs are then subjected to canonical discriminant analysis to establish the potential differences between right and left samples based upon the Mahalanobis' squared distances between sample means.

For the femur, the equal best separation of sides is achieved using 80% of total variance. This assessment was reached after separate discriminant and cross-validation analyses were carried out using the PC scores accounting for between c.50% to 100% of total variance. Results are summarised in Figure 3.1. A decision was made to use the greatest number of PC scores where crossvalidation correctly assigned 100% of specimens to groups.

The Mahalanobis' squared distance generated by discriminant analysis between the means of right and left samples is 35.71; this is statistically significant at $p= 0.001$, indicating that the two sides can be separated on some aspect of shape of the distal femur.

Population	Mean Right	Mean Left	Diff. Rt against Lt mm	% diff. Rt against Lt	t =	*p* =
African American Males	144.77	144.52	0.25	0.17	0.15	0.88
African American Females	125.37	124.36	1.01	0.81	0.67	0.51
African American Pooled	135.66	135.06	0.60	0.45	0.26	0.79
Caucasian Americans Males	140.41	139.90	0.51	0.37	0.16	0.88
Caucasian Americans Females	126.95	126.80	0.15	0.12	0.07	0.94
Caucasian Americans Pooled	133.95	133.66	0.29	0.21	0.11	0.91
Spitalfields Males	136.24	135.31	0.93	0.69	0.37	0.70
Spitalfields Females	121.48	120.08	1.40	1.17	0.97	0.33
Spitalfields Pooled	126.69	125.46	1.23	0.98	0.64	0.52
Arikara Males	140.96	139.61	1.35	0.97	0.86	0.40
Arikara Females	122.85	120.82	2.03	1.68	1.59	0.14
Arikara Pooled	135.45	133.89	1.56	1.16	0.55	0.58
Chinese Males	127.84	127.74	0.10	0.08	0.06	0.95

Table 3.10: Comparisons of centroid size of the knee joint between right and left tibiae in 5 populations. Figures in black denote sexed groups; figures in red denote pooled-sex populations.

PCs	Prop.	Cumul.	PCs	Prop.	Cumul.	PCs	Prop.	Cumul.
PC1	11.20	11.20	PC26	1.03	88.00	PC51	0.15	98.80
PC2	9.37	20.60	PC27	0.98	89.00	PC52	0.15	99.00
PC3	6.43	27.00	PC28	0.90	89.90	PC53	0.14	99.10
PC4	5.81	32.90	PC29	0.78	90.70	PC54	0.12	99.20
PC5	5.42	38.30	PC30	0.74	91.40	PC55	0.11	99.30
PC6	4.64	42.90	PC31	0.69	92.10	PC56	0.10	99.40
PC7	4.28	47.20	PC32	0.65	92.70	PC57	0.09	99.50
PC8	4.23	51.40	PC33	0.57	93.30	PC58	0.07	99.60
PC9	3.86	55.30	PC34	0.52	93.80	PC59	0.06	99.70
PC10	3.64	58.90	PC35	0.48	94.30	PC60	0.06	99.70
PC11	3.32	62.20	PC36	0.47	94.80	PC61	0.05	99.80
PC12	2.90	65.10	PC37	0.41	95.20	PC62	0.04	99.80
PC13	2.76	67.90	PC38	0.39	95.60	PC63	0.04	99.80
PC14	2.34	70.20	PC39	0.38	95.90	PC64	0.03	99.90
PC15	2.21	72.50	PC40	0.35	96.30	PC65	0.03	99.90
PC16	1.94	74.40	PC41	0.32	96.60	PC66	0.03	99.90
PC17	1.84	76.20	PC42	0.30	96.90	PC67	0.02	100.00
PC18	1.77	78.00	PC43	0.28	97.20	PC68	0.02	100.00
PC19	1.55	79.50	PC44	0.26	97.40	PC69	0.01	100.00
PC20	1.45	81.00	PC45	0.23	97.70	PC70	0.01	100.00
PC21	1.38	82.40	PC46	0.22	97.90	PC71	0.01	100.00
PC22	1.26	83.60	PC47	0.20	98.10			
PC23	1.20	84.80	PC48	0.20	98.30			
PC24	1.09	85.90	PC49	0.19	98.50			
PC25	1.03	87.00	PC50	0.18	98.70			

Table 3.11: Asymmetry in the femur of African Americans. The proportion and accumulated variance for PCs 1-71, which account for 100% of total variance.

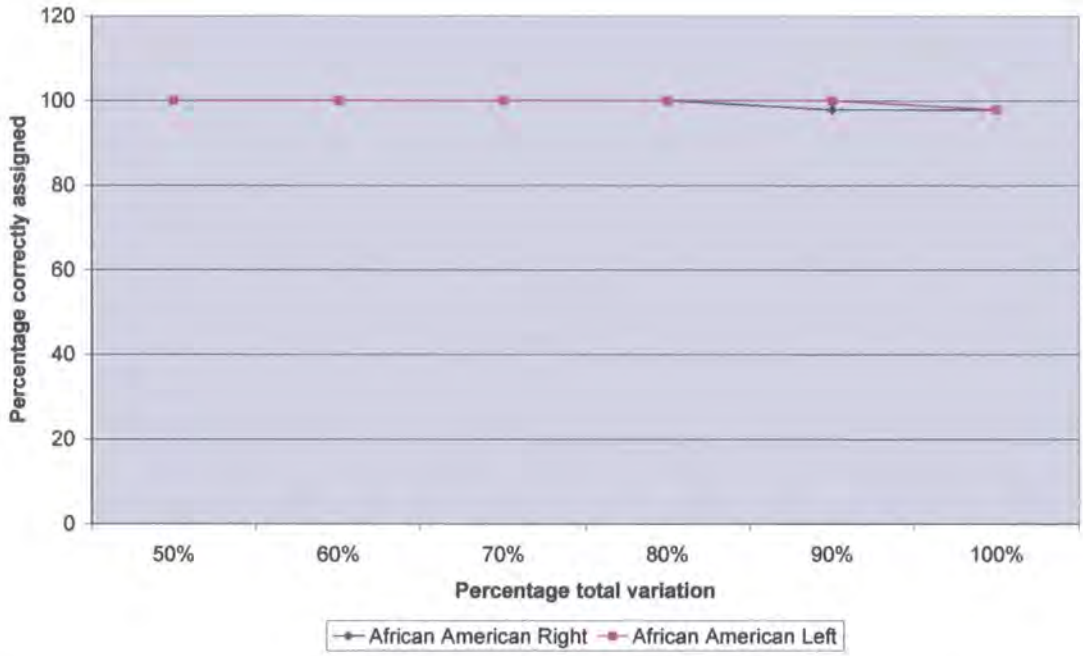

Figure 3.1: Asymmetry in the femur of African Americans. Summary of separate discriminant analyses and cross-validation analyses using the PC scores accounting for c.50% of total variance (PCs 1-8), c.60% (PCs 1-10), c.70% (PCs 1-14), c.80% (PCs 1-19), c.90% (PCs 1-28) and 100% (PCs 1-71).

Using cross-validation analysis, the separation of African American right and left specimens using the scores of each individual on the resultant PCs shows that 100% of right and left specimens are correctly assigned to group.

An alternative analysis of morphological differences between right and left distal femora for the African American sample is carried out using EDMA (see section 3.3 above). Table 3.12 shows the results generated by EDMA comparing the two datasets with right specimens as the numerator sample and left specimens as the denominator sample. T_{obs} indicates a difference in form at a high level of statistical significance between the two samples (p= 0.004). As the difference in centroid size between the two samples is negligible (30.674mm for the right, 30.492mm for the left) with a ratio of left to right samples at 0.994, virtually all morphological differences can be attributable to shape alone.

Femur	Measurements generated by EDMA	Results
African Americans Form	T_{obs} statistic	1.493
	p value	**0.004**
African Americans Shape	*Z* statistic upper-lower	0.128 0.158 to -0.159
	Sneath scaling centroid Rt	30.674
	Sneath scaling centroid Lt	30.492
	Scaling difference	0.182
	Ratio of Lt centroid to Rt centroid	0.994
	Total number of *ilds* in sample	325
	Number of *ilds* not different after scaling with 90% confidence	204
	Number of *ilds* different after scaling with 90% confidence	121
	% of *ilds* different with 90% confidence	37.23%

Table 3.12: Results generated by EDMA for analyses of asymmetry in form and shape of the distal femur of African Americans. For abbreviations and interpretation of statistics, see Chapter 2 section 2.2.3b

Results produced by EDMA for the distal femur therefore indicate highly significant differences in shape between specimens of the right and left sides, thus reinforcing results produced by the superimposition methods using GPA in the *morphologika*© programme.

34.3a(ii) Femur: Description of differences in shape between right and left sides

Using PCs accounting for the initial c.80% of total variance within the sample (PCs 1 to 20), only PCs 1 and 5 separate the right and left sides significantly. Using the Student's t-test, PC1 significantly separates right and left specimens at t= 17.65, $p<0.0001$, and PC5 at t= 2.45, $p= 0.02$. Together, PCs 1 and 5 account for a total of 16.62% of total variance and significantly separate right and left specimens at t= 10.50, $p<0.0001$.

Figure 3.2 shows an almost complete separation of specimens on PC1 with all right sided specimens in the negative section of the scale and all left specimens in the centre and towards the positive section. PC1 explains a difference in the orientation of the condyles relative to the patella articular surface, although such differences are particularly noticeable across the lateral condyle. For left sided specimens, the condyles project further in an inferior direction relative to the position of the condyles in right sided specimens. This is exemplified in the positions of landmarks 17 and 23 relative to landmarks 25 and 26. Figure 3.2 shows this difference in the mean configuration in the distal plane but is further clarified by the images in Figure 3.3 shown in the lateral plane. This relative difference between sides is further demonstrated in Figure 3.4. These figures show the morphological differences between the right and left means displaying the maximum deformation of the TPS over both condyles but with particular emphasis over the lateral condyle, in (a) the anteroposterior plane and (b) the distal plane. The difference in position of the condyles between sides appears to have repercussions for the orientation of the knee joint relative to the shaft, such that in right sided specimens the angle between joint and shaft is more acute relative to left sided specimens.

Figure 3.2:

Asymmetry in African American femur, total sample. Bivariate plot of PC1 with PC5 showing a separation of right and left sided specimens. Images represent the mean configuration if warped to the extremes of PC1 (at 0.09 and -0.06) and PC5 (at 0.06 and -0.06). The larger image at the positive extreme of PC5 highlights landmarks discussed in the text (section 3.4.3a(ii)).

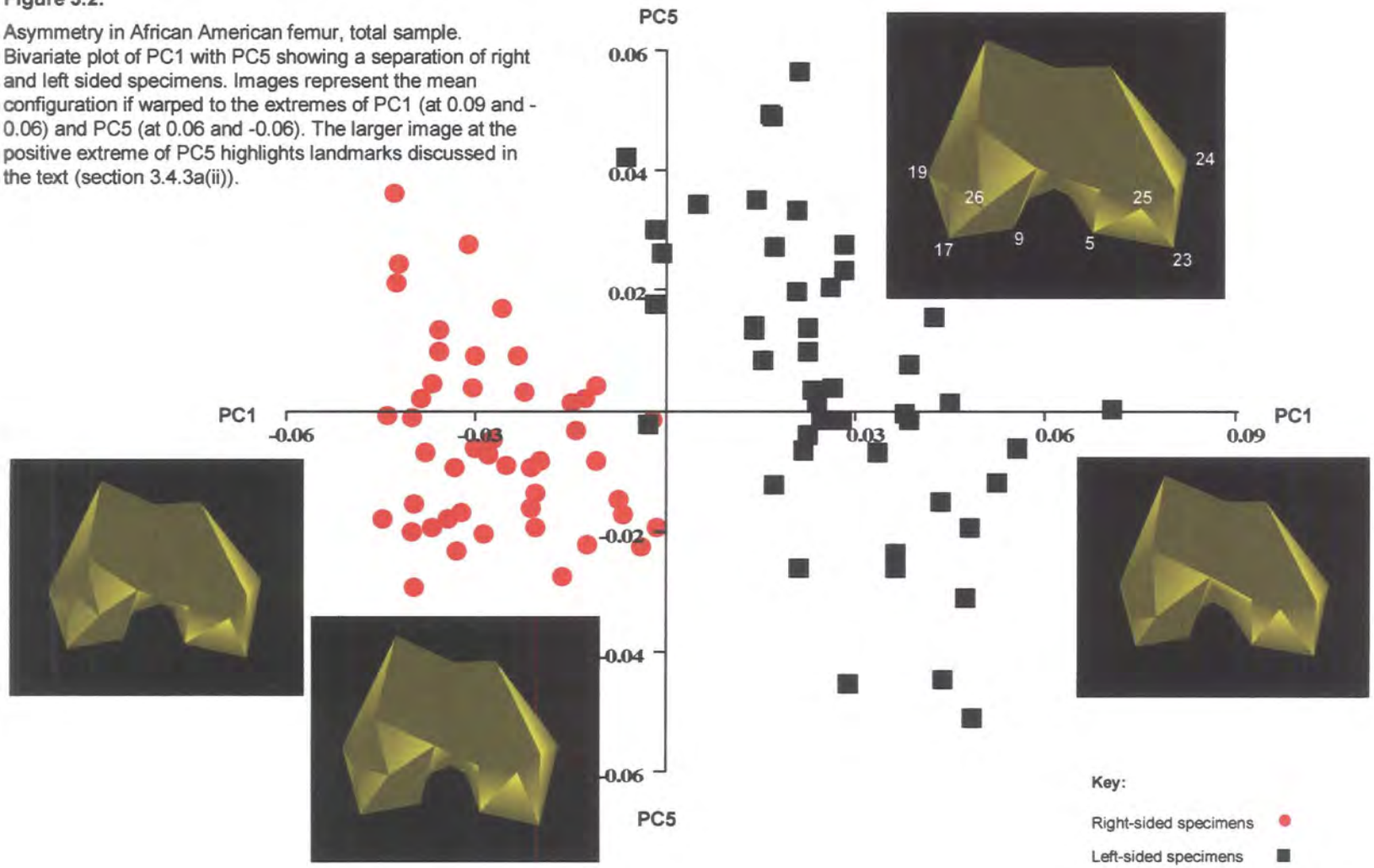

Figure 3.3:

Asymmetry in African American femur, total sample. Bivariate plot of PC1 with PC5 showing a separation of right and left sided specimens. Images represent the mean configuration if warped to the extremes of PC1 (at 0.09 and -0.06) and PC5 (at 0.06 and -0.06). The larger image includes landmarks discussed in the text (section 3.4.3a(ii))

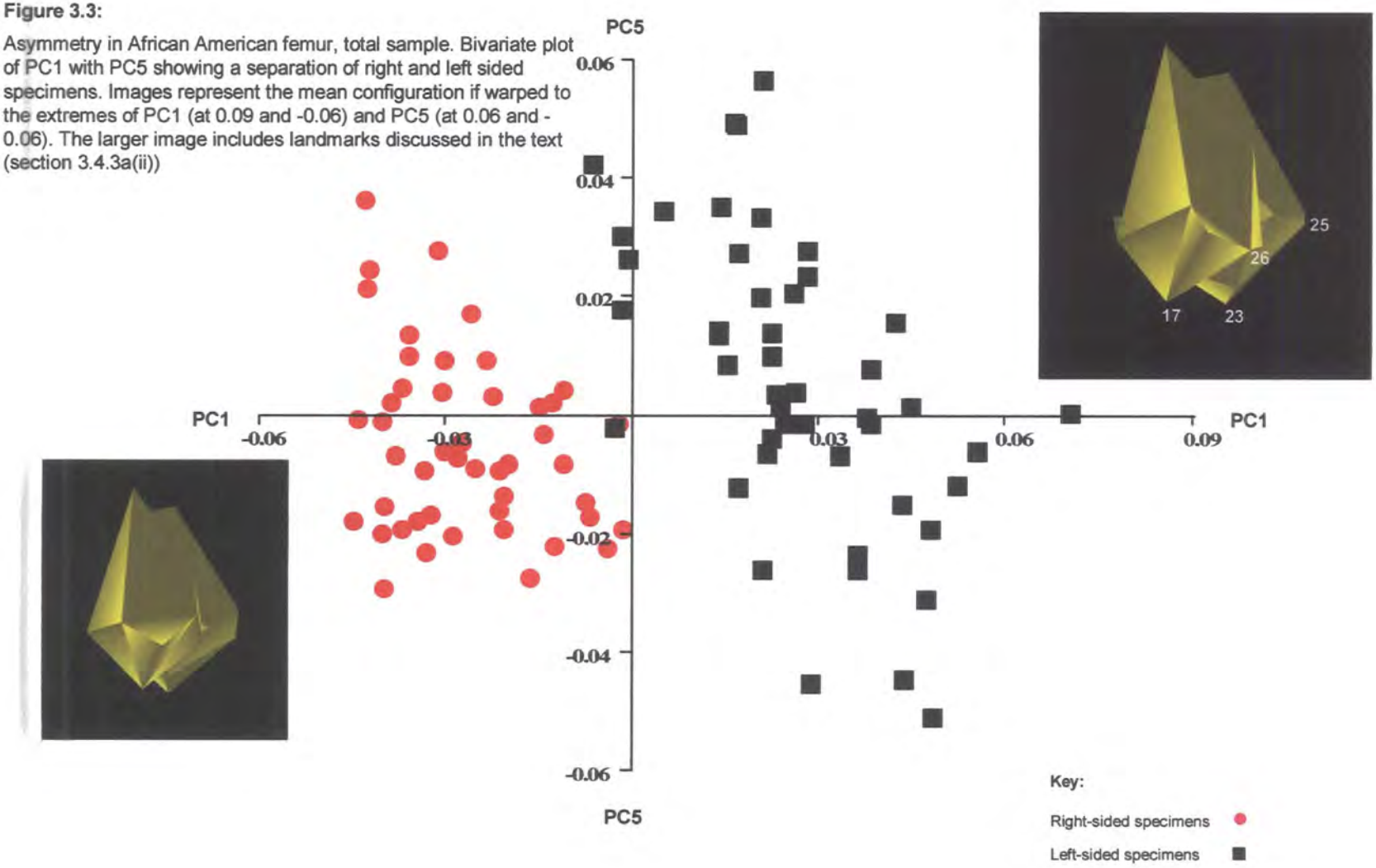

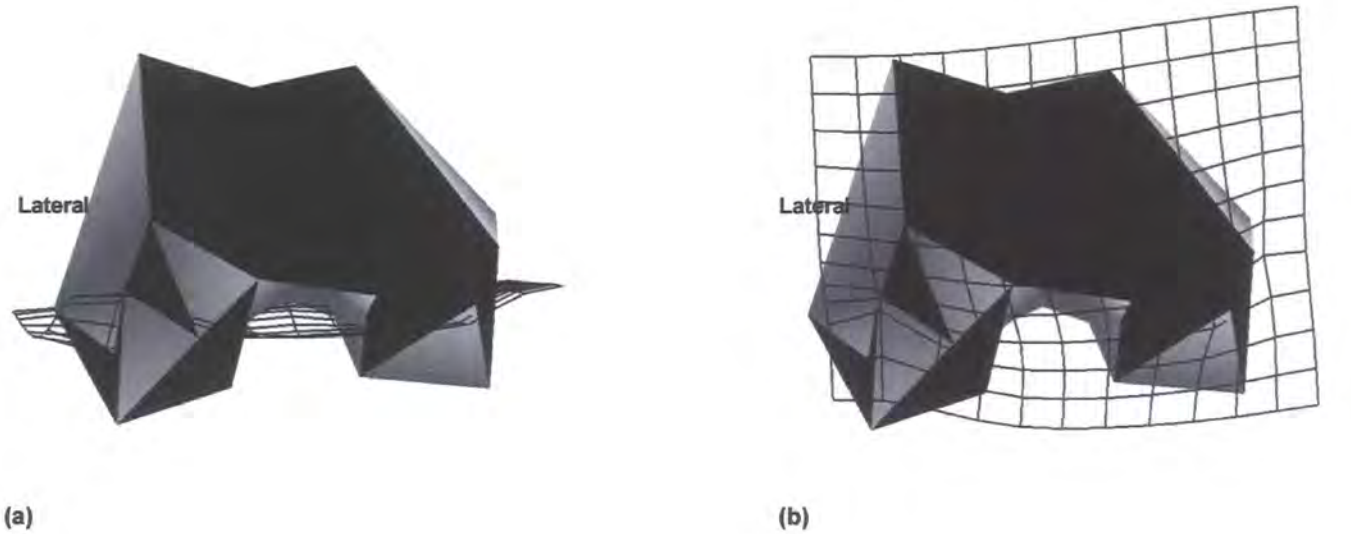

Figure 3.4: Asymmetry in African American femur with sexes pooled: Representations of femoral shape with TPS taken from PC1 using sample means, showing regions of bone giving maximum difference in shape between the right and left samples. (a) represents TPS view in the anterior-posterior plane; (b) in the distal plane. Images are presented to give the best indication of maximum difference in shape and are not necessarily taken from the same perspective as the mean configurations in Figure 3.2.

Although there is a difference between right and left sided specimens at a statistically significant level on PC5, Figure 3.2 shows a complete overlap of right and left specimens along this scale; probably due to the difficulties of representing complex three-dimensional data in two dimensions. Variation on PC5 explains overall mediolateral width between landmarks 19 and 24 and particularly across the condyles (landmarks 17 to 23) and the intercondylar fossa (landmarks 5 to 9). Because of the overlap of specimens, it is therefore difficult to determine specific shape differences between sides on PC5.

3.4.3b(i) Tibia: African Americans using the total sample

Differences in shape of the left and right proximal tibiae from 49 individuals are analysed using the Procrustes fitted co-ordinates and by subjecting the data to PCA. Table 3.13 gives the proportional and accumulated variance for PCs 1 to 56, which represents the total variance within the sample. The scores for each specimen on the resultant PCs are then subjected to canonical discriminant analysis to establish the degree of difference between right and left samples based upon the Mahalanobis' squared distances between sample means.

For the tibia, the best separation of sides is achieved using 90% of total variance. This assessment was reached after separate discriminant and cross-validation analyses were carried out using the PC scores accounting for between c.50% to 100% of total variance. Results are summarised in Figure 3.5.

The Mahalanobis' squared distance generated by discriminant analysis between the means of right and left samples is 12.66 and statistically significant at $p= 0.001$, indicating that the two sides can be separated on some aspect of shape of the proximal tibia. Using cross-validation analysis, the separation of African American right and left specimens using the scores of each individual on the resultant PCs shows that 93.88% of right sided specimens and 85.71% of left sided specimens are correctly assigned to group.

PCs	Prop.	Cumul.	PCs	Prop.	Cumul.	PCs	Prop.	Cumul.
PC1	20.20	20.20	PC21	1.15	86.80	PC41	0.26	98.30
PC2	8.45	28.60	PC22	1.02	87.90	PC42	0.22	98.50
PC3	7.85	36.50	PC23	0.97	88.80	PC43	0.20	98.70
PC4	6.64	43.10	PC24	0.94	89.80	PC44	0.19	98.90
PC5	4.90	48.00	PC25	0.89	90.70	PC45	0.16	99.10
PC6	4.49	52.50	PC26	0.80	91.50	PC46	0.15	99.20
PC7	4.33	56.80	PC27	0.77	92.20	PC47	0.13	99.30
PC8	3.97	60.80	PC28	0.64	92.90	PC48	0.13	99.50
PC9	3.38	64.20	PC29	0.61	93.50	PC49	0.11	99.60
PC10	3.12	67.30	PC30	0.59	94.10	PC50	0.09	99.70
PC11	2.83	70.20	PC31	0.57	94.60	PC51	0.08	99.70
PC12	2.46	72.60	PC32	0.53	95.20	PC52	0.07	99.80
PC13	2.13	74.70	PC33	0.50	95.70	PC53	0.06	99.90
PC14	2.02	76.80	PC34	0.44	96.10	PC54	0.05	99.90
PC15	1.89	78.70	PC35	0.37	96.50	PC55	0.04	100.00
PC16	1.58	80.20	PC36	0.36	96.80	PC56	0.04	100.00
PC17	1.48	81.70	PC37	0.33	97.20			
PC18	1.39	83.10	PC38	0.30	97.50			
PC19	1.31	84.40	PC39	0.30	97.80			
PC20	1.28	85.70	PC40	0.27	98.00			

Table 3.13: Asymmetry in the tibia of African Americans. The proportion and accumulated variance for PCs 1-56, which accounts for 100% of total variance

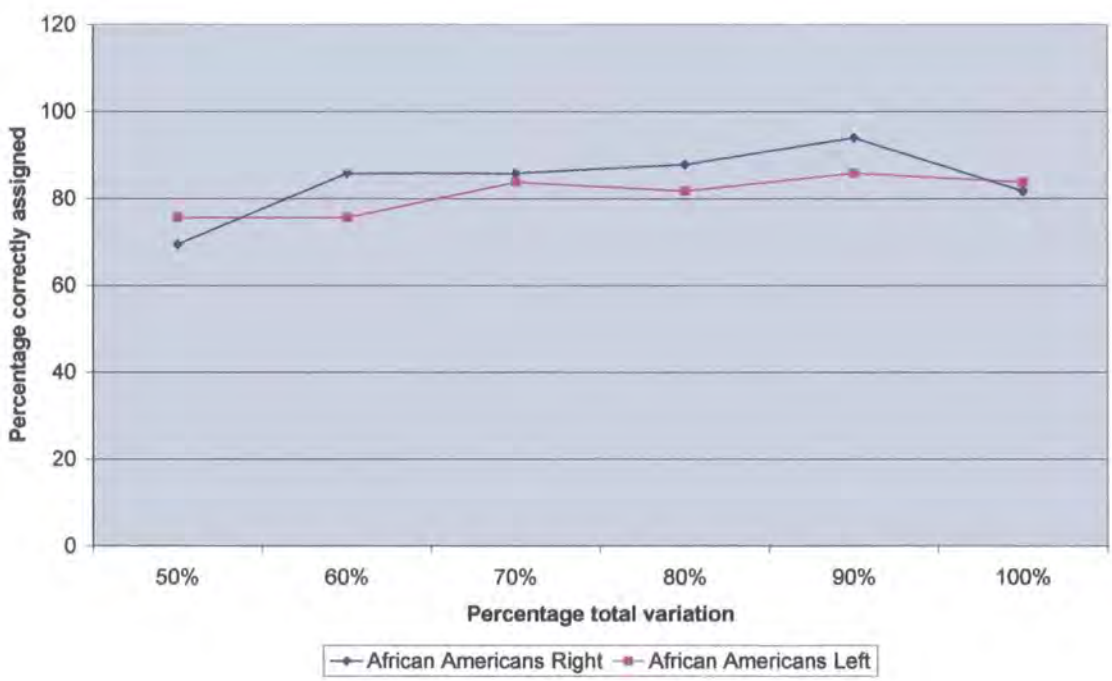

Figure 3.5: Asymmetry in the tibia of African Americans. Summary of separate discriminant analyses and cross-validation analyses using the PC scores accounting for c.50% of total variance (PCs 1-5), c.60% (PCs 1-8), c.70% (PCs 1-11), c.80% (PCs 1-16), c.90% (PCs 1-24) and 100% (PCs 1-56).

An alternative analysis of morphological differences between right and left distal femora for the African American sample is carried out using EDMA (see section 3.3 above).

Table 3.14 shows the results generated by EDMA comparing the two datasets with right specimens as the numerator sample and left specimens as the denominator sample. T_{obs} indicates a difference in form at a high level of statistical significance between the two samples (p= 0.001). As the difference in centroid size between the two samples is negligible (29.287mm for the right, 29.157mm for the left) with a ratio of left to right samples at 0.995, virtually all morphological differences can be attributable to shape alone.

Results produced by EDMA for the proximal tibia therefore indicate highly significant differences in shape between specimens of the right and left sides, thus reinforcing results produced by the superimposition methods using GPA in the *morphologika*© programme.

3.4.3b(ii) Tibia: Description of differences in shape between right and left sides

Using the initial c.90% of total variance within the sample (PCs 1 to 24), only PCs 3, 5, 7 and 12 separate the right and left sides at a level of statistical significance. Using the Student's t-test, PC3 significantly separates right and left specimens at t= 6.62, p<0.0001; PC5 at t= 2.60, p= 0.01; PC7 at t= 3.30, p= 0.001 and PC12 at t=2.29, p= 0.02. Collectively, PCs 3, 5, 7 and 12 account for a total of 19.54% of total variance and significantly separate right and left specimens at t= 2.51; p= 0.01.

PC3 primarily explains a difference between right and left sided specimens in the orientation of the proximal tibiae relative to the diaphyses. Figure 3.6 shows more left sided specimens concentrated towards the positive section of the scale and right sided specimens concentrated in the negative section, although there is considerable overlap between sides. Whilst the relative positions of the intercondylar tubercles (landmarks 1 and 8) appear to remain relatively unchanged as the mean configuration is morphed along PC3, the tibial plateau is seen to be rotated more to the medial side in right compared to left sided specimens.

Tibia	Measurements generated by EDMA	Results
African Americans Form	T_{obs} statistic	1.316
	p value	**0.001**
African Americans Shape	*Z* statistic upper-lower	0.080 0.098 to -0.109
	Sneath scaling centroid Rt	29.287
	Sneath scaling centroid Lt	29.157
	Scaling difference	0.130
	Ratio of Lt centroid to Rt centroid	0.996
	Total number of *ilds* in sample	210
	Number of *ilds* not different after scaling with 90% confidence	71
	Number of *ilds* different after scaling with 90% confidence	139
	% of *ilds* different with 90% confidence	66.19%

Table 3.14: Results generated by EDMA for analyses of asymmetry in form and shape of the proximal tibia of African Americans For abbreviations and interpretation of statistics, see Chapter 2 section 2.2.3b

Figure 3.6:

Asymmetry in African American tibia, total sample. Bivariate plot of PC3 with PC5 showing a separation of right and left sided specimens. Images represent the mean configuration if warped to the extremes of PC3 (at 0.06 and -0.12) and PC5 (at 0.06 and -0.06).

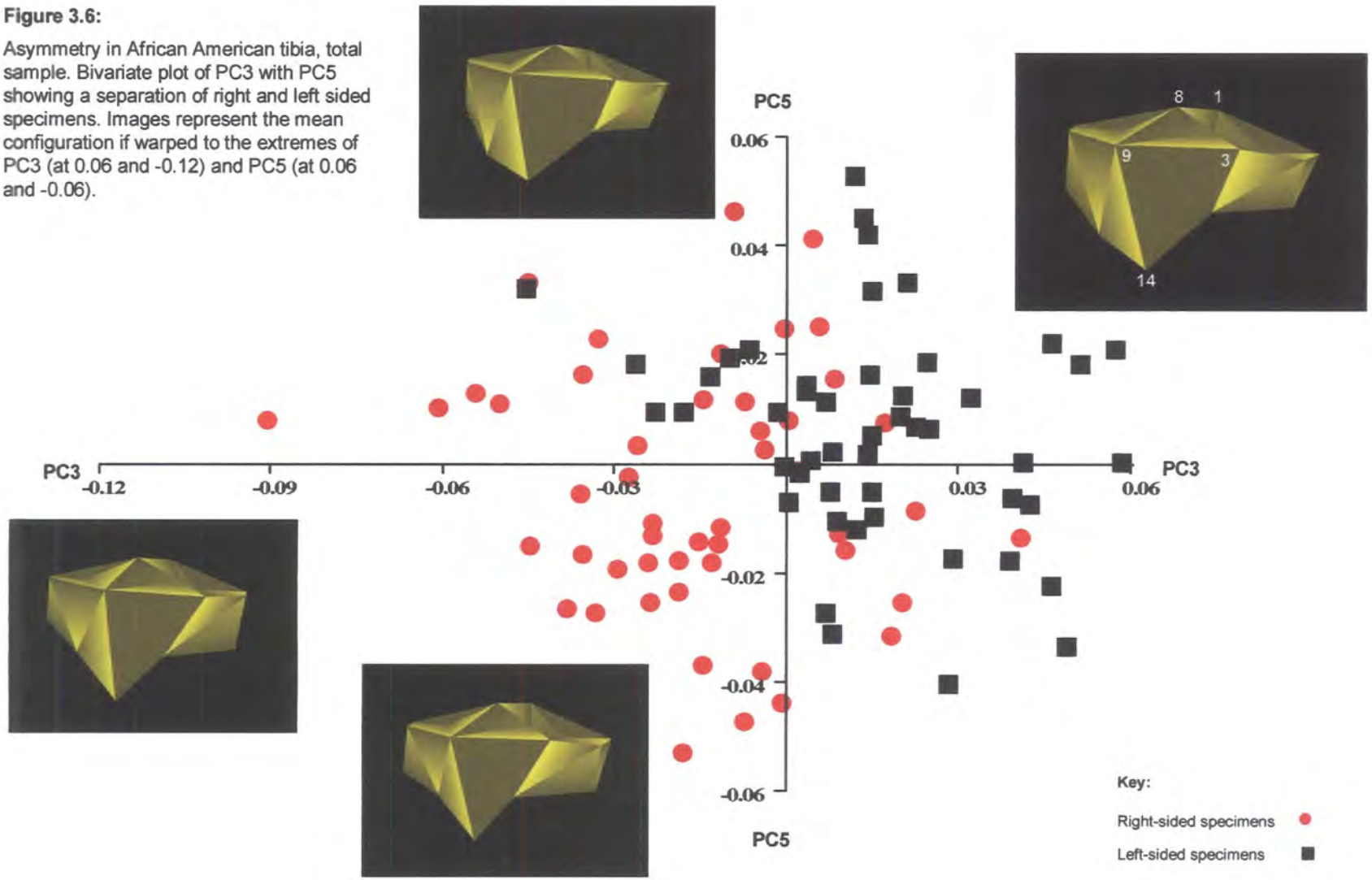

This is seen clearly in the relative position of landmarks 9 and 3 at the anterior edge of the tibial plateau, relative to landmark 14 at the inferior end of the tibial tuberosity. The deformation of the TPS seen in Figure 3.7 for PC3 highlights the differences across the anterior section, noted in Figure 3.6.

Although Figure 3.6 shows considerable overlap of right and left specimens on PC5, results show a statistically significant difference in shape between sides for this PC at $p= 0.01$. The mean configuration shows differences in the relative projection of the tibial shelf, particularly on the lateral side, when morphed along PC5. This is more clearly shown in the relative position of landmark 15 on the lateral side of the tibial tuberosity (compared to both landmarks 9 and 14), in that it is positioned further anteriorly for specimens at the positive end of the scale relative to those at the negative extreme. A slightly higher proportion of right sided specimens are concentrated at the negative extreme and vice versa. Differences explained by PC5 can be clearly seen in Figure 3.7 showing the maximum deformation of the TPS in the lateral side of the anterior region around landmark 15.

PCs 7 and 12 are the two remaining PCs that show a statistically significant difference between sides within the initial 90% of total variance. As shown in Figure 3.8, however, the overlap of right and left specimens on both PC7 and PC12 is extensive and morphological differences between sides are therefore difficult to interpret. PC7 primarily explains differences in the proportions of the tibial shelf. The mean configuration shows increasing depth of the shelf in specimens towards the negative extreme relative to those at the positive extreme. Differences are exemplified in the distances between landmarks 5 and 6 (edge of the tibial plateau; medial) and 21 (posterior; medial) and landmarks 3 (edge of the tibial plateau; anterior) and 15 (anterior region; medial). On the lateral side, differences are noted in the change in distance between landmarks 9 (edge of the tibial plateau; anterior) and 16 (anterior). Greater visibility of landmark 20 (posterior) also shows this relative difference in proportions. PC12 appears to reflect similar differences to those explained by PC7. Despite the high degree of overlap of specimens on PC7, a slightly higher proportion of left sided specimens are positioned towards the negative extreme. For PC12, however, any concentration of specimens of either side towards one extreme appears marginal in the two-dimensional graph.

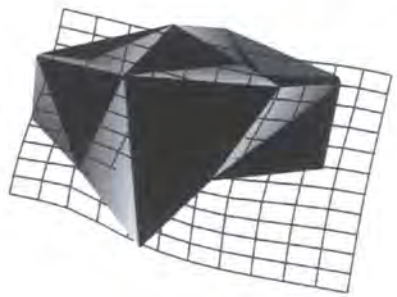

(a): PC3

(b): PC3

(c): PC5

(d): PC5

Figure 3.7: Asymmetry in African American tibia with sexes pooled. Representations of tibial shape with TPS taken from PC3 and PC5 using sample means, showing regions of bone giving maximum difference in shape between the right and left samples. (a) and (c) represent TPS in the transverse plane; (b) and (d) in the proximal plane. Images are presented in to give the best indication of maximum difference in shape and are not necessarily taken from the same perspective as the mean configurations in Figure 3.6.

Figure 3.8:

Asymmetry in African American tibia, total sample). Bivariate plot showing the positions of right and left sided specimens on PC7 and PC12. Images represent the mean configuration if warped to the extremes of PC7 (at 0.06 and -0.06) and PC12 (at 0.04 and -0.04). The larger image at the positive extreme of PC7 highlights landmarks discussed in the text (section 3.4.3b(ii)).

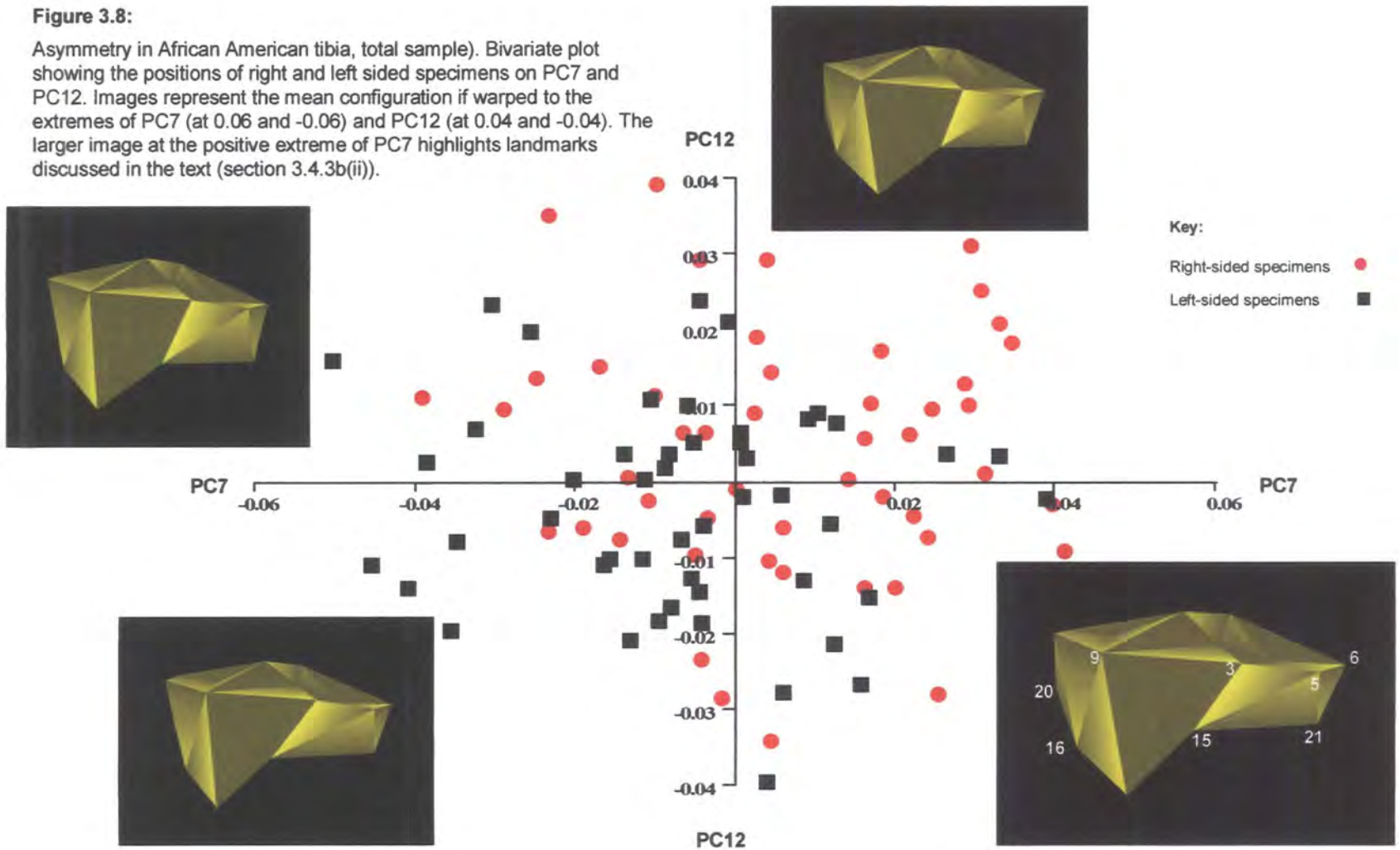

Figure 3.9 summarises where the maximum differences between right and left sides lie by using the right and left sample means. With only two means, the single resultant PC explains all of total variance between sample means and emphasises the two aspects of difference highlighted by PC3 and PC5 in Figure 3.6, i.e., differences in the angle created by the joint relative to the diaphysis, with the greatest effect seen in the anterior region, particularly over the lateral side. Although these differences appear subtle, they can be seen in the differences in the mean configurations in Figure 3.9, in the relative positions of landmarks 14 (anterior) and 20 and of 11 and 12 (edge of the tibial plateau; lateral) and 20, when the image is presented in the frontal plane.

To summarise, asymmetry in the knee joint for both femur and tibia primarily appears to relate to the angle created by the joint relative to the diaphysis. In the femur, this difference in angle appears to be either caused by or itself causes a change in the angle of the condyles relative to the patella articular surface. Whilst asymmetric differences affect both medial and lateral sides of both femur and tibia, maximum difference is concentrated in the lateral side of the joint.

3.4.4 Asymmetry of shape of the knee joint of five populations

3.4.4a(i) Femur: Analyses using the total sample

Differences in shape of the 338 specimens are analysed using the Procrustes fitted co-ordinates and by subjecting the data to PCA. Table 3.15 gives the proportional and accumulated variance for PCs 1 to 71, which represents the total variance within the sample. The scores for each specimen on the resultant PCs are then subjected to canonical discriminant analysis to establish the relationships between populations based upon the Mahalanobis' squared distances between population means. For the femur, the best separation of samples of right and left sides for the five populations is achieved using 90% of total variance. This assessment was reached after separate discriminant and cross-validation analyses were carried out using the PC scores accounting for between c.50% to 100% of total variance. Results are summarised in Figure 3.10.

Figure 3.9:

Asymmetry in African American tibia, means. Separation of right and left means of African Americans on PC1. Images represent the mean configuration if warped to the extremes of PC1 (at 0.02 and -0.02). Image at the positive extreme shows landmarks discussed in the text (section 3.4.3b(ii)).

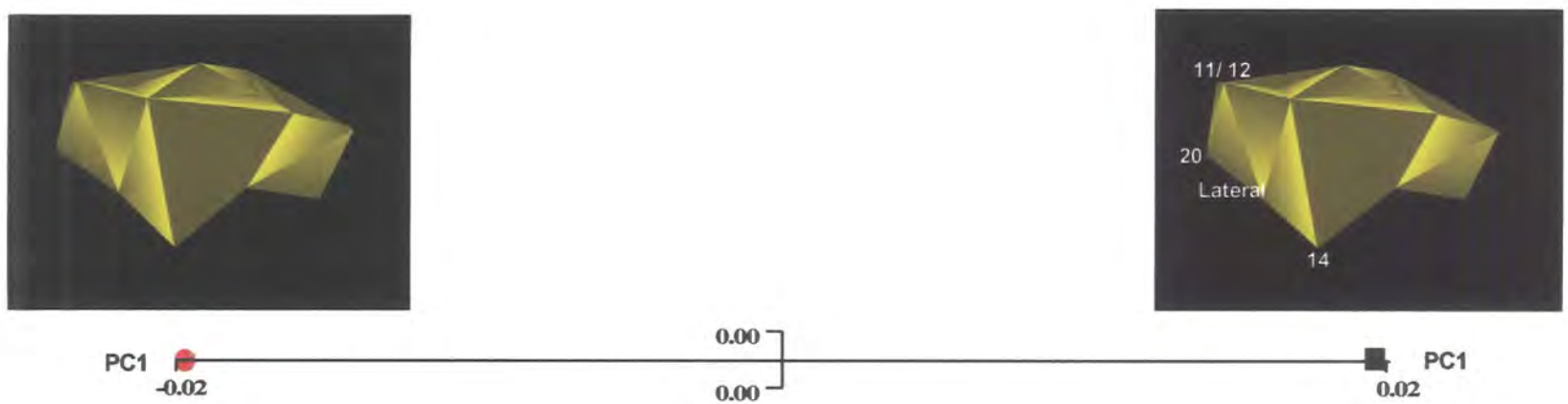

Key:

African Americans Right Mean ●

African Americans Left Mean ■

PCs	Prop.	Cumul.	PCs	Prop.	Cumul.	PCs	Prop.	Cumul.
PC1	9.01	9.0	PC26	1.16	80.9	PC51	0.33	96.4
PC2	6.63	15.6	PC27	1.11	82.0	PC52	0.31	96.8
PC3	6.06	21.7	PC28	0.98	83.0	PC53	0.28	97.0
PC4	5.30	27.0	PC29	0.93	83.9	PC54	0.27	97.3
PC5	5.19	32.2	PC30	0.91	84.8	PC55	0.26	97.6
PC6	4.08	36.3	PC31	0.85	85.7	PC56	0.23	97.8
PC7	4.00	40.3	PC32	0.79	86.5	PC57	0.22	98.0
PC8	3.72	44.0	PC33	0.78	87.2	PC58	0.21	98.2
PC9	3.37	47.3	PC34	0.77	88.0	PC59	0.20	98.4
PC10	3.19	50.5	PC35	0.72	88.7	PC60	0.19	98.6
PC11	3.14	53.7	PC36	0.70	89.4	PC61	0.17	98.8
PC12	2.99	56.7	PC37	0.66	90.1	PC62	0.17	99.0
PC13	2.60	59.3	PC38	0.63	90.7	PC63	0.15	99.1
PC14	2.46	61.7	PC39	0.58	91.3	PC64	0.15	99.3
PC15	2.27	64.0	PC40	0.57	91.9	PC65	0.14	99.4
PC16	1.97	66.0	PC41	0.54	92.4	PC66	0.13	99.5
PC17	1.88	67.8	PC42	0.50	92.9	PC67	0.11	99.7
PC18	1.84	69.7	PC43	0.49	93.4	PC68	0.10	99.7
PC19	1.69	71.4	PC44	0.46	93.8	PC69	0.09	99.8
PC20	1.62	73.0	PC45	0.43	94.3	PC70	0.08	99.9
PC21	1.54	74.5	PC46	0.40	94.7	PC71	0.08	100.0
PC22	1.43	76.0	PC47	0.39	95.1			
PC23	1.31	77.3	PC48	0.37	95.4			
PC24	1.27	78.6	PC49	0.35	95.8			
PC25	1.18	79.7	PC50	0.34	96.1			

Table 3.15: Asymmetry in the femur in 5 populations. The proportion and accumulated variance for PCs 1-71, which accounts for 100% of total variance

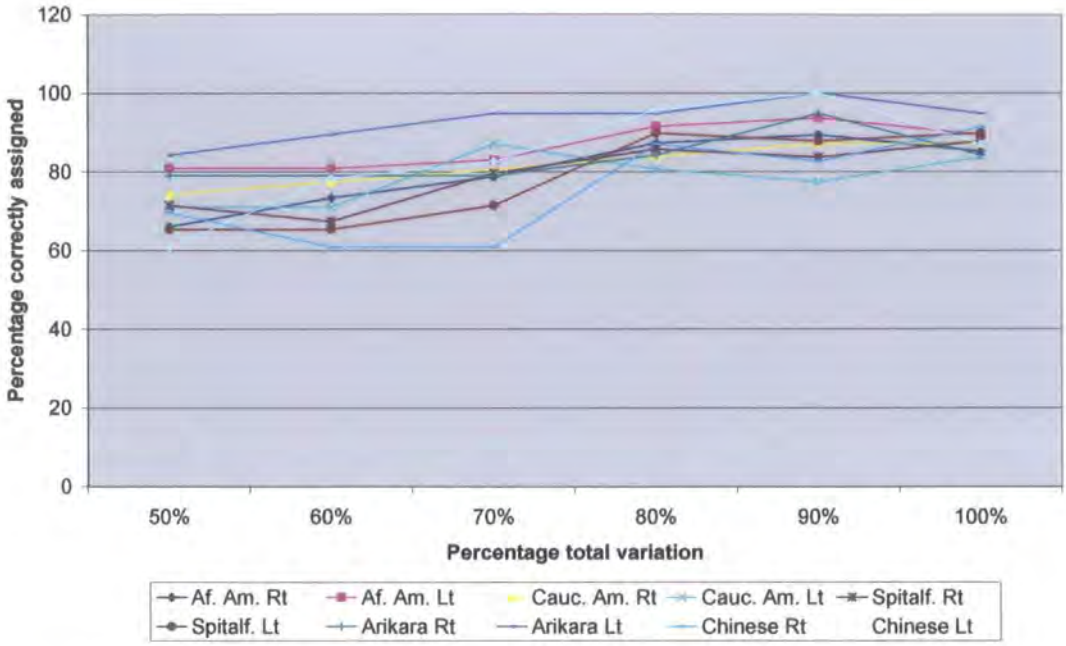

Figure 3.10: Asymmetry in the femur of 5 Populations. Summary of separate discriminant and cross-validation analyses were carried out using PCs accounting for c.50% of total variance (PCs 1-10), 60% (PCs 1-13), 70% (PCs 1-18), 80% (PCs 1-25), 90% (PCs 1-37) and 100% (PCs 1-71).

The Mahalanobis' squared distances between right and left sample means, generated by discriminant analysis are shown in Table 3.16. All distances between samples are at a high level of statistical significance, indicating that right and left groups can be separated on some aspect of shape of the distal femur. Table 3.17 illustrates the relationship of each sample to all others on the basis of the generated Mahalanobis' squared distances by showing the distance of each primary sample to all others and ranking them accordingly from the closest sample (at position 1) to the most distant (at position 9).

With the exception of the left Spitalfields sample, in each case the closest sample in shape is of the same side from another population, before the matching joint from the same population. In addition, with the exception of the two Spitalfields groups, samples from the other four populations are closest in shape to *all* other samples from the same side but different populations before any other sample of the opposite side, including the matching joint from their own population. It is apparent from Tables 3.16 and 3.17 that the Caucasian American samples shows the greatest degree

African Am.	0									
Right	1.000									
African Am.	36.59	0								
Left	0.0001	1.000								
Ca. Am.	18.95	55.67	0							
Right	0.0001	0.0001	1.000							
Ca. Am.	56.32	23.01	67.54	0						
Left	0.0001	0.0001	0.0001	1.000						
Spitalfields	17.87	37.92	40.63	47.67	0					
Right	0.0001	0.0001	0.0001	0.0001	1.000					
Spitalfields	37.61	18.81	55.34	24.60	18.74	0				
Left	0.0001	0.0001	0.0001	0.0001	0.0001	1.000				
Arikara	23.50	67.01	27.28	73.44	39.45	64.78	0			
Right	0.0001	0.0001	0.0001	0.0001	0.0001	0.0001	1.000			
Arikara	59.24	27.94	62.55	20.71	54.18	39.53	48.10	0		
Left	0.0001	0.0001	0.0001	0.0001	0.0001	0.0001	0.0001	1.000		
Chinese	17.88	50.59	27.48	55.58	26.45	45.90	12.72	46.33	0	
Right	0.0001	0.0001	0.0001	0.0001	0.0001	0.0001	0.0001	0.0001	1.000	
Chinese	54.95	20.61	67.15	17.90	45.54	27.63	62.57	14.58	37.41	0
Left	0.0001	0.0001	0.0001	0.0001	0.0001	0.0001	0.0001	0.0001	0.0001	1.000
	Af. Am. Right	**Af. Am. Left**	**Ca. Am. Right**	**Ca. Am. Left**	**Spitalf. Right**	**Spitalf. Left**	**Arikara Right**	**Arikara Left**	**Chinese Right**	**Chinese Left**

Table 3.16: Asymmetry in femur of 5 populations. Results from the canonical discriminant analysis of right and left groups from 5 populations, on the basis of 90% total variance. The upper value in red gives the Mahalanobis' squared distance between groups, lower value in black gives the Hotelling's t^2 *p*-value.

Group	1	2	3	4	5	6	7	8	9
African Am. Rt	Sp Rt	Ch Rt	CA Rt	SD Rt	AA Lt	Sp Lt	Ch Lt	CA Lt	SD Lt
African Am. Lt	Sp Lt	Ch Lt	CA Lt	SD Lt	AA Rt	Sp Rt	Ch Rt	CA Rt	SD Rt
Cauc. Am. Rt	AA Rt	SD Rt	Ch Rt	Sp Rt	Sp Lt	AA LT	SD Lt	Ch Lt	CA Lt
Cauc. Am. Lt	Ch Lt	SD Lt	AA Lt	Sp Lt	Sp Rt	Ch Rt	AA Rt	CA Rt	SD Rt
Spitalfields Rt	AA Rt	Sp Lt	Ch Rt	AA Lt	SD Rt	CA Rt	Ch Lt	CA Lt	Sd Lt
Spitalfields Lt	Sp Rt	AA Lt	CA Lt	Ch Lt	AA Rt	SD Lt	Ch Rt	CA Rt	SD Rt
Arikara Rt	Ch Rt	AA Rt	CA Rt	Sp Rt	SD Lt	Ch Lt	Sp Lt	AA Lt	CA Lt
Arikara Lt	Ch Lt	CA Lt	AA Lt	Sp Lt	Ch Rt	SD Rt	Sp Rt	AA Rt	CA Rt
Chinese Rt	SD Rt	AA Rt	Sp Rt	CA Rt	Ch Lt	Sp Lt	Sd Lt	AA Lt	CA Lt
Chinese Lt	SD Lt	CA Lt	AA Lt	Sp Lt	Ch Rt	Sp Rt	AA Rt	SD Rt	CA Rt

Table 3.17: Asymmetry in the femur in 5 populations. The order of proximity in distance of each primary right and left group from the other groups of the 5 populations, on the basis of their Mahalanobis squared distances, as shown in Table 3.16.

of asymmetry, with the Spitalfields samples showing the least degree of asymmetry of the five populations.

Table 3.18 shows the results of cross-validation analysis using 90% of total variance for the ten samples. Samples correctly assigned to groups range from 77.42% for Caucasian Americans (left side) to 100% for the Arikara (left side) and Chinese (left side), indicating that the shape of the distal femur is specific to each right and left sample.

3.4.4a(ii) Femur: Analyses using sample means

Because of the high degree of overlap on the bivariate plots of selected PCs when using all specimens in the data set (see section 3.4.4a above), the population means are used to help determine the specific morphologies of each right and left sample and to explore the relationships between them.

Number of Observations and Percent Classified into Group											
From Group	African Am. Right	African Am. Left	Caucasian Am. Right	Caucasian Am. Left	Spitalf. Right	Spitalf. Left	Arikara Right	Arikara Left	Chinese Right	Chinese Left	Total
African Am. Right	42 89.36	0 0	0 0	0 0	2 4.26	0 0	1 2.13	0 0	2 4.26	0 0	47 100
African Am. Left	0 0	44 93.62	0 0	0 0	0 0	1 2.13	0 0	1 2.13	0 0	1 2.13	47 100
Cauc. Am. Right	1 3.23	0 0	27 87.1	0 0	0 0	0 0	2 6.45	0 0	1 3.23	0 0	31 100
Cauc. Am. Left	0 0	2 6.45	0 0	24 77.42	0 0	2 6.45	0 0	0 0	0 0	3 9.68	31 100
Spitalfields Right	2 4.08	0 0	0 0	0 0	41 83.67	4 8.16	0 0	0 0	2 4.08	0 0	49 100
Spitalfields Left	1 2.04	3 6.12	0 0	1 2.04	1 2.04	43 87.76	0 0	0 0	0 0	0 0	49 100
Arikara Right	0 0	0 0	1 5.26	0 0	0 0	0 0	18 94.74	0 0	0 0	0 0	19 100
Arikara Left	0 0	0 0	0 0	0 0	0 0	0 0	0 0	19 100	0 0	0 0	19 100
Chinese Right	2 8.7	0 0	0 0	0 0	0 0	0 0	2 8.7	0 0	19 82.61	0 0	23 100
Chinese Left	0 0	0 0	0 0	0 0	0 0	0 0	0 0	0 0	0 0	23 100	23 100
Total	48 14.2	49 14.5	28 8.28	25 7.4	44 13.02	50 14.79	23 6.8	20 5.92	24 7.1	27 7.99	338 100

Table 3.18: Separation of right and left femora from 5 populations using 90% total variation selected by cross-validation analysis. Upper figure denotes number of individuals; lower figure denotes percentage. Red figures denote number of individuals placed into their correct group.

For the femur, there is a correlation at a high level of statistical significance between the Procrustes distances between sample means (Table 3.19) and the Mahalanobis' squared distances in Table 3.16 (r=0.77; p <0.0001) indicating that similar shape relationships are represented by both datasets. The Procrustes mean co-ordinates have been calculated from separate GPAs of each population's right and left samples and these have then been subjected to a joint GPA and PCA. The proportion and accumulated variance of the PCs generated in the analysis of population means is given in Table 3.20:

PCs	Proportion	Cumulative	PCs	Proportion	Cumulative
PC1	30.7	30.7	PC6	4.64	94.1
PC2	27.8	58.4	PC7	3.48	97.5
PC3	13.6	72.0	PC8	1.73	99.3
PC4	8.85	80.8	PC9	0.73	100.0
PC5	8.58	89.4			

Table 3.20: Proportion and accumulative variance represented by PCs 1-9 for the femur which accounts for total sample variance for population means.

The first four PCs account for over 80% of total variance in the sample and the exploration of shape differences between sides will concentrate on these four PCs.

Figure 3.11 shows the location of the ten means relative to each other on PC1 and PC2, which cumulatively account for 58.4% of total variance. Figures 3.12 and 3.13 show the mean configuration warped to the extremes of PC1 and PC2, respectively. On PC1, means from the same population are placed relatively adjacent to one another. In four of the five pairs of means from each population, the right sided mean is placed more positively than the left. For the fifth pair of means, the Arikara, the left mean is placed more positively than the right. Having described the detailed nature of morphological differences between right and left sides in the analysis of the African American samples (section 3.4.3a(ii) above), it can be deduced from the pattern of relationships between means along PC1 that shape differences similar in nature, if not identical in degree, are evident in the other three populations, showing the same spatial relationships as seen for the African American means.

African American Rt	0									
African American Lt	1.49	0								
Caucasian American Rt	0.24	1.47	0							
Caucasian American Lt	1.50	0.11	1.49	0						
Spitalfields Rt	0.42	1.43	0.53	1.44	0					
Spitalfields Lt	1.50	0.34	1.48	0.38	1.49	0				
Arikara Rt	0.34	1.45	0.36	1.46	0.22	1.50	0			
Arikara Lt	1.52	0.15	1.50	0.09	1.46	0.36	1.48	0		
Chinese Rt	0.55	1.47	0.47	1.48	0.92	1.41	0.79	1.49	0	
Chinese Lt	1.51	0.40	1.51	0.31	1.42	0.57	1.46	0.29	1.53	0
	African Am Rt	African Am Lt	Caucasian Am Rt	Caucasian Am Lt	Spitalfields Rt	Spitalfields Lt	Arikara Rt	Arikara Lt	Chinese Rt	Chinese Lt

Table 3.19: Asymmetry in the femur of 5 Populations. Procrustes distances between sample means of right and left groups for 5 populations. Correlation between Procrustes distances and Mahalanobis' distances generated by stepwise discriminant analysis (Table 3.16) is: r= 0.77; $p<0.0001$

Figure 3.11:

Asymmetry of femur in 5 population means. Bivariate plot of PC1 with PC2, showing a separation of right and left means of 5 populations. Arrows point from right to left means from each population.

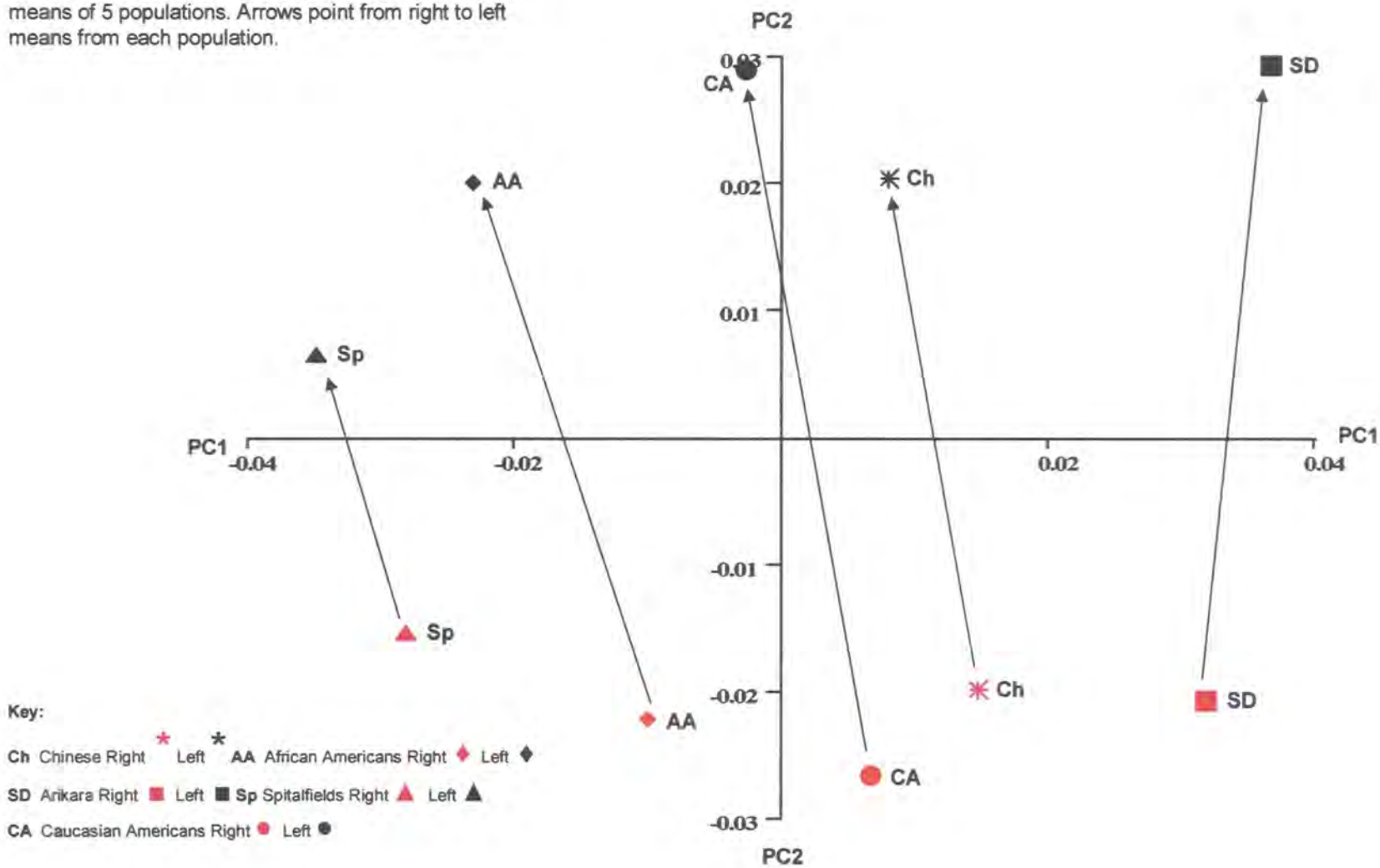

Figure 3.12:

Separation of right and left means of femur in 5 populations on PC1. Images represent the mean configuration if warped to the extremes of PC1 (at 0.04 to –0.04). The image at the positive extreme includes landmarks discussed in the text (section 3.4.4a(ii)).

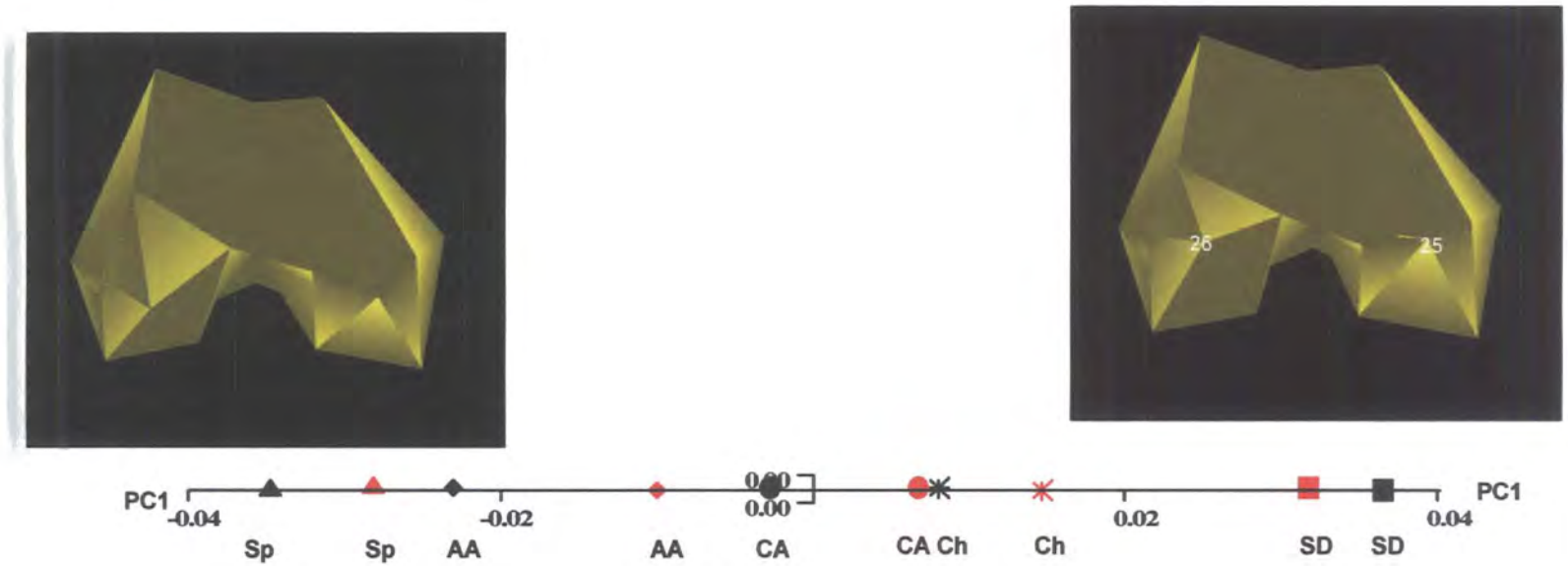

Key:

Ch Chinese Right * Left * AA African Americans Right ♦ Left ♦

SD Arikara Right ■ Left ■ Sp Spitalfields Right ▲ Left ▲

CA Caucasian Americans Right ● Left ●

Figure 3.13:

Asymmetry in femur of 5 population means. Separation of right and left means of 5 populations on PC2. Images represent the mean configuration if warped to the extremes of PC2 (at 0.04 to –0.04). The image at the positive extreme includes landmarks discussed in the text (section 3.4.4a(ii)).

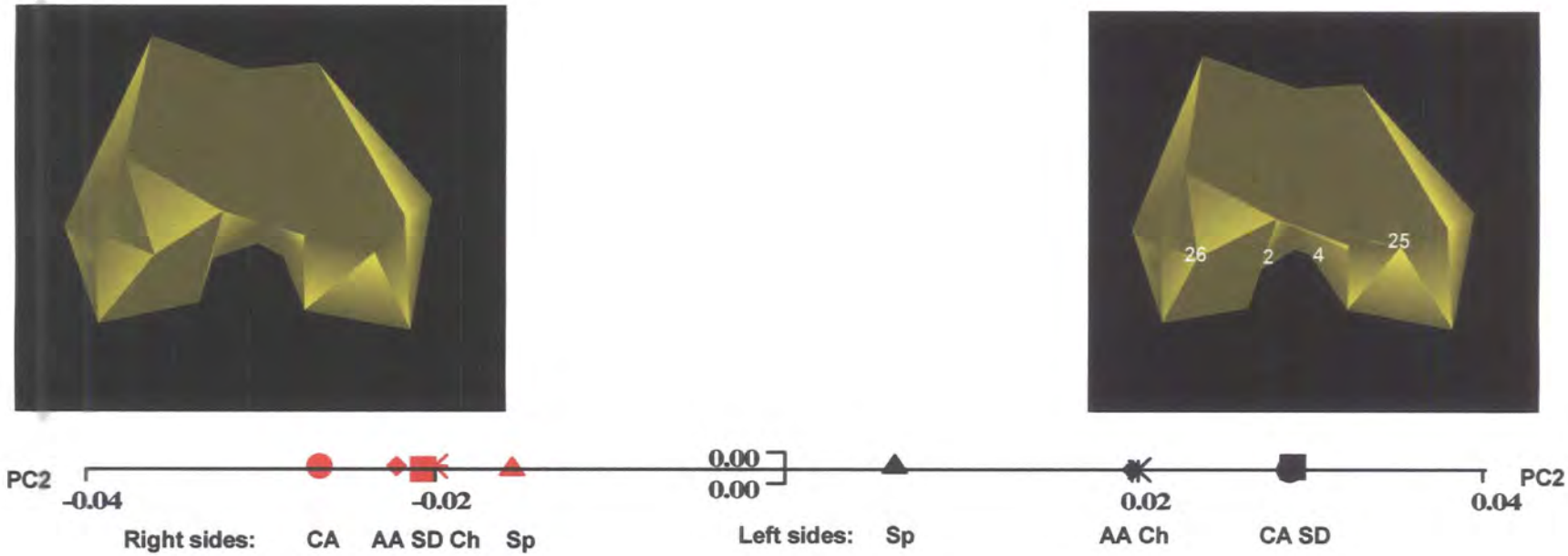

Thus, differences in the orientation of the condyles relative to the patella articular surface seen for African Americans also apply to the Caucasian Americans, Spitalfields and Chinese, as shown in Figure 3.12. This pattern of orientation between right and left sides appears to be reversed in the Arikara joint, which shows the opposite relationship of right and left means relative to the other four populations.

For the femur, all right and left sided means are fully separated along PC2 at t=9.28; $p<0.0001$. No other PC separates right and left means at a level of statistical significance. Therefore, PC2 explains shape differences between right and left sides more specifically than any other PC.

On PC2, all right means are placed towards the negative side of the scale and all left towards the positive extreme. The degree of difference in shape varies between the pairs of means for each population, with less shape difference noted between the Spitalfields pair of means relative to, for example, the Caucasian Americans. Morphological differences between all right and all left means along PC2 are primarily explained in terms of the orientation of the distal femur to the diaphysis in the mediolateral plane with a lesser degree of difference in the relative proportions of the joint. The differences in orientation of the joint to the shaft can be seen in the mean configurations in Figure 3.13, by noting the difference in position of the maximum height of the condyles (landmarks 25 and 26) relative to landmarks 2 and 4 across the posterior side of the intercondylar fossa.

PCs 3 and 4 both appear to explain slight differences in the proportions of the joint, rather than in the orientation of the joint relative to the diaphysis. As shown in Figure 3.14 along PC3, differences appear to be of a similar nature for four of the five pairs of population means (African Americans, Spitalfields, Arikara and Chinese), with the right side of each pair placed towards the positive end of the scale. For the fifth pair of means, the Caucasian Americans, this pattern is reversed with the left mean placed towards the negative extreme. There is also greater distance between the Caucasian American means, compared to the distances between the remaining four pairs, which appear relatively small. The nature of differences, which appears to be

Figure 3.14:

Asymmetry in femur of 5 population means. Bivariate plot of PC3 with PC4 showing a separation of right and left means of 5 populations. Arrows indicate right to left means from each population. Images represent the mean configuration if warped to the extremes of PC3 (at 0.02 to -0.04) and PC4 (0.03 to -0.02).

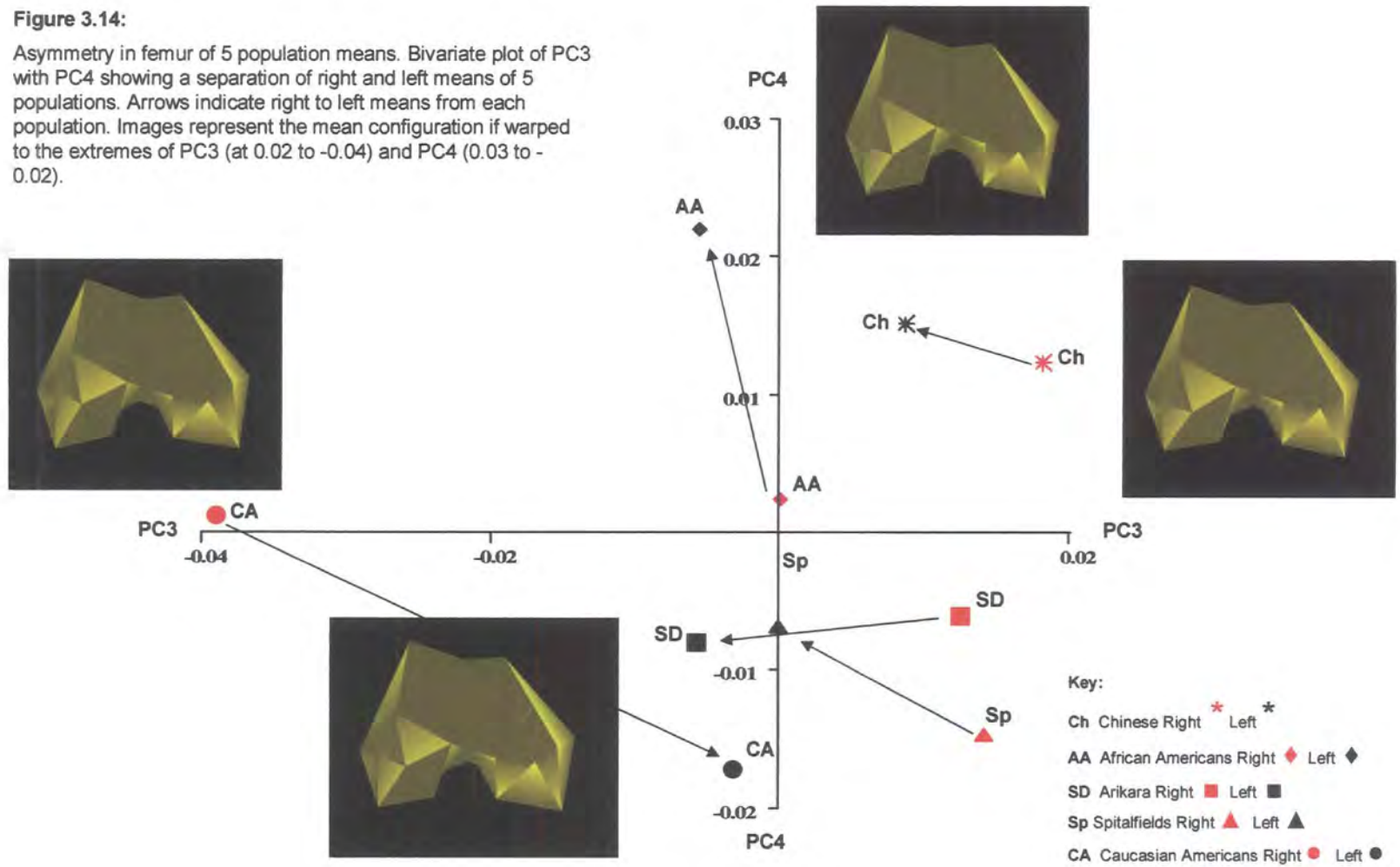

greatest across the lateral condyle, is also very subtle and difficult to assess from the mean configuration in Figure 3.14. There is no consistent pattern in the positions of right and left sample means on PC4 and any morphological asymmetries explained by PC4 between the five pairs of means are too subtle to be assessed.

3.4.4b(i) Tibia: Analyses using the total sample

Differences in shape of the 360 specimens are analysed using the Procrustes fitted co-ordinates and by subjecting the data to PCA. Table 3.21 gives the proportional and accumulated variance for PCs 1 to 56, which represents the total variance within the sample. The scores for each specimen on the resultant PCs are then subjected to canonical discriminant analysis to establish the relationships between populations based upon the Mahalanobis' squared distances between population means.

For the tibia, the best separation of samples of right and left sides for the five populations is achieved using 100% of total variance. This assessment was reached after separate discriminant and cross-validation analyses were carried out using the PC scores accounting for between c.50% to 100% of total variance. Results are summarised in Figure 3.15.

The Mahalanobis' squared distances between right and left sample means, generated by discriminant analysis are shown in Table 3.22. All distances between samples are statistically significant indicating that right and left samples can be separated on the basis of shape of the proximal tibia. Table 3.23 illustrates the relationship of each sample to all others on the basis of the generated Mahalanobis' squared distances by showing the distance of each primary sample to all others and ranking them accordingly from the closest sample (at position 1) to the most distant (at position 9).

For the tibia, in three of the ten samples (Spitalfields right and left and Chinese left) the matching limb from the same population is seen to be the most similar in shape to the primary sample. For the other seven samples, the closest sample is of the same side from a different population although the matching limb of the opposite side from the same population is never further than the third position from the primary sample.

PCs	Prop.	Cumul.	PCs	Prop.	Cumul.	PCs	Prop.	Cumul.
PC1	25.70	25.70	PC21	1.17	83.00	PC41	0.37	96.60
PC2	8.43	34.10	PC22	1.03	84.00	PC42	0.34	96.90
PC3	6.49	40.60	PC23	1.02	85.00	PC43	0.33	97.30
PC4	5.91	46.50	PC24	0.99	86.00	PC44	0.31	97.60
PC5	3.77	50.30	PC25	0.93	87.00	PC45	0.30	97.90
PC6	3.40	53.70	PC26	0.90	87.90	PC46	0.29	98.10
PC7	3.26	57.00	PC27	0.84	88.70	PC47	0.27	98.40
PC8	2.93	59.90	PC28	0.77	89.50	PC48	0.24	98.70
PC9	2.47	62.40	PC29	0.75	90.20	PC49	0.22	98.90
PC10	2.32	64.70	PC30	0.70	90.90	PC50	0.21	99.10
PC11	2.24	66.90	PC31	0.66	91.60	PC51	0.20	99.30
PC12	2.12	69.10	PC32	0.64	92.20	PC52	0.20	99.50
PC13	2.05	71.10	PC33	0.61	92.80	PC53	0.14	99.60
PC14	1.87	73.00	PC34	0.57	93.40	PC54	0.13	99.80
PC15	1.79	74.80	PC35	0.54	94.00	PC55	0.12	99.90
PC16	1.55	76.30	PC36	0.52	94.50	PC56	0.11	100.00
PC17	1.50	77.80	PC37	0.48	95.00			
PC18	1.47	79.30	PC38	0.47	95.40			
PC19	1.29	80.60	PC39	0.41	95.80			
PC20	1.24	81.80	PC40	0.39	96.20			

Table 3.21: Asymmetry in the tibia of 5 populations. The proportion and accumulated variance for PCs 1-56, which accounts for 100% of total variance

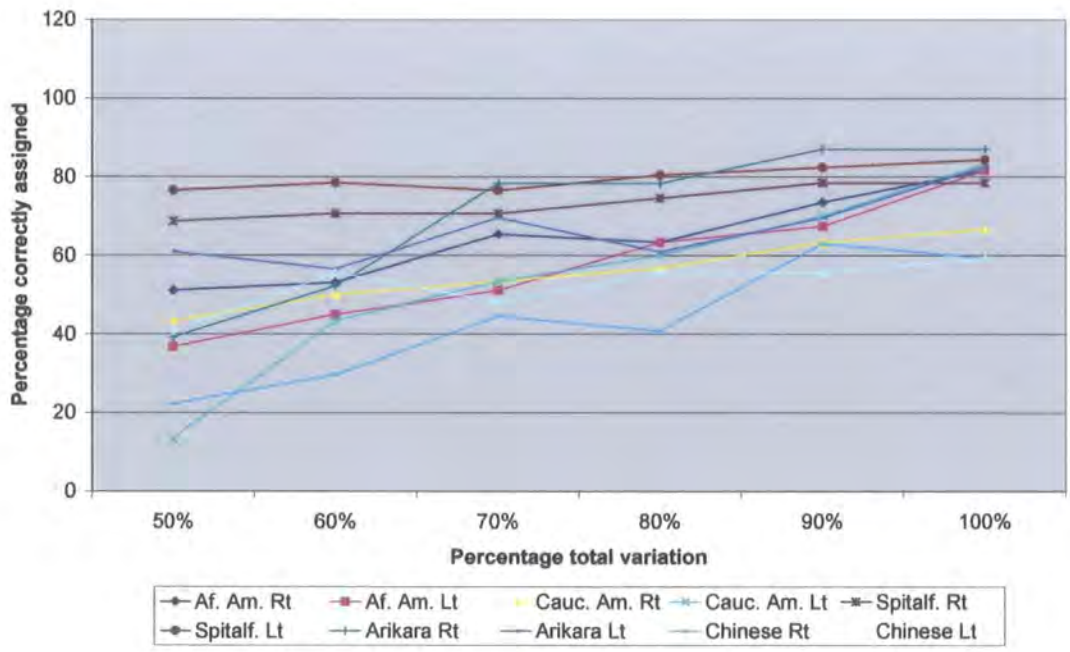

Figure 3.15: Asymmetry in the tibia of 5 Populations. Summary of separate discriminant and cross-validation analyses were carried out using PCs accounting for c.50% of total variance (PCs 1-15), 60% (PCs 1-8), 70% (PCs 1-12), 80% (PCs 1-19), 90% (PCs 1-29) and 100% (PCs 1-56).

African Am. Right	0 1.000									
African Am. Left	20.24 0.0001	0 1.000								
Ca. Am. Right	16.25 0.0001	21.60 0.0001	0 1.000							
Ca. Am. Left	21.82 0.0001	15.99 0.0001	18.00 0.0001	0 1.000						
Spitalfields Right	61.47 0.0001	69.69 0.0001	76.39 0.0001	82.37 0.0001	0 1.000					
Spitalfields Left	59.32 0.0001	56.13 0.0001	75.44 0.0001	65.20 0.0001	11.64 0.0001	0 1.000				
Arikara Right	26.14 0.0001	35.91 0.0001	19.79 0.0001	27.77 0.0001	99.55 0.0001	92.23 0.0001	0 1.000			
Arikara Left	42.94 0.0001	25.54 0.0001	33.49 0.0001	31.36 0.0001	102.73 0.0001	91.21 0.0001	24.55 0.0001	0 1.000		
Chinese Right	25.22 0.0001	29.93 0.0001	10.95 0.0001	25.47 0.0001	80.48 0.0001	79.43 0.0001	18.19 0.0001	31.50 0.0001	0 1.000	
Chinese Left	33.74 0.0001	18.91 0.0001	21.48 0.0001	18.20 0.0001	88.21 0.0001	76.80 0.0001	29.00 0.0287	19.44 0.0001	12.14 0.0001	0 1.000
	Af. Am. Right	**Af. Am. Left**	**Ca. Am. Right**	**Ca. Am. Left**	**Spitalf. Right**	**Spitalf. Left**	**Arikara Right**	**Arikara Left**	**Chinese Right**	**Chinese Left**

Table 3.22: Asymmetry in the tibia in 5 populations: Results from the canonical discriminant analysis of right and left groups from 5 populations, on the basis of 100% total variance. The upper value in red gives the Mahalanobis' squared distance between groups, lower value in black gives the Hotelling's t^2 *p*-value.

Group	1	2	3	4	5	6	7	8	9
African Am. Rt	CA Rt	AA Lt	CA Lt	Ch Rt	SD Rt	Ch Lt	SD Lt	Sp Lt	Sp Rt
African Am. Lt	CA Lt	Ch Lt	AA Rt	CA Rt	SD Lt	Ch Rt	SD Rt	Sp Lt	Sp Rt
Cauc. Am. Rt	Ch Rt	AA Rt	CA Lt	SD Rt	SD Lt	Ch Lt	SD Lt	Sp Lt	Sp Rt
Cauc. Am. Lt	AA Lt	CA Rt	Ch Lt	AA Rt	Ch Rt	SD Rt	SD Lt	Sp Lt	Sp Rt
Spitalfields Rt	Sp Lt	AA Rt	AA Lt	CA Rt	Ch Rt	CA Lt	Ch Lt	SD Rt	SD Lt
Spitalfields Lt	Sp Rt	AA Lt	AA Rt	CA Lt	CA Rt	Ch Lt	Ch Rt	SD Lt	SD Rt
Arikara Rt	Ch Rt	CA Rt	SD Lt	AA Rt	CA Lt	CA Rt	AA Lt	Sp Lt	Sp Rt
Arikara Lt	Ch Lt	SD Rt	AA Lt	Ch Rt	CA Lt	CA Rt	AA Rt	Sp Lt	Sp Rt
Chinese Rt	CA Rt	Ch Lt	SD Rt	AA Rt	CA Lt	AA Lt	SD Lt	Sp Lt	Sp Rt
Chinese Lt	Ch Rt	AA Lt	CA Lt	SD Lt	CA Rt	SD Rt	AA Lt	Sp Lt	Sp Rt

Table 3.23: Asymmetry in the tibia of 5 populations. The order of proximity in distance of each primary right and left group from the other groups of the 5 populations, on the basis of their Mahalanobis squared distances, as shown in Table 3.22.

It appears, therefore, that the pattern of asymmetry for the proximal tibia is more difficult to interpret than in the distal femur, particularly in relation to the Caucasian Americans. In the Spitalfields group, the reduced asymmetry relative to the other four populations noted for the femur is repeated in the tibia. Whilst the Spitalfields femora are not noticeably distant from the other samples, however, the left and particularly the right Spitalfields tibiae are markedly distant from all other population samples. This extreme distance is shown in the positions of Spitalfields left and right tibiae relative to other population groups at positions 8 and 9 respectively in Table 3.23 and is also apparent in Figures 3.16 and 17 (the bivariate plot of PCs 1 and 2 and on PC1, respectively, using sample means; see below). This extreme distance in the Spitalfields tibiae noted here in relation to asymmetry, is explored further in relation to inter-population variation at the knee joint in Chapter 6.

Table 3.24 shows the results of cross-validation analysis using 100% of total variance for the ten samples. Samples correctly assigned to groups range from 59.26% for both Chinese right and left sides to 86.96% for the Arikara right side.

Number of Observations and Percent Classified into Greoup											
From Group	African Am. Right	African Am. Left	Caucasian Am. Right	Caucasian Am. Left	Spitalf. Right	Spitalf. Left	Arikara Right	Arikara Left	Chinese Right	Chinese Left	Total
African Am. Right	40 81.63	2 4.08	4 8.16	2 4.08	0 0	0 0	0 0	0 0	1 2.04	0 0	49 100
African Am. Left	3 6.12	40 81.63	2 4.08	2 4.08	0 0	0 0	0 0	1 2.04	0 0	1 2.04	49 100
Cauc. Am. Right	1 3.33	3 10	20 66.67	0 0	0 0	0 0	2 6.67	0 0	4 13.33	0 0	30 100
Cauc. Am. Left	0 0	2 6.67	1 3.33	25 83.33	0 0	0 0	0 0	0 0	0 0	2 6.67	30 100
Spitalfields Right	0 0	0 0	1 1.96	0 0	40 78.43	10 19.61	0 0	0 0	0 0	0 0	51 100
Spitalfields Left	0 0	1 1.96	0 0	0 0	6 11.76	43 84.31	0 0	0 0	0 0	1 1.96	51 100
Arikara Right	1 4.35	0 0	1 4.35	0 0	0 0	0 0	20 86.96	0 0	1 4.35	0 0	23 100
Arikara Left	0 0	2 8.7	0 0	0 0	0 0	0 0	1 4.35	19 82.61	0 0	1 4.35	23 100
Chinese Right	0 0	0 0	3 11.11	1 3.7	0 0	0 0	3 11.11	0 0	16 59.26	4 14.81	27 100
Chinese Left	0 0	1 3.7	0 0	2 7.41	0 0	0 0	0 0	3 11.11	5 18.52	16 59.26	27 100
Total	45 12.5	51 14.17	32 8.89	32 8.89	46 12.78	53 14.72	26 7.22	23 6.39	27 7.5	25 6.94	360 100

Table 3.24: Separation of right and left tibiae from 5 populations using 100% total variation selected by cross-validation analysis. Upper figure denotes number of individuals; lower figure denotes percentage. Red figures denote number of individuals placed into their correct group.

Although the percentage of specimens correctly assigned to groups is seen to be less than that for the femur, the vast majority of misplaced individuals are either placed into the categories of the matching limb of the same population or into the same side of different populations.

3.4.4b(ii) Tibia: Analyses using sample means

Because of the high degree of overlap on the bivariate plots of selected PCs when using the total sample (see section 3.4.4b(i) above), right and left population means are used to help determine the specific morphologies and to explore the relationships between them. For the tibia, the correlation between the Procrustes distances shown in Table 3.25 and the Mahalanobis' squared distances shown in Table 3.22 is not statistically significant (r= 0.09; $p = 0.56$). This result implies that it may therefore be problematic to infer the relative relationships between entire populations solely from the relationships between population means. It can be seen, however, from Tables 3.22 and 3.23 and Figures 3.16 and 3.17 (see below) that not only is there is agreement between results of the two types of analyses regarding the relationship between the right and left Spitalfields samples (as conspicuously distant relative to all other samples) but also the relative lack of asymmetry in the Caucasian American tibia compared to the relatively marked asymmetry in the femur.

The Procrustes mean co-ordinate means have been calculated from separate GPAs of each population's right and left samples and have been subjected to a joint GPA and PCA. The proportion and accumulated variance of the PCs generated in the analysis of population means is given in Table 3.26:

African American Rt	0									
African American Lt	1.45	0								
Caucasian American Rt	0.39	1.44	0							
Caucasian American Lt	1.46	0.19	1.43	0						
Spitalfields Rt	0.59	1.41	0.54	1.39	0					
Spitalfields Lt	1.4	0.6	1.33	0.56	1.38	0				
Arikara Rt	0.31	1.45	0.41	1.43	0.32	1.4	0			
Arikara Lt	1.43	0.29	1.39	0.31	1.4	0.35	1.43	0		
Chinese Rt	0.45	1.4	0.46	1.42	0.9	1.31	0.68	1.35	0	
Chinese Lt	1.45	0.15	1.42	0.25	1.42	0.49	1.45	0.16	1.37	0
	African Am Rt	African Am Lt	Caucasian Am Rt	Caucasian Am Lt	Spitalfields Rt	Spitalfields Lt	Arikara Rt	Arikara Lt	Chinese Rt	Chinese Lt

Table 3.25: Asymmetry in the tibia of 5 Populations. Procrustes distances between sample means of right and left groups for 5 populations. Correlation between Procrustes distances and Mahalanobis' distances generated by stepwise discriminant analysis (Table 3.22) is: r= 0.09; *p*= 0.56.

PCs	Proportion	Cumulative	PCs	Proportion	Cumulative
PC1	70.20	70.20	PC6	2.11	97.90
PC2	10.50	80.70	PC7	1.02	98.90
PC3	7.63	88.30	PC8	0.72	99.60
PC4	4.59	92.90	PC9	0.39	100.00
PC5	2.84	95.80			

Table 3.26: Proportion and accumulative variance represented by PCs 1-9 for the tibia, which accounts for 100% of total variance for sample means.

The first four PCs account for over 90% of total variance in the sample and the exploration of shape differences between sides will concentrate on these four PCs.

Figure 3.16 shows the location of the ten means on PC1 with PC2, which cumulatively account for over 80% of total variance. Figures 3.16 and 3.17 show the mean configuration warped to the extremes of PC1 and PC2, respectively.

On PC1, the right mean is placed more positively than the left mean for the Caucasian Americans, Chinese and Arikara. Placement is almost identical on PC1 for the African Americans and Spitalfields right and left means. As previously noted in section 3.4.4b(i), the Spitalfields pair is positioned at the extreme negative end of the scale of PC1 and at a considerable distance from all other means. Although the variation in shape explained by PC1 shows some degree of separation between right and left sides in three populations, much of the variation along this PC relates to the differences between specific populations (exemplified in the separation of the Spitalfields pair relative to the other four population means). Differences in shape explained by this PC appears to centre on the anterior region of bone; in the mean configuration shown in Figure 3.17, this is seen in the relatively changed positions of landmarks 14, 15 and 16 and in the depth of the of the tibial shelf (landmarks 3 and 5 on the edge of the tibial plateau and landmark 16 on the medial side.

Figure 3.16:

Asymmetry in tibia of 5 Population means. Bivariate plot of PC1 with PC2, showing a separation of right and left means of 5 populations. Arrows point from right to left means from each population.

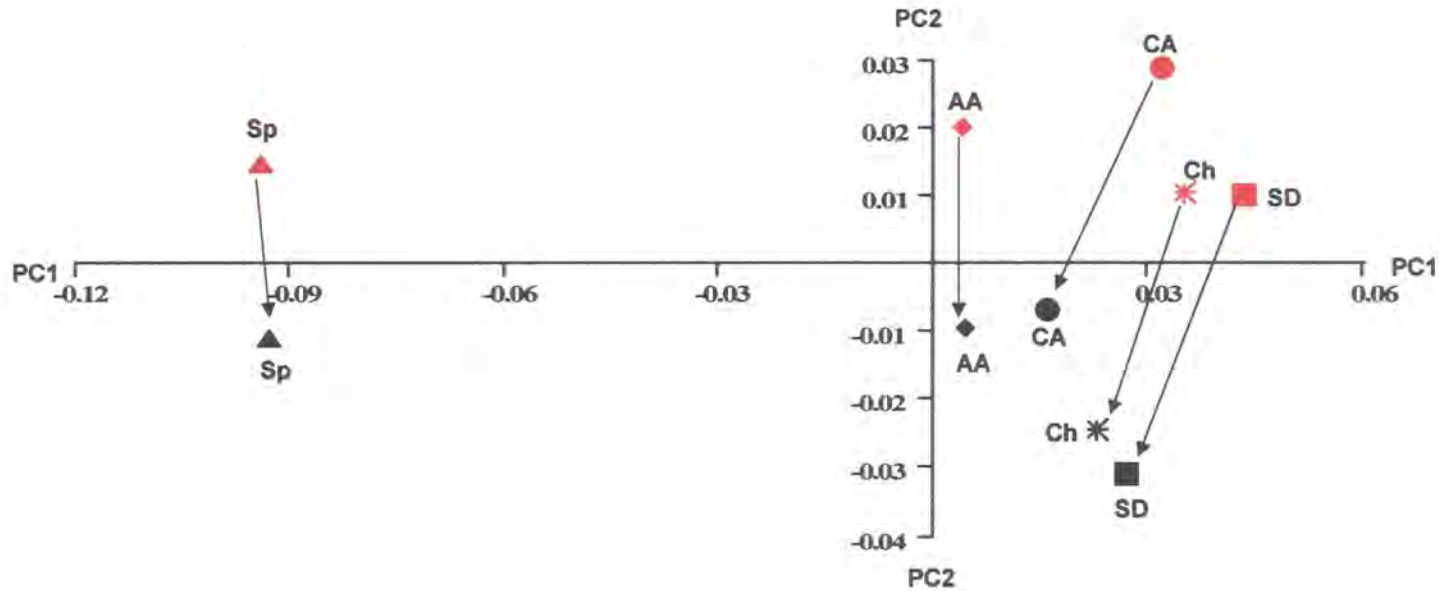

Key:

Ch Chinese Right Left

AA African Americans Right Left

SD Arikara Right Left

Sp Spitalfields Right Left

CA Caucasian Americans Right Left

Figure 3.17:

Asymmetry in tibia of 5 Population means. Separation of right and left means of 5 populations on PC1. Images represent the mean configuration if warped to the extremes of PC1 (at 0.06 to –0.12). The image at the positive extreme shows landmarks discussed in the text (section 3.4.4b(ii)).

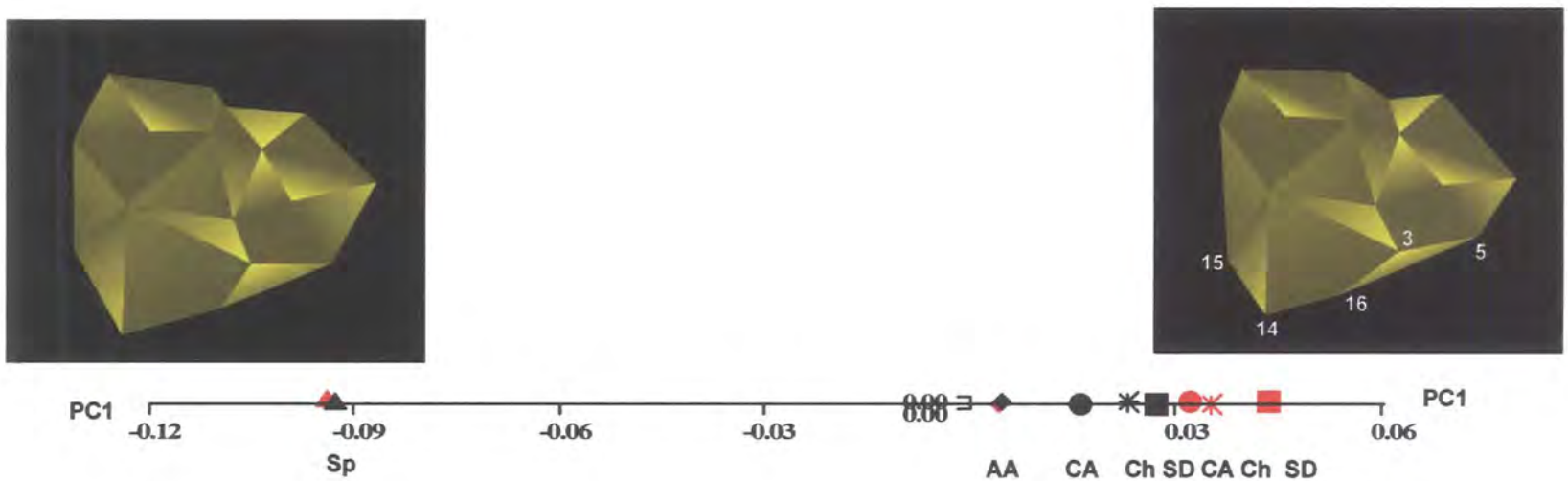

Key:

Ch Chinese Right * Left * AA African Americans Right ♦ Left ♦

SD Arikara Right ■ Left ■ Sp Spitalfields Right ▲ Left ▲

CA Caucasian Americans Right ● Left ●

Like the femur, PC2 fully separates all right and left sided tibiae at t= 5.69; p= 0.0005. No other PC separates right and left sides at a level of statistical significance. Tibial shape asymmetry is therefore primarily explained by PC2.

Figures 3.16 and 3.18 show this clear separation of right and left sides with all right means scoring towards the positive side of the scale and all left scoring towards the negative extreme. The degree of separation in shape appears to be relatively uniform between the five population pairs, with each right and left mean showing a relatively similar degree of separation between sides. Figure 3.18 shows that differences between sides in the five population means are likely to relate to the orientation of the joint to the shaft, showing the tibial plateau rotated more towards the medial side in right compared to left sided individuals. This is highlighted in Figure 3.18 in the change of position of landmarks 3, 5 and 16 on the medial side of the tibial shelf.

PCs 3 and 4, accounting for a cumulative 12.22% of total variance, both appear to explain slight differences in the proportions of the joint, rather than the orientation of the joint relative to the diaphysis. Figure 3.19, the bivariate plot of PC3 with PC4 shows that there is a similar relationship between right and left sides in all five populations for PC3, with all right means being placed more positively than their corresponding left; although the difference in shape between two of the pairs (African Americans and Arikara) is marginal. PC3 explains greater projection of the anterior region over the lateral side; this is highlighted in Figure 3.19 in the relative difference in position of landmarks 9 (edge of the tibial plateau) and landmarks 14 and 15.

PC4 seems to be unrelated to asymmetry, as the right and left mean from each population lay closely adjacent to each other, with the right mean placed more negatively than the left mean in four of the five populations. This relative position is reversed in the Spitalfields pair. Shape variation explained by this PC relates to a slight difference in proportions of the anterior region; specifically the relative change in position of landmarks 3, 9, 14, 15 and 16 in Figure 3.19.

Figure 3.18:

Asymmetry in tibia of 5 Population means. Separation of right and left means of 5 populations on PC2. Images represent the mean configuration if warped to the extremes of PC2 (at 0.04 to –0.04). The image at the positive extreme shows landmarks discussed in the text (section 3.4.4b(ii)).

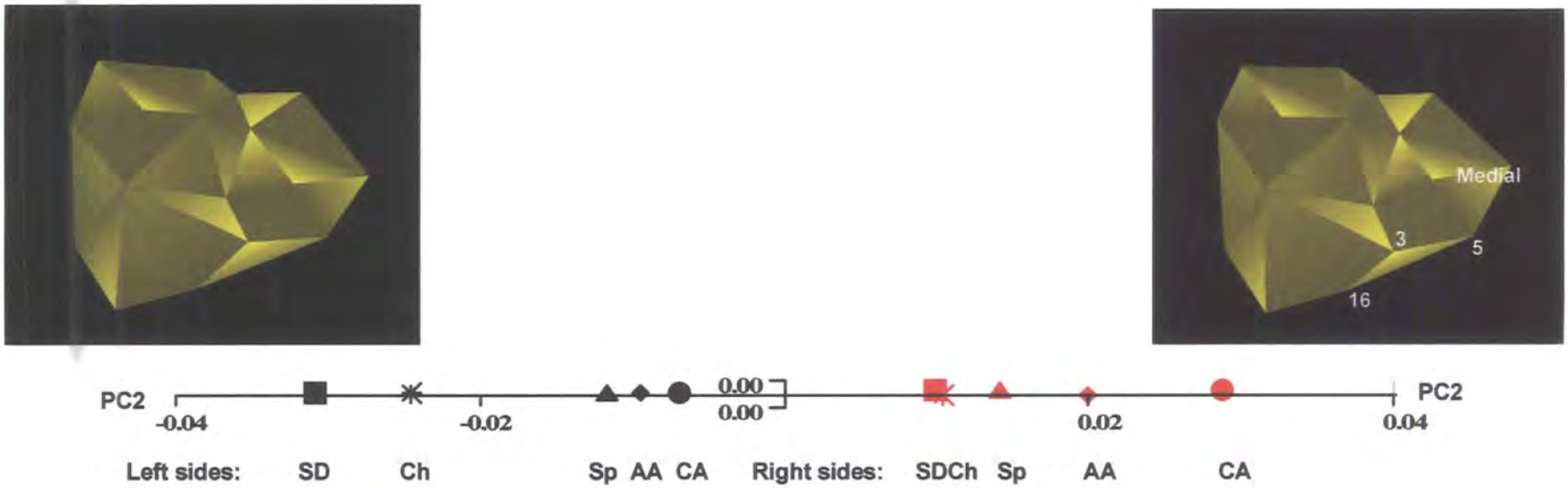

Key:

Ch Chinese Right * Left * **AA** African Americans Right ♦ Left ♦

SD Arikara Right ■ Left ■ **Sp** Spitalfields Right ▲ Left ▲

CA Caucasian Americans Right ● Left ●

Figure 3.19:

Asymmetry in tibia of 5 population means. Bivariate plot of PC3 with PC4, showing a separation of right and left means of 5 populations. Images represent the mean configuration if warped to the extremes of PC1 (at 0.04 to –0.04) and PC2 (at 0.02 to -0.02). The image at the positive extreme of PC3 shows landmarks discussed in the text (section 3.4.4b(ii)).

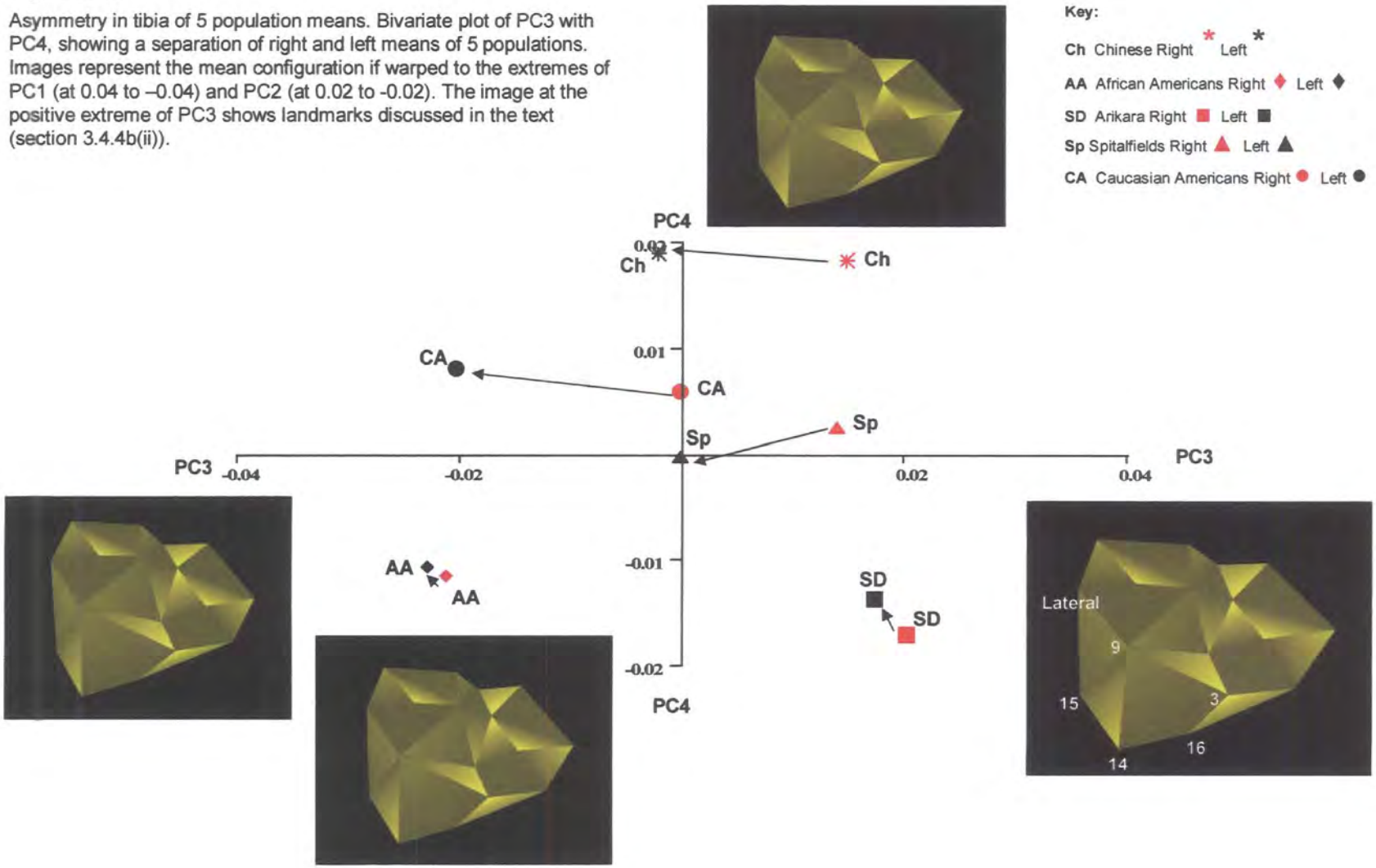

3.4.5 Asymmetry of shape of the knee joint of males and females of three populations

3.4.5a(i) Femur: Analyses using the total sample

Three populations are used for the analysis comparing males and females in relation to asymmetry of the knee joint; African and Caucasian Americans and the Spitalfields sample. Differences in shape of the 254 specimens are analysed using the Procrustes fitted co-ordinates and by subjecting the data to PCA. Table 3.27 gives the proportional and accumulated variance for PCs 1 to 71, which represents the total variance within the sample. The scores for each specimen on the resultant PCs are then subjected to canonical discriminant analysis to establish the relationships between populations based upon the Mahalanobis' squared distances between population means.

For the femur, the best separation of samples is achieved using 90% of total variance. This assessment was reached after separate discriminant and cross-validation analyses were carried out using the PC scores accounting for between c.50% to 100% of total variance. Results are summarised in Figure 3.20.

The Mahalanobis' squared distances between male and female, right and left sample means, generated by discriminant analysis are shown in Table 3.28. Distances between samples of African American and Spitalfields samples are highly statistically significant, indicating that male and female, right and left samples can be separated on the basis of some aspect of shape of the distal femur for these two populations. For the Caucasian Americans, right and left groups are separated at a level of statistical significance but males and females of the same side are not separated at a significant level (between Caucasian American right sided males and females p= 0.3076; between left sided males and females p= 0.3073). Table 3.29, p192, illustrates the distance of each sample to all others on the basis of the generated Mahalanobis' squared distances, by showing the distance of each primary sample to all others and ranking them accordingly from the closest sample (at position 1) to the most distant (at position 11).

PCs	Prop.	Cumul.	PCs	Prop.	Cumul.	PCs	Prop.	Cumul.
PC1	11.20	11.20	PC26	1.03	88.00	PC51	0.15	98.80
PC2	9.37	20.60	PC27	0.98	89.00	PC52	0.15	99.00
PC3	6.43	27.00	PC28	0.90	89.90	PC53	0.14	99.10
PC4	5.81	32.90	PC29	0.78	90.70	PC54	0.12	99.20
PC5	5.42	38.30	PC30	0.74	91.40	PC55	0.11	99.30
PC6	4.64	42.90	PC31	0.69	92.10	PC56	0.10	99.40
PC7	4.28	47.20	PC32	0.65	92.70	PC57	0.09	99.50
PC8	4.23	51.40	PC33	0.57	93.30	PC58	0.07	99.60
PC9	3.86	55.30	PC34	0.52	93.80	PC59	0.06	99.70
PC10	3.64	58.90	PC35	0.48	94.30	PC60	0.06	99.70
PC11	3.32	62.20	PC36	0.47	94.80	PC61	0.05	99.80
PC12	2.90	65.10	PC37	0.41	95.20	PC62	0.04	99.80
PC13	2.76	67.90	PC38	0.39	95.60	PC63	0.04	99.80
PC14	2.34	70.20	PC39	0.38	95.90	PC64	0.03	99.90
PC15	2.21	72.50	PC40	0.35	96.30	PC65	0.03	99.90
PC16	1.94	74.40	PC41	0.32	96.60	PC66	0.03	99.90
PC17	1.84	76.20	PC42	0.30	96.90	PC67	0.02	100.00
PC18	1.77	78.00	PC43	0.28	97.20	PC68	0.02	100.00
PC19	1.55	79.50	PC44	0.26	97.40	PC69	0.01	100.00
PC20	1.45	81.00	PC45	0.23	97.70	PC70	0.01	100.00
PC21	1.38	82.40	PC46	0.22	97.90	PC71	0.01	100.00
PC22	1.26	83.60	PC47	0.20	98.10			
PC23	1.20	84.80	PC48	0.20	98.30			
PC24	1.09	85.90	PC49	0.19	98.50			
PC25	1.03	87.00	PC50	0.18	98.70			

Table 3.27: Asymmetry in the femur of males and females of 3 populations. The proportion and accumulated variance for PCs 1-71, which accounts for 100% of total variance.

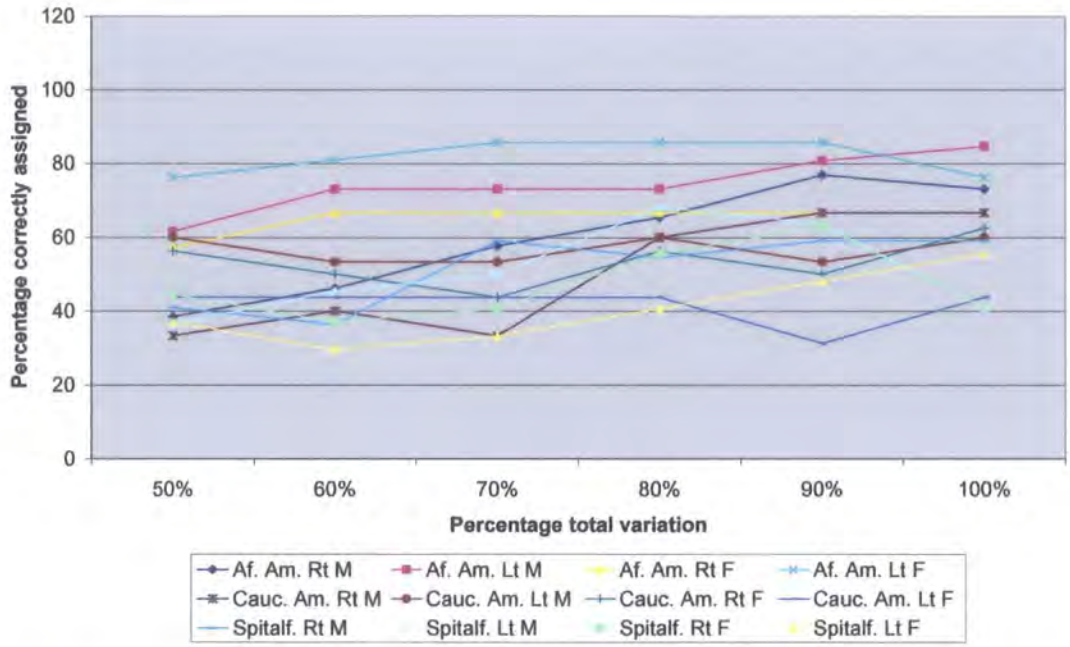

Figure 3.20: Asymmetry in the femur of males and females of 3 populations. Summary of separate discriminant and cross-validation analyses were carried out using PCs accounting for c.50% of total variance (PCs 1-10), 60% (PCs 1-13), 70% (PCs 1-18), 80% (PCs 1-25), 90% (PCs 1-36) and 100% (PCs 1-71).

In each case, the closest sample is the same side from the opposite sex of the same population. With the exception of the Spitalfields groups, for at least the next three subsequent positions, samples are closest in shape to all other samples from the same side but from different populations before any other sample of the opposite side, including the matching bone from their own population. In addition, the distances of groups from the primary group subsequent to the first position are positioned largely irrespective of sex. These results therefore indicate that asymmetry of shape is a more powerful determinant of shape variation than sexual dimorphism.

Table 3.30 shows the results of cross-validation analysis using 90% of total variance for the twelve samples. Samples correctly assigned to groups range from 31.25% for Caucasian Americans (female, left side) to 85.71% for the African Americans (female, left side).

AA Rt. Male	0 1.000											
AA Lt. Male	53.70 0.0001	0 1.000										
AA Rt. Female	16.65 0.0046	63.38 0.0001	0 1.000									
AA Lt. Female	59.91 0.0001	24.95 0.0001	48.22 0.0001	0 1.000								
CA Rt. Male	40.19 0.0001	81.81 0.0001	39.40 0.0001	70.33 0.0001	0 1.000							
CA Lt. Male	77.72 0.0001	46.60 0.0001	88.43 0.0001	63.35 0.0001	88.50 0.0001	0 1.000						
CA Rt. Female	60.18 0.0001	101.52 0.0001	46.53 0.0001	74.61 0.0001	19.95 0.3076	108.74 0.0001	0 1.000					
CA Lt. Female	90.69 0.0001	54.51 0.0001	92.42 0.0001	60.40 0.0001	103.90 0.0001	15.45 0.3073	106.57 0.0001	0 1.000				
Sp Rt. Male	44.38 0.0001	69.92 0.0001	66.22 0.0001	79.62 0.0001	68.42 0.0001	66.95 0.0001	92.83 0.0205	79.79 0.0001	0 1.000			
Sp Lt. Male	51.61 0.0001	40.64 0.0001	60.28 0.0001	48.82 0.0001	73.29 0.0001	47.45 0.0001	87.38 0.0287	49.84 0.0001	29.47 0.0001	0 1.000		
SP Rt. Female	35.83 0.0001	68.45 0.0001	44.28 0.0001	64.88 0.0001	59.44 0.0001	74.14 0.0001	73.17 0.0001	78.74 0.0001	13.33 0.0106	29.59 0.0001	0 1.000	
Sp Lt. Female	59.43 0.0001	39.06 0.0001	59.43 0.0001	33.56 0.0001	73.71 0.0001	48.23 0.0001	78.61 0.0001	44.14 0.0001	40.65 0.0001	13.71 0.0126	28.92 0.0001	0 1.000
	AA Rt. Male	AA Lt. Male	AA Rt. Female	AA Lt. Female	CA Rt. Male	CA Lt. Male	CA Rt. Female	CA Lt. Female	Sp Rt. Male	Sp Lt. Male	Sp Rt. Female	Sp Lt. Female

Table 3.28: Asymmetry in the femur of males and females of 3 populations. Results from the canonical discriminant analysis of right and left, male and female groups from 3 populations, on the basis of 90% total variance. The upper value in red gives the Mahalanobis' squared distance between groups, lower value in black gives the Hotelling's t^2 *p*-value; values in blue denote non-significant results.

Group	1	2	3	4	5	6	7	8	9	10	11
African Am. Rt Male	AARF	SpRF	SpRM	CARM	CARF	SpLM	AALF	SpLF	AALM	CALM	CALF
African Am. Lt Male	AALF	SpLF	CALM	SpLM	CALF	AARM	SpRF	SpLM	AARF	CARM	CARF
African Am. Rt Female	AARM	CARM	SpRF	CARF	AALF	SpRM	SpLF	SpLM	AALM	CALM	CALF
African Am. Lt Female	AALM	SpLF	SpLM	CALF	CALM	AARF	AARM	SpRF	SpRM	CARM	CARF
Cauc. Am. Rt Male	CARF	CAARF	AARM	SpRF	AALF	SpRM	SpLF	SpLM	AALM	CALM	CALF
Cauc. Am. Lt Male	CALF	AALM	SpLF	SpLM	AALF	SpRF	SpRM	AARM	AARF	CARM	CARF
Cauc. Am. Rt Female	CARM	AARF	AARM	SpRF	AALF	SpLF	SpRM	SpLM	AALM	CALF	CALM
Cauc. Am. Lt Female	CALM	AALM	SpLF	SpLM	CALF	SpRF	SpRM	AARM	AARF	CARF	CARM
Spitalfields Rt Male	SpRF	SpLM	AARM	SpLF	AARF	AALM	AALF	CALM	CARM	CALF	CARF
Spitalfields Lt Male	SpLF	SpRM	SpRF	AALM	AALF	CALM	CALF	AARM	AARF	CARM	CARF
Spitalfields Rt Female	SpRM	AARM	SpLM	SpLF	AARF	AALF	AALM	CARM	CARF	CALM	CALF
Spitalfields Lt Female	SpLM	SpRF	AALM	AALF	CALF	SpRM	CALM	AARM	AARF	CARM	CARF

Table 3.29: Asymmetry in the femur of males and females from 3 populations. The order of proximity in distance of each primary right and left, male and female group from the other groups of the 3 populations, on the basis of their Mahalanobis squared distances, as shown in Table 3.28. Figures in red highlight the opposite sex group of the same side and population to the primary group.

Number of Observations and Percent Classified into Group using 90% total variance													
From Group	Af. Am. Rt M	Af. Am. Lt.M	Af. Am. Rt F	Af. Am. Lt F	Ca. Am. Rt M	Ca. Am. Lt M	Ca. Am. Rt F	Ca. Am. Lt F	Spitaf. Rt M	Spitalf. Lt M	Spitalf. Rt F	Spitalf. Lt F	Total
Af. Am. Rt M	20	0	3	0	1	0	1	0	1	0	0	0	26
	76.92	0	11.54	0	3.85	0	3.85	0	3.85	0	0	0	100
Af. Am. Lt M	0	21	0	4	0	0	0	1	0	0	0	0	26
	0	80.77	0	15.38	0	0	0	3.85	0	0	0	0	100
Af. Am. Rt F	6	0	14	0	1	0	0	0	0	0	0	0	21
	28.57	0	66.67	0	4.76	0	0	0	0	0	0	0	100
Af. Am. Lt F	0	2	0	18	0	0	0	0	0	0	0	1	21
	0	9.52	0	85.71	0	0	0	0	0	0	0	4.76	100
Ca. Am. Rt M	0	0	0	0	10	0	5	0	0	0	0	0	15
	0	0	0	0	66.67	0	33.33	0	0	0	0	0	100
Ca. Am. Lt M	0	0	0	0	0	8	0	5	0	1	0	1	15
	0	0	0	0	0	53.33	0	33.33	0	6.67	0	6.67	100
Ca. Am. Rt F	0	0	1	0	7	0	8	0	0	0	0	0	16
	0	0	6.25	0	43.75	0	50	0	0	0	0	0	100
Ca. Am. Lt F	0	0	0	2	0	8	0	5	0	0	0	1	16
	0	0	0	12.5	0	50	0	31.25	0	0	0	6.25	100
Spitalf. Rt M	1	0	0	0	0	0	0	0	13	2	6	0	22
	4.55	0	0	0	0	0	0	0	59.09	9.09	27.27	0	100
Spitalf. Lt M	0	0	0	0	0	0	0	0	0	14	0	8	22
	0	0	0	0	0	0	0	0	0	63.64	0	36.36	100
Spitalf. Rt F	1	0	1	0	0	0	0	0	7	0	17	1	27
	3.7	0	3.7	0	0	0	0	0	25.93	0	62.96	3.7	100
Spitalf. Lt F	0	1	0	3	0	0	0	0	0	8	2	13	27
	0	3.7	0	11.11	0	0	0	0	0	29.63	7.41	48.15	100
Total	28	24	19	27	19	16	14	11	21	25	25	25	254
	11.02	9.45	7.48	10.63	7.48	6.3	5.51	4.33	8.27	9.84	9.84	9.84	100

Table 3.30: Asymmetry in the femur of males and females of 3 populations. Separation of right and left, male and female groups from 3 populations using 90% total variance selected by cross-validation analysis. Upper figure denotes number of individuals; lower figure denotes percentage. Red figures denote number of individuals placed into their correct group; blue figures denote misplaced individuals from the opposite sex of the same side and population.

Although the percentage of individuals correctly assigned are low in several instances, in all cases the majority of misplaced individuals are of the same side and population but of the opposite sex. These results again emphasise the greater influence of shape variation caused by asymmetry compared to that which may be caused by sexual dimorphism.

3.4.5a(ii) Femur: Analyses using sample means

Because of the high degree of overlap on the bivariate plots of selected PCs when using the total sample (see section 3.4.5a(i) above), the sample means are used to help determine the specific morphologies of each male and female, right and left sample and to explore the relationships between them. For the femur, there is a correlation (at a high level of statistical significance) between the Procrustes distances shown in Table 3.31 and the Mahalanobis' squared distances shown in Table 3.28 ($r= 0.67$; $p < 0.0001$), indicating that similar shape relationships are represented by both datasets.

The Procrustes mean co-ordinates have been calculated from separate GPAs of each population's right and left sides for males and females and have been subjected to a joint GPA and PCA.

The proportion and accumulated variance of the PCs generated in the analysis of population means is given in Table 3.32:

African Am. Rt Male	0											
African Am. Lt Male	1.50	0										
African Am. Rt Female	0.16	1.47	0									
African Am. Lt Female	1.49	0.06	1.46	0								
Caucasian Am. Rt Male	0.24	1.48	0.13	1.47	0							
Caucasian Am. Lt Male	1.51	0.11	1.48	0.11	1.49	0						
Caucasian Am. Rt Female	0.07	1.50	0.17	1.49	0.21	1.51	0					
Caucasian Am. Lt Female	1.51	0.24	1.49	0.23	1.50	0.14	1.51	0				
Spitalfields Rt Male	0.43	1.44	0.42	1.43	0.53	1.45	0.47	1.44	0			
Spitalfields Lt Male	1.51	0.34	1.49	0.35	1.48	0.38	1.50	0.45	1.50	0		
Spitalfields Rt Female	0.36	1.46	0.38	1.45	0.49	1.46	0.40	1.46	0.09	1.50	0	
Spitalfields Lt Female	1.51	0.47	1.49	0.47	1.49	0.48	1.50	0.50	1.51	0.20	1.51	0
	Af. Am. Rt Male	Af. Am. Lt Male	Af. Am. Rt Fem.	Af. Am. Lt Fem.	Ca. Am. Rt Male	Ca. Am. Lt Male	Ca. Am. Rt Fem.	Ca. Am. Lt Fem.	Spitalf. Rt Male	Spitalf. Lt Male	Spitalf. Rt Fem.	Spitalf. Lt Fem.

Table 3.31: Asymmetry in the femur of males and females of 3 populations. Procrustes distances between sample means of right and left, male and female groups of 3 populations. Correlation between Procrustes distances and Mahalanobis' distances generated by stepwise discriminant analysis (Table 3.28) is: $r = 0.67$; $p < 0.0001$.

PCs	Proportion	Cumulative	PCs	Proportion	Cumulative
PC1	32.6	32.6	PC7	2.9	94.7
PC2	21.9	54.5	PC8	2.2	96.8
PC3	15.6	70.0	PC9	1.2	98.0
PC4	9.9	79.9	PC10	1.2	99.2
PC5	8.0	87.9	PC11	0.8	100.0
PC6	3.9	91.8			

Table 3.32: Proportion and accumulative variance represented by PCs 1-11 for the femur, which accounts for 100% of total variance for sample means.

The first four PCs account for nearly 80% of total variance in the sample and the exploration of shape differences between sides will concentrate on these four PCs.

Figure 3.21 shows the relative location of the twelve samples on PC1 and PC2, as well as a depiction of the mean configuration morphed to the extremes of PC1 and PC2. PC1 and PC2 cumulatively account for 54.4% of total variance.

On PC1, all right sided means are placed more positively than all left sided means, irrespective of sex and population. PC1 more clearly differentiates right and left means than other PCs, with a slightly greater shape variation between the left sided means of the three populations than in the right sided means. In accordance with results using the five populations (sexes pooled), Figure 3.21 shows that the Caucasian American male and female means have the greatest degree of asymmetry with the Spitalfields means showing the least degree. Male and female means of the same side and same population also remain more closely positioned on both PC1 and PC2 than same-sex groups of the opposite side. These results therefore imply that both males and females share a similar degree of asymmetry at the knee joint and that one sex is not more greatly asymmetric than the other.

As male and female means show little sexual dimorphism in relation to asymmetry, with regard to the nature of morphological variation explained by PCs 1 and 2, the same descriptions apply to those given in section 3.4.4a(ii) above; namely, a reorientation of the joint to the diaphysis in the mediolateral plane.

Figure 3.21:

Asymmetry in femur of males and females of 3 population means. Bivariate plot of PC1 with PC2, showing a separation of right and left, male and female means of 3 populations. Arrows point from right to left means of the same sex and same population. Images represent the mean configuration if warped to the extremes of PC1 (0.06 to -0.04) and PC2 (0.04 to -0.03). The image at the positive extreme of PC1 highlights landmarks discussed in the text (section 3.4.5a(ii)).

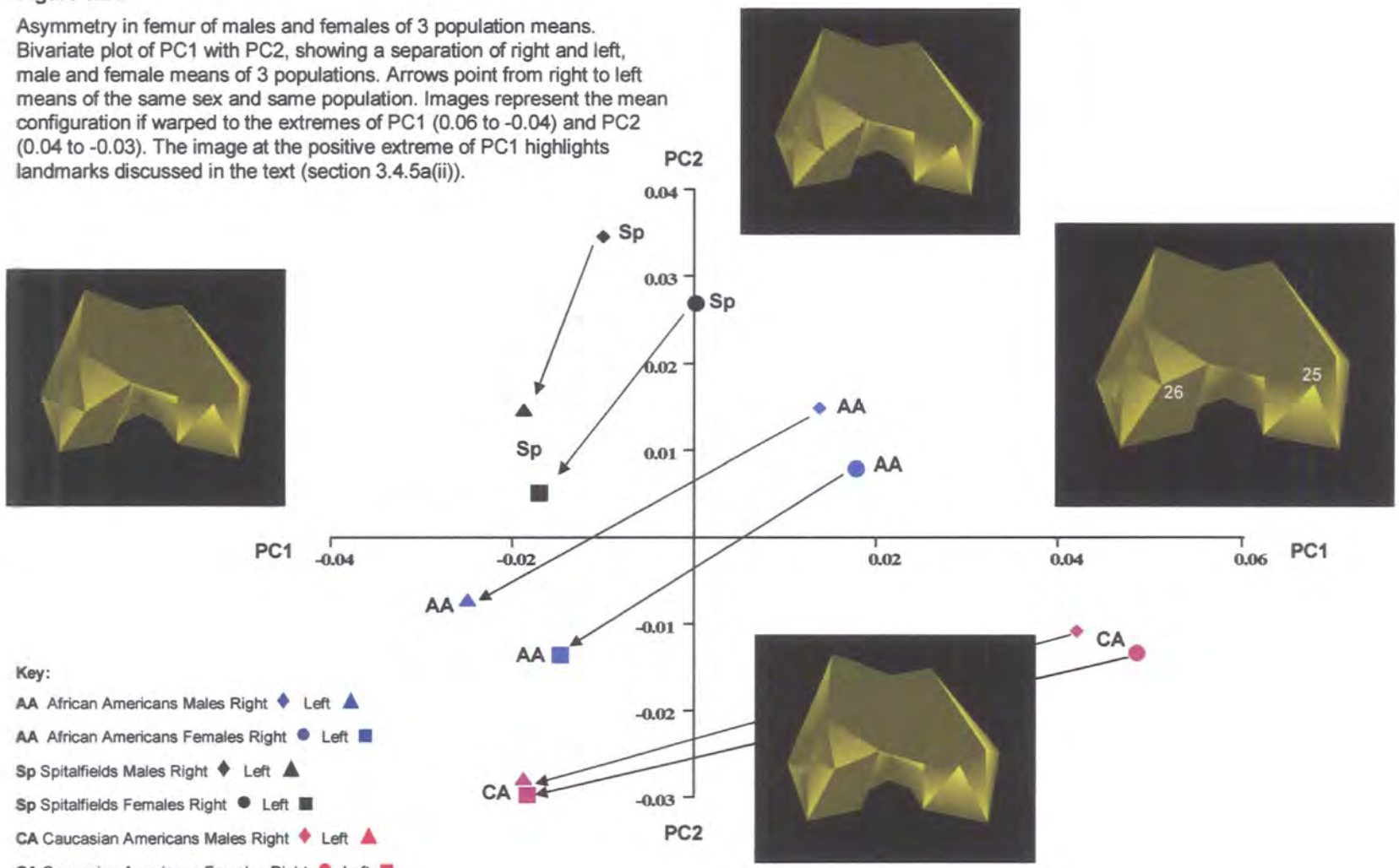

Again, this is best appreciated by observing the relative positions of landmarks 25 and 26, the maximum height of the medial and lateral condyles respectively, although differences are subtle.

Given a relative similarity between males and females of each side and population, the descriptions of morphological variation with sexes pooled explained by both PCs 3 and 4 (section 3.4.4a(ii) above), also apply to this analysis with sexes differentiated. Both PCs 3 and 4 explain slight differences in the proportions of the joint but, as previously noted, whilst the African Americans and the Spitalfields means share similar differences in proportions between right and left sides, the nature of these differences is reversed in the Caucasian Americans. Figure 3.22 shows that along PC3, differences in proportions of the bone appears to relate to an increase in mediolateral width towards the negative extreme (landmarks 19 and 24) relative to anteroposterior length (landmarks 17 to 18 and 21 to 23) towards the positive extreme. Whilst right sided African American and Spitalfields means tend toward greater mediolateral width and left sided means have greater anteroposterior length, this is reversed for the Caucasian American specimens. Differences are small, however, especially between the Spitalfields means.

3.4.5b(i) Tibia: Analyses using the total sample

Differences in shape of the 260 specimens are analysed using the Procrustes fitted co-ordinates and by subjecting the data to PCA. Table 3.33 gives the proportional and accumulated variance for PCs 1 to 56, which represents the total variance within the sample. The scores for each specimen on the resultant PCs are then subjected to canonical discriminant analysis to establish the relationships between populations based upon the Mahalanobis' squared distances between population means.

For the tibia, the best separation of samples of right and left sides for males and females of the three populations is achieved using 90% of total variance. This assessment was reached after separate discriminant and cross-validation analyses were carried out using the PC scores accounting for between c.50% to 100% of total variance. Results are summarised in Figure 3.23.

Figure 3.22:

Asymmetry in femur of males and females of 3 population means. Bivariate plot of PC3 with PC4, showing a separation of right and left, male and female means of 3 populations. Arrows point from right to left means of the same sex and same population. Images represent the mean configuration if warped to the extremes of PC3 (0.04 to -0.04) and PC4 (0.03 to -0.03). The image at the positive extreme of PC1 highlights landmarks discussed in the text (section 3.4.5a(ii)).

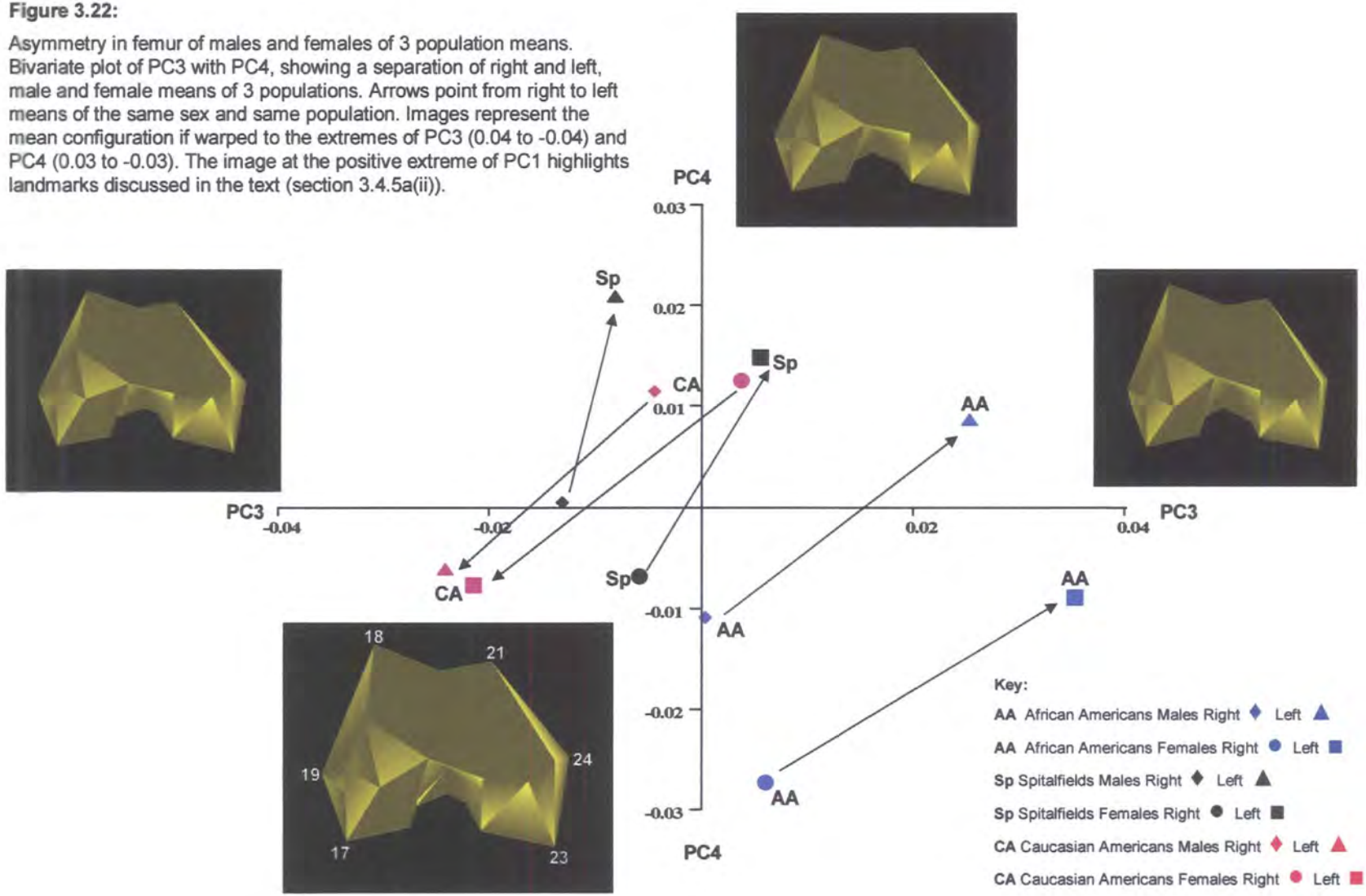

PCs	Prop.	Cumul.	PCs	Prop.	Cumul.	PCs	Prop.	Cumul.
PC1	25.50	25.50	PC21	1.14	83.70	PC41	0.33	97.00
PC2	9.89	35.40	PC22	1.09	84.80	PC42	0.33	97.30
PC3	6.29	41.60	PC23	1.02	85.80	PC43	0.29	97.60
PC4	5.52	47.20	PC24	0.98	86.80	PC44	0.29	97.90
PC5	4.05	51.20	PC25	0.92	87.70	PC45	0.26	98.10
PC6	3.48	54.70	PC26	0.89	88.60	PC46	0.25	98.40
PC7	3.27	58.00	PC27	0.87	89.40	PC47	0.24	98.60
PC8	2.77	60.70	PC28	0.77	90.20	PC48	0.21	98.80
PC9	2.61	63.30	PC29	0.73	90.90	PC49	0.21	99.00
PC10	2.45	65.80	PC30	0.66	91.60	PC50	0.18	99.20
PC11	2.22	68.00	PC31	0.64	92.20	PC51	0.17	99.40
PC12	2.15	70.20	PC32	0.62	92.90	PC52	0.17	99.50
PC13	1.90	72.10	PC33	0.59	93.40	PC53	0.13	99.70
PC14	1.78	73.80	PC34	0.55	94.00	PC54	0.12	99.80
PC15	1.72	75.50	PC35	0.53	94.50	PC55	0.11	99.90
PC16	1.59	77.10	PC36	0.48	95.00	PC56	0.10	100.00
PC17	1.49	78.60	PC37	0.44	95.40			
PC18	1.38	80.00	PC38	0.42	95.90			
PC19	1.33	81.30	PC39	0.40	96.30			
PC20	1.19	82.50	PC40	0.37	96.60			

Table 3.33: Asymmetry in the tibia of males and females of 3 populations: The proportion and accumulated variance for PCs 1-56, which accounts for 100% of total variance.

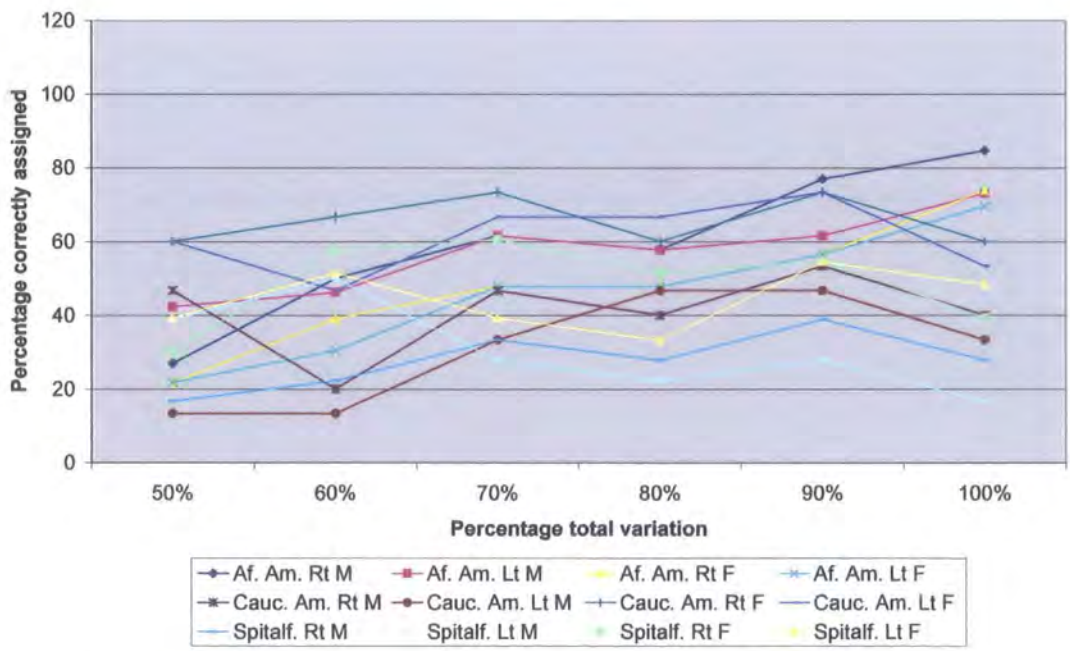

Figure 3.23: Asymmetry in the tibia of males and females of 3 populations. Summary of separate discriminant and cross-validation analyses were carried out using PCs accounting for c.50% of total variance (PCs 1-5), 60% (PCs 1-8), 70% (PCs 1-12), 80% (PCs 1-18), 90% (PCs 1-28) and 100% (PCs 1-56).

The Mahalanobis' squared distances between male and female, right and left sample means, generated by discriminant analysis are shown in Table 3.34. Only those distances between the four African American samples are statistically significant to a high degree, indicating that the male and female, right and left samples of this population can be separated on the basis of some aspect of shape of the proximal tibia. For the Caucasian Americans and Spitalfields population, right and left samples are separated at a level of statistical significance, but for the Spitalfields population males and females of the same side are not separated at a significant level (between right sided males and females p= 0.08; between left sided males and females p= 0.16). For the Caucasian Americans, whilst the left sided males and females are separated at a low level of statistical significance (p= 0.04), the right sided samples cannot be separated (p= 0.09). Table 3.35 illustrates the relationship of each sample to all others on the basis of the generated Mahalanobis' squared distances by showing the distance of each primary sample to all others and ranking them accordingly from the closest sample (at position 1) to the most distant (at position 11).

With two exceptions (African American, right males and right females) the closest sample to the primary sample is the same side from the opposite sex of the same population. In contrast to the femur, however, there is a poorer distinction between right and left sided tibiae to the primary sample; for example, for African American left sided males, three right sided samples remain within the first five positions relative to the primary sample.

In addition, there appears to be little close association within samples of either sex in terms of distance to the primary sample; an indication that asymmetry in shape variation at the proximal tibia is greater than that which may be caused by sexual dimorphism, albeit to a lesser degree than is seen for the femur. As previously noted (section 3.4.4b(ii)) in relation to the analysis examining the five populations with sexes pooled, all four Spitalfields samples show the greatest distance and dissimilarity of shape from all other samples.

AA Rt. Male	0											
	1.000											
AA Lt. Male	9.33	0										
	0.0001	1.000										
AA Rt. Female	14.57	16.01	0									
	0.0001	0.0001	1.000									
AA Lt. Female	16.76	6.69	10.47	0								
	0.0001	0.0001	0.0001	1.000								
CA Rt. Male	14.07	12.04	9.43	9.34	0							
	0.0001	0.0001	0.0001	0.0001	1.000							
CA Lt. Male	21.60	15.74	8.22	9.60	9.03	0						
	0.0001	0.0001	0.0003	0.0001	0.0001	1.000						
CA Rt. Female	20.92	19.29	12.65	15.66	5.89	14.90	0					
	0.0001	0.0001	0.0001	0.0001	0.0923	0.0001	1.000					
CA Lt. Female	28.65	21.93	11.05	12.28	16.97	6.56	15.34	0				
	0.0001	0.0001	0.0001	0.0001	0.0001	0.0407	0.0001	1.000				
Sp Rt. Male	42.29	49.03	47.02	55.66	54.70	57.71	66.44	70.35	0			
	0.0001	0.0001	0.0001	0.0001	0.0001	0.0001	0.0001	0.0001	1.000			
Sp Lt. Male	42.02	41.75	50.51	49.37	58.08	53.61	74.99	67.44	8.26	0		
	0.0001	0.0001	0.0001	0.0001	0.0001	0.0001	0.0001	0.0001	0.0001	1.000		
SP Rt. Female	42.84	48.41	45.12	55.12	52.31	55.56	62.49	67.99	3.85	11.75	0	
	0.0001	0.0001	0.0001	0.0001	0.0001	0.0001	0.0001	0.0001	0.0841	0.0001	1.000	
Sp Lt. Female	40.09	38.25	44.18	45.11	49.03	43.89	64.27	59.34	8.25	3.48	8.25	0
	0.0001	0.0001	0.0001	0.0001	0.0001	0.0001	0.0001	0.0001	0.0001	0.1588	0.0001	1.000
	AA Rt. Male	**AA Lt. Male**	**AA Rt. Female**	**AA Lt. Female**	**CA Rt. Male**	**CA Lt. Male**	**CA Rt. Female**	**CA Lt. Female**	**Sp Rt. Male**	**Sp Lt. Male**	**Sp Rt. Female**	**Sp Lt. Female**

Table 3.34: Asymmetry in the tibia of males and females of 3 populations. Results from the canonical discriminant analysis of right and left, male and female groups from 3 populations, on the basis of 90% total variance. The upper value in red gives the Mahalanobis' squared distance between groups, lower value in black gives the Hotelling's t^2 *p*-value; values in blue denote non-significant results.

Group	1	2	3	4	5	6	7	8	9	10	11
African Am. Rt Male	AALM	CARM	AARF	AALF	CARF	CALM	CALF	SpLF	SpLM	SpRM	SpRF
African Am. Lt Male	AALF	AARM	CARM	CALM	AARF	CARF	CALF	SpLF	SpLM	SpRF	SpRM
African Am. Rt Female	CALM	CARM	AALF	CALF	CARF	AARM	AALM	SpLF	SpRF	SpRM	SpLM
African Am. Lt Female	AALM	CARM	CALM	AARF	CALF	CARF	AARM	SpLM	SpLF	SpRF	SpRM
Cauc. Am. Rt Male	CARF	CALM	AALF	AARF	AALM	AARM	CALF	SpLF	SpRF	SpRM	SpLM
Cauc. Am. Lt Male	CALF	AARF	CARM	AALF	CARF	AALM	AARM	SpLF	SpLM	SpRF	SpRM
Cauc. Am. Rt Female	CARM	AARF	CALM	CALF	AALF	AALM	AARM	SpRF	SpLF	SpRM	SpLM
Cauc. Am. Lt Female	CALM	AARF	AALF	CARF	CARM	AALM	AARM	SpLF	SpLM	SpRF	SpRM
Spitalfields Rt Male	SpRF	SpLF	SpLM	AARM	AARF	AALM	CARM	AALF	CALM	CARF	CALF
Spitalfields Lt Male	SpLF	SpRM	SpRF	AALM	AARM	AALF	AARF	CALM	CARM	CALF	CARF
Spitalfields Rt Female	SpRM	SpLF	SpLM	AARM	AARF	AALM	CARM	AALF	CALM	CARF	CALF
Spitalfields Lt Female	SpLM	SpRF	SpRM	AALM	AARM	CALM	AARF	AALF	CARM	CALF	CARF

Table 3.35: Asymmetry in the tibia of males and females from 3 populations. The order of proximity in distance of each primary right and left, male and female group from the other groups of the 3 populations, on the basis of their Mahalanobis squared distances, as shown in Table 3.34. Figures in red highlight the opposite sex group of the same side and population to the primary group.

Table 3.36 shows the results of cross-validation analysis using the twelve samples. Specimens correctly assigned range from 38.89% for Spitalfields right males to 76.92% for African American right males. Although the percentage of individuals correctly assigned is low in several instances, in most cases the majority of misplaced individuals are of the same side and population but opposite sex. These results again emphasise that for the tibia, shape variation caused by asymmetry is of greater influence than that caused by sexual dimorphism, although this finding is less clear-cut than in the femur.

3.4.5b(ii) Tibia: Analyses using sample means

Because of the high degree of overlap on the bivariate plots of selected PCs (see section 3.4.5b(i) above) when using the total sample, the sample means are used to help determine the specific morphologies of each right and left, male and female sample and to explore the relationships between them. For the tibia, the correlation between the Procrustes distances shown in Table 3.37 and the Mahalanobis' squared distances shown in Table 3.34 is not statistically significant ($r= 0.08$, $p= 0.52$). This result therefore implies that it may be problematic to infer the relative relationships between entire samples solely from the relationships between the sample means. However, it can be seen from Tables 3.34 and 3.35 and Figure 3.24 (the bivariate plot of PCs 1 and 2, using sample means, see below) that there is agreement between results of the two types of analyses, which show the four Spitalfields samples to be more distant relative to all other samples.

The Procrustes mean co-ordinates have been calculated from separate GPAs of each population's right and left side and have been subjected to a joint GPA and PCA.

The proportion and accumulated variance of the PCs generated in the analysis of population means is given in Table 3.38.

Number of Observations and Percent Classified into Group using 90% total variance													
From Group	Af. Am. Rt M	Af. Am. Lt.M	Af. Am. Rt F	Af. Am. Lt F	Ca. Am. Rt M	Ca. Am. Lt M	Ca. Am. Rt F	Ca. Am. Lt F	Spitaf. Rt M	Spitalf. Lt M	Spitalf. Rt F	Spitalf. Lt F	Total
Af. Am. Rt M	20	0	3	1	2	0	0	0	0	0	0	0	26
	76.92	0	11.54	3.85	7.69	0	0	0	0	0	0	0	100
Af. Am. Lt M	0	16	2	4	2	1	1	0	0	0	0	0	26
	0	61.54	7.69	15.38	7.69	3.85	3.85	0	0	0	0	0	100
Af. Am. Rt F	3	0	13	0	2	3	1	1	0	0	0	0	23
	13.04	0	56.52	0	8.7	13.04	4.35	4.35	0	0	0	0	100
Af. Am. Lt F	1	3	1	13	3	1	1	0	0	0	0	0	23
	4.35	13.04	4.35	56.52	13.04	4.35	4.35	0	0	0	0	0	100
Ca. Am. Rt M	1	1	1	0	8	1	3	0	0	0	0	0	15
	6.67	6.67	6.67	0	53.33	6.67	20	0	0	0	0	0	100
Ca. Am. Lt M	0	1	2	0	1	7	0	4	0	0	0	0	15
	0	6.67	13.33	0	6.67	46.67	0	26.67	0	0	0	0	100
Ca. Am. Rt F	0	0	0	0	4	0	11	0	0	0	0	0	15
	0	0	0	0	26.67	0	73.33	0	0	0	0	0	100
Ca. Am. Lt F	0	0	0	0	1	3	0	11	0	0	0	0	15
	0	0	0	0	6.67	20	0	73.33	0	0	0	0	100
Spitalf. Rt M	0	0	0	0	1	0	0	0	7	1	6	3	18
	0	0	0	0	5.56	0	0	0	38.89	5.56	33.33	16.67	100
Spitalf. Lt M	0	1	0	0	0	0	0	0	3	5	0	9	18
	0	5.56	0	0	0	0	0	0	16.67	27.78	0	50	100
Spitalf. Rt F	0	0	0	0	0	0	0	0	10	2	18	3	33
	0	0	0	0	0	0	0	0	30.3	6.06	54.55	9.09	100
Spitalf. Lt F	0	0	0	0	0	0	0	0	3	10	2	18	33
	0	0	0	0	0	0	0	0	9.09	30.3	6.06	54.55	100
Total	25	22	22	18	24	16	17	16	23	18	26	33	260
	9.62	8.46	8.46	6.92	9.23	6.15	6.54	6.15	8.85	6.92	10	12.69	100

Table 3.36: Asymmetry in the tibia of males and females of 3 populations. Separation of right and left, male and female groups from 3 populations using 90% total variance selected by cross-validation analysis. Upper figure denotes number of individuals; lower figure denotes percentage. Red figures denote number of individuals placed into their correct group; blue figures denote misplaced individuals from the opposite sex of the same side and population.

African Am. Rt Male	0											
African Am. Lt Male	1.45	0										
African Am. Rt Female	0.20	1.44	0									
African Am. Lt Female	1.45	0.14	1.44	0								
Caucasian Am. Rt Male	0.39	1.43	0.21	1.42	0							
Caucasian Am. Lt Male	1.46	0.20	1.45	0.19	1.43	0						
Caucasian Am. Rt Female	0.47	1.42	0.30	1.42	0.16	1.42	0					
Caucasian Am. Lt Female	1.44	0.15	1.44	0.18	1.43	0.31	1.43	0				
Spitalfields Rt Male	0.59	1.40	0.56	1.41	0.54	1.38	0.48	1.43	0			
Spitalfields Lt Male	1.39	0.60	1.37	0.49	1.33	0.56	1.34	0.61	1.38	0		
Spitalfields Rt Female	0.44	1.43	0.44	1.43	0.48	1.41	0.46	1.45	0.18	1.40	0	
Spitalfields Lt Female	1.39	0.37	1.37	0.30	1.36	0.46	1.37	0.31	1.42	0.42	1.42	0
	Af. Am. Rt Male	Af. Am. Lt Male	Af. Am. Rt Fem.	Af. Am. Lt Fem.	Ca. Am. Rt Male	Ca. Am. Lt Male	Ca. Am. Rt Fem.	Ca. Am. Lt Fem.	Spitalf. Rt Male	Spitalf. Lt Male	Spitalf. Rt Fem.	Spitalf. Lt Fem.

Table 3.37: Asymmetry in the tibia of males and females of 3 populations. Procrustes distances between sample means of right and left, male and female groups of 3 populations. Correlation between Procrustes distances and Mahalanobis' distances generated by stepwise discriminant analysis (Table 3.34) is: $r = 0.08$; $p = 0.52$

PCs	Proportion	Cumulative	PCs	Proportion	Cumulative
PC1	72.7	72.7	PC7	1.3	97.5
PC2	9.1	81.8	PC8	0.8	98.3
PC3	6.9	88.7	PC9	0.8	99.1
PC4	3.3	91.9	PC10	0.5	99.6
PC5	2.3	94.2	PC11	0.4	100.0
PC6	2.0	96.2			

Table 3.38: Proportion and accumulative variance represented by PCs 1-11 for the tibia, which accounts for 100% total variance for sample means.

The first two PCs account for over 80% of total variance in the sample and the exploration of shape differences between sides will concentrate on these two PCs.

Figure 3.24 shows the location of the twelve means on the bivariate plot of PC1 with PC2, as well as a depiction of the mean configuration morphed to the extremes of PC1 and PC2.

PC1 separates the four Spitalfields means relative to both the African and Caucasian American means. Within each of the three populations, the mean representing both sex and side cluster closely. Morphological variation along PC1 therefore primarily relates to differences between the three populations. Morphological variation at the knee joint between populations is examined in greater detail in Chapter 6.

Morphological variation caused by asymmetry is better explained by PC2, which shows right sided means of both sexes scoring towards the positive extreme of PC2, and all left sided means scoring towards the negative extreme. As the mean configuration is morphed from the positive to negative extremes, it shows the reorientation of the tibial plateau more towards the medial side relative to the diaphysis in right compared to left sided means, as previously noted in section 3.4.4b(ii) above. There also appears, however, to be a small degree of sexual difference in this difference in orientation of joint relative to diaphysis, as all female right or left means are placed more positively than the corresponding right or left male means within the same population. In other words, the knee joint of each

Figure 3.24:

Asymmetry in tibia of males and females of 3 population mean. Bivariate plot of PC1 with PC2, showing a separation of right and left, male and female means of 3 populations. Arrows point from right to left means of the same sex and same population. Images represent the mean configuration if warped to the extremes of PC1 (0.09 to -0.09) and PC2 (0.04 to -0.04). The image at the positive extreme of PC1 highlights landmarks discussed in the text (section 3.4.5b(ii)).

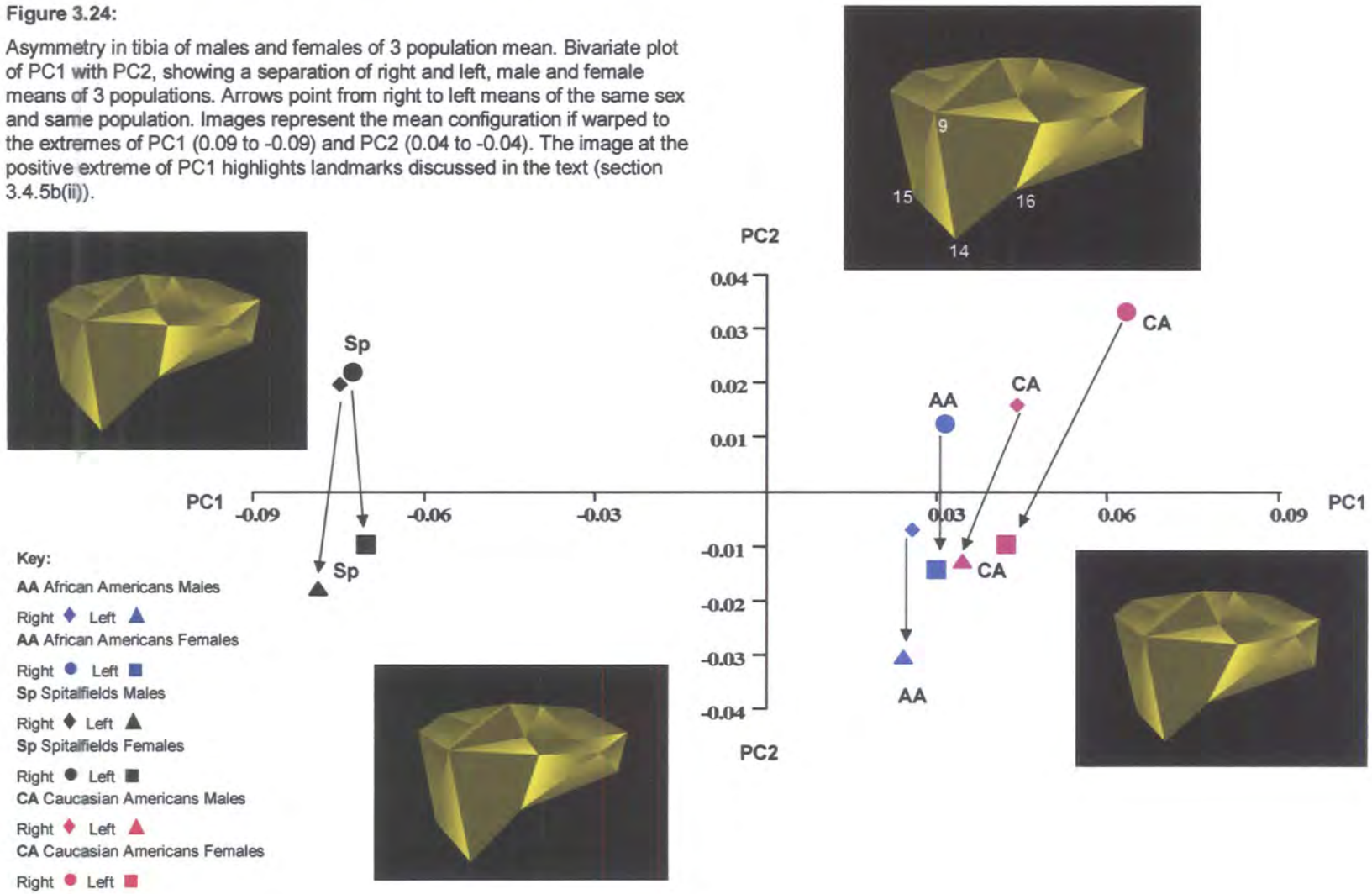

female individual appears to be slightly more oriented towards the medial side relative to the corresponding male mean of their own population. In the mean configuration in Figure 3.24, the difference in orientation can be seen in the respective positions of landmarks 9, 14, 15 and 16 in the anterior region of the joint.

3.5 Discussion

For the femur, results show marginally greater length of the left limb relative to the right (at approximately 1% or less of total length), which supports previous research by Inglemark (1943, 1974), Huelster (1953), Marsk (1953), Latimer and Lowrance (1957), Chibber and Singh (1970), and Hayes et al. (1978). In no instance, however, are results statistically significant. The results for the tibia show less consistency with one of the five populations (the Arikara) showing hypertrophy on the right side. Like the femur, the percentage differences between sides is less than 1% for the tibia, with the exception of the Arikara, and all cases fail to reach a level of statistical significance.

Results show there is no consistent directional asymmetry in the robusticity of the diaphyses for either the femur or tibia between the five populations. In comparisons of right and left diaphyses, percentage differences are small with a maximum for pooled-sex populations of 1.30% for the femur (Arikara) and 1.41% for the tibia (Arikara), and in no instance do results reach a level of statistical significance. Results also show that there is no great disparity in asymmetry in the length or the robusticity between the sexes. Although small differences are apparent, for example in the difference in length between right and left sides of female Spitalfields limbs relative to males, the overall percentage differences remain small and statistically non-significant.

Hypothesis H.3.1 states that there is no significant difference in the means of the lengths and means of the robusticity indices between right and left femora and tibiae in *Homo sapiens* for the five populations examined in this study. Despite indicating a notional degree of directional asymmetry, results for both femur and tibia are not significant and hypothesis H.3.1 is therefore supported.

For the centroid size of the knee joint, all results show that differences between right and left sides are marginal at approximately 1% or less for both femur and tibia (with the exception of the Spitalfields female distal femur), and, although the right side is consistently hypertrophic, results do not reach statistical significance in any case. Therefore, any significant differences in the form of the knee joint must be ascribed to shape.

For the shape of the knee joint, results from this study show that differences exist between right and left joints for both femur and tibia in the African American sample, at a high level of statistical significance (p=0.001). Analyses conducted on the African American sample using GPA and PCA reaching conclusions of asymmetry of shape, are supported by results obtained using the invariant approach to statistical analysis using EDMA.

The African American samples are included in analyses comparing specimens of right and left knee joints with those of four additional populations. Results indicate that for both femur and tibia, there is a clear and statistically significant difference in shape between right and left sides in all five population samples.

For the femur, the directional asymmetry in this part of the skeleton is strong with samples from all populations being most similar in shape to other samples of the same side but from different populations. In two of the five populations (the Arikara and Chinese), the assignment of specimens to the correct group reaches 100% accuracy. For the tibia, the indication of asymmetry between sides remains statistically significant in all cases but the degree of asymmetry is less pronounced than in the femur. PC2 clearly separates all right from all left sided means. For four of the five populations, the relationship of right and left sides appears similar in nature. As these four pairs of means include the African Americans, the asymmetric differences in shape noted for this population when using the total sample, which primarily relates to the orientation of the knee joint to the diaphysis, must therefore be similar in nature to the other four populations with the same spatial relationships. In the fifth population, the Arikara, the relationship between the right and left means is reversed; therefore it can be assumed that the orientation of the knee joint to the shaft is also reversed, relative to the other four populations. Asymmetric shape

differences in the proportions of both knee joints appears to be of lesser significance compared to those relating to the orientation of the joints relative to the diaphyses and are expressed in the higher PCs.

For the tibia, PC2 also clearly separates the five pairs of right and left means. The relationship between pairs of means and thus the nature of the asymmetry is relatively similar in four of the five population pairs (including the African Americans) and reversed in the fifth, Spitalfields population. Additional reference to the analysis of African American tibiae using the total sample confirms that the nature of the asymmetric shape variation, like the femur, is primarily related to the orientation of the knee joint to the diaphysis in the mediolateral plane. The fifth, sample, Spitalfields, shows not only a difference in the nature of asymmetry but also an overall difference in the shape of the right and left pair relative to the other four samples.

For the distal femur, the degree of asymmetry between the five populations is variable and there is a clear difference between the Spitalfields sample (with a relatively small degree of asymmetry, compared to the Caucasian Americans with the greatest degree of asymmetry) between the five samples. For the tibia, the degree to which asymmetry is expressed between the five samples is relatively similar, particularly on PC2.

The results of this study showing the statistically significant nature of the asymmetry at the knee joint for both the femur and tibia must be regarded as a clear expression of directional asymmetry, as random differences at the level of the individual, creating fluctuating asymmetry, would be equalised at the level of the population. The nature of this asymmetry is not identical in every population and, particularly in relation to the distal femur, is not identical in degree. These results therefore support evidence produced by previous workers such as Sadeghi (2000), who showed that the lower limbs do *not* behave symmetrically in normal, able-bodied walking; conclusions that also support work by Kettlekamp et al. (1970). Subsequent research by Nordin and Frankel (2001) also show that different phases of gait produce different results for the means of degrees of movement for each knee (see section 3.2), again lending support to the concept of asymmetry of shape at the knee joint.

Whilst differences in size between right and left sides are not statistically significant for either the knee joint or the diaphyses, the differences in knee joint shape are highly statistically significant. Therefore, if only a single size measurement, such as maximum intercondylar notch height is used to compare different samples (e.g., Craig, 1995; Gill, 2001) it would be valid to use the best preserved side from each specimen. If research requires overall knee joint shape to be compared between samples, however, results here indicate that it is not viable to use both right and left bones within any single data set.

From these results, it appears that hypothesis H.3.2, (that there is no significant difference in asymmetry in the size and shape of the knee joint in *Homo sapiens*), can only be supported in relation to size. With respect to differences in shape between right and left knee joints for both femur and tibia, results show the presence of directional asymmetry at a high level of statistical significance, which partly falsifies hypothesis H.3.2

Hypothesis H.3.3 states that there is a no significant difference in asymmetry in the shape of the knee joint between males and females in *Homo sapiens.* The results from this study show that, for both femur and tibia, there is a statistically significant difference in asymmetry between the knee joints of males and females of the same population in some (but not all) cases. It is also apparent that shape differences due to sexual dimorphism within each population are secondary to those due to asymmetry.

Results show that the degree of asymmetric differences between males and females varies between the three population samples, with the Caucasian Americans showing the greatest degree of asymmetry overall (particularly in relation to the femur) but showing little difference in that expressed by males and females. In terms of the nature of asymmetric variation between males and females, it is apparent from the relationships of means on PC2 for the femur and PC2 for the tibia, which best separate groups in the two analyses, that the degree of orientation of the female joint relative to the shaft is greater than that of the corresponding male, in some (but not all) cases; exceptions being, Caucasian American left males relative to left females

for the femur and tibia; Caucasian American right males relative to right females for the tibia and Spitalfields right males relative to right females for the tibia.

The number of instances where a statistically significant difference in asymmetry is apparent between males and females of the same population lends weight to the research of Ruff (1984, 1994, 2000), Bridges (1985, 1989), Freesia et al. (1990) and Larsen (1997), amongst others. Whilst such research states that differences in asymmetry are present in both the internal and external architecture of the diaphyses between males and females, this study has also shown that differences are present between male and female right sided and male and female left sided knee joint specimens. Therefore, whilst it is not possible to conclusively falsify hypothesis H.3.3, results indicate that a degree of asymmetric variation is present between the sexes in some populations.

Results from this study, showing the knee joint in *Homo sapiens* to be asymmetric in shape, is possibly predictable in the light of previous knowledge. Research has shown that asymmetry in behavioural traits is deeply embedded in the human condition, probably affecting all aspects of the human body and psychology and extending far enough back to include other species of *Homo*, even as far distant as *Homo erectus* (Coren and Porac, 1977; Steele, 2000). Indeed, behavioural asymmetry appears to be deeply embedded in the behaviour of many species, including other primate species, together with other mammals, birds and reptiles (McManus, 2003), although probably not to the same degree as in humans (Steele, 2000). This strong tendency towards both right handedness and footedness is also known to be largely genetically controlled (McManus, 2003; Faurie and Raymond, 2004). It develops at an acutely early foetal stage (Ruff and Jones, 1981; McManus, 2003), and results in frequently inexplicable associations between physiological conditions and behavioural traits (McManus et al., 2004). Researchers have attributed a direct association between the development of behavioural laterality with the embryonic lateralisation of the cortex of the brain, but recent evidence points to an even earlier development in asymmetry (Irving et al., 1974; Hepper et al., 1998). Plochocki (2002), (supporting earlier work by Huelster (1953)), indicates that directional asymmetry in the sacrum shows a strong correlation with handedness but little correlation with age (or sex). This lack of change in the sacrum associated with

age suggested to Plochocki (2002, p353) that "asymmetry is developed in most individuals during endochondral bone growth and is maintained through adulthood". This conclusion supports other studies that show a marked asymmetry in the lengths of the femur and foot in human foetuses as young as four months gestation, well before significant activity-related stress factors are operative (Ruff and Jones, 1981). It also supports work that shows behavioural asymmetry in arm and leg movements in foetuses as young as ten weeks gestation; even before the neurons in the brain have become connected to the spinal cord (Hepper et al., 1998; Steele, 2000; McManus, 2003). Research into this early stage of development, however, is rudimentary and not all results have proved conclusive (Steele and Mays, 1995; Steele, 2000). At whatever stage of early development asymmetries become evident, however, side preference appears to be present prior to the development of greater skill in using the preferred side but greater usage of the preferred side will inevitably create developmental asymmetry (Inglemark, 1974; McManus, 2003).

Research indicates that there is some degree of sexual dimorphism in relation to directional asymmetry embedded into the genetic make-up of humans (Annett, 1985) and accentuated by behavioural patterns (Ruff, 2000, 1994, 1984; Larsen, 1997; Bridges, 1985, 1989; Freesia et al., 1990; Sakaue, 1998; Roy et al., 1994, amongst others). Whilst the proportion of left-handed to right-handed individuals is known to vary within a limited range between societies (Steele, 2000; Faurie and Raymond, 2004), in all societies the proportion of left-handed males to females is always greater with an average of five males to four females (Steele, 2000; McManus, 2003). Evidence of a higher proportion of females with right-sided dominance in the upper limbs (specifically humeral length) compared to males from a variety of cross-cultural contexts has also been reported (Schultz, 1937; Wilczak, 1998). Various researchers have attempted to explain the origins of sexual dimorphism in the asymmetry of bilateral traits, including the suggestion of a direct genetic causation; possibly in the X-chromosome but reflecting the action of a modifying gene or genes (McManus, 2003). Such conclusions are tentative, however, and at this stage of research there appears to be relatively little understanding of sexual dimorphism in relation to handedness, let alone other forms of sidedness.

3.6 Implications of results and direction of future research

It has been clearly established that there is a statistically significant difference in shape between right and left knee joints in *Homo sapiens*. Therefore, it is not valid to use both right and left specimens in any data set, when comparing shape between samples.

Given this premise, implications of these results arise from two further assertions. The first is that cerebral lateralisation leading to preferential footedness in *Homo sapiens* is partly or wholly responsible for asymmetry of shape between sides in the lower limbs and feet. This assumption is based on previous research that indicates an early development for this preferential footedness *in utero* (Ruff and Jones, 1981; Irving et al., 1974; Hepper et al., 1998; Steele, 2000; McManus, 2003; Plockocki, 2003). The second is that because of the innate predisposition in humans for using their legs differentially (Kettlekamp et al., 1970; Sadeghi, 2000; Nordin and Frankel, 2001), greater loading pressure on one side will accentuate any differences in the morphology of that side relative to the other.

Because it is known that the lower limbs do not behave symmetrically in normal able-bodied walking, it can be hypothesised that this difference in use between sides is an expression of preferential footedness. It also implies that preferential footedness is itself, highly correlated with the habitual bipedalism of *Homo sapiens*. As outlined in section 3.5, previous research indicates that, although asymmetry is embedded in the behaviour of many non-human species as well as *Homo sapiens,* preferential handedness and footedness is rarely expressed as strongly at the species level as in humans. With respect to other primate species, there are few conclusive results of a species-level handedness in monkeys and apes, although individuals often show strong handed preferences, particularly in relation to specific tasks and even preferences in handedness by one sex over the other in relation to the same task (Hopkins, 1996; Singer and Schwibbe, 1999; Parnell, 2001; Wesley et al., 2002; Hopkins et al., 2003; Corp and Byrne, 2004).

Future research should therefore be directed towards an assessment of the degree and nature of asymmetry in the knee joint of other non-human species; principally, other

primate species. If no significant asymmetry is found in non-human primates, it can be inferred that there is a positive correlation in humans between the phenomena of strong preferential sidedness, habitual bipedalism and skeletal asymmetry. If, however, significant degrees of asymmetry are found in the knee joint of other species that are not habitually bipedal, it would appear that there is a relatively tenuous link between the expressed degree of laterality of handedness and footedness at the species level and asymmetry of shape of the limbs and joints. In these circumstances, therefore, either the normal mode of locomotion of non-human species is eliciting the same response in creating or accentuating morphological asymmetry in the joints that bipedalism does in *Homo sapiens,* or that the cerebral laterality in many vertebrate and bird species (McManus, 2002), is fundamentally responsible for causing a degree of shape asymmetry in the limbs, or indeed that a combination of both these factors (and, possibly, more) are responsible.

The second assumption implies that asymmetrically applied loading pressures throughout the individual's lifetime will accentuate differences in morphology between the joints. An extreme example of this is the greater degree and earlier manifestation of osteoarthritis in one limb that is used to operate machinery; such as, for example, the type of weaving handloom that required the direct use of one leg only, used in early industrial processes (Bythell, 1969).

The condyles of the knee joint, particularly the proximal tibia, accept significant weight-bearing in relation to the downward pressure of the body's mass (see Chapter 1 sections 1.5.2 and 1.7.2). In those individuals involved in occupations exerting great pressure on the knee, this is thought to be expressed in relatively greater *size* of the condyles, particularly the lateral condyle, which accepts three-fifths of the downward pressure (Heberden Society, 1969). In individuals using one limb excessively, greater asymmetry in centroid size of the condyles, especially of the proximal tibia, would therefore be predicted. Results here indicate, however, that in no instance is there a statistically significant difference in centroid size between joints for either the distal femur or proximal tibia. This applies even to the Spitalfields population, which is known to have included handloom silk weavers (although for this sample, it is not known how many individuals were themselves weavers or if the machinery used required the direct use of one or both legs).

Given the above expectation that asymmetrically applied abnormal loading is more likely to affect the relative *size* of the articular surfaces in some (but unlikely, all) individuals within a sample, the implication for these results is that the asymmetry of *shape* found in these samples tested is neither atypical nor pathological. In addition, results using the African Americans as a sample population show that the right and left specimens for both femur and tibia are clearly asymmetric in shape for *all* individuals. Therefore, the implications from these results are that asymmetry in the knee joint is *primarily* innate. It appears, therefore, that environmental pressures are likely to be of secondary influence, determining how the population-specific aspect of this asymmetry is manifest.

3.7 Direct implications of results for this study

As the morphology of right and left knee joints differs at a high level of statistical significance, specimens from one side only (the right) will be used for all subsequent analyses. Although differences in the lengths of the long bones are not found to be statistically significant, for consistency throughout the study, only right limbs will be used for comparisons in subsequent analyses.

Chapter 4

Sexual dimorphism in the form of the knee joint of six populations of *Homo sapiens*

4.1 Introduction

This chapter assesses the possible presence of sexual dimorphism in the form of the knee joint and size of the lower limbs in *Homo sapiens*. One population, (African Americans), is used for detailed analyses into possible sex differences in the morphology of knee joint surfaces for the distal femur and proximal tibia. This population is chosen for detailed analysis as it has a greater number of sexed specimens in the collection than other samples. Five additional populations, (Caucasian Americans, the Spitalfields collection, the Aleut, Arikara and Pachacama), are then included for comparing and contrasting any possible shape differences found between African American males and females with those found in other samples. Supplementary analyses comparing the length and robusticity of the femora and tibiae are included to provide additional insight into possible form differences between male and female knee joints.

4.2 Examination of issues relating to sexual dimorphism in the lower limbs

Recent literature has concentrated upon two aspects of sexual dimorphism in the postcranium; firstly, the estimation of sex from fragmentary remains for diagnostic purposes and secondly, the effects of changes in subsistence strategies on the skeleton.

Diagnosis of sex from fragmentary remains of the lower limb bones is based on features recognised to be more dimorphic in size rather than shape, such as shaft length and circumference, proportions of the femoral head and epicondylar breadth. Size has always been considered of paramount importance, as males are on average bigger than females. The most gracile elements are therefore likely to be female as some skeletal elements can be up to 20% bigger in males (White, 2000). In one of the best-referenced works on sexing the femur, Black (1978) stated that sexual dimorphism in width and circumference often exceeds sexual dimorphism in length. This belief was reiterated by

Dittrick and Suchey (1986) who produced better separation of the sexes using the ends of long bones rather than the lengths of shafts and suggested a change of emphasis from the diaphyses to the bone ends in future research.

Iscan and co-workers (1984a, 1984b, 1986, 1994, 1996) investigated sexual dimorphism in the tibia, together with a comparison of the degree of sexual dimorphism in the tibia compared to the femur. They stated that previous authors had found the tibia to be the more sexually dimorphic bone, although such research had concentrated upon shaft dimensions as the benchmark, namely around the nutrient foremen in the tibia and at the mid-shaft in the femur. When using a more complete set of measurements, however, they found that (in shaft dimensions alone), the tibia was indeed the more dimorphic bone but by extending these measurements to include the ends of the bones, and more especially the femoral head, the femur was found to be the more dimorphic. A later study by Steyn and Iscan (1997) found the tibia and femur to be almost equally dimorphic across various measurements in Caucasian Americans, but concluded that such findings would not apply to all populations or indeed to the same population through time. This reinforced their previous findings that tibial shaft circumference was a better sex assessor for Caucasian Americans but that length was a better sex assessor for African Americans and native North Americans (Iscan and Millar-Shaivitz, 1984b).

Iscan and Millar-Shaivitz (1984b) concluded that sexual dimorphism in both the femur and tibia is a population specific phenomenon. They also stated that the effects of changes in musculoskeletal activity and therefore differences in growth and subsequent remodelling of bone between the sexes as well as between geographic variants, may increase (or decrease) expected dimorphism. This viewpoint has been extended in numerous pieces of research into the skeletal implications of changes in subsistence strategies including, Ruff and Hayes (1983), Brock and Ruff (1988), Bridges (1989), Hawkey and Merbs (1995), Larsen (1995). All such research indicates that declining levels in the sexual division of labour from hunter-gatherer economies to agriculture and industrialisation have reduced levels of sexual dimorphism.

In the light of previous research, this chapter will focus on four aspects of sexual dimorphism;

1. To evaluate the degree and nature of sexual dimorphism in the size of the femur and tibia and in the size and shape of the knee joint.
2. To evaluate whether sexual dimorphism in the two bones is a population specific phenomenon.
3. To determine whether the shape of the knee joint of males and females of the same population is more similar to each other relative to the shapes of other groups.
4. To determine whether the degree of sexual dimorphism in the tibia is greater than that of the femur.

Issues raised by previous research will suggest the following hypotheses:

H.4.1 The degree of sexual dimorphism in maximum length measurements and the robusticity indices of the femur and tibia are identical across the six populations.

H.4.2 The degree of sexual dimorphism in the centroid size of the knee joint is identical across the six populations.

H.4.3 The degree and nature of sexual dimorphism in the femur and tibia is a population-specific phenomenon.

H.4.4 The shape of the knee joint of males and females from the same population is more similar relative to the shape of the knee joint of any other group.

H.4.5 The tibia is a more sexually dimorphic bone compared to the femur.

4.3 Materials and Methods

The six different population samples of modern humans used in the analyses of shape and the analyses of centroid size of the knee joint include 185 right male and 161 right female femora and 177 right male and 160 right female tibiae. The same population samples used for the analyses of size measurements of the long bones include 179 right male and 160 right female femora and 178 right male and 165 right female tibiae. The composition and original locations of the data sets are shown in Tables 4.1 and 4.2.

All analyses of shape are conducted on all landmarks for both distal femur and proximal tibia. The specimens are superimposed using Generalised Procrustes Analysis (GPA) and the Procrustes fitted data are subjected to Principal Components Analysis (PCA). These methods are described in Chapter 2 sections 2.2.3c and 2.2.3d.

The centroid sizes used for comparisons of size of the knee joints are calculated in *morphologika*© as part of the GPA analyses. The correlation analyses of size relating to the centroid sizes of the knee joint and to the maximum length and robusticity indices of the long bones are calculated using Microsoft Excel. All comparisons of size between males and females are expressed as a percentage of the female size relative to a percentage of the male size. Use of the t-test is described in Chapter 2 sections 2.2.3k.

Population	Femur Males	Femur Females	Tibia Males	Tibia Females	Location of collection
African Americans	63	59	57	59	NMNH
Caucasian Americans	30	28	30	28	NMNH
Spitalfields	35	42	36	45	NHM
Arikara	24	10	22	10	NMNH
Aleut	15	11	17	9	NMNH
Pachacama	18	11	15	9	NMNH
Total number	185	161	177	160	

Table 4.1: The composition and original locations of the data sets used for the analyses of shape and centroid size of the femur and tibia.

Population	Femur Males	Femur Females	Tibia Males	Tibia Females	Location of collection
African Americans	63	58	63	66	NMNH
Caucasian Americans	30	29	30	29	NMNH
Spitalfields	34	37	32	37	NHM
Arikara	24	12	21	11	NMNH
Aleut	18	12	20	12	NMNH
Pachacama	10	12	12	10	NMNH
Total number	179	160	178	165	

Table 4.2: The composition and original locations of the data sets used for the analyses of maximum length (M2) and robusticity indices (RI) of the femur and tibia.

NMNH: National Museum of Natural History, Smithsonian Institution, Washington, DC
NHM: Natural History Museum, London

4.4 Results

4.4.1 Sexual dimorphism of the maximum length and robusticity indices of the diaphyses of the femur and tibia

4.4.1a Femur

Tables 4.3 and 4.4 show comparisons of maximum length measurements and robusticity indices of specimens of male and female femora from the six samples. Table 4.3 gives the means of maximum length measurements for the six populations and, using the Student's t-test, shows a statistically significant difference between males and females of each sample. The greatest degree of sexual dimorphism lies with the Aleutians, with female size as a percentage of male size at 91.19% and the least difference with the Caucasian Americans at 94.41%. The percentage difference between males and females using the total sample is 92.64%. Results therefore indicate that the difference between male and female maximum length is highly significant at t= 9.49; $p<0.0001$.

Table 4.4 shows that the pattern of male size being consistently greater than female size seen in maximum length, is repeated for femoral robusticity indices. The percentage difference between males and females ranges from the Spitalfields group with the least degree of sexual dimorphism at 98.75% to the Pachacama with the greatest degree at 93.48%. Results, however, reveal that only in the African and Caucasian American samples is female robusticity statistically significantly different relative to male robusticity. Despite the differences within separate samples, when using the total sample, the difference between male and female robusticity indices is highly significant at t= 4.28; $p<0.0001$ with a percentage difference in size between males and females of 96.55%.

Population	Male Mean Length	M. Min-Max Range	Female Mean Length	F. Min-Max Range	% of mean F to M size	t =	*p* =
African Americans	470.68	408-431	435.79	380-487	92.59	7.63	<0.0001
Caucasian Americans	453.2	402-530	427.86	384-465.	94.41	4.07	<0.0001
Spitalfields	438.18	394-480	408.95	320-465	93.33	4.67	<0.0001
Arikara	445.43	390-485	410.33	381-434	92.12	4.66	<0.0001
Aleut	417.61	363-449	380.83	350-420	91.19	4.68	<0.0001
Pachacama	409.7	383-432	377.83	351-402	92.22	5.34	<0.0001
All Individuals	449.54	363-531	417.88	320-487	92.963	9.49	<0.0001

Table 4.3: Comparison of maximum length measurements of the femur between males and females of 6 populations using the total sample.

Population	Male Mean Robusticity	Male Min-Max Range	Female Mean Robusticity	Female Min-Max Range	% of mean F to M size	t =	*p* =
African Americans	6.21	4.85-7.05	6.05	5.27-6.90	97.42	2.15	0.03
Caucasian Americans	6.37	5.35-7.04	5.96	4.93-6.94	93.56	3.49	0.0009
Spitalfields	6.40	5.75-8.73	6.32	5.31-8.12	98.75	0.62	0.54
Arikara	6.42	5.45-7.69	6.15	5.75-6.47	95.79	1.80	0.08
Aleut	6.81	6.29-7.39	6.66	6.02-7.71	97.80	1.01	0.32
Pachacama	6.60	5.31-7.30	6.17	5.55-6.65	93.48	2.00	0.06
All Individuals	6.38	4.85-8.73	6.16	4.93-8.12	96.55	4.28	<0.0001

Table 4.4: Comparison of robusticity indices of the femur between males and females of 6 populations using the total sample.

4.4.1b Tibia

Tables 4.5 and 4.6 show the results of size comparisons of maximum length and robusticity indices of specimens of male and female tibiae from the six populations. Table 4.5 gives the means of maximum length for the six populations and shows a statistically significant difference between males and females from each sample. The greatest degree of sexual dimorphism lies with the Arikara at 91.17% and the population with the least sexual dimorphism, like the femur, is the Caucasian Americans at 94.33%. The percentage difference, using the total sample is 92.44% and is statistically significant at t= 8.02; $p<0.0001$.

Table 4.6 shows that the pattern of male size being consistently greater than female size in maximum length of the shaft is repeated for the robusticity indices. Although males are seen as relatively more robust in all cases, however, results fail to reach statistical significance in two of the six samples. The greatest degree of difference between male and female robusticity indices lies with the Pachacama, with female robusticity as a percentage of male size at 90.66% and the least difference lies with the Arikara at 98.54%. The percentage difference between males and females, using the total sample is 98.49% and is statistically significant at t=5.81; p<0.0001.

For maximum length measurements for the total sample, the femur and tibia are seen to be identical in the degree of sexual dimorphism with a percentage size difference between males and females of 92.96. For the six samples analysed separately, the range between those with the least degree of sexual dimorphism (Caucasian Americans for both bones) to the greatest degree (Aleut for the femur and Arikara for the tibia) is also relatively close at between 91.19% and 94.41% (3.22% difference) for the femur and 91.17% and 94.33% (3.16% difference) for the tibia.

Population	Male Mean Length	M. Min-Max Range	Female Mean Length	F. Min-Max Range	% of mean F to M size	t =	*p* =
African Americans	403.17	311-471	371.38	320-437	92.11	7.01	<0.0001
Caucasian Americans	375.7	330-447	354.41	322-393	94.33	3.86	0.0003
Spitalfields	365.53	329-394	334.97	289-391	91.64	5.99	<0.0001
Arikara	381.81	342-419	348.09	330-370	91.17	4.92	<0.0001
Aleut	335.15	299-376	310	280-333	92.5	3.54	0.001
Pachacama	347.92	329-380	323.2	299-343	92.89	4.18	0.0005
All Individuals	377.89	299-471	351.3	280-437	92.964	8.02	<0.0001

Table 4.5: Comparison of maximum length measurements of the tibia between males and females of 6 populations using the total sample.

Population	Male Mean Robusticity	Male Min-Max Range	Female Mean Robusticity	Female Min-Max Range	% of mean F to M size	t =	*p* =
African Americans	7.7	5.96-10.53	7.45	6.28-8.68	96.75	2.27	0.02
Caucasian Americans	7.9	6.10-9.39	7.23	6.54-8.09	91.52	4.60	<0.0001
Spitalfields	7.88	6.55-8.86	7.65	6.10-8.97	97.08	1.60	0.12
Arikara	7.73	6.14-8.48	7.62	6.60-8.37	98.58	0.60	0.55
Aleut	8.69	7.61-10.56	8.02	6.82-9.13	92.29	2.67	0.01
Pachacama	7.85	7.15-8.62	7.11	6.52-7.71	90.57	3.88	0.0009
All Individuals	7.89	5.96-10.56	7.49	6.10-9.13	94.93	5.81	<0.0001

Table 4.6: Comparison of robusticity indices of the tibia between males and females of 6 populations using the total sample.

For robusticity, the tibia is seen as the more sexually dimorphic of the two bones with a female-to-male size for the total sample of 94.93%, compared to 96.55% for the femur. The tibia is also seen as the more variable bone in degrees of relative robusticity between males and females of the six separate samples, with a range of 8.50% difference between samples from the least degree of sexual dimorphism to the greatest. The femur shows less variation, with a range of 5.27% between samples from the least degree of sexual dimorphism to the greatest.

4.4.2 Sexual dimorphism of centroid size of the knee joint

4.4.2a Femur

Table 4.7 shows that the difference in means of centroid size of the femoral knee joint between males and females of each sample is statistically significant to a high degree. Results also show that sexual dimorphism is greater in the centroid size of the knee joint in each sample than that of either maximum length or robusticity indices of the femur. The most sexually dimorphic group is the African American population with a percentage difference of 88.77%, and the least dimorphic is the Spitalfields population at 90.89%. The percentage difference between males and females using the total sample is 90.02%. This is statistically significant at $t=16.92$; $p<0.0001$.

4.4.2b Tibia

Table 4.8 shows that for the tibia, like the femur, the difference between males and females for each population is statistically significant to a high degree. Results show that sexual dimorphism is greater in the centroid size of the proximal tibia in each sample than in either maximum length or robusticity indices. As with the femur, the most sexually dimorphic sample for the tibia is the African Americans with a percentage difference of 87.55% and the least sexually dimorphic is the Caucasian Americans at 89.99%. The percentage difference between males and females using the total sample is 88.86%, and is statistically significant at $t= 20.14$; $p<0.0001$.

Population	Mean Male Centroid size	Mean Female Centroid size	% of mean F to M size	t =	*p* =
African Americans	166.71	147.99	88.77	15.35	<0.0001
Caucasian Americans	162.28	146.12	90.03	7.87	<0.0001
Spitalfields	157.59	143.23	90.89	7.41	<0.0001
Arikara	160.17	143.93	89.86	7.18	<0.0001
Aleut	157.49	142.18	90.28	5.25	<0.0001
Pachacama	146.31	131.47	89.86	5.81	<0.0001
All Individuals	160.69	144.65	90.02	16.92	<0.0001

Table 4.7: Comparison of centroid size of the distal femur between males and females of 6 populations using the total sample.

Population	Mean Male Centroid size	Mean Female Centroid size	% of mean F to M size	t =	*p* =
African Americans	145.31	127.21	87.55	15.56	<0.0001
Caucasian Americans	140.78	126.69	89.99	7.93	<0.0001
Spitalfields	135.36	121.56	89.81	9.98	<0.0001
Arikara	141.09	124.6	88.32	9.8	<0.0001
Aleut	134.71	118.46	87.94	6.69	<0.0001
Pachacama	132.99	118.43	89.05	6.65	<0.0001
All Individuals	139.93	124.36	88.87	20.14	<0.0001

Table 4.8: Comparison of centroid size of the proximal tibia between males and females of 6 populations using the total sample.

4.4.2c Summary of size measurements

In relation to the centroid size, the tibia is the more sexually dimorphic bone using the total sample, with a percentage size difference of 11.14% between male and female specimens. This compares to a difference of 10.05% for the distal femur. For both bones, the degree of sexual dimorphism in the size of the knee joint is considerably greater than in maximum length of the long bone (7.04% size difference between males and females, for both femur and tibia) and, especially, in the robusticity of the shaft (3.45% size difference for the femur and 5.07% for the tibia). Results are summarised in Table 4.9.

Size Measurement	Femur: Female size as percentage Male size	Femur: Range of percentage diff. in size bet. samples	Tibia: Female size as percentage Male size	Tibia: Range of percentage diff. in size bet. samples
Maximum Length of Shaft	92.96	7.04	92.96	7.04
Robusticity Indices of Shaft	96.55	3.45	94.93	5.07
Centroid Size of Knee Joint	89.95	10.05	88.86	11.14

Table 4.9: Summary of female-to-male size comparisons of maximum length and robusticity indices of the diaphyses and centroid sizes of the knee joint, using the total sample.

4.4.3 Sexual dimorphism of shape of the knee joint: African Americans

The African American sample is used as an example to establish the presence of sexual dimorphism in one population of modern humans. If found to be present in this sample, the nature and degree of dimorphism will be used to compare and contrast results and the description of sex differences with five additional populations.

4.4.3a(i) Femur

Differences in shape of the femur in 122 specimens from 63 males and 59 females are analysed using the Procrustes fitted co-ordinates and by subjecting the data to PCA. Table 4.10 gives the proportional and accumulated variance for PCs 1 to 71, which represents the total variance within the sample. The scores for each specimen on the resultant PCs are then subjected to canonical discriminant analysis to establish the relationships between male and female samples based upon the Mahalanobis' squared distances between sample means.

Because sex differences are likely to form only a small proportion of the overall variation within the sample, the use of scores on all PCs (i.e., the total variance in the sample) may not adequately discriminate differences due to sex alone. Therefore, canonical stepwise discriminant function analysis is used to determine which PCs relate more specifically to sexual dimorphism. Table 4.11 shows the PCs selected by the stepwise discriminant analyses for the African American sample. Predictably, the best separation of male and female specimens is achieved using the PCs selected by the stepwise discriminant analysis. The results using PCs accounting for c.50% to 100% of total variation and those used in the stepwise discriminant function analyses are summarised in Figure 4.1.

The Mahalanobis' squared distance generated by stepwise discriminant analysis between the means of male and female samples is 6.04 and statistically significant at $p<0.0001$,

PCs	Prop.	Cumul.	PCs	Prop.	Cumul.	PCs	Prop.	Cumul.
PC1	9.21	9.2	PC26	1.13	84.3	PC51	0.22	98
PC2	7.53	16.7	PC27	1.02	85.3	PC52	0.20	98.2
PC3	6.78	23.5	PC28	0.99	86.3	PC53	0.18	98.4
PC4	6.44	30.0	PC29	0.89	87.2	PC54	0.18	98.6
PC5	5.03	35.0	PC30	0.84	88.0	PC55	0.16	98.8
PC6	4.71	39.7	PC31	0.82	88.9	PC56	0.14	98.9
PC7	4.32	44.0	PC32	0.81	89.7	PC57	0.13	99.0
PC8	4.06	48.1	PC33	0.77	90.4	PC58	0.12	99.2
PC9	3.67	51.8	PC34	0.66	91.1	PC59	0.12	99.3
PC10	3.07	54.8	PC35	0.65	91.8	PC60	0.11	99.4
PC11	2.89	57.7	PC36	0.61	92.4	PC61	0.09	99.5
PC12	2.87	60.6	PC37	0.60	93.0	PC62	0.09	99.6
PC13	2.56	63.1	PC38	0.53	93.5	PC63	0.08	99.6
PC14	2.40	65.6	PC39	0.50	94.0	PC64	0.07	99.7
PC15	2.21	67.8	PC40	0.48	94.5	PC65	0.07	99.8
PC16	2.00	69.8	PC41	0.46	94.9	PC66	0.05	99.8
PC17	1.91	71.7	PC42	0.42	95.3	PC67	0.05	99.9
PC18	1.77	73.4	PC43	0.40	95.7	PC68	0.04	99.9
PC19	1.65	75.1	PC44	0.39	96.1	PC69	0.03	100
PC20	1.62	76.7	PC45	0.34	96.5	PC70	0.02	100
PC21	1.44	78.2	PC46	0.30	96.8	PC71	0.02	100
PC22	1.34	79.5	PC47	0.28	97.1			
PC23	1.25	80.7	PC48	0.27	97.3			
PC24	1.24	82.0	PC49	0.26	97.6			
PC25	1.20	83.2	PC50	0.23	97.8			

Table 4.10: Sexual Dimorphism in the femur in African Americans. The proportion and accumulated variance for PCs 1-71, which accounts for 100% of total variance

Order	Entered	Order	Entered	Order	Entered
1	PC1	8	PC11	15	PC17
2	PC7	9	PC26	16	PC29
3	PC33	10	PC12	17	PC19
4	PC10	11	PC4	18	PC20
5	PC27	12	PC9	19	PC62
6	PC3	13	PC8	20	PC44
7	PC28	14	PC56	21	PC21

Table 4.11: PCs selected by stepwise discriminant analysis and the order of entry of selected PCs for the femur.

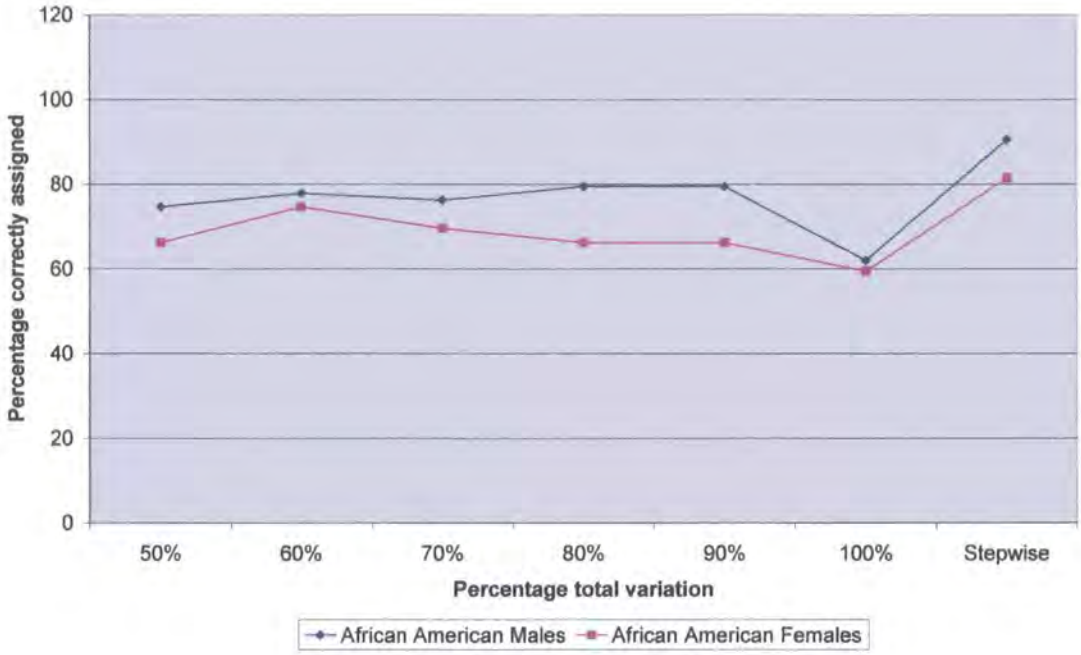

Figure 4.1: Sexual Dimorphism in the femur in African Americans. Summary of separate discriminant and cross-validation analyses using PCs accounting for c.50% of total variance (PCs 1-9), c.60% (PCs 1-12), c.70% (PCs 1-16), c.80% (PCs 1-22), c.90% (PCs 1-32), 100% (PCs 1-71) and stepwise discriminant analysis.

indicating that the two sexes can be separated on some aspect of shape of the distal femur. The crossvalidation of African American male and female specimens using discriminant function analysis generated by the selected PC scores, results in 90.48% of males and 81.36% of females being correctly assigned to group.

4.4.3a(ii) Femur: Description of differences in shape between males and females

PCs 1, 7, 33 and 10 are the first four PCs selected by stepwise discriminant analysis. Using the Student's t-test, these four are the only PCs with significantly differently scores for male and female specimens; PC1 at t= 4.20, $p<0.0001$; PC7 at t= 3.88, $p<0.0001$; PC33 at t= 2.41, $p= 0.02$; and PC10 at t= 2.28, $p= 0.02$.

Figure 4.2 shows a bivariate plot of PC1 with PC7, which account for 9.21% and 4.32% of total variance, respectively. Figure 4.2 shows a tendency for more male specimens to concentrate on the positive side of the scale of PC1, with females towards the negative

Figure 4.2:

Sexual Dimorphism in the African American femur, total sample. Bivariate plot, showing the overlap of male and female specimens along the scales of PCs 1 and 7 (first and second PCs selected by stepwise discriminant analysis). Images represent the mean configuration at the extremes of PC1 (at 0.06 and -0.09) and PC7 (at 0.05 and -0.05). Larger image at the positive extreme of PC1 includes landmarks discussed in section 4.4.3a(ii).

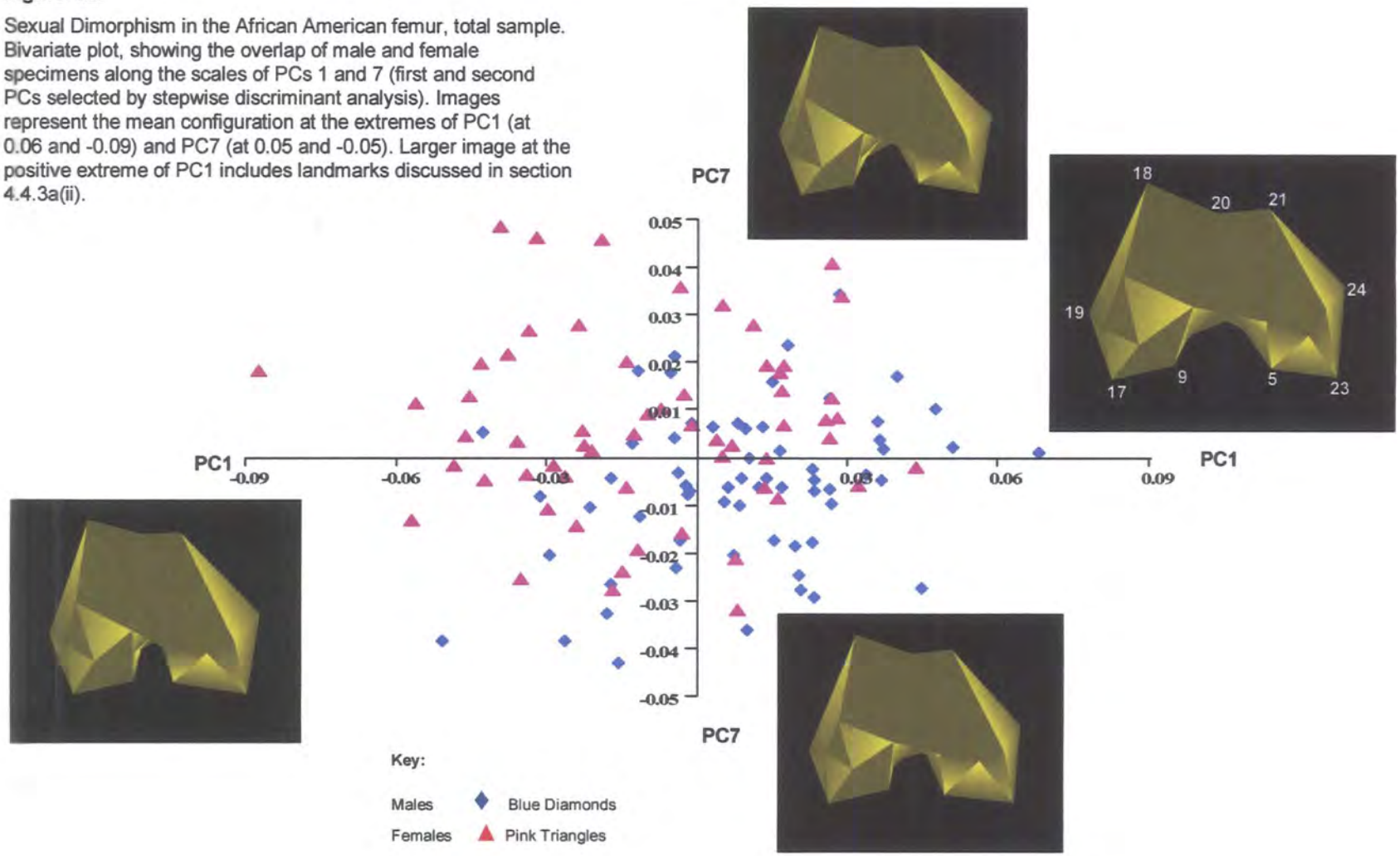

extreme. There is, however, too great an overlap of males and females to allow an assessment of any morphological differences between them. The greatest shape variation explained by PC1 is in overall mediolateral width; both epicondylar width (as represented by landmarks 19 to 24) and across the intercondylar fossa (landmarks 5 to 9). This difference in width can also be seen across the anterior patella surface (landmarks 18, 20 and 21). The increase in mediolateral width is accompanied by a decrease in anteroposterior length (landmarks 17 to 18 and 21 to 23), together with a slight repositioning of the joint relative to the shaft on the lateral side. This orientation of the joint towards the lateral side is seen more in specimens on the negative side of the scale, which includes more females than males.

PC7 accounts for variation in the relative positions of the condyles in the mediolateral plane. The degree of overlap between individuals of both sexes, however, is even greater for PC7 than for PC1. Because of the overlap between the majority of male and female specimens, variation explained by PCs 1 and 7 should largely be construed as attributable to the range of morphological differences throughout the complete sample rather than to specific sexual dimorphism within the sample. As individual PCs selected by stepwise analysis, including PCs1 and 7, fail to show any apparent degree of separation of male and female specimens in bivariate plots using the total sample, it is assumed that the statistically significant separation of the two sexes ($p<0.0001$) results from the accumulation of incremental degrees of variance contributed by all relevant PCs. Therefore, the sample means of each of the two sexes have also been used to help distinguish specific variation due to sexual dimorphism.

The Procrustes mean co-ordinates have been calculated from the two separate GPAs of the male and female samples and have been subjected to a joint GPA and PCA. Because it calculates on the basis of two specimens only, PC1 accounts for 100% of total variance. Whilst the visually obvious increase in mediolateral width between landmarks 19 to 24 and 5 to 9 in Figure 4.2 is less apparent when using the male and female sample means, the mean configuration at each end of the scale in Figure 4.3 emphasises the

Figure 4.3:

Sexual Dimorphism in the African American femur. Separation of mean male and female specimens of African Americans on PC1. Images represent the mean configuration if warped to the extremes of PC1 (at 0.04 to –0.04). The images at the positive extreme include landmarks discussed in the text (section 4.4.3a(ii)).

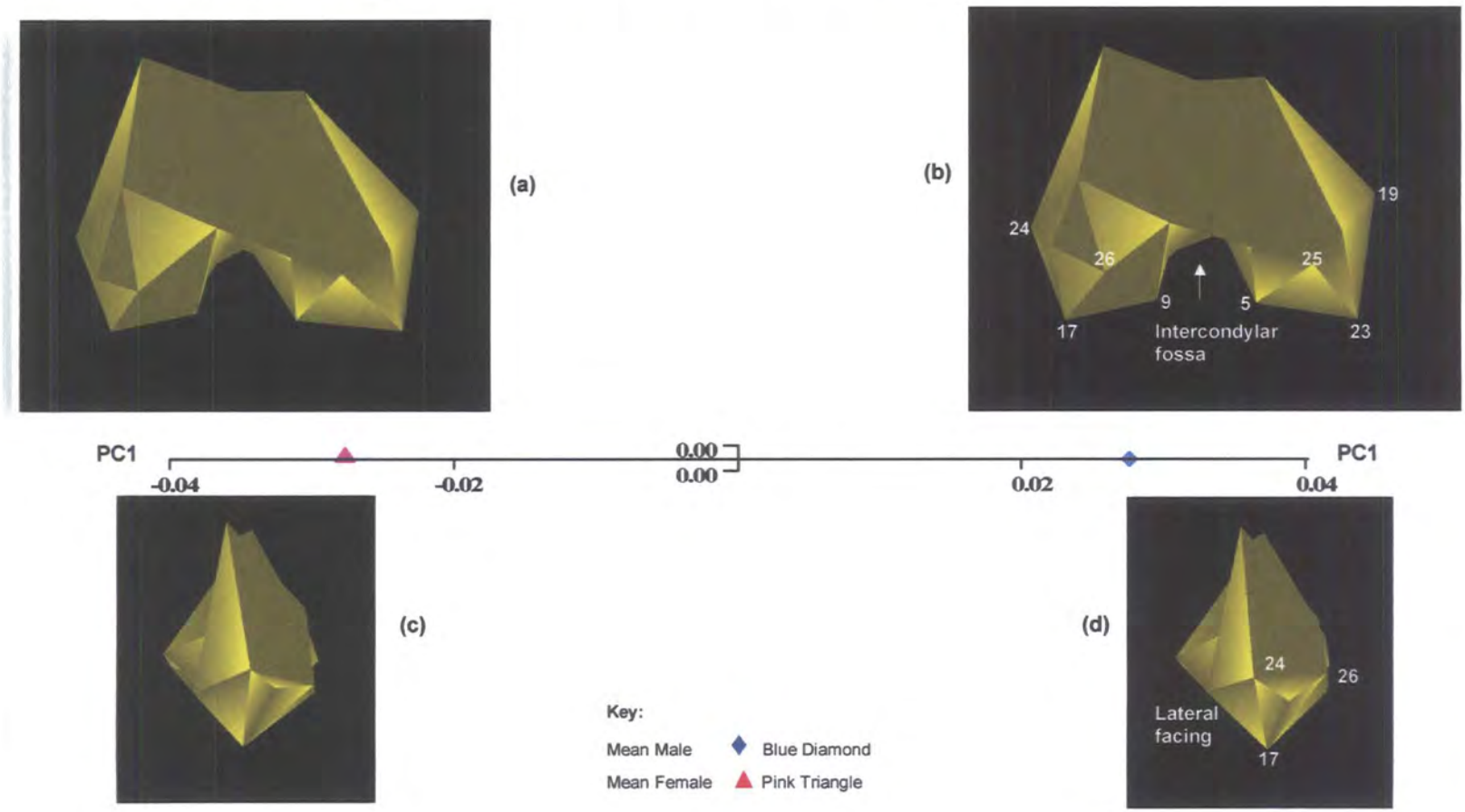

difference in the position of the joint relative to the shaft particularly on the lateral side, also noted in the description of Figure 4.2 above. This is most clearly seen in the difference in the visible area of the intercondylar fossa between the male mean at the positive end of the scale and the female on the negative side, although the actual dimensions of the fossa do not appear to alter when the mean configuration is morphed between the two extremes (Fig. 4.3 (a) and (b)). The relative change in position of the more laterally oriented female mean compared to the male is also seen in the relative positions of landmarks 23 to 25 (on the medial side) and 17 to 26 (on the lateral side) and by comparing the shape of images in Figs. 4.3 (c) and (d) when viewed laterally. The greater sexual dimorphism in the lateral side of the joint is emphasised in Figure 4.4, which shows the maximum degree of deformation of the TPS on PC1 over the lateral condyle in both the anteroposterior and distal planes.

4.4.3b(i) Tibia

Differences in shape of the 116 specimens from 57 males and 59 females are analysed using the Procrustes fitted co-ordinates and by subjecting the data to PCA. Table 4.12 gives the proportional and accumulated variance for PCs 1 to 56, which represents the total variance within the sample. The scores for each specimen on the resultant PCs are then subjected to canonical discriminant analysis to establish the relationships between male and female samples based upon the Mahalanobis' squared distances between sample means.

Stepwise discriminant analysis is also used for the proximal tibia to determine which PCs more specifically relate to shape differences caused by sexual dimorphism. Table 4.13 shows the PCs selected by the stepwise discriminant analyses for the African American sample. Predictably, the best separation of male and female specimens is achieved using the PCs selected by stepwise discriminant analysis. The results using PCs accounting for c.50% to 100% of total variation and those used in the stepwise discriminant function analyses are summarised in Figure 4.5. The Mahalanobis' squared distance between the sexes is 16.96 and is statistically significant at $p<0.0001$,

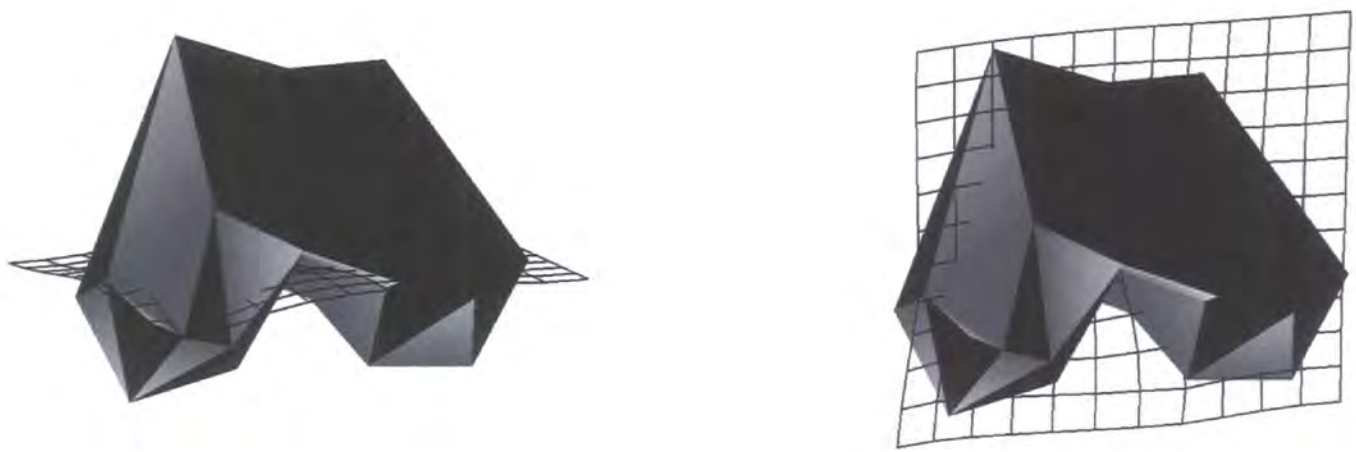

(a) (b)

Figure 4.4: Sexual Dimorphism in the African American femur. Representations of femoral shape with TPS taken from PC1 using male and female sample means, showing regions of bone giving maximum difference in shape between means. Figures 4.4(a) represents TPS view in anterior-posterior plane; 4.4(b) in distal plane. Images are presented in Figure 4.4 to give the best indication of maximum difference in shape on PC1 and are not necessarily taken from the same perspective as the mean configurations in Figure 4.3.

PCs	Prop.	Cumul.	PCs	Prop.	Cumul.	PCs	Prop.	Cumul.
PC1	12.80	12.8	PC21	1.29	84.3	PC41	0.30	97.7
PC2	9.16	21.9	PC22	1.18	85.5	PC42	0.29	98.0
PC3	7.48	29.4	PC23	1.14	86.7	PC43	0.24	98.2
PC4	6.79	36.2	PC24	1.07	87.7	PC44	0.23	98.4
PC5	6.01	42.2	PC25	0.97	88.7	PC45	0.21	98.6
PC6	5.20	47.4	PC26	0.91	89.6	PC46	0.21	98.9
PC7	4.30	51.7	PC27	0.83	90.4	PC47	0.20	99.1
PC8	3.69	55.4	PC28	0.76	91.2	PC48	0.18	99.2
PC9	3.50	58.9	PC29	0.71	91.9	PC49	0.15	99.4
PC10	3.29	62.2	PC30	0.65	92.6	PC50	0.13	99.5
PC11	3.10	65.3	PC31	0.64	93.2	PC51	0.12	99.6
PC12	2.76	68.1	PC32	0.61	93.8	PC52	0.10	99.7
PC13	2.63	70.7	PC33	0.58	94.4	PC53	0.09	99.8
PC14	2.38	73.1	PC34	0.54	94.9	PC54	0.07	99.9
PC15	2.14	75.2	PC35	0.48	95.4	PC55	0.07	99.9
PC16	1.88	77.1	PC36	0.46	95.9	PC56	0.05	100
PC17	1.75	78.8	PC37	0.40	96.3			
PC18	1.47	80.3	PC38	0.38	96.7			
PC19	1.44	81.8	PC39	0.36	97.0			
PC20	1.31	83.1	PC40	0.35	97.4			

Table 4.12: Sexual Dimorphism in the tibia of African Americans. The proportion and accumulated variance for PCs 1-56, which accounts for 100% of total variance

Order	Entered	Order	Entered	Order	Entered	Order	Entered
1	PC1	8	PC14	15	PC53	22	PC20
2	PC6	9	PC44	16	PC24	23	PC15
3	PC5	10	PC19	17	PC51	24	PC7
4	PC32	11	PC42	18	PC31	25	PC33
5	PC2	12	PC10	19	PC37	26	PC54
6	PC11	13	PC49	20	PC16	27	PC27
7	PC4	14	PC9	21	PC55	28	PC39

Table 4.13: PCs selected by stepwise discriminant analysis and the order of entry of selected PCs for the tibia.

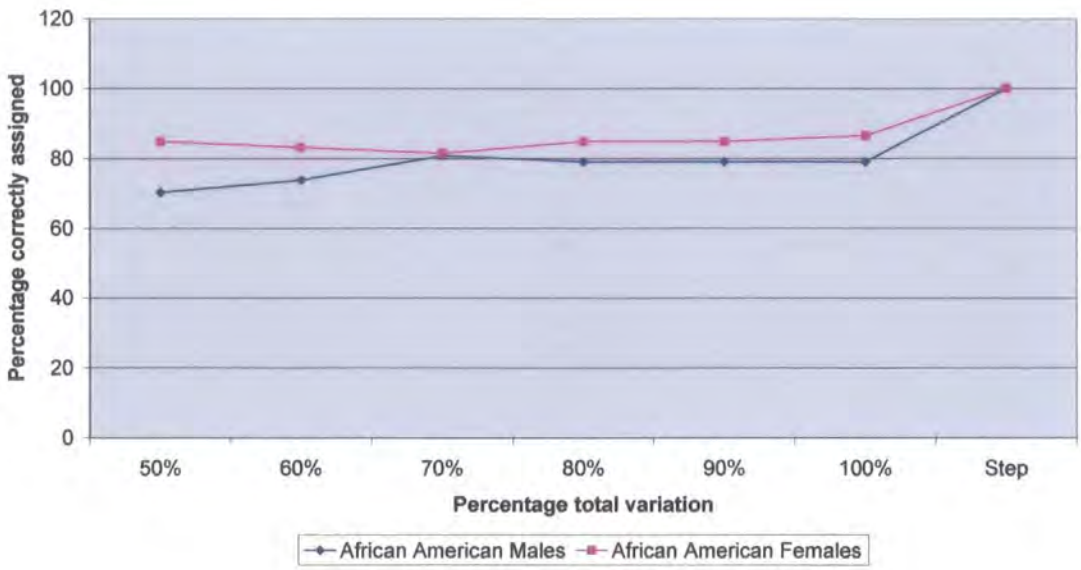

Figure 4.5: Sexual Dimorphism in the tibia in African Americans. Summary of separate discriminant and cross-validation analyses using PCs accounting for c.50% of total variance (PCs 1-7), c.60% (PCs 1-9), c.70% (PCs 1-13), c.80% (PCs 1-18), c.90% (PCs 1-27), 100% (PCs 1-56) and stepwise discriminant analysis

indicating that the two sexes can be separated on some aspect of shape of the proximal tibia. The crossvalidation of African American male and female specimens results in 100% of male and female specimens being correctly assigned to group.

4.4.3b(ii) Tibia: Description of differences in shape between males and females

PCs 1, 6, 5 and 32 are the first four PCs selected by stepwise discriminant analysis. Using the Student's t-test, these four are the only PCs with significantly different scores for male and female specimens; PC1 at t= 4.91, $p<0.0001$; PC6 at t= 4.60, $p<0.0001$; PC5 at t= 3.59, $p= 0.0005$; and PC32 at t= 3.02, $p= 0.003$. Figure 4.6 shows a bivariate plot of PC1 with PC6 which account for 12.80% and 5.20% of total variance respectively. As for the femur, PCs 1 and 6 for the tibia show a considerable overlap of male and female specimens, although there is a slightly higher concentration of males on

Figure 4.6:

Sexual Dimorphism in the African American tibia, total sample. Bivariate plot, showing the overlap of male and female specimens on PCs 1 and 6 (first and second PCs selected by stepwise discriminant analysis). Images represent the mean configuration if warped to the extremes of PCs 1 (at 0.16 and -0.08) and PC6 (at 0.05 and -0.05). Larger image at the positive extreme of PC1 includes landmarks discussed in section 4.4.3b(ii).

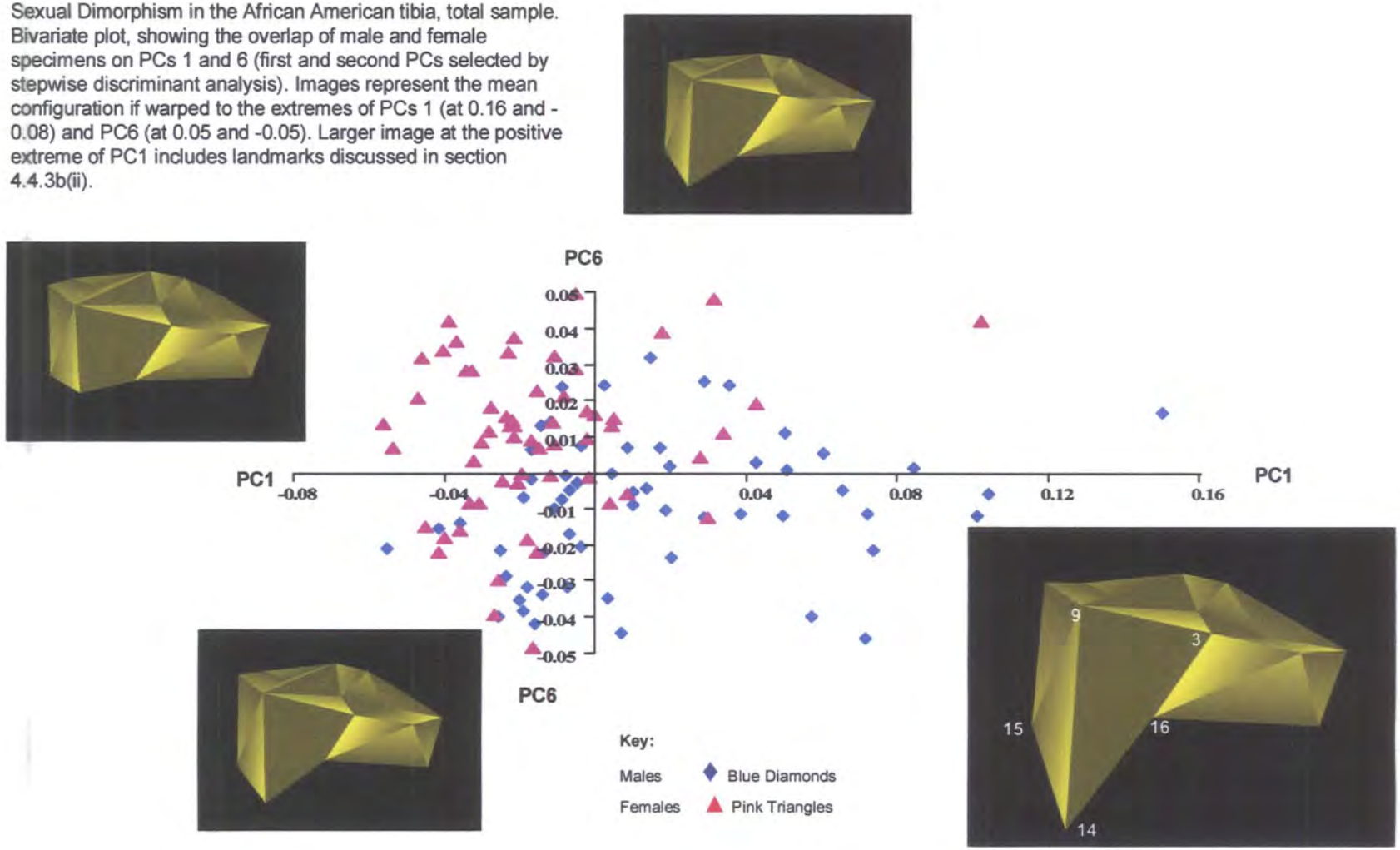

the positive side of PC1. When using the total sample, the most visually apparent variation explained by PC1 is in the length of the anterior section. The greatest distance between the tibial tuberosity (landmarks 14, 15 and 16) and the edge of the tibial plateau (landmarks 3 and 9) is seen in specimens towards the positive extreme of the scale, which has a higher concentration of males.

PC6 explains a slightly greater degree of relative projection of the anterior section of the tibial tuberosity in specimens scoring more positively relative to those on the negative side. The overlap of male and female specimens is high along the scale of PC6, although there are a slightly higher proportion of females placed more positively.

Like the femur, because of the high degree of overlap in specimens shown in Figure 4.6 and apparent in other PCs selected by stepwise analysis, including PCs 5 and 32 (not shown), it must be assumed that the statistically significant separation of the two sexes ($p<0.0001$) results from the accumulation of small degrees of variance contributed by all relevant PCs. For the tibia, the sample means of each of the two sexes have also been used to help distinguish variation due to sexual dimorphism.

The Procrustes mean co-ordinates have been calculated from the two separate GPAs of the male and female samples and have been subjected to a joint GPA and PCA. Because it calculates on the basis of two specimens only, PC1 accounts for 100% of total variance.

The notable difference between specimens in the length of the anterior section seen in Figure 4.6, using the total sample, is reflected to a lesser degree in Figure 4.7 when using male and female sample means. Figure 4.7 shows that the male mean has slightly greater anterior length between the tibial tuberosity and the edge of the tibial plateau relative to the female mean; seen in the relative distances between landmarks 14, 15 and 16 and landmarks 3 and 9, in Figure 4.7(a) and (b). Although the degree of difference in anterior length is smaller when using the means, there remain distinct implications for

Figure 4.7:

Sexual Dimorphism in the African American tibia. Separation of African American male and female means on PC1. Images represent the mean configuration if warped to the extremes of PC1 (at 0.04 to –0.04). The images at the positive extreme (b) and (d) include landmarks discussed in the text (section 4.4.3b(ii)).

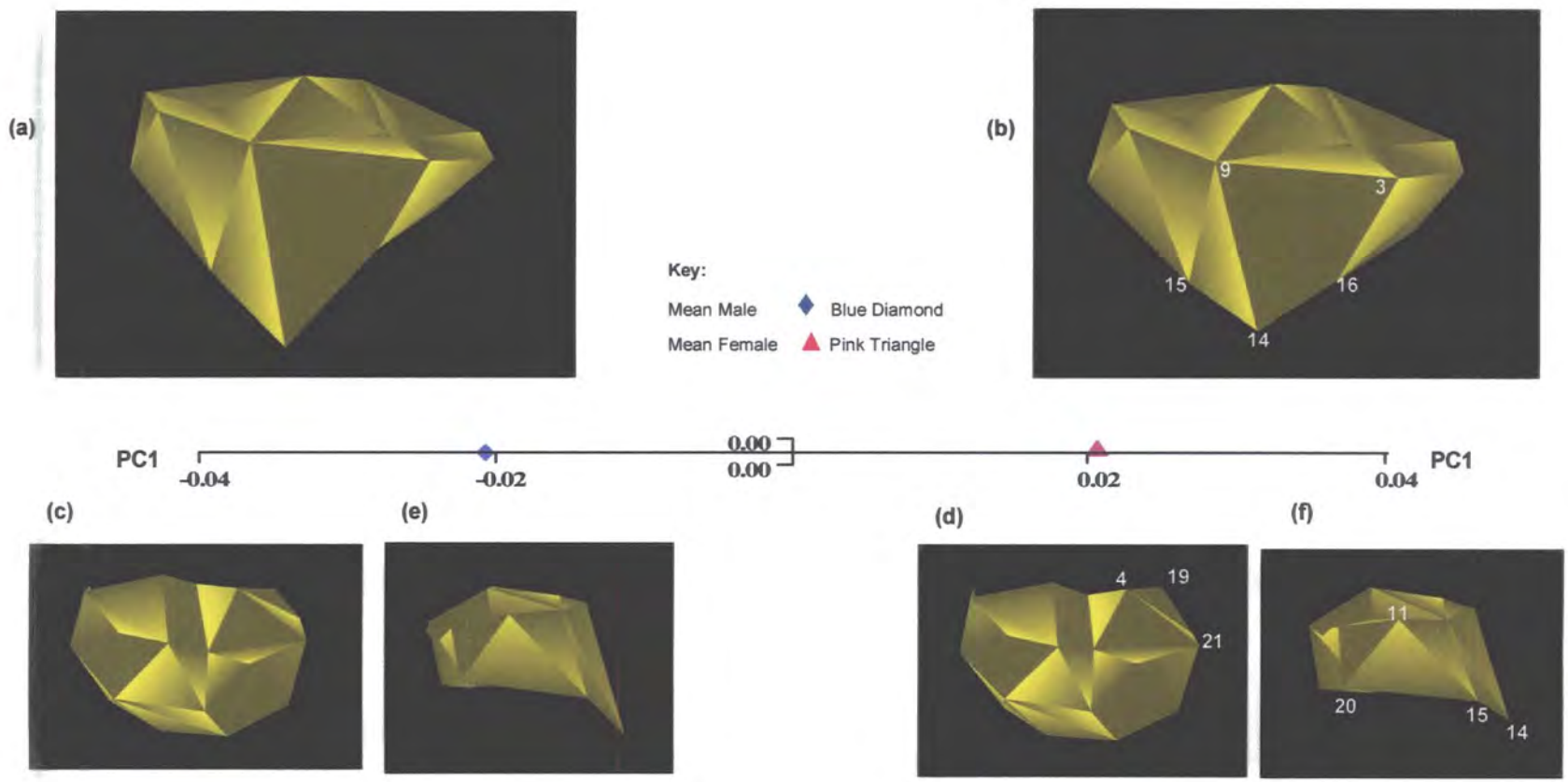

for the proportions of the tibial shelf. This difference is optimally seen in the relative difference in angle between landmark 4 (at the medial posterior edge of the tibial plateau) and landmarks 19 and 21 on the medial side of the tibial shelf and in (e) and (f) in the relative difference in angles made between landmarks 11, 15 and 20 and 14, 15 and 20 on the lateral side of the tibial shelf. If any differences occur in mediolateral width or anteroposterior length across the tibial plateau between the male and female means, they are less visibly obvious.

Figure 4.8, which shows the deformation of the TPS on PC1 across the tibia in three planes, confirms the maximum difference between male and female means is in the anterior section. The greater degree of sexual dimorphism observed in the lateral side of the femur is also apparent in the tibia, although to a less obvious degree. This is confirmed by the slight deformation over the lateral side seen in Figure 4.8(c).

4.4.4 Sexual dimorphism in the shape of the knee joint; six populations analysed jointly

The analyses of the African American samples have established the presence of sexual dimorphism in the knee joint for both the distal femur and proximal tibia. This section seeks to determine the presence of sexual differences in five other population samples in addition to the African Americans and compares sexual dimorphism in these groups with that found in the African Americans. The five populations include the Caucasian Americans, Spitalfields, the Arikara, Aleut and Pachacama.

4.4.4a(i) Femur

Differences in shape of the 347 specimens from 185 males and 162 females are analysed using the Procrustes fitted co-ordinates and by subjecting them to PCA. Table 4.14 gives the proportional and accumulated variance for PCs 1 to 71, which represents the total variance within the sample.

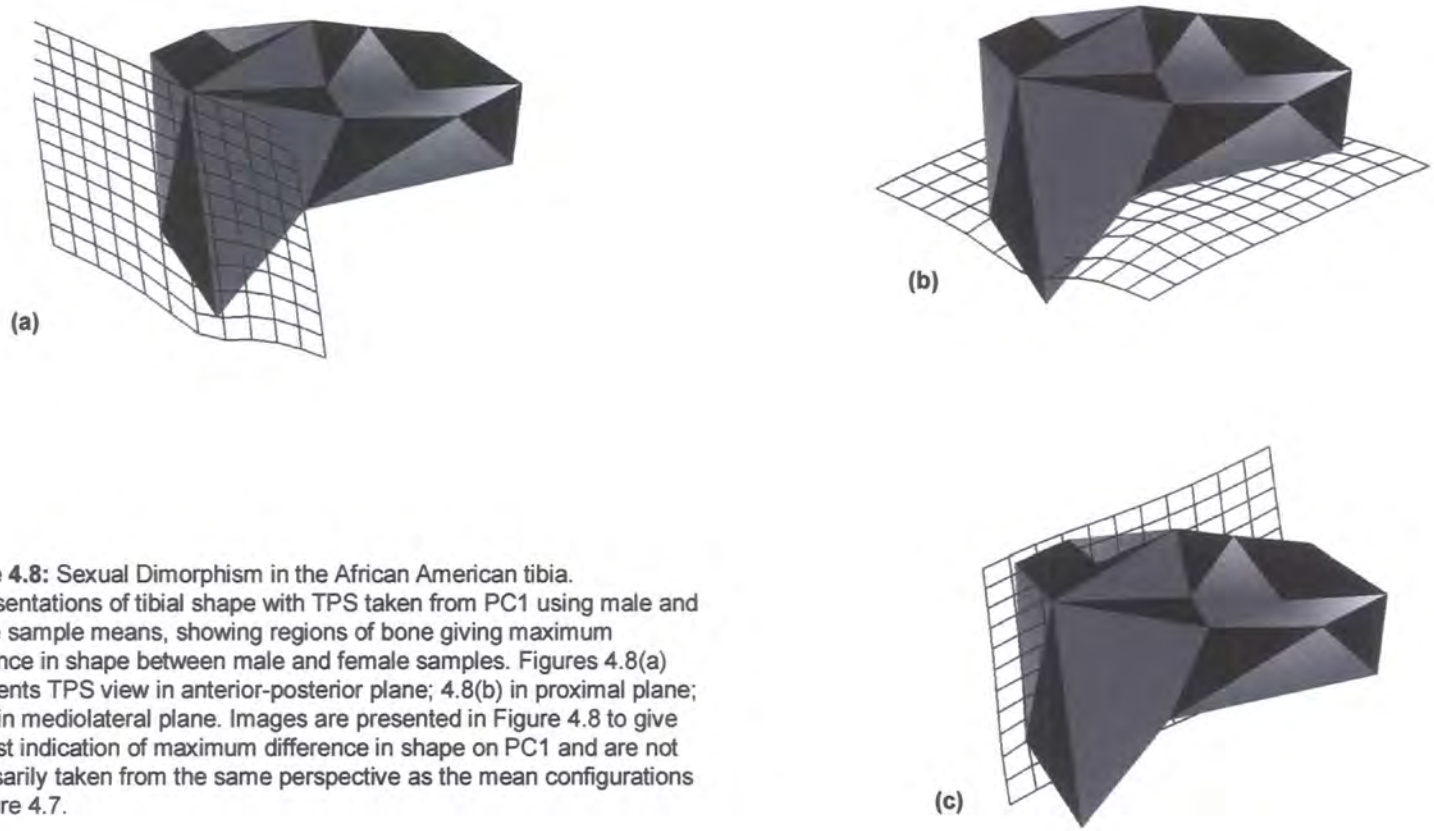

Figure 4.8: Sexual Dimorphism in the African American tibia. Representations of tibial shape with TPS taken from PC1 using male and female sample means, showing regions of bone giving maximum difference in shape between male and female samples. Figures 4.8(a) represents TPS view in anterior-posterior plane; 4.8(b) in proximal plane; 4.8(c) in mediolateral plane. Images are presented in Figure 4.8 to give the best indication of maximum difference in shape on PC1 and are not necessarily taken from the same perspective as the mean configurations in Figure 4.7.

PCs	Prop.	Cumul.	PCs	Prop.	Cumul.	PCs	Prop.	Cumul.
PC1	10.20	10.20	PC26	1.09	80.10	PC51	0.34	96.30
PC2	6.91	17.10	PC27	1.04	81.10	PC52	0.31	96.60
PC3	6.42	23.50	PC28	1.02	82.20	PC53	0.29	96.90
PC4	5.62	29.10	PC29	0.97	83.10	PC54	0.27	97.20
PC5	4.42	33.50	PC30	0.94	84.10	PC55	0.27	97.50
PC6	4.25	37.80	PC31	0.90	85.00	PC56	0.25	97.70
PC7	4.02	41.80	PC32	0.86	85.80	PC57	0.24	98.00
PC8	3.47	45.30	PC33	0.85	86.70	PC58	0.22	98.20
PC9	3.18	48.40	PC34	0.78	87.50	PC59	0.21	98.40
PC10	3.05	51.50	PC35	0.76	88.20	PC60	0.19	98.60
PC11	2.76	54.20	PC36	0.70	88.90	PC61	0.19	98.80
PC12	2.58	56.80	PC37	0.69	89.60	PC62	0.16	98.90
PC13	2.43	59.30	PC38	0.67	90.30	PC63	0.16	99.10
PC14	2.28	61.50	PC39	0.61	90.90	PC64	0.15	99.20
PC15	2.03	63.60	PC40	0.58	91.50	PC65	0.14	99.40
PC16	2.02	65.60	PC41	0.55	92.00	PC66	0.13	99.50
PC17	1.90	67.50	PC42	0.55	92.60	PC67	0.12	99.60
PC18	1.75	69.20	PC43	0.49	93.10	PC68	0.11	99.70
PC19	1.67	70.90	PC44	0.47	93.50	PC69	0.10	99.80
PC20	1.53	72.40	PC45	0.46	94.00	PC70	0.09	99.90
PC21	1.45	73.90	PC46	0.43	94.40	PC71	0.08	100.00
PC22	1.39	75.30	PC47	0.42	94.80			
PC23	1.32	76.60	PC48	0.41	95.20			
PC24	1.29	77.90	PC49	0.39	95.60			
PC25	1.13	79.00	PC50	0.36	96.00			

Table 4.14: Sexual Dimorphism in the femur of 6 populations: The proportion and accumulated variance for PCs 1-71, which accounts for 100% of total variance.

The scores for each specimen on the resultant PCs are then subjected to canonical discriminant analysis to establish the relationships between male and female specimens based upon the Mahalanobis' squared distances between sample means.

For the femur, the best separation of groups is achieved using 100% of total variance. This conclusion was reached after separate discriminant and cross-validation analyses were carried out using PC scores accounting for c.50% to 100% of total variance. Results are summarised in Figure 4.9.

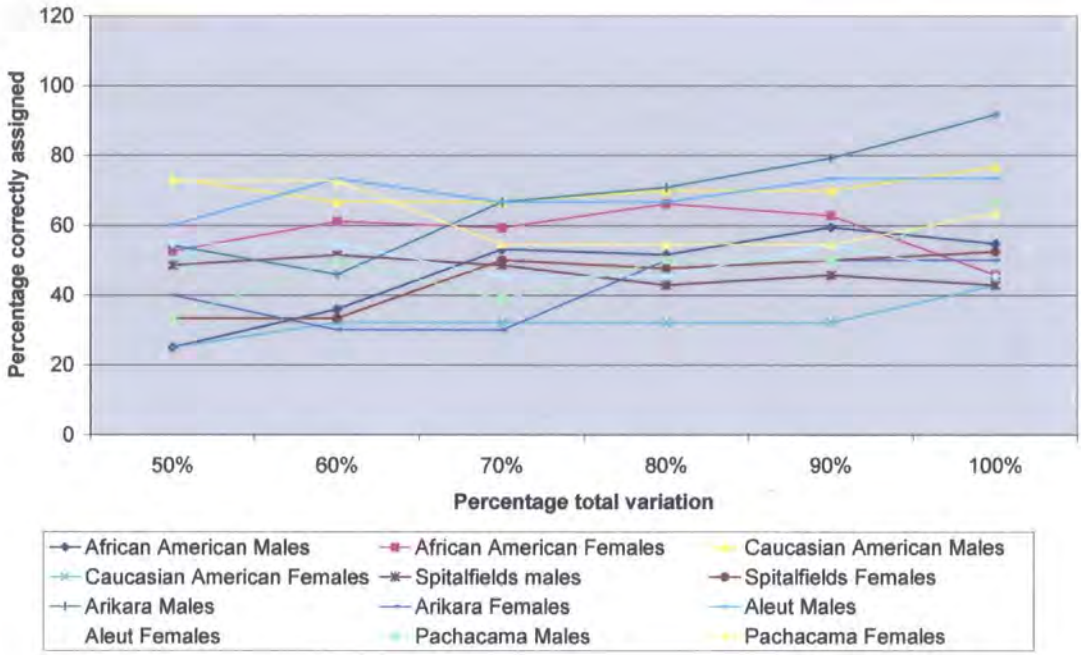

Figure 4.9: Sexual Dimorphism in the femur of 6 Populations: Summary of separate discriminant and cross-validation analyses using PC scores accounting for c. 50% of total variance (PCs 1-10), c.60% (PCs 1-13), c.70% (PCs 1-18), c.80% (PCs 1-26), c.90% (PCs 1-38) and 100% (PCs 1-70).

The Mahalanobis' squared distances between male and female sample means generated by discriminant analysis are shown in Table 4.15. Distances between samples reach a level of statistical significance with one exception, indicating that male and female groups can be separated on the basis of shape of the distal femur. The notable exception is between the male and female Pachacama at a level close to statistical significance at $p= 0.058$. Table 4.16 illustrates the relationship of each sample to all others on the basis of the generated Mahalanobis' squared distances by showing the distance of each primary sample to all others and ranking them accordingly from the closest sample (at position 1) to the furthest (at position 11). In every case the closest sample is that of the opposite sex of the same population.

Af. American Males	0											
	1.000											
Af. American Females	7.20	0										
	0.0001	1.0000										
Cauc. American Males	17.02	24.27	0									
	0.0001	0.0001	1.0000									
Cauc. American Females	20.43	17.21	15.34	0								
	0.0001	0.0001	0.0001	1.0000								
Spitalfields Males	16.62	26.07	21.25	24.17	0							
	0.0001	0.0001	0.0001	0.0001	1.0000							
Spitalfields Females	19.66	22.20	24.39	19.78	7.35	0						
	0.0001	0.0001	0.0001	0.0001	0.017	1.0000						
Arikara Males	30.04	31.25	36.30	30.05	37.49	38.49	0					
	0.0001	0.0001	0.0001	0.0001	0.0001	0.0001	1.0000					
Arikara Females	38.28	29.47	49.65	37.59	52.16	50.22	19.33	0				
	0.0001	0.0001	0.0001	0.0001	0.0001	0.0001	0.024	1.0000				
Aleut Males	62.08	61.02	67.97	49.67	71.09	66.13	39.00	55.06	0			
	0.0001	0.0001	0.0001	0.0001	0.0001	0.0001	0.0001	0.0001	1.0000			
Aleut Females	66.82	60.19	78.45	55.90	73.72	67.35	41.00	40.81	20.34	0		
	0.0001	0.0001	0.0001	0.0001	0.0001	0.0001	0.0001	0.0001	0.049	1.0000		
Pachacama Males	36.53	34.76	44.42	26.18	45.17	42.75	21.53	31.14	30.22	38.46	0	
	0.0001	0.0001	0.0001	0.0001	0.0001	0.0001	0.0001	0.0001	0.0001	0.0001	1.0000	
Pachacama Females	56.62	50.49	65.94	41.91	64.19	58.39	38.11	45.83	52.19	62.09	18.61	0.00
	0.0001	0.0001	0.0001	0.0001	0.0001	0.0001	0.0001	0.0001	0.0001	0.0001	0.058	1.0000
	Af. Am Males	**Af. Am. Females**	**Ca. Am. Males**	**Ca. Am. Females**	**Spitalf. Males**	**Spitalf. Females**	**Arikara Males**	**Arikara Females**	**Aleut Males**	**Aleut Females**	**Pachac. Males**	**Pachac. Females**

Table 4.15: Sexual Dimorphism in the femur of 6 populations. Results of canonical discriminant analysis of the male and female groups from 6 population samples, on the basis of 100% variance. The upper value in red gives the Mahalanobis' squared distance between groups, lower value in black gives the Hotelling's t^2 *p*-value. Figures in blue indicate a statistically non-significant value.

Group	1	2	3	4	5	6	7	8	9	10	11
African American Males	AA F	Sp M	CA M	Sp F	CA F	SD M	Pu M	SD F	Pu F	At M	At F
African American Females	AA M	CA F	Sp F	CA M	Sp M	SD F	SD M	Pu M	Pu F	At F	At M
Cauc. American Males	CA F	AA M	Sp M	AA F	Sp F	SD M	Pu M	SD F	Pu F	At M	At F
Cauc. American Females	CA M	AA F	Sp F	AA M	Sp M	Pu M	SD M	SD F	Pu F	At M	At F
Spitalfields Males	Sp F	AA M	CA M	CA F	AA F	SD M	Pu M	SD F	Pu F	At M	At F
Spitalfields Females	Sp M	AA M	CA F	AA F	CA M	SD M	Pu M	SD F	Pu F	At M	At F
Arikara Males	SD F	Pu M	AA M	CA F	AA F	CA M	Sp M	Sp F	Pu F	At M	At F
Arikara Females	SD M	AA F	Pu M	CA F	AA M	At F	Pu F	CA M	Sp F	Sp M	At M
Aleut Males	At F	Pu M	SD F	SD M	Pu F	CA F	AA F	AA M	Sp F	Sp M	CA M
Aleut Females	At M	Pu M	SD F	SD M	Pu F	CA F	AA F	AA M	Sp F	Sp M	CA M
Pachacama Males	Pu F	SD M	CA F	At M	SD F	AA F	AA M	At F	Sp F	CA M	Sp M
Pachacama Females	Pu M	SD M	CA F	SD F	AA F	At M	AA M	Sp F	At F	Sp M	CA M

Table 4.16: Sexual Dimorphism in the femur of 6 Populations. The order of proximity in distance of each primary male and female group from the other groups of the 6 populations, on the basis of their Mahalanobis squared distances, as shown in Table 4.15. Figures in red indicate the group of the opposite sex from the same population.

Table 4.17 shows the results of a cross-validation analysis using 100% of total variance for the twelve samples. Samples correctly assigned to groups range from 42.86% for Caucasian Americans females and Spitalfields males to 91.67% for the Arikara males. Although the percentage of specimens correctly assigned is relatively low for four of the groups (below 50%), the vast majority of misplaced individuals are placed into the opposite sex group of the same population. If the percentages of the two sexes are amalgamated, the combined percentage of specimens correctly assigned to each population rises to between 71.43% and 100% of individuals.

With respect to the Pachacama sample, to clarify the non-significant result, the following analysis investigates the presence of significant sexual dimorphism within this sample, when analysed separately. Results from this analysis are used to give greater insight into results when all populations are analysed jointly.

Differences in shape of the 29 Pachacama, (18 males and 11 females) are analysed using the Procrustes fitted co-ordinates and by subjecting the data to PCA. Table 4.18 gives the proportional and accumulated variance for all PCs, which represent the total variance within the sample. Table 4.19 shows which PCs relate more specifically to sexual dimorphism when using canonical stepwise discriminant function analysis. Figure 4.10 summarises the best separation of male and female specimens when using PCs accounting for c.50% to 100% of total variation and those used in the stepwise discriminant function analysis. The scores for each specimen on the resultant PCs are subjected to canonical discriminant analysis to establish the relationships between the male and female specimens based upon the Mahalanobis' squared distance between sample means. The distance generated by stepwise discriminant analysis is 1576827 ($p<0.0001$), with crossvalidation assigning 100% of males and 100% of females to the correct group, indicating that the two sexes can be separated on some aspect of shape of the distal femur.

Number of Observations and Percent Classified into Group using 100% PCs													
From Group	Af. Amer. Males	Af. Amer. Females	Ca Am. Males	Ca Am. Females	Spitalf. Males	Spitalf. Females	Arikara Males	Arikara Females	Aleut Males	Aleut Females	Pachac. Males	Pachac. Females	Total
Af. Amer. Males	35	13	3	1	5	4	1	0	1	0	1	0	64
	54.69	20.31	4.69	1.56	7.81	6.25	1.56	0	1.56	0	1.56	0	100
Af. Amer. Females	17	27	3	4	0	4	1	3	0	0	0	0	59
	28.81	45.76	5.08	6.78	0	6.78	1.69	5.08	0	0	0	0	100
Ca. Amer. Males	1	1	23	2	2	1	0	0	0	0	0	0	30
	3.33	3.33	76.67	6.67	6.67	3.33	0	0	0	0	0	0	100
Ca. Amer. Females	0	3	8	12	1	2	0	0	0	0	2	0	28
	0	10.71	28.57	42.86	3.57	7.14	0	0	0	0	7.14	0	100
Spitalfields Males	3	0	3	2	15	12	0	0	0	0	0	0	35
	8.57	0	8.57	5.71	42.86	34.29	0	0	0	0	0	0	100
Spitalfields Females	0	2	0	3	14	22	0	0	1	0	0	0	42
	0	4.76	0	7.14	33.33	52.38	0	0	2.38	0	0	0	100
Arikara Males	0	0	0	0	0	0	22	0	0	0	2	0	24
	0	0	0	0	0	0	91.67	0	0	0	8.33	0	100
Arikara Females	0	1	0	0	0	0	3	5	1	0	0	0	10
	0	10	0	0	0	0	30	50	10	0	0	0	100
Aleut Males	0	0	0	0	0	0	0	0	11	4	0	0	15
	0	0	0	0	0	0	0	0	73.33	26.67	0	0	100
Aleut Females	0	0	0	0	0	0	0	0	6	5	0	0	11
	0	0	0	0	0	0	0	0	54.55	45.45	0	0	100
Pachacama Males	0	0	0	1	0	0	1	0	2	0	12	2	18
	0	0	0	5.56	0	0	5.56	0	11.11	0	66.67	11.11	100
Pachacama Females	0	0	0	0	0	0	0	0	0	0	4	7	11
	0	0	0	0	0	0	0	0	0	0	36.36	63.64	100
Total	56	47	40	25	37	45	28	8	22	9	21	9	347
	16.14	13.54	11.53	7.2	10.66	12.97	8.07	2.31	6.34	2.59	6.05	2.59	100

Table 4.17: Sexual Dimorphism in the femur of 6 populations using 100% total variance. Upper figure denotes number of individuals correctly assigned; lower figure denotes percentage. Red figures denote number and percentage of individuals placed into their correct group; blue figures denote number of individuals and percentage correctly assigned to the opposite sex of the same population.

PCs	Prop.	Cumul.	PCs	Prop.	Cumul.
PC1	13.20	13.20	PC16	1.88	89.70
PC2	11.40	24.50	PC17	1.70	91.40
PC3	10.30	34.80	PC18	1.50	92.80
PC4	8.49	43.30	PC19	1.33	94.20
PC5	7.27	50.60	PC20	1.26	95.40
PC6	5.53	56.10	PC21	1.02	96.50
PC7	5.25	61.40	PC22	0.83	97.30
PC8	4.83	66.20	PC23	0.79	98.10
PC9	4.20	70.40	PC24	0.68	98.80
PC10	3.56	74.00	PC25	0.50	99.30
PC11	3.38	77.30	PC26	0.43	99.70
PC12	3.01	80.40	PC27	0.32	100.00
PC13	2.81	83.20			
PC14	2.51	85.70			
PC15	2.10	87.80			

Table 4.18: Sexual Dimorphism in the femur for the Pachacama. The proportion and accumulated variance for PCs 1-27, which accounts for 100% of total variance

Order	Entered	Order	Entered	Order	Entered	Order	Entered
1	PC29	8	PC28	15	PC27	22	PC20
2	PC16	9	PC3	16	PC11	23	PC12
3	PC1	10	PC2	17	PC22	24	PC25
4	PC13	11	PC5	18	PC26	25	PC15
5	PC8	12	PC14	19	PC19		
6	PC9	13	PC18	20	PC17		
7	PC4	14	PC6	21	PC23		

Table 4.19: PCs selected by stepwise discriminant function analysis and the order entered into subsequent discriminant function analyses for the femur (Pachacama).

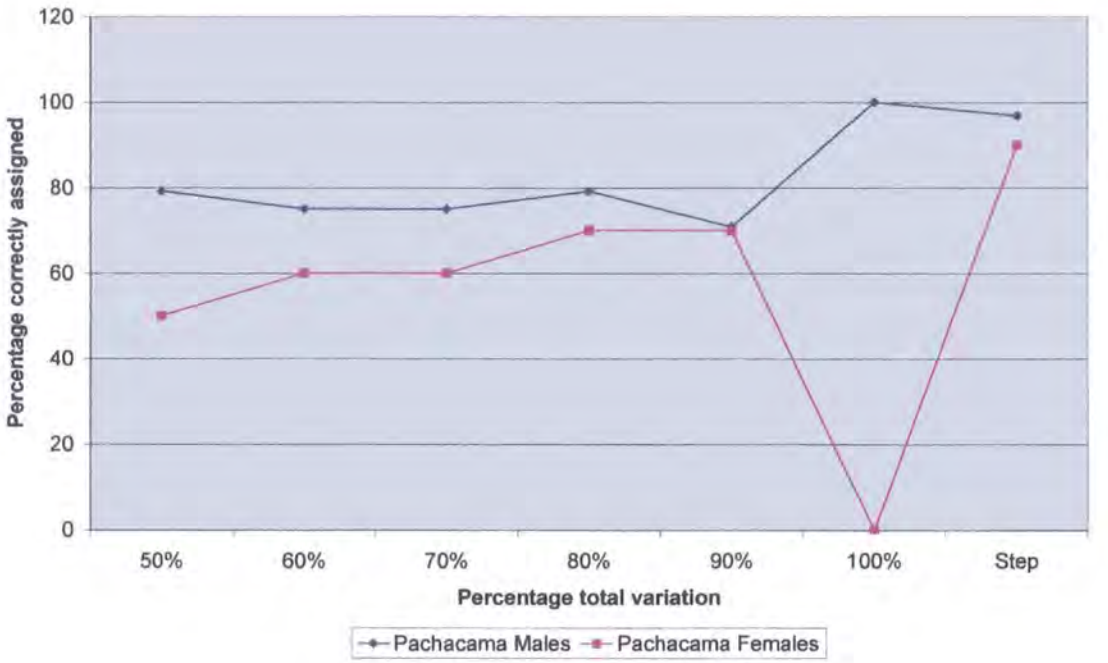

Figure 4.10: Sexual Dimorphism in the Pachacama femur. Summary of separate discriminant and cross-validation analyses using PCs accounting for c.50% of total variance PCs 1-5, c.60% PCs 1-7, c.70% PCs 1-9, c.80% PCs 1-12, c.90% PCs 1-16, 100% PCs 1-29 and stepwise discriminant analysis.

Despite the non-significant result when the Pachacama sample is included in the joint analysis with five other populations, results here indicate from the analysis of male and female Pachacama specimens have established the presence of sexual dimorphism in this sample when analysed separately.

4.4.4a(ii) Femur: Description of differences in shape between males and females

Figures 4.11 and 4.12 show the bivariate plots of PC1 with PC2 and PC3 with PC4, accounting for a cumulative 29.10% of total variance. It is evident from these two figures that the overlap between male and female specimens from the six populations is too extensive to assess any degree of separation between the samples and to establish any relationships between male and female groups within or between populations.

Figure 4.11:

Sexual Dimorphism in the femur of 6 Populations, total sample. Bivariate plot of PC1 with PC2 which shows the overlap of specimens from different groups and the difficulty of assessing the separation of males and females of the 6 populations when using the total sample.

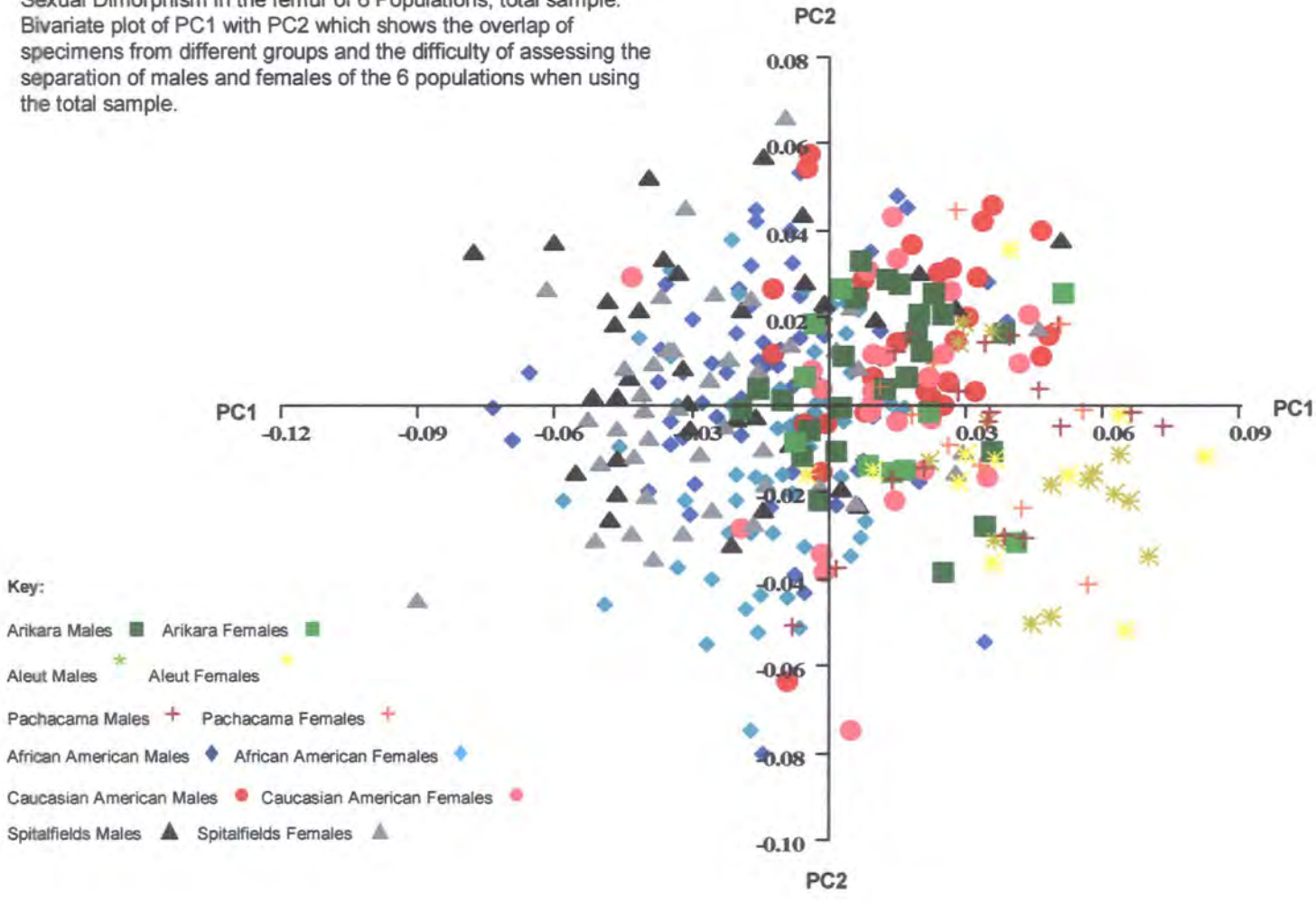

Figure 4.12:

Sexual Dimorphism in the femur of 6 Populations, total sample. Bivariate plot of PC3 with PC4 which shows the overlap of specimens from different groups and the difficulty of assessing the separation of males and females of the 6 populations when using the total sample.

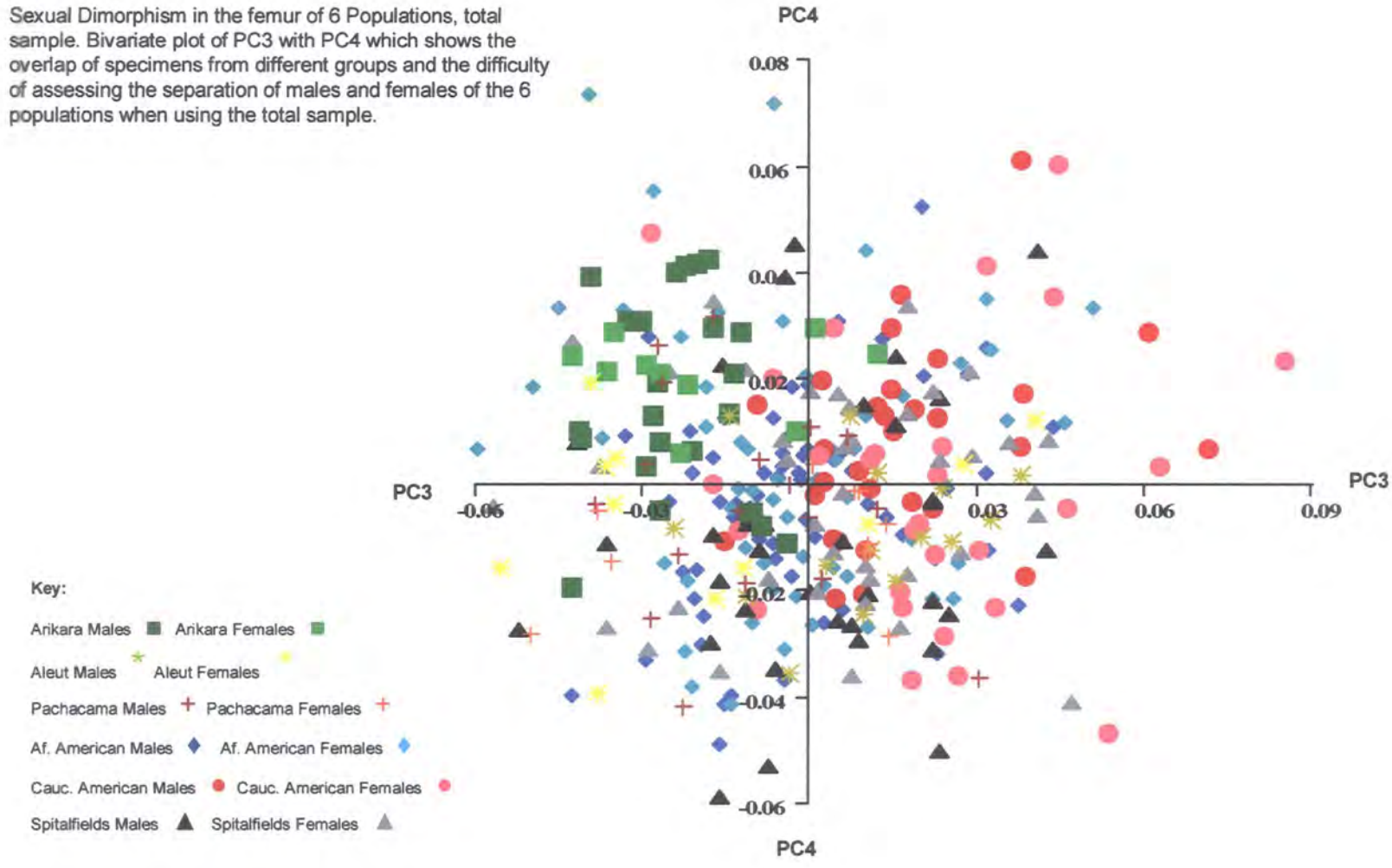

Although in Figure 4.11 it is possible to distinguish a separation of some population samples (e.g., between the majority of Spitalfields individuals and the Aleut), any distinguishable concentrations of separate populations are seen to comprise both male and female specimens. This overlap of individuals applies equally to all higher PCs in addition to those seen in PCs 1 to 4. Therefore, the sample means of the two sexes for each of the six populations have been used to help distinguish specific variation due to sexual dimorphism.

For the femur, the correlation between the Procrustes distances using the population means shown in Table 4.20 and the Mahalanobis' distances shown in Table 4.15 does not reach a level of statistical significance ($r= 0.21$; $p= 0.10$). This result therefore implies that it may be problematic to infer the relationships between populations solely from the relationships between the population means.

The Procrustes mean co-ordinate have been calculated from the separate GPAs and have been subjected to a joint GPA and PCA.

The proportion and accumulated variance of the PCs generated in the analysis of population means is given in Table 4.21.

African American Males	0											
African American Females	0.14	0										
Caucasian American Males	0.11	0.13	0									
Caucasian American Females	0.23	0.17	0.21	0								
Spitalfields Males	0.12	0.13	0.19	0.24	0							
Spitalfields Females	0.42	0.39	0.48	0.48	0.32	0						
Arikara Males	0.30	0.27	0.36	0.36	0.20	0.15	0					
Arikara Females	0.31	0.27	0.36	0.38	0.21	0.15	0.05	0				
Aleut Males	0.35	0.26	0.37	0.24	0.28	0.34	0.26	0.28	0			
Aleut Females	0.34	0.23	0.33	0.21	0.29	0.40	0.30	0.30	0.11	0		
Pachacama Males	0.25	0.17	0.20	0.10	0.28	0.52	0.40	0.40	0.28	0.22	0	
Pachacama Females	0.16	0.13	0.09	0.20	0.21	0.49	0.36	0.36	0.36	0.31	0.16	0
	Af. Am. Males	Af. Am. Females	Ca. Am. Males	Ca. Am. Females	Spitalf. Males	Spitalf. Females	Arikara Males	Arikara Females	Aleut Males	Aleut Females	Pachac. Males	Pachac. Females

Table 4.20: Sexual Dimorphism in the femur of 6 Populations. Procrustes distances between sample means for males and females of 6 populations. Correlation between Procrustes distances and Mahalanobis' distances (Table 4.15) is significant at: $r = 0.21$; $p = 0.10$.

PCs	Proportion	Cumulative	PCs	Proportion	Cumulative
PC1	41.70	41.7	PC7	3.19	94.7
PC2	17.80	59.5	PC8	2.02	96.7
PC3	12.70	72.2	PC9	1.73	98.5
PC4	9.80	82.0	PC10	0.97	99.4
PC5	5.74	87.7	PC11	0.56	100
PC6	3.83	91.5			

Table 4.21: Proportion and accumulative variance represented by PCs 1-11 which accounts for total sample variance for population means for the femur.

The first four PCs account for 82% of total variance in the sample and the exploration of shape differences between sexes will concentrate on these four PCs.

Figure 4.13 indicates that sexual dimorphism within the six populations is not identical, either in nature or degree and that sexual dimorphism in the African Americans is not shared in all aspects by the other populations. For PC1, male and female means of each population remain in closer proximity to each other than to any other means, particularly for the Aleut and Spitalfields groups, where the male and female means show relatively little sexual dimorphism for this PC. Differences in morphology on PC1 must therefore primarily reflect differences between the populations comprising both male and female elements. Variation explained by PC1 between the twelve means, primarily explains the angle of attachment of the knee joint to the diaphyses, with the male and female Spitalfields joint at the positive extreme displaying a more acute angle relative to that of the Aleut at the negative extreme. In addition, means towards the negative extreme are seen to be relatively more laterally oriented than those at the negative extreme. This difference in position can be best assessed in Figure 4.14(a) and (d) in the relative positions of landmarks 17 and 23 relative to landmarks 25 and 26 respectively (indicating the maximum extent and height of the condyles) and in the lateral views in Figure 4.14(b) and (c), which also includes landmark 19, which indicates the maximum width of the lateral epicondyle.

Figure 4.13:

Sexual Dimorphism in the femur of 6 Populations. Bivariate plot of PC1 and PC6, showing a separation of male and female means. Arrows point from male to female means from each population.

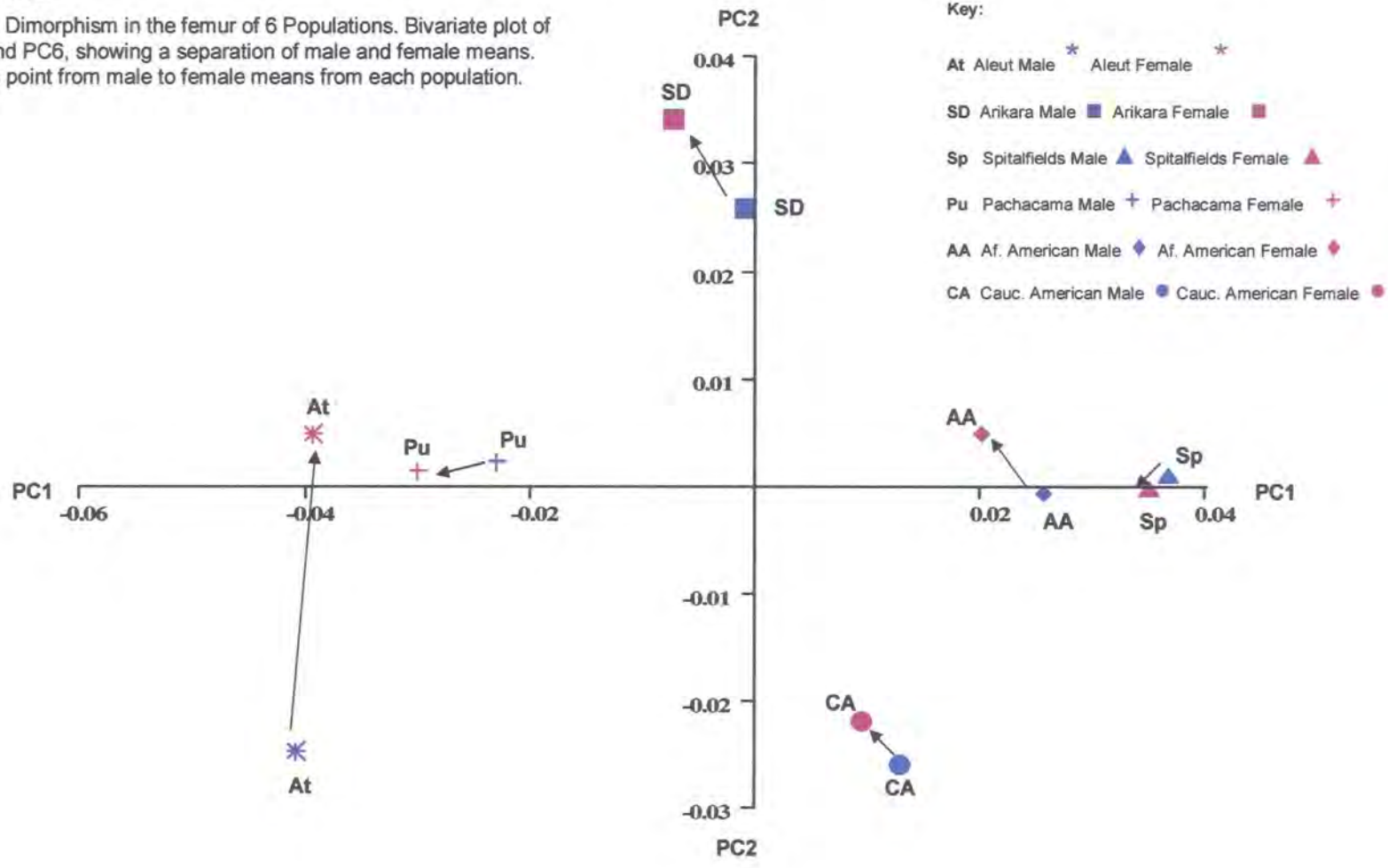

Figure 4.14:

Sexual Dimorphism in the femur of 6 Populations. Separation of male and female means of 6 populations on PC1. Images represent the mean configuration if warped to the extremes of PC1 (at 0.04 to –0.06). Images (c) and (d) include landmarks discussed in the text (section 4.4.4a(ii)).

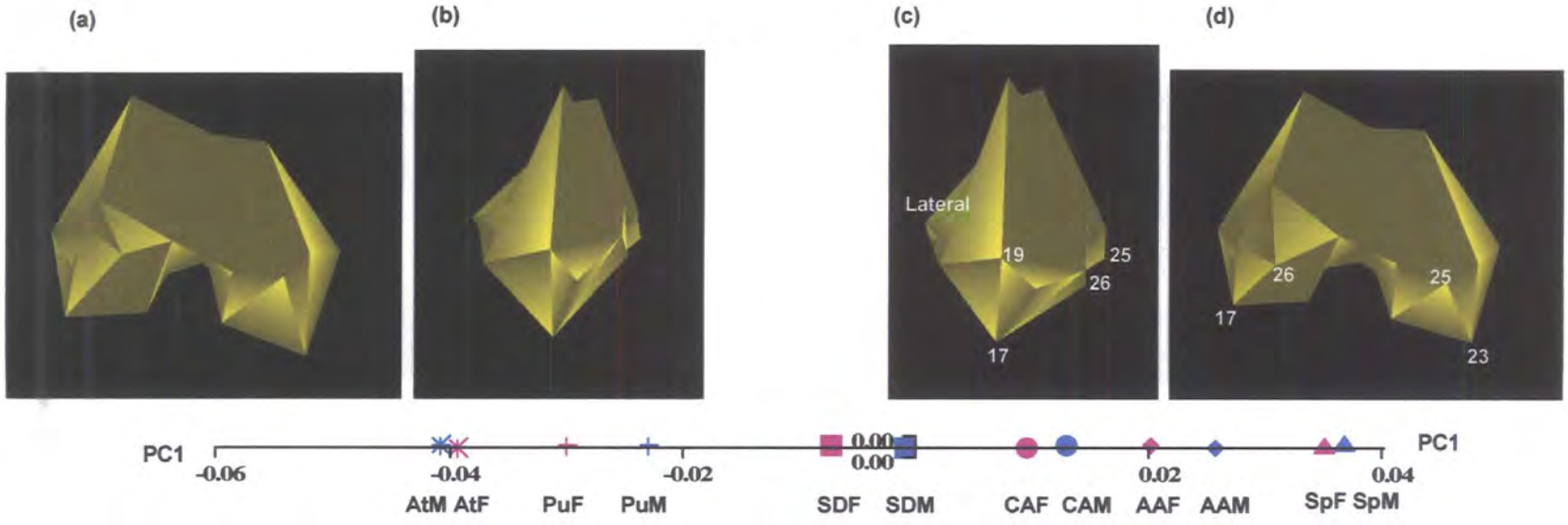

Within each population sample on PC1, however, the mean male is placed more positively relative to the mean female in five of the six populations, including that of the African Americans. These males are therefore likely to exhibit the more acute angle of attachment of joint relative to shaft, relative to the corresponding females. The description of the African American samples (section 4.4.3a(ii) above) also noted that the joint of the female mean is seen to be more laterally oriented relative to the shaft, compared to the male mean. This lateral orientation would therefore also apply to the other similarly positioned means. For the sixth population, (the Aleut), the relative positions of the male and female means are reversed, indicating that the sex specific angle of attachment and the orientation of the joint relative to the shaft are also reversed relative to the other five pairs of means.

Variation explained by PC2 explains the position of the height of the condyles relative to the anterior edge of the patella surface and the maximum extent of the condyles. As with PC1, the difference between the mean configuration in Figure 4.15 at the two extremes of the scale is more easily appreciated in the relationships between landmarks 17 and 26 (lateral side) and 23 and 25 (medial side) and in the degree of visibility in the area of the intercondylar fossa, exemplified in the relative positions of landmarks 2 and 4 on the posterior edge of the intercondylar fossa. The relative positions of the African American male and female means is shared by the Caucasian Americans, Aleut and Arikara and therefore indicates some similarity in the nature of sexual dimorphism, although this pattern is reversed in the Spitalfields samples and the Pachacama. The degree of sexual difference for PC2 varies, however, with little dimorphism in five of the populations, but considerable dimorphism in the Aleut.

For PCs 3 and 4 in Figure 4.16, morphological variation between the pairs of means for each population is slight and difficult to assess. It is apparent, however, that the morphological relationship between the sexes in each population differs both in nature and degree relative to the other populations. Whilst the Arikara, Pachacama and Spitalfields show a similar pattern of variation, the degree to which the sexes differ is wide, with the Pachacama showing considerably greater dimorphism relative to the other

Figure 4.15:

Sexual Dimorphism in the femur of 6 Populations. Separation of male and female means of 6 populations on PC2. Images represent the mean configuration if warped to the extremes of PC2 (at 0.04 to –0.04). Image at positive extreme includes landmarks discussed in the text (section 4.4.4a(ii)).

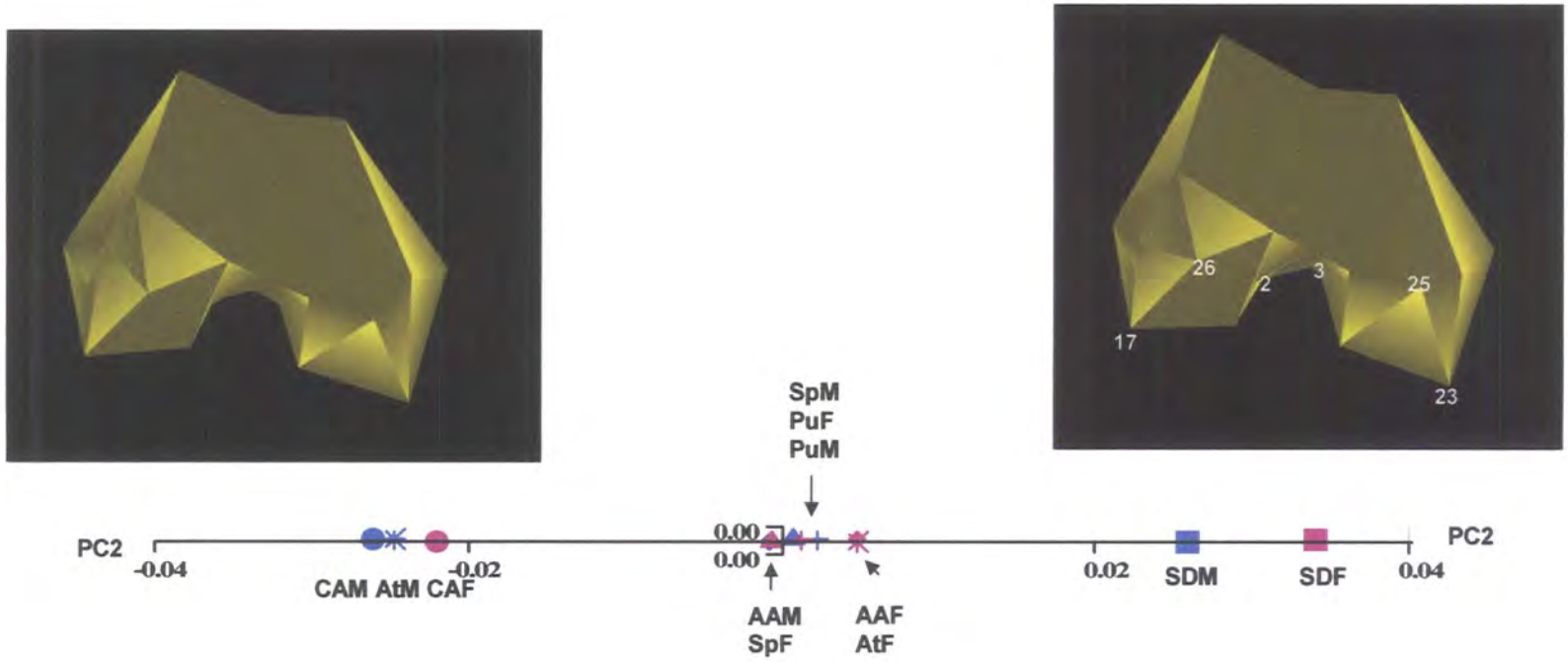

Key:

At Aleut Male * Aleut Female * CA Cauc. American Male ● Cauc. American Female ●

SD Arikara Male ■ Arikara Female ■ AA Af. American Male ♦ Af. American Female ♦

Sp Spitalfields Male ▲ Spitalfields Female ▲ Pu Pachacama Male + Pachacama Female +

Figure 4.16:

Sexual Dimorphism in the femur of 6 Populations. Bivariate plot of Pc3 and PC4, showing a separation of male and female means. Arrows point from male to female means from each population. Images represent the mean configuration if warped to the extremes of PC3 (at 0.04 to –0.04) and PC4 (at 0.03 to -0.03).

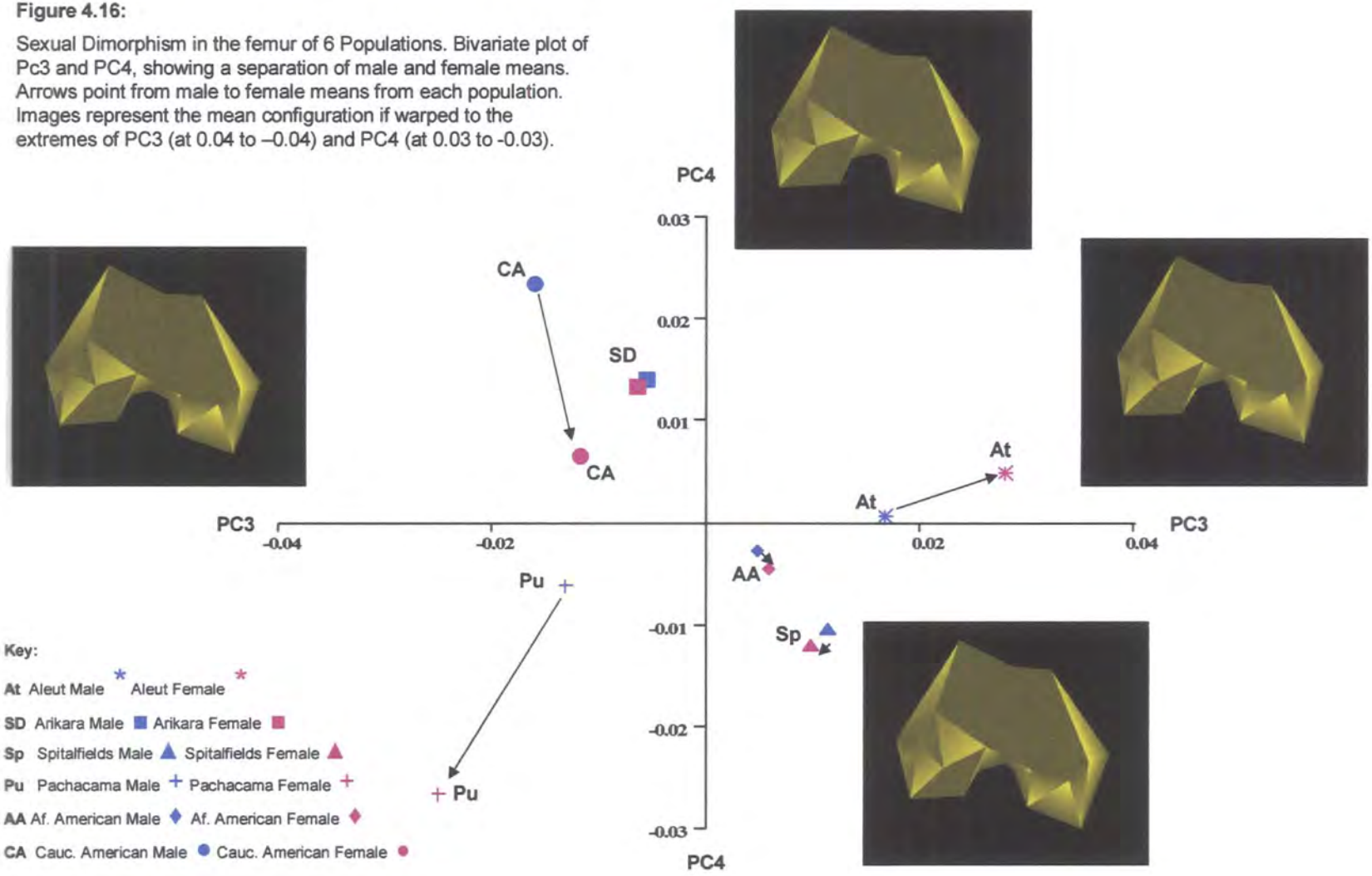

two groups for both PCs 3 and 4. Again, the African and Caucasian Americans show similarity of nature but with variation in degree and the Aleut shows a unique pattern for these two PCs relative to the other five populations.

The areas of greatest difference across all populations can be seen in Figure 4.17 which shows where the maximum deformation of the TPS lies on PC1. Because the differences between mean male and female pairs within each population are too small to allow an accurate interpretation from such diagrams, each mean configuration can only show how differences affect the total sample. Further interpretation of sexual differences must therefore take into account the relationships between the pairs of means described above. Figure 4.17 (a) and (b) reaffirms differences noted above in the relative height and extent of the condyles, particularly over the lateral side.

4.4.4b(i) Tibia

Differences in shape of the 337 specimens from 177 males and 160 females are analysed using the Procrustes fitted co-ordinates and by subjecting them to PCA. Table 4.22 gives the proportional and accumulated variance for PCs 1 to 56, which represents the total variance within the sample. The scores for each specimen on the resultant PCs are then subjected to canonical discriminant analysis to establish the relationships between male and female specimens based upon the Mahalanobis' squared distances between sample means.

For the tibia, the best separation of groups is achieved using 100% of total variance. This conclusion was reached after separate discriminant and cross-validation analyses were carried out using PC scores accounting for c.50% to 100% of total variance. Results are summarised in Figure 4.18.

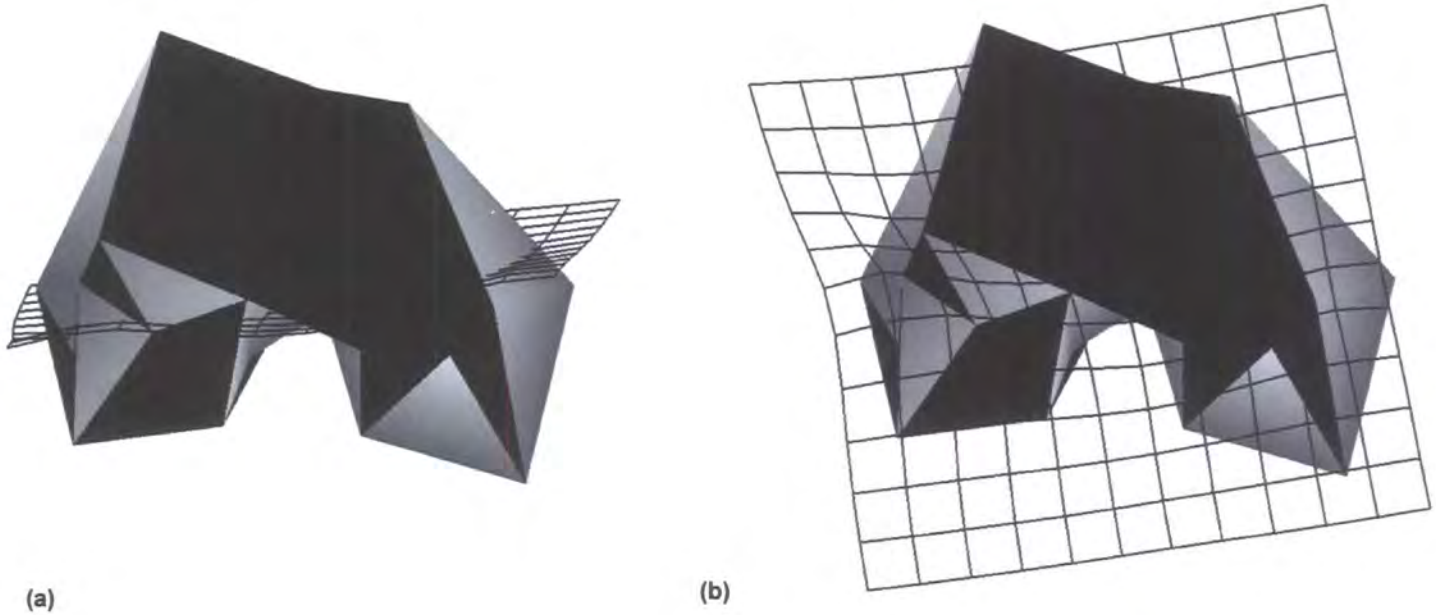

Figure 4.17: Sexual Dimorphism in the femur of 6 Populations. Representations of femoral shape with TPS taken from PC1 using male and female sample means, showing regions of bone giving maximum difference in shape between means. Figures 4.17(a) represents TPS view in anterior-posterior plane; 4.17(d) in distal plane. Images are presented in Figure 4.17 to give the best indication of maximum difference in shape on PC1 and are not necessarily taken from the same perspective as the mean configurations in Figure 4.14.

PCs	Prop.	Cumul.	PCs	Prop.	Cumul.	PCs	Prop.	Cumul.
PC1	23.60	23.60	PC21	1.18	81.90	PC41	0.41	96.30
PC2	7.50	31.10	PC22	1.13	83.10	PC42	0.40	96.70
PC3	6.10	37.20	PC23	1.11	84.20	PC43	0.36	97.00
PC4	5.10	42.30	PC24	1.03	85.20	PC44	0.34	97.40
PC5	4.64	46.90	PC25	0.96	86.20	PC45	0.33	97.70
PC6	4.06	51.00	PC26	0.91	87.10	PC46	0.30	98.00
PC7	3.60	54.60	PC27	0.88	88.00	PC47	0.28	98.30
PC8	3.20	57.80	PC28	0.86	88.80	PC48	0.26	98.50
PC9	2.83	60.60	PC29	0.81	89.60	PC49	0.25	98.80
PC10	2.52	63.10	PC30	0.77	90.40	PC50	0.22	99.00
PC11	2.37	65.50	PC31	0.73	91.10	PC51	0.21	99.20
PC12	2.28	67.80	PC32	0.65	91.80	PC52	0.20	99.40
PC13	2.09	69.90	PC33	0.62	92.40	PC53	0.16	99.60
PC14	1.89	71.80	PC34	0.57	93.00	PC54	0.15	99.70
PC15	1.73	73.50	PC35	0.55	93.50	PC55	0.14	99.90
PC16	1.60	75.10	PC36	0.53	94.00	PC56	0.13	100.00
PC17	1.58	76.70	PC37	0.49	94.50			
PC18	1.47	78.20	PC38	0.48	95.00			
PC19	1.38	79.50	PC39	0.45	95.40			
PC20	1.22	80.70	PC40	0.44	95.90			

Table 4.22: Sexual Dimorphism in the tibia of 6 populations. The proportion and accumulated variance for PCs 1-56, which accounts for 100% of total variance.

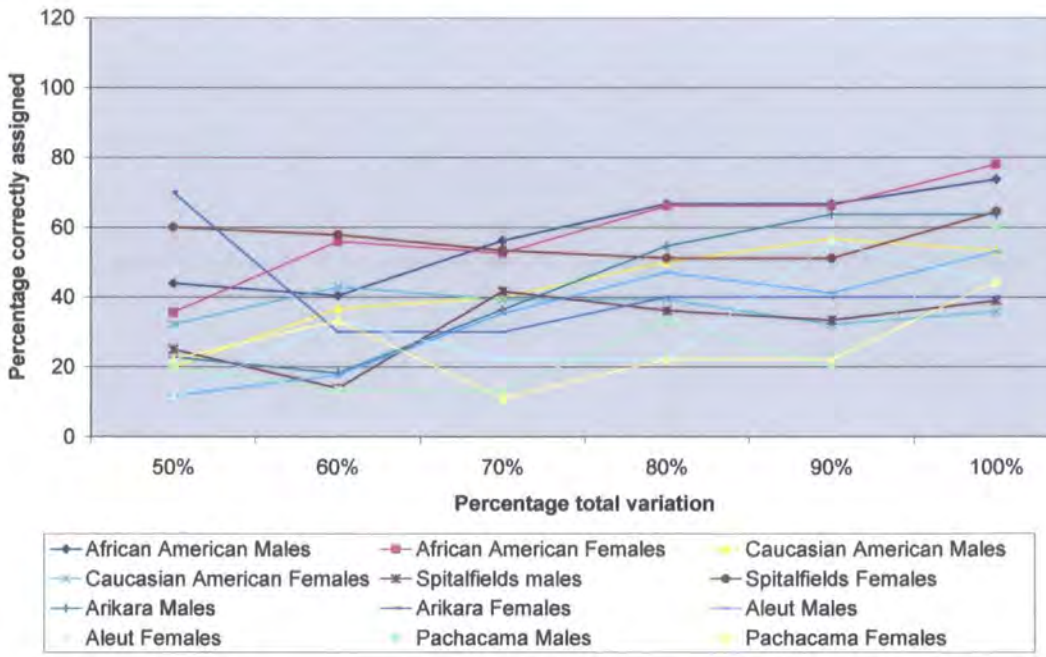

Figure 4.18: Sexual Dimorphism in the tibia of 6 Populations. Summary of separate discriminant and cross-validation analyses using PCs accounting for c.50% of total variance (PCs 1-6), c.60% (PCs 1-9), c.70% (PCs 1-13), c.80% (PCs 1-20), c.90% (PCs 1-30) and 100% (PCs 1-56).

The Mahalanobis' squared distances between male and female sample means, generated by discriminant analysis are shown in Table 4.23. Distances between samples are highly statistically significant with three notable exceptions. Although male and female groups can be separated on the shape of the proximal tibia across different populations and between the African and Caucasian American and Spitalfields males and females, sexual dimorphism does not reach a level of statistical significance between males and females of each of the three Native American populations, when all populations are analysed jointly.

Table 4.24 illustrates the relationship of each sample to all others on the basis of the generated Mahalanobis' squared distances by showing the distance of each primary sample to all others and ranking them accordingly from the closest sample (at position 1) to the furthest (at position 11). In contrast to the femur where Table 4.16 shows that the closest group to any sexed sample is the opposite sex of the same population, Table 4.23 shows that for the tibia, the Aleut male sample is seen to be marginally closer to the Arikara male sample than to the Aleut female sample (a distance of 17.00 to Arikara males compared to 17.42 to Aleut females). However, the distance between the Aleut males and Arikara males remains statistically significant, in contrast to that between the Aleut males and females, which is not significant.

Table 4.25 shows the results of cross-validation analysis using 100% of total variance for the twelve samples. Samples correctly assigned to groups range from 35.71% for Caucasian Americans females to 77.97% for the African American females. Although for five of the groups, the percentage of specimens correctly assigned is relatively low at below 50%, the majority of misplaced individuals are placed into the opposite sex group of the same population. If the percentages of the two sexes are amalgamated, the combined percentage of specimens from each population rises to between 64.7% and 90% of individuals.

Af. American Males	0 1.000											
Af. American Females	10.48 0.0001	0 1.000										
Cauc. American Males	20.15 0.0001	21.74 0.0001	0 1.000									
Cauc. American Females	15.03 0.0001	13.22 0.0001	8.90 0.0014	0 1.000								
Spitalfields Males	20.62 0.0001	26.64 0.0001	17.21 0.0001	21.05 0.0001	0 1.000							
Spitalfields Females	25.32 0.0001	26.07 0.0001	20.18 0.0001	22.29 0.0001	8.92 0.0001	0 1.000						
Arikara Males	20.62 0.0001	21.65 0.0001	21.56 0.0001	16.39 0.0001	35.09 0.0001	36.46 0.0001	0 1.000					
Arikara Females	32.67 0.0001	28.49 0.0001	29.58 0.0001	25.05 0.0001	49.03 0.0001	49.19 0.0001	8.88 0.8004	0 1.000				
Aleut Males	35.27 0.0001	33.11 0.0001	39.16 0.0001	29.73 0.0001	44.21 0.0001	46.90 0.0001	17.00 0.0001	19.52 0.0031	0 1.000			
Aleut Females	48.73 0.0001	45.02 0.0001	38.80 0.0001	41.61 0.0001	50.80 0.0001	49.40 0.0001	33.32 0.0001	33.56 0.0001	17.42 0.393	0 1.000		
Pachacama Males	27.33 0.0001	24.98 0.0001	25.86 0.0001	18.27 0.0001	37.37 0.0001	44.47 0.0001	16.58 0.0001	21.68 0.0012	23.12 0.0001	41.74 0.0001	0 1.000	
Pachacama Females	43.97 0.0001	42.45 0.0001	31.81 0.0001	28.55 0.0001	46.67 0.0001	47.66 0.0002	25.00 0.0001	29.82 0.0001	24.57 0.0001	35.05 0.0001	18.15 0.414	0.00 1.000
	Af. Am Males	**Af. Am. Females**	**Ca. Am. Males**	**Ca. Am. Females**	**Spitalf. Males**	**Spitalf. Females**	**Arikara Males**	**Arikara Females**	**Aleut Males**	**Aleut Females**	**Pachac. Males**	**Pachac. Females**

Table 4.23: Sexual Dimorphism in the tibia in 6 populations. Results of canonical discriminant analysis of male and female groups from 6 population samples, on the basis of 100% variance. The upper value in red gives the Mahalanobis' squared distance between groups, lower value in black gives the Hotelling's t^2 *p*-value. Figures in blue indicate statistically non-significant values.

Group	1	2	3	4	5	6	7	8	9	10	11
African American Males	BA F	CA F	CA M	Sp M	SD M	Sp F	Pu M	Sd F	At M	Pu F	At F
African American Females	BA M	CA F	SD M	CA M	Pu M	Sp F	Sp M	SD F	At M	Pu M	At F
Cauc. American Males	CA F	Sp M	BA M	Sp F	SD M	BA F	Pu M	SD F	Pu F	At F	At M
Cauc. American Females	CA M	BA F	BA M	SD M	Pu M	Sp M	Sp F	SD F	Pu F	At M	At F
Spitalfields Males	Sp F	CA M	BA M	CA F	BA F	SD M	Pu M	At M	Pu F	SD F	At F
Spitalfields Females	Sp M	CA M	CA F	BA M	BA F	SD M	Pu M	At M	Pu F	SD F	At F
Arikara Males	SD F	CA F	Pu M	At M	BA M	CA M	BA F	SD M	At F	Sp M	Sp F
Arikara Females	SD M	At M	Pu M	CA F	CA M	BA F	Pu F	BA M	At F	Sp M	Sp F
Aleut Males	SD M	At F	SD F	PU M	Pu F	CA F	BA F	BA M	CA F	Sp M	Sp F
Aleut Females	At M	SD M	SD F	Pu F	CA M	CA F	Pu M	BA F	BA M	Sp F	Sp M
Pachacama Males	Pu F	SD M	CA F	SD F	At M	BA F	CA M	BA M	Sp M	At F	Sp F
Pachacama Females	Pu M	At M	SD M	CA F	SD F	CA M	At F	BA F	BA M	Sp M	Sp F

Table 4.24: Sexual Dimorphism in the tibia of 6 Populations. The order of proximity in distance of each primary male and female group from the other groups of the 6 populations, on the basis of their Mahalanobis squared distances, shown Table 4.21. Figures in red indicate the group of the opposite sex from the same population.

Number of Observations and Percent Classified into Group using 100% PCs													
From Group	Af. Amer. Males	Af. Amer. Females	Ca Am. Males	Ca Am. Females	Spitalf. Males	Spitalf. Females	Arikara Males	Arikara Females	Aleut Males	Aleut Females	Pachac. Males	Pachac. Females	Total
Af. Amer. Males	42	4	3	4	1	0	3	0	0	0	0	0	57
	73.68	7.02	5.26	7.02	1.75	0	5.26	0	0	0	0	0	100
Af. Amer. Females	5	46	0	4	2	1	0	1	0	0	0	0	59
	8.47	77.97	0	6.78	3.39	1.69	0	1.69	0	0	0	0	100
Ca. Amer. Males	1	2	16	8	0	1	2	0	0	0	0	0	30
	3.33	6.67	53.33	26.67	0	3.33	6.67	0	0	0	0	0	100
Ca. Amer. Females	3	4	6	10	0	0	1	1	1	0	1	1	28
	10.71	14.29	21.43	35.71	0	0	3.57	3.57	3.57	0	3.57	3.57	100
Spitalfields Males	2	0	5	2	14	12	0	0	0	1	0	0	36
	5.56	0	13.89	5.56	38.89	33.33	0	0	0	2.78	0	0	100
Spitalfields Females	1	1	3	2	8	29	0	0	0	0	0	1	45
	2.22	2.22	6.67	4.44	17.78	64.44	0	0	0	0	0	2.22	100
Arikara Males	0	0	0	0	0	0	14	5	2	0	1	0	22
	0	0	0	0	0	0	63.64	22.73	9.09	0	4.55	0	100
Arikara Females	0	0	0	0	0	0	5	4	1	0	0	0	10
	0	0	0	0	0	0	50	40	10	0	0	0	100
Aleut Males	0	1	0	0	0	0	3	2	9	2	0	0	17
	0	5.88	0	0	0	0	17.65	11.76	52.94	11.76	0	0	100
Aleut Females	0	0	0	0	0	0	1	0	4	4	0	0	9
	0	0	0	0	0	0	11.11	0	44.44	44.44	0	0	100
Pachacama Males	1	0	0	0	0	0	2	0	0	0	9	3	15
	6.67	0	0	0	0	0	13.33	0	0	0	60	20	100
Pachacama Females	0	0	0	0	0	0	1	0	0	0	4	4	9
	0	0	0	0	0	0	11.11	0	0	0	44.44	44.44	100
Total	55	58	33	30	25	43	32	13	17	7	15	9	337
	16.32	17.21	9.79	8.9	7.42	12.76	9.5	3.86	5.04	2.08	4.45	2.67	100

Table 4.25: Sexual Dimorphism in the tibia of 6 populations. Separation of male and female groups from 6 populations using 100% total variance. Upper figure denotes number of individuals correctly assigned; lower figure denotes percentage. Red figures denote number and percentage of individuals placed into their correct group; blue figures denote number of individuals and percentage correctly assigned to the opposite sex of the same population.

With respect to the three Native American samples, to clarify the non-significant results, the following analyses investigate the presence of significant sexual dimorphism within the samples when analysed separately. Results from these analyses are used to give greater insight into results when all populations are analysed jointly.

Differences in shape of the 32 Arikara, (22 males and 10 females), 26 Aleut (17 males and 9 females) and 24 Pachacama (15 males and 9 females) are analysed using the Procrustes fitted co-ordinates and by subjecting the data to PCA. Table 4.26 gives the proportional and accumulated variance for all PCs, which represent the total variance within each sample. Table 4.27 shows which PCs relate more specifically to sexual dimorphism when using canonical stepwise discriminant function. Figures 4.19, 4.20 and 4.21 summarise the best separation of male and female specimens when using PCs accounting for c.50% to 100% of total variation and those used in the stepwise discriminant function analysis. The scores for each specimen on the resultant PCs are subjected to canonical discriminant analysis to establish the relationships between the male and female specimens based upon the Mahalanobis' squared distance between sample means. The distance generated by stepwise discriminant analysis between males and females for the Arikara is 457.3 ($p<0.0001$), for the Aleut is 11.12 ($p<0.0001$) and for the Pachacama is 227984 ($p<0.0001$). Crossvalidation analyses assign 100% of males and 100% of females to the correct group in each sample. These analyses indicate, therefore, that the two sexes can be separated on some aspect of shape of the proximal tibia for each Native American sample.

Despite the non-significant result when the Arikara, Aleut and Pachacama samples are included in the joint analysis with the three other populations, results here have established the presence of sexual dimorphism in each sample when analysed separately.

Arikara			Aleut			Pachacama		
PCs	Prop.	Cumul.	PCs	Prop.	Cumul.	PCs	Prop.	Cumul.
PC1	13.6	13.6	PC1	18.70	18.7	PC1	15.00	15.0
PC2	11.5	25.1	PC2	12.70	31.4	PC2	11.90	26.9
PC3	9.71	34.8	PC3	9.42	40.8	PC3	11.50	38.4
PC4	7.22	42.0	PC4	7.74	48.6	PC4	9.48	47.8
PC5	6.25	48.3	PC5	6.62	55.2	PC5	6.85	54.7
PC6	5.87	54.1	PC6	6.28	61.5	PC6	5.99	60.7
PC7	5.58	59.7	PC7	5.52	67.0	PC7	5.27	65.9
PC8	4.79	64.5	PC8	5.09	72.1	PC8	4.69	70.6
PC9	4.35	68.8	PC9	3.56	75.6	PC9	4.46	75.1
PC10	4.02	72.9	PC10	3.30	78.9	PC10	4.31	79.4
PC11	3.47	76.3	PC11	2.98	81.9	PC11	3.56	83.0
PC12	3.33	79.7	PC12	2.73	84.7	PC12	2.98	85.9
PC13	2.74	82.4	PC13	2.14	86.8	PC13	2.39	88.3
PC14	2.57	85.0	PC14	1.92	88.7	PC14	2.21	90.5
PC15	2.35	87.3	PC15	1.89	90.6	PC15	1.85	92.4
PC16	1.77	89.1	PC16	1.70	92.3	PC16	1.64	94.0
PC17	1.66	90.8	PC17	1.48	93.8	PC17	1.33	95.4
PC18	1.56	92.3	PC18	1.31	95.1	PC18	1.11	96.5
PC19	1.15	93.5	PC19	1.09	96.2	PC19	1.03	97.5
PC20	1.07	94.5	PC20	1.02	97.2	PC20	0.80	98.3
PC21	0.99	95.5	PC21	0.80	98.0	PC21	0.72	99.0
PC22	0.79	96.3	PC22	0.65	98.6	PC22	0.50	99.5
PC23	0.76	97.1	PC23	0.57	99.2	PC23	0.48	100.0
PC24	0.62	97.7	PC24	0.51	99.7			
PC25	0.55	98.2	PC25	0.27	100.0			
PC26	0.48	98.7						
PC27	0.37	99.1						
PC28	0.31	99.4						
PC29	0.25	99.7						
PC30	0.20	99.8						
PC31	0.15	100.0						

Table 4.26: Sexual Dimorphism in the tibia of the Arikara, Aleut and Pachacama. The proportion and accumulated variance for PCs accounting for 100% of total variance.

Arikara		Aleut		Pachacama	
Order	Entered	Order	Entered	Order	Entered
1	PC1	1	PC8	1	PC8
2	PC15	2	PC4	2	PC1
3	PC10	3	PC23	3	PC3
4	PC4	4	PC2	4	PC9
5	PC24	5	PC7	5	PC12
6	PC20	6	PC12	6	PC23
7	PC26	7	PC17	7	PC10
8	PC29	8	PC16	8	PC19
9	PC30	9	PC5	9	PC16
10	PC16	10	PC10	10	PC20
11	PC25			11	PC21
12	PC8			12	PC17
13	PC3			13	PC6
14	PC19			14	PC7
15	PC7			15	PC13
16	PC27			16	PC18
17	PC6			17	PC15
18	PC31			18	PC14
19	PC12			19	PC4
20	PC23			20	PC22
21	PC18				

Table 4.27: Sexual Dimorphism in the tibia of the Arikara, Aleut and Pachacama. PCs selected by Stepwise discriminant function analysis and the order entered into subsequent discriminant function analyses.

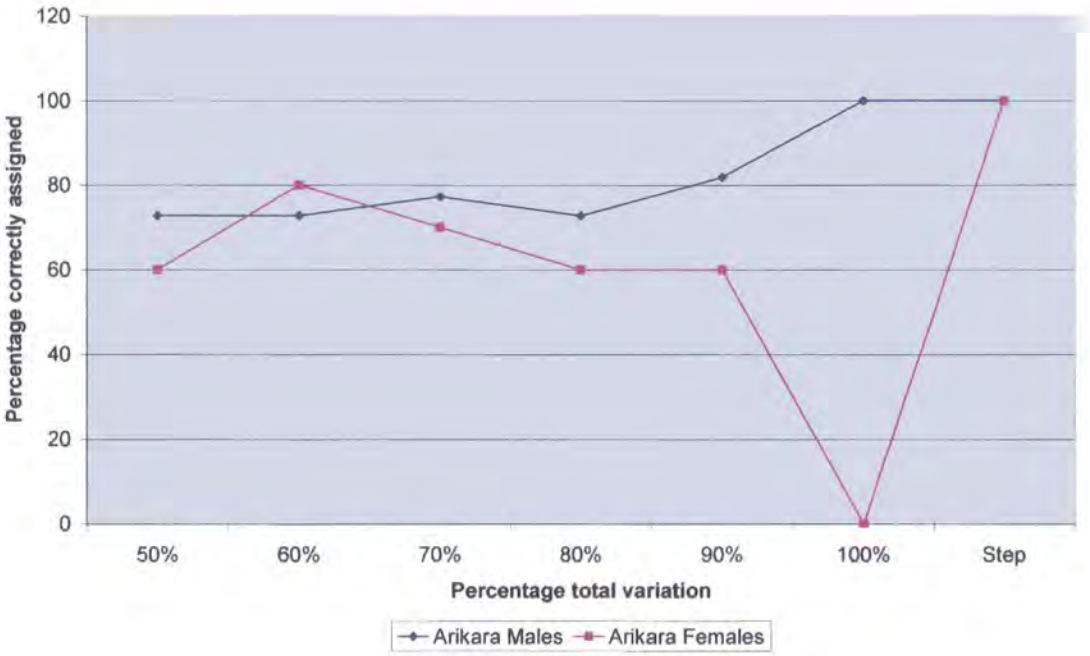

Figure 4.19: Sexual Dimorphism in the tibia of the Arikara. Summary of separate discriminant and cross-validation analyses using PCs accounting for c.50% of total variance PCs 1-5, c.60% PCs 1-7, c.70% PCs 1-9, c.80% PCs 1-12, c.90% PCs 1-17, 100% PCs 1-32 and stepwise discriminant analysis.

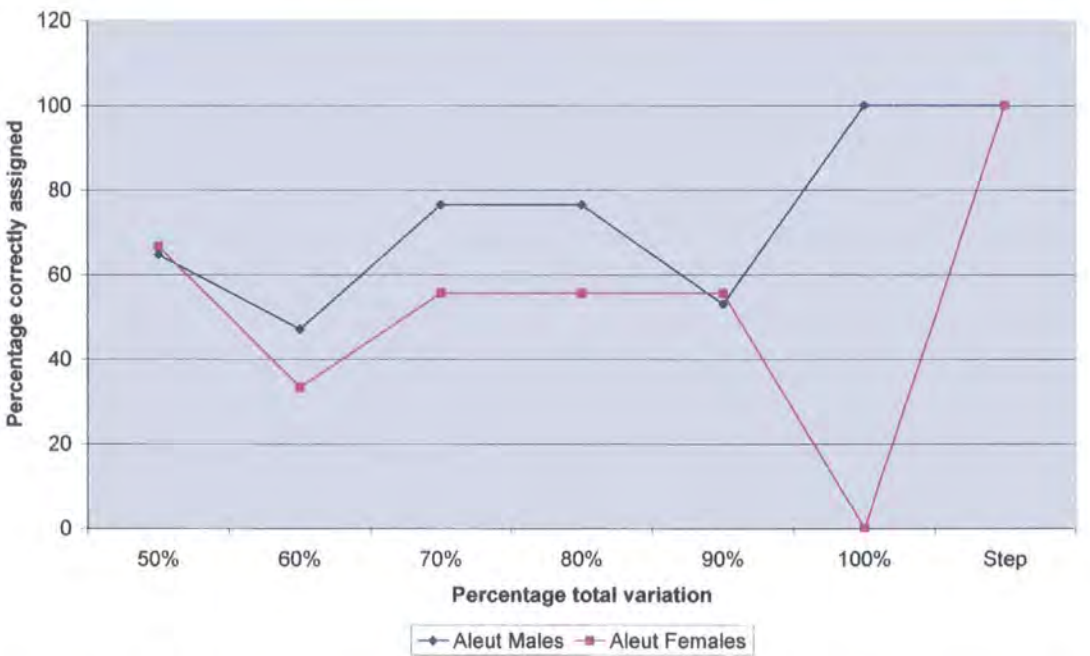

Figure 4.20: Sexual Dimorphism in the tibia of the Aleut. Summary of separate discriminant and cross-validation analyses using PCs accounting for c.50% of total variance PCs 1-4, c.60% PCs 1-6, c.70% PCs 1-8, c.80% PCs 1-10, c.90% PCs 1-15, 100% PCs 1-26 and stepwise discriminant analysis

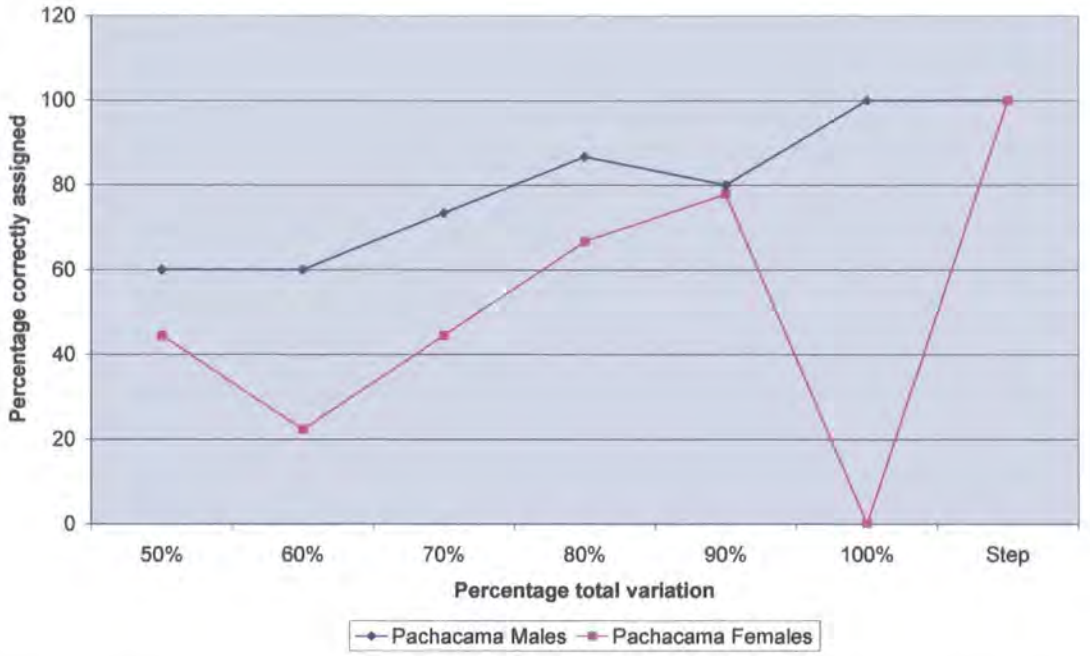

Figure 4.21: Sexual Dimorphism in the tibia of the Pachacama. Summary of separate discriminant and cross-validation analyses using PCs accounting for c.50% of total variance PCs 1-4, c.60% PCs 1-6, c.70% PCs 1-8, c.80% PCs 1-10, c.90% PCs 1-14, 100% PCs 1-24 and stepwise discriminant analysis.

4.4.4b(ii) Tibia: Description of differences in shape between males and females

Figures 4.22 and 4.23 show the bivariate plots of PC1 with PC2 and PC3 with PC4, accounting for a cumulative 42.30% of total variance. It is evident from these two figures that the overlap between male and female specimens from the six populations is too extensive to assess any degree of separation within each population sample and to establish any relationships between male and female groups across populations. It is also apparent from Figure 4.20 on PC1 (alone accounting for 23.6% of total variance) that the principal variation in the total sample is between the Spitalfields collection (including male and female elements) and the other five populations.

Figure 4.22:

Sexual Dimorphism in the tibia of 6 Populations, total sample. Bivariate plot of PC1 with PC2 which shows the overlap of specimens from different groups and the difficulty of assessing the separation of males and females of the 6 populations when using the total sample.

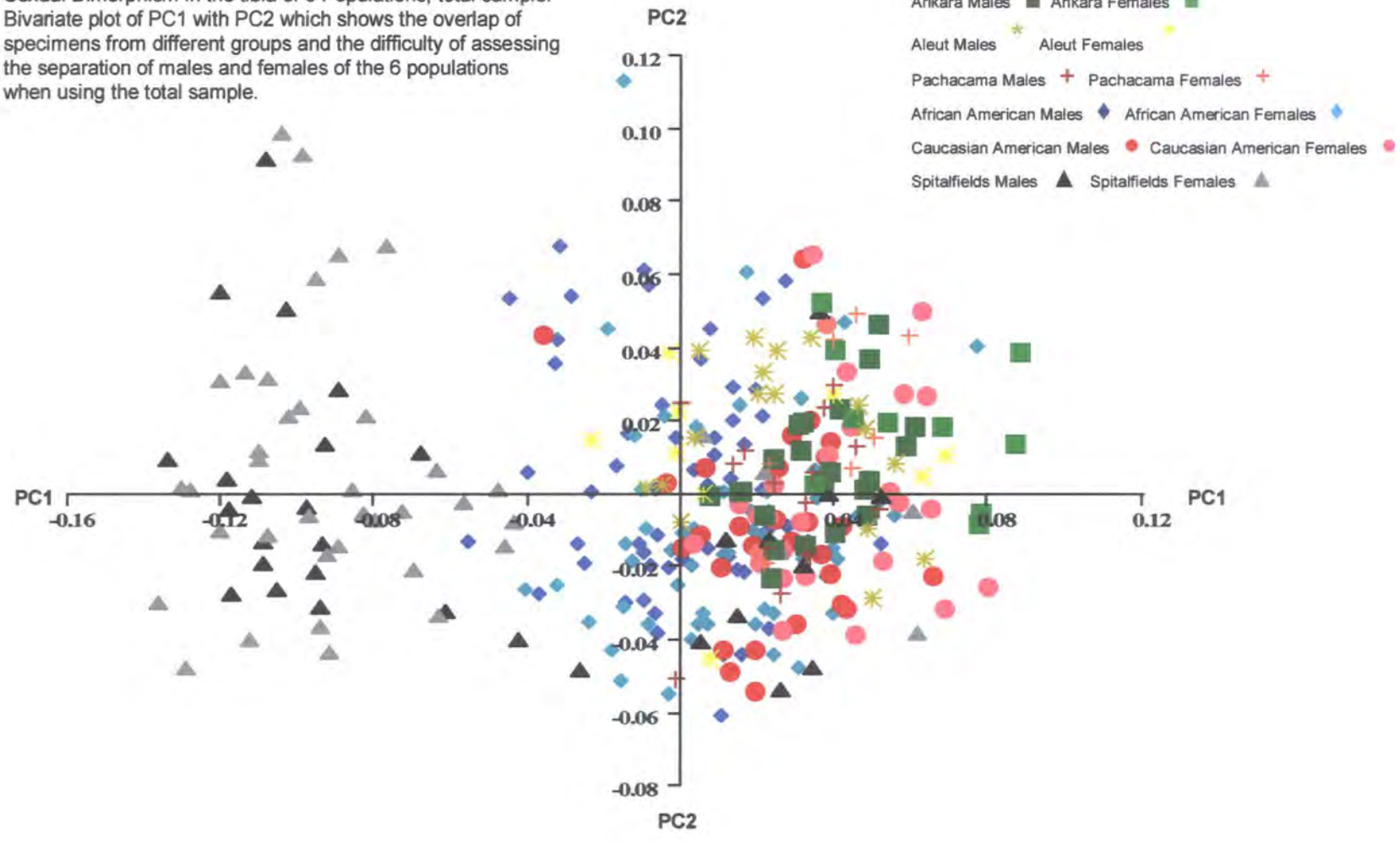

Figure 4.23:

Sexual Dimorphism in the tibia of 6 Populations, total sample. Bivariate plot of PC3 with PC4 which shows the overlap of specimens from different groups and the difficulty of assessing the separation of males and females of the 6 populations when using the total sample.

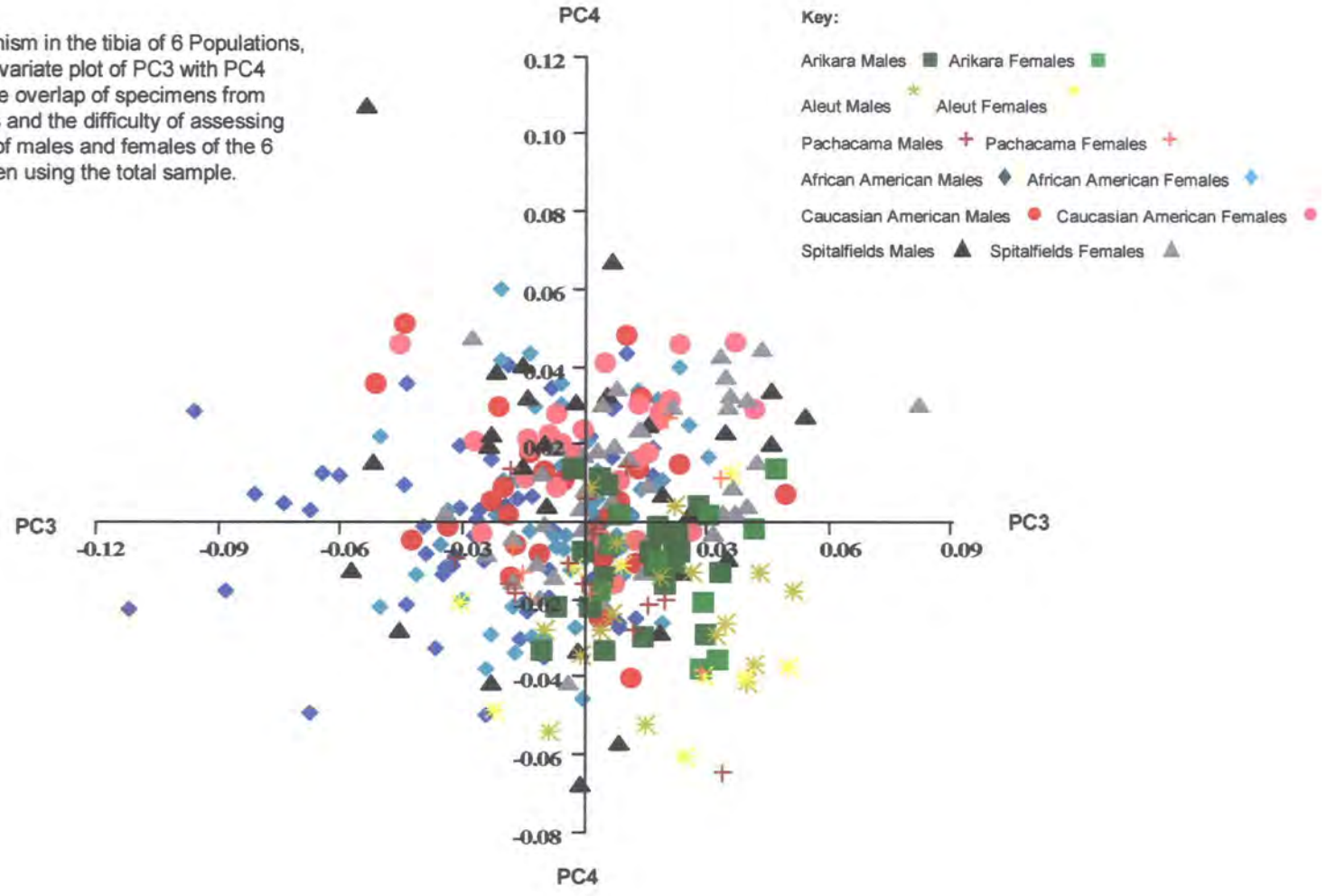

This obvious differentiation between one population sample and the other five is not repeated for subsequent PCs. It is too difficult to assess any other separation within the total sample for higher PCs, particularly between males and females. The causes for this apparent separation of the Spitalfields sample from the other populations will be examined further in Chapter 6 in comparing inter-population morphology.

Because of the high degree of overlap between individuals when using the total sample, the sample means of the two sexes for each of the six populations have been used to help distinguish specific variation due to sexual dimorphism. For the tibia, the correlation between the Procrustes distances using the population means shown in Table 4.28 and the Mahalanobis' squared distances shown in Table 4.23 does not reach a level of statistical significance (r= 0.11; p= 0.39). Figure 4.22 using the total sample and Figure 4.24 using sample means (see below), however, indicate the same primary separation of the Spitalfields males and females from all other groups in both analyses. The description of sexual dimorphism in the African American samples (section 4.4.3b(ii) above) is again used as an example, in order to compare and contrast results with the other five populations and to help interpret the relationships between the sexes in these additional samples.

The Procrustes mean co-ordinates have been calculated from the separate GPAs and have been subjected to a joint GPA and PCA. The proportion and accumulated variance of the PCs generated in the analysis of population means is given in Table 4.29:

PCs	Proportion	Cumulative	PCs	Proportion	Cumulative
PC1	61.10	61.1	PC7	2.50	95.6
PC2	13.40	74.5	PC8	1.54	97.1
PC3	6.47	80.9	PC9	1.28	98.4
PC4	5.08	86.0	PC10	0.84	99.2
PC5	3.76	89.8	PC11	0.75	100
PC6	3.33	93.1			

Table 4.29: Proportion and accumulative variance represented by PCs 1-11 which accounts for total sample variance for population means for the tibia.

African American Males	0											
African American Females	0.29	0										
Caucasian American Males	0.22	0.21	0									
Caucasian American Females	0.13	0.30	0.16	0								
Spitalfields Males	0.37	0.56	0.53	0.47	0							
Spitalfields Females	0.34	0.44	0.48	0.45	0.18	0						
Arikara Males	0.31	0.33	0.41	0.41	0.31	0.17	0					
Arikara Females	0.29	0.42	0.44	0.39	0.20	0.16	0.16	0				
Aleut Males	0.19	0.47	0.36	0.23	0.36	0.41	0.42	0.33	0			
Aleut Females	0.21	0.46	0.31	0.21	0.39	0.43	0.44	0.36	0.15	0		
Pachacama Males	0.35	0.52	0.34	0.25	0.61	0.64	0.63	0.58	0.30	0.25	0	
Pachacama Females	0.37	0.10	0.27	0.38	0.61	0.49	0.37	0.47	0.54	0.53	0.58	0
	Af. Am. Males	Af. Am. Females	Ca. Am. Males	Ca. Am. Females	Spitalf. Males	Spitalf. Females	Arikara Males	Arikara Females	Aleut Males	Aleut Females	Pachac. Males	Pachac. Females

Table 4.28: Sexual Dimorphism in the tibia in 6 Populations. Procrustes distances between mean individuals of right and left groups for males and females of 6 populations. Correlation between Procrustes distances and Mahalanobis' distances (Table 4.23) is not significant at $r = 0.11$; $p = 0.39$).

The first four PCs account for 86% of total variance and the exploration of shape differences between sexes will concentrate on these four PCs.

Figure 4.24 indicates that for the tibia, sexual dimorphism within the six populations is not identical, either in nature or degree, and that sexual dimorphism in the African Americans is not shared in all aspects by the other population groups. In Figure 4.25 (PC1), the mean configuration at the negative extreme shows a slightly greater length of tibial tuberosity relative to the edge of the plateau (landmarks 14, 15 and 16 relative to landmarks 3 and 9), compared to the mean configuration at the positive extreme. This difference appears to be less significant than the difference in proportions of the tibial shelf and the repercussions this creates in the posterior region.

For means from all six populations, the Spitalfields pair at the negative extreme is seen to have the longest anterior section, while the Arikara female mean at the positive extreme has the shortest length. In addition to the greater anterior length, the posterior section in the Spitalfields pair is seen to be slightly protruding from the edge of the shelf relative to other groups. The most visible expression of difference between all groups is in the angle created between the three landmarks 14, 15 and 20, in Figure 4.25(d). This difference in morphology of the tibial shelf on PC1 was also noted between male and female African American means (section 4.4.3b(ii) above) where a change in length of the tibial tuberosity was accompanied by a change in proportions of the tibial shelf. In Figures 4.7 and 4.25, the African American male mean is placed more negatively relative to the female mean (and therefore closer to the Spitalfields pair) and shows relatively greater length of tibial tuberosity compared to the female, with the more acute angle created between landmarks 14, 15 and 20. This similarity of positioning (and therefore shape) also applies to the Caucasian Americans, Arikara and Pachacama. The Spitalfields mean male and female pair, however, together with the Aleut, shows a reversed positioning and therefore a comparative difference in sexual dimorphism relative to the other four pairs of means. Figure 4.25 shows that the degree of sexual dimorphism is relatively similar in five of the populations, with the Arikara showing slightly greater dimorphism for the characteristics explained by PC1.

Figure 4.24:

Sexual Dimorphism in the tibia of 6 Populations. Bivariate plot of PC1 with PC2, showing the separation of male and female means. Arrows point from male to female means from each population. Images represent the mean configuration if warped to the extremes of PC1 (at 0.04 to –0.06) and PC2 (at 0.04 to -0.03).

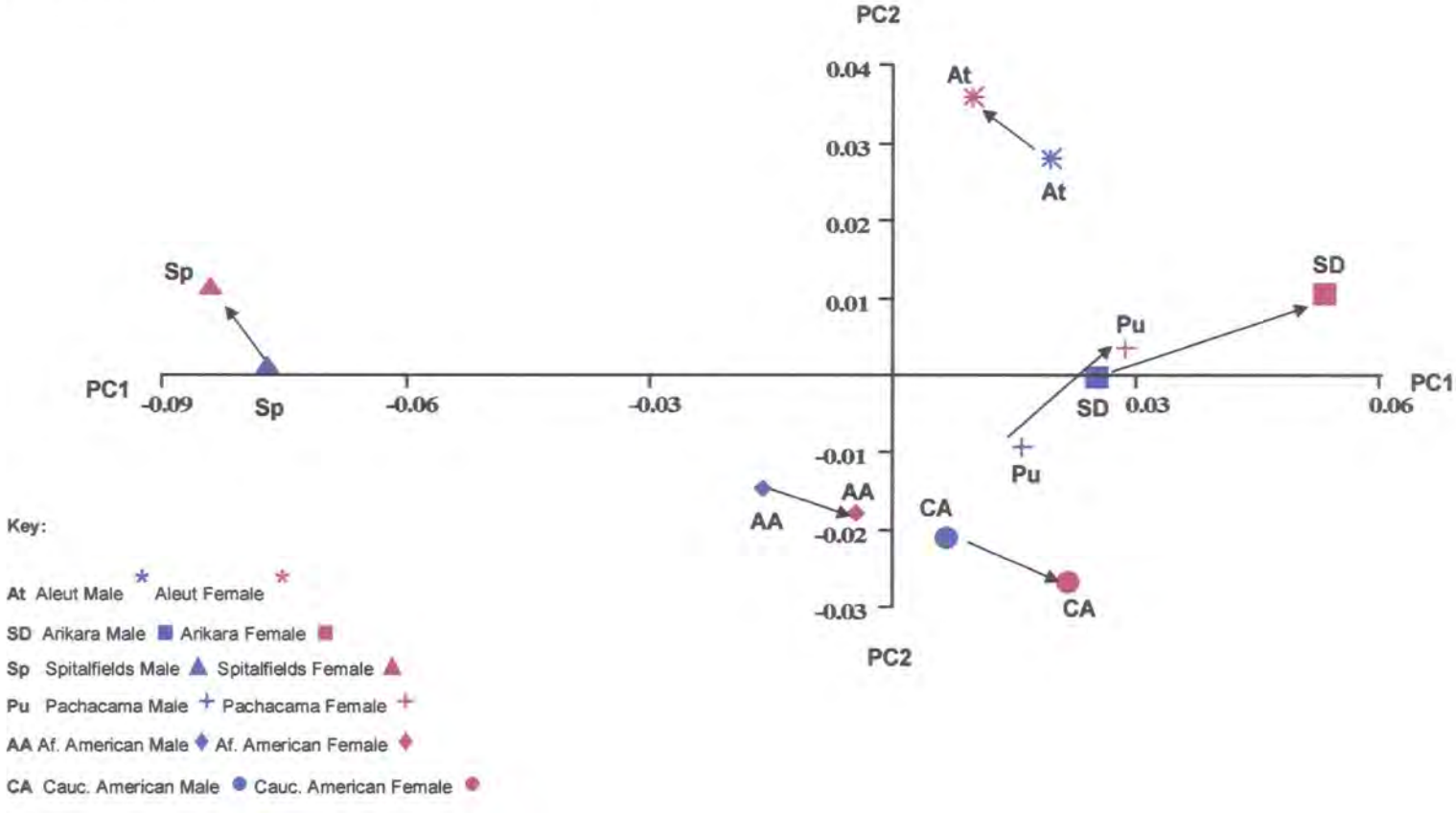

Figure 4.25:

Sexual Dimorphism in the tibia of 6 Populations. Separation of male and female means of 6 populations on PC1. Images represent the mean configuration if warped to the extremes of PC1 (at 0.06 to –0.09). Images (c) and (d) include landmarks discussed in the text (section 4.4.4b(ii)).

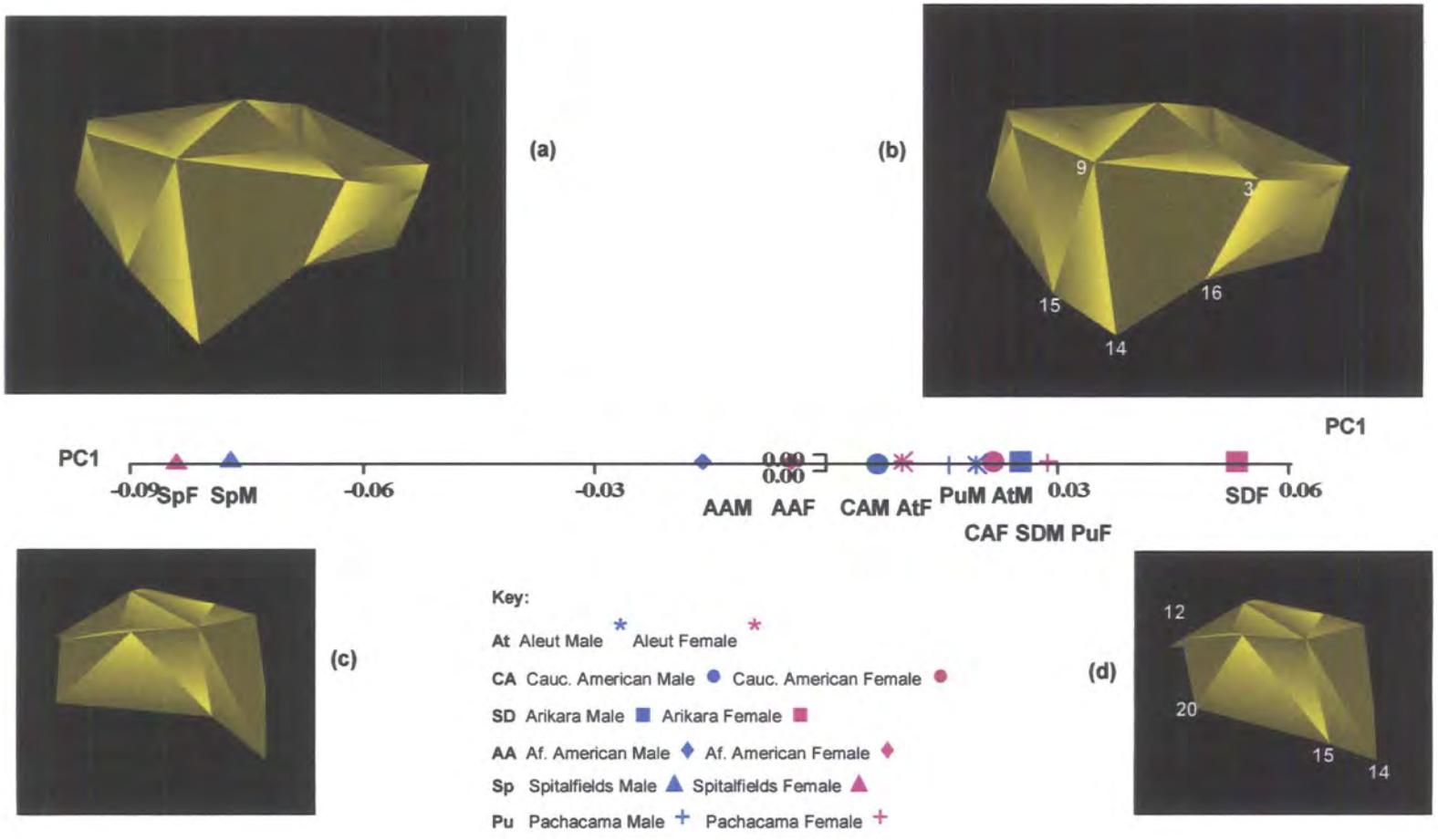

Variation explained by PC2 is less easily appreciated than in PC1 but appears to reflect differences in the relative protrusion or retraction of the posterior section of bone under the tibial shelf. This is most clearly visible in the relationship between the two landmarks 12 and 20 in Figure 4.26(d). For this trait, the African and Caucasian American male means are placed more positively than their corresponding females, indicating that the posterior section of bone is relatively more retracted in males relative to females. This positioning and therefore difference in shape is reversed in the Spitalfields, Arikara, Aleut and Pachacama pairs compared to the African and Caucasian American pairs. For PC2, the degree of sexual dimorphism is relatively similar for four of the population samples, with the African and Caucasian American samples showing slightly less dimorphism than in the other four populations.

It is difficult to interpret the variation between males and females expressed by PCs 3 and 4 in Figure 4.27, although, once again, it appears to reflect differences in the shape of the tibial shelf. For PC3, this is concentrated in the depth of the shelf over the lateral side and most clearly appreciated in the distance between landmark 9 at the anterior edge of the tibial plateau and landmark 15 at the inferior edge of the tibial shelf. Greater depth in this region does not appear to be a specifically male or female trait, with three male means and three female means showing greater depth relative to the corresponding sex of the same population. Only 5.08% of variation is accounted for by PC4, with little visual difference between the twelve means. Again, the variation accounted for by PC4 is not a specifically male or female trait, as five of the six males are placed more positively relative to their respective females, with the sixth (the Pachacama), showing the reversed position. The degree of sexual dimorphism appears to vary for this PC, with considerable dimorphism shown for the African Americans and a negligible amount for the Aleut.

The areas of greatest difference across all means can be seen in Figure 4.28 which shows where the maximum deformation of the TPS lies on PC1. Because the differences between male and female pairs of means within each population are too small

Figure 4.26:

Sexual Dimorphism in the tibia of 6 Populations. Separation of male and female means of 6 populations on PC2. Images represent the mean configuration if warped to the extremes of PC2 (at 0.04 to –0.04). Image (d) includes landmarks discussed in the text (section 4.4.4b(ii)).

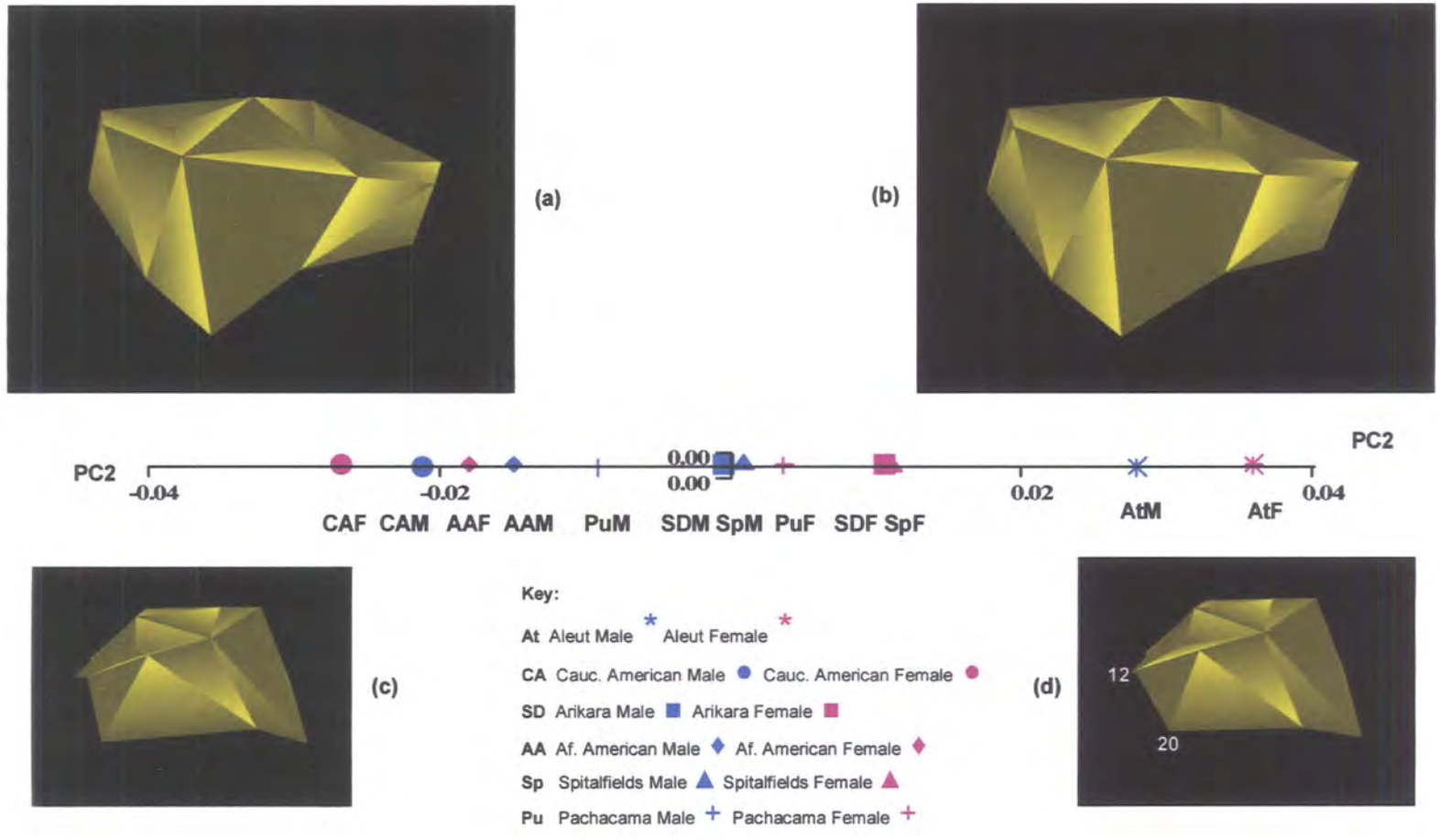

Figure 4.27:

Sexual Dimorphism in the tibia of 6 Populations. Bivariate plot of PC3 and PC4, showing a separation of male and female means. Arrows point from male to female means from each population. Images represent the mean configuration if warped to the extremes of PC3 (at 0.04 to –0.04) and PC4 (at 0.02 to -0.02). The image at the positive extreme of PC3 shows landmarks discussed in the text (section 4.4.4b(ii)).

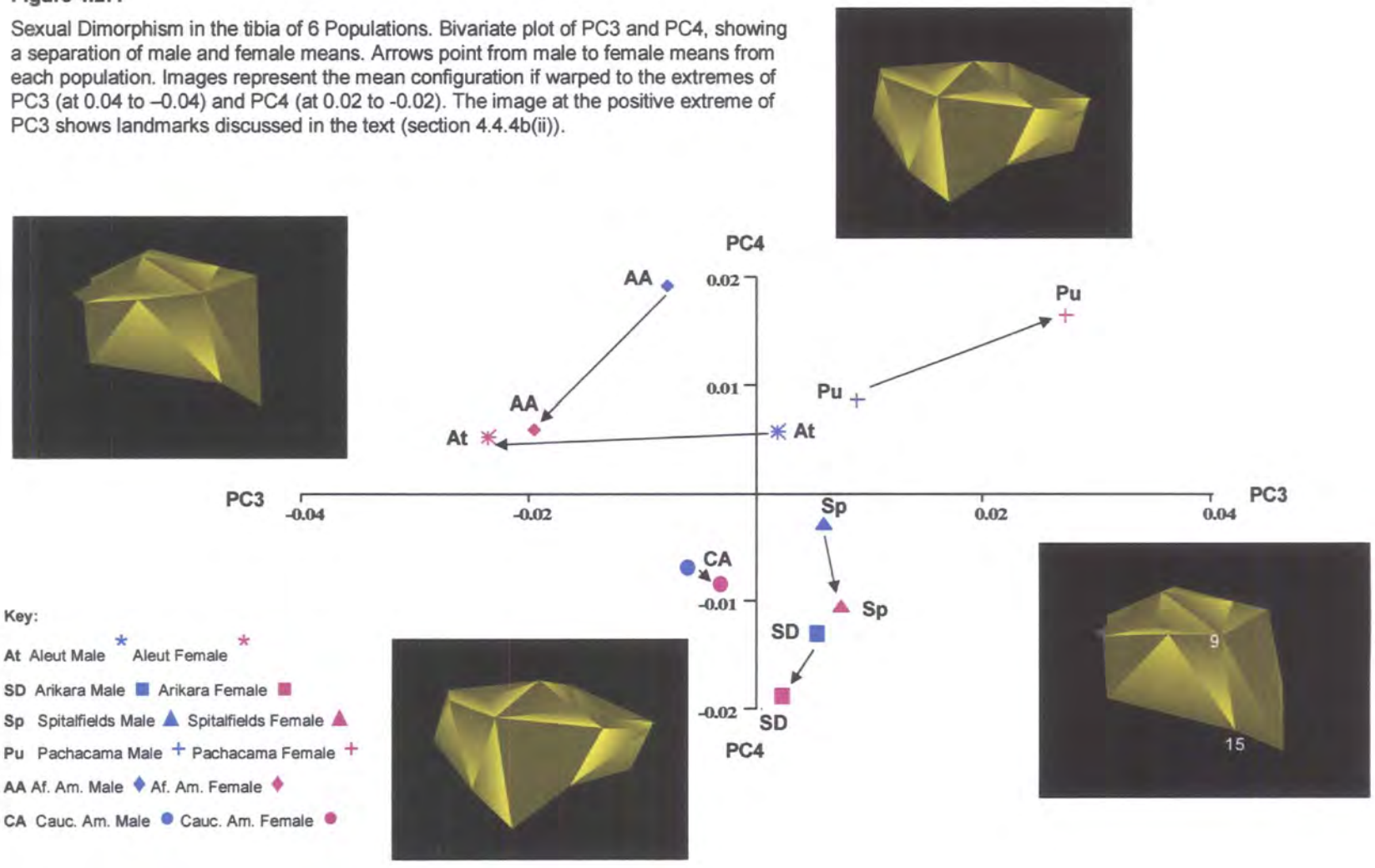

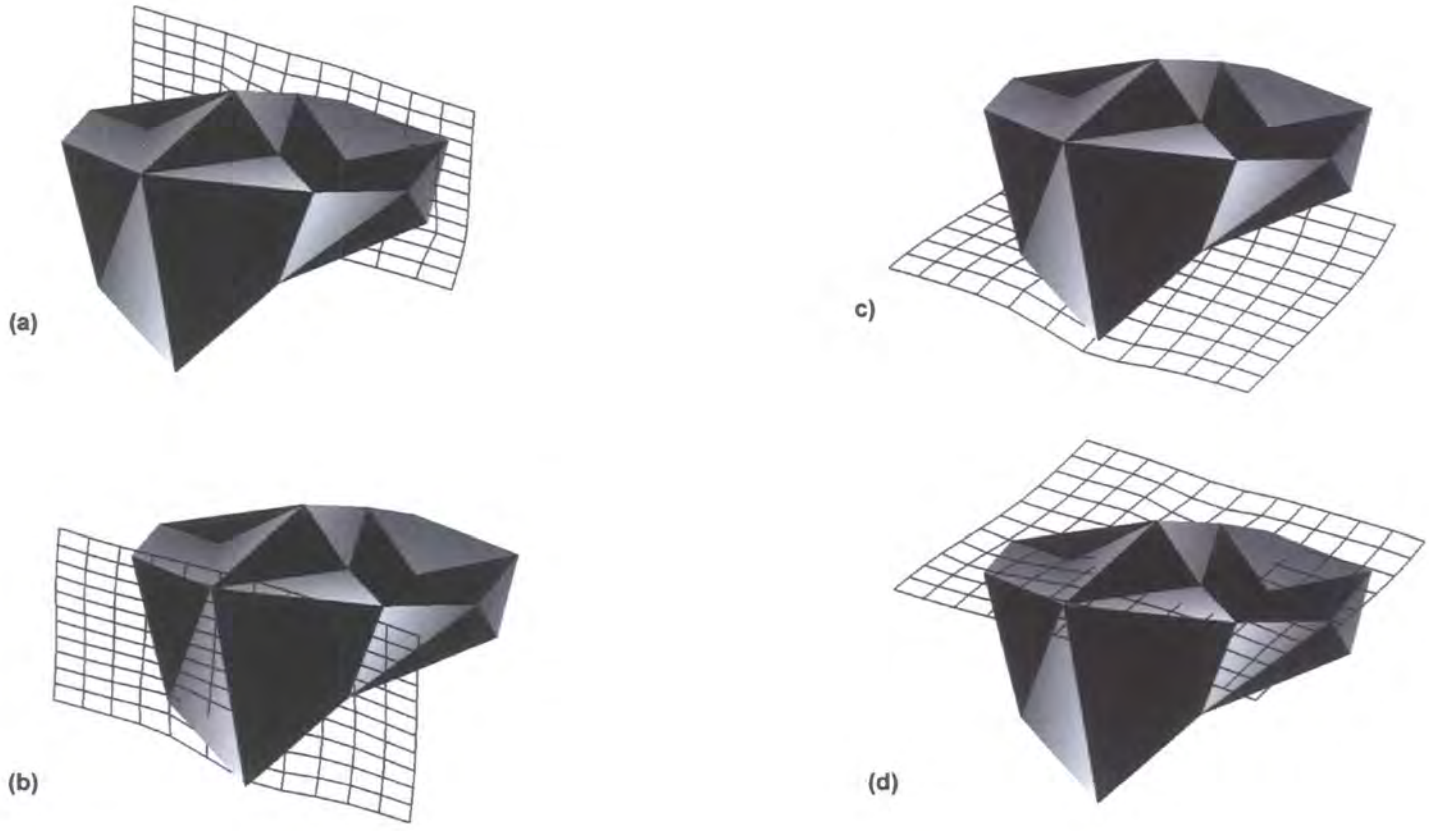

Figure 4.28: Sexual dimorphism in the tibia of 6 Populations. Representations of tibial shape with TPS taken from PC1 using male and female sample means, showing regions of bone giving maximum difference in shape between means. Figures 4.26 (a) and (b) represents TPS view in anterior-posterior plane; 4.26 (c) and (d) in proximal plane. Images are presented in Figure 4.26 to give the best indication of maximum difference in shape on PC1 and are not necessarily taken from the same perspective as the mean configurations in Figure 4.23.

to interpret from such diagrams, each figure can only show maximum differences across all twelve means. Further interpretation of sexual differences must therefore take into account the relationships between the sample pairs described above. Figure 4.28(a) to (c) reaffirm differences noted above in the anterior region, affecting the length of the tibial tuberosity, in the depth of the tibial shelf and across the posterior section.

4.5 Discussion

Sexual dimorphism in the size of many postcranial skeletal parts for any sample is frequently visually obvious. Previous research conducted on hard tissue and muscle insertion sites of both the postcranium and cranium confirms the presence of sexual dimorphism in size in all populations studied, both in relation to specific skeletal parts within populations and in the degree of sexual differences between populations (Wood and Lynch, 1996; Wilczak, 1998). Males, on average, are bigger and more robust than females, although many skeletal parts from gracile and smaller males will always be confused with bigger and more robust females around the centre of any distribution. Also, although some male parts can be up to 20% bigger than those of females from the same population, the distinctions between skeletal samples becomes complex when heavier and more robust populations are compared with smaller and lighter ones (White, 2000).

In this analysis, sexual dimorphism in the maximum length of both femur and tibia is readily established for each population. Using the total sample, the sexual difference in size is identical for femur and tibia at 92.96%, at a high level of statistical significance. Whilst, sexual dimorphism in relation to the robusticity indices of the long bones only reaches statistical significance in 50% of analyses, the variation between populations in the degree of dimorphism is considerably greater in terms of robusticity than in maximum length or indeed, in the centroid size of the knee joint. This degree of variation in robusticity compared to length is predictable in the light of previous research. Significant differences in mediolateral and anteroposterior diaphyseal measurements both between populations and within the same population over time, has

been used to demonstrate the adaptive properties of bone relative to the specific environment of distinct populations, in addition to the inherent functional implications of the difference in shape of the male and female pelvis. (e.g., Larsen, 1981, 1995; Ruff and Hayes, 1983; Ruff et al., 1984; Brock and Ruff, 1988; Bridges, 1989; Collier, 1989; Hawkey and Merbs, 1995; Ruff, 1997; Churchill and Morris, 1998).

The calculation of robusticity indices here is a simple measurement compared to more sophisticated cross-sectional geometric analyses. Although cross-sectional analyses are now routinely used, as they provide more informed results by comparing internal as well as external dimensions and properties of bone, there is a high correlation in results when using both methods (Larsen, 1999). Significant sex differences have been shown in cross-sectional values between different populations as a whole, such as the various North American Indian groups during the transitional stages from foraging to agriculture (e.g., Larsen, 1981, 1995; Ruff and Hayes, 1983; Ruff et al., 1984; Brock and Ruff, 1988; Bridges, 1989; Hawkey and Merbs, 1995; Ruff, 1997) and for groups from the same population but undertaking significantly different activities (Stirland, 1993).

Sex differences in bone size and structure are therefore complex and strongly linked to the sexual division of labour and loading pressures of different activities undertaken by men and women, and the terrain where each primarily carries out his or her allotted tasks (Murdock and Provost, 1973; Larsen, 2000; Ruff, 2000). The energy requirement for males, who tend to be bigger and have a higher proportion of metabolically-active lean tissue, is therefore greater than for nonpregnant females. As such, environmental stressors and the alleviation of those stressors will have a greater impact on male growth and development and will proportionately affect male shape to a greater degree than female shape (Stini, 1985). Ruff (1987) attributed a decrease in sexual dimorphism of cross-sectional geometric values in the lower limbs of Georgia coast native North American samples in the transitional phase to a reduction of anteroposterior bending loads. This reduction of anteroposterior bending loads applied particularly to the knees of males no longer participating in activities requiring fast running. With a reduction of

bone being distributed in the anteroposterior plane, the male shape became more feminised.

In relation to the functional repercussions of sex differences in pelvic shape, Burr et al. (1983) examined the biomechanical implications for locomotion. They conclude that the principal contribution to male-female discrimination in patterns of locomotion is caused by the differential loading on abductor muscles of the hip and, through them, differential pressure on the femoral head. Sexual dimorphism in body size is less likely to be a major contributory factor to biomechanical variability (Lovejoy et al., 1973), although it should still be considered a necessary component. Van Gerven (1972) states that the greater width of the female pelvis combined with the shorter femur implies an increase in the bicondylar angle that increases femoral torsion in females over males. By implication, any differential loading on the proximal femur will affect shape variability of the distal femur and leg.

In addition, the physical changes in women during reproduction create many and varied effects on the skeletal tissue itself, primarily in the pelvis (Cox, 2000) but also in the lower limbs (Mensforth and Lovejoy, 1985). There is a significant depletion of calcium, iron and mid-shaft femur bone in women from societies where high levels of fertility over a long period are encouraged; to the extent that in some highly fertile groups, significant bone loss is seen throughout the third decade of female life with improvement during the middle of the fourth decade and a decrease thereafter with the onset of the menopause (Mensforth and Lovejoy, 1985). Differences in cortical bone structure caused by differential rates of parturition will therefore have an effect upon the overall degree of sexual dimorphism in lower limb form, both within and between populations.

This study shows that for maximum length, all populations are sexually dimorphic to a statistically significant level within a close range, i.e., a c.3% difference between the least dimorphic samples (the Caucasian Americans at 94.41% for the femur and 94.33% for the tibia) and those with the highest degree (the Aleut at 91.19% for the femur and

the Arikara at 91.17% for the tibia). In relation to femoral and tibial robusticity, although there appears to be less sexual dimorphism overall in comparison to maximum length, there is considerable variability in the degree of robusticity between populations. Results show there is a difference of 5.27% for the femur and 8.50% for the tibia between the least sexually dimorphic samples (the Spitalfields group at 98.75% for the femur and at 97.08% for the tibia) and the greatest degree of sexual dimorphism (the Pachacama at 93.48% for the femur and 90.57% for the tibia).

Hypothesis H.4.1 was erected to test whether the degree of sexual dimorphism in maximum length measurements and the robusticity of the femur and tibia is identical across all six populations examined. This study falsifies this hypothesis by showing that the degree of sexual dimorphism varies between the six populations. Whilst the range of variation is relatively close between samples in terms of maximum length, it is considerably wider in terms of robusticity.

In relation to centroid size, results show that those of males are bigger than those of females of the same population to a statistically significant degree. They also show that the degree of sexual dimorphism in size is greater in the knee joints than in the diaphyses, with an average size difference of 10.05% for the femur and 11.13% for the tibia between the sexes, using the total sample, (compared to 7.04% for both femur and tibia in length). The six population means range between the groups with the least degree of sexual dimorphism (Spitalfields at 90.89% for the femur and Caucasian Americans at 89.99% for the tibia) to the greatest degree (African Americans at 88.77% and 87.55% for the femur and tibia respectively), a difference of 2.12% for the femur and 2.44% for the tibia. This is a relatively smaller differential between samples compared to maximum length and, especially, robusticity.

The relatively small range of variation in rates of sexual dimorphism between different population samples in knee joint size (compared to diaphyseal robusticity) accords with research such as that by Rafferty and Ruff (1994), Ruff et al. (1994) and Lieberman et al. (2001), who argue that articular joint size and shape does not respond to alterations in

mechanical loading to the same degree as diaphyseal structure, in that the articular joints are less developmentally plastic than the diaphyses. Macho (1990), Holland (1991), Iscan et. al. (1994), Iscan and Shihai (1995), King et al. (1998) and Asala et al. (2004), however, have all shown that epicondylar width in the femur and proximal epiphyseal width in the tibia can be the most sexually dimorphic and diagnostically useful of all femoral and tibial measurements, including bone length. They are also capable of demonstrating clear sex differences within and between such diverse populations as native Africans, South Africans of European extraction, Thai, Chinese, African and Caucasian Americans and modern Japanese.

To some degree, the results of this study concur with both sets of findings. The range of difference in degrees of sexual dimorphism in knee joint size between samples is shown to be relatively low and therefore supports the conclusions by Rafferty and Ruff (1994), Ruff et al. (1994) and Lieberman et al. (2001). These results also support the findings of Macho (1990) and the second groups of workers named above, however, in that, whilst the range of difference in sexual dimorphism between populations is relatively low, the degree of sexual dimorphism within each sample is relatively high and is therefore likely to provide a good indication of sex. It should be noted, however, that this later group of researchers, use only one specific measurement per bone for assessment, in comparison to this study, which compares overall size.

Interestingly, Purkait (2002) and Purkait and Chandra (2004) found that comparisons of head measurements proved more reliable and produced more accurate results for estimating sexual variation in the Indian femur, than comparisons of epicondylar width. This contrast with the results by Macho (1990) and the groups of workers listed above and lends support to the conclusion that sexual dimorphism is a population-specific phenomenon, (discussed in relation to hypothesis H.4.3 below).

Hypothesis H.4.2 was erected to test whether the degree of sexual dimorphism in the centroid size of the knee joint is identical across all six populations examined. This study falsifies this hypothesis by showing that the degree of sexual dimorphism in centroid

size varies between the six populations, although the degree of variation between populations is relatively small.

Results of this study show that in relation to knee joint shape, all six populations are sexually dimorphic to some degree in both the femur and tibia. For the African and Caucasian Americans and the Spitalfields populations, sexual dimorphism appears to be relatively strong, with results reaching a high level of statistical significance when analysed both separately (for the African Americans) and jointly with all six populations. For the three Native American populations, analyses have indicated a degree of sexual dimorphism when each sample is analysed separately, but this distinction becomes weaker when all groups are analysed jointly. Particularly for the tibia, the statistically significant level of sexual dimorphism within each of the three Native American samples when analysed separately, fails to reach a level of significance when all populations are analysed jointly. In addition, although the level of sexual dimorphism appears relatively high for the African and Caucasian Americans and the Spitalfields samples compared to the three Native American populations, there is an almost complete overlap of individuals in the bivariate plots when using the total sample and even for the African American sample when analysed alone. It is therefore likely that sexual dimorphism is not the most influential variable for knee joint shape between populations. With no clear separation of the sexes when using the total sample, it is only possible to decipher morphological differences by using the sample means, despite the lack of significant correlation between the two methods of analysis.

From using the sample means, it is clear that the degree and nature of sexual dimorphism seen in the African American sample is not shared in all aspects by the other five populations. Whilst is it evident that sexual dimorphism is concentrated in certain characteristics across populations, each population appears to show variation in how these differences are expressed. For example, for the femur the more lateral orientation of the joint relative to the diaphysis expressed by PC1, is seen in females relative to males in five of the six samples and is reversed in the Pachacama. For variation explained by PC2, five populations appear to show only a small degree of

dimorphism, whilst the Aleut show considerably more variation. For the tibia, primary variation is concentrated in the length of the anterior section, with males showing greater length relative to females in four populations, but with greater length being shown by females in the Spitalfields and Aleut samples. For PC4, there is considerable variation shown between the sexes for the African Americans, but only a negligible degree in the Aleut. These results indicate that both the nature and degree of sexual dimorphism in both femur and tibia is unique to each sample.

The results of this study point towards a relatively low level of sexual dimorphism in the shape of the articular surfaces, a conclusion that indicates that the shape of the surfaces may be less responsive to developmental changes than the diaphyses. However, even if the joints *are* less responsive to the normal environmental pressures acting upon the form of the diaphyses (e.g., climate, altitude, lifestyles, nutrition and pathologies), they are proportionately more prone to the degenerative diseases of osteophytosis and osteoarthritis (see Chapter 5). Researchers have noted clear differences in the incidence and sites of such diseases between different populations, in the onset of disease in different populations and (in relation to this chapter) in the different patterns of disease between males and females within the same population (Chapman, 1972; Larsen, 1982, 1999, 2000; Bridges, 1991, 1992; Molleson, 1994; Grieve, 1996; Aufderheide and Rodriguez-Martin, 1998). In addition, they have outlined how the incidence of joint disease between males and females alters with changes in subsistence and activity patterns between groups and within groups at different times (Larsen, 1999). Bridges (1991) notes that whilst there are few sexual differences in the incidence of joint diseases in Archaic hunter-gatherer groups in northwest Alabama, differences start to increase in farmers of the Mississipian period, when severe osteoarthritis is seen to affect men and women at different rates in different joints. In relation to the knee, all degenerative joint diseases affect this joint more than any other and, overall, affect more women than men and the femur more than the tibia (Aufderheide and Rodriguez-Martin, 1998). Although all specimens used for this study were chosen as ostensibly healthy and disease-free, results from Chapter 5 suggest that shape changes occur prior to any

external signs of disease (Riddle et al., 1988; Rodgers et al., 1990; Roberts and Manchester, 1997).

Hypothesis H.4.3 was erected to test whether sexual dimorphism in knee joint shape is a population specific phenomenon. Results of this study show that each population has a unique pattern of sexual dimorphism in both the distal femur and proximal tibia and therefore support the hypothesis.

For the femur, results show that despite the finding of sexual dimorphism in knee joint shape, males from each population are more similar in shape to the females of their own population than to any other group. For the tibia, results also show that males and females from the same population are more similar in shape relative to all other groups, with one exception. The distance between males and females in this exceptional case, however, is not significant. Therefore, results appear to hold sufficiently well to allow male and female specimens and those of unknown sex of the same population to be combined into a single sample for analyses comparing shape differences between populations, without significantly compromising results.

Hypothesis H.4.4 was erected to test whether the morphologies of the knee joints of males and females of the same population are more similar to each other relative to the shape of joints of all other groups. This study therefore supports hypothesis H.4.4.

Early research by Iscan and co-workers (1984a, 1984b, 1986) originally implied that the tibia is the more sexually dimorphic bone compared to the femur and hypothesis H.4.5 was erected to test this assertion.

The results in this study for the three size measurements, suggest that the tibia shows the greatest degree of sexual dimorphism in 80% of analyses. In each of the six samples for the centroid size of the knee joint, the tibia is seen to be the more dimorphic bone. For robusticity, only the Arikara show a greater degree of dimorphism in the femur compared to the tibia; for maximum length, only the Aleut and Pachacama show a

greater degree of dimorphism in the femur. Using the total sample, results suggest that the tibia is identical to the femur in degrees of sexual dimorphism in length and although variation in the degrees of sexual dimorphism between the six samples is greater for the tibia, it is by a negligible amount only. For robusticity of the shaft, using the total sample, the tibia is the more dimorphic bone and is also seen as the more variable in degrees of sexual dimorphism between populations. In centroid size of the knee joint, the tibia is again the more sexually dimorphic bone, but by a small degree only, with a marginally greater degree of variation in the tibia between the six samples.

In terms of knee joint shape, whilst it is not feasible to directly compare results for the femur with those of the tibia, it appears that distances between samples in the femur between males and females of the same population are statistically significant in more cases than in the tibia, when all six populations are analysed jointly. For the femur, only one male-female pair failed to reach a level of statistical significance, although this remained close to significance at $p= 0.058$. For the tibia, results for three male-female pairs failed to reach statistical significance at $p= 0.80$, $p= 0.39$ and $p= 0.41$. These results therefore provide some limited indication that for knee joint shape, the femur is the more sexually dimorphic bone. If these indications are accepted, the difference between the tibia being more sexually dimorphic in shaft dimensions and the femur being more dimorphic in relation to the bone ends therefore lends support to this earlier research by Iscan and co-workers (1984a, 1984b, 1986).

In the light of the support for hypothesis H.4.3, (the degree and nature of sexual dimorphism in the femur and tibia is a population-specific phenomenon), it is not feasible to uphold hypothesis H.4.5, however, as the tibia cannot be seen to be the more sexually dimorphic bone *as a generalisation.*

These results therefore lend support to the conclusions reached in later research by Iscan and co-workers (1994,1995), who concluded that inter- and intra-specific variation precludes making generalisations about the degree and nature of sexual dimorphism in lower limb form, as each sample shows its own unique pattern.

4.6 Implications of results and direction of future research

Results here have established the presence of sexual dimorphism in knee joint shape in the six populations examined. They show that the degree of sexual dimorphism is relatively more pronounced in some populations, and that its nature varies between populations. Results also indicate that sexual dimorphism is unlikely to be the most influential variable for knee joint shape between populations. In addition, it has been established that there is a significant degree of sexual dimorphism in the centroid size of the knee joint and that this relative difference in size is greater than that of length for both the femur and tibia.

The implication of these results arises from two assertions. Firstly, these differences in size and shape at the knee joint are innate, arising from general differences in the morphology of the skeleton (particularly the pelvis), and influenced by the dimorphism in body weight, creating differential stresses on the limbs (Van Gerven, 1972; Lovejoy et al., 1973; White, 2000). Secondly, sex differences are exacerbated by differing loading stresses placed upon them by the different tasks undertaken by males and females throughout life (Larsen, 1981, 1995; Ruff and Hayes, 1983; Ruff et al., 1984; Brock and Ruff, 1988; Bridges, 1989; Stirland, 1993; Hawkey and Merbs, 1995; Ruff, 1997).

To determine the degree to which innate factors such as differential body weight places upon the knee joint relative to differential loading pressures caused by differing lifeways, future research should be directed towards an understanding of the morphology of the knee joint in non-human primates. Rowe (1999) estimates the ratio of female to male body weight in humans at approximately 80% (based upon an average female weight of 55kg compared to males at 68kg). The ratio between male and female common chimpanzees (*Pan troglodytes*), for example, is approximately 79% (average female weight of 31kg compared to males at 39kg), and in western lowland gorillas (*Gorilla gorilla*), the ratio is approximately 42%, (average female weight of 72kg compared to males at 170kg). Analyses using knee joint specimens from species such as

these two, would help determine the relative importance of innate factors such as body weight differentials relative to those arising from differing lifeways. Analyses should take into account differences in patterns of behaviour between the sexes, for example, male and female chimpanzees show relatively few substantive differences in behaviour (both sexes being equally arboreal), whilst male gorillas spend more time resting and feeding on the ground, being considerably less agile than females because of the significant difference in body weight. Non-significant results of sexual dimorphism of knee joint shape in chimpanzees (which share the same body weight ratio as humans) might therefore emphasise the importance of differing economic strategies in humans in determining significant sexual dimorphism in knee joint shape. Non-significant results in analyses using male and female gorilla specimens, which are considerably different in body weight, would reinforce this conclusion. Equally, significant results in non-human primate species might emphasise the relative importance of innate factors and differences in general morphology relative to those of differing lifeways in determining sex differences in knee joint shape in humans.

4.7 Direct implications of results for this study

Males and females of each population will be combined into discrete samples for future inter-population analyses.

Chapter 5

The effects of ageing on the morphology of the knee joint in *Homo sapiens*

5.1 Introduction

This chapter assesses the morphology of the distal femur and proximal tibia at different stages of adulthood by analysing the degree and nature of shape differences between age groups. One population (African Americans) is used for the detailed analyses of shape differences with ageing, using both sexed and unsexed samples. In the third set of analyses, two additional populations (Caucasian Americans and Spitalfields) are included to compare and contrast shape differences associated with ageing between populations.

5.2 The effects of ageing on the lower limbs

Medical literature has concentrated on two aspects of ageing in the postcranium: firstly, the changing internal and external architecture and cross-sectional properties of bone with age caused by the decrease in bone mineral content (BMC) and secondly, the increasing incidence of degenerative joint diseases with their effect upon the appearance and structure of bone and the soft tissue of the joints (White, 2000;. Aufderheide and Rodriguez-Martin, 1998).

BMC is age and sex related and strongly influenced by genetic and environmental factors, with considerable variation between populations. The most obvious symptom of abnormally low BMC (osteoporosis) in the long bones is a complex alteration of the trabecular patterns in the metaphyseal areas and a tendency towards fracture, particularly in the femoral neck, with females being more at risk overall and at an earlier age than males in all populations (Aufderheide and Rodriguez-Martin, 1998). The external manifestations of low BMC are less obvious. Periosteal expansion in the cortical bone of the diaphyses through remodelling is greater in males than in females and in individuals or populations with higher levels of physical activity. This

added degree of external expansion gives some added protection against fracture (Ruff and Hayes, 1988; Ruff, 2000; Seeman, 2002). In diathrodial joints the thinning of trabecular bone is a normal concomitant of ageing, although the extent of thinning is often not appreciated internally without using invasive or X-ray techniques. Rates of trabecular bone loss appear to be less sex-related than cortical bone loss, in some (if not in all areas) of the skeleton (Seeman, 1995; Brickly, 1999).

The second indication of shape changes in ageing joints is the presence of disease; in diathrodial joints such as the knee, this is primarily in a form of arthritis. Arthritic disease can be divided into two broad categories; that which is inflammatory and caused by an autoimmune response (rheumatoid arthritis), and that which is degenerative, causing an alteration of the joint by the destruction of the articular cartilage and the formation of additional adjacent bone (osteoarthritis) (White, 2000).

Rheumatoid arthritis causes the lining of the joint to become thickened, invading the articular cartilaginous surface and producing additional chemicals, which further attack the cartilage. The incidence of this autoimmune disease is affected by genetic and environmental factors, with some populations being more at risk than others. For instance, whilst an estimated 2.1 million or 1% of modern Americans suffer from rheumatoid arthritis (Handy, 2001), Gregg and Gregg report that few if any Arikaran individuals have been identified with the disease (Gregg and Gregg, 1987). Usually starting in youth or middle life and affecting more women than men, this disease can remain active into old age and frequently results in deformed and twisted joints. Although rheumatoid arthritis may affect the elderly more than younger people, it is not a disease strictly caused by ageing or wear and tear, as physical symptoms usually begin between 20 and 50 years of age (White, 2000; Aufderheide and Rodriguez-Martin, 1998).

In contrast to rheumatoid arthritis, osteoarthritis is more directly associated with the elderly, being caused by degeneration of the articular cartilage and contiguous bone within the diathrodial joints. It is also highly correlated with those subsistence strategies requiring hard, physically demanding activity levels (Hadler, 1977; Molleson, 1994; Larson, 2000) As the cartilage becomes softened and broken down during the normal ageing process, after chronic injury or through continuous

excessive loading pressures, the subchondral bone becomes eburnated, i.e., smoothed and 'polished' following contact with other articulating bone surfaces, as the cartilage between them is destroyed. As the exposed bone becomes increasingly damaged, the surface tissue becomes increasingly modified, until this modification becomes visually obvious by the appearance of osteophytic spurs or 'lipping' (Figure 5.1) (White, 2000)..

Recent research indicates that osteoarthritis may be more of a long term progressive disease than previously thought. Although the elderly express the obvious symptoms of pain, stiffness, eburnation and osteophytosis to a greater degree than younger adults, the earlier less apparent signs may be accumulating in the forties, thirties and even twenties, well before old age is reached (Roberts and Manchester, 1997; Wright, 2003). Modern medical techniques show that only 50% of individuals with either radiologic evidence or with abnormal X-ray findings of osteoarthritis in the soft tissues present osteoarthritic symptoms (Felson, 1988). Osteoarthritis therefore appears to be a 'silent' complaint for much of its history until sufficient degeneration has accumulated to cause pain and other external evidence, if such external manifestations ever occur. As a result, judging the extent of osteoarthritis in archaeological populations by observation of the external morphology of skeletal remains is necessarily problematic and likely to underestimate its occurrence.

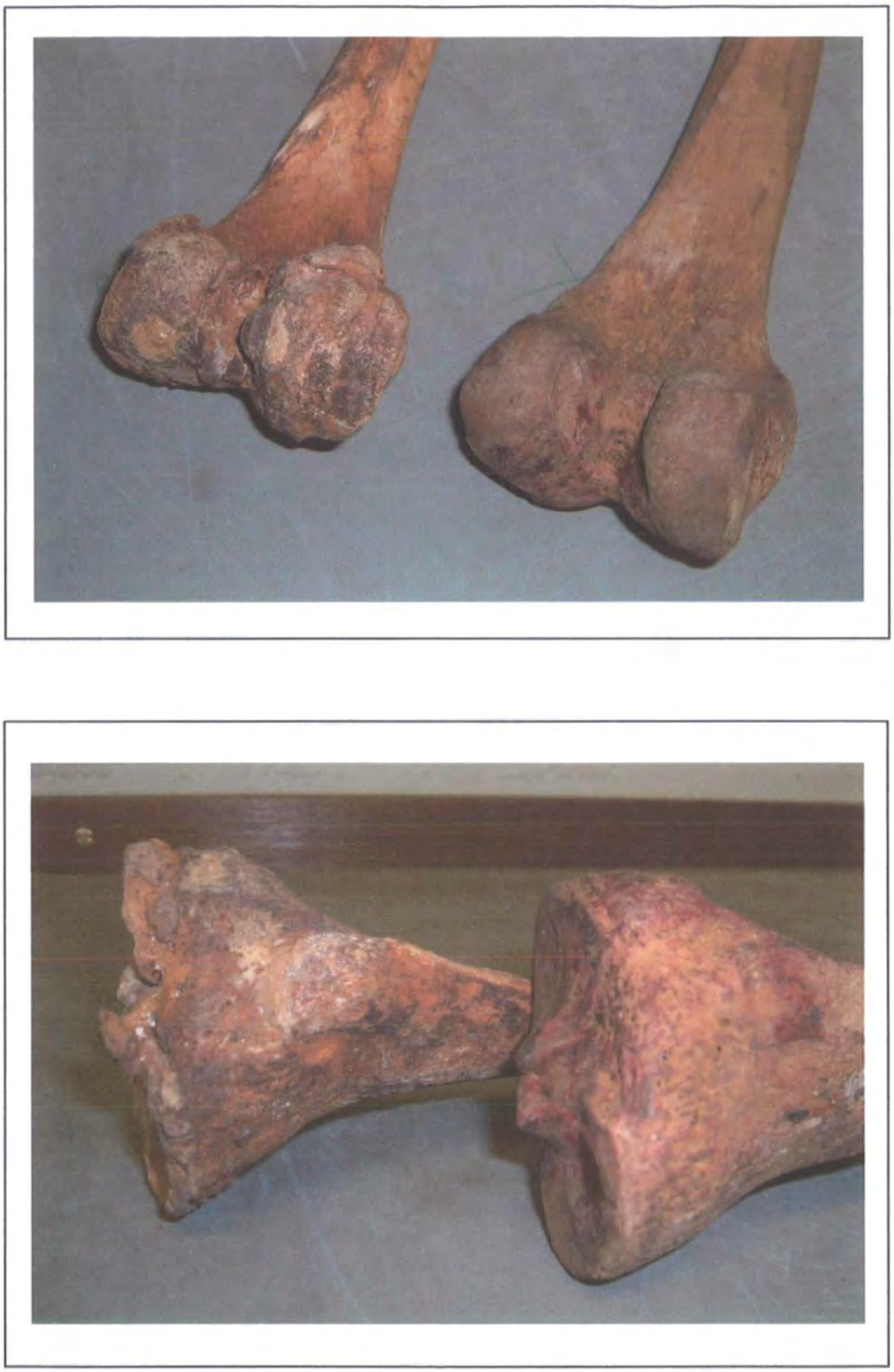

Figure 5.1: Comparisons of a healthy and disease-free distal femur and proximal tibia (right) with bones affected by degeneration and osteophyte growth caused by osteoarthritis (left).

5.3 Examination of issues relating to the changing shape of the knee joint during ageing

In the light of previous research, this chapter will analyse whether the changes in shape of the knee joint during ageing are evident in ostensibly non-pathological bone and will focus on three aspects of morphological differences:

1. To determine the degree and nature of any shape differences in the knee joint during the ageing process in both femur and tibia.
2. To determine whether the nature of shape changes associated with ageing is similar in males and females.
3. To determine whether changes relating to ageing are more or less pronounced than those morphological differences associated with sexual dimorphism or differences between population samples.

To examine issues raised by previous research, this study will therefore seek to support or reject the following hypotheses:

H.5.1 The shape of the knee joint in non-pathological bone does not change throughout the ageing process.

H.5.2 If H.5.1 is falsified, differences in shape of the knee joint associated with ageing are similar in males and females.

H.5.3 If H.5.1 is falsified, the degree and nature of differences in shape associated with ageing will be less than any morphological differences that may exist between distinct population samples.

5.4 Materials and Methods

Data from the African American population is used to analyse morphological differences between pooled-sex samples and between males and females because this sample has the greatest number of specimens of both femora and tibiae available, with well documented records of sex and age at death (see Chapter 2, section 2.1.2f). Not only is it necessary to have a sufficient number of specimens of each age group available for these analyses, but it is essential that specimens are in good condition and exhibiting no pathological signs of disease. Any bones with signs of disease (primarily eburnation and osteophytosis) had been discarded at the initial stages of data collection. This was necessary on two counts; firstly the presence of osteophytes or other pathological growths on the bone surface create problems for the use of morphometric methods, as landmarks can no longer be safely located and digitised. (see Figure 5.1). Secondly, only disease-free bones are used in order to determine whether ostensibly *normal* bone changes shape throughout the individual's lifetime prior to the advent of any pathological deformities.

The Caucasian American and Spitalfields samples are also used with the African American sample to test hypothesis H.5.3. Like the African Americans, both populations include specimens with reliable information regarding age of death and possess sufficient numbers to choose sound, non-pathological specimens from each age group (Chapter 2, sections 2.1.2f and 2.1.2l). Tables 5.1 (femur) and 5.2 (tibia) give the numbers of specimens used for the analyses of shape differences.

The primary method of analysis subdivides the total sample into three age groups; the youngest adults from epiphyseal fusion to 39 years of age, middle aged adults from 40 to 59 years of age and elderly adults from 60 years and above. In comparing and contrasting different age sets, this study makes use of the precedents set by many previous studies when examining structural changes in bone during ageing (Eriksen, 1976; Ruff and Hayes, 1983; Gregg and Gregg, 1987; Wilczak, 1998; Brickley, 1999; Drusini, 2000; Roguecka et al., 2001; Dittmar, 2002; Snodgrass, 2004). Supplementary comparisons in the first set of analyses using the pooled-sex African American sample have also been used in correlating the total sample against specific PCs.

No attempt has been made to analyse age differences in the size of the diaphyses or of the centroid size of the knee joint. Greater numbers of specimens than are currently available in this study would be needed to reliably determine such differences because of the wide variation in size of the lower limbs within any one age group for any single population. It is possible that analyses comparing and contrasting shape between age groups may be similarly problematic. Whilst this study has shown that there is considerable variation in the centroid size of the knee joint within each sample (see Chapter 4, section 4.4.2(a) and (b)), it is probable that *shape* is initially less variable than size. Whilst this may be true for both the diaphyses as well as the articular joints, Rafferty and Ruff (1994), Ruff et al. (1994), Tanaka (1999) and Lieberman et al. (2001) have argued that the joints do not respond to alterations in mechanical loading to the same degree as diaphyseal structure, in that the articular joints are less developmentally plastic than the diaphyses. If this argument is accepted, the smaller degrees of variation in knee joint shape specifically caused by ageing are more likely to become apparent during analysis.

To determine the degree and significance of differences in knee joint shape between age groups of adult African Americans and between the three populations, specimens are superimposed using GPA and the Procrustes fitted data subjected to PCA. Because differences with age are likely to form only a small proportion of the overall variation within the sample, the use of scores on all PCs (i.e., the total variance) in the sample may not adequately discriminate differences due to age alone. Therefore, canonical stepwise discriminant function analysis is used to determine which PCs relate more specifically to changes with ageing. All analyses of shape are conducted on all landmarks for both distal femur and proximal tibia.

(a)

Population (Femur)	Youngest adults to 39yrs	Middle adults 40-59yrs	Oldest adults 60+yrs	Total
African Americans Sexes pooled	40	40	41	121
African Americans Males	22	21	20	63
African American Females	18	19	21	58
Caucasian Americans	18	20	20	58
Spitalfields	20	23	24	67

(b)

Population (Tibia)	Youngest adults to 39yrs	Middle adults 40-59yrs	Oldest adults 60+yrs	Total
African Americans Sexes pooled	42	41	38	120
African Americans Males	23	21	18	62
African American Females	19	20	20	58
Caucasian Americans	18	20	20	58
Spitalfields	21	21	29	71

Tables 5.1: (a) Femur and (b) Tibia. The composition of the data sets used for the analyses of shape of the distal femur and proximal tibia during the ageing process.

African and Caucasian American specimens originate from the NMNH, Smithsonian Institution, Washington, DC; the Spitalfields specimens originate from the NHM, London.

5.5 Results

5.5.1 Analysis of differences between three age groups using African Americans (pooled-sex sample).

5.5.1a(i) Femur

Differences in shape of the 121 specimens divided by age group are analysed using the Procrustes fitted co-ordinates and by subjecting the data to PCA. Table 5.2 gives the proportional and accumulated variance for PCs 1 to 71, which represents the total variance within the sample. The scores for each specimen on the resultant PCs are then subjected to canonical discriminant analysis to establish the relationships between samples of the three age groups based upon the Mahalanobis' squared distances between sample means.

PCs	Prop.	Cumul.	PCs	Prop.	Cumul.	PCs	Prop.	Cumul.
PC1	9.14	9.14	PC26	1.07	84.40	PC51	0.21	98.00
PC2	7.37	16.50	PC27	1.00	85.40	PC52	0.19	98.20
PC3	6.67	23.20	PC28	0.96	86.40	PC53	0.18	98.40
PC4	6.33	29.50	PC29	0.87	87.20	PC54	0.18	98.60
PC5	5.09	34.60	PC30	0.82	88.00	PC55	0.17	98.80
PC6	4.65	39.30	PC31	0.80	88.80	PC56	0.15	98.90
PC7	4.47	43.70	PC32	0.78	89.60	PC57	0.13	99.00
PC8	4.08	47.80	PC33	0.74	90.40	PC58	0.12	99.20
PC9	3.87	51.70	PC34	0.73	91.10	PC59	0.12	99.30
PC10	3.56	55.20	PC35	0.64	91.70	PC60	0.10	99.40
PC11	2.90	58.10	PC36	0.61	92.30	PC61	0.09	99.50
PC12	2.75	60.90	PC37	0.59	92.90	PC62	0.08	99.60
PC13	2.56	63.40	PC38	0.52	93.50	PC63	0.08	99.60
PC14	2.31	65.70	PC39	0.49	93.90	PC64	0.07	99.70
PC15	2.15	67.90	PC40	0.48	94.40	PC65	0.07	99.80
PC16	2.05	69.90	PC41	0.45	94.90	PC66	0.06	99.80
PC17	1.94	71.90	PC42	0.44	95.30	PC67	0.05	99.90
PC18	1.81	73.70	PC43	0.41	95.70	PC68	0.04	99.90
PC19	1.66	75.40	PC44	0.38	96.10	PC69	0.03	100.00
PC20	1.54	76.90	PC45	0.35	96.50	PC70	0.03	100.00
PC21	1.43	78.30	PC46	0.33	96.80	PC71	0.02	100.00
PC22	1.34	79.70	PC47	0.30	97.10			
PC23	1.29	81.00	PC48	0.27	97.30			
PC24	1.22	82.20	PC49	0.25	97.60			
PC25	1.15	83.30	PC50	0.23	97.80			

Table 5.2: Ageing in the femur of African Americans. The proportional and accumulated variance for PCs 1-71 accounting for 100% of total variance in African Americans.

Table 5.3 shows the PCs selected by stepwise discriminant analyses for the African American sample, used to determine which PCs relate more specifically to ageing.

Order	Entered	Order	Entered	Order	Entered	Order	Entered
1	PC3	8	PC31	15	PC29	22	PC56
2	PC9	9	PC2	16	PC54	23	PC61
3	PC41	10	PC68	17	PC42	24	PC25
4	PC7	11	PC44	18	PC55	25	PC23
5	PC1	12	PC37	19	PC12		
6	PC20	13	PC38	20	PC57		
7	PC18	14	PC16	21	PC6		

Table 5.3: PCs selected by stepwise discriminant analysis for the three age groups of African Americans (sexes pooled) for the femur. Stepwise PCs account for a cumulative 55.09% of total variance.

The results using PCs accounting for c.50% to 100% of total variance and those used in the stepwise discriminant function analyses are summarised in Figure 5.2.

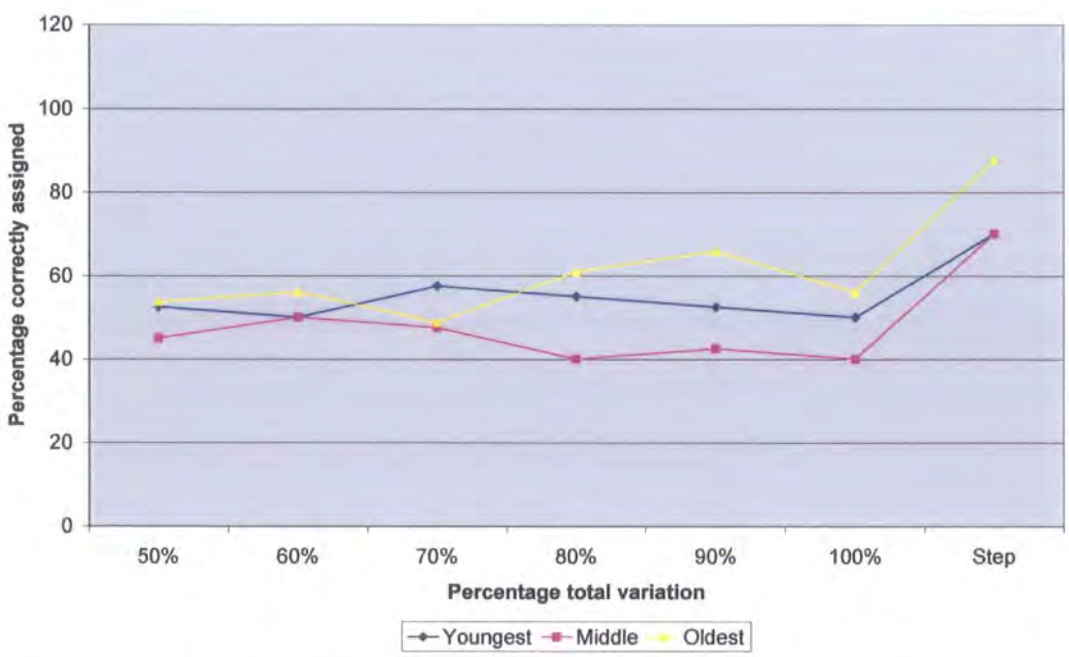

Figure 5.2: Ageing in the femur of African Americans (sexes pooled). Summary of separate discriminant and cross-validation analyses using PCs accounting for c.50% of total variance (PCs 1-6), c.60% (PCs 1-9), c.70% (PCs 1-12), c.80% (PCs 1-16), c.90% (PCs 1-33) and 100% (PCs 1-71) and stepwise discriminant analysis.

To test the validity of using PCs selected by stepwise discriminant analysis for subsequent analyses, initial stepwise PCs are correlated with the ages of all individuals. Table 5.4 shows that only four of the initial five stepwise PCs show a correlation with age at a level of statistical significance; PC3 at a moderate level of correlation and the remaining three showing a weak correlation only. PC41 explains only a very small percentage of total variance at 0.33%, which may be influencing the significance of this result. Using the initial c.50% of total variance and the first ten stepwise PCs, no other PCs achieved a statistically significant level of correlation with age.

PC3	v Age	PC9	v Age	PC41	v Age	PC7	v Age	PC1	v Age
r=	*p*=	r=	*p*=	r=	*p*=	r=	*p*=	r=	*p*=
0.42	<0.0001	0.26	0.0003	0.15	0.11	0.23	0.01	0.26	0.004

Table 5.4: Results of correlation of age with PC scores for initial PCs selected by stepwise discriminant analysis for the femur. Figures in blue indicate a non-significant result.

Figures 5.3 to 5.6 highlight the three age groups and the spread of individuals in an age continuum against those stepwise PCs that show a degree of correlation at a level of statistical significance.

The Mahalanobis' squared distances between the three age groups, generated from the PC scores selected by stepwise discriminant analysis are shown in Table 5.5, which indicates that all distances between the three age groups are statistically significant at $p<0.0001$. The three age groups can therefore be separated on some aspect of shape of the distal femur. The distances are smaller between the youngest and middle and middle and oldest groups and greatest between the youngest and oldest groups, indicating that age related shape changes are progressive.

Table 5.6 shows the result of cross-validation analysis, with between 70% and 87.8% of specimens from the three age groups correctly assigned to group. The greatest distance between the youngest and oldest groups seen in Table 5.5 is reflected in the percentages of misplaced individuals from these two groups, with a higher percentage in both categories being placed into the middle aged category.

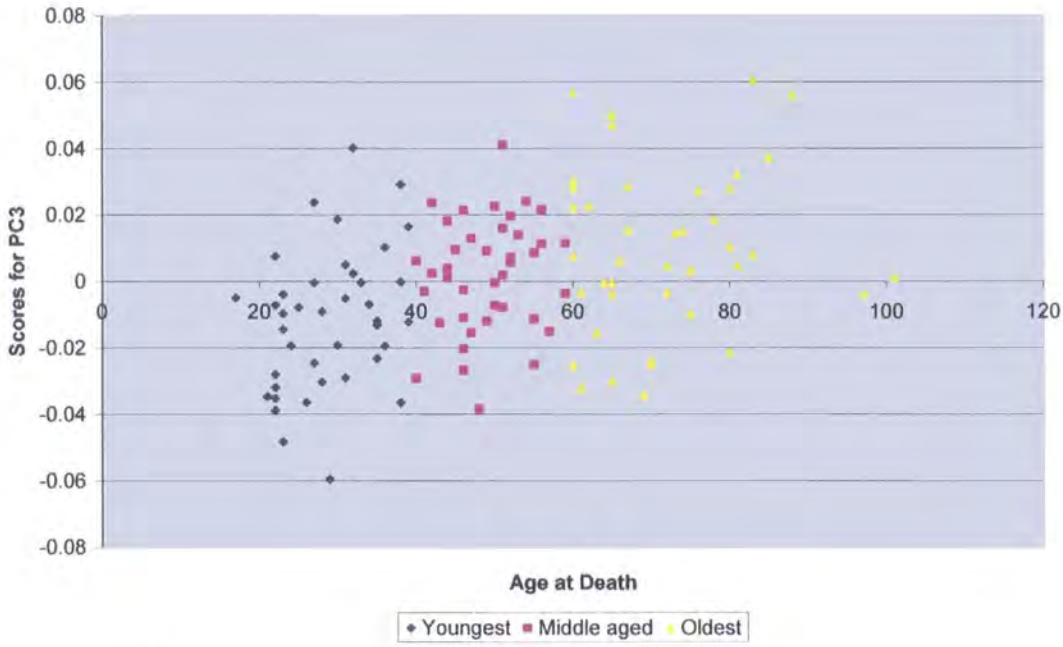

(a)

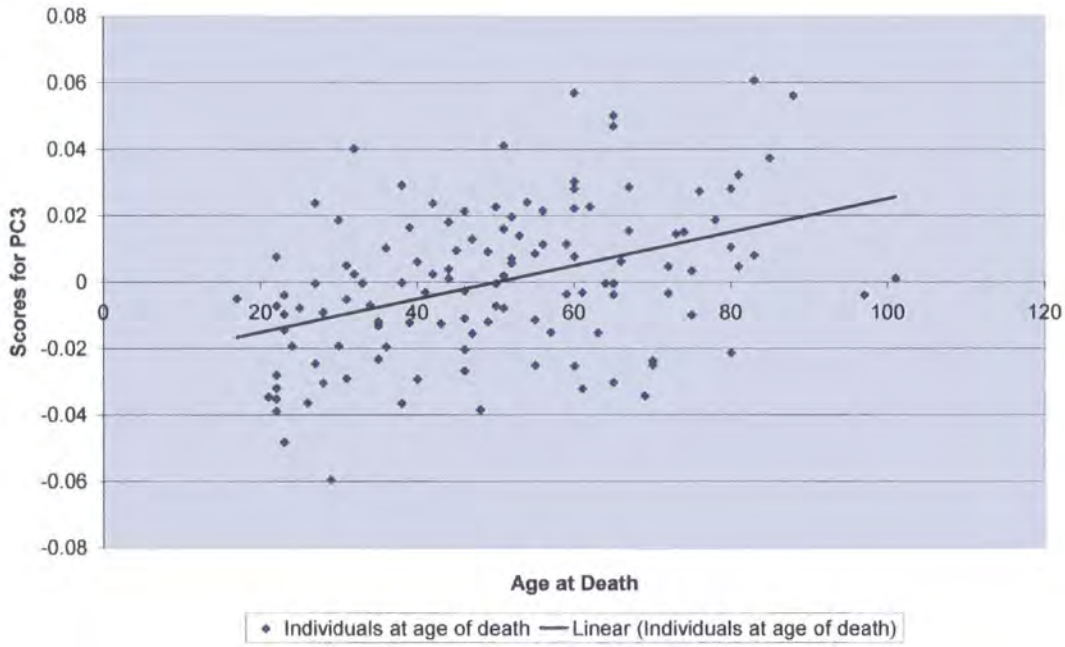

(b)

Figure 5.3: Ageing in the femur of African Americans. Correlation of age at death with scores of PC3 highlighting (a) the 3 age groups and (b) the linear trendline ($r = 0.42$; $p < 0.0001$).

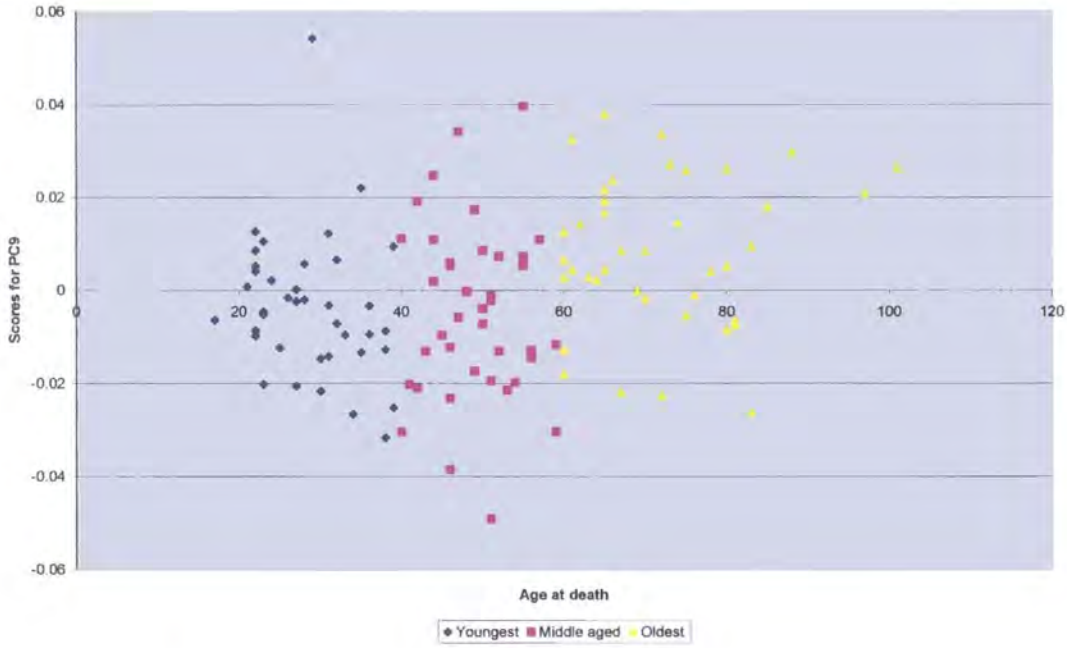

(a)

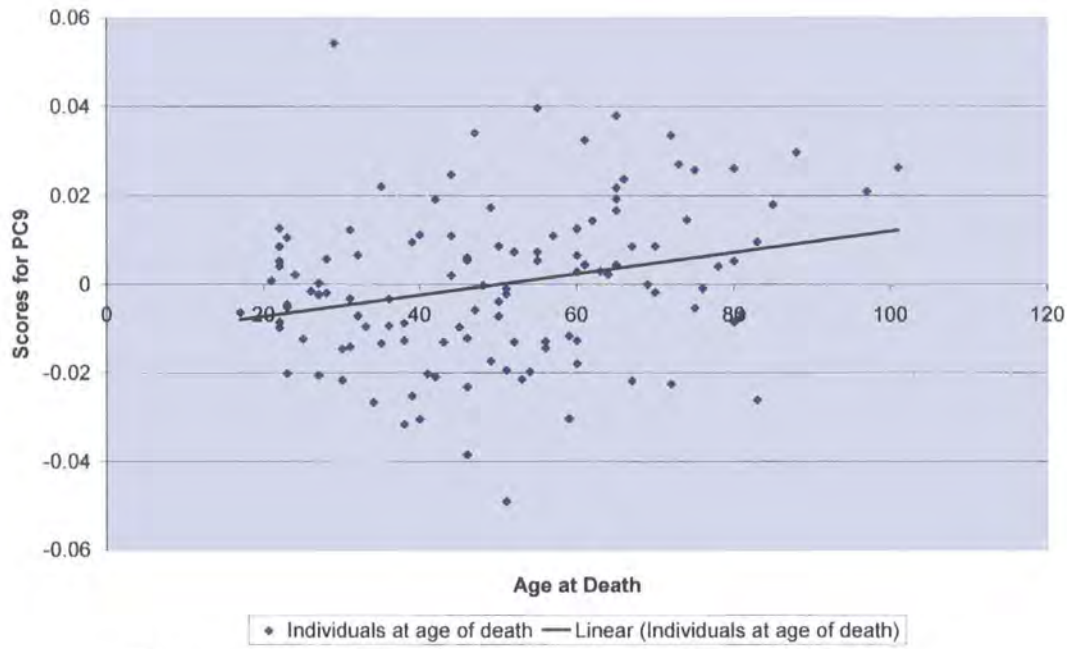

(b)

Figure 5.4: Ageing in the femur of African Americans. Correlation of age at death with scores of PC9 highlighting (a) the 3 age groups and (b) the linear trendline ($r = 0.26$; $p = 0.0003$)

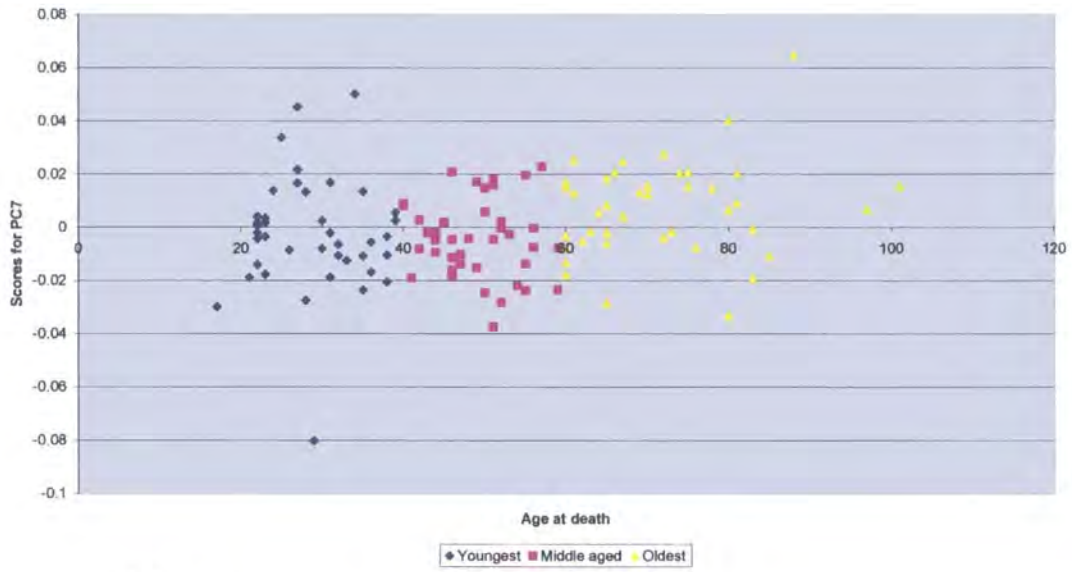

(a)

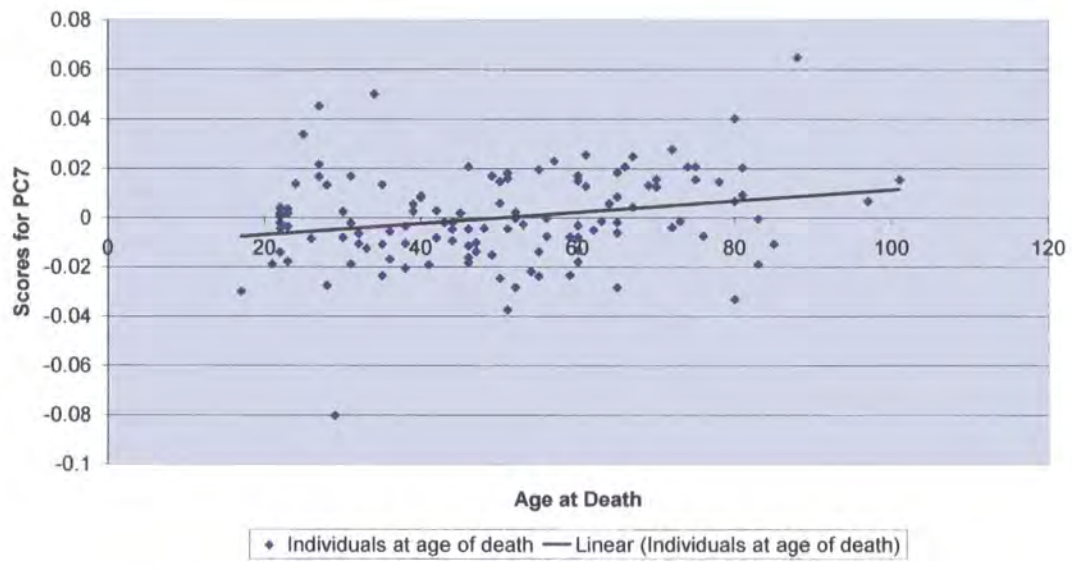

(b)

Figure 5.5: Ageing in the femur of African Americans. Correlation of age at death with scores of PC7 highlighting (a) the 3 age groups and (b) the linear trendline ($r = 0.23$; $p = 0.01$).

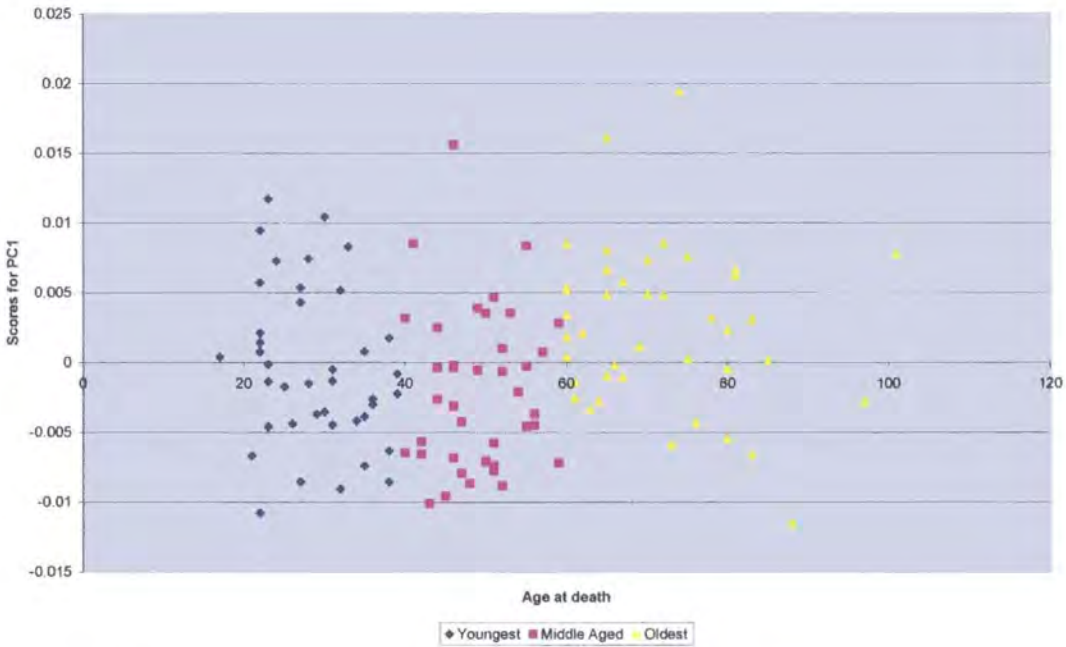

(a)

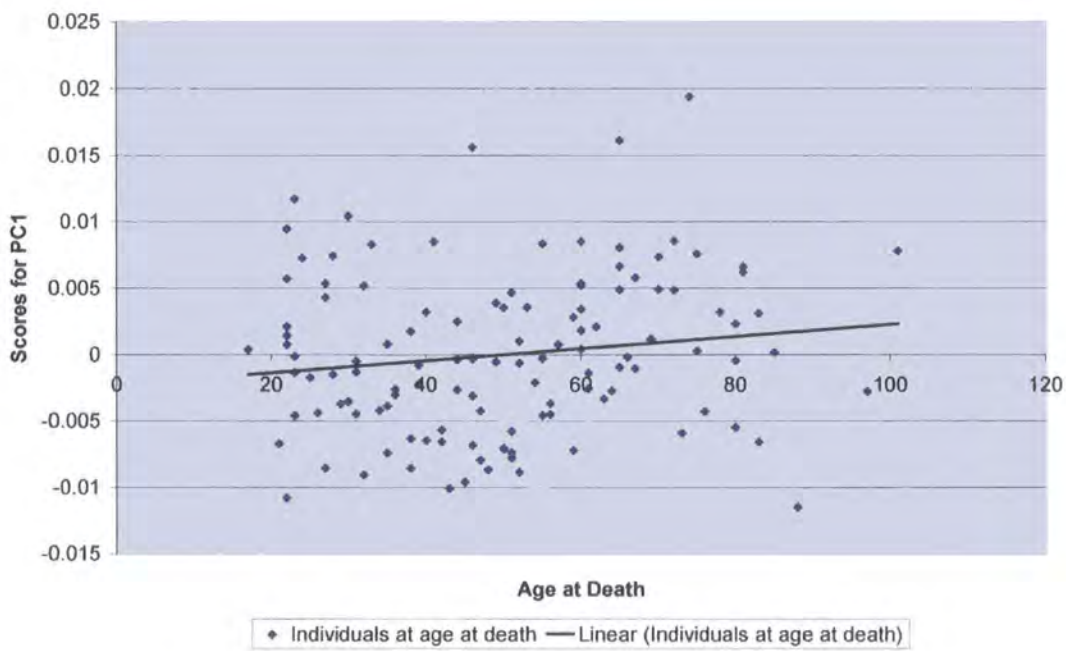

(b)

Figure 5.6: Ageing in the femur of African Americans. Correlation of age at death with scores of PC1 highlighting (a) the 3 age groups and (b) the linear trendline ($r = 0.26$; $p = 0.004$).

Youngest	0		
	1.000		
Middle	4.65	0	
	0.0001	1.000	
Oldest	14.13	9.36	0
	0.0001	0.0001	1.000
	Youngest	Middle	Oldest

Table 5.5: Ageing in the femur of African Americans (sexes pooled). The Mahalanobis' squared distances between the means of the 3 age groups, generated by stepwise discriminant analysis. The upper value in red gives the Mahalanobis' squared distance between species, the lower value in black gives the Hotelling's t^2 *p*-value.

Number of Observations and Percent Classified into Groups using Stepwise PCs				
From Group	Youngest	Middle	Oldest	Total
	28	9	3	40
Youngest	70	22.5	7.5	100
	8	28	4	40
Middle	20	70	10	100
	0	5	36	41
Oldest	0	12.2	87.8	100
	36	42	43	121
Total	29.75	34.71	35.54	100

Table 5.6: Ageing in the femur of African Americans (sexes pooled). Results of cross validation analysis of the 3 age groups using PCs selected by stepwise discriminant analysis. Upper figure denotes the number of individuals; lower figure denotes percentage. Red figures denote number of individuals placed into their correct groups.

5.5.1a(ii) Femur: Description of morphological differences between three age groups

PCs 3 and 9 are the first two PCs selected by stepwise discriminant analysis and account for 6.67% and 3.87% of total variance respectively. These two stepwise PCs will initially be used to examine the relationships between specimens in the bivariate plot shown in Figure 5.6. Using the Student's t-test in pairwise comparisons, at least the youngest and oldest groups are separated at a statistically significant level for both PC3 and PC9 in Table 5.7.

PC3	t=	*p*=	PC9	t=	*p*=
Groups 1 and 2	3.13	0.002	Groups 1 and 2	0.18	0.86
Groups 1 and 3	4.16	<0.0001	Groups 1 and 3	3.50	0.0008
Groups 2 and 3	1.69	0.10	Groups 2 and 3	3.30	0.001

Table 5.7 Femur: Results of Student's t-test between the three age groups for the femur with PC3 and PC9, the first two PCs selected by stepwise discriminant analysis. Figures in blue indicate a non-significant result.

Despite both PC3 and PC9 showing a correlation with age at a level of statistical significance, the bivariate plot of PC3 with PC9 in Figure 5.6 shows a complete overlap of all specimens from the three age groups. As individual PCs selected by stepwise analysis, including PCs 3 and 9, fail to show any apparent separation of specimens of the three age groups in bivariate plots using the total sample, it is assumed that the significant separation of groups results from the accumulation of incremental degrees of variation contributed by all relevant PCs. Therefore, the sample means of each of the three age groups have been used to help distinguish specific variation due to ageing.

Figure 5.7:

Ageing in the femur of African Americans, total sample. Bivariate plot, showing the overlap of specimens of 3 age groups on PCs 3 and 9 (first and second PCs selected by stepwise discriminant analysis).

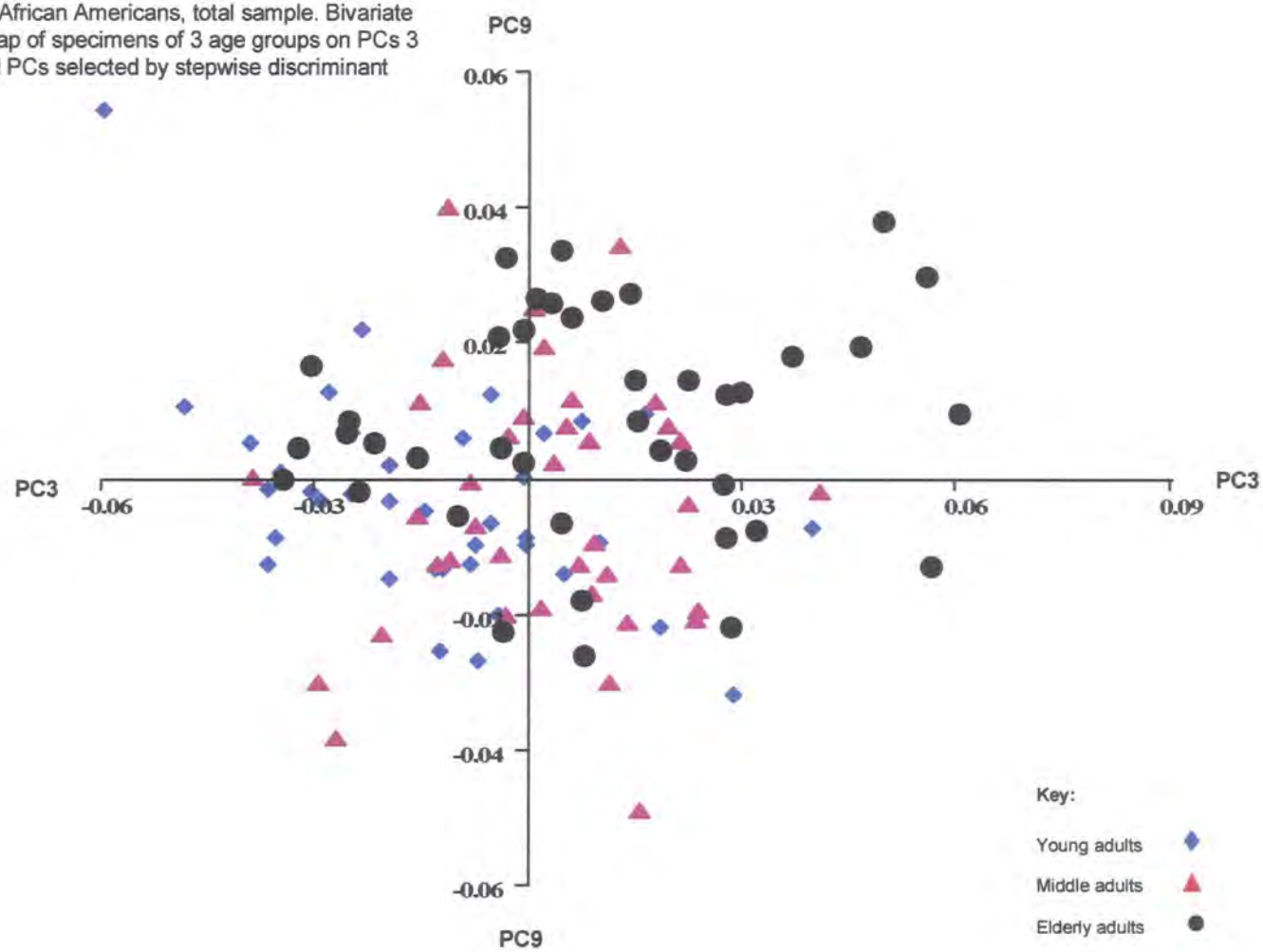

For the femur, the correlation between the Procrustes distances using the population means shown in Table 5.8 and the Mahalanobis' squared distances shown in Table 5.5 does not reach a level of statistical significance (r= 0.96, p= 0.19). This non-significant result may result from the Mahalanobis' squared distances being generated from a selected number of PCs only. Although results do not reach statistical significance, however, both Mahalanobis' and Procrustes distances are greatest between the youngest and oldest groups.

Youngest	0		
Middle	0.14	0	
Oldest	0.19	0.15	0
	Youngest	Middle	Oldest

Table 5.8: Procrustes distances between the 3 age groups in the femur of African Americans.

The Procrustes mean co-ordinates have been calculated from the separate GPAs for each age group and have been subjected to a joint GPA and PCA. With a sample of three specimens, PC1 accounts for 73% and PC2 for 27% of total variance.

Figure 5.8 shows a separation of the three means along the scale of PC1 with the youngest mean at the positive extreme and the oldest mean at the negative extreme. The middle aged mean lies mid-way between the two extremes. The shape differences between the three means appear marginal. There is a slight difference in the angle of attachment of the joint relative to the diaphysis such that the angle is more acute in the mean configuration of the youngest mean relative to the oldest, particularly on the medial side of the joint. The condyles are also seen to be more inward-facing towards the mid-line of the joint in the oldest mean relative to the youngest. Although these differences are difficult to appreciate in Figure 5.8(a) and (b), the mean configuration shows greater width across the intercondylar fossa (landmarks 5 and 9) and in the relative change in positions of landmarks 17 and 23 at the maximum extent of the condyles, as it is warped between the two extremes. The difference in the angle of attachment is better appreciated in Figure 5.8 (c) and (d), in the relationship between landmarks 25 and 26 (the maximum height of the condyles)

Figure 5.8:

Ageing in the femur of African Americans. Bivariate plot of PC1 with PC2, showing the separation of sample means of 3 age groups. Images represent the mean configuration if warped to the extremes of PC1 (at 0.02 and -0.02). Figs. 5.7(a) and (b) are distal view; (c) and (d) sagittal view (medial side). Images (b) and (d) include landmarks discussed in section 5.5.1a(ii)

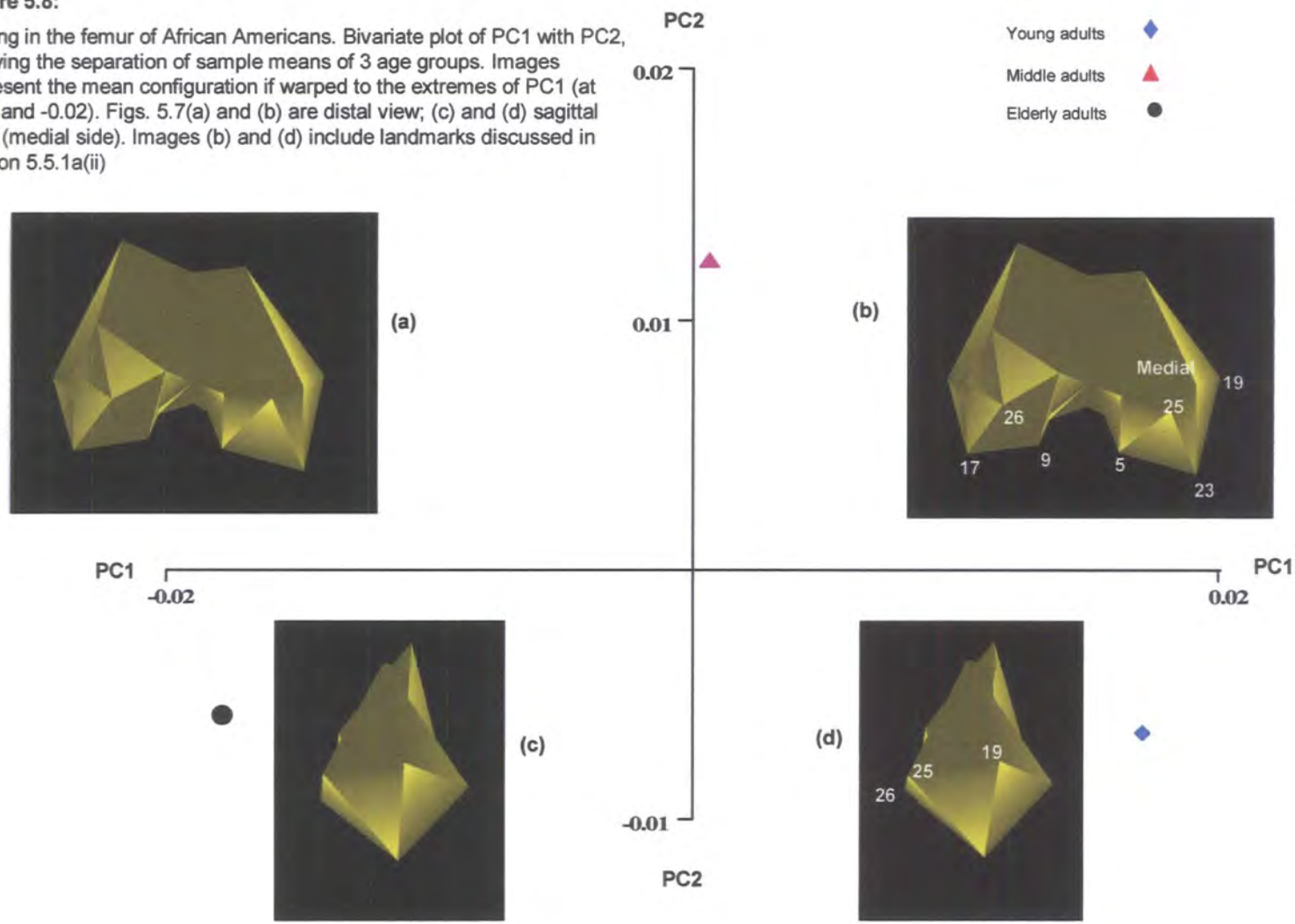

and in the relative position of landmark 19 (the greatest width of the medial epicondyle). This greater degree of difference on the medial side can also be appreciated from Figure 5.9, showing the maximum deformation of the TPS relative to all three means.

Shape variation explained by PC2 is slight and difficult to interpret. No separation is seen between the youngest and oldest means, which cluster together at a marginal distance from the middle aged mean; indicating that shape variation on PC2 is unlikely to relate solely to differences with ageing.

5.5.1b(i) Tibia

Differences in shape of the 120 specimens divided by age group are analysed using the Procrustes fitted co-ordinates and by subjecting the data to PCA. Table 5.9 gives the proportional and accumulated variance for PCs 1 to 56, which represents the total variance within the sample.

PCs	Prop.	Cumul.	PCs	Prop.	Cumul.	PCs	Prop.	Cumul.
PC1	14.30	14.30	**PC21**	1.25	84.20	**PC41**	0.33	97.60
PC2	9.19	23.50	**PC22**	1.14	85.30	**PC42**	0.29	97.90
PC3	7.16	30.60	**PC23**	1.09	86.40	**PC43**	0.27	98.10
PC4	6.42	37.00	**PC24**	1.04	87.50	**PC44**	0.23	98.40
PC5	5.79	42.80	**PC25**	0.96	88.40	**PC45**	0.22	98.60
PC6	4.95	47.80	**PC26**	0.90	89.30	**PC46**	0.21	98.80
PC7	4.24	52.00	**PC27**	0.83	90.20	**PC47**	0.20	99.00
PC8	3.68	55.70	**PC28**	0.78	90.90	**PC48**	0.18	99.20
PC9	3.55	59.30	**PC29**	0.73	91.70	**PC49**	0.16	99.30
PC10	3.43	62.70	**PC30**	0.72	92.40	**PC50**	0.13	99.50
PC11	2.99	65.70	**PC31**	0.67	93.10	**PC51**	0.12	99.60
PC12	2.68	68.40	**PC32**	0.61	93.70	**PC52**	0.11	99.70
PC13	2.55	70.90	**PC33**	0.58	94.20	**PC53**	0.10	99.80
PC14	2.29	73.20	**PC34**	0.53	94.80	**PC54**	0.08	99.90
PC15	2.08	75.30	**PC35**	0.49	95.30	**PC55**	0.07	99.90
PC16	1.85	77.10	**PC36**	0.46	95.70	**PC56**	0.06	100.00
PC17	1.71	78.80	**PC37**	0.41	96.10			
PC18	1.42	80.30	**PC38**	0.40	96.50			
PC19	1.41	81.70	**PC39**	0.37	96.90			
PC20	1.29	83.00	**PC40**	0.36	97.20			

Table 5.9: Ageing in the tibia of African Americans. The proportional and accumulated variance for PCs 1-56 accounting for 100% of total variance in African Americans.

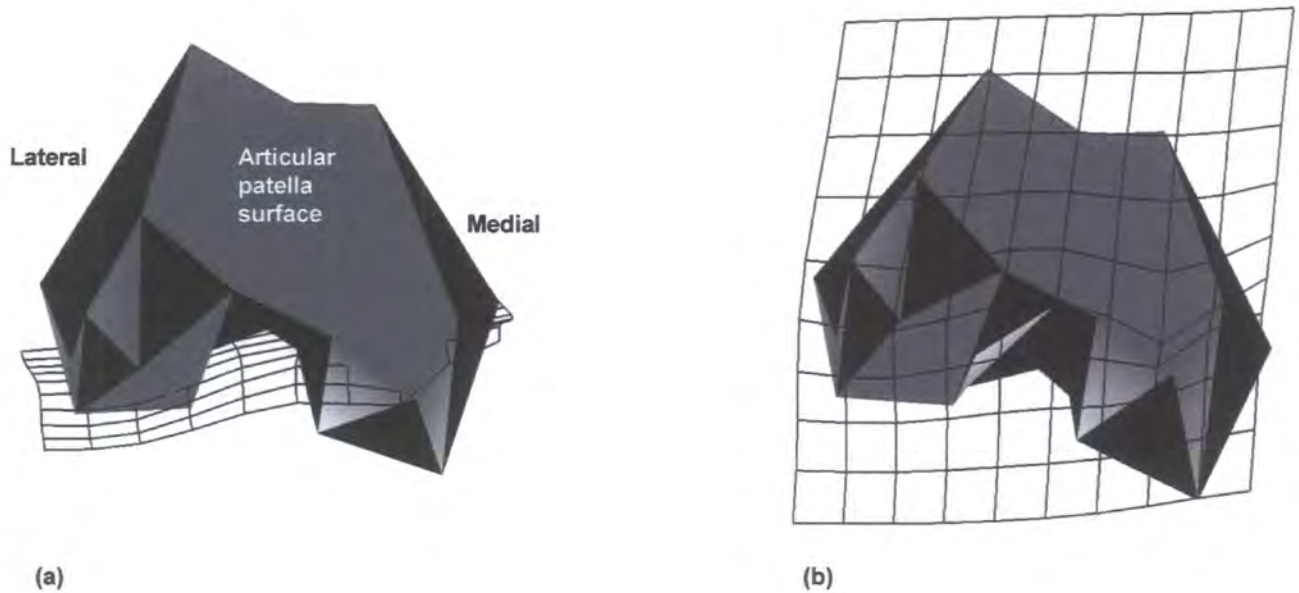

Fig 5.9: Ageing in the femur of African Americans (sexes pooled). Representations of femoral shape with TPS taken from PC3 (first PC selected by stepwise discriminant analysis) showing region of bone (over medial side) giving maximum difference in shape between the means of the 3 age groups. (a) TPS view in anteroposterior plane; (b) in distal plane. Images are presented to give the best indication of maximum difference in shape and are not necessarily taken from the same perspective as the mean configurations in Figure 5.8.

As for the femur, canonical stepwise discriminant function analysis is used to determine which PCs relate more specifically to differences related to ageing. PCs selected by stepwise canonical discriminant analysis for the three age groups of African Americans are shown in Table 5.10. The results using PCs accounting for c.50% to 100% of total variance and those used in the stepwise discriminant function analyses are summarised in Figure 5.10.

Order	Entered	Order	Entered	Order	Entered	Order	Entered
1	PC11	7	PC4	13	PC3	19	PC39
2	PC9	8	PC43	14	PC27	20	PC45
3	PC2	9	PC29	15	PC26	21	PC40
4	PC7	10	PC54	16	PC41	22	PC28
5	PC6	11	PC59	17	PC20	23	PC8
6	PC30	12	PC52	18	PC19		

Table 5.10: PCs selected by stepwise discriminant analysis for the tibia for the 3 age groups of African Americans. Stepwise PCs account for a cumulative 50.58% of total variance.

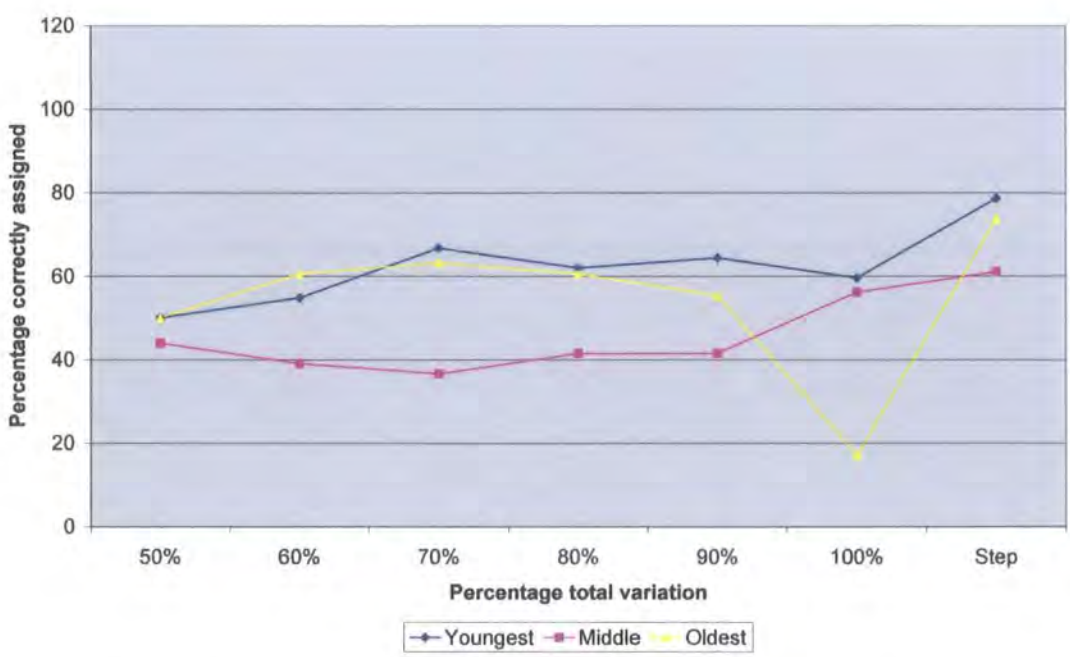

Figure 5.10: Ageing in the tibia of African Americans (sexes pooled). Summary of separate discriminant and cross-validation analyses using PCs accounting for c.50% of total variance (PCs 1-7), c.60% (PCs 1-9), c.70% (PCs 1-13), c.80% (PCs 1-18), c.90% (PCs 1-27) and 100% (PCs 1-56) and stepwise discriminant analysis.

The initial stepwise PCs are also correlated with the ages of all individuals for the tibia. Table 5.11 shows that six of the initial stepwise PCs show a correlation with age at a level of statistical significance; PC9 achieves a moderate level of correlation with all others remaining at a weak level only. Using the initial c.50% of total variance and the first ten stepwise PCs, no other PCs achieved a statistically significant level of correlation with age.

PC11	v Age	PC9	v Age	PC2	v Age	PC7	v Age	PC6	v Age	PC30	v Age
r=	*p*=	r=	*p*=	r=	*p*=	r=	*p*=	r=	*p*=	r=	*p*=
0.25	0.006	0.32	<0.0001	0.25	0.007	0.21	0.02	0.2	0.03	0.24	0.009

Table 5.11: Results of correlation of age with PC scores for initial PCs selected by stepwise discriminant analysis for the tibia.

Figures 5.11 to 5.16 highlight the three age groups and the spread of individuals in an age continuum against those stepwise PCs that show a degree of correlation at a level of statistical significance.

The Mahalanobis' squared distances between the three age groups, generated from the PC scores selected by stepwise discriminant analysis, are shown in Table 5.12, which indicates that all distances between groups are statistically significant at $p<0.0001$. The three age groups can therefore be separated on some aspect of shape of the proximal tibia. The distances are smaller between the youngest and middle and middle and oldest groups and greatest between the youngest and oldest groups; indicating that age related shape changes are progressive.

Table 5.13 shows the result of cross-validation analysis, with between 60.98% and 78.57% of specimens from the three age groups correctly assigned to group. Table 5.12 shows the distance between the youngest and oldest groups to be only marginally greater than that between the youngest and middle group and this marginal difference appears to be reflected in the percentages of misplaced individuals in the youngest group with a higher percentage being placed into the oldest rather than middle aged category. For the oldest group, a higher percentage is misplaced into the middle-aged category.

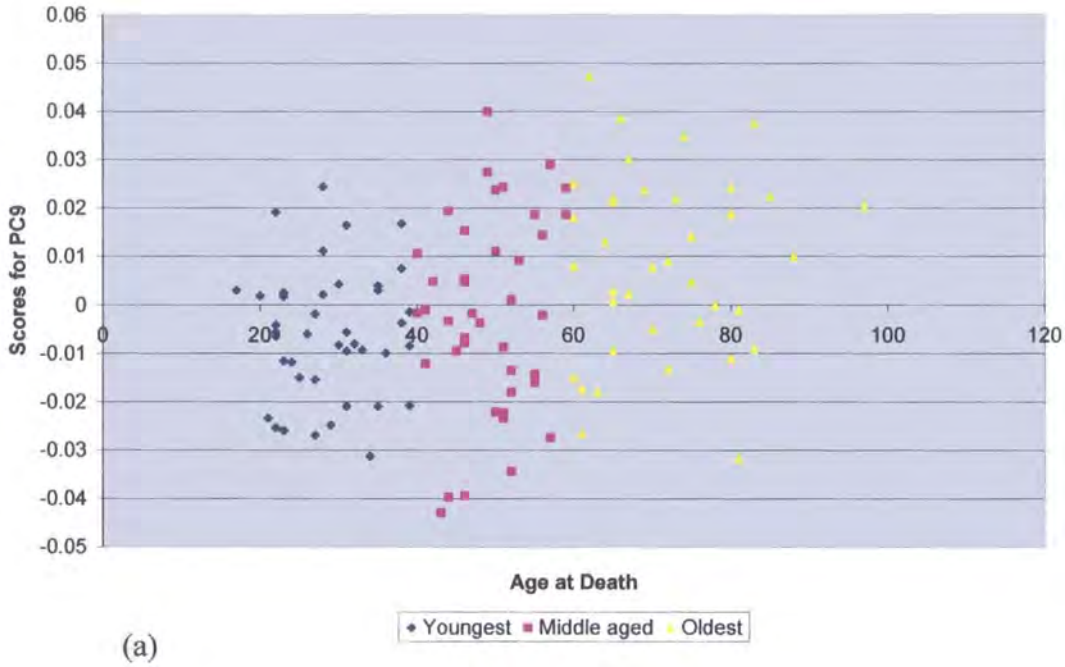

(a)

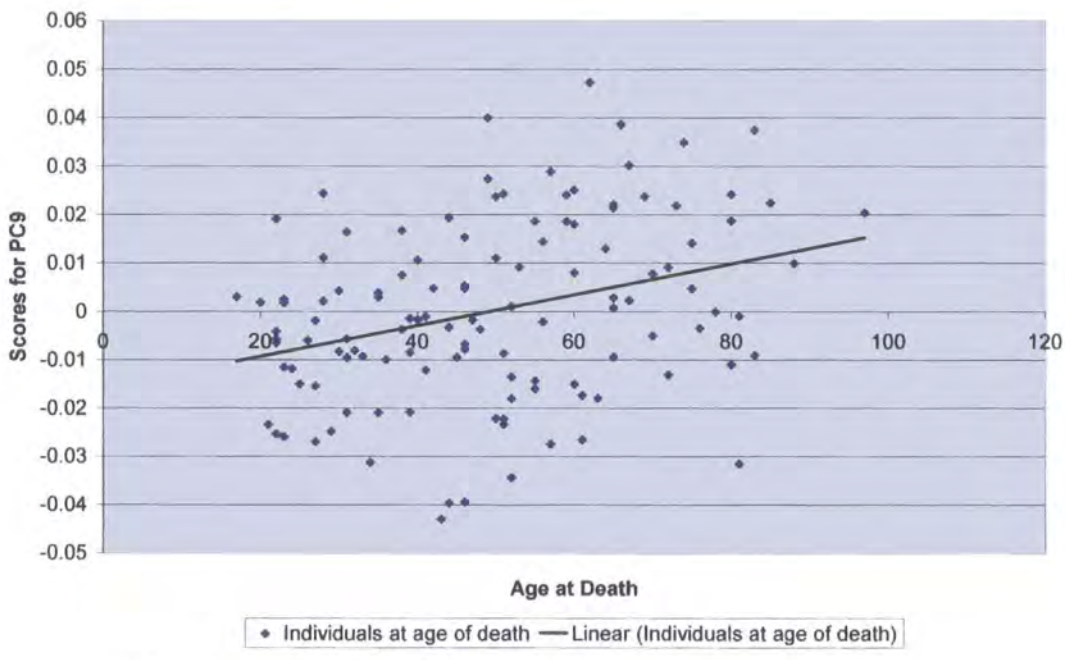

(b)

Figure 5.11: Ageing in the tibia of African Americans. Correlation of age at death with scores of PC9 highlighting (a) the 3 age groups and (b) the linear trendline ($r = 0.32$; $p<0.0001$).

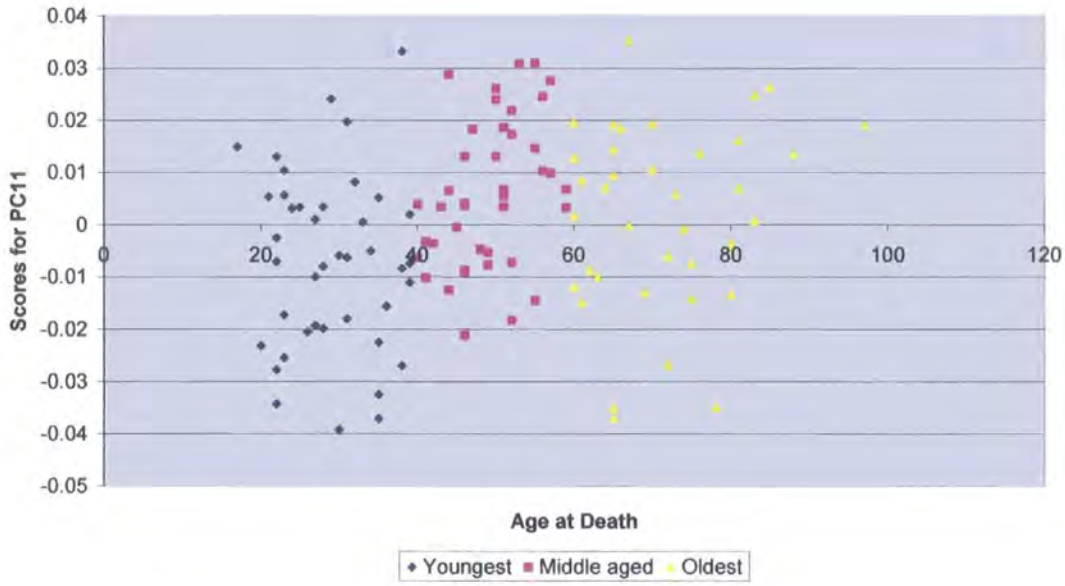

(a)

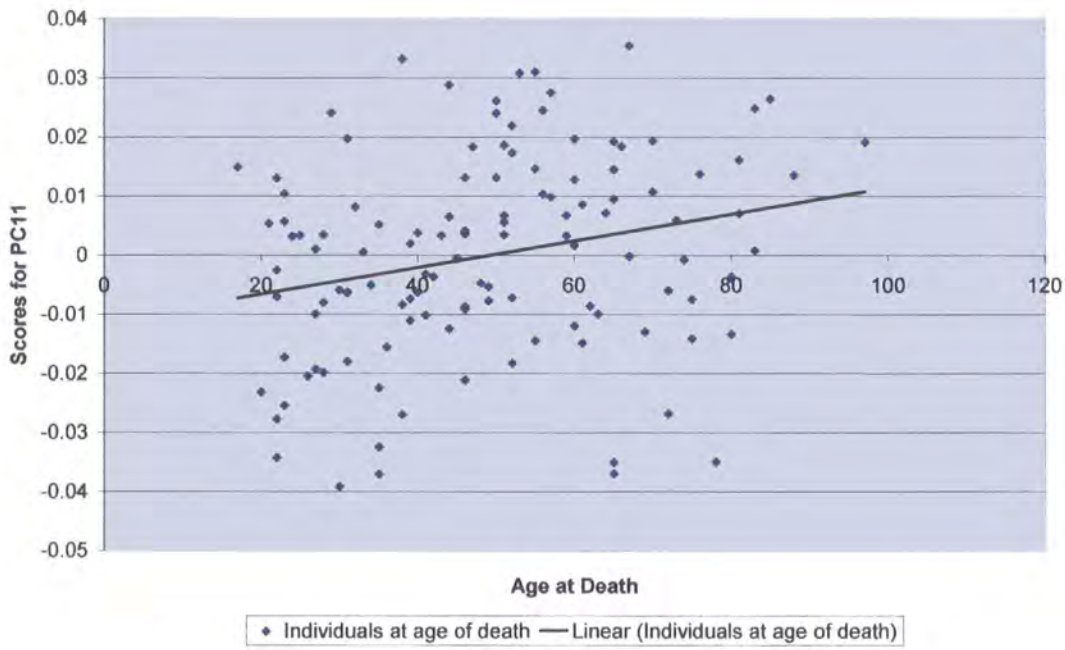

(b)

Figure 5.12: Ageing in the tibia of African Americans. Correlation of age at death with scores of PC11 highlighting (a) the 3 age groups and (b) the linear trendline ($r = 0.25$; $p = 0.0006$).

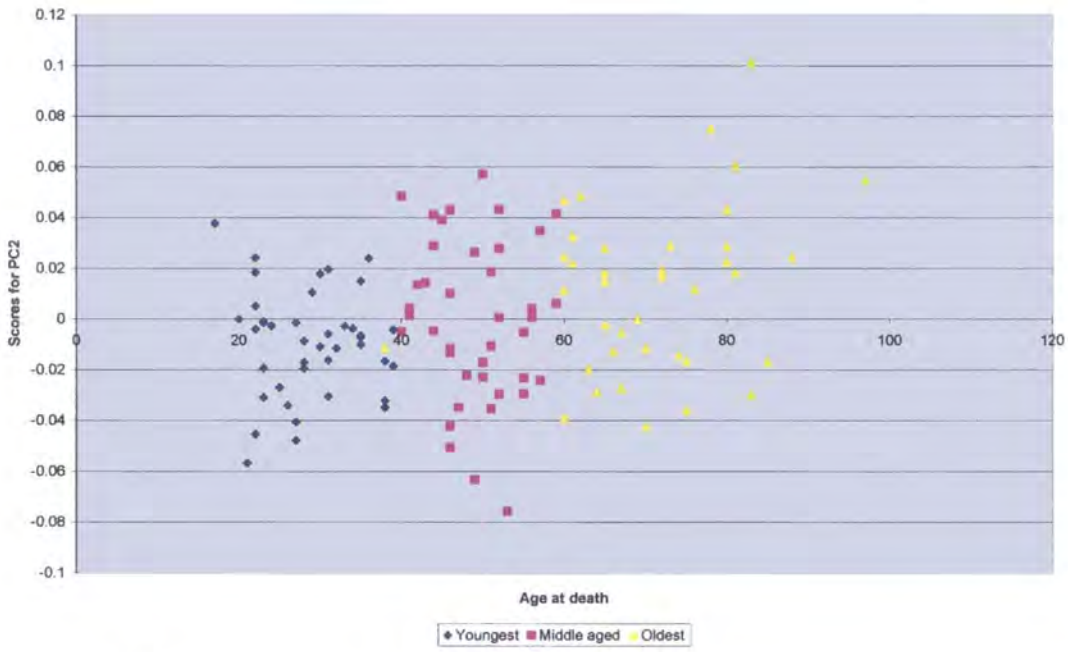

(a)

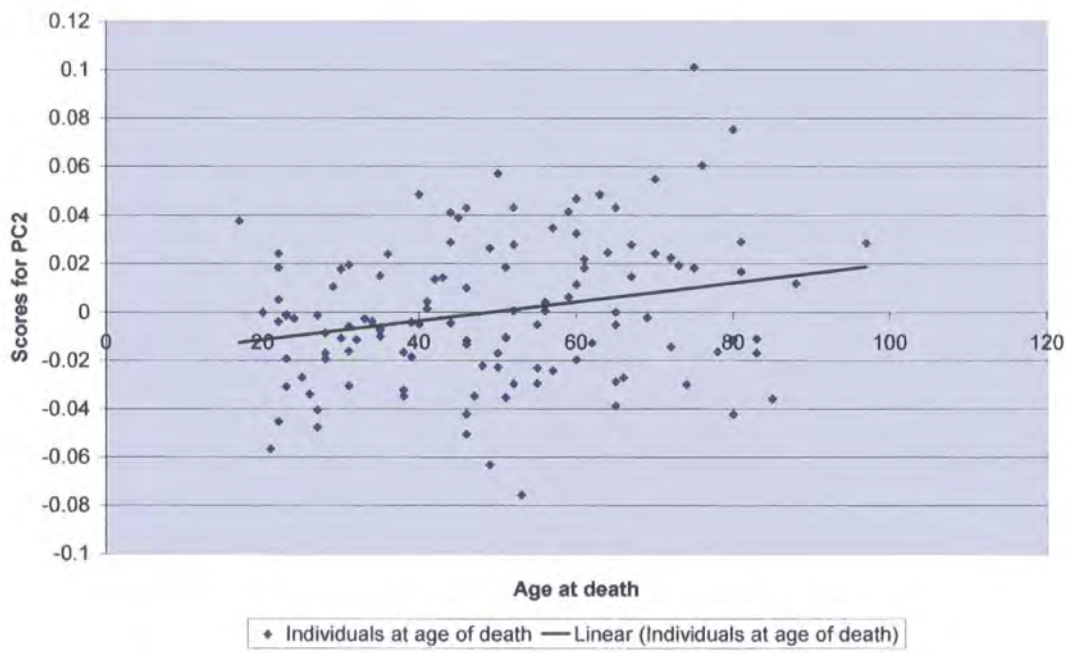

(b)

Figure 5.13: Ageing in the tibia of African Americans. Correlation of age at death with scores of PC2 highlighting (a) the 3 age groups and (b) the linear trendline ($r = 0.25$; $p = 0.007$).

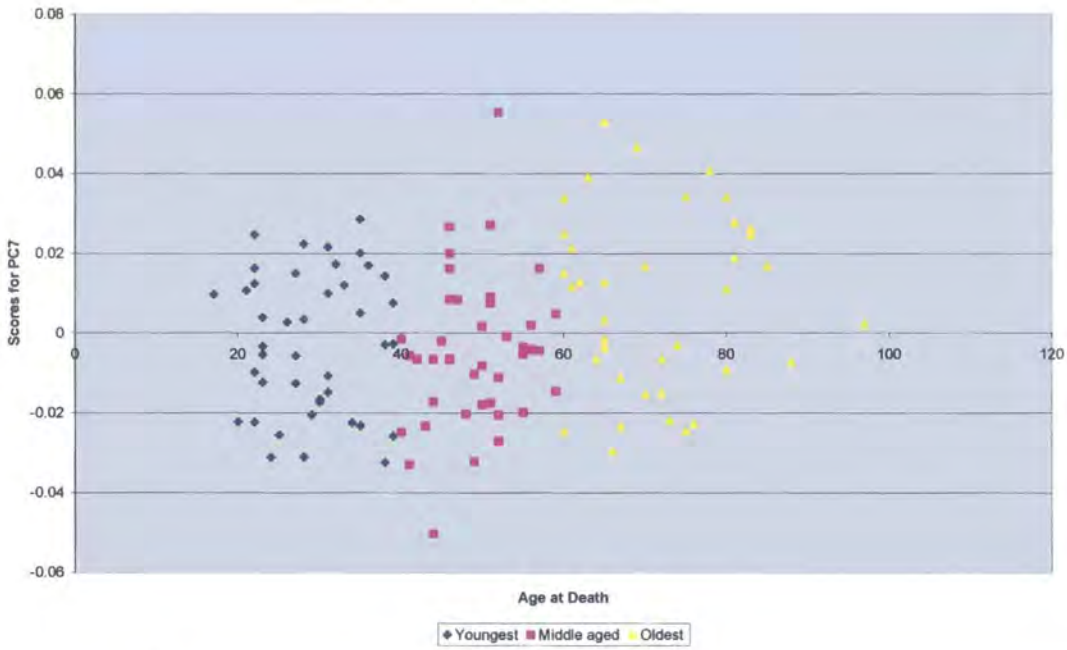

(a)

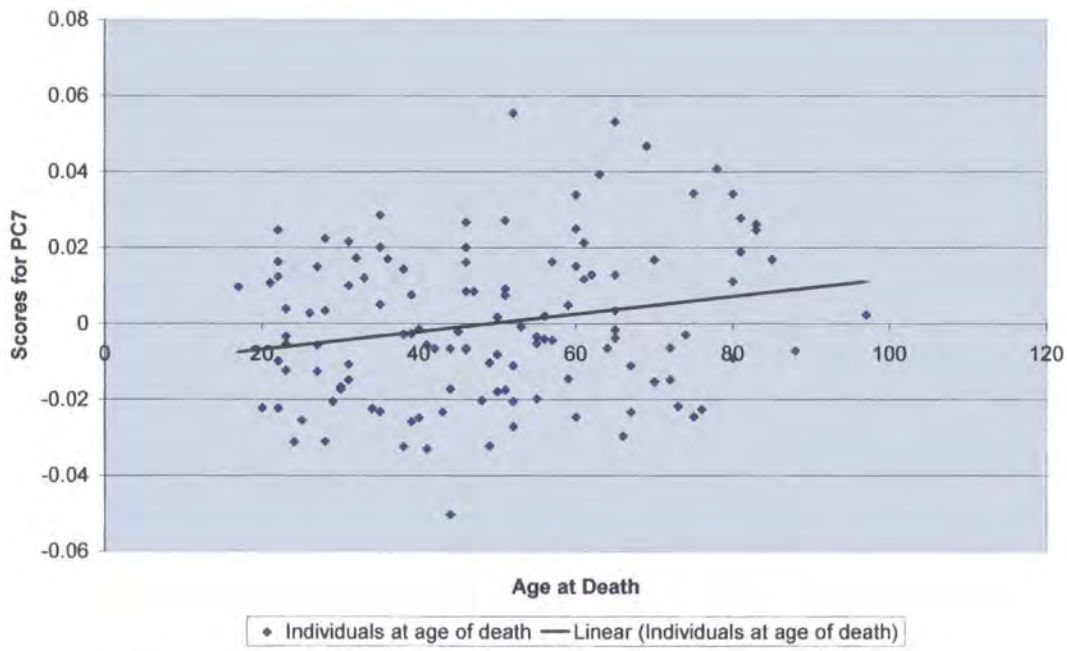

(b)

Figure 5.14: Ageing in the tibia of African Americans. Correlation of age at death with scores of PC7 highlighting (a) the 3 age groups and (b) the linear trendline ($r = 0.21$; $p = 0.007$).

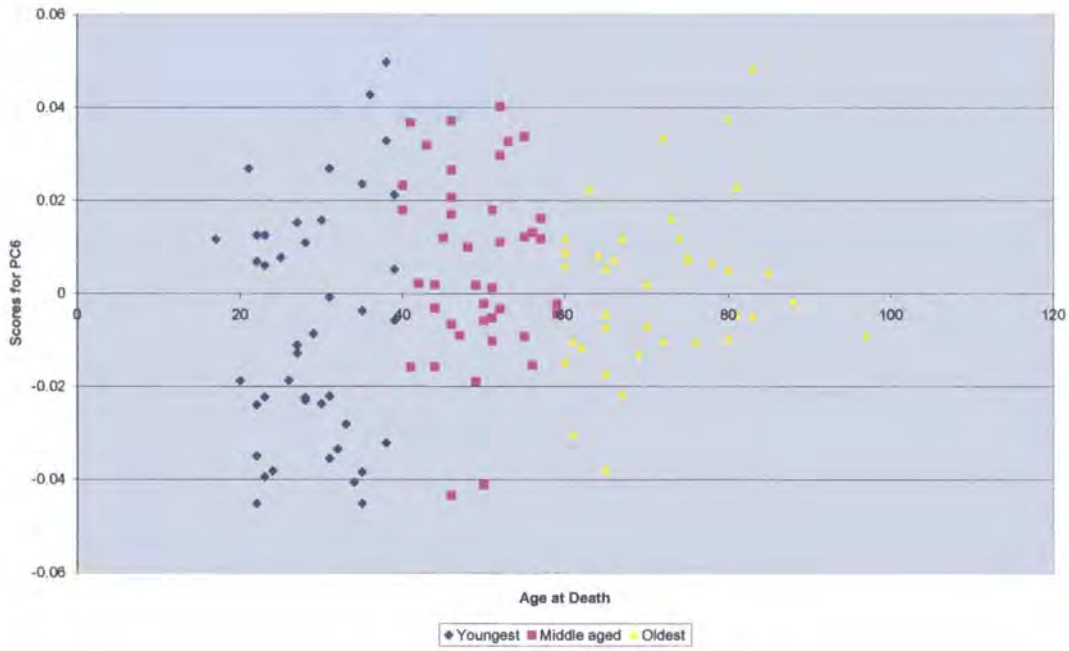

(a)

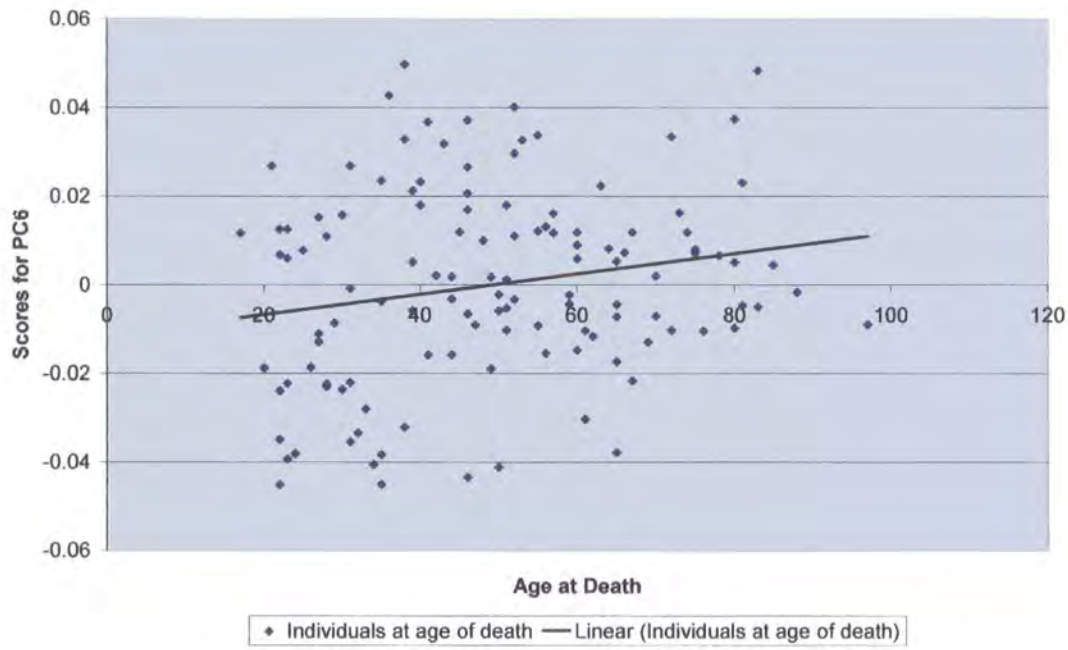

(b)

Figure 5.15: Ageing in the tibia of African Americans. Correlation of age at death with scores of PC6 highlighting (a) the 3 age groups and (b) the linear trendline ($r = 0.20$; $p = 0.03$).

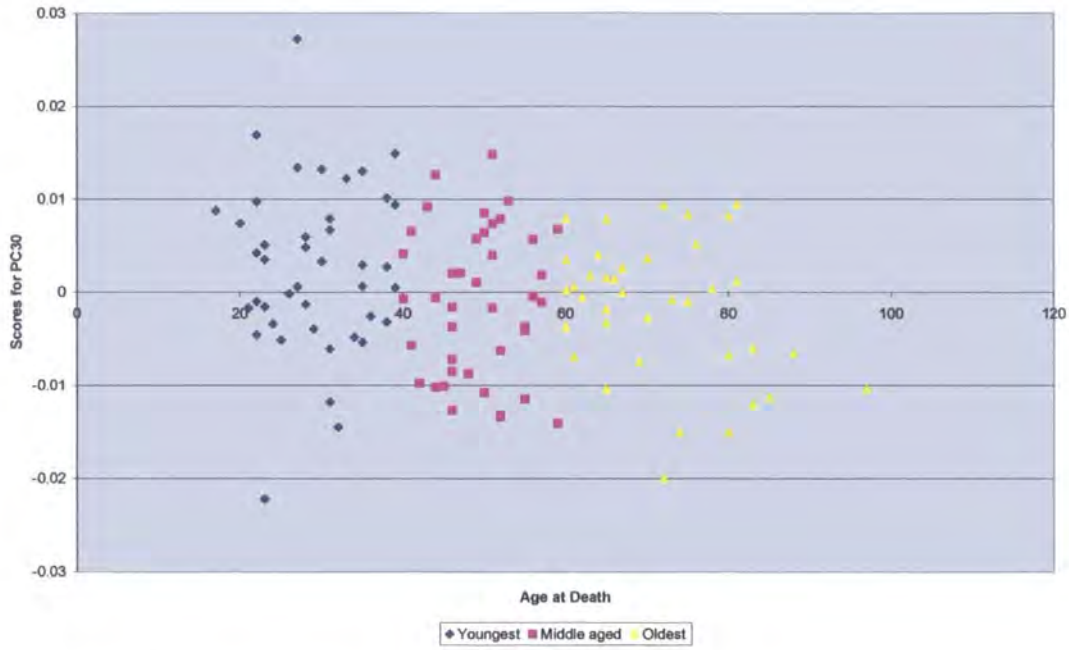

(a)

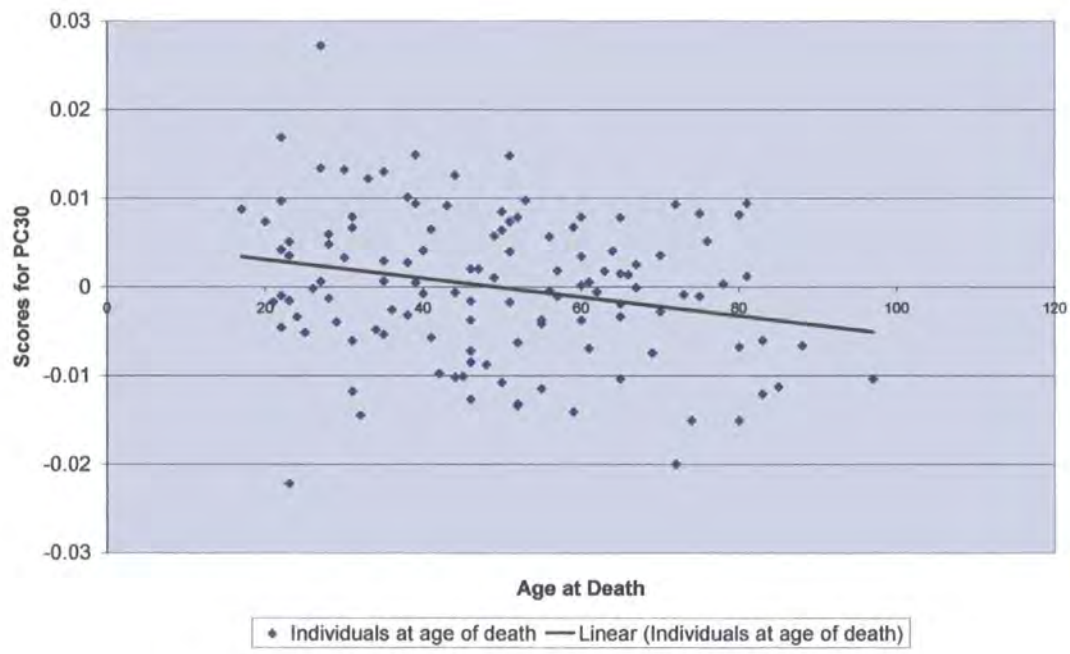

(b)

Figure 5.16: Ageing in the tibia of African Americans. Correlation of age at death with scores of PC30 highlighting (a) the 3 age groups and (b) the linear trendline ($r = 0.24$; $p = 0.009$).

Youngest	0		
	1.000		
Middle	6.33	0	
	0.0001	1.000	
Oldest	7.59	6.10	0
	0.0001	0.0001	1.000
	Youngest	Middle	Oldest

Table 5.12: Ageing in the tibia of African Americans (sexes pooled). The Mahalanobis' squared distances between the means of the 3 age groups, generated by stepwise discriminant analysis. The upper value in red gives the Mahalanobis' squared distance between species, the lower value in black gives the Hotelling's t^2 *p*-value.

Number of Observations and Percent Classified into Groups using Stepwise PCs				
From Group	Youngest	Middle	Oldest	Total
	33	3	6	42
Youngest	78.57	7.14	14.29	100
	8	25	8	41
Middle	19.51	60.98	19.51	100
	4	6	28	38
Oldest	10.53	15.79	73.68	100
	45	34	42	121
Total	37.19	28.1	34.71	100

Table 5.13: Ageing in the tibia of African Americans (sexes pooled). Results of cross validation analysis of the 3 age groups using PCs selected by stepwise discriminant analysis. Upper figure denotes the number of individuals; lower figure denotes percentage. Red figures denote number of individuals placed into their correct groups.

5.5.1b(ii) Tibia: Description of morphological differences between three age groups

PCs 11 and 9 are the first two PCs selected by stepwise discriminant analysis and account for 2.99% and 3.55% of total variance respectively. These two stepwise PCs will initially be used to examine the relationships between specimens in the bivariate plot shown in Figure 5.17. Using the Student's t-test in pairwise comparisons, at least the youngest and oldest samples are separated at a statistically significant level for both PC11 and PC9 in Table 5.14.

PC11	t=	*p*=	PC9	t=	*p*=
Groups 1 and 2	3.87	0.0002	Groups 1 and 2	1.08	0.28
Groups 1 and 3	2.31	0.02	Groups 1 and 3	3.91	0.0002
Groups 2 and 3	1.2	0.23	Groups 2 and 3	2.28	0.03

Table 5.14 Tibia: Results of Student's t-test between the 3 age groups for the tibia with PC11 and PC9, the first two PCs selected by stepwise discriminant analysis. Figures in blue indicate a non-significant result.

Despite both PC11 and PC9 showing a correlation with age at a level of statistical significance, the bivariate plot of PC11 with PC9 in Figure 5.17 shows an overlap of all specimens. As individual PCs selected by stepwise analysis, including PCs 11 and 9, fail to show any apparent separation of specimens in bivariate plots using the total sample, it is assumed that the significant separation of groups results from the accumulation of incremental degrees of variation contributed by all relevant PCs. Therefore, the sample means of each of the two sexes have also been used to help distinguish specific variation due to ageing.

For the tibia, the correlation between the Procrustes distances using the population means shown in Table 5.15 and the Mahalanobis' squared distances shown in Table 5.12 does not reach a level of statistical significance ($r= 0.09$, $p= 0.94$). In contrast to the Mahalanobis' distances, the Procrustes distances are seen to be greater between the middle and oldest groups than between the youngest and oldest.

Figure 5.17:

Ageing in the tibia of African Americans, total sample. Bivariate plot, showing a complete overlap of specimens of 3 age groups on PCs 11 and 9 (first and second PCs selected by stepwise discriminant analysis).

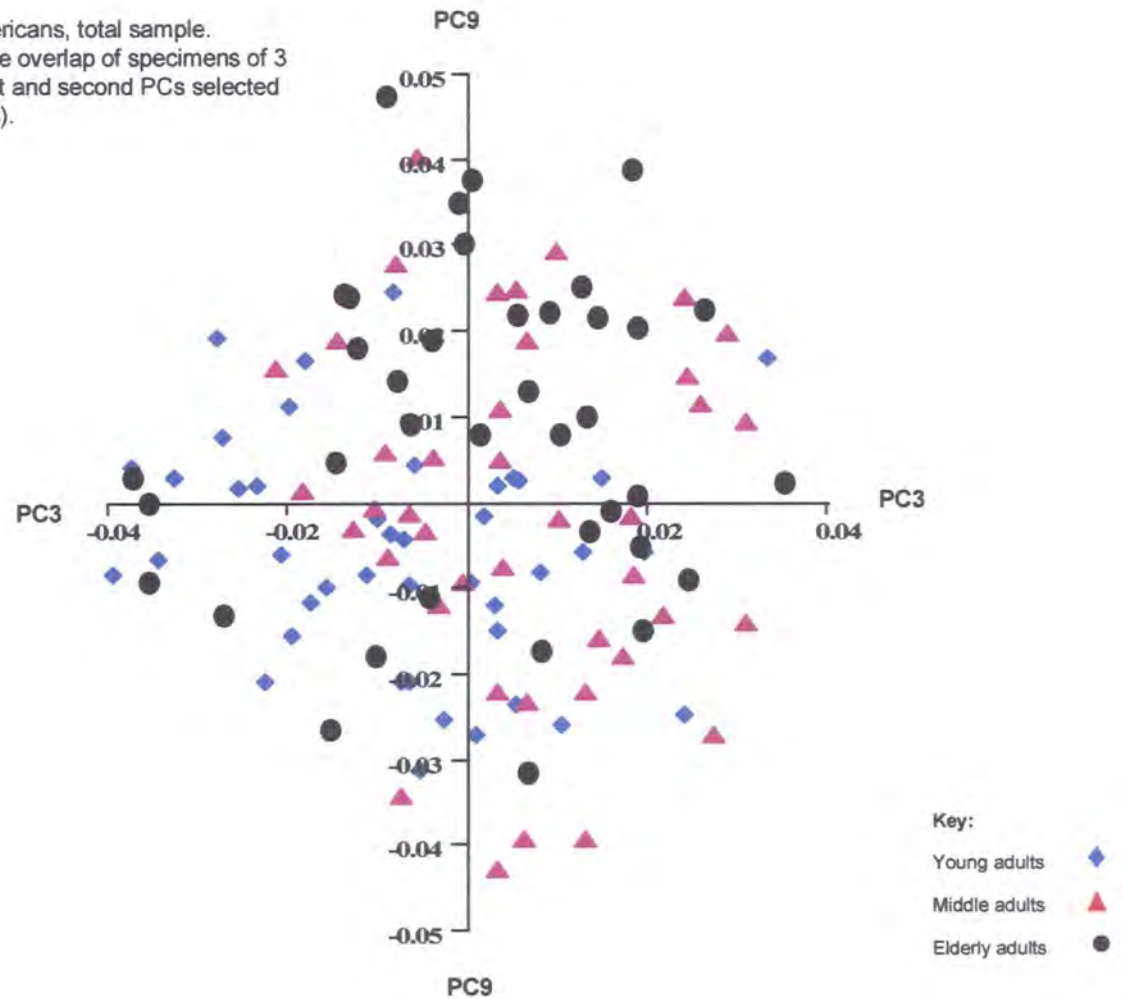

This difference in results should be borne in mind when comparing subsequent results using the two methods.

Youngest	0		
Middle	18.75	0	
Oldest	43.76	57.40	0
	Youngest	Middle	Oldest

Table 5.15: Procrustes distances between the 3 age groups in the tibia of African Americans.

The Procrustes mean co-ordinates have been calculated from the separate GPAs and have been subjected to a joint GPA and PCA. With a sample of three specimens, PC1 accounts for 63.8% and PC2 for 36.2% of total variance.

Figure 5.18 shows a separation of the three sample means in the bivariate plot of PC1 with PC2. On PC1 the youngest mean scores towards the negative extreme, with the oldest at the positive extreme and the middle aged mean scoring mid-way between the two.

As the mean configuration is warped along PC1, it is possible to appreciate a slight difference in the angle of the joint relative to the diaphysis between sample means at the two extremes. This difference in angle appears to compliment the similar change in angle between epiphysis and diaphysis noted between the sample means in the distal femur (section 5.5.1a(ii)). Although difficult to appreciate in the mean configuration, the difference in angle can be judged from the visible change in distance between landmarks 19 and 21 in the posterior section of the tibial shelf, and in the degree of visibility of landmark 15 at the inferior edge of the shelf, on the lateral side of the tibial tuberosity.

As with the femur, variation explained by PC2 is slight and difficult to interpret. Again, no separation is seen between the youngest and oldest means, which cluster together at a distance from the middle group, indicating that shape variation along the scale of PC2 does not appear to be solely related to differences with ageing.

Figure 5.18:

Ageing in the tibia of African Americans. Bivariate plot of PC1 with PC2, showing the separation of sample means of 3 age groups. Images represent the mean configuration if warped to the extremes of PC1 (at 0.02 and -0.02). Image at the positive extreme includes landmarks discussed in section 5.5.1b(ii).

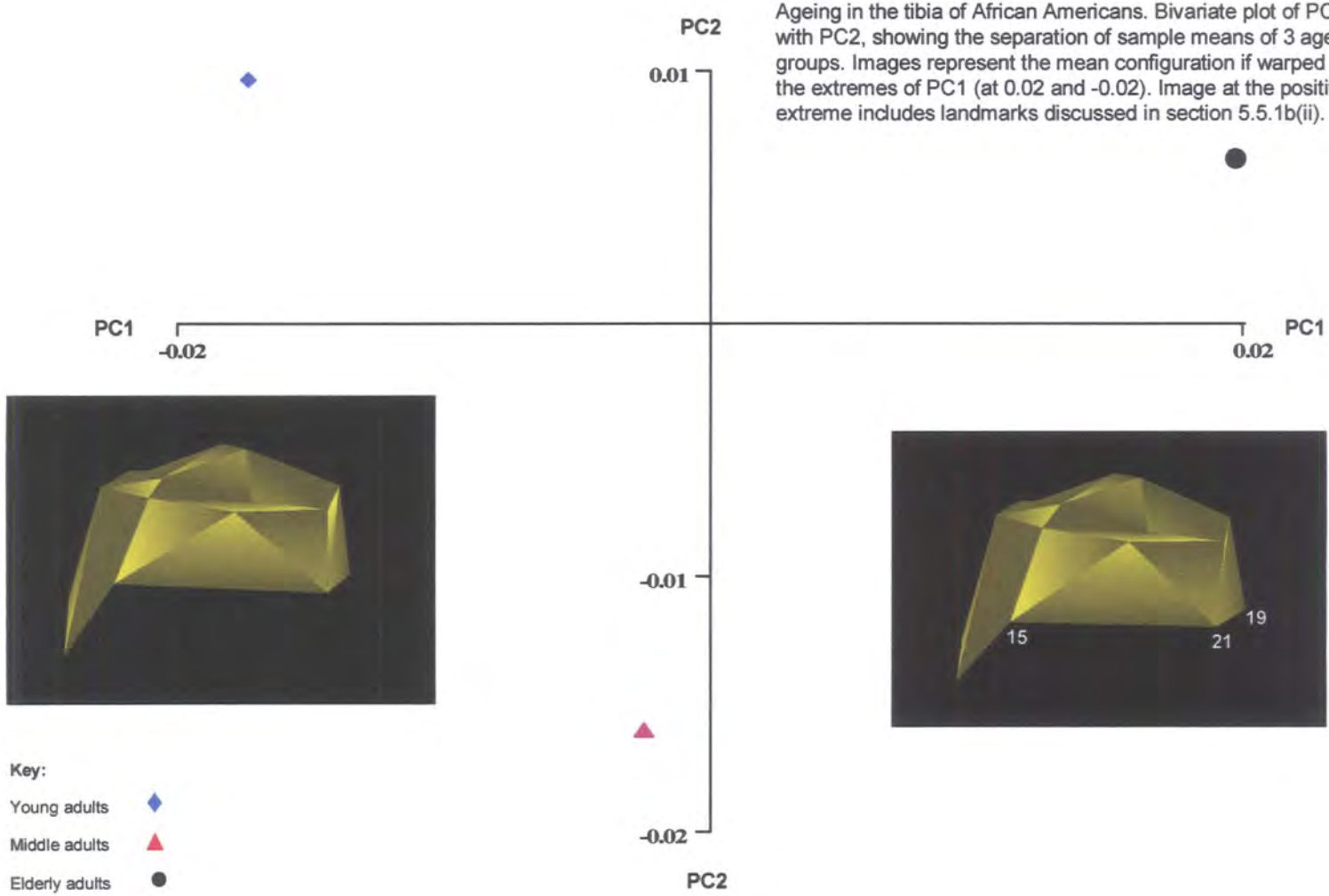

The mean configuration showing the maximum deformation of the TPS on PC1 in Figure 5.18 highlights a difference between the three sample means in the anterior section of bone, particularly on the lateral side. Although the difference in the anterior section has been noted above in the context of the change in angle between the youngest and oldest specimens, any change in the proportions of the joint are difficult to appreciate in the mean configuration at the two extremes. The deformation of the TPS, however, implies that there is also a marginal difference between specimens in the proportions of the bone, particularly across the tibial plateau.

5.5.2 Analysis of morphological differences between males and females of three age groups using African Americans

5.5.2a(i) Femur

Differences in shape of the 63 male and 58 female specimens divided by age group are analysed using the Procrustes fitted co-ordinates and by subjecting the data to PCA. Table 5.2 gives the proportional and accumulated variance for PCs 1 to 71, which represents the total variance within the sample.

A canonical stepwise discriminant function analysis is used to determine which PCs relate more specifically to differences between male and female age groups of African Americans. PCs selected by stepwise canonical discriminant analysis are shown in Table 5.16. The results using PCs accounting for c.50% to 100% of total variance and those used in the stepwise discriminant function analyses are summarised in Figure 5.20.

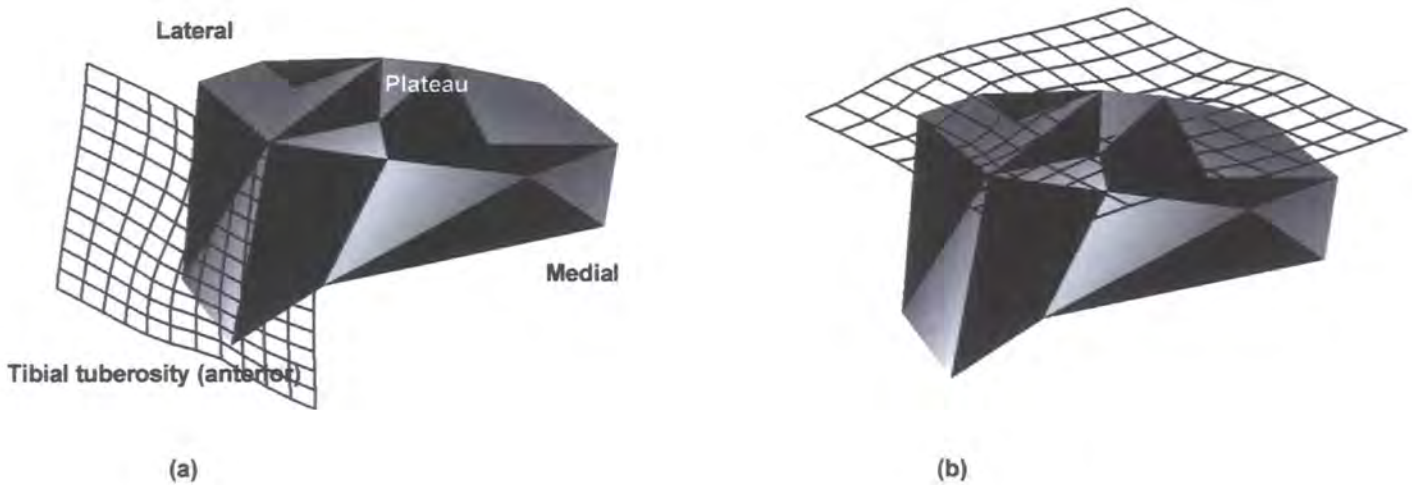

Fig 5.19: Ageing in the tibia of African Americans (sexes pooled). Representations of tibial shape with TPS taken from PC11 (first PC selected by stepwise discriminant analysis) using sample means, showing regions of bone (tibial tuberosity and plateau) giving maximum difference in shape between the means of the 3 age groups. (a) TPS view in anteroposterior plane; (b) in proximal plane. Images are presented to give the best indication of maximum difference in shape and are not necessarily taken from the same perspective as the mean configurations in Figure 5.18.

Order	Entered	Order	Entered	Order	Entered	Order	Entered
1	PC1	9	PC18	17	PC51	25	PC33
2	PC54	10	PC11	18	PC14	26	PC38
3	PC3	11	PC4	19	PC44	27	PC35
4	PC41	12	PC27	20	PC29	28	PC25
5	PC9	13	PC8	21	PC31	29	PC57
6	PC7	14	PC5	22	PC37		
7	PC16	15	PC20	23	PC30		
8	PC6	16	PC2	24	PC68		

Table 5.16 PCs selected by stepwise discriminant analysis for the males and females of the three age groups of African Americans for the femur. Stepwise PCs account for a cumulative 70.80% of total variance.

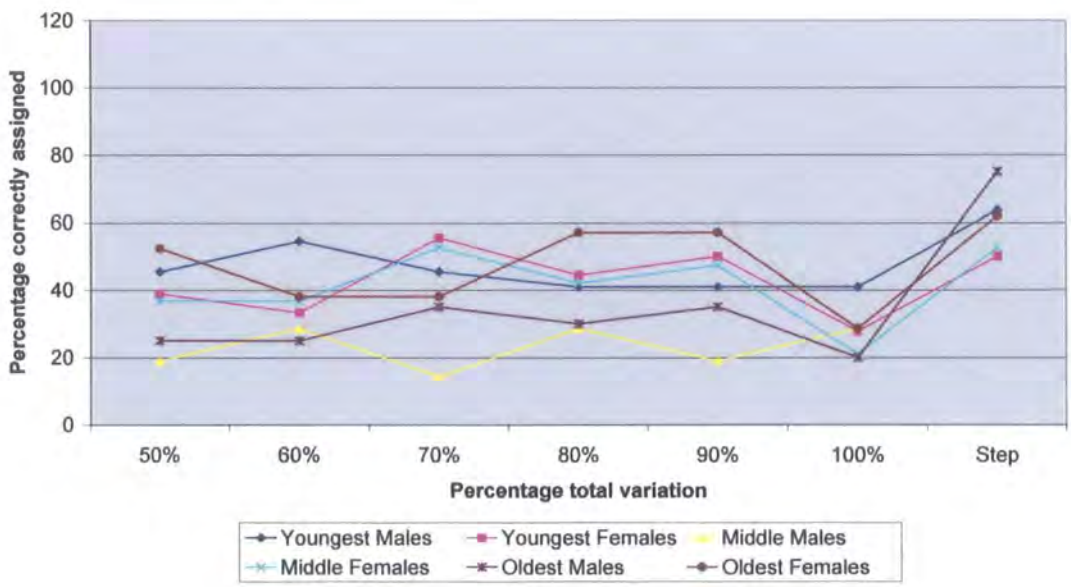

Figure 5.20: Ageing in the femur of African American males and females. Summary of separate discriminant and cross-validation analyses using PCs accounting for c.50% of total variance (PCs 1-9), c.60% (PCs 1-12), c.70% (PCs 1-16), c.80% (PCs 1-22), c.90% (PCs 1-33) and 100% (PCs 1-71) and stepwise discriminant analysis.

The Mahalanobis' squared distances between the male and female age groups, generated by stepwise discriminant analysis are shown in Table 5.17.

Males Youngest	0 1.000					
Females Youngest	11.68 0.0032	0 1.000				
Males Middle	9.81 0.3009	7.62 0.1732	0 1.000			
Females Middle	15.14 0.0001	7.11 0.024	9.15 0.005	0 1.000		
Males Oldest	17.65 0.0122	19.09 0.0002	10.40 0.3953	14.54 0.0001	0 1.000	
Females Oldest	21.33 0.0010	16.18 0.0001	16.06 0.0009	14.81 0.0001	13.81 0.0014	0 1.0000
	Males Youngest	Females Youngest	Males Middle	Females Middle	Males Oldest	Females Oldest

Table 5.17: Ageing in the femur of African American males and females. Results of canonical stepwise discriminant analysis of males and females of the 3 age groups. The upper value in red gives the Mahalanobis' squared distance between groups, lower value in black gives the Hotelling's t^2 *p*-value. Figures in blue indicate a statistically non-significant value.

Only 12 of the total 15 Mahalanobis' squared distances are statistically significant. For the three male groups, the distance between the youngest and oldest groups remains statistically significant, as are distances between all three female groups. Table 5.18 illustrates the relationship of each sample to all others on the basis of the generated Mahalanobis' squared distances by showing the distance of each primary sample to all others and ranking them accordingly from the closest sample (at position 1) to the furthest (at position 5).

Group	1	2	3	4	5
Males Youngest	MM	FY	FM	MO	FO
Females Youngest	FM	MM	MY	FO	MO
Males Middle	FY	FM	MM	MO	FO
Females Middle	FY	MM	MO	FO	MY
Males Oldest	MM	FO	FM	MY	FY
Females Oldest	MO	FM	MM	FY	MY

Table 5.18: The order of proximity in distance of each primary male and female aged group from other groups for the femur in the dataset on the basis of their Mahalanobis squared distances, as shown in Table 5.17.

The relatively low degree of separation of groups highlighted in Table 5.18 is reflected in Table 5.19 which shows the results of cross-validation analysis with between 50% and 75% of specimens from the male and female age groups correctly assigned to group. Remaining specimens appear to be misplaced at random with a relatively high proportion being placed within groups of the opposite sex. However, Table 5.18 shows that the youngest and oldest primary groups are always separated by the middle aged groups. The sex of the primary group is also the same sex as the group in position 4 and opposite to that of position 5.

Number of Observations and Percent Classified into Groups using Stepwise PCs

From Group	Males Youngest	Females Youngest	Males Middle	Females Middle	Males Oldest	Females Oldest	Total
Males Youngest	14	2	3	2	1	0	22
	63.64	9.09	13.64	9.09	4.55	0	100
Females Youngest	1	9	3	3	1	1	18
	5.56	50	16.67	16.67	5.56	5.56	100
Males Middle	2	3	13	0	2	1	21
	9.52	14.29	61.9	0	9.52	4.76	100
Females Middle	0	4	4	10	0	1	19
	0	21.05	21.05	52.63	0	5.26	100
Males Oldest	1	0	2	1	15	1	20
	5	0	10	5	75	5	100
Females Oldest	1	1	0	2	4	13	21
	4.76	4.76	0	9.52	19.05	61.9	100
Total	19	19	25	18	23	17	121
	15.7	15.7	20.66	14.88	19.01	14.05	100

Table 5.19: Ageing in the femur of African American males and females. Results of cross validation analysis of the males and females of the 3 age groups using PCs selected by stepwise discriminant analysis. Upper figure denotes the number of individuals; lower figure denotes percentage. Red figures denote number of individuals placed into their correct groups.

Tables 5.17, 5.18 and 5.19 all imply that shape differences accruing with age at the knee joint are progressive. Chapter 4 also verifies that knee joint shape is sexually dimorphic and this is apparent in relation to age, albeit weakly, in some results outlined above. In relation to the femur, however, it appears that neither shape differences due to ageing nor those due to sexual dimorphism are so strong as to mask the influence of the other.

5.5.2a(ii) Femur: Description of morphological differences between males and females of the three age groups

The exploration of shape differences due to ageing between the two sexes by visual means is problematic, as it is necessary to differentiate between shape differences due to ageing and those due to sexual dimorphism. All PCs, including initial stepwise PCs, show an overlap of all male and female specimens from the three age groups and fail to separate groups in any bivariate plot using the total sample. Therefore, the sample means of each of the two sexes and three age groups have been used to help distinguish specific variation due to ageing.

For the femur, the correlation between the Procrustes distances using the population means shown in Table 5.20 and the Mahalanobis' squared distances shown in Table 5.17 does not reach a level of statistical significance (r= 0.05; p= 0.87). This lack of a statistically significant correlation in results should be borne in mind when comparing results from the two methods.

Males Youngest	0					
Females Youngest	14.21	0				
Males Middle	13.92	10.77	0			
Females Middle	18.98	23.32	14.81	0		
Males Oldest	18.83	10.77	14.97	23.85	0	
Females Oldest	18.60	11.20	13.51	26.63	20.11	0
	Males Youngest	Females Youngest	Males Middle	Females Middle	Males Oldest	Females Oldest

Table 5.20: Ageing in 3 age groups for the femur of African American males and females. Procrustes distances between mean individuals of males and females of 3 age groups. Correlation between Procrustes distances and Mahalanobis' distances generated by stepwise discriminant analysis (Table 5.17) is not significant at: r=0.048; p=0.87.

The Procrustes mean co-ordinates have been calculated from the separate GPAs and have been subjected to a joint GPA and PCA. As the first four PCs account for a cumulative 94.20% of total variance in the sample (PC1 for 38.4%, PC2 for 27.9%, PC3 for 12.70% and PC4 for 9.55%), the exploration of shape differences will concentrate on these four PCs.

In Figure 5.21, the bivariate plot of PC1 with PC2, PC1 shows a complete separation of all three male means and all three female means. Variation explained by these two PCs is of the same nature and degree to that described between the three pooled-sex age groups in section 5.5.1a(ii) above, i.e., with an emphasis on the angle of attachment of joint relative to shaft, particularly on the medial side. PC1 explains a sexually dimorphic separation of the six sexed groups with the three male means placed more positively than the three female means. With the two middle-aged groups positioned in close proximity and towards the centre of the scale of PC1 and with the oldest female and youngest male at the two extremes, there are no clear relationships between the three age groups. For PC2 also, there are no clear relationships between means based either on shape variation due to sexual dimorphism or differences due to ageing.

Figure 5.22, the bivariate plot of PC3 with PC4 also shows for PC3 that the oldest female mean is separated from the youngest and middle means by all three male means. On PC4, the youngest male mean is separated from the middle and oldest male means by all three female means. As with PC2, therefore, PCs 3 and 4 demonstrate no clear relationships between means, based either on shape variation due to sexual dimorphism or differences due to ageing.

5.5.2b(i) Tibia

Differences in shape between the 62 male and 58 female specimens divided by age group are analysed using the Procrustes fitted co-ordinates and by subjecting the data to PCA. Table 5.9 gives the proportional and accumulated variance for PCs 1 to 56, which represents the total variance within the sample.

Figure 5.21:

Ageing in the femur of African American males and females. Bivariate plot of PC1 with PC2, showing the separation of male and female means of 3 age groups. Images represent the mean configuration if warped to the extreme corners of upper right and lower left quadrants.

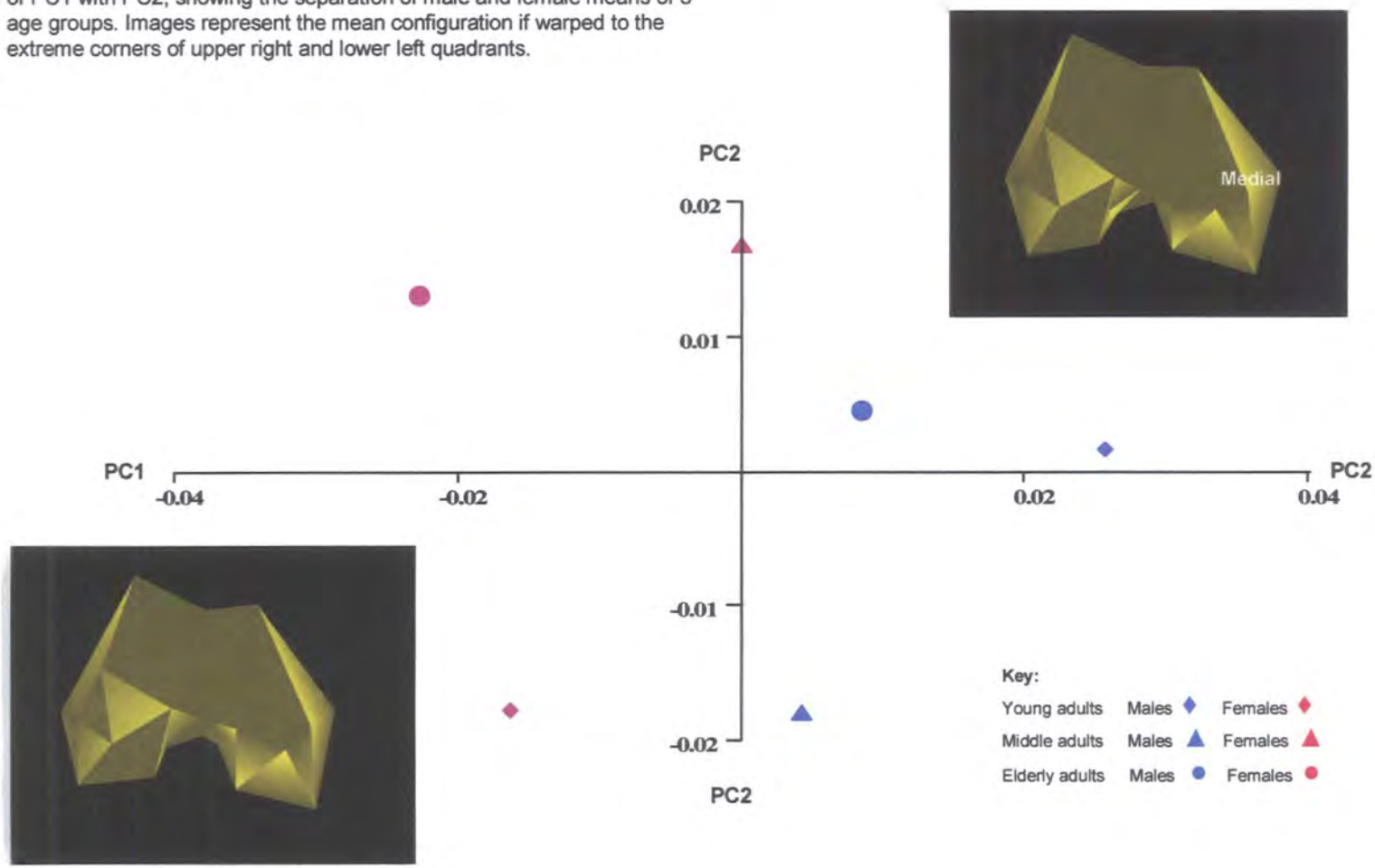

Figure 5.22:

Ageing in the femur of African American males and females. Bivariate plot of PC3 with PC4, showing the separation of male and female means of 3 age groups. Images represent the mean configuration if warped to the extreme corners of PC3 (0.02 and -0.02).

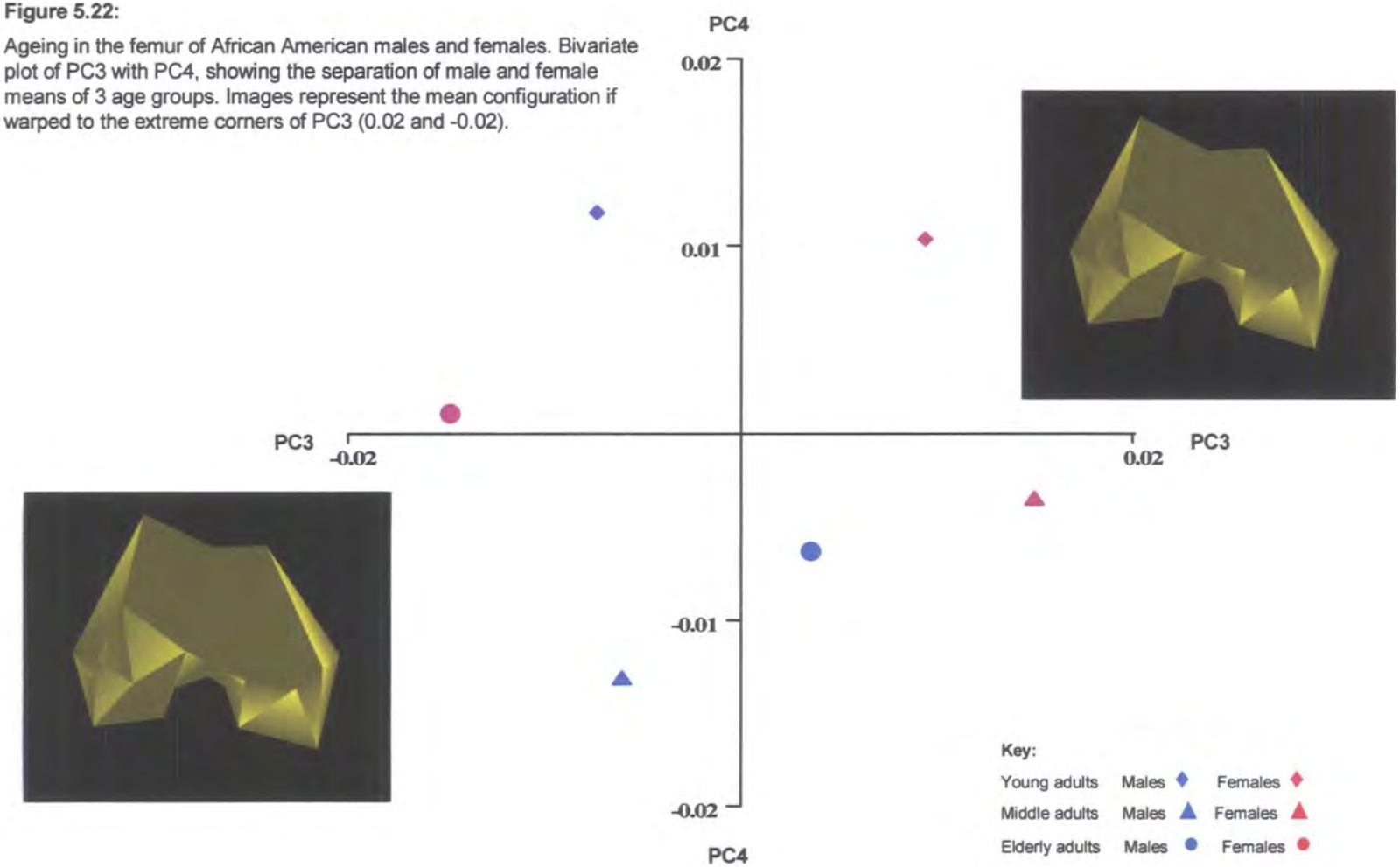

A canonical stepwise discriminant function analysis is used to determine which PCs relate more specifically to differences between male and female age groups of African Americans. PCs selected by stepwise canonical discriminant analysis for the male and female groups are shown in Table 5.21. The results using PCs accounting for c.50% to 100% of total variance and those used in the stepwise discriminant function analyses are summarised in Figure 5.23.

Order	Entered	Order	Entered	Order	Entered	Order	Entered
1	PC6	7	PC9	13	PC22	19	PC54
2	PC5	8	PC29	14	PC52	20	PC59
3	PC1	9	PC33	15	PC21	21	PC42
4	PC2	10	PC7	16	PC44	22	PC24
5	PC11	11	PC30	17	PC14		
6	PC4	12	PC8	18	PC43		

Table 5.21: PCs selected by stepwise discriminant analysis for the males and females of the 3 age groups for the tibia of African Americans. Stepwise PCs account for a cumulative 63.84% of total variance.

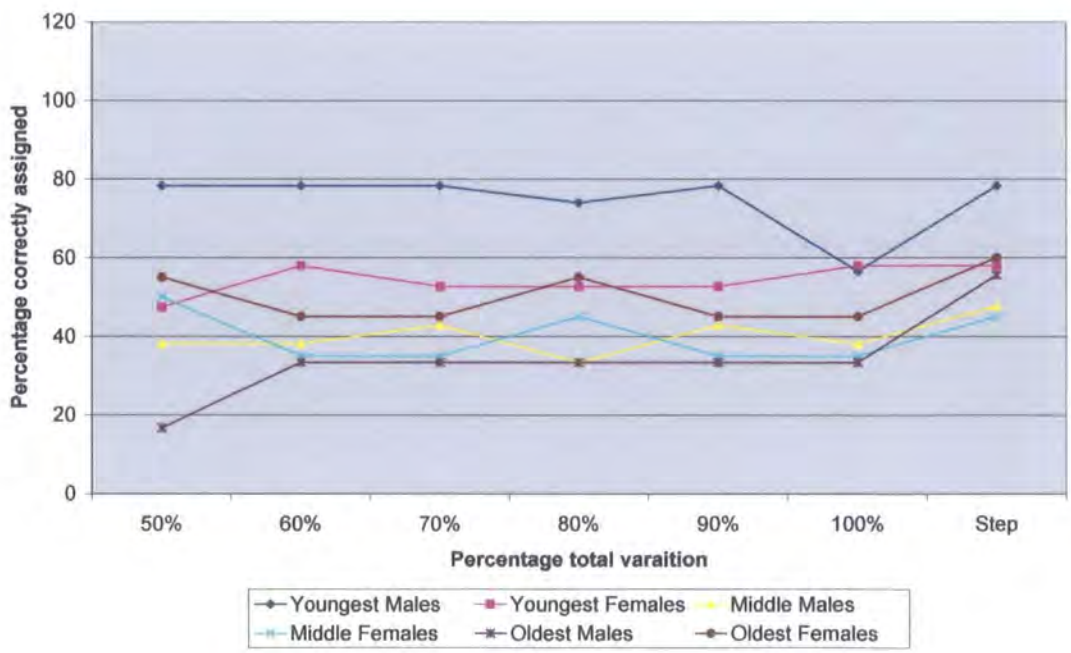

Figure 5.23: Ageing in the tibia of African American males and females. Summary of separate discriminant and cross-validation analyses using PCs accounting for c.50% of total variance (PCs 1-6), c.60% (PCs 1-9), c.70% (PCs 1-13), c.80% (PCs 1-18), c.90% (PCs 1-27) and 100% (PCs 1-56) and stepwise discriminant analysis.

The Mahalanobis' squared distances between the male and female age groups, generated by stepwise discriminant analysis are shown in Table 5.22. For the tibia, all Mahalanobis' squared distances between groups are statistically significant. Table 5.23 illustrates the relationship of each sample to all others on the basis of the generated Mahalanobis' squared distances by showing the distance of each primary sample to all others and ranking them accordingly from the closest sample (at position 1) to the furthest (at position 5).

Males	0					
Youngest	1.0000					
Females	23.69	0				
Youngest	0.0001	1.0000				
Males	9.90	15.30	0			
Middle	0.0001	0.0001	1.0000			
Females	28.16	7.79	17.02	0		
Middle	0.0001	0.0003	0.0001	1.0000		
Males	13.65	13.93	10.27	11.60	0	
Oldest	0.0001	0.0001	0.0001	0.0001	1.0000	
Females	19.36	9.18	13.52	5.53	8.30	0
Oldest	0.0001	0.0001	0.0001	0.0091	0.0002	1.0000
	Males Youngest	Females Youngest	Males Middle	Females Middle	Males Oldest	Females Oldest

Table 5.22: Ageing in the tibia of African American males and females. Results of canonical stepwise discriminant analysis of males and females of the three age groups. The upper value in red gives the Mahalanobis' squared distance between groups, lower value in black gives the Hotelling's t^2 *p*-value.

Group	1	2	3	4	5
Males Youngest	M M	M O	F O	F Y	F M
Females Youngest	F M	F O	M O	M M	M Y
Males Middle	M Y	M O	F O	F Y	F M
Females Middle	F O	F Y	M O	M M	M Y
Males Oldest	F O	M M	F M	M Y	F Y
Females Oldest	F M	M O	F Y	M M	M Y

Table 5.23 Tibia: The order of proximity in distance of each primary male and female aged group from other groups in the dataset on the basis of their Mahalanobis squared distances, as shown in Table 5.22.

Despite Table 5.22 indicating that all groups are separated at a level of statistical significance, Table 5.24, which gives the results of cross-validation analysis, shows that (for five of the six groups) only 60% or less of specimens are correctly assigned to groups. For the youngest and middle aged groups, the majority of misplaced specimens are assigned to other groups of the same sex; reinforcing the placement of groups relative to the primary group seen in Table 5.23. The closer association of the primary group to other groups of the same sex is less pronounced in the oldest adults, suggesting some similarity of shape in older bones regardless of sex.

Number of Observations and Percent Classified into Groups using Stepwise PCs							
From Group	Males Youngest	Females Youngest	Males Middle	Females Middle	Males Oldest	Females Oldest	Total
Males Youngest	18	0	4	0	0	1	23
	78.26	0	17.39	0	0	4.35	100
Females Youngest	0	11	0	3	3	2	19
	0	57.89	0	15.79	15.79	10.53	100
Males Middle	5	1	10	1	3	1	21
	23.81	4.76	47.62	4.76	14.29	4.76	100
Females Middle	0	3	1	9	2	5	20
	0	15	5	45	10	25	100
Males Oldest	0	1	1	2	10	4	18
	0	5.56	5.56	11.11	55.56	22.22	100
Females Oldest	0	1	1	4	2	12	20
	0	5	5	20	10	60	100
Total	23	17	17	19	20	25	121
	19.01	14.05	14.05	15.7	16.53	20.66	100

Table 5.24: Ageing in the tibia of African American males and females. Results of cross validation analysis of the males and females of the three age groups using PCs selected by stepwise discriminant analysis. Upper figure denotes the number of individuals; lower figure denotes percentage. Red figures denote number of individuals placed into their correct groups.

5.5.2b(ii) Tibia: Description of morphological differences between males and females of the three age groups

The exploration of shape differences due to ageing between the two sexes by visual means is particularly problematic for the tibia as it is difficult to differentiate between shape differences due to ageing and those due to sexual dimorphism.

All PCs, including initial stepwise PCs, show an overlap of all male and female specimens from the three age groups and fail to separate groups in any bivariate plot using the total sample. Therefore, the sample means of each of the two sexes and three age groups have been used to help distinguish specific variation due to ageing.

For the tibia, the correlation between the Procrustes distances using the population means shown in Table 5.25 and the Mahalanobis' squared distances shown in Table 5.22 does not reach a level of statistical significance ($r = 0.15$; $p = 0.59$). This lack of a statistically significant correlation in results using the two methods should be borne in mind when comparing results from the two methods.

Males Youngest	0					
Females Youngest	28.96	0				
Males Middle	19.04	19.41	0			
Females Middle	42.27	60.87	55.58	0		
Males Oldest	43.81	64.39	57.50	7.25	0	
Females Oldest	9.95	33.66	20.00	43.71	44.38	0
	Males Youngest	Females Youngest	Males Middle	Females Middle	Males Oldest	Females Oldest

Table 5.25; Ageing in 3 age groups for the tibia of African American males and females. Procrustes distances between mean individuals of males and females of 3 age groups. Correlation between Procrustes distances and Mahalanobis' distances generated by stepwise discriminant analysis (Table 5.18) is not significant at:
$r = 0.15$; $p = 0.59$

The Procrustes mean co-ordinates have been calculated from the separate GPAs and have been subjected to a joint GPA and PCA. As the first two PCs account for a cumulative 70.5% of total variance in the sample (PC1 for 49.9% and PC2 for 20.6%), the exploration of shape differences will concentrate on these two PCs. No PC beyond PC2 shows any degree of separation of age groups for males and females.

In Figure 5.24, PC1 separates means primarily on a sexual rather than an age-group basis with all three male means lying on the positive side of the scale and all three female means on the negative side. There is no similarity in the relationship of male

Figure 5.24:

Ageing in the tibia of African American males and females. Bivariate plot of PC1 with PC2, showing the separation of male and female means of 3 age groups. Images (a) and (b) represent the mean configuration if warped to the extremes of PC1 (at 0.04 and -0.04) and (c) and (d) at the extremes of PC2 (at 0.03 and -0.03). Images (b) and (d) include landmarks discussed in the text (section 5.5.2b(ii)).

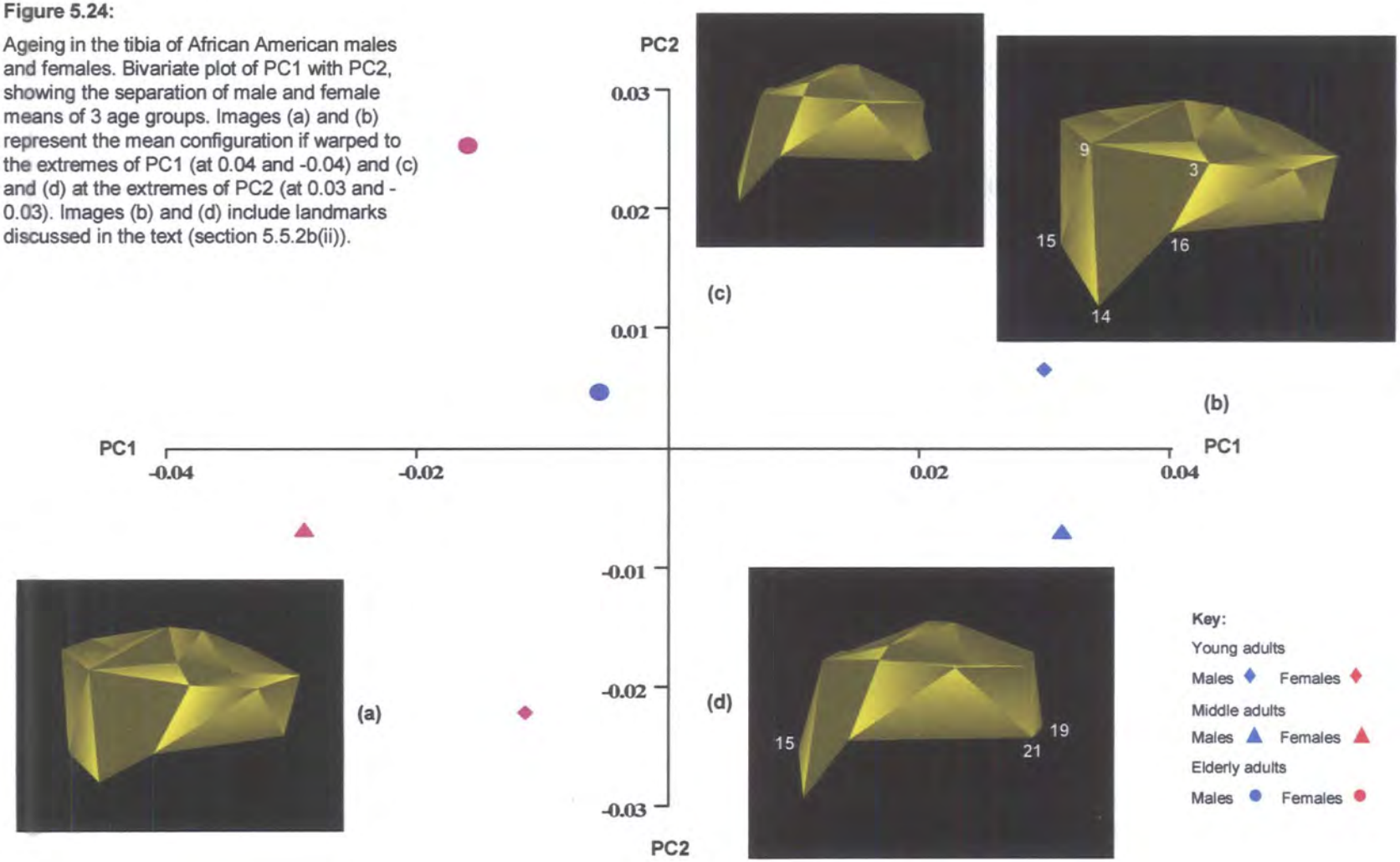

age groups relative to those of females. The mean configuration at the extremes of PC1 (Figure 5.24(a) and (b)), shows a clear difference in the length of the tibial tuberosity from the edge of the plateau (landmarks 14, 15 and 16 from landmarks 3 and 9) with male groups at the positive extreme showing greater length relative to female groups at the negative extreme. The results of Chapter 4 (section 4.4.3b(ii)) noted that the length of the anterior section is a primary distinguishing characteristic between males and females, with males showing significantly greater anterior length relative to females.

Although there is no clear association of either the three male means or the three female means on PC2, any more than for PC1, variation explained by PC2 more closely reflects the differences between age groups noted in section 5.5.1b(ii) above in the slight difference in the angle of attachment between the joint relative to the diaphysis. The mean configuration in Figure 5.24(c) and (d) illustrate this difference in the visible distance between landmarks 19 and 21 in the posterior section of the tibial shelf and in the degree of visibility of landmark 15 at the inferior edge of the shelf, on the lateral side of the tibial tuberosity.

5.5.3 Analysis of morphological differences between the three age groups of three populations

5.5.3a(i) Femur

Differences in shape of the 246 specimens from the African and Caucasian American and Spitalfields samples divided into three age groups are analysed using the Procrustes fitted co-ordinates and by subjecting the data to PCA. Table 5.26 gives the proportional and accumulated variance for PCs 1 to 71, which represents the total variance within the sample.

A canonical stepwise discriminant function analysis is used to determine which PCs relate more specifically to differences between age groups. PCs selected by stepwise canonical discriminant analysis are shown in Table 5.27. The results using PCs accounting for c.50% to 100% of total variance and those used in the stepwise discriminant function analyses are summarised in Figure 5.25.

PCs	Prop.	Cumul.	PCs	Prop.	Cumul.	PCs	Prop.	Cumul.
PC1	9.05	9.05	**PC26**	1.12	80.60	**PC51**	0.31	96.50
PC2	7.23	16.30	**PC27**	1.06	81.70	**PC52**	0.30	96.80
PC3	6.52	22.80	**PC28**	1.06	82.70	**PC53**	0.28	97.10
PC4	5.88	28.70	**PC29**	1.02	83.70	**PC54**	0.27	97.40
PC5	4.58	33.20	**PC30**	0.96	84.70	**PC55**	0.25	97.60
PC6	4.54	37.80	**PC31**	0.88	85.60	**PC56**	0.25	97.90
PC7	3.95	41.70	**PC32**	0.83	86.40	**PC57**	0.23	98.10
PC8	3.61	45.30	**PC33**	0.80	87.20	**PC58**	0.21	98.30
PC9	3.27	48.60	**PC34**	0.76	88.00	**PC59**	0.21	98.50
PC10	2.91	51.50	**PC35**	0.74	88.70	**PC60**	0.19	98.70
PC11	2.88	54.40	**PC36**	0.70	89.40	**PC61**	0.18	98.90
PC12	2.81	57.20	**PC37**	0.67	90.10	**PC62**	0.16	99.10
PC13	2.48	59.70	**PC38**	0.63	90.70	**PC63**	0.15	99.20
PC14	2.27	62.00	**PC39**	0.60	91.30	**PC64**	0.14	99.30
PC15	2.15	64.10	**PC40**	0.59	91.90	**PC65**	0.12	99.50
PC16	2.02	66.10	**PC41**	0.54	92.40	**PC66**	0.11	99.60
PC17	1.86	68.00	**PC42**	0.53	92.90	**PC67**	0.11	99.70
PC18	1.82	69.80	**PC43**	0.50	93.40	**PC68**	0.10	99.80
PC19	1.68	71.50	**PC44**	0.47	93.90	**PC69**	0.09	99.90
PC20	1.50	73.00	**PC45**	0.45	94.40	**PC70**	0.07	99.90
PC21	1.47	74.50	**PC46**	0.43	94.80	**PC71**	0.07	100.00
PC22	1.35	75.80	**PC47**	0.39	95.20			
PC23	1.30	77.10	**PC48**	0.37	95.50			
PC24	1.23	78.30	**PC49**	0.35	95.90			
PC25	1.12	79.50	**PC50**	0.33	96.20			

Table 5.26: Ageing in the femur of 3 populations. The proportional and accumulated variance for PCs 1-71 accounting for 100% of total variance using the total sample of 3 age groups from 3 populations.

Order	Entered	Order	Entered	Order	Entered	Order	Entered
1	PC1	10	PC21	19	PC58	28	PC44
2	PC2	11	PC6	20	PC32	29	PC59
3	PC14	12	PC9	21	PC55	30	PC40
4	PC4	13	PC37	22	PC34	31	PC67
5	PC10	14	PC73	23	PC45	32	PC61
6	PC7	15	PC3	24	PC17	33	PC30
7	PC5	16	PC8	25	PC23	34	PC49
8	PC11	17	PC43	26	PC19	35	PC51
9	PC15	18	PC20	27	PC42		

Table 5.27: PCs selected by stepwise discriminant analysis for the femur of the three age groups from the three population samples. Stepwise PCs account for a cumulative 74.01% of total variance

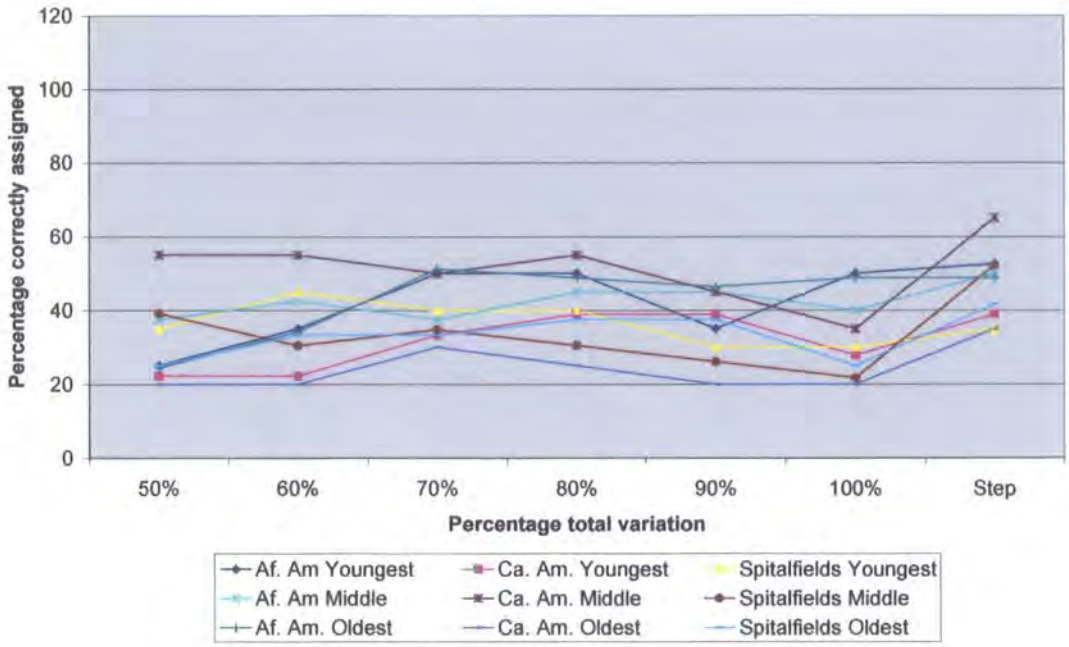

Figure 5.25: Ageing in the femur of 3 populations. Summary of separate discriminant and cross-validation analyses using PCs accounting for c. 50% of total variance (PCs 1-9), c.60% (PCs 1-13), c.70% (PCs 1-18), c.80% (PCs 1-25), c.90% (PCs 1-37) and 100% (PCs 1-71) and stepwise discriminant analysis.

The Mahalanobis' squared distances between the three age groups from the three population samples, generated by stepwise discriminant analysis are shown in Table 5.28. Four of the total 36 Mahalanobis' squared distances shown in Table 5.28 are not statistically significant; including those between all three Caucasian American groups and between the youngest and oldest Spitalfields groups.

Table 5.29 illustrates the relationship of each sample to all others on the basis of the generated Mahalanobis' squared distances by showing the distance of each primary sample to all others and ranking them accordingly from the closest sample (at position 1) to the furthest (at position 8). In every case the two closest samples in shape to the primary group are the two remaining samples from the same population. From position 3 onwards, groups are placed relatively at random with little priority given to the same age category of any population relative to the age category of the primary group.

Af. Am.	0								
Youngest	1.000								
Ca. Am.	14.00	0							
Youngest	0.0001	1.000							
Spitalfs.	18.27	14.60	0						
Youngest	0.0001	0.0001	1.000						
Af. Am.	3.23	13.06	16.45	0					
Middle	0.0061	0.0001	0.0001	1.000					
Ca. Am.	25.69	6.07	22.11	24.16	0				
Middle	0.0001	0.0599	0.0001	0.0001	1.000				
Spitalfs.	14.71	15.33	6.32	11.27	18.74	0			
Middle	0.0001	0.0001	0.0060	0.0001	0.0001	1.000			
Af. Am.	6.6	7.71	17.64	4.95	14.81	12.9	0		
Oldest	0.0001	0.0001	0.0001	0.0001	0.0001	0.0001	1.0000		
Ca. Am.	16.95	5.44	12.96	12.93	5.62	9.12	8.60	0	
Oldest	0.0001	0.1522	0.0001	0.0001	0.0680	0.0001	0.0001	1.000	
Spitalfs.	20.30	15.69	4.87	17.43	21.54	5.01	16.93	11.64	0
Oldest	0.0001	0.0001	0.0560	0.0001	0.0001	0.0009	0.0001	0.0001	1.000
	Af. Am. Youngest	Ca. Am. Youngest	Spitalfs. Youngest	Af. Am. Middle	Ca. Am. Middle	Spitalfs. Middle	Af. Am. Oldest	Ca. Am. Oldest	Spitalfs. Oldest

Table 5.28 Ageing in the femur of 3 Population. Results of canonical stepwise discriminant analysis of age groups from 3 populations. The upper value in red gives the Mahalanobis' squared distance between groups, lower value in black gives the Hotelling's t^2 *p*-value. Figures in blue indicate a statistically non-significant value.

Group	1	2	3	4	5	6	7	8
African American Youngest	AA M	AA O	CA Y	Sp M	CA O	Sp Y	Sp O	CA M
Caucasian American Youngest	CA O	CA M	AA O	AA M	AA Y	Sp Y	Sp M	Sp O
Spitalfields Youngest	Sp O	Sp M	CA O	CA Y	AA M	AA O	AA Y	CA M
African American Middle	AA Y	AA O	Sp M	CA O	CA Y	Sp Y	Sp O	CA M
Caucasian American Middle	CA O	CA Y	AA O	Sp M	Sp O	Sp Y	AA M	AA Y
Spitalfields Middle	Sp O	Sp Y	CA O	AA M	AA O	AA Y	CA Y	CA M
African American Oldest	AA M	AA Y	CA Y	CA O	Sp M	CA M	Sp O	Sp Y
Caucasian American Oldest	CA Y	CA M	AA O	Sp M	Sp O	AA M	Sp Y	AA Y
Spitalfields Oldest	Sp Y	Sp M	CA O	CA Y	AA O	AA M	AA Y	CA M

Table 5.29 Femur: The order of proximity in distance of each primary age group from other groups in the dataset on the basis of their Mahalanobis squared distances, as shown in Table 5.28. Key: Y Youngest; M Middle aged; O Oldest.

Table 5.28 also shows that whilst the average distance between the three sets of intra-population groups is 5.35, the average distance between groups across different populations is 15.76. This is confirmed by the ranking of groups in Table 5.29. This low degree of separation between groups of the same population is also reflected in Table 5.30 which, whilst showing a poor separation of groups correctly assigned at between only 35% and 65%, shows a high percentage of misplaced individuals coming from the same population.

5.5.3a(ii) Femur: Description of morphological differences between the three age groups of the three populations

The exploration of shape differences due to ageing between the three population samples by visual means is problematic. The results of Tables 5.28, 5.29 and 5.30 strongly suggest that any shape differences due to ageing within each population are of secondary influence compared to the overriding shape differences between populations.

Figure 5.26 shows the bivariate plots of PC1 with PC2 (the first two stepwise PCs), accounting for a cumulative 16.30% of total variance. It is evident from this figure that the overlap between specimens of the three age groups from the three populations is too extensive to assess any degree of separation between the samples and to establish any relationships between groups within or between populations. This overlap of specimens applies equally to all higher PCs. Therefore, the sample means of the three age groups have been used to help distinguish shape variation due to ageing in the three populations.

For the femur, the correlation between the Procrustes distances using the population means shown in Table 5.31 and the Mahalanobis' distances shown in Table 5.28 does not reach a level of statistical significance ($r= 0.12$, $p= 0.49$). This lack of a statistically significant correlation in results using the two methods should be borne in mind when comparing results from the two methods. The Procrustes mean co-ordinates have been calculated from the separate GPAs and have been subjected to a joint GPA and PCA. The proportion and accumulated variance of the PCs generated in the analysis of group means is given in Table 5.32.

Number of Observations and Percent Classified into Group using 100% PCs										
From Group	Af. Am. Youngest	Ca. Am. Youngest	Spitalfield Youngest	Af. Am. Middle	Ca. Am. Middle	Spitalfield Middle	Af. Am. Oldest	Ca. Am. Oldest	Spitalfield Oldest	Total
Af. Amer. Youngest	21	0	0	15	0	1	2	1	0	40
	52.5	0	0	37.5	0	2.5	5	2.5	0	100
Ca. Amer. Youngest	1	7	1	0	3	0	1	5	0	18
	5.56	38.89	5.56	0	16.67	0	5.56	27.78	0	100
Spitalfields Youngest	0	0	7	0	0	3	1	1	8	20
	0	0	35	0	0	15	5	5	40	100
Af. Amer. Middle	9	0	0	20	0	1	8	2	0	40
	22.5	0	0	50	0	2.5	20	5	0	100
Ca. Amer. Middle	0	4	0	0	13	0	0	3	0	20
	0	20	0	0	65	0	0	15	0	100
Spitalfields Middle	1	0	3	1	0	12	0	1	5	23
	4.35	0	13.04	4.35	0	52.17	0	4.35	21.74	100
Af. Amer. Oldest	3	5	2	7	0	1	20	0	3	41
	7.32	12.2	4.88	17.07	0	2.44	48.78	0	7.32	100
Ca. Amer. Oldest	0	4	0	0	5	1	1	7	2	20
	0	20	0	0	25	5	5	35	10	100
Spitalfields Oldest	1	1	5	0	1	6	0	0	10	24
	4.17	4.17	20.83	0	4.17	25	0	0	41.67	100
Total	36	21	18	43	22	25	33	20	28	246
	14.63	8.54	7.32	17.48	8.94	10.16	13.41	8.13	11.38	100

Table 5.30: Ageing in the femur of 3 populations. Results of cross-validation analysis of age groups from 3 populations using PCs selected by stepwise discriminant analysis. Upper figure denotes the number of individuals; lower figure denotes percentage. Red figures denote number of individuals placed into their correct groups.

Figure 5.26:

Ageing in the femur of African Americans, Caucasian Americans and Spitalfields (total sample). Bivariate plot, showing the overlap of specimens of the total sample of 3 age groups on PC1 and PC2 (first and second PCs selected by stepwise discriminant analysis).

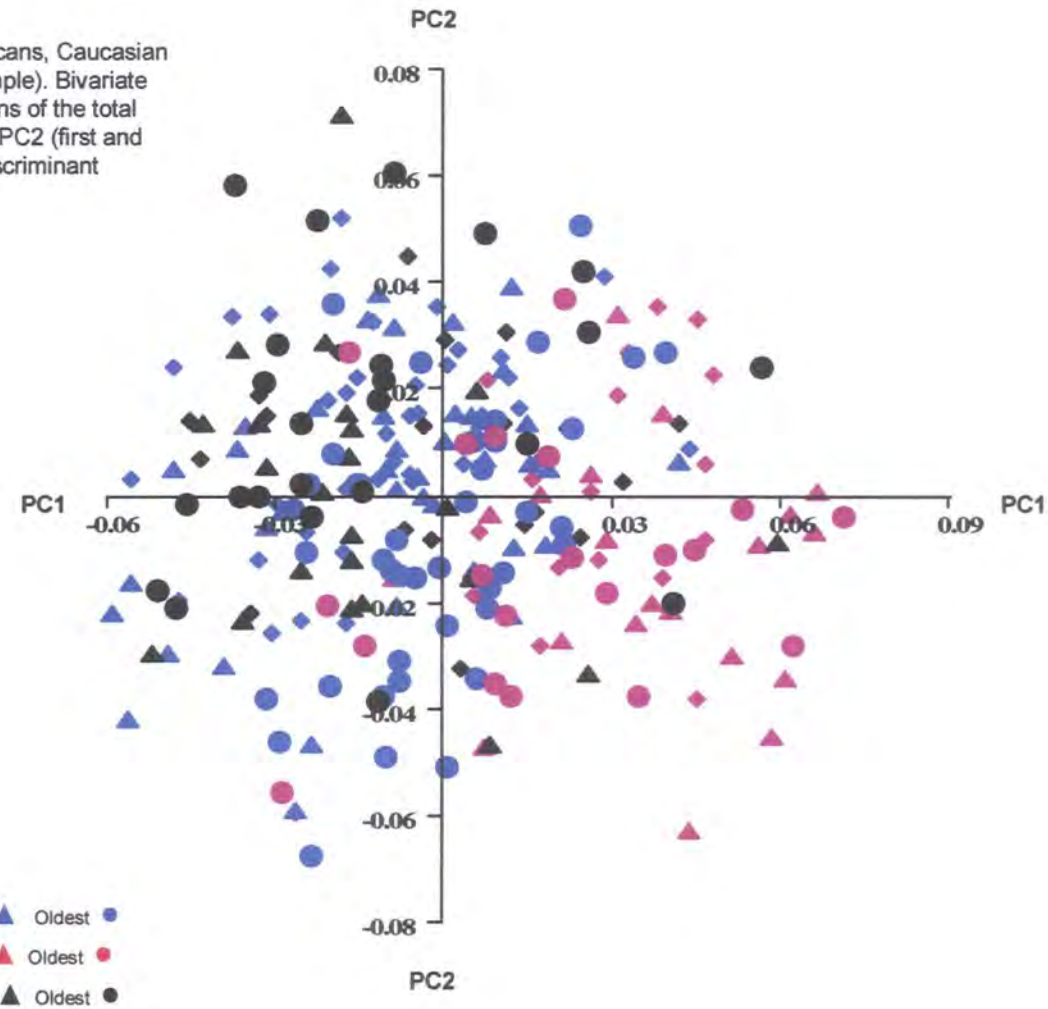

Af. Ams. Youngest	0								
Ca. Ams. Youngest	10.61	0							
Spitalfields Youngest	11.86	18.18	0						
Af. Ams. Middle	13.87	11.02	16.56	0					
Ca. Ams. Middle	21.68	16.63	22.82	20.33	0				
Spitalfields Middle	25.25	30.25	16.38	28.90	25.53	0			
Af. Ams. Oldest	18.80	12.79	21.70	14.94	7.68	27.61	0		
Ca. Ams. Oldest	10.88	6.00	19.79	12.10	21.79	33.33	17.57	0	
Spitalfields Oldest	106.47	102.11	114.96	106.60	107.11	122.65	104.35	100.38	0
	Af. Ams. Youngest	Ca. Ams. Youngest	Spitalfields Youngest	Af. Ams. Middle	Ca. Ams. Middle	Spitalfields Middle	Af. Ams. Oldest	Ca. Ams. Oldest	Spitalfields Oldest

Table 5.31: Ageing in the femur of 3 age groups of 3 populations. Procrustes distances between sample means of 3 age groups from 3 populations. Correlation between Procrustes distances and Mahalanobis' distances generated by stepwise discriminant analysis (Table 5.28) is not significant at: $r = 0.12$; $p = 0.49$

PCs	Proportion	Cumulative	PCs	Proportion	Cumulative
PC1	48.7	48.7	PC6	4.09	95.2
PC2	19.1	67.8	PC7	3.11	98.3
PC3	9.19	77.0	PC8	1.71	100
PC4	8.62	85.6			
PC5	5.47	91.1			

Table 5.32: Proportion and accumulative variance represented by PCs 1-8 which accounts for total sample variance for age group means for the femur.

The first four PCs account for over 85% of total variation in the sample and the exploration of shape differences between age groups will concentrate on these four PCs.

Figure 5.27, the bivariate plot of PC1 against PC2 when using sample means, clearly shows that the nine means cluster by population. Variation explained by PC1, which accounts for nearly 50% of total variance, is primarily concentrated in those shape differences between the three populations and shows no distinct pattern of relationships within each of the three age-group sets.

Like PC1, PC2 also highlights the separation of the three populations. PC2 explains variation in the position of the condyles, such that in means at the negative extreme (the three African American means), the condyles are more inward-facing towards the mid-line of the joint, resulting in a smaller intercondylar fossa relative to those at the positive extreme. In the mean configuration where the condyles are more inward-facing, the mediolateral width is noticeably wider relative to those at the opposite extreme; particularly across the anterior edge of the patella surface (landmarks 18, 20 and 21). This difference can be best appreciated in Figure 5.28 (a) and (b) in the relative positions of landmarks 18, 20 and 21, landmarks 5 and 9 across the intercondylar fossa and in the relative positions of landmarks 17 and 23, the maximum extent of the lateral and medial condyles respectively. Differences can also be seen in the lateral views in Figure 5.28 (c) and (d), in the relative positions of landmarks 17, 23 and in landmark 19, the maximum extent of the lateral epicondyle.

Figure 5.27:

Ageing in the femur of African Americans, Caucasian Americans & Spitalfields. Bivariate plot of PC1 with PC2, showing the separation of sample means of 3 age groups of 3 populations. Images represent the mean configuration if warped to the extremes of PC1 (at 0.04 and -0.04).

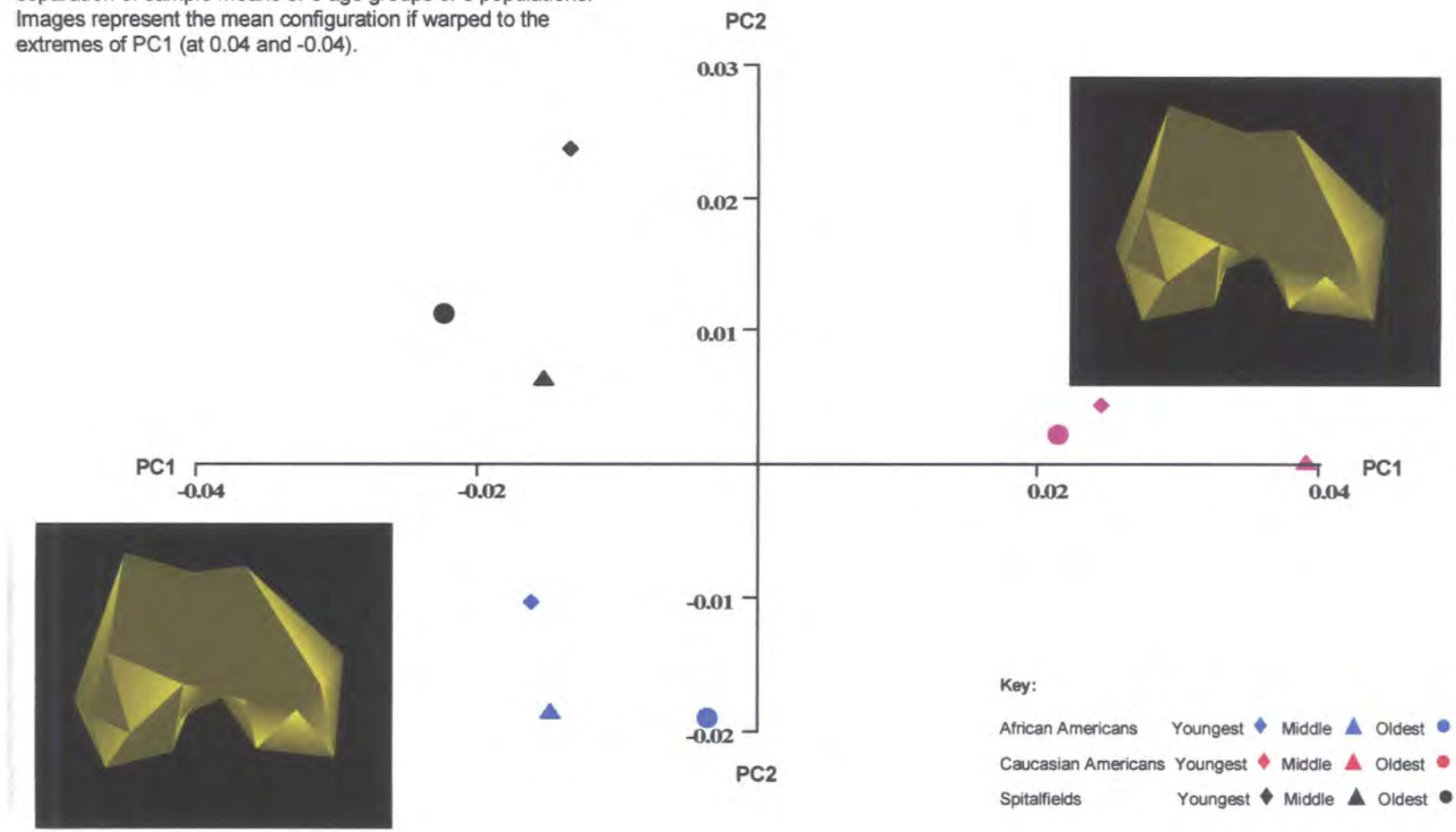

Figure 5.28:

Ageing in African Americans, Caucasian Americans & Spitalfields. Separation of sample means of 3 age groups of 3populations. Images represent the mean configuration at the extremes of PC2 (at 0.03 and -0.02). Images (b) and (d) include landmarks discussed in the text (section 5.5.3a(ii)).

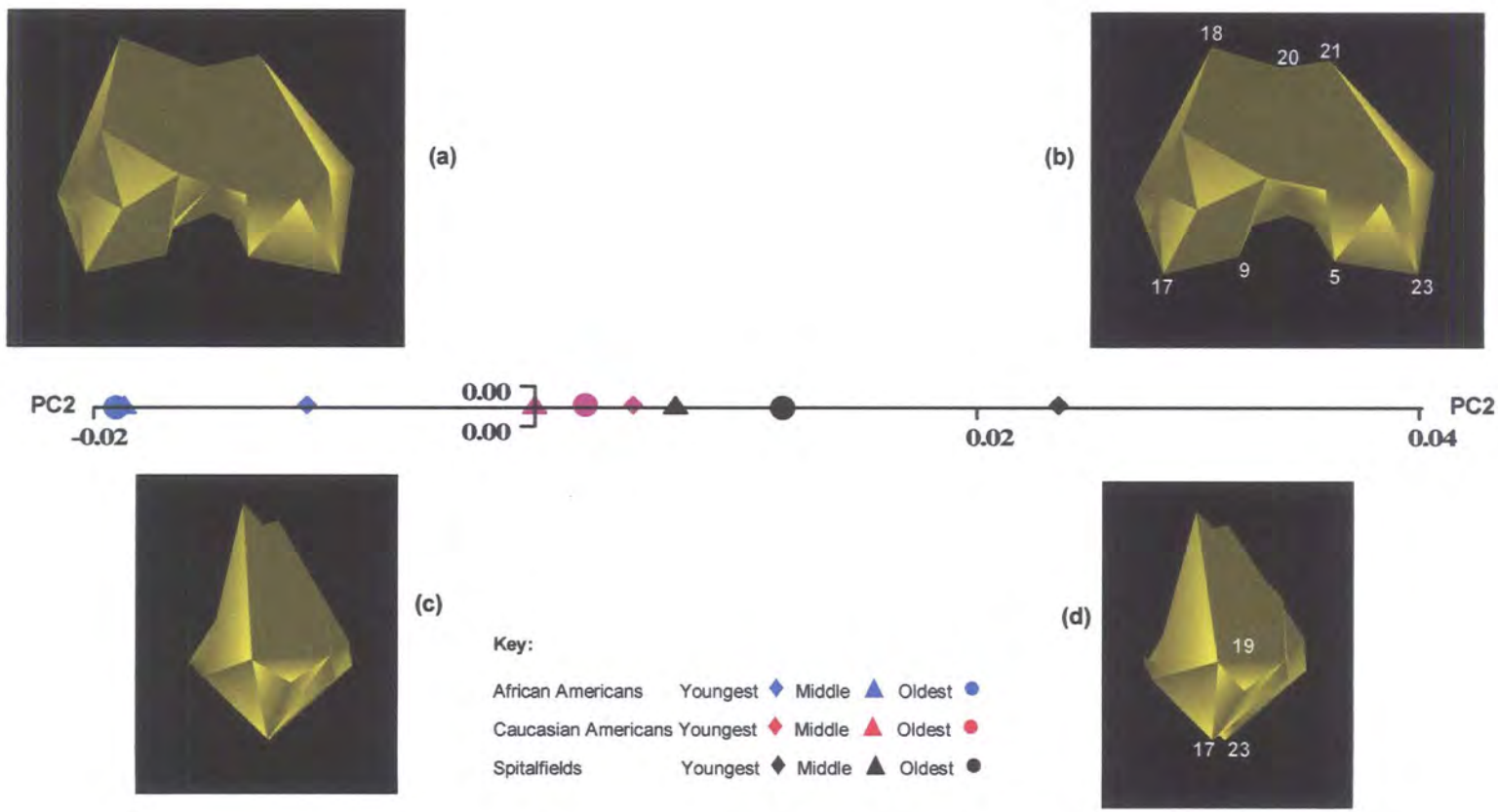

PC2 shows the youngest age group of each population sample is positioned on the positive side of the middle and oldest means, implying that the condyles turn relatively more inward-facing with age. This change during ageing was noted in the separate analysis using the African American sample (section 5.5.1a(ii) above). The degree of this change throughout adulthood appears to be greatest in the Spitalfields population.

Figure 5.29 shows the bivariate plot of PC3 with PC4. Figure 5.30, which specifically highlights PC3, explains variation in the orientation of the joint mediolaterally, such that means at the positive extreme represent a joint that is positioned in a more lateral orientation relative to the shaft, relative to those at the negative extreme. In each of the three population age sets, the youngest mean is positioned on the positive side of the oldest, indicating that the joint is more laterally oriented in younger rather than older individuals. Although sample means are well separated along PC3 in all three population age sets, the overall scale of difference is small.

Visible differences explained by PC4 appear too slight to be easily appreciated when the mean configuration is warped along the scale. Although differences between means are primarily related to the maximum height of the condyles, seen in Figure 5.29 in the relative positions of landmarks 25 and 26 on PC4, there is no clear pattern of relationships between the sample means of the three age group sets.

The deformation of the TPS in the mean configuration in on PC2 in Figure 5.31 shows that the maximum differences between age groups lies across the condyles. Although the degree of deformation would be greater for PC1, this would primarily indicate the overriding differences between population samples rather than those between the three age groups within each population sample. For PC2, the degree of TPS deformation is extremely subtle, confirming the low level of separation between age groups within each population sample.

Figure 5.29:

Ageing in the femur of African Americans, Caucasian Americans & Spitalfields. Bivariate plot of PC3 and PC4, showing the separation of sample means of 3 age groups of 3 populations. Images (a) and (b) represent the mean configuration if warped to the extremes of PC4 (at 0.01 and -0.03). Image at the negative extreme includes landmarks discussed in the text (section 5.5.3a(ii)).

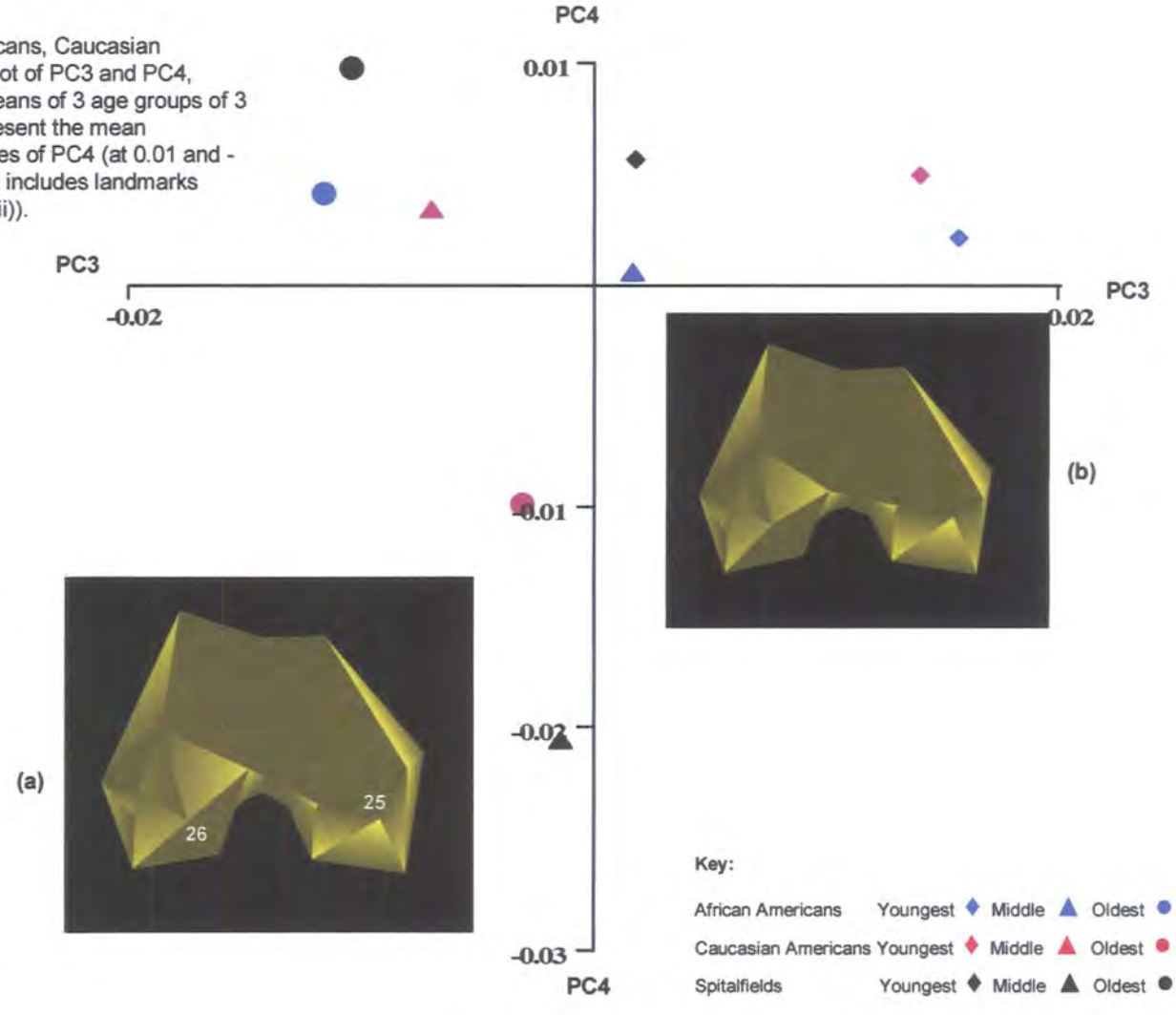

Figure 5.30:

Ageing in the femur of African Americans, Caucasian Americans & Spitalfields. Separation of sample means of 3 age groups of 3 populations on PC3. Images represent the mean configuration if warped to the extremes of PC3 (at 0.02 and -0.02). Image at the positive extreme includes landmarks discussed in the text (section 5.5.3a(ii)).

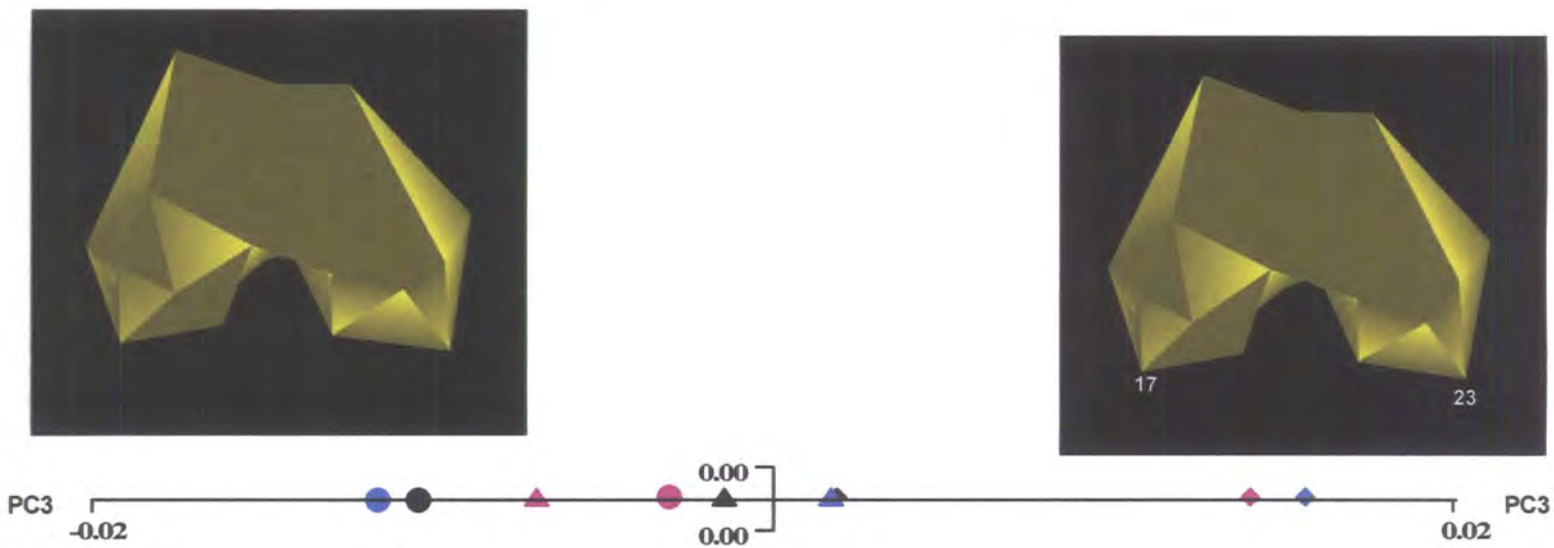

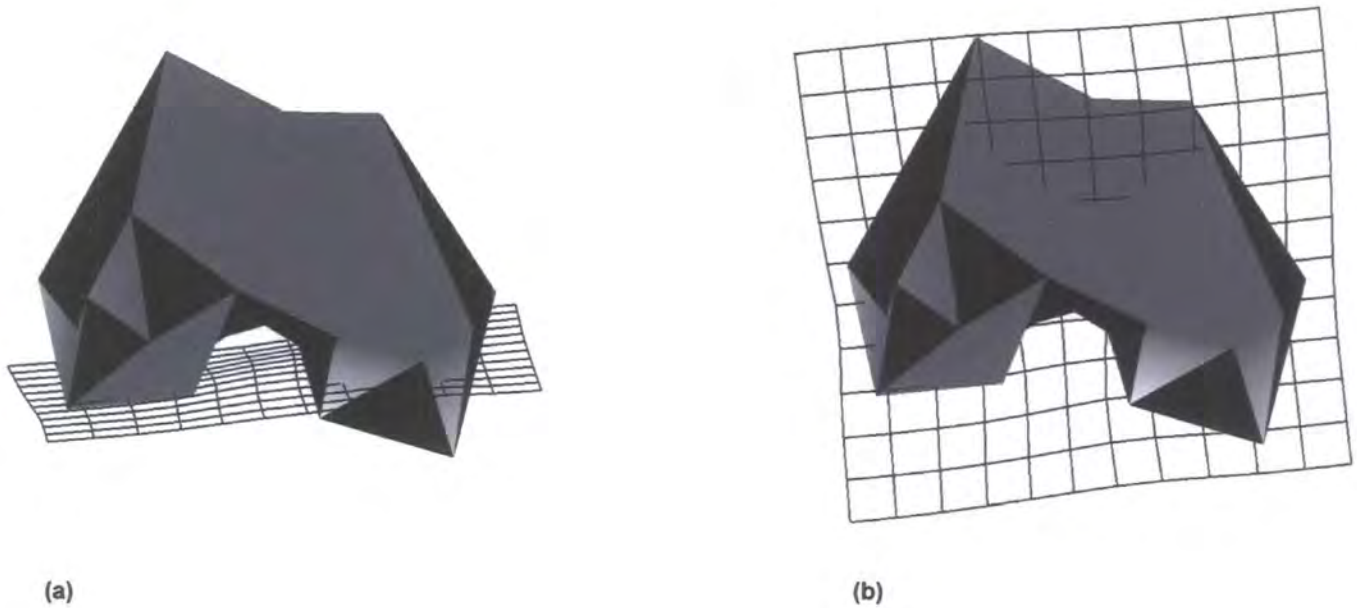

Fig 5.31: Ageing in the femur of African Americans, Caucasian Americans and Spitalfields. Representations of femoral shape with TPS taken from PC2 using sample means, showing region of bone giving maximum difference in shape between means. (a) TPS view in anteroposterior plane; (b) in distal plane. Images are presented to give the best indication of maximum difference in shape and are not necessarily taken from the same perspective as the mean configurations in Figure 5.28.

5.5.3b(i) Tibia

Differences in shape between the 246 specimens from the African and Caucasian American and Spitalfields samples divided into three age groups are analysed using the Procrustes fitted co-ordinates and by subjecting the data to PCA. Table 5.33 gives the proportional and accumulated variance for PCs 1 to 56, which represents the total variance within the sample.

PCs	Prop.	Cumul.	PCs	Prop.	Cumul.	PCs	Prop.	Cumul.
PC1	24.00	24.00	**PC21**	1.18	82.90	**PC41**	0.37	96.70
PC2	9.07	33.10	**PC22**	1.16	84.10	**PC42**	0.36	97.10
PC3	6.19	39.30	**PC23**	1.04	85.10	**PC43**	0.35	97.40
PC4	4.77	44.10	**PC24**	1.02	86.10	**PC44**	0.32	97.70
PC5	4.12	48.20	**PC25**	0.95	87.10	**PC45**	0.28	98.00
PC6	4.02	52.20	**PC26**	0.88	88.00	**PC46**	0.26	98.30
PC7	3.37	55.60	**PC27**	0.86	88.80	**PC47**	0.24	98.50
PC8	3.06	58.60	**PC28**	0.80	89.60	**PC48**	0.23	98.70
PC9	2.81	61.40	**PC29**	0.77	90.40	**PC49**	0.21	99.00
PC10	2.58	64.00	**PC30**	0.72	91.10	**PC50**	0.20	99.10
PC11	2.44	66.50	**PC31**	0.69	91.80	**PC51**	0.19	99.30
PC12	2.22	68.70	**PC32**	0.63	92.40	**PC52**	0.18	99.50
PC13	2.09	70.80	**PC33**	0.58	93.00	**PC53**	0.15	99.70
PC14	1.84	72.60	**PC34**	0.55	93.60	**PC54**	0.12	99.80
PC15	1.78	74.40	**PC35**	0.51	94.10	**PC55**	0.11	99.90
PC16	1.66	76.10	**PC36**	0.50	94.60	**PC56**	0.10	100.00
PC17	1.58	77.60	**PC37**	0.47	95.00			
PC18	1.49	79.10	**PC38**	0.45	95.50			
PC19	1.32	80.50	**PC39**	0.43	95.90			
PC20	1.28	81.70	**PC40**	0.41	96.30			

Table 5.33: Ageing in the tibia of 3 populations. The proportional and accumulated variance for PCs 1-56 accounting for 100% of total variance in 3 age groups from 3 populations.

A canonical stepwise discriminant function analysis is used to determine which PCs relate more specifically to differences between age groups. PCs selected by stepwise canonical discriminant analysis are shown in Table 5.34. The results using PCs accounting for c.50% to 100% of total variance and those used in the stepwise discriminant function analyses are summarised in Figure 5.32.

Order	Entered	Order	Entered	Order	Entered	Order	Entered
1	PC1	8	PC9	15	PC16	22	PC11
2	PC3	9	PC5	16	PC31	23	PC43
3	PC8	10	PC44	17	PC13	24	PC39
4	PC15	11	PC38	18	PC49	25	PC26
5	PC32	12	PC7	19	PC23	26	PC20
6	PC14	13	PC44	20	PC10	27	PC25
7	PC23	14	PC34	21	PC21	28	PC18

Table 5.34: PCs selected by stepwise discriminant analysis for the three age groups from the three population samples for the tibia. Stepwise PCs account for a cumulative 67.75% of total variance.

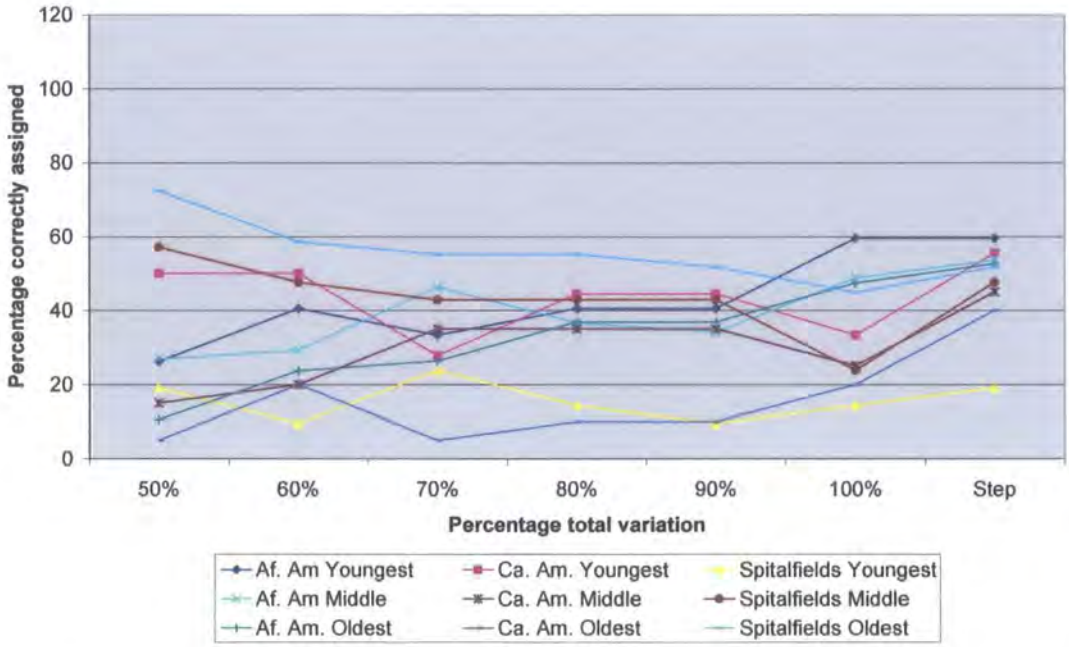

Figure 5.32 Ageing in the tibia of 3 populations. Summary of separate discriminant and cross-validation analyses using PCs accounting for c.50% of total variance (PCs 1-5), c.60% (PCs 1-8), c.70% (PCs 1-13), c.80% (PCs 1-19), c.90% (PCs 1-29) and 100% (PCs 1-56) and stepwise discriminant analysis.

The Mahalanobis' squared distances between the three age groups from the three populations, generated by stepwise discriminant analysis, are shown in Table 5.35. Four of the total 36 distances between groups are not statistically significant including those between the youngest and oldest and middle aged and oldest Caucasian Americans and the middle aged and oldest of the Spitalfields samples. Table 5.36 illustrates the relationship of each sample to all others on the basis of the generated Mahalanobis' squared distances by showing the distance of each primary sample to all others and ranking them accordingly from the closest sample

Af. Am.	0								
Youngest	1.000								
Ca. Am.	5.55	0							
Youngest	0.0001	1.000							
Spitalfs.	9.60	6.99	0						
Youngest	0.0001	0.0001	1.000						
Af. Am.	2.28	6.82	11.48	0					
Middle	0.0022	0.0001	0.0001	1.000					
Ca. Am.	7.01	2.55	8.42	7.22	0				
Middle	0.0001	0.2774	0.0001	0.0001	1.000				
Spitalfs.	10.88	11.95	3.52	12.65	14.28	0			
Middle	0.0001	0.0001	0.0242	0.0001	0.0001	1.000			
Af. Am.	2.88	3.72	8.38	2.57	3.47	12.2	0		
Oldest	0.0002	0.0033	0.0001	0.0009	0.0033	0.0001	1.0000		
Ca. Am.	6.21	1.82	7.66	6.45	1.33	13.74	3.48	0	
Oldest	0.0001	0.6583	0.0001	0.0001	0.8683	0.0001	0.0032	1.000	
Spitalfs.	12.15	12.71	3.12	15.37	14.52	2.37	12.82	14.06	0
Oldest	0.0001	0.0001	0.0191	0.0001	0.0001	0.1268	0.0001	0.0001	1.000
	Af. Am. Youngest	Ca. Am. Youngest	Spitalfs. Youngest	Af. Am. Middle	Ca. Am. Middle	Spitalfs. Middle	Af. Am. Oldest	Ca. Am. Oldest	Spitalfs. Oldest

Table 5.35: Ageing in the tibia of 3 populations. Results of canonical stepwise discriminant analysis of age groups from 3 populations. The upper value in red gives the Mahalanobis' squared distance between groups, lower value in black gives the Hotelling's t^2 *p*-value. Figures in blue indicate a statistically non-significant value.

Group	1	2	3	4	5	6	7	8
African American Youngest	AA M	AA O	CA O	CA Y	CA M	Sp Y	Sp M	Sp O
Caucasian American Youngest	CA O	CA M	AA Y	AA O	AA M	Sp Y	Sp O	Sp M
Spitalfields Youngest	Sp O	Sp M	CA M	CA O	AA O	CA Y	AA Y	AA M
African American Middle	AA Y	AA O	CA O	CA M	CA Y	Sp Y	Sp M	Sp O
Caucasian American Middle	CA O	CA Y	AA O	AA M	Sp Y	AA Y	Sp M	Sp O
Spitalfields Middle	Sp O	Sp Y	CA M	AA Y	CA O	AA O	AA M	CA Y
African American Oldest	AA M	AA Y	CA M	CA O	CA Y	Sp Y	Sp M	Sp O
Caucasian American Oldest	CA M	CA Y	AA O	AA M	AA Y	Sp Y	Sp O	Sp M
Spitalfields Oldest	Sp M	Sp Y	CA M	CA O	CA Y	AA Y	AA O	AA M

Table 5.36: Ageing in the tibia of 3 populations. The order of proximity in distance of each primary age group from other groups in the dataset on the basis of their Mahalanobis squared distances, as shown in Table 5.35. Key: Y Youngest; M Middle aged; O Oldest.

(at position 1) to the furthest (at position 8). As with the femur, in every case the two closest samples in shape to the primary group are the two remaining samples from the same population. From position 3 onwards, groups are placed relatively at random with little priority given to the same age category of any population relative to the age of the primary group.

Table 5.35 shows that whilst the average distance between the three sets of intra-population groups is 4.38, the average distance between groups across different populations is 13.77. Again, this reinforces the ranked positions of groups seen in Table 5.37. Like the femur, the low degree of separation between groups of the same population is also reflected in Table 5.37 which shows a poor separation of groups correctly assigned (19.05% and 59.52%). Although a high percentage of misplaced individuals come from the same population, many others are seemingly placed at random.

5.5.3b(ii) Tibia: Description of morphological differences between the three age groups of the three populations

As with the femur, the exploration of shape differences due to ageing between the tibial samples of the three populations by visual means is problematic as the results of Tables 5.35, 5.36 and 5.38 strongly suggest that any shape differences due to ageing within each population are of secondary influence compared to the overriding shape differences between populations.

Figure 5.33 shows the bivariate plot of PC1 with PC3, which accounts for 30.19% of total variance. The overlap between specimens of the three age groups is too extensive to assess any degree of separation between the aged samples. It is also apparent from PC1 (alone accounting for 24% of total variance), however, that the principal shape variation in the total sample is between the majority of Spitalfields individuals, including specimens from all three age groups, and the remaining two populations. This obvious differentiation between one population and the other two is not repeated for subsequent PCs. It is too difficult to assess any separation within the total sample for PCs higher than PC1, particularly between different age groups.

Number of Observations and Percent Classified into Group using 100% PCs										
From Group	Af. Am. Youngest	Ca. Am. Youngest	Spitalfield Youngest	Af. Am. Middle	Ca. Am. Middle	Spitalfield Middle	Af. Am. Oldest	Ca. Am. Oldest	Spitalfield Oldest	Total
Af. Amer. Youngest	25	2	0	8	0	1	4	2	0	42
	59.52	4.76	0	19.05	0	2.38	9.52	4.76	0	100
Ca. Amer. Youngest	1	10	0	1	2	0	2	2	0	18
	5.56	55.56	0	5.56	11.11	0	11.11	11.11	0	100
Spitalfields Youngest	0	1	4	0	4	5	0	2	5	21
	0	4.76	19.05	0	19.05	23.81	0	9.52	23.81	100
Af. Amer. Middle	8	4	0	22	1	0	5	1	0	41
	19.51	9.76	0	53.66	2.44	0	12.2	2.44	0	100
Ca. Amer. Middle	0	3	0	2	9	0	1	5	0	20
	0	15	0	10	45	0	5	25	0	100
Spitalfields Middle	0	0	1	0	1	10	2	1	6	21
	0	0	4.76	0	4.76	47.62	9.52	4.76	28.57	100
Af. Amer. Oldest	6	2	0	6	4	0	20	0	0	38
	15.79	5.26	0	15.79	10.53	0	52.63	0	0	100
Ca. Amer. Oldest	2	3	0	1	6	0	0	8	0	20
	10	15	0	5	30	0	0	40	0	100
Spitalfields Oldest	0	1	3	0	2	7	1	0	15	29
	0	3.45	10.34	0	6.9	24.14	3.45	0	51.72	100
Total	42	26	8	40	29	23	35	21	26	250
	16.8	10.4	3.2	16	11.6	9.2	14	8.4	10.4	100

Table 5.37: Ageing in the tibia of 3 populations. Results of cross-validation analysis of age groups from 3 populations using PCs selected by stepwise discriminant analysis. Upper figure denotes the number of individuals; lower figure denotes percentage. Red figures denote number of individuals placed into their correct groups.

Figure 5.33:

Ageing in the tibia of African Americans, Caucasian Americans & Spitalfields. Bivariate plot of PC1 with PC3 showing the overlap of individuals using the total sample of 3 age groups of 3 populations. PC1 shows the separation of the majority of the Spitalfields collection, including specimens of all 3 age groups, from the other population datasets.

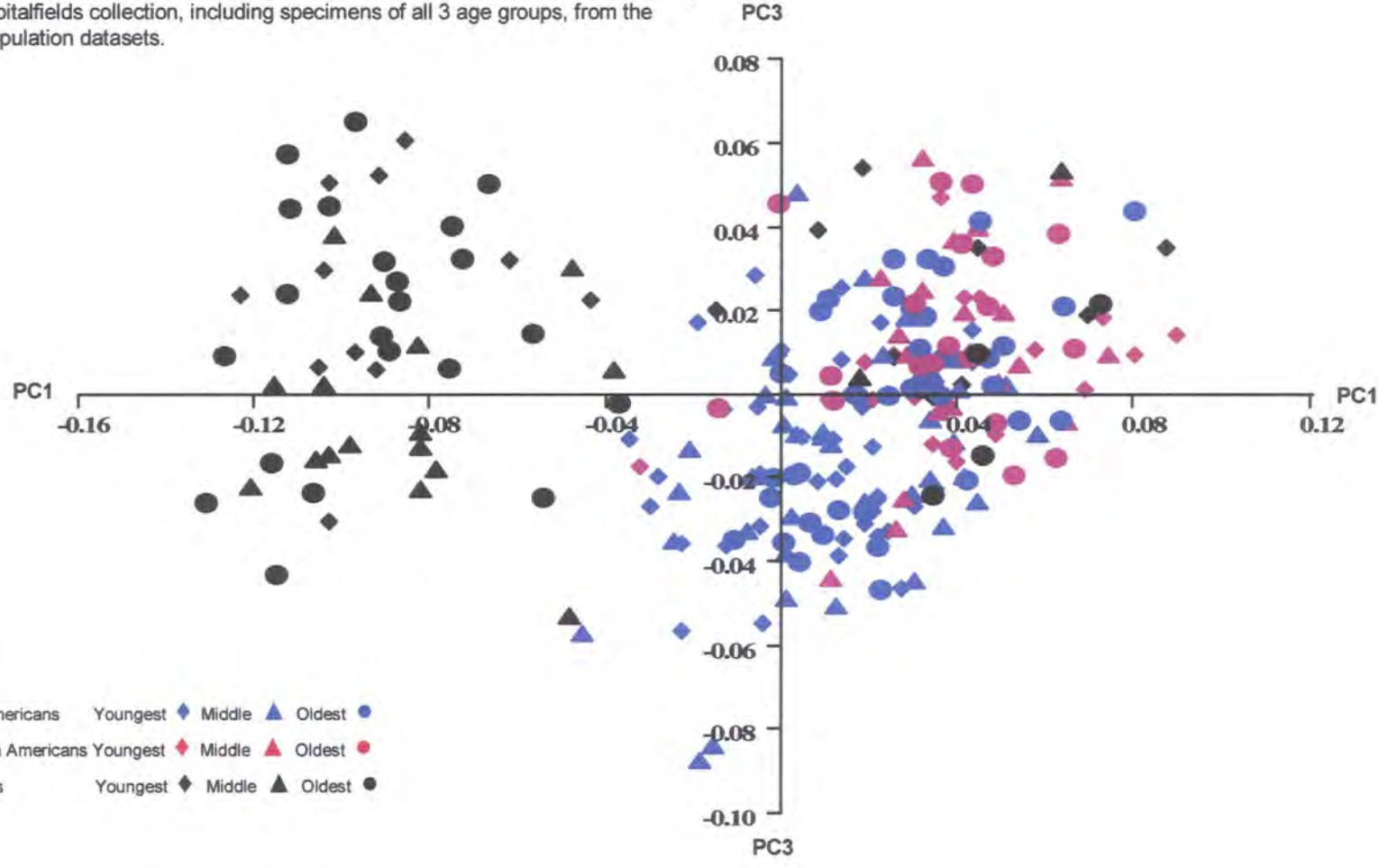

Because the overlap of specimens is seen on all PCs when using the total sample, the sample means of the three age groups for the three populations have been used to help distinguish shape variation due to ageing.

For the tibia, the correlation between the Procrustes distances using the population means shown in Table 5.38 and the Mahalanobis' squared distances shown in Table 5.35 does not reach a level of statistical significance ($r= 0.22$; $p= 0.19$). Despite this non-significant result, however, PC1 in Figure 5.33 (using the total sample) and PC1 in Figure 5.34 (see below using the sample means) both show the same separation of the Spitalfields groups from samples of the other two populations.

The Procrustes mean co-ordinates have been calculated from the separate GPAs and have been subjected to a joint GPA and PCA. The proportion and accumulated variance of the PCs generated in the analysis of age group means is given in Table 5.39.

PCs	Proportion	Cumulative	PCs	Proportion	Cumulative
PC1	78.1	78.1	PC6	1.59	98.0
PC2	10.1	88.3	PC7	1.03	99.1
PC3	3.39	91.6	PC8	0.93	100
PC4	2.78	94.4			
PC5	2.02	96.4			

Table 5.39: Proportion and accumulative variance represented by PCs 1-8 which accounts for total sample variance for age group means for the tibia.

The first four PCs account for nearly 95% of total variance in the sample and the exploration of shape differences between sides will concentrate on these four PCs.

Figure 5.34, the bivariate plot of PC1 against PC2 (using the sample means), clearly shows that the nine means cluster into three distinct populations groups. Shape variation explained by PC1, which accounts for nearly 80% of total variance, is primarily concentrated in shape differences between the three populations and shows no similarity in the pattern of relationships between the three age-group sets.

Af. Ams. Youngest	0								
Ca. Ams. Youngest	22.06	0							
Spitalfields Youngest	18.78	23.93	0						
Af. Ams. Middle	18.75	20.73	18.93	0					
Ca. Ams. Middle	17.38	10.94	17.61	22.05	0				
Spitalfields Middle	17.38	25.43	6.47	17.99	20.00	0			
Af. Ams. Oldest	43.76	46.72	57.67	57.40	45.62	57.20	0		
Ca. Ams. Oldest	17.58	10.41	14.77	16.03	7.68	17.25	51.05	0	
Spitalfields Oldest	108.25	95.41	106.56	110.01	97.33	107.75	95.94	100.37	0
	Af. Ams. Youngest	Ca. Ams. Youngest	Spitalfields Youngest	Af. Ams. Middle	Ca. Ams. Middle	Spitalfields Middle	Af. Ams. Oldest	Ca. Ams. Oldest	Spitalfields Oldest

Table 5.38: Ageing in the tibia of 3 age groups of 3 populations. Procrustes distances between sample means of 3 age groups from 3 populations. Correlation between Procrustes distances and Mahalanobis' distances generated by stepwise discriminant analysis (Table 5.36) is not significant at: $r = 0.22$; $p = 0.19$.

Figure 5.34:

Ageing in the tibia of African Americans, Caucasian Americans & Spitalfields. Bivariate plot of PC1 with PC2 showing the separation of sample means of 3 age groups of 3 populations. Images represent the mean configuration if warped to the extremes of PC1 (a) and (b) (at 0.06 and -0.09) and PC2 (c) and (d) (at 0.02 and -0.03) . Image (d) includes landmarks discussed in the text (section 5.5.3b(ii))

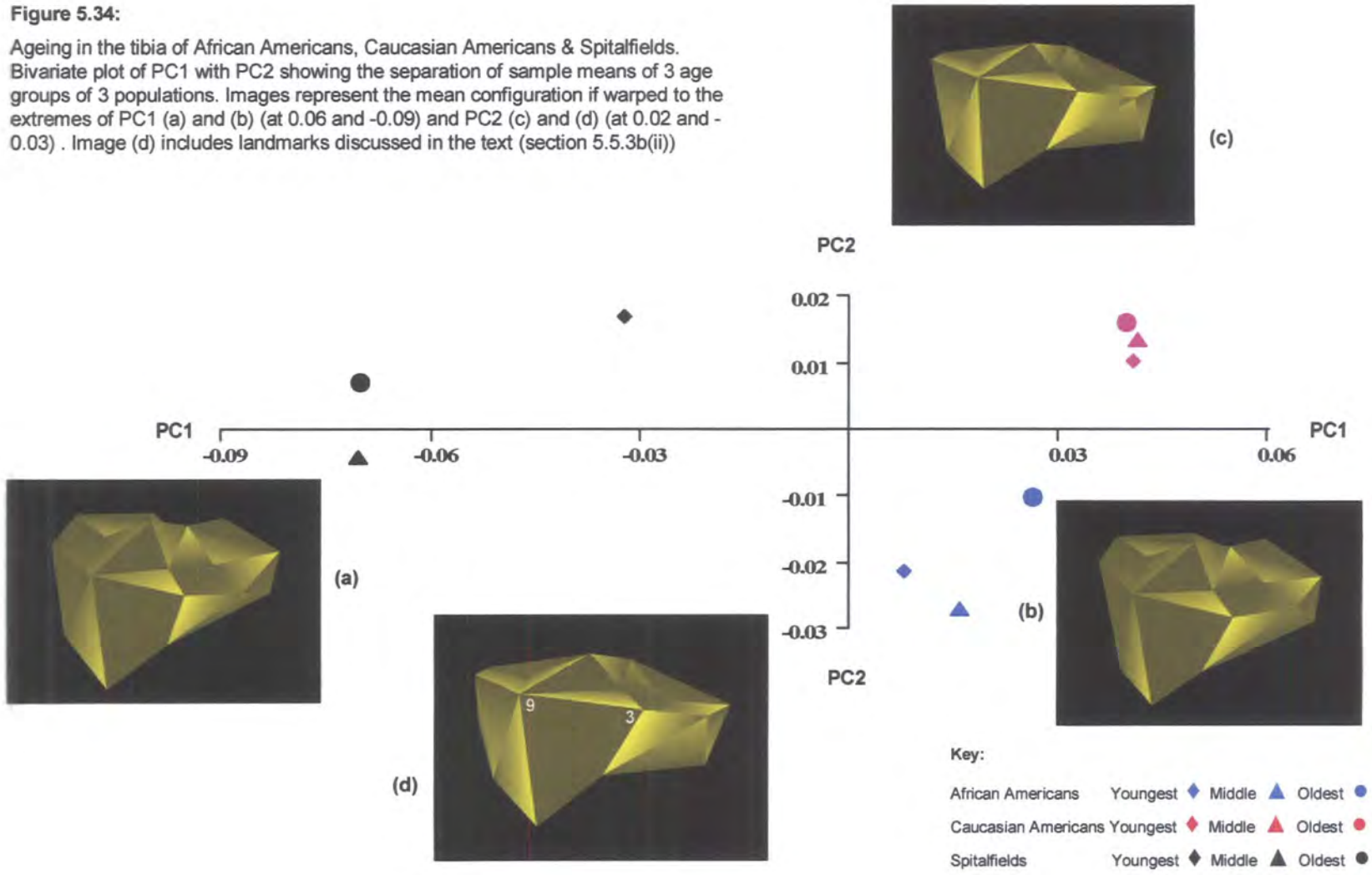

PCs 2, 3 and 4 in Figures 5.34 and 5.35 explain small degrees of variation relating to the proportions of the tibial plateau and shelf and of the tibial tuberosity. PC2 explains a greater degree of lateral orientation (also noted in relation to differences between age groups in the distal femur; section 5.5.3a(ii) above), together with greater mediolateral width across the anterior edge of the tibial plateau in means at the negative extreme relative to those at the positive extreme (between landmarks 3 and 9). PC3 explains greater depth of the tibial shelf in means at the positive extreme relative to those at the negative extreme (landmarks 9 to 15) and PC4 explains a greater degree of lateral orientation of the tibial tuberosity in means at the positive extreme relative to those at the negative extreme (noted in the different positions of landmarks 3 and 9 relative to 14). For PCs 2, 3 and 4, however, there is no obvious similarity in the pattern of relationships of the three aged groups of the three populations; with little to indicate that the patterns seen between groups are anything other than a random arrangement.

The deformation of the TPS in Figure 5.36 on PC2, shows that the maximum differences between age groups lies across the tibial plateau and anterior region. For the tibia (and to an even greater extent than for the femur), the degree of deformation on the TPS would be greater for PC1 than for PC2. However variation on PC1 primarily relates to the overriding differences between populations rather than variation relating to differences between age groups of the same population. For PC2, the degree of TPS deformation is extremely subtle and difficult to appreciate. Despite the statistically significant distances in 32 of the 36 distances between groups (Table 5.36), the subtlety of this deformation on PC2 confirms the low level of separation between age groups within each population sample.

5.6 Discussion

Arking (1998) states that ageing is a highly complex process that proceeds at different rates at both the population and individual level. In addition, not only do individuals age at different rates within populations, but also the organs and tissues within the same body age at different rates. It is also a universal phenomenon of human biology that bone loses mass with age and occurs regardless of gender, race, occupation, habitual physical activity, dietary habits, economic development

Figure 5.35:

Ageing in the tibia of African Americans, Caucasian Americans & Spitalfields. Bivariate plot of PC3 with PC4 showing the separation of sample means of 3 age groups of 3 populations. Images represent the mean configuration if warped to the extremes of PC1 (a) and (b) (at 0.02 and -0.02) and PC2 (c) and (d) (at 0.02 and -0.02) . Images (b) and (d) include landmarks discussed in the text (section 5.5.3b(ii)).

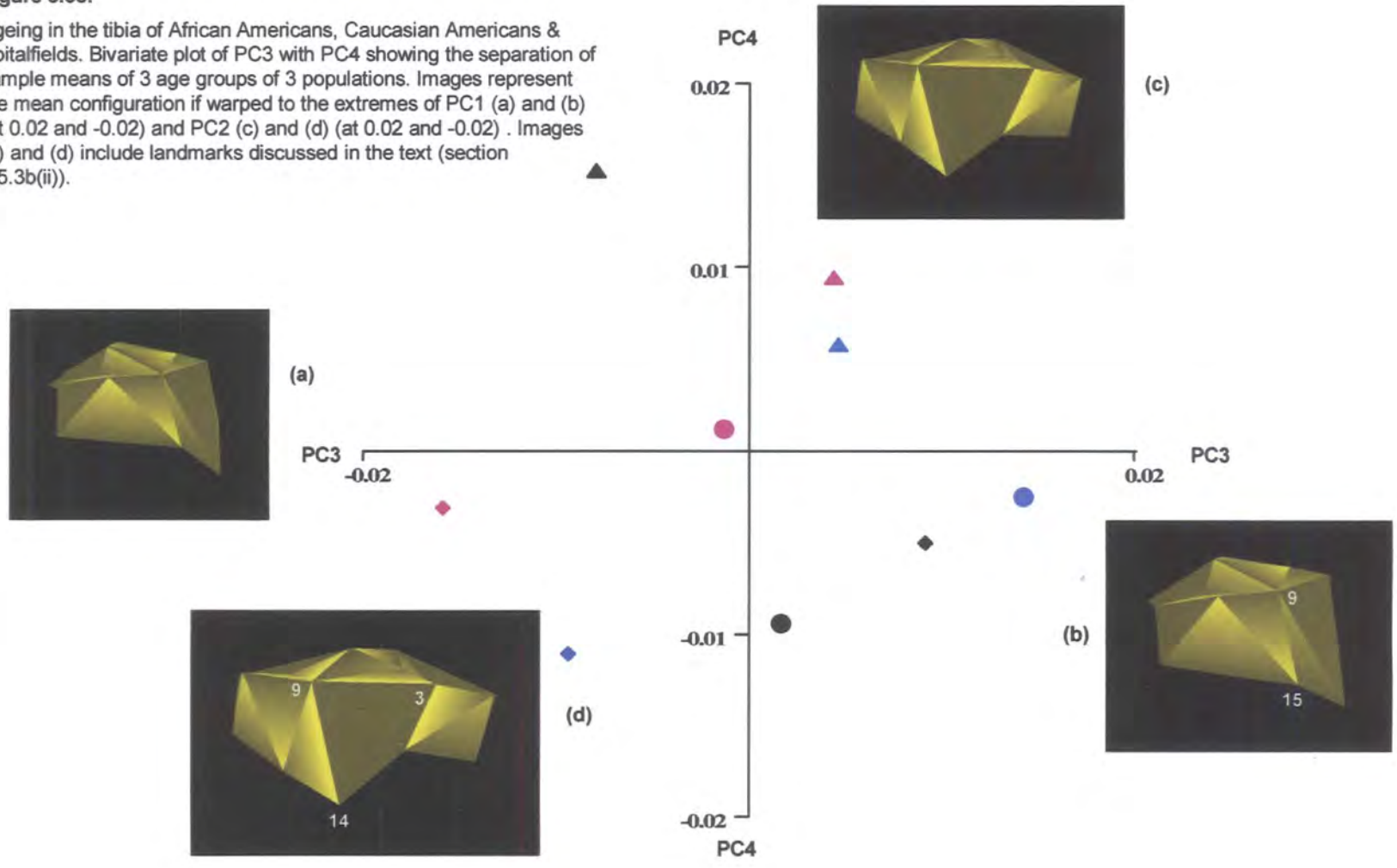

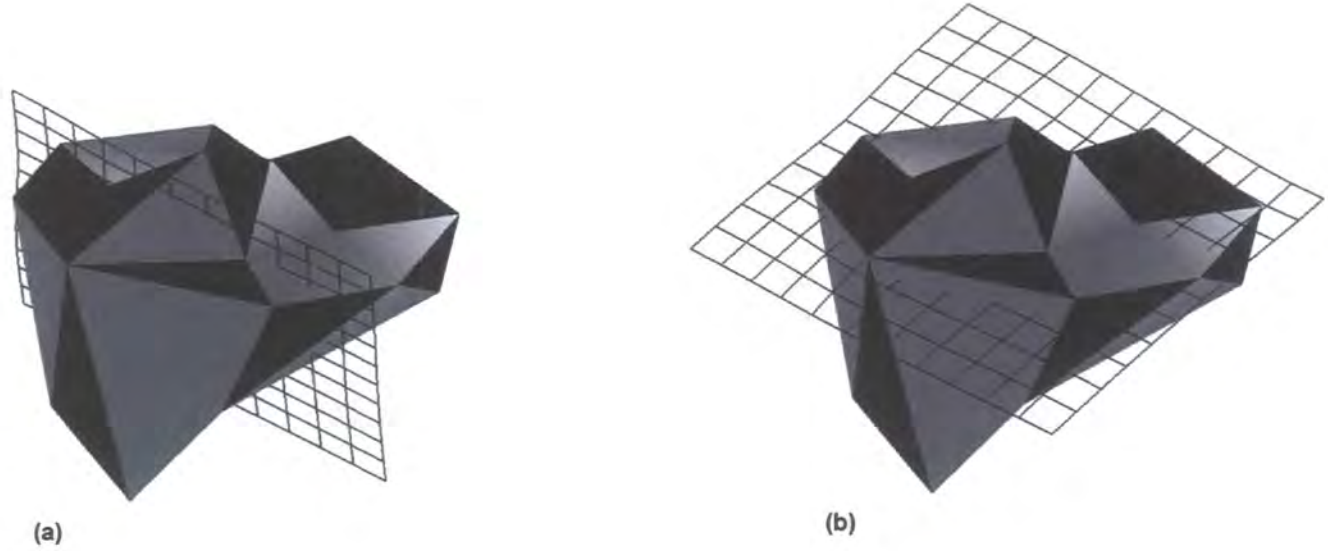

Fig 5.36: Ageing in the tibia of African Americans, Caucasian Americans and Spitalfields. Representations of tibial shape with TPS taken from PC2 using population means, showing region of bone giving maximum difference in shape between means. (a) TPS view in transverse plane; (b) in proximal plane. Images are presented to give the best indication of maximum difference in shape and are not necessarily taken from the same perspective as the mean configurations in Figure 5.34.

or geographic location (Parfitt, 1991). Two linked factors contribute towards this universal loss: firstly, the remodelling process is not completely efficient at any stage in the individual's lifetime and a small deficit in bone remains after the remodelling cycle is complete (Marcus, 1987), and secondly, hormonal changes in later life accelerate the rate of bone deficit during remodelling. For post-menopausal women, oestrogen deficiency not only increases the rate of remodelling, but as each remodelling cycle leaves a bone deficit, overall loss is greatly increased. Although there is no equivalent change in older men, both sexes are affected by generally poorer efficiency of hormonal production, which causes both cortical and trabecular thinning (Seeman, 2002). In addition, whilst periosteal expansion continues in both sexes during ageing as a compensatory mechanism for internal bone loss, such bone formation on the cortical surface is greater in men than in women (Martin and Atkinson, 1977; Ruff and Hayes, 1988; Beck et al., 1992; Waldron, 1992; Seeman, 1995, 2002; Ruff, 2000). Even when declining levels of BMC are taken into account, the accumulation of remodelled bone at different sites caused by differing loading pressures in the lower limbs over time, will necessarily affect the geometry of the bone throughout the individual's lifetime (Ruff and Hayes, 1984).

Therefore, whilst being universal, the rate of BMC loss with age is variable between males and females; it is also variable between individuals of the same sex, between different time periods and between different populations. High impact, weight-bearing activity throughout adulthood stimulates bone density and strength through the direct loading of force to the bone, although such loading is frequently site-specific. In addition, good nutrition must be combined with high impact loading to maintain any benefits to the bone. If either stimulus is deficient or lacking, benefits may be negligible or even detrimental (Zanker and Cooke, 2004). The universality of bone loss with age must therefore be tempered by gender, nutritional status, environment and the subsistence strategies undertaken.

As a result, both the internal and external appearance of the lower limb diaphyses will change throughout adulthood and the direction of change will be progressive, even in ostensively healthy bone. For the diathrodial joints, changes are likely to be of a different nature to the diaphyses for two reasons: firstly, the internal bone structure of the joint is primarily trabecular and, it has been suggested, age-related

loss is more similar in men and women in trabecular bone (Seeman, 1995; Brickly, 1999; Cordey and Nolte, 1998), and secondly, the joints are more prone to the age-related arthritic diseases, primarily osteoarthritis, than the diaphyses. This, the most common joint disorder, is thought to affect the majority of people aged 65 years and over in the USA, and 80% of those aged 75 years and over (Felson, 1988). Also, incipient osteoarthritis appears to be 'silent' for much of its aetiology, creating small progressive changes internally, prior to the overtly visible changes in external appearance (Riddle et al., 1988; Rodgers et al., 1990; Wright, 2003). Although initially these changes will affect cartilage and soft tissue, prolonged exposure will slowly begin to change the shape of the articular bone surface. Maquet (1983) describes such changes in the proximal tibia as involving the formation of a dense triangle of bone forming under the medial condyle, with a reduction in the sub-chondral sclerosis and cancellous trabeculae from beneath the lateral condyle.

In the analysis of age-related shape changes at the knee joint in African Americans, results establish some degree of statistically significant correlation of the scores of initial PCs selected by stepwise discriminant analysis with the ages of all individuals in the total sample. For the femur, four of the stepwise PCs show this degree of correlation, although results of only one PC (PC3) approach a moderate level of correlation ($r= 0.42$; $p<0.0001$). For the tibia, six of the initial stepwise PCs show a statistically significant correlation with age, but at a relatively weak level only, the best being PCs 11 and 9 at $r=0.25$; $p=0.006$ and $p=0.007$ respectively. When specimens are subdivided into groups of young, middle aged and elderly adults, however, the Mahalanobis' squared distances between groups are seen to be statistically significant with progressive magnitude between the youngest and oldest groups. This applies to both the distal femur and proximal tibia although the separation between groups appears clearer for the femur than for the tibia. The distances between age groups, however, appear to be relatively small and visualisation of the differences indicates that shape changes are very subtle in nature. For the femur, most differences concentrate on the medial side of the joint and this is confirmed by TPS deformation. For the tibia, changes appear to be concentrated across the tibial plateau, with some degree of change in the anterior region although the techniques available cannot clarify this more accurately.

Despite the subtleties of shape changes, therefore, results indicate statistically significant differences between age groups of African American adults, which appear to be cumulative in nature. This evidence, therefore, refutes hypothesis H.5.1 that the shape of the knee joint in non-pathological bone does not change throughout the ageing process.

Results therefore show that the shape of the knee joint changes during ageing between groups of African Americans with sexes pooled. Previous research, however, indicates that for the diaphyses (central medullary, cortical and subperiosteal areas), the internal and external appearance and properties of bone change more in women than in men and that such changes increase at a non-linear rate, particularly in women. Ruff and Hayes's study (1983) found an average decrease in rates of cortical femoral mid-shaft bone area of 1% between younger and older Pecos Pueblo male adults, with an average 10% decline in females; for the subperiosteal area, the decline was 7% in males and 11% in females. With the ensuing cortical bone loss, the central medullary area increased in volume; with an increase of 39% in females compared to 19% in males. They also found differences in rates of loss between the diaphyses of the femur compared to the tibia with relatively greater subperiosteal expansion of the femur in females. Although all measurements relate to the diaphyses rather than the joint ends, Ruff and Hayes's (1983) first measurements, taken at the distal end of the femoral shaft and proximal end of the tibial shaft, indicate statistically significant differences in rates of loss between younger and older females (for the cortical area of the femur $p<0.01$; for the cortical area of the tibia, $p<0.0001$ and for the periosteal area of the tibia, $p<0.05$). For males, only the loss of cortical area of the distal femoral shaft reached a level of statistical significance ($p<0.05$). Ruff and Hayes's study (1983) has been supported more recently with findings of sex-related changes in ageing by Drusini et al. (2000), who looked at cortical bone dynamics in three Italian samples.

In addition, osteoarthritis is thought to affect different joints in both nature and degree between the sexes and at different time periods within any one population. Overall, however, osteoarthritis of the knee joint is said to be the most common form of the illness (Aufderheide and Rodriguez-Martin, 1998). In the USA, Felson (1988) states that its prevalence increases from negligible in young people up to 20 years of

age to between 20% to 40% in the 75 years and above age group. More men than women are known to be affected up to 45 years of age; the reverse is true after 45 years, with a dramatic increase in the numbers of women affected relative to men. Some estimates have put the ratio of men to women affected by age 65 years at 1:5 (Hernborg and Nillson, 1973).

In the light of such research, it is predicted that substantial differences will be found in the degree and nature of morphological change in the knee joint between males and females with ageing. For the femur, this study finds that in relation to the African American sample, statistically significant distances are found between all three female groups and between the youngest and oldest males. Male and female groups remain at a statistically significant distance from one another with one exception (between youngest females and middle aged males). Visual representations of shape changes appear so subtle that ascribing morphological differences to changes with ageing is problematic relative to the differences due to sexual dimorphism. A similar conclusion is reached for the tibia, although all distances between groups remain statistically significant. As with the femur, visual representations of shape changes for the tibia appear too subtle to allow for precise identification of morphological differences between age groups. The relatively shallow distances between groups lead to the conclusion that the separation of age-specific male and female groups is at a relatively low level. Although differences due to sexual dimorphism are generally more pronounced, however, they are not so strong as to totally mask the influence of shape changes due to age.

The results of this study, which fail to show a clear distinction between male and female age groups, do not add strong support to that of previous research relating to the diaphyses. In relation to the knee joint, there is a relatively low separation between the three age groups of the two sexes in African Americans. Although the strongest group affiliations are primarily between same-sex groups, distances include a non-significant result for a male-female combination for the femur. Also, the average Mahalanobis' distances between the three male groups are 12.62 for the femur and 11.27 for the tibia. For the three female groups, distances are 12.70 and 7.50, respectively. These figures indicate that for the femur, males and females show the same degree of age-related change. For the tibia, females appear to show a

reduced degree of change compared to males, which contrasts with expectations. All distances remain greater between the youngest and oldest groups relative to the middle aged groups, however, and this implies that morphological changes with age are equally progressive for both sexes. This study is therefore unable to reject hypothesis H.5.2, that the degree and nature of differences in shape of the knee joint associated with ageing is similar in males and females.

Two factors may be affecting the discrepancy in the two sets of results; firstly, because BMC loss in the trabecular bone of the diathrodial joints is thought to be more similar between the sexes than in cortical bone (see above and Chapter 1 section 1.3), and secondly, if sex-related changes in morphology with ageing are population-specific (see discussion below), it is possible that this African American sample shows fewer sex-related changes at the knee joint compared to other populations. In addition, this group may have experienced a lower incidence of osteoarthritis at the knee during the period the people were living, or males and females may have shared a similar degree of disease. It is interesting to note that Snodgrass (2004) found that, in using the same African American sample (from the Terry Collection; see Chapter 2 section 2.2.1f), males and females show 'remarkably similar' patterns of age-related changes in osteophyte development in the vertebral column.

Previous research indicates that there is significant variation in the rate of BMC loss, which is thought to have a strong genetic determination (Dvornyk et al., 2003) and in the incidence and prevalence of osteoarthritis in the lower limbs between populations. Roguecka et al. (2001), in a study using femoral specimens from a Polish male sample, showed that peak bone mass is reached in early middle age, with a rapid decline thereafter. In contrast, Gregg and Gregg (1987) found that Arikaran males gained more cortical bone mass during growth and young adulthood. This early peak for the Arikara contrasts with the Polish males and with both Eskimo and New Mexico Pueblo skeletons (Eriksen, 1976). For the latter two groups, cortical bone loss is known to have peaked in middle age, although the Eskimo and Pueblo males lost BMC more slowly than the Arikara thereafter. Females consistently suffered greater bone loss than males of the same three Native American groups but the timing of peak loss and the overall degree of loss by old age varied between the

three female groups (Eriksen, 1976). In addition, although osteoarthritis is a universal phenomenon, it is strongly influenced by the age structure and longevity of the population and the degree and nature of physical activity undertaken. In both modern and archaeological rural populations, osteophytosis in skeletal remains is frequently found at far greater levels in the younger age groups than in urban, industrial societies (such as that of the urban African American sample, see discussion above) (Larsen, 2000; Molleson, 1994). The type of research above is also supported by Schmitt et al. (2002) who, by observing the variability in bone indicators of ageing on the ilium and pubic symphysis, have drawn attention to the population-specific patterning of age-related changes.

In the light of such research, this study predicted that the morphology at the knee joint of each age group will be specific to each population. Therefore, the specific morphology of each age group is unlikely to show any greater similarity to the corresponding age group of other populations than to other age groups of the same population.

Results here indicate that changes with age in knee joint morphology are so subtle for both the femur and tibia, that age groups are far closer to other age groups of the same population than to corresponding same-age groups of other populations. The bivariate plots of PCs 1 and 2 using sample means (Figures 5.27 for the femur and 5.34 for the tibia), highlight a clear separation of samples into three population age-sets. The close association of means for the Caucasian Americans in Figures 5.27 and 5.34, reflecting the Mahalanobis' squared distances, shows only one statistically significant distance between groups for this population (between the youngest and middle aged groups for the tibia). All distances remain statistically significant between African American groups, with significant results for four of the six distances between Spitalfields groups (femur and tibia). This indicates that age-related changes in some populations may be relatively more acute than in others. Differences in the mean configuration between sample means at the extremes of PCs 1 and 2 appear to relate primarily to differences in morphology between populations with few obvious similarities in the pattern of relationships between the three age groups of the three populations; the exception being for PC2 for the femur (using sample means).

These results for the knee joint reflect conclusions by previous researchers that age-related changes in morphology in the diaphyses are population-specific. Although the knee is the most commonly affected of joints for all people, the occurrence and degree of degenerative joint diseases are sex, age, environment and activity-related and therefore highly variable between populations. These results therefore verify hypothesis H.5.3; the degree and nature of changes in shape associated with ageing will be less than any morphological differences that may exist between specimens from different population samples.

5.7 Implications of results and direction of future research

Results here show that for any population, at a specific period of time, there will be a relatively 'normal' rate of BMC loss in the trabecular bone of the epiphysis of the knee during ageing. In addition, the incidence of degenerative joint disease within that population is likely to increase the rate of bone degeneration to a greater or lesser extent. It is likely that the combination of these two factors will be responsible for the alteration in the shape of the joint with ageing, noted in this study. The population-specific aspect of ageing at the knee demonstrated here accords with previous results using the diaphyses of the femur and tibia.

Results here imply, however, that the degree and nature of morphological changes noted for the diaphysis cannot be applied equally to the epiphysis. Using the African Americans as a sample population, it was noted that whilst the degree of change is relatively strong overall, there appears to be little difference in the rate of those changes between males and females. This is contrary to expectations from previous results using the diaphysis.

As previous research into the effects of ageing has been directed more specifically towards the diaphysis (Eriksen, 1976; Gregg and Gregg, 1987; Roguecka et al., 2000; Dvornyk et al., 2003), future research should be directed towards a better understanding of the degree and nature of BMC loss in the epiphysis, and more specifically, the difference in rates of loss between the sexes within populations and between populations. In addition, research should be directed towards an understanding of how degenerative joint disease in its earliest stages may affect the

epiphysis, and how this is manifest between different groups. Given the population-specific aspect of morphological changes with ageing, comparison of results using sexed Caucasian American and Spitalfields samples would help towards a better understanding of results of the African American male and female samples tested here.

5.8 Direct implications of results for this study

Populations comprising adult specimens of different ages and of unknown age will be combined into discrete samples for future inter-population analyses.

Chapter 6

Differences in form of the knee joint between thirteen populations of *Homo sapiens.*

6.1 Introduction

The majority of studies comparing and contrasting different populations of modern humans have taken either of two lines of approach; by analysing and comparing skeletal measurements or by comparing genetic differences between groups. Within the first approach, the majority of studies have compared measurements of the skull and facial skeleton (e.g., Giles and Elliott, 1962; Howells, 1970, 1973, 1989; Krogman and Iscan, 1986; Bass, 1987; Relethford, 1994; Hanihara, 1996; Viðarsdóttir, 1999), although some have used features of the appendicular skeleton (Craig, 1995; Gill, 2000). The second approach categorises human populations into genetically defined groups by comparing and contrasting the prevalence of numbers of specified alleles at polymorphic loci. Research using this approach includes work by Nei and Roychoudhury (1974), O'Rourke et al., (1985), Nei and Takezaki (1996), Dvornyk et al. (2003) and the numerous papers and books by Cavelli-Sforza and co-workers, much of whose work was collated and expanded in *The History and Geography of Human Genes* (1994).

The use of cranial (as opposed to postcranial) measurements is likely to be a more accurate tool for comparing morphology between populations because of the inherently greater degree of stability of cranial form throughout each individual's lifetime. The form of the cranium is less influenced by local reaction to stress and subsequent bone remodelling than the postcranium; any changes in cranial shape are largely confined to the systemic hormonal influences experienced by the entire skeleton (Lieberman, 1996). Therefore, craniofacial form is therefore subject to fewer short-term influences within populations, and the distinct differences in morphology seen between populations result from more long term changes. The frequently dramatic changes in size noted in the postcrania of first and second generation migrants, and between different generations undergoing rapid and stressful change, emphasises the importance of using cranial rather than postcranial

data for distinguishing between groups (Owsley and Jantz, 1985; Endo et al., 1993; Loesch et al., 2000; Bogin et al., 2002; Padez, 2002).

Studies using cranial measurements, exemplified in the work of Howells (1973) have produced inferred relationships between populations that contrast with studies using the genetic data, exemplified in the work of Cavelli-Sforza et al. (1994) and Nei and Takezaki (1996). Howells acknowledged that shape and size constitute two separate components to form and that determining relationships between populations without separating these two components will affect results. In his later work, Howells (1989) tried to remove the size element and, although results in comparing form were similar, they were not identical.

Even when size differences are removed from Howells' analyses, the most obvious disparity between the two approaches is that craniofacial data group Australians and Melanesians with Andaman Islanders and Africans, whilst molecular results draw a sharp distinction between Africans and all non-Africans; a distinction that Cavelli-Sforza et al. (1994) attribute to phylogeny reflecting environmental factors, principally climate, more closely that genetic traits. Neither approach used all of the same populations within their analyses that are used in the present study although broad comparisons can be made. Seven of Howells' 28 populations (Howells, 1989) and nine of the 42 populations used by Cavelli-Sforza et al. (1994) are broadly comparable. These comparisons will be examined further in Discussion section 6.5.4.

It is likely that the effects of parallel evolution of form between different populations sharing similar conditions in the physical environment (temperature, rainfall and humidity, altitude and terrain) will mask underlying genetic differences, thus creating discrepancies between results (Ruff, 1994). In addition, it is acknowledged that cultural differences between populations also affect skeletal structures; examples being the ability of the Japanese to rotate the knee more extensively than Caucasian groups because of their greater use of squatting (Freeman, 2001), and the increased incidence of degenerative diseases in the hip and back reflecting the acquisition of horses amongst Native American groups (Larsen, 2000). Rossi (2005) describes the changes that occur in the biomechanics of gait between 'normal' locomotion in cultures that are shod and 'natural' locomotion in societies that are unshod (Chapter 1

section 1.6.2). Therefore, environmental factors such as climate, altitude, habitual footwear and subsistence lifestyles are likely to constitute the most influential variables affecting the skeletal form of the lower limbs.

6.2 Examination of issues relating to differences in form in the lower limbs and knee joint

This chapter will examine differences in skeletal form at the knee joint between populations of modern humans. Differences in the size of the lower limbs will also be examined and results from these analyses will be compared with results examining knee joint form to help interpret such differences. Results of any differences in knee joint form and of size differences in the long bones (maximum length measurements and robusticity indices) will then be analysed in relation to various environmental factors (climate, use of footwear and subsistence strategies) that may be instrumental in governing shape and size. These results will then be compared to results of the relationships established in the previous research outlined in section 6.1 above.

Because of the inherent high weight-bearing function on a relatively unstable joint, the knee joint is probably subject to the greatest degree of localised stress and remodelling in the skeleton (Chapter 1, sections 1.6 and 1.7.2). External factors, such as extreme temperatures, high altitude, harsh terrain and a physically hard working environment are thus likely to create greater variability at the knee joint between individuals and ultimately populations than would be predicted for the cranium or facial skeleton. Therefore, relationships between populations based upon knee joint form are predicted to differ from those based upon cranial measurements or upon genotype.

It has been established above (Chapters 3, 4 and 5) that the shape of the knee joint differs within and between the restricted number of populations examined. It has also been established (Chapters 3 and 4) that the size of the knee joint varies in some populations. This chapter seeks to establish whether differences are present in the form of the knee joint between the full dataset of thirteen populations of modern humans. In doing so, it will establish whether such differences, if present, are primarily differences in shape or differences in size and whether both shape and size factors are equally influential in governing form.

The following hypotheses are therefore erected:

H.6.1 There is no significant difference in the shape of the knee joint between the thirteen populations of *Homo sapiens*.

H.6.2 There is no significant difference in the centroid size of the knee joint between the thirteen populations of *Homo sapiens*.

If H.6.1 and H.6.2 are falsified, the following hypothesis will be examined:

H.6.3 The degree of difference in the shape of the knee joint between the thirteen populations is highly correlated with the degree of difference in centroid size.

Jacob (1985) proposed that changing environmental conditions affect the length of different parts of the anatomy at differing rates; for example, tibial length reacts at a different rate to femoral length. Holliday and Ruff (2001) analysed the lengths of the two proximal and two distal limbs within and between populations and concluded that the distal segments are the more variable pair and that the tibia is more variable than the femur. In an extension of both Jacob's (1985) and Holliday and Ruff's (2001) research, this study proposes to examine whether different aspects of size of the same bone (centroid size of the knee joint and maximum length and robusticity of the external proportions of the shaft) respond differently to the various genetic or environmental forces acting upon them. It will also examine whether comparable features of the femur and tibia react similarly to these forces. The following hypothesis is therefore erected:

H.6.4 In a comparison of the femur with the tibia and within each bone separately, the three component size measurements (centroid size, maximum length and robusticity of the diaphyses) react to the various genetic and environmental forces influencing them to the same degree across different populations.

Allen's and Bergmann's Rules both state that climate and specifically ambient temperature, is fundamental in affecting body shape and proportions. Although, these Rules were proposed in the late 19th century and are described in most textbooks on human biology (e.g., Weiss and Mann, 1989), they were recently tested, updated and

endorsed by Ruff (1994b). In addition, Cavelli-Sforza et al. (1994) state their belief that both human skeletal shape as well as size is strongly influenced by climatic variables. This appears to be borne out by the results of phylogenies based upon cranial form, which cluster populations sharing similar climatic conditions. However, as phylogenies based upon ancestral relationships such as those by Cavelli-Sforza et al. (1994) result in an alternate set of relationships to those based upon cranial morphology, the next section will examine the degree to which climatic and environmental influences are fundamental in affecting the form of the knee joint and lower limbs and whether closeness in terms of ancestral relationships also determines similarity in knee joint morphology.

Therefore the following hypothesis is erected:

H.6.5 Similarity in the shape of the knee joint between different populations is related to similarity of craniofacial shape or molecular history or both.

As the postcranial skeleton (and the knee joint in particular), is also subject to the high degrees of loading pressures not directly experienced by the cranium, it is possible that lower limbs will be more strongly influenced by additional environmental factors than the cranium. If these forces appear to be sufficiently powerful in affecting knee joint shape, such that hypothesis H.6.5 is falsified, this section will then examine whether the relationships between populations based upon similarity of knee joint shape are based solely upon similarity of environmental background. Finally, therefore, the following hypothesis is erected:

H.6.6 Similarity of form of the knee joint between different populations is highly correlated with similarity of their environmental background.

6.3 Materials and Methods

Specimens of 387 right femora and 369 right tibiae from thirteen distinct populations of modern humans are studied in the analyses of shape and centroid sizes of the knee joint. The sample sizes for some populations, notably the Ibo, are small. To give relative balance of sample sizes throughout the thirteen populations, the African, Caucasian American and Spitalfields populations are restricted to forty specimens

each. For these three populations, individuals are chosen from the numerous specimens available, with male and female numbers equalised and specimens taken from across all age groups. Of the remaining ten populations, data sets comprise individuals of known and unknown sex and of unknown age. The details and composition of the data sets is shown in Tables 6.1 and 6.2.

The centroid sizes of specimens are calculated from the same specimens used for the analyses of shape during GPA analysis. Although the majority of individuals used for analyses exploring the form of the knee joint and the size of the diaphyses are the same, the small discrepancy in numbers is to maximise data (see Chapter 2 section 2.1.1). Tables 6.3 and 6.4 detail specimens used in the analyses using maximum length and robusticity indices of the femoral and tibial long bones.

All analyses of shape are conducted on all landmarks for both femora and tibiae. The specimens are superimposed using Generalised Procrustes Analysis (GPA) and the Procrustes fitted data are subjected to Principal Components Analysis (PCA). These methods are described in Chapter 2 Sections 2.2.3c and 2.2.3d.

Because ten of the populations comprise samples of pooled males, females and those of unknown sex, the validity of using such pooled samples in size comparisons between populations.

Five of the thirteen populations used in the following size analyses (Australians, Ibo, Andaman Islanders, Sri Lankans and Khoisan) consist of pooled-sex samples, including a high proportion of those of unknown sex. Three of the remaining eight populations (African and Caucasian Americans and Spitalfields) have sufficient numbers in the original collections to use an equal number of known male and female specimens. Four of the populations (Aleut, Pachacama, Arikara and Egyptians) comprise a number of specimens of known sex but need to use additional specimens of unknown sex or an excess number of one sex over the other to make up an adequately sized sample. The thirteenth population (Chinese) is a male-only sample. Chapter 4 shows that there is significant sexual dimorphism in both the centroid size of the knee joint and in diaphyseal length and robusticity.

Population	Total	Males	Females	Unknown	Collection
Aleut	26	15	11	0	NMNH
Pachacama	29	18	11	0	NMNH
Arikara	34	21	13	0	NMNH
Chinese	25	25	0	0	NMNH
Australian	32	5	7	20	NMNH, NHM
African American	40	20	20	0	NMNH
Ibo	14	4	7	3	NMNH, NHM
Andaman Islanders	34	7	8	19	NHM
Sri Lankans	18	5	13	0	NHM
Khoisan	22	10	11	1	NMNH, NHM
Egyptians	33	12	10	11	NHM
Spitalfields	40	20	20	0	NHM
Caucasian Americans	40	20	20	0	NMNH, NHM
Total Number	387	182	151	54	

Table 6.1: The composition of the data sets used for the analyses of shape and calculation of centroid size of the proximal tibia for 13 populations and location of collections.

Population	Total	Males	Females	Unknown	Collection
Aleut	26	17	9	0	NMNH
Pachacama	27	15	9	3	NMNH
Arikara	32	22	10	0	NMNH
Chinese	29	29	0	0	NMNH
Australian	28	5	10	13	NMNH, NHM
African American	40	20	20	0	NMNH
Ibo	9	2	7	0	NMNH, NHM
Andaman Islanders	33	9	9	15	NHM
Sri Lankans	13	4	8	1	NHM
Khoisan	23	14	8	1	NMNH, NHM
Egyptians	30	15	10	5	NHM
Spitalfields	40	20	20	0	NHM
Caucasian Americans	40	20	20	0	NMNH, NHM
Total Number	370	192	140	38	

Table 6.2: The composition of the data sets used for the analyses of shape and calculation of centroid size of the proximal tibia for 13 populations and location of collections.

NMNH: National Museum of Natural History, Smithsonian Institution, Washington, DC. NHM: Natural History Museum, London

Population	Total	Males	Females	Unknown	Collection
Aleut	30	18	12	0	NMNH
Pachacama	22	10	12	0	NMNH
Arikara	36	23	13	0	NMNH
Chinese	29	29	0	0	NMNH
Australian	32	5	9	18	NMNH, NHM
African American	40	20	20	0	NMNH
Ibo	20	5	6	9	NMNH, NHM
Andaman Islanders	25	2	2	21	NHM
Sri Lankans	22	5	12	5	NHM
Khoisan	25	7	10	8	NMNH, NHM
Egyptians	36	12	10	14	NHM
Spitalfields	40	20	20	0	NHM
Caucasian Americans	40	20	20	0	NMNH, NHM
Total Number	397	176	146	75	

Table 6.3: The composition of the data sets used for the calculation of maximum length and robusticity indices of the femur for 13 populations and location of collections.

Population	Total	Males	Females	Unknown	Collection
Aleut	32	20	12	0	NMNH
Pachacama	22	12	10	0	NMNH
Arikara	32	21	11	0	NMNH
Chinese	30	30	0	0	NMNH
Australian	32	5	8	19	NMNH, NHM
African American	40	20	20	0	NMNH
Ibo	19	3	7	9	NMNH, NHM
Andaman Islanders	33	9	9	15	NHM
Sri Lankans	20	4	10	6	NHM
Khoisan	21	6	9	6	NMNH, NHM
Egyptians	45	16	16	13	NHM
Spitalfields	40	20	20	0	NHM
Caucasian Americans	40	20	20	0	NMNH, NHM
Total Number	406	186	152	68	

Table 6.4: The composition of the data sets used for the calculation of maximum length and robusticity indices of the tibia for 13 populations and location of collections.

NMNH: National Museum of Natural History, Smithsonian Institution, Washington, DC. NHM: Natural History Museum, London

In order to assess the feasibility of using pooled samples of males and females in analyses of size, this analysis focuses upon the four populations with small but matching numbers of sexed individuals (minimum nine specimens of each sex per sample) and compares them with the comparable group from their own population, which includes the specimens of unknown sex or extra individuals of one sex. The four are embedded within the two sets of tables which compare all thirteen samples. All tables are sorted into ascending order of size.

6.3.1 Results of the analysis comparing size measurements:

6.3.1a Femur:

For the femur, Tables 6.5, 6.6 and 6.7 show the comparison of the unmatched samples (a) in relation to the matched samples (b).

Differences between the four example populations in the two samples for the centroid size of the knee joint, shown in Table 6.5, range from 0.81mm (0.55%) for the Egyptians, to 2.65mm (1.88%) for the Pachacama; a mean percentage difference of 1.25% across the four populations.

Population	Centroid Size
Sri Lankan	130.62
Andaman Islands	131.55
Khoisan	139.04
Pachacama	140.68
Australian	145.22
Ibo	145.80
Egyptian	146.92
Chinese	148.32
Aleut	151.01
Spitalfields	151.68
Caucasian American	153.53
Arikara	155.39
African American	157.71

(a) Unmatched dataset

Population	Centroid Size
Sri Lankan	130.62
Andaman Islands	131.55
Pachacama	138.03
Khoisan	139.04
Australian	145.22
Ibo	145.80
Egyptian	146.11
Chinese	148.32
Aleut	148.95
Spitalfields	151.68
Caucasian American	153.53
Arikara	153.55
African American	157.71

(b) Matched dataset

Table 6.5: Inter-population variation in the femur (centroid size). Comparison of datasets using (a) pooled male and female specimens in the Aleut, Pachacama, Arikara and Egyptians and (b) matched numbers of male and female specimens. Figures in red highlight results for the example populations.

Differences between the four example populations in the two samples for the maximum length of the diaphysis, shown in Table 6.6, range from 0.87mm (0.20%) for the Egyptians, to 1.88mm (0.48%) for the Pachacama; a mean percentage difference of 0.31% across the four populations.

Differences between the four example populations in the two samples for the robusticity indices of the diaphysis, shown in Table 6.7, range from 0.00 (0%) for the Pachacama, to 0.04 (0.68%) for the Egyptians; a mean percentage difference of 0.25% across the four populations.

Population	M2 Length
Andaman Islands	384.96
Pachacama	395.28
Sri Lankan	400.67
Aleut	404.85
Khoisan	417.18
Chinese	427.96
Spitalfields	428.67
Arikara	430.55
Ibo	437.00
Egyptian	437.29
Caucasian American	437.97
African American	454.89
Australian	455.24

(a) Unmatched dataset

Population	M2 Length
Andaman Islands	384.96
Pachacama	393.40
Sri Lankan	400.67
Aleut	403.58
Khoisan	417.18
Chinese	427.96
Spitalfields	428.67
Arikara	429.54
Egyptian	436.42
Ibo	437.00
Caucasian American	437.97
African American	454.89
Australian	455.24

(b) Matched dataset

Table 6.6: Inter-population variation in the femur (maximum length). Comparison of datasets using (a) pooled male and female specimens in the Aleut, Pachacama, Arikara and Egyptians and (b) matched numbers of male and female specimens. Figures in red highlight results for the example populations.

Population	RI
Sri Lankan	5.57
Andaman Islands	5.74
Australian	5.82
Ibo	5.89
Egyptian	5.91
Khoisan	5.94
African American	6.13
Caucasian American	6.15
Chinese	6.18
Arikara	6.18
Spitalfields	6.29
Pachacama	6.39
Aleut	6.77

(a) Unmatched dataset

Population	RI
Sri Lankan	5.57
Andaman Islands	5.74
Australian	5.82
Ibo	5.89
Khoisan	5.94
Egyptian	5.95
African American	6.13
Caucasian American	6.15
Chinese	6.18
Arikara	6.19
Spitalfields	6.29
Pachacama	6.39
Aleut	6.76

(b) Matched dataset

Table 6.7: Inter-population variation in the femur (robusticity indices). Comparison of datasets using (a) pooled male and female specimens in the Aleut, Pachacama, Arikara and Egyptians and (b) matched numbers of male and female specimens. Figures in red highlight results for the example populations.

6.3.1b Tibia:

For the tibia, Tables 6.8, 6.9 and 6.10 show the comparison of the unmatched samples (a) in relation to the matched samples (b). Differences between the four example populations in the two samples for the centroid size of the knee joint, shown in Table 6.8, range from 0.98mm (0.77%) for the Egyptians, to 2.08mm (1.62%) for the Pachacama; a mean percentage difference of 1.22% across the four populations.

Population	Centroid Size
Andaman Islands	115.08
Sri Lankan	117.99
Khoisan	123.66
Ibo	124.58
Australian	125.53
Spitalfields	125.89
Egyptian	127.57
Pachacama	128.12
Chinese	128.15
Aleut	129.08
Caucasian American	133.69
Arikara	135.94
African American	136.85

(a) Unmatched dataset

Population	Centroid Size
Andaman Islands	115.08
Sri Lankan	117.99
Khoisan	123.66
Ibo	124.58
Australian	125.53
Spitalfields	125.89
Pachacama	126.04
Egyptian	126.59
Aleut	127.81
Chinese	128.15
Caucasian American	133.69
Arikara	133.87
African American	136.85

(b) Matched dataset

Table 6.8: Inter-population variation in the tibia (centroid size). Comparison of datasets using (a) pooled male and female specimens in the Aleut, Pachacama, Arikara and Egyptians and (b) matched numbers of male and female specimens. Figures in red highlight results for the example populations.

Differences between the four example populations in the two samples for the maximum length of the diaphysis, shown in Table 6.9, range from 0.86mm (0.23%) for the Egyptians, to 3.34mm (0.98%) for the Pachacama; a mean percentage difference of 0.54% across the four populations.

Differences between the four example populations in the two samples for the robusticity indices of the diaphysis, shown in Table 6.10, range from 0.02mm (0.26%) for the Arikara, to 0.10mm (1.26%) for the Aleut; a mean percentage difference of 0.68% across the four populations.

Population	M2 Length
Andaman Islands	322.68
Aleut	329.24
Pachacama	340.24
Chinese	340.83
Spitalfields	347.72
Sri Lankan	348.50
Khoisan	357.83
Arikara	361.85
Caucasian American	364.88
Ibo	375.00
Egyptian	377.05
Australian	378.11
African American	388.19

(a) Unmatched dataset

Population	M2 Length
Andaman Islands	322.68
Aleut	331.17
Pachacama	336.90
Chinese	340.83
Spitalfields	347.72
Sri Lankan	348.50
Khoisan	357.83
Arikara	360.59
Caucasian American	364.88
Ibo	375.00
Egyptian	376.19
Australian	378.11
African American	388.19

(b) Matched dataset

Tables 6.9: Inter-population variation in the tibia (maximum length). Comparison of datasets using (a) pooled male and female specimens in the Aleut, Pachacama, Arikara and Egyptians and (b) matched numbers of male and female numbers of specimens. Figures in red highlight results for the example populations.

Population	RI
Egyptian	6.91
Ibo	6.96
Andaman Islands	7.00
Khoisan	7.02
Sri Lankan	7.07
Australian	7.12
Caucasian American	7.49
African American	7.52
Pachacama	7.53
Arikara	7.67
Chinese	7.76
Spitalfields	7.90
Aleut	8.28

(a) Unmatched dataset

Population	RI
Ibo	6.96
Egyptian	6.97
Andaman Islands	7.00
Khoisan	7.02
Sri Lankan	7.07
Australian	7.12
Caucasian American	7.49
Pachacama	7.50
African American	7.52
Arikara	7.69
Chinese	7.76
Spitalfields	7.90
Aleut	8.38

(b) Matched dataset

Table 6.10: Inter-population variation in the tibia (robusticity indices). Comparison of datasets using (a) pooled male and female specimens in the Aleut, Pachacama, Arikara and Egyptians and (b) matched numbers of male and female specimens. Figures in red highlight results for the example populations.

6.3.1c Summary:

Results show that the greatest difference between the matched and unmatched samples for the three size measurements is in centroid size, with a mean 1.24% difference for the femur and tibia across the four example populations. The mean percentage difference for both bones in maximum length and robusticity is only 0.45%

The Pachacama shows the greatest difference between samples in centroid size for both the femur and tibia. For the femur, Table 6.5 shows the matched position of the Pachacama to be transposed with the Khoisan. All other populations remain in the same positions relative to each other in both the matched and unmatched samples.

Table 6.8 for the tibia, shows that two transpositions occur between matched and unmatched samples for centroid size, between the Pachacama and the Egyptians, and the Aleut and Chinese. Only 1.51mm difference lies between all four groups in the unmatched sample, but this distance is increased to 2.11mm in the matched sample. All other populations remain in the same positions relative to each other.

For the maximum lengths of the femoral shaft (Tables 6.6), one transposition occurs between the Egyptians and Ibo, where the difference between the two populations of 0.29mm in the unmatched sample is increased to 0.58mm in the matched sample. For the tibia, all positions remain unchanged relative to length in Tables 6.9.

For the robusticity of the femoral shaft in (Tables 6.7), one transposition occurs between the Egyptians and Khoisan, because of the increase in the Egyptian index from 5.91 to 5.95 between matched and unmatched samples. For the tibia, Table 6.10 shows that the increase in the robusticity index in the Egyptians also causes a transposition with the Ibo, with a second transposition between the Pachacama and the African Americans.

6.3.1d Conclusion

Results show that measurements of the centroid size of the knee joint reveal a greater degree of difference between the matched and unmatched samples, compared to those for the length and robusticity of the shafts. The positions of the populations in the comparative tables are undoubtedly affected when using pooled-sex populations, but to a relatively minor degree and only between pairs of samples in an adjacent position. Using pooled-sex samples is not ideal when comparing the means of size measurements. As this analysis has shown, however, in relation to these samples, the differences in means appear relatively small and in order to maximise available data, analyses comparing size measurements will continue to use pooled-sex samples.

6.4 Results

6.4.1 Population differences in the shape of the knee joint

6.4.1a Femur:

Table 6.11 gives the proportional and accumulated variance for PCs 1 to 71 for the 387 specimens, which represents the total variance within the sample. The scores for each specimen on the resultant PCs are then subjected to canonical discriminant analysis to establish the relationships between populations based upon the Mahalanobis' squared distances between population means.

For the femur, the best separation of populations is achieved using 100% of total variance. This assessment was reached after separate discriminant and cross-validation analyses were carried out using PCs accounting for between c.50% to 100% of total variance. Results are summarised in Figure 6.1.

PCs	Prop.	Cumul.	PCs	Prop.	Cumul.	PCs	Prop.	Cumul.
PC1	10.50	10.50	PC26	1.08	81.30	PC51	0.31	96.40
PC2	8.21	18.70	PC27	1.03	82.40	PC52	0.30	96.70
PC3	6.47	25.20	PC28	0.98	83.40	PC53	0.28	97.00
PC4	5.92	31.10	PC29	0.88	84.20	PC54	0.26	97.20
PC5	4.90	36.00	PC30	0.87	85.10	PC55	0.26	97.50
PC6	4.48	40.50	PC31	0.81	85.90	PC56	0.24	97.70
PC7	3.97	44.50	PC32	0.80	86.70	PC57	0.23	98.00
PC8	3.68	48.10	PC33	0.76	87.50	PC58	0.21	98.20
PC9	2.98	51.10	PC34	0.72	88.20	PC59	0.20	98.40
PC10	2.78	53.90	PC35	0.68	88.90	PC60	0.20	98.60
PC11	2.72	56.60	PC36	0.66	89.50	PC61	0.18	98.80
PC12	2.67	59.30	PC37	0.61	90.20	PC62	0.17	98.90
PC13	2.27	61.60	PC38	0.60	90.80	PC63	0.16	99.10
PC14	2.13	63.70	PC39	0.58	91.30	PC64	0.15	99.20
PC15	2.04	65.70	PC40	0.54	91.90	PC65	0.14	99.40
PC16	1.87	67.60	PC41	0.53	92.40	PC66	0.12	99.50
PC17	1.80	69.40	PC42	0.49	92.90	PC67	0.12	99.60
PC18	1.76	71.20	PC43	0.47	93.40	PC68	0.11	99.70
PC19	1.53	72.70	PC44	0.45	93.80	PC69	0.10	99.80
PC20	1.42	74.10	PC45	0.42	94.20	PC70	0.09	99.90
PC21	1.37	75.50	PC46	0.42	94.70	PC71	0.08	100.00
PC22	1.36	76.80	PC47	0.40	95.10			
PC23	1.17	78.00	PC48	0.35	95.40			
PC24	1.14	79.20	PC49	0.35	95.80			
PC25	1.10	80.30	PC50	0.34	96.10			

Table 6.11: Inter-population variation in the femur. The proportion and accumulated variance for PCs 1-71, which accounts for 100% of total variance using 13 populations.

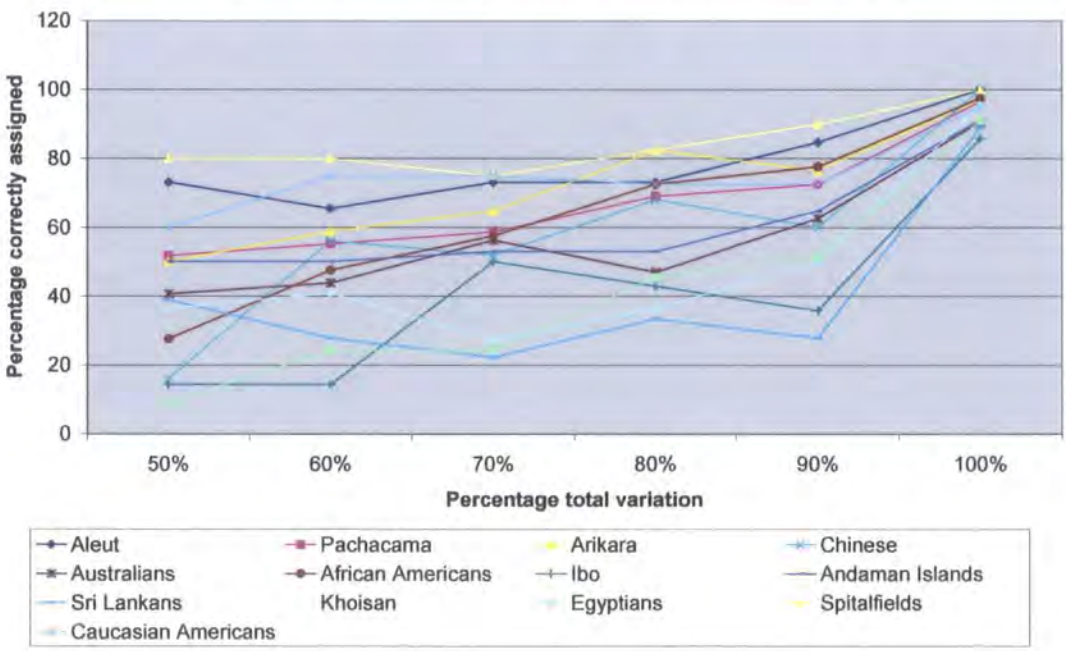

Figure 6.1: Inter-population variation in the femur. Summary of separate discriminant and cross-validation analyses using PCs accounting for c.50% (PCs 1-9), 60% (PCs 1-12), 70% (PCs 1-17), 80% (PCs 1-25), 90% (PCs 1-37) and 100% (PCs 1-71).

The Mahalanobis' squared distances between populations, generated by the discriminant analysis are shown in Table 6.12. All distances between populations are highly statistically significant indicating that groups can be separated on the basis of shape of the distal femur. Distances range from the closest pairs at Mahalanobis' D^2 =15.20, shared equally between the Ibo and Khoisan and the Egyptians and Sri Lankans, to the most distant at MD^2 =74.18 between the Aleut and the Spitalfields sample.

Table 6.13 illustrates the relationship of each sample to all others on the basis of the generated Mahalanobis' squared distances by showing the distance of each primary sample to all others and ranking them accordingly from the closest sample (at position 1) to the furthest (at position 12). Table 6.13 shows the Spitalfields population to be the most distant from all other populations in nine of the possible twelve positions. For two of the remaining three comparisons, the Andaman Islanders are the most distant.

Table 6.14 shows the results of cross-validation analysis using the thirteen populations. Individuals correctly assigned to groups range from 85.71% for the Ibo to 100% for the Aleut, Chinese and Spitalfields. The mean percentage for all individuals correctly assigned to groups is 94.53%, indicating that the shape of the distal femur is largely specific to each population analysed in this study.

It is apparent from the results of the cross-validation analysis that there is a strong shape signal for each population sample. However, because of the high number of specimens in the total sample and the high degree of overlap between specimens on the bivariate plots of selected PCs when using the total sample, the population means are used to help determine the specific morphologies of each sample and to explore the relationships between them. For the femur, there is a statistically significant correlation between the Procrustes distances shown in Table 6.15 and the Mahalanobis' squared distances shown in Table 6.12 ($r= 0.25$; $p= 0.03$). An anomaly is seen in the high values for the Sri Lankan sample in Table 6.15 compared to average values for this sample seen in Table 6.12. See Chapter 2 section 2.1.2i and Discussion section 6.5.5c(iv) for a discussion and possible causes for this anomaly.

Aleut	0												
	1.000												
Pach.	26.18	0											
	0.0001	1.000											
Arikara	30.37	23.62	0										
	0.0001	0.0001	1.000										
Chinese	34.18	24.45	16.26	0									
	0.0001	0.0001	0.0001	1.000									
Australian	45.90	36.72	21.97	27.54	0								
	0.0001	0.0001	0.0001	0.0001	1.000								
African	47.59	42.61	28.49	25.86	37.32	0							
Americans	0.0001	0.0001	0.0001	0.0001	0.0001	1.000							
Ibo	46.37	36.86	25.70	27.48	22.37	27.89	0						
	0.0001	0.0001	0.0001	0.0001	0.0001	0.0001	1.000						
Andaman	54.35	48.94	36.02	44.37	20.61	48.41	36.55	0					
	0.0001	0.0001	0.0001	0.0001	0.0001	0.0001	0.0001	1.000					
Sri Lankan	32.45	30.52	23.17	19.34	22.80	31.26	16.93	35.92	0				
	0.0001	0.0001	0.0001	0.0001	0.0001	0.0001	0.0205	0.0001	1.000				
Khoisan	48.24	47.48	27.94	35.38	19.37	35.96	15.20	27.02	21.86	0			
	0.0001	0.0001	0.0001	0.0001	0.0001	0.0001	0.0287	0.0001	0.0001	1.000			
Egyptians	38.02	34.81	25.81	25.19	16.29	38.71	20.28	29.04	15.20	15.24	0		
	0.0001	0.0001	0.0001	0.0001	0.0001	0.0001	0.0001	0.0001	0.0001	0.0001	1.000		
Spitalfields	74.18	70.14	49.88	35.83	52.40	29.82	46.66	60.35	44.46	53.44	46.76	0	
	0.0001	0.0001	0.0001	0.0001	0.0001	0.0001	0.0001	0.0001	0.0001	0.0001	0.0001	1.000	
Caucasian	44.39	34.34	29.64	27.04	39.54	19.49	32.32	49.55	29.57	41.15	34.72	40.57	0.00
Americans	0.0001	0.0001	0.0001	0.0001	0.0001	0.0001	0.0001	0.0001	0.0001	0.0001	0.0001	0.0001	1.000
	Aleut	**Pach.**	**Arikara**	**Chinese**	**Aust.**	**Af Am**	**Ibo**	**Andam.**	**Sri L.**	**Khoi**	**Egypts.**	**Spitalfs.**	**Ca. Am**

Table 6.12: Inter-population variation in the femur. Results from the canonical discriminant analysis of the 13 populations, on the basis of 100% variance.The upper value in red gives the Mahalanobis' squared distance between populations, lower value in black gives the Hotelling's t^2 *p*-value

Population	1	2	3	4	5	6	7	8	9	10	11	12
Aleut	Pu	SD	SL	Ch	Eg	CA	Au	Ibo	BA	Kh	Al	Sp
Pachacama	SD	Ch	At	SL	CA	Eg	Au	Ibo	BA	Al	Kh	Sp
Arikara	Ch	Au	SL	Pu	Ibo	Eg	Kh	BA	CA	At	Al	Sp
Chinese	SD	SL	Pu	Eg	BA	CA	Ibo	Au	At	Kh	Sp	Al
Australians	Eg	Kh	Al	SD	Ibo	SL	Ch	Pu	BA	CA	At	Sp
African Americans	CA	Ch	Ibo	SD	Sp	SL	Kh	Au	Eg	Pu	At	Al
Ibo	Kh	SL	Eg	Au	SD	Ch	BA	CA	Al	Pu	At	Sp
Andaman Islands	Au	Kh	Eg	SL	Ibo	SD	Ch	BA	Pu	CA	At	Sp
Sri Lankan	Eg	Ibo	Ch	Kh	Au	SD	CA	Pu	BA	At	Al	Sp
Khoisan	Eg	Ibo	Au	SL	Al	SD	Ch	BA	CA	Pu	At	Sp
Egyptian	SL	Kh	Au	Ibo	Ch	SD	Ai	CA	Pu	At	BA	Sp
Spitalfields	BA	Ch	CA	SL	Ibo	Eg	SD	Au	Kh	Al	Pu	At
Cauc. Americans	BA	Ch	SL	SD	Ibo	Pu	Eg	Au	Sp	Kh	At	Al

Table 6.13: Inter-population variation in the femur. The order of proximity in distance of each primary population sample from other samples in the dataset on the basis of their Mahalanobis squared distances, as shown in Table 6.12.

Number of Observations and Percent Classified into Group using 100% PCs														
From Group	Aleut	Peru	Arikara	Chinese	Australia	Af. Amer.	Ibo	Andam.	Sri Lanka	Khoisan	Egypt	Spitalfs.	Ca. Amer.	Total
Aleut	26 100	0 0	0 0	0 0	0 0	0 0	0 0	0 0	0 0	0 0	0 0	0 0	0 0	26 100
Peru	1 3.45	28 96.55	0 0	0 0	0 0	0 0	0 0	0 0	0 0	0 0	0 0	0 0	0 0	29 100
Arikara	0 0	0 0	33 97.06	0 0	1 2.94	0 0	0 0	0 0	0 0	0 0	0 0	0 0	0 0	34 100
Chinese	0 0	0 0	0 0	25 100	0 0	0 0	0 0	0 0	0 0	0 0	0 0	0 0	0 0	25 100
Australia	0 0	0 0	0 0	0 0	29 90.63	0 0	1 3.13	1 3.13	0 0	1 3.13	0 0	0 0	0 0	32 100
Af. Amer.	0 0	0 0	0 0	0 0	0 0	39 97.5	1 2.5	0 0	0 0	0 0	0 0	0 0	0 0	40 100
Ibo	0 0	0 0	0 0	0 0	1 7.14	0 0	12 85.71	0 0	1 7.14	0 0	0 0	0 0	0 0	14 100
Andaman	0 0	0 0	0 0	0 0	0 0	0 0	0 0	31 91.18	1 2.94	2 5.88	0 0	0 0	0 0	34 100
Sri Lanka	0 0	0 0	0 0	1 5.56	0 0	0 0	0 0	0 0	16 88.89	0 0	1 5.56	0 0	0 0	18 100
Khoisan	0 0	0 0	1 4.55	0 0	0 0	0 0	0 0	0 0	0 0	21 95.45	0 0	0 0	0 0	22 100
Egyptian	0 0	0 0	0 0	0 0	0 0	0 0	0 0	0 0	1 3.03	2 6.06	30 90.91	0 0	0 0	33 100
Spitalfs.	0 0	0 0	0 0	0 0	0 0	0 0	0 0	0 0	0 0	0 0	0 0	40 100	0 0	40 100
Ca. Amer.	0 0	0 0	1 2.5	1 2.5	0 0	0 0	0 0	0 0	0 0	0 0	0 0	0 0	38 95	40 100
Total	27 6.98	28 7.24	35 9.04	27 6.98	31 8.01	39 10.08	14 3.62	32 8.27	19 4.91	26 6.72	31 8.01	40 10.34	38 9.82	387 100

Table 6.14: Inter-population variation in the femur. Cross-validation with number and percentages of individuals from 13 populations based on 100% total variance. Upper figure denotes number; lower figure denotes percentage. Red figures denote number of individuals placed into their correct group.

Aleut	0												
Pachacama	0.28	0											
Arikara	0.26	0.4	0										
Chinese	0.72	0.46	0.75	0									
Australians	0.26	0.09	0.36	0.48	0								
African Americans	0.35	0.25	0.3	0.49	0.21	0							
Ibo	0.33	0.09	0.41	0.41	0.09	0.21	0						
Andaman Islands	0.32	0.13	0.37	0.43	0.11	0.18	0.1	0					
Sri Lankans	1.64	1.7	1.6	1.7	1.69	1.67	1.7	1.7	0				
Khoisan	0.18	0.16	0.26	0.57	0.12	0.21	0.18	0.17	1.67	0			
Egyptians	0.26	0.4	0.05	0.76	0.36	0.31	0.41	0.37	1.6	0.26	0		
Spitalfields	0.28	0.51	0.22	0.9	0.48	0.48	0.54	0.52	1.55	0.38	0.22	0	
Cauc. Americans	0.33	0.13	0.38	0.42	0.12	0.16	0.09	0.09	1.7	0.18	0.38	0.53	0
	Aleut	Pachac.	Arikara	Chinese	Aust.	Af. Amer.	Ibo	And. Islands	Sri Lanka	Khoisan	Egypt.	Spitalf.	Cauc. Amer.

Table 6.15: Inter-population variation in the femur. Procrustes distances between sample means of 13 populations. Correlation between Procrustes distances and Mahalanobis' distances generated by stepwise discriminant analysis (Table 6.12) is: $r = 0.25$; $p = 0.03$).

The Procrustes mean co-ordinates have been calculated from separate GPAs of each population sample and have been subjected to a joint GPA and PCA. The proportion and accumulated variance of the PCs generated in the analysis of population means is given in Table 6.16.

PCs	Proportion	Cumulative	PCs	Proportion	Cumulative
PC1	29.00	29.0	PC8	3.40	92.3
PC2	20.10	49.2	PC9	2.92	95.3
PC3	16.90	66.0	PC10	1.78	97.0
PC4	8.09	74.1	PC11	1.59	98.6
PC5	6.03	80.2	PC12	1.38	100.0
PC6	4.86	85.0			
PC7	3.91	88.9			

Table 6.16 Proportion and accumulative variance represented by PCs 1-12 which accounts for total sample variance for population means for the femur.

The first four PCs account for 74.1% of total variance in the sample and the exploration of morphological differences will concentrate on these four PCs.

Figure 6.2 shows the location of the thirteen population means on PC1 and PC2, which cumulatively account for nearly 50% of total variation. Figure 6.3 shows the morphology of the mean configuration warped to the extremes of PC1 and PC2. On PC1, the Spitalfields mean is placed at the extreme negative end of the scale with the Andaman Island mean at the positive extreme. The other populations are spread relatively evenly along PC1. PC1 explains a difference in position of the joint relative to the shaft in the mean configuration between the positive and negative extremes. As the image is morphed along PC1, the posterior region of the condyles (landmarks 17 and 23) appears to 'tilt' progressively in a relatively inferior direction. This difference in relative position is best indicated by the change in position of landmarks 25 and 26 (the points of maximum height on the medial and lateral condyles respectively) in Figures 6.3 and 6.4. At the same time, the mean configuration increases in relative width across the epicondyles (landmarks 19 and 24). Therefore, the Andaman Island mean at the positive extreme displays considerably greater mediolateral width with relatively greater protrusion of the medial epicondyle (landmark 24), relative to the Spitalfields mean at the negative extreme. The regions of the joint where the maximum differences in shape can be

Figure 6.2:

Inter-population variation in the femur in 13 populations. Bivariate plot of PC1 with PC2, showing a separation of 13 population means. Mean individuals inside the circle represent 6 of the 7 populations from year-round warm climates.

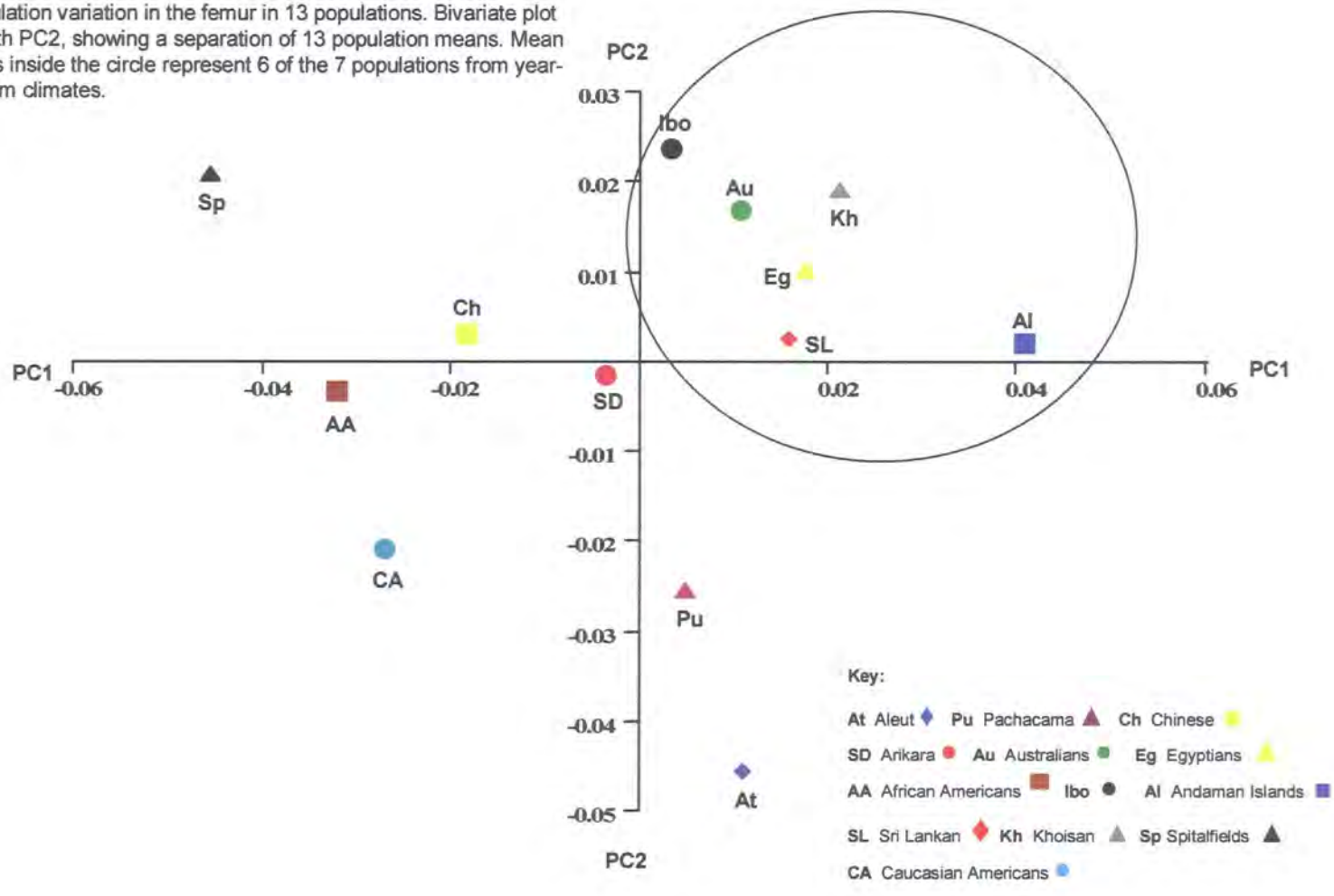

Figure 6.3:

Inter-population variation in the femur in 13 populations. Images represent the mean configuration if warped to the extremes of PCs 1 (at 0.06 and -0.06) and PC2 (at 0.03 and -0.05). Image at negative extreme of PC2 shows landmarks discussed in text (section 6.4.1a). The bivariate plot is shown in larger scale in Figure 6.2.

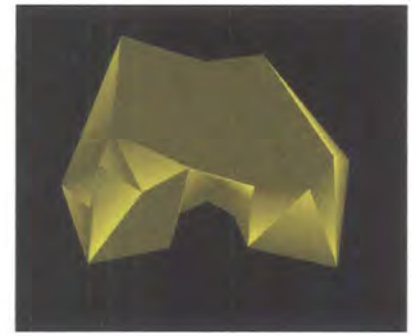

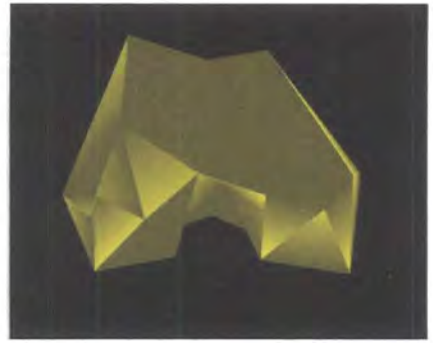

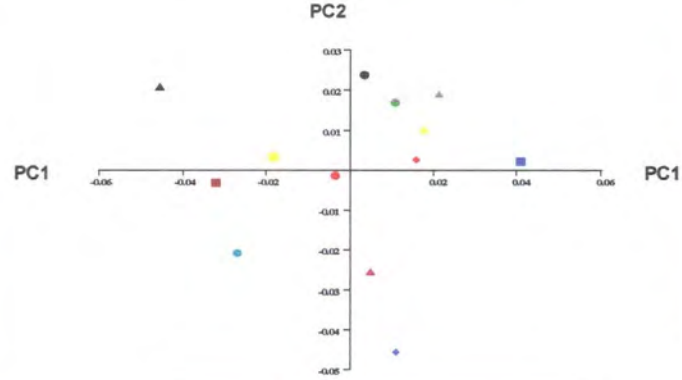

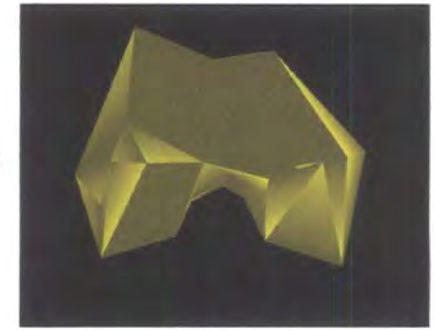

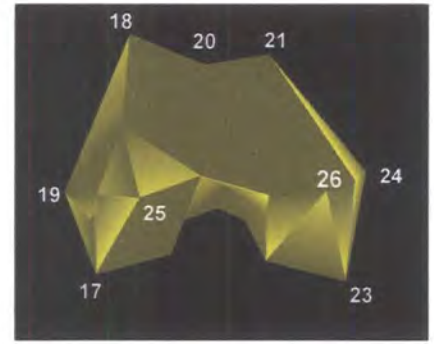

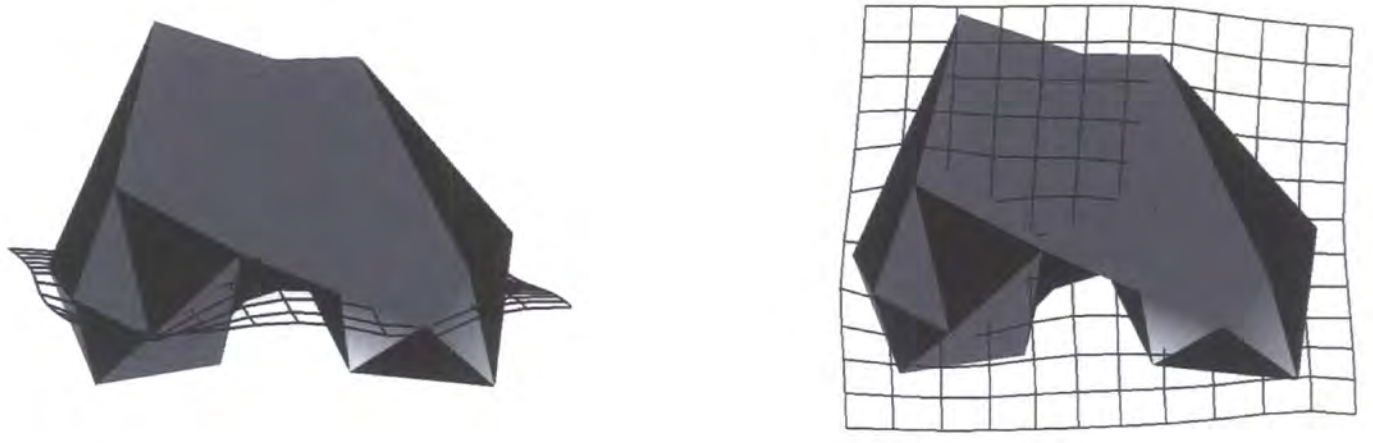

(a)

(b)

Figure 6.4: Inter-population variation in the femur in 13 populations. Representations of femoral shape with TPS taken from PC1 using sample means, showing regions of bone giving maximum difference in shape between the 13 populations (a) TPS view in anterior-posterior plane, (b) in distal plane. Images are presented to give the best indication of maximum difference in shape and are not necessarily taken from the same perspective as the mean configurations in Figure 6.2.

seen between all means, primarily those relating to the maximum height of the condyles and across the epicondyles, are highlighted by the deformation of the TPS in Figure 6.4.

PC2 explains a relative narrowing of the posterior proportions across the condyles, as the mean configuration is warped from positive to the negative extremes of the scale. Landmarks 17 and 23, indicating the greatest length of the condyles are positioned relatively more medially and laterally, giving the joint a relatively more squared shape in means at the negative extreme (Spitalfields and Ibo) relative to those at the positive end of the scale (culminating in the Aleut). This change in width across the condyles is balanced by an increase in width across the anterior proportions of the patella surface (landmarks 18, 20 and 21).

When PC1 is plotted against PC2, the scatter of means highlighted in the positive quadrant is a cluster from year-round warmer climates (the Ibo, Andaman Islanders, Sri Lankan, Khoisan and Egyptians and Australians). Remaining means are relatively distinct from this first group. The exception to the first, wholly warm-climate group of means is the Pachacama, which is placed at a distance from this initial group. The possible reason for this exclusion is that this sample may have originated from a colder more mountainous region away from the warm coastal region of recovery (see Chapter 2 section 2.1.2b).

Figure 6.5 shows the location of the thirteen populations on PC3 with PC4, which together account for nearly 25% of total variance. As the mean configuration is morphed along PC3 from the Sri Lankan and Ibo means at the positive extreme to the Spitalfields and Andaman Islanders means at the negative extreme, the image shows a relative reduction in the length of the condyles (landmarks 17 to 18 and 23 to 21). This reduction in length appears to be balanced by a relative increase in the depth of the joint from landmarks 12 to 25 and 13 to 26. At the same time, the joint becomes relatively more protruding and rotated towards the medial side. Thus, the Sri Lankan joint at the positive extreme is longer and narrower relative to that of the Andaman Island mean at the negative extreme.

Figure 6.5:

Inter-population variation in the femur in 13 populations. Bivariate plot of PC3 with PC4, showing a separation of 13 population means. Images represent the mean configuration if warped to the extremes of PC3 (at 0.04 and -0.06) and PC4 (at 0.03 and -0.02). Larger image at positive extreme of PC3 includes landmarks used in the text (section 6.4.1a). Figures in red denote landmarks 'behind' the image.

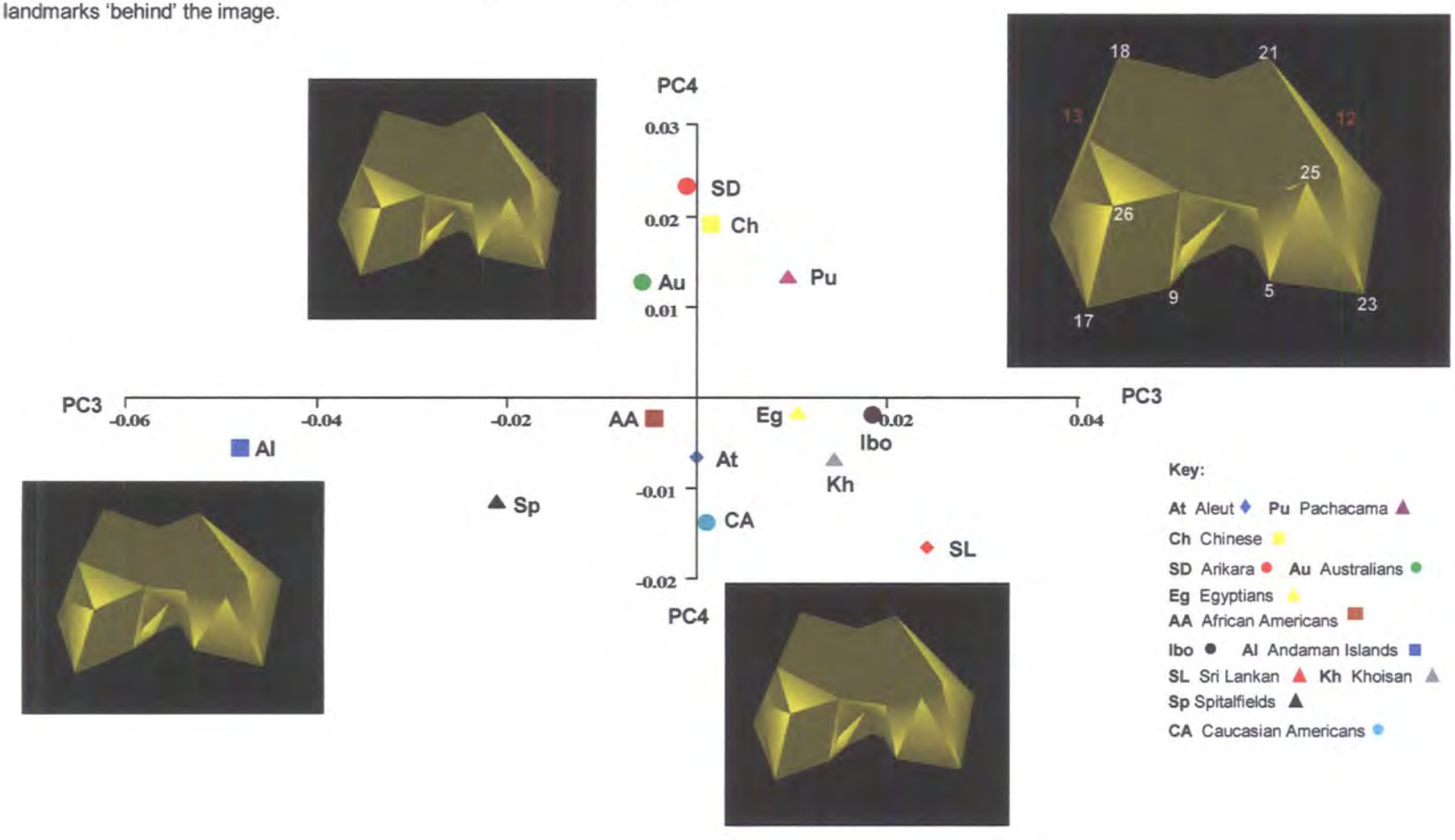

PC4 explains a relative decrease in width of the condyles and therefore the width of the intercondylar fossa (landmarks 17 to 23 and 5 to 9). Figure 6.5 shows the mean configuration warped to the two extremes of PC4 from the Arikaran mean at the positive extreme to the Sri Lankan mean at the negative extreme.

6.4.1b Tibia:

Differences in shape of the 369 specimens are analysed by GPA and subjecting the Procrustes fitted co-ordinates to PCA. Table 6.17 gives the proportional and accumulated variance for PCs 1 to 56, which represents the total variance within the sample. The scores for each specimen on the resultant PCs are then subjected to canonical discriminant analysis to establish the relationships between populations based upon the Mahalanobis' squared distances between population means.

For the tibia, the best separation of populations is achieved using 100% of total variance. This assessment was reached after separate discriminant and cross-validation analyses were carried out using PCs accounting for between c.50% to 100% of total variance. Results are summarised in Figures 6.6.

PCs	Prop.	Cumul.	PCs	Prop.	Cumul.	PCs	Prop.	Cumul.
PC1	21.00	21.00	PC21	1.27	81.20	PC41	0.42	96.20
PC2	8.02	29.00	PC22	1.18	82.40	PC42	0.39	96.60
PC3	6.63	35.60	PC23	1.15	83.50	PC43	0.37	96.90
PC4	5.64	41.30	PC24	1.10	84.60	PC44	0.35	97.30
PC5	4.77	46.00	PC25	1.06	85.70	PC45	0.34	97.60
PC6	3.80	49.80	PC26	1.02	86.70	PC46	0.31	97.90
PC7	3.63	53.50	PC27	0.95	87.70	PC47	0.30	98.20
PC8	2.99	56.50	PC28	0.86	88.50	PC48	0.27	98.50
PC9	2.93	59.40	PC29	0.81	89.30	PC49	0.26	98.70
PC10	2.82	62.20	PC30	0.78	90.10	PC50	0.22	99.00
PC11	2.36	64.60	PC31	0.71	90.80	PC51	0.21	99.20
PC12	2.18	66.80	PC32	0.65	91.50	PC52	0.21	99.40
PC13	2.07	68.80	PC33	0.64	92.10	PC53	0.18	99.60
PC14	2.03	70.80	PC34	0.60	92.70	PC54	0.16	99.70
PC15	1.68	72.50	PC35	0.59	93.30	PC55	0.15	99.90
PC16	1.65	74.20	PC36	0.55	93.80	PC56	0.12	100.00
PC17	1.57	75.70	PC37	0.50	94.30			
PC18	1.46	77.20	PC38	0.49	94.80			
PC19	1.38	78.60	PC39	0.47	95.30			
PC20	1.34	79.90	PC40	0.44	95.70			

Table 6.17: Inter-population variation in the tibia. The proportion and accumulated variance for PCs 1-56, which accounts for 100% of total variance.

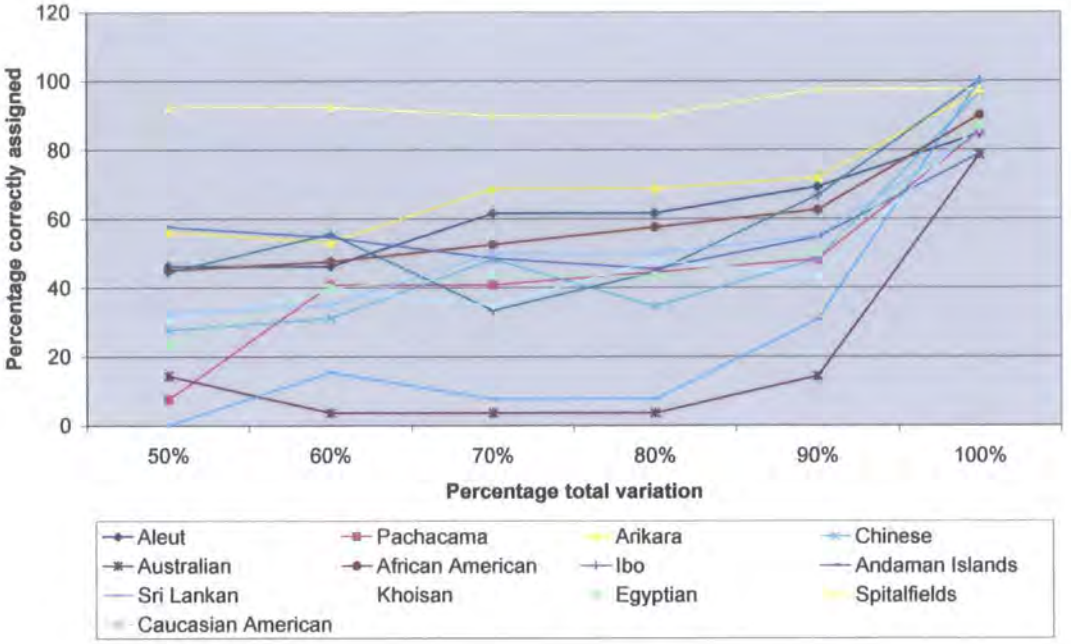

Figure 6.6 Inter-population variation in the tibia. Summary of separate discriminant and cross-validation analyses using PCs accounting for c.50% (PCs 1-6), 60% (PCs 1-9), 70% (PCs 1-14), 80% (PCs 1-20), 90% (PCs 1-30) and 100% (PCs 1-56).

The Mahalanobis' squared distances between population means, generated by a discriminant analysis, are shown in Table 6.18. All distances between populations are highly statistically significant indicating that groups can be separated on the basis of shape of the proximal tibia. Distances range from Mahalanobis' D^2 =9.98 between the Caucasian Americans and Chinese to MD^2 =72.63 between the Spitalfields sample and the Arikara.

Table 6.19 illustrates the relationship of each sample to all others on the basis of the generated Mahalanobis' squared distances by showing the distance of each primary sample to all others and ranking them accordingly from the closest sample (at position 1) to the furthest (at position 12). In all cases, the Spitalfields group lies at the greatest distance from all other populations. Distances between populations are generally smaller in the tibia than in the femur, with the notable exception of the Spitalfields population, which is even more distinct from the other samples. Table 6.20 shows the results of cross-validation analysis with population samples correctly assigned to groups, ranging from 78.57% for the Australians to 100% for the Ibo and Sri Lankans (the mean percentage correctly assigned to groups being 89.75%). These results indicate that, like the femur, the shape of the proximal tibia is specific to each population.

Aleut	0												
	1.000												
Pach.	16.20	0											
	0.0001	1.000											
Arikara	13.20	13.14	0										
	0.0001	0.0001	1.000										
Chinese	25.44	16.39	14.45	0									
	0.0001	0.0001	0.0001	1.000									
Australian	13.79	13.09	11.42	16.34	0								
	0.0001	0.0001	0.0001	0.0001	1.000								
African	28.03	22.52	22.14	19.86	18.34	0							
Americans	0.0001	0.0001	0.0001	0.0001	0.0001	1.000							
Ibo	39.80	30.13	33.62	30.15	22.81	24.24	0						
	0.0001	0.0001	0.0001	0.0001	0.0001	0.0001	1.000						
Andaman	22.94	26.92	29.91	34.22	17.24	30.12	32.23	0					
	0.0001	0.0001	0.0001	0.0001	0.0001	0.0001	0.0001	1.000					
Sri Lankan	30.45	22.35	27.02	24.34	18.14	22.23	30.02	22.85	0				
	0.0001	0.0001	0.0001	0.0001	0.0001	0.0001	0.0001	0.0001	1.000				
Khoisan	23.91	23.26	18.17	21.64	12.90	13.20	22.44	19.17	15.86	0			
	0.0001	0.0001	0.0001	0.0001	0.0001	0.0001	0.0001	0.0001	0.0005	1.000			
Egyptians	17.56	16.25	20.35	22.51	10.85	20.65	21.33	17.60	19.93	17.12	0		
	0.0001	0.0001	0.0001	0.0001	0.0001	0.0001	0.0001	0.0001	0.0001	0.0001	1.000		
Spitalfields	70.74	67.76	72.63	57.41	53.12	45.15	46.56	53.48	48.24	48.15	39.74	0	
	0.0001	0.0001	0.0001	0.0001	0.0001	0.0001	0.0001	0.0001	0.0001	0.0001	0.0001	1.000	
Caucasian	24.81	18.38	16.01	9.98	16.83	12.86	35.33	34.66	27.87	19.59	23.78	51.08	0
Americans	0.0001	0.0001	0.0001	0.0001	0.0001	0.0001	0.0001	0.0001	0.0001	0.0001	0.0001	0.0001	1.000
	Aleut	**Pach.**	**Arikara**	**Chinese**	**Aust.**	**Af Am**	**Ibo**	**Andam.**	**Sri L.**	**Khoi**	**Egypts.**	**Spitalfs.**	**Ca. Am**

Table 6.18: Inter-population variation in the tibia. Results from the canonical discriminant analysis of the 13 populations, on the basis of 100% variance.The upper value in red gives the Mahalanobis' squared distance between populations, lower value in black gives the Hotelling's t^2 *p*-value

Population	1	2	3	4	5	6	7	8	9	10	11	12
Aleut	SD	Au	Pu	Eg	Al	Kh	CA	Ch	BA	SL	Ibo	Sp
Pachacama	Au	SD	At	Eg	Ch	CA	SL	BA	Kh	Al	Ibo	Sp
Arikara	Au	Pu	At	Ch	CA	Kh	Eg	BA	SL	Al	Ibo	Sp
Chinese	CA	SD	Au	Pu	BA	Kh	Eg	SL	At	Ibo	Al	Sp
Australians	Eg	SD	Kh	Pu	At	Ch	CA	Al	SL	BA	Ibo	Sp
African Americans	CA	Kh	Au	Ch	Eg	SD	SL	Pu	Ibo	At	Al	Sp
Ibo	Eg	Kh	Au	BA	SL	Pu	Ch	SD	Al	CA	At	Sp
Andaman Islands	Au	Eg	Kh	SL	At	Pu	SD	BA	Ibo	Ch	CA	Sp
Sri Lankan	Kh	Au	Eg	BA	Pu	Al	Ch	SD	CA	Ibo	At	Sp
Khoisan	Au	BA	SL	Eg	SD	Al	CA	Ch	Pu	At	Ibo	Sp
Egyptian	Au	Pu	Kh	At	Al	SL	SD	BA	Ibo	Ch	CA	Sp
Spitalfields	Eg	BA	Ibo	Kh	SL	CA	Au	Al	Ch	Pu	At	SD
Cauc. Americans	Ch	BA	SD	Au	Au	Kh	Eg	At	SL	Al	Ibo	Sp

Table 6.19: Inter-population variation in the tibia. The order of proximity in distance of each primary population sample from other samples in the dataset on the basis of their Mahalanobis squared distances, as shown in Table 6.18.

Number of Observations and Percent Classified into Group using 100% PCs														
From Group	Aleut	Peru	Arikara	Chinese	Australia	Af. Amer.	Ibo	Andam.	Sri Lanka	Khoisan	Egypt	Spitalfs.	Ca. Amer.	Total
Aleut	22	0	2	0	0	0	0	0	1	0	1	0	0	26
	84.62	0	7.69	0	0	0	0	0	3.85	0	3.85	0	0	100
Peru	0	23	0	2	0	1	0	0	0	0	1	0	0	27
	0	85.19	0	7.41	0	3.7	0	0	0	0	3.7	0	0	100
Arikara	0	0	31	0	1	0	0	0	0	0	0	0	0	32
	0	0	96.88	0	3.13	0	0	0	0	0	0	0	0	100
Chinese	0	0	1	28	0	0	0	0	0	0	0	0	0	29
	0	0	3.45	96.55	0	0	0	0	0	0	0	0	0	100
Australia	0	1	1	0	22	0	0	2	1	0	1	0	0	28
	0	3.57	3.57	0	78.57	0	0	7.14	3.57	0	3.57	0	0	100
Af. Amer.	0	0	0	1	1	36	0	0	0	2	0	0	0	40
	0	0	0	2.5	2.5	90	0	0	0	5	0	0	0	100
Ibo	0	0	0	0	0	0	9	0	0	0	0	0	0	9
	0	0	0	0	0	0	100	0	0	0	0	0	0	100
Andaman	2	0	0	0	0	0	0	26	1	1	3	0	0	33
	6.06	0	0	0	0	0	0	78.79	3.03	3.03	9.09	0	0	100
Sri Lanka	0	0	0	0	0	0	0	0	13	0	0	0	0	13
	0	0	0	0	0	0	0	0	100	0	0	0	0	100
Khoisan	1	0	0	0	0	1	0	0	0	20	1	0	0	23
	4.35	0	0	0	0	4.35	0	0	0	86.96	4.35	0	0	100
Egyptian	1	0	1	1	0	0	0	0	0	1	26	0	0	30
	3.33	0	3.33	3.33	0	0	0	0	0	3.33	86.67	0	0	100
Spitalfs.	0	0	0	0	0	0	0	0	0	0	0	39	1	40
	0	0	0	0	0	0	0	0	0	0	0	97.5	2.5	100
Ca. Amer.	0	0	0	2	1	2	0	0	0	1	0	0	34	40
	0	0	0	5	2.5	5	0	0	0	2.5	0	0	85	100
Total	26	24	36	34	25	40	9	28	16	25	33	39	35	370
	7.03	6.49	9.73	9.19	6.76	10.81	2.43	7.57	4.32	6.76	8.92	10.54	9.46	100

Table 6.20: Inter-population variation in the tibia. Cross-validation with number and percentages of individuals from 13 populations based on 100% total variance. Upper figure denotes number; lower figure denotes percentage. Red figures denote number of individuals placed into their correct group.

As for the femur, the population means are used to help determine the specific morphologies of each sample and to explore the relationships between them because of the high number of specimens in the total sample and the high degree of overlap when using all specimens on the bivariate plots of selected PCs, when using the total sample. The Procrustes distances are calculated from separate GPAs of each population and then subjected to a joint GPA and PCA. The Procrustes distances between population means are shown in Table 6.21.

The Procrustes distances between population means show no significant correlation with the Mahalanobis' distances between the full population sample (r= 0.004; p=0.97). Therefore, the positions of means on the PC plots cannot be said to reveal the same relative shape relationships as would the full populations. It can be seen from Tables 6.18 and 6.19 and Figures 6.7 and 6.8 (using sample means, see below), however, that there is agreement between results of the two types of analyses regarding the relationship between the Spitalfields sample as conspicuously distant relative to all other samples. The Andaman Islanders' position is also seen as relatively distant to the remaining eleven populations and, to a lesser extent, that of the Ibo in analyses generated from both Mahalanobis' and Procrustes distances. As for the femur, an anomaly is seen in the high values for the Sri Lankan sample in Table 6.15 compared to the average values for this sample seen in Table 6.18 (see Chapter 2 section 2.1.2i and Discussion section 6.5.5c(iv) for a discussion and possible cause of this anomaly). The proportion and accumulated variance of the PCs generated in the analysis of population means is given in Table 6.22.

PCs	Proportion	Cumulative	PCs	Proportion	Cumulative
PC1	52.4	52.4	PC8	2.14	95.4
PC2	16.8	69.2	PC9	1.60	97.0
PC3	7.96	77.2	PC10	1.42	98.4
PC4	5.58	82.8	PC11	0.98	99.4
PC5	5.04	87.8	PC12	0.63	100
PC6	2.86	90.7			
PC7	2.55	93.2			

Table 6.22: Proportion and accumulative variance represented by PCs 1-12 which accounts for total sample variance for population means for the tibia.

Aleut	0												
Pachacama	0.30	0											
Arikara	0.42	0.63	0										
Chinese	0.76	0.68	0.68	0									
Australians	0.32	0.18	0.65	0.81	0								
African Americans	0.19	0.34	0.31	0.61	0.40	0							
Ibo	0.40	0.40	0.40	0.41	0.49	0.24	0						
Andaman Islands	0.19	0.20	0.46	0.65	0.25	0.19	0.29	0					
Sri Lankans	1.48	1.52	1.49	1.62	1.50	1.52	1.57	1.53	0				
Khoisan	0.14	0.29	0.37	0.68	0.31	0.13	0.30	0.12	1.51	0			
Egyptians	0.31	0.52	0.14	0.66	0.55	0.19	0.33	0.34	1.49	0.26	0		
Spitalfields	0.50	0.59	0.29	0.46	0.66	0.32	0.24	0.45	1.56	0.42	0.27	0	
Cauc. Americans	0.36	0.34	0.41	0.46	0.42	0.22	0.11	0.24	1.56	0.26	0.34	0.31	0
	Aleut	Pachac.	Arikara	Chinese	Aust.	Af. Amer.	Ibo	And. Islands	Sri Lanka	Khoisan	Egypt.	Spitalf.	Cauc. Amer.

Table 6.21: Inter-population variation in the tibia. Procrustes distances between sample means of 13 populations. Correlation between Procrustes distances and Mahalanobis' distances generated by stepwise discriminant analysis (Table 6.18) is not significant at: r = 0.004; p = 0.97).

The first four PCs account for 82.8% of total variance in the sample and the exploration of morphological differences will concentrate on these four PCs.

Figure 6.7 shows the location of the thirteen population means on PC1 and PC2, which cumulatively accounts for nearly 70% of total variance. Figure 6.8 shows the morphology of the mean configuration morphed to the extremes of PC1 and PC2. On PC1, most population means appear relatively tightly clustered, with the Arikara mean at the positive extreme closely followed by two groups of means; the Chinese, Pachacama and Caucasian Americans in one group and the Aleut, Khoisan, Australians and Sri Lankans in the second group. The Spitalfields mean is placed at the negative extreme of PC1, at a considerable distance from all other populations. The separation of the Spitalfields mean from the others on PC1 reinforces the distinctiveness of their morphology noted in the discriminant analysis of the total sample (Table 6.18).

The Spitalfields mean shows a relatively greater degree of depth of the anterior region, from the edge of the tibial plateau to the tibial tuberosity relative to that of other means (landmarks 3 to 14 and 9 to 14). This is accompanied by relatively greater depth of the lateral side of the tibial shelf from landmarks 9 to 15 and 11 to 15. This difference in morphology between means (primarily between the Spitalfields mean relative to that of the other means) is highlighted in Figure 6.9 by the deformation of the TPS around the anterior section of the joint. The angle of retroversion of the tibial knee joint relative to the shaft is considerably more obtuse in the Spitalfields joint compared to that of other populations. This relative increase in the angle is also accompanied by a relatively more rounded appearance in the tibial plateau as mediolateral width (landmarks 5 to 11 and 6 to 12) decreases relative to anteroposterior length (landmarks 3 to 4 and 9 to 10) and as the posterior section contracts under the tibial shelf. This difference in degree of retraction in the posterior region of the bone is seen in those means placed towards the negative extreme of the scale and again, primarily in the Spitalfields mean. This visualised difference in the posterior section of the tibial shelf is reinforced by the deformation of the TPS in the same posterior region, seen in Figure 6.9.

Figure 6.7:

Inter-population variation in the tibia in 13 populations. Bivariate plot of PC1 with PC2, showing a separation of 13 population means.

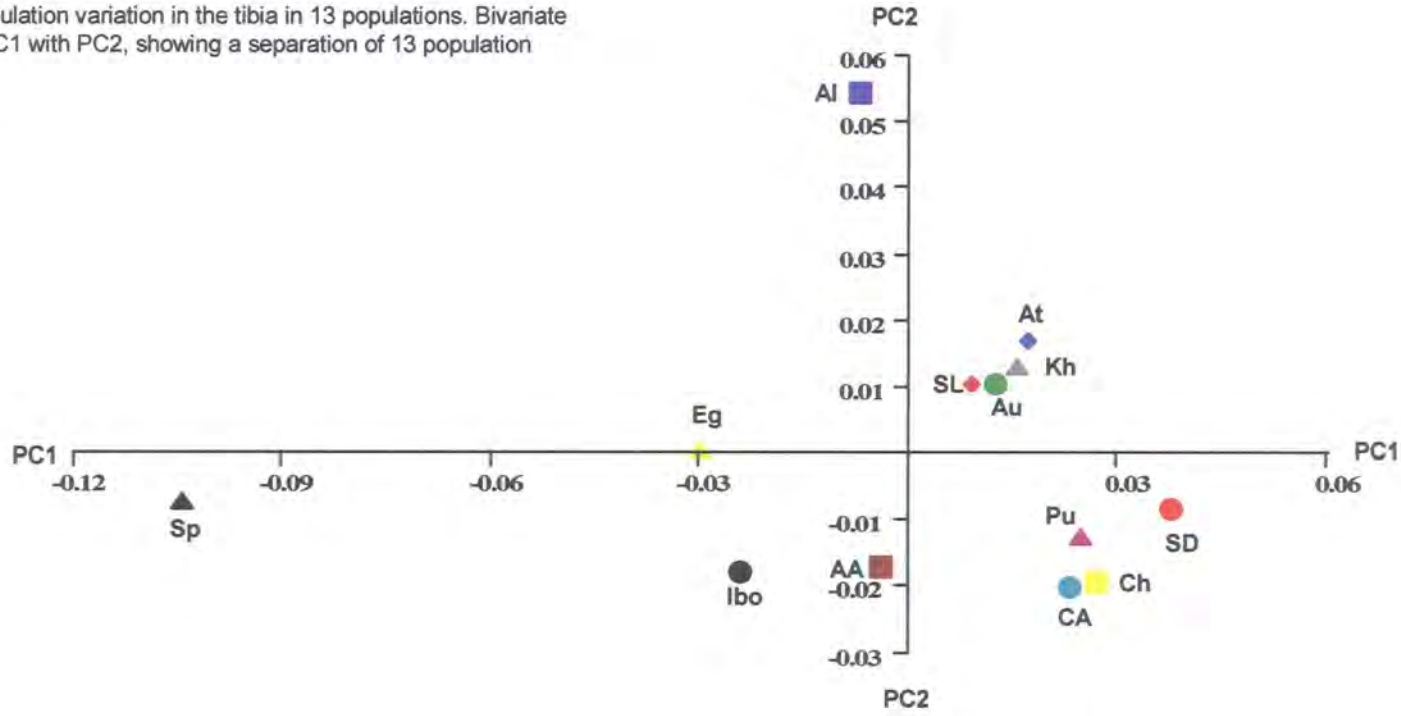

Key:

At Aleut Pu Pachacama Ch Chinese
SD Arikara Au Australians Eg Egyptians
AA African Americans Ibo Al Andaman Islands
SL Sri Lankan Kh Khoisan Sp Spitalfields
CA Caucasian Americans

Figure 6.8:

Inter-population variation in the tibia in 13 populations. Images represent the mean configuration if warped to the extremes of PCs 1 (at 0.06 and -0.012) and PC2 (at 0.06 and -0.03). Image at negative extreme of PC2 shows landmarks discussed in text (section 6.4.1b). The bivariate plot is shown in larger scale in Figure 6.7.

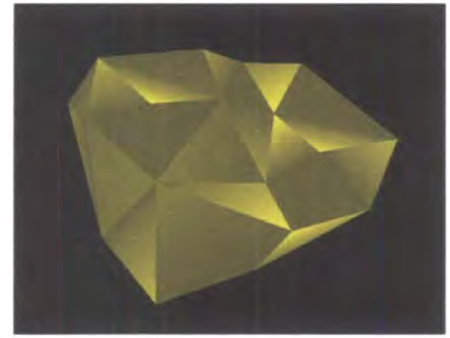

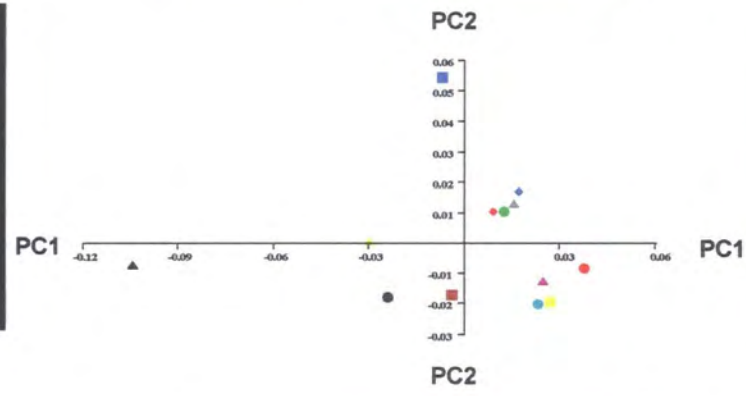

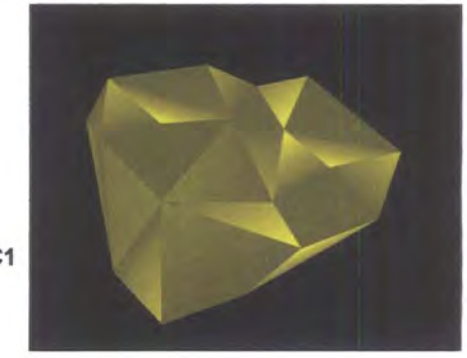

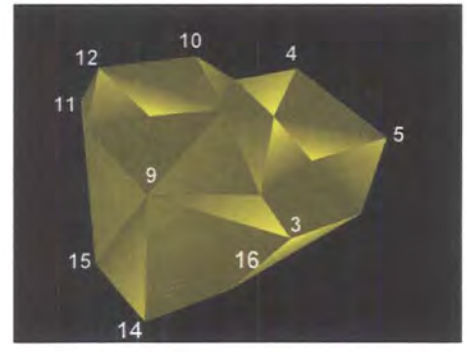

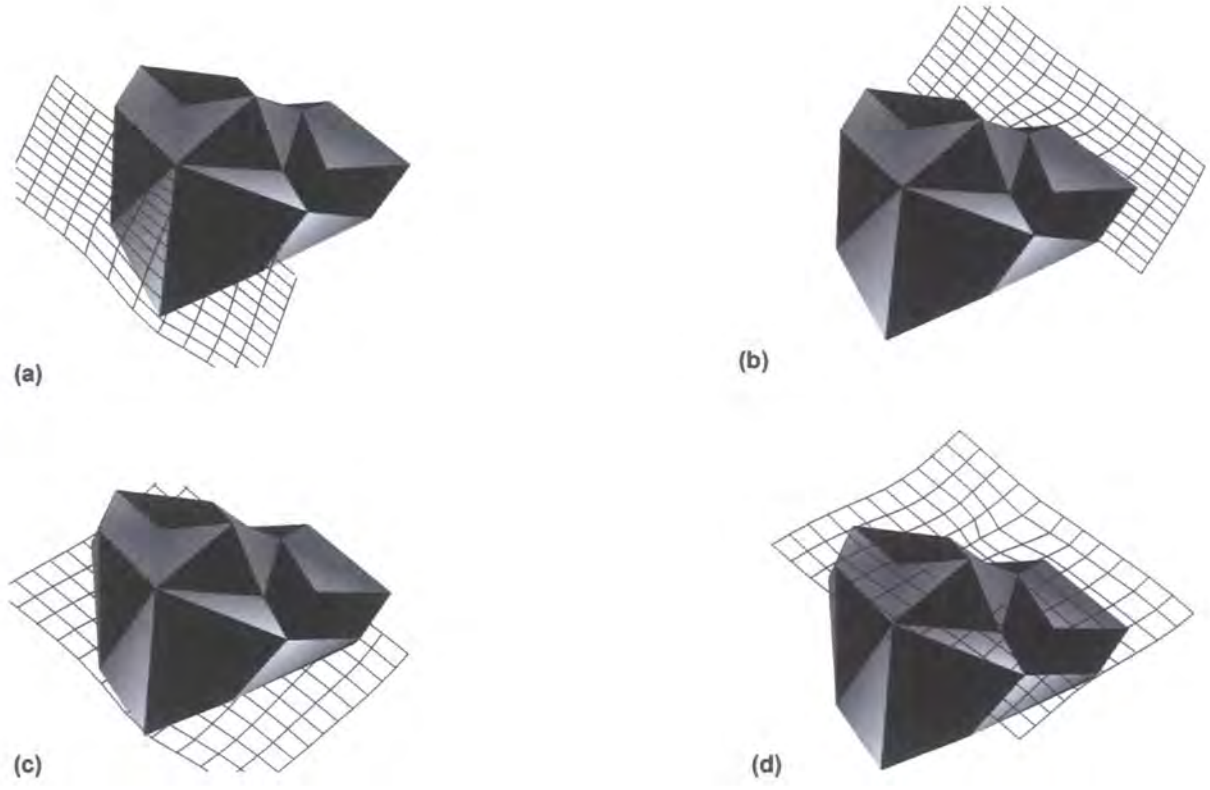

Figure 6.9; Inter-population variation in the tibia in 13 populations. Representations of tibial shape with TPS taken from PC1 using sample means, showing regions of bone giving maximum difference in shape between the 13 populations (a) and (b) in anterior-posterior plane, (c) and (d) in proximal plane. Images give the best indication of maximum difference in shape and are not necessarily taken from the same perspective as the mean configurations in Figure 6.7.

PC2 shows the Andaman Island mean placed at the positive extreme and at a considerable distance from all other means, thus driving the differences in shape for this PC. All other means, including the Spitalfields mean, are tightly clustered between the centre of the scale and the negative extreme. PC2 represents differences in anteroposterior length (landmarks 3 to 4 and 9 to 10), which increases as the mean configuration is morphed from the positive to negative extremes of PC2. This is particularly apparent on the medial side of the plateau.

Figure 6.10 shows PC3 with PC4, which together account for 13.54% of total variance and appears to explain slight differences between means in the alignment of the tibial plateau relative to the shaft. As the mean configuration is morphed along PC3, from the Caucasian American and Khoisan means at the negative extreme to the Ibo at the positive extreme, the lateral side of the bone is seen to project further anteriorly relative to the medial side. Thus, landmark 15 is positioned further forward in the Caucasian American and Khoisan means relative to landmark 16 in the Ibo mean. Along PC4, the Ibo mean lies at the positive extreme, at some distance from the other means, with the Australians, African Americans and Khoisan grouped together towards the centre of the scale and all other populations are tightly grouped from the centre towards the negative extreme. On PC4, shape differences highlighted as the mean configuration is warped between means, are subtle and appear to relate to a slight shift of the position of the tibial tuberosity towards the medial side.

6.4.2 Differences in the form of the knee joint and the size of the lower limbs.

Differences in the form of the knee joint rely both on differences in shape and differences in size. This section will test the relationship between the shape and centroid size of the knee joint. It will also examine the relationships and detail the results of comparisons, between the centroid size of the knee joint compared to the maximum length and robusticity indices of the shafts.

Figure 6.10:

Variation in the tibia in 13 populations. Bivariate plot of PC3 with PC4, showing a separation of sample means of 13 populations. Images represent the mean configuration if warped to the extremes of PC3 (at 0.04 and -0.04) and PC4 (at 0.03 and -0.02). Image at the negative extreme of PC3 includes landmarks used in the text (section 6.4.1b).

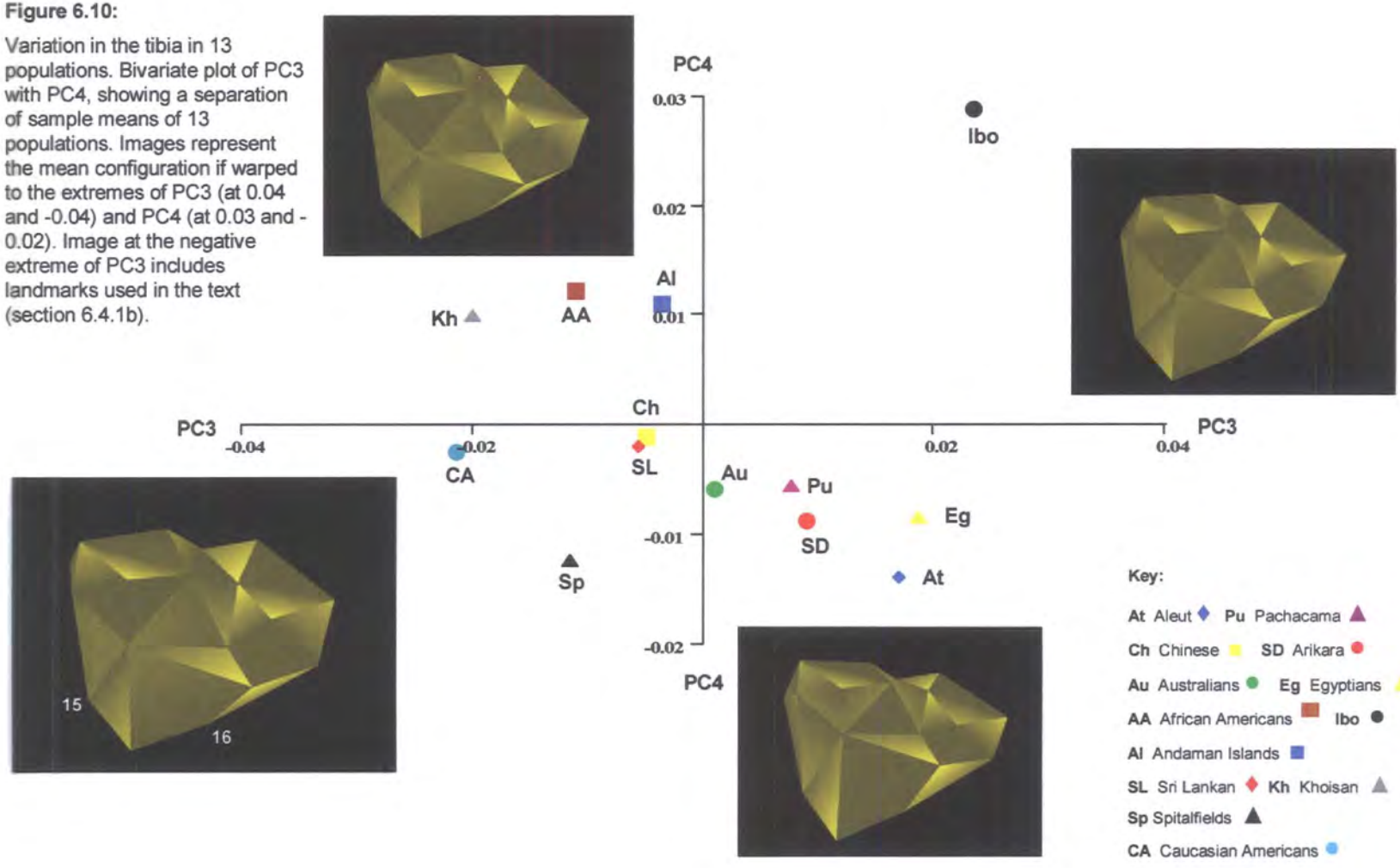

6.4.2a Femur: Differences in centroid size compared to shape

The centroid sizes of the femoral knee joint for the 387 specimens are calculated in GPA. Table 6.23 shows the pairwise comparisons of the centroid size of each sample against the other twelve; of the 78 comparisons, only 54 (69.23%) are significant. This contrasts with the results of the discriminant analysis (Table 6.12) where, Mahalanobis' squared distances between groups are statistically significant in 100% of comparisons. When distances between groups for centroid size are correlated with the Mahalanobis' squared distances between groups, results show no significant correlation ($r= 0.06$; $p= 0.63$).

These results indicate that centroid size and knee joint shape are independent variables and that larger distal femora are not hypermorphic versions of the same shapes of the smaller bones. Differences in shape are therefore not dependent on differences in size.

6.4.2b Femur: Centroid size of knee joint and maximum length measurements and robusticity indices of the diaphysis

The maximum length measurements (M2) and robusticity indices (RI) of the diaphysis are calculated for the 397 femoral specimens (Table 6.24). Table 6.25 shows results of correlation analyses conducted on the three measurements of centroid size of the knee joint, maximum length and robusticity of the shafts. Analyses between centroid size and length and robusticity measurements use only those 294 individuals with both digitised distal femora and measured leg bones. This table shows that for the total sample, centroid size is significantly correlated with both maximum length ($r=0.51$; $p<0.0001$) and robusticity ($r=0.31$; $p<0.0001$). The breakdown of populations, however, shows that the degree of correlation is not uniform, ranging from a strong correlation between centroid size and maximum length with no significant correlation between centroid size and robusticity in the Aleut and African Americans, and a relatively strong correlation between centroid size and both maximum length and robusticity in the Pachacama. Only in the Khoisan is centroid size more highly correlated with robusticity than with length.

	Aleut	Pach.	Arikara	Chinese	Aust.	Af Am	Ibo	Andam.	Sri L.	Khoi	Egypts.	Spitalfs.	Ca. Am
Aleut	0												
	1.000												
Pach.	10.34	0											
	0.0004	1.000											
Arikara	4.380	14.71	0										
	0.098	0.0001	1.000										
Chinese	2.700	7.640	7.070	0									
	0.239	0.002	0.003	1.000									
Australian	5.80	4.54	10.17	3.01	0								
	0.022	0.054	0.00002	0.141	1.000								
African	6.70	17.03	2.32	9.39	12.50	0							
Americans	0.033	0.0001	0.04	0.002	0.0001	1.000							
Ibo	5.22	5.12	9.60	2.52	0.58	11.92	0						
	0.191	0.172	0.009	0.461	0.861	0.006	1.000						
Andaman	19.46	9.12	23.84	16.76	13.66	26.16	14.24	0					
	0.0001	0.0002	0.0001	0.0001	0.0001	0.0001	0.0001	1.000					
Sri Lankan	20.39	10.06	24.77	17.70	14.60	27.09	15.17	0.93	0				
	0.0001	0.005	0.0001	0.0001	0.0001	0.0001	0.004	0.758	1.000				
Khoisan	11.98	1.64	16.35	9.28	6.18	18.67	6.76	7.49	8.42	0			
	0.001	0.612	0.0001	0.004	0.038	0.0001	0.151	0.012	0.050	1.000			
Egyptians	4.10	6.24	8.47	1.40	1.70	10.79	1.12	15.36	16.30	7.88	0		
	0.124	0.014	0.0006	0.554	0.444	0.0002	0.751	0.0001	0.0001	0.013	1.000		
Spitalfields	0.66	11.00	3.71	3.36	6.46	6.04	5.88	20.12	21.05	12.64	4.76	0	
	0.808	0.00005	0.127	0.178	0.007	0.003	0.113	0.0001	0.0001	0.0001	0.054	1.000	
Caucasian	2.51	12.85	1.86	5.21	8.31	4.18	7.73	21.97	22.91	14.49	6.61	1.85	0
Americans	0.359	0.0001	0.443	0.040	0.0007	0.127	0.04	0.0001	0.0001	0.0001	0.0008	0.451	1.000

Table 6.23: Inter-population variation in the femur. Pairwise comparisons of centroid size of the knee joint between 13 populations. Upper figures in red denote distance between population means in mm; lower figures in black denote Hotelling's t^2 *p*-values. Figures in blue denote results not statistically significant.

Population	Centroid size
Sri Lankan	130.62
Andaman Islands	131.55
Khoisan	139.04
Pachacama	140.68
Australian	145.22
Ibo	145.80
Egyptian	146.92
Chinese	148.32
Aleut	151.01
Spitalfields	151.68
Cauc. American	153.53
Arikara	155.39
African American	157.71

(a) Means of Centroid size

Population	M2 Length
Andaman Islands	384.96
Pachacama	395.28
Sri Lankan	400.67
Aleut	404.85
Khoisan	417.18
Chinese	427.96
Spitalfields	428.67
Arikara	430.55
Ibo	437.00
Egyptian	437.29
Cauc. American	437.97
African American	454.89
Australian	455.24

(b) Means of maximum length

Population	RI
Sri Lankan	5.57
Andaman Islands	5.74
Australian	5.82
Ibo	5.89
Egyptian	5.91
Khoisan	5.94
African American	6.13
Cauc. American	6.15
Arikara	6.18
Chinese	6.18
Spitalfields	6.29
Pachacama	6.39
Aleut	6.77

(c) Means of RI

Table 6.24: Inter-population variation in the femur. The means of the centroid sizes of the knee joint and of maximum length measurements (in mm) and robusticity indices of the diaphysis for the 13 populations, sorted in ascending order of size (sexes pooled).

Population	Centroid size v Length	Centroid size v Robusticity	Length v Robusticity
All Populations	0.51 **<0.0001**	0.31 **<0.0001**	0.68 **<0.0001**
Aleut	0.78 **<0.0001**	0.07 0.76	0.68 **<0.0001**
Pachacama	0.76 **0.0003**	0.55 **0.02**	0.57 **0.005**
Arikara	0.57 **0.006**	0.47 **0.03**	0.68 **<0.0001**
Chinese	0.15 0.50	0.35 0.10	0.47 **0.01**
Australian	0.04 0.85	0.19 0.36	0.62 **<0.0001**
African American	0.75 **<0.0001**	0.15 0.39	0.62 **<0.0001**
Ibo	0.03 0.92	0.20 0.52	0.65 **0.0002**
Andaman Islands	0.26 0.24	0.10 0.65	0.68 **<0.0001**
Sri Lankan	0.32 0.24	0.30 0.27	0.77 **<0.0001**
Khoisan	0.39 0.13	0.58 **0.02**	0.79 **<0.0001**
Egyptian	0.21 0.32	0.06 0.79	0.62 **<0.0001**
Spitalfields	0.71 **0.0009**	0.14 0.59	0.46 **<0.0001**
Caucasian American	0.57 **0.0002**	0.51 **0.001**	0.62 **<0.0001**

Table 6.25: Inter-population variation in the femur. Correlations between the centroid size of the knee joint and the maximum length (M2) and robusticity indices (RI) of the femoral shaft and between the maximum length and robusticity of the femoral shaft. Upper figure in red denotes the correlation co-efficient; lower figure in black denotes the associated *p*-values; bold indicates statistically significant results.

For the correlation between maximum length and robusticity indices in this context, only a simplified equation is used to signify robusticity (i.e., the transverse plus sagittal measurements), thus avoiding using maximum length within the robusticity index.

Table 6.25 also shows that maximum length is highly correlated with robusticity of the shaft in all samples. For the total sample, maximum length and robusticity is correlated at a high level of statistical significance (r=0.68; $p<0.0001$). For each population, correlation ranges between r=0.79, ($p<0.0001$) for the Khoisan to r=0.46, ($p<0.0001$) for the Spitalfields sample.

When comparing population means of these three measurements Table 6.24 demonstrates that, to some degree, the size of these measurements may be independently influenced by differing factors, either genetic or environmental, acting upon them. For example, although the Sri Lankans and Andaman Islanders remain consistently small throughout all three measurements, others such as the Aleut show wider variability, with moderate centroid size and femoral length but high robusticity. This aspect of comparability of size will be examined in section 6.5.3.

6.4.2c Tibia: Differences in centroid size compared to shape

The centroid sizes of the femoral knee joint of the 370 specimens are calculated in GPA. Table 6.26 shows the pairwise comparison of the difference in centroid size of each sample against the other twelve samples. It shows that of 78 comparisons, only 42 (53.85%) are significantly different. This contrasts with the results of the discriminant analysis shown in Table 6.18, where Mahalanobis' squared distances between groups are statistically significant in 100% of comparisons. When distances between samples for centroid size are correlated with the Mahalanobis' squared distances, results show no significant correlation (r= 0.03; p= 0.79).

As for the femur, results for the tibia indicate that centroid size and knee joint shape are independent variables and that larger proximal tibiae are not hypermorphic versions of the same shapes of the smaller bones. Differences in shape are therefore not dependent on differences in size.

Aleut	0												
	1.000												
Pach.	0.97	0											
	0.7120	1.000											
Arikara	6.850	7.82	0										
	0.007	0.002	1.000										
Chinese	0.930	0.040	7.780	0									
	0.663	0.986	0.0002	1.000									
Australian	3.55	2.59	10.40	2.62	0								
	0.174	0.30	0.0001	0.197	1.000								
African	7.77	8.74	0.92	8.70	11.32	0							
Americans	0.002	0.0004	0.680	0.0001	0.0001	1.000							
Ibo	4.51	3.54	11.36	3.58	0.96	12.28	0						
	0.261	0.352	0.003	0.209	0.799	0.002	1.000						
Andaman	14.00	13.04	20.85	13.07	10.45	21.77	9.49	0					
	0.0001	0.0001	0.0001	0.0001	0.0001	0.0001	0.002	1.000					
Sri Lankan	11.09	10.13	17.94	10.16	7.54	18.86	6.58	2.91	0				
	0.01	0.015	0.0001	0.004	0.061	0.0001	0.301	0.537	1.000				
Khoisan	5.43	4.46	12.28	4.50	1.88	13.20	0.92	8.57	5.66	0			
	0.072	0.121	0.0001	0.059	0.506	0.0001	0.833	0.0005	0.213	1.000			
Egyptians	1.51	0.54	8.36	0.58	2.04	9.28	3.00	12.49	9.58	3.92	0		
	0.517	0.807	0.0002	0.739	0.355	0.0001	0.359	0.0001	0.01	0.126	1.000		
Spitalfields	3.19	2.23	10.04	2.26	0.36	10.96	1.32	10.81	7.90	2.24	1.68	0	
	0.185	0.335	0.0001	0.246	0.874	0.0001	0.713	0.0001	0.031	0.388	0.417	1.000	
Caucasian	4.61	5.57	2.25	5.54	8.16	3.17	9.11	18.61	15.70	10.03	6.11	7.08	0
Americans	0.074	0.026	0.33	0.01	0.001	0.159	0.022	0.0001	0.0001	0.0005	0.007	0.0006	1.000
	Aleut	**Pach.**	**Arikara**	**Chinese**	**Aust.**	**Af Am**	**Ibo**	**Andam.**	**Sri L.**	**Khoi**	**Egypts.**	**Spitalfs.**	**Ca. Am**

Table 6.26: Inter-population variation in the tibia. Pairwise comparisons of centroid size of the knee joint between 13 populations. Upper figures in red denote distance between population means in mm; lower figures in black denote Hotelling's t^2 *p*-values. Figures in blue denote results not statistically significant.

6.4.2d Tibia: Centroid size of knee joint and maximum length measurements and robusticity indices of the diaphysis

The maximum length measurements (M2) and robusticity indices (RI) of the diaphysis are calculated for the 406 tibial specimens (Table 6.27). Table 6.28 shows results of correlation analyses conducted on the three measurements of centroid size of the knee joint, maximum length and robusticity of the shafts. Analyses between centroid size and length and robusticity measurements use only those 281 individuals with both digitised proximal tibiae and measured leg bones.

Table 6.28 shows that for the total sample, centroid size is correlated to a high level of statistical significance with maximum length (r=0.49, $p<0.0001$) and with robusticity (r=0.24; $p<0.0001$). The breakdown by population, however, shows that the degree of correlation is not uniform, following the same pattern of populations as for the femur. In no instance is centroid size more highly correlated with robusticity than with maximum length and a statistically significant correlation is reached in only two populations, the Pachacama and Caucasian Americans.

Table 6.28 shows that maximum length is highly correlated with robusticity of the shaft for the total sample at r=0.62, ($p<0.0001$) and in twelve of the thirteen samples, with the exception of the Ibo. For the remaining twelve populations, significant correlation ranges between r=0.48, ($p=0.008$) for the Chinese and r=0.82, ($p<0.0001$) for the Australians and Sri Lankans equally. The weak and statistically non-significant correlation at r=0.18, ($p=0.47$) for the Ibo appears to stem from exaggerated measurements for 5 of the 20 individuals in the sample (1 transverse and 4 sagittal measurements; used in the calculation of the robusticity index). Although the femora for this sample appear regular in shape and showed a strong correlation between maximum length and robusticity of the diaphyses (r= 0.65; $p= 0.0002$), measurements for the 5 irregular tibiae appear to have influenced results for this sample. The tibia with the exaggerated transverse measurement showed a 49.57% increase is size over the mean size for the remaining 19 individuals in the sample; the mean for the 4 individuals with the exaggerated sagittal measurements showed an increase over the mean for the remaining 16 individuals of 21.44%.

Population	Centroid size
Andaman Islands	115.08
Sri Lankan	117.99
Khoisan	123.66
Ibo	124.58
Australian	125.53
Spitalfields	125.89
Egyptian	127.57
Pachacama	128.12
Chinese	128.15
Aleut	129.08
Cauc. American	133.69
Arikara	135.94
African American	136.85

(a) Means of Centroid size

Population	M2 Length
Andaman Islands	322.68
Aleut	329.24
Pachacama	340.24
Chinese	340.83
Spitalfields	347.72
Sri Lankan	348.50
Khoisan	357.83
Arikara	361.85
Cauc. American	364.88
Ibo	375.00
Egyptian	377.05
Australian	378.11
African American	388.19

(b) Means of maximum length

Population	RI
Egyptian	6.91
Ibo	6.96
Andaman Islands	7.00
Khoisan	7.02
Sri Lankan	7.07
Australian	7.12
Cauc. American	7.49
African American	7.52
Pachacama	7.53
Arikara	7.67
Chinese	7.76
Spitalfields	7.90
Aleut	8.28

(c) Means of RI

Table 6.27: Inter-population variation in the tibia. The means of the centroid sizes of the knee joint and of maximum length measurements (in mm) and robusticity indices of the diaphysis for the 13 populations, sorted in ascending order of size (sexes pooled).

Population	Centroid size v Length	Centroid size v Robusticity	Length v Robusticity
All Populations	0.49 <0.0001	0.24 <0.0001	0.62 <0.0001
Aleut	0.73 0.0009	0.27 0.30	0.55 0.001
Pachacama	0.65 0.005	0.74 0.0008	0.62 0.002
Arikara	0.73 0.0003	0.23 0.329	0.69 <0.0001
Chinese	0.35 0.06	0.03 0.87	0.48 0.008
Australian	0.01 0.98	0.66 0.83	0.82 <0.0001
African American	0.71 <0.0001	0.03 0.86	0.54 <0.0001
Ibo	0.27 0.52	0.32 0.44	0.18 0.47
Andaman Islands	0.05 0.83	0.08 0.73	0.60 0.002
Sri Lankan	0.17 0.61	0.38 0.22	0.82 <0.0001
Khoisan	0.42 0.17	0.02 0.94	0.78 <0.0001
Egyptian	0.39 0.09	0.42 0.07	0.79 <0.0001
Spitalfields	0.26 0.18	0.26 0.18	0.50 <0.0001
Cauc. American	0.78 <0.0001	0.40 0.01	0.69 <0.0001

Table 6.28: Inter-population variation in the tibia. Correlations between the centroid size of the knee joint and the maximum length (M2) and robusticity indices (RI) of the femoral shaft and between the maximum length and robusticity of the femoral shaft Upper figure in red denotes the correlation co-efficient; lower figure in black denotes the associated *p*-values; bold indicates statistically significant results.

For the correlation between maximum length and robusticity indices in this context, only a simplified equation is used to signify robusticity (i.e., the transverse plus sagittal measurements), thus avoiding using maximum length within the robusticity index.

The individual with the exaggerated transverse measurement was not one of the four individuals with the exaggerated sagittal measurements; this specimen did not represent an abnormally large individual.

In the same manner as the femur, comparing sample means of these three measurements (Table 6.27) demonstrates that to some degree, the size of the measurements may be independently influenced by differing factors, either genetic or environmental, which may be acting upon them. Again, like the femur, although the Sri Lankans and Andaman Islanders remain consistently small for all three size measurements, others such as the Aleut show greater robusticity compared to centroid size or maximum length.

6.4.3 The femur in relation to the tibia: the shape and size of the knee joint and the size of the diaphyses

For the following analyses comparing the femur with the tibia, only those individuals are used which have matching right femora and right tibiae. For the comparisons of centroid size using the total sample, 235 individuals from twelve of the thirteen populations are used; the Pachacama are excluded because all femoral and tibial specimens are unmatched. For comparisons of centroid size between populations, four populations are excluded for having insufficient numbers of matching specimens; the Aleut, Ibo, Sri Lankans and Egyptians (although the small number of matched pairs are included in the total sample).

For the comparisons of maximum length and robusticity indices using the total sample, 264 individuals from twelve of the thirteen populations are used; again, the Pachacama are excluded because all femoral and tibial specimens are unmatched. For individual population comparisons, the Ibo are also excluded for having insufficient numbers of matched pairs, although the few available are included in the total sample.

For the correlation of the shape of the distal femur with the proximal tibia using the total sample, the Procrustes distances are calculated for each matched pair and compared using matrix correlation. Results show a highly statistically significant

correlation at r= 0.72, (p<0.0001). For comparisons of size measurements (Table 6.29) show results for all pairs.

In summary, using the total sample, these results indicate that within the knee joint there is a predictably close fit between the distal femur and proximal tibia, with both the shape and centroid size of each bone being highly correlated with that of the other. There is also a strong correlation between the maximum length measurements and the robusticity indices of the diaphyses.

Table 6.29(a) also shows that there is a highly significant and strong correlation in the centroid size of the femur against the tibia in the eight populations tested with little variability between them. The range of tibial centroid size as a percentage of femoral size shows only a 2.97% difference between all samples. Table 6.29(b) shows that for maximum length measurements there is also a strong and highly significant correlation between the two bones in the eleven populations tested. The tibio-femoral indices for the eleven populations tested lies between 80.30% for the Aleut and 86.43% for the Sri Lankans; a range of 6.13% between samples. The tibio-femoral index (tibial maximum length as a percentage of femoral maximum length) is recognised as a useful indicator in the prediction of racial affiliation (Rathbun and Buikstra, 1984).

Despite the strong and highly significant correlation of femoral against tibial robusticity indices for the total sample, Table 6.29(c) shows relatively wide variability between the eleven populations. The range of difference in robusticity lies between the Egyptians at 117.62% for tibial size as a percentage of femoral size and the Chinese at 126.77%; (a 9.15% difference). Correlation between the robusticity indices of three of the samples (the Arikara, Chinese and Australians) does not reach a level of statistical significance.

	Femur	Tibia	%Tp to Fd Cent. Size	Correlation r =	Correlation *p* =
All Populations	149.01	128.76	86.37	0.93	<0.0001
Arikara	154.97	136.50	88.08	0.95	<0.0001
Chinese	148.11	128.05	86.46	0.95	<0.0001
Australians	147.17	128.43	87.26	0.96	<0.0001
African Americans	155.74	134.56	86.40	0.98	<0.0001
Andaman Islanders	132.40	114.86	86.76	0.89	<0.0001
Khoisan	135.77	117.95	86.78	0.99	<0.0001
Spitalfields	151.17	128.66	85.11	0.94	<0.0001
Cauc. Americans	153.76	133.24	86.65	0.97	<0.0001

(a)

	Femur	Tibia	%Tp to Fd Max Length	Correlation r =	Correlation *p* =
All Populations	434.35	367.37	84.58	0.88	<0.0001
Aleut	413.00	331.63	80.30	0.80	0.02
Arikara	429.24	369.68	86.12	0.85	<0.0001
Chinese	427.91	354.45	82.83	0.87	<0.0001
Australians	454.43	386.71	85.10	0.93	0.002
African Americans	454.28	388.07	85.42	0.86	<0.0001
Andaman Islanders	381.56	323.22	84.71	0.92	<0.0001
Sri Lankans	407.18	351.94	86.43	0.97	<0.0001
Khoisan	412.81	353.19	85.56	0.93	<0.0001
Egyptians	430.53	370.59	86.07	0.83	<0.0001
Spitalfields	423.27	352.78	83.35	0.76	<0.0001
Cauc. Americans	440.66	365.00	82.83	0.93	<0.0001

(b)

	Femur	Tibia	%Tp to Fd Robusticity	Correlation r =	Correlation *p* =
All Populations	6.13	7.51	122.43	0.59	<0.0001
Aleut	6.61	8.28	125.27	0.80	0.02
Arikara	6.33	7.76	122.52	0.12	0.57
Chinese	6.13	7.78	126.77	0.07	0.75
Australians	5.96	7.12	119.46	0.64	0.12
African Americans	6.13	7.57	123.40	0.52	<0.0001
Andaman Islanders	5.77	7.01	121.61	0.72	0.00
Sri Lankans	5.71	6.83	119.73	0.56	0.02
Khoisan	6.02	7.19	119.47	0.73	0.00
Egyptians	5.93	6.98	117.62	0.57	0.02
Spitalfields	6.37	7.75	121.71	0.40	0.00
Cauc. Americans	6.16	7.56	122.75	0.73	<0.0001

(b)

Table 6.29: Inter-population variation between the femur and tibia. Comparison of (a) centroid size of the knee joint, (b) maximum length measurements and (c) robusticity indices of the femur against the tibia. Datasets include total sample.

6.4.4 Factors affecting the shape and size of the knee joint and the diaphysis

Results highlighted in sections 6.4.1a and 6.4.1b above indicate that the morphology of the knee joint is specific to each of the thirteen populations studied. This section seeks to determine which forces account for the variations in shape and size of the knee joint between different populations.

Previous research has indicated that several factors account for variability of bone morphology between populations, including:

1. Differences in climatic conditions (Howells, 1973, 1989; Van Vark, 1985; O'Rourke et al., 1985; and Cavelli-Sforza et al., 1994).
2. Differences due to ancestral history (Nei and Roychoudhury, 1974; O'Rourke et al., 1985; Cavelli-Sforza et al., 1994; Nei and Takezaki, 1996, Cavelli-Sforza, 2001; Dvornyk et al., 2003).
3. Differences in habitual use of footwear (Rossi, 2005; Trinkaus, 2005).
4. Differences in subsistence strategies (for example, Ruff and Hayes, 1983; Brock and Ruff, 1988; Bridges, 1989; Hawkey and Merbs, 1995; Larsen, 1995).
5. Nutrition and disease (Zanker, and Cooke, 2004).
6. A combination of some or all of the above factors.

For more detailed information about the thirteen populations, see Chapter 2, section 2.1.2.

6.4.4a Differences in climatic conditions

The climatic conditions experienced by the thirteen populations are shown in Table 6.30. All statistics are current and have been taken from worldclimate.com (2003). They are used to give an indication of the temperature, annual rainfall and altitude likely to have been experienced by the populations when living, although there may be differences between the two time periods (as for example, in relation to the Spitalfields sample, see Chapter 2 section 2.1.2l and Molleson and Cox, 1993). In addition, as the history of each group may not be sufficient to place them in an exact

Population	Country of Origin	Mean Annual Temperatures °C (average and range)	Average Temperature °C (mid-winter) (average and range)	Average Temperature °C (mid-summer) (average and range)	Average yearly rainfall in mm (average and range)	Altitude approx above sea level in metres (average and range)
Aleut	Aleutian Islands	2 (1.7 to 2.3)	-7.9 (-5.4 to -10.3)	12.8 (11.0 to 14.6)	1413 (416 to 2410)	29 (sea level to 59)
Pachacama	Peru	18.2	15.3	21.4	25	139
Arikara	South Dakota, USA	6.8	-10.6	23	418	525
Chinese	Northern China	7.6 (3.3 to 11.8)	-12.2 (-4.6 to -19.6)	24.0 (23.0 to 24.7)	634 (552 to 715)	93 (31 to 155)
Australians	Australia	20.2 (16.8 to 31.8)	14.4 (11.1 to 24.9)	25.4 (16.8 to 27.8)	896 (281 to 1,757)	281 (18 to 545+)
African Americans	St Louis, Missouri, USA	13.3	-1.5	26.5	940	176
Ibo	SE Nigeria	26.5 (21.3 to 31.8)	24.6 (24.4 to 24.9)	28.5 (28.1 to 28.9)	1,866 (1,740 to 1,991)	122 (41 to 203)
Andamanese	Andaman Islands	27.3	26.6	29.1	2,983	74
Sri Lankans	Sri Lanka	26.5 (24.7 to 27.6)	25.0 (23.6 to 26.3)	27.9 (26.1 to 29.7)	1,748 (1,255 to 2,241)	245 (3 to 487)
Khoisan	S and SW Africa	18.5 (17.5 to 20.1)	11.1 (10.1 to 11.7)	25.1 (23.1 to 27.7)	305 (189 to 420)	1,034 (850 to 1,218)
Egyptians	Egypt	24 (21 to 26.6)	14.5 (12.4 to 16.6)	31.0 (28.1 to 33.9)	27	68 (33 to 102)
Spitalfields	London, UK	11.7	5.5	18.9	752	23
Caucasian Americans	St Louis, Missouri, USA	13.3	-1.5	26.5	940	176

Table 6.30: Climate and Altitude experienced by the 13 populations. Data taken from WorldClimate.com (2003). Cities and regions from where data has been collected: **Aleut**: Bristol Bay and Chinik, Aleutian Islands, Alaska; **Pachacama:** Lima, Peru; **Arikara:** Mobridge, S. Dakota; **Chinese:** Beijing, Harbin and Shenyang, N. China; **Australians:** Alice Springs, Darwin, Adelaide and Perth, Australia; **African and Caucasian Americans:** St. Louis, Missouri, USA; **Ibo:** Lagos, Ibadan and Benin City, Nigeria; **Andaman Islanders**: Port Blair, S. Andaman; **Sri Lankans:** Colombo, Kandy and Jaffna, Sri Lanka; **Khoisan:** Upington, Kimberley, Okiep, South Africa and Karasburg, Namibia; **Egyptians:** Cairo and Aswan, Egypt; **Spitalfields:** London, England.

location, these statistics must remain broad indications only, for example, in relation to the Pachacama (see Chapter 2, section 2.1.2b).

6.4.4a(i) Femur: The shape and size of the knee joint in relation to climate

Figure 6.2, the bivariate plot of PC1 with PC2 using sample means, highlights a group of populations from year-round warm climates in the positive quadrant of the plot. This section therefore explores further the effect of three climatic variables on the shape and size of the knee joint: temperature (mean annual, mid-winter and mid-summer temperatures), annual rainfall and altitude.

Using the total sample, Table 6.31 shows the correlation of the first eight PCs (accounting for nearly 50% of total variance) taken from the analysis of shape, together with the centroid sizes of the distal femur taken from the analysis of size, against the three aspects of climate.

Table 6.31 shows that there is a statistically significant correlation between shape and climatic variables in 28 of the 40 comparisons, although many correlations remain relatively weak. Comparisons approaching moderate strength ($r<0.30$) include those between the scores of PC1 and mean annual temperature ($r= 0.40$; $p<0.0001$), PC1 and mid-winter temperatures ($r= 0.41$; $p<0.0001$) and PC1 and annual rainfall ($r= 0.33$; $p<0.0001$). Any significant correlations after PC6 are very weak and no significant correlations are registered beyond PC8.

Centroid size shows a significant and moderately strong correlation with mean annual temperatures ($r=0.45$; $p<0.0001$), mid-winter temperatures ($r=0.49$; $p<0.0001$) and a statistically significant but weaker correlation with annual rainfall ($r=0.29$, $p<0.0001$).

In these analyses, shape shows only a very weak correlation with altitude (PCs 1, 2, 3, 4 and 6) and centroid size shows no correlation with altitude.

Therefore, the most significant factors affecting the shape of the knee joint is temperature and, to a lesser extent, the amount of annual rainfall. More specifically,

Environment/ PCs	Mean Annual Temperature ^{0}C	Mid-Winter Temperature ^{0}C	Mid-Summer Temperature ^{0}C	Annual Rainfall in mm	Altitude in feet above sea level
PC1	**0.40**	**0.41**	**0.23**	**0.33**	**0.13**
	<0.0001	**<0.0001**	**<0.0001**	**<0.0001**	**0.01**
PC2	0.04	0.01	**0.10**	**0.25**	**0.19**
	0.38	0.82	**0.05**	**<0.0001**	**0.0001**
PC3	**0.27**	**0.24**	**0.25**	0.08	**0.1**
	<0.0001	**<0.0001**	**<0.0001**	0.10	**0.05**
PC4	**0.10**	**0.11**	0.02	**0.21**	**0.23**
	0.04	**0.03**	0.73	**<0.0001**	**<0.0001**
PC5	**0.14**	0.05	**0.25**	0.08	0.07
	0.007	0.29	**<0.0001**	0.12	0.14
PC6	**0.22**	**0.28**	0.01	**0.11**	**0.1**
	<0.0001	**<0.0001**	0.81	**0.02**	**0.05**
PC7	**0.18**	**0.19**	0.08	**0.12**	0.02
	0.005	**0.0002**	0.11	**0.02**	0.64
PC8	0.05	0.06	0.02	**0.10**	**0.12**
	0.36	0.2	0.72	**0.05**	**0.02**
Centroid size	**0.45**	**0.49**	**0.19**	**0.29**	0.05
	<0.0001	**<0.0001**	**0.0002**	**<0.0001**	0.31

Table 6.31: Inter-population variation in the femur. Correlations between scores of PCs 1 to 8 (using total sample), accounting for 48.10% of total variation with aspects of climate and altitude and of the centroid size of the knee joint with aspects of climate and altitude Upper figures in red denote the correlation statistic, r; lower figures in black denote the associated *p* value. Bold figures indicate statistically significant correlations.

in those PCs where mean annual temperature shows a significant and strong correlation, with only one exception, mid-winter temperatures show an even stronger degree of correlation, with mid-summer temperatures remaining correlated to a lesser degree. These results therefore indicate that cold temperature has a greater effect in shaping the femoral knee joint than warm temperature.

In relation to centroid size, Table 6.32 ranks the means of centroid sizes in ascending order against mid-winter temperatures. The thirteen populations are loosely divided into two categories; those with colder mid-winter temperatures (the Aleut, Arikara, Chinese, African and Caucasian Americans and the Spitalfields group) and those from year-round warmer climates (the Pachacama, Australians, Ibo, Sri Lankans,

Khoisan and Egyptians). This table shows that the populations from warmer winter climates are also those with smaller femoral knee joints. Thus temperature, and more specifically cold winter temperature, constitutes an important factor influencing the size of the knee joint.

Population	Centroid size	Mid-Winter Temps ^{0}C	Winter Climates
Sri Lankan	130.62	25.0	Warmer
Andaman Islands	131.55	26.6	Warmer
Khoisan	139.04	11.1	Warmer
Pachacama	140.68	15.3	Warmer
Australian	145.22	14.4	Warmer
Ibo	145.80	26.3	Warmer
Egyptian	146.92	14.5	Warmer
Chinese	148.32	-12.2	Colder
Aleut	151.01	-7.9	Colder
Spitalfields	151.68	5.5	Colder
Cauc. American	153.53	-1.5	Colder
Arikara	155.39	-10.6	Colder
African American	157.71	-1.5	Colder

Table 6.32: Populations sorted in ascending order of centroid size of the femur in relation to mid-winter temperatures.

6.4.4a(ii) Femur: Maximum length and robusticity of the diaphysis in relation to climate

Table 6.33 shows the correlation of maximum length and robusticity indices of the femur against the three features of the climate:

Measures	Mean Annual Temps. °C	Mid-Winter Temperature °C	Mid-Summer Temperature °C	Annual Rainfall in mm	Altitude in feet above sea level
M2	0.11	0.27	0.25	0.20	0.03
	0.01	<0.0001	<0.0001	<0.0001	0.56
RI	0.40	0.31	0.41	0.14	0.04
	<0.0001	<0.0001	<0.0001	0.001	0.33

Table 6.33: Maximum length and robusticity indices of the femur correlated with the three features of the climate. Upper figures in red denote the correlation coefficient; lower figures in black denote the associated *p* value. Bold figures indicate statistically significant correlations.

Table 6.33 shows that temperature and rainfall are more strongly correlated with size measurements than altitude and that the robusticity of the femoral shaft appears to be more greatly influenced by temperature than its length. This is clearly seen in Table 6.34 which uses the two categories previously used for the analysis comparing centroid size and mid-winter temperatures.

Although no clear pattern emerges in relation to maximum length, the populations with smaller robusticity indices are those from warmer mid-winter climates, with the one exception of the Pachacama. It is not know whether the Pachacama specimens originated from much colder regions than the year-round warm Pachacamac site. If so, this may provide insight into this exception (Chapter 2 section 2.1.2b).

6.4.4.a(iii) Tibia: The shape and size of the knee joint in relation to climate

Using the total sample, Table 6.35 shows the correlation of the first eight PCs (accounting for 56.5% of total variance) taken from the analysis of shape and the centroid size of the proximal tibia taken from the analysis of size, against the three climatic variables.

Table 6.35 shows that there is a statistically significant correlation between shape and climatic variables in 13 of the 40 comparisons, although many remain relatively weak. Comparisons approaching moderate strength ($r<0.3$) include those between PC1 and altitude ($r= 0.32$; $p<0.0001$), PC2 and mean annual temperature ($r= 0.30$; $p<0.0001$), PC2 and mid-winter temperature ($r= 0.37$; $p<0.0001$), PC2 and annual rainfall ($r= 0.42$; $p<0.0001$), PC3 and annual rainfall ($r= 0.32$; $p<0.0001$) and PC8 and altitude ($r=0.30$; $p<0.0001$). No significant correlations are registered beyond PC8 for any of the three climatic variables.

Like the femur, the tibia shows a significant and moderate correlation between shape and temperature and more specifically with mid-winter temperature (PC2). There is also a stronger correlation between shape and annual rainfall (PCs 2 and 3) and shape and altitude (PCs 1 and 8) in the tibia compared to the femur.

Population	M2 Length	Mid-Winter Temps ^{0}C	Winter Climates
Andaman Isles	384.96	26.6	Warmer
Pachacama	395.28	15.3	Warmer
Sri Lankan	400.67	25.0	Warmer
Aleut	404.85	-7.9	Colder
Khoisan	417.18	11.1	Warmer
Chinese	427.96	-12.2	Colder
Spitalfields	428.67	5.5	Colder
Arikara	430.55	-10.6	Colder
Ibo	437.00	26.3	Warmer
Egyptian	437.29	14.5	Warmer
Cauc. American	437.97	-1.5	Colder
African American	454.89	-1.5	Colder
Australian	455.24	14.4	Warmer

(a)

Population	RI	Mid-Winter Temps ^{0}C	Winter Climates
Sri Lankan	5.57	25.0	Warmer
Andaman Isles	5.74	26.6	Warmer
Australian	5.82	14.4	Warmer
Ibo	5.89	26.3	Warmer
Egyptian	5.91	14.5	Warmer
Khoisan	5.94	11.1	Warmer
African American	6.13	-1.5	Colder
Cauc. American	6.15	-1.5	Colder
Arikara	6.18	-10.6	Colder
Chinese	6.18	-12.2	Colder
Spitalfields	6.29	5.5	Colder
Pachacama	6.39	15.3	Warmer
Aleut	6.77	-7.9	Colder

(b)

Table 6.34: Inter-population variation in the femur. Populations sorted in ascending order of size for (a) maximum length measurements and (b) robusticity indices of the diaphysis in relation to mid-winter temperatures

Environment/ PCs	Mean Annual Temperature ^{0}C	Mid-Winter Temperature ^{0}C	Mid-Summer Temperature ^{0}C	Annual Rainfall in mm	Altitude in feet above sea level
PC1	**0.10**	**0.20**	**0.12**	0.14	**0.32**
	0.05	**0.0001**	**0.02**	0.78	**<0.0001**
PC2	**0.30**	**0.37**	0.07	**0.42**	0.01
	<0.0001	**<0.0001**	0.17	**<0.0001**	0.81
PC3	**0.15**	**0.18**	0.06	**0.32**	0.04
	0.003	**0.0004**	0.27	**<0.0001**	0.49
PC4	0.07	0.07	0.07	0.05	0.07
	0.19	0.21	0.20	0.33	0.17
PC5	0.08	0.04	**0.13**	**0.12**	**0.09**
	0.13	0.44	**0.01**	**0.02**	**0.09**
PC6	0.06	0.04	0.08	0.02	0.03
	0.25	0.43	0.15	0.64	0.51
PC7	0.04	0.09	0.08	0.04	0.16
	0.45	0.09	0.13	0.50	0.76
PC8	0.03	0.03	0.03	0.04	**0.30**
	0.52	0.63	0.51	0.47	**<0.0001**
Centroid size	**0.37**	**0.43**	0.09	**0.32**	0.04
	<0.0001	**<0.0001**	0.07	**<0.0001**	0.45

Table 6.35: Inter-population variation in the tibia. Correlations between scores of PCs 1 to 8, accounting for 56.50% of total variation, with aspects of climate and altitude and of the centroid size of the knee joint with aspects of climate and altitude Upper figures in red denote the correlation statistic, r; lower figures in black denote the associated *p* value. Bold figures indicate statistically significant correlations.

Centroid size shows a significant and moderate correlation with annual temperature (r= 0.36; $p<0.0001$), especially mid-winter temperature (r= 0.42; $p<0.0001$) and a significant and moderate correlation with annual rainfall (r=0.31; $p<0.0001$). It therefore appears that tibial shape is influenced by cold temperatures, annual rainfall and altitude. The most significant factors affecting centroid size are cold temperatures and annual rainfall.

Table 6.36 ranks the population means of centroid size in ascending order against the mid-winter temperatures. The thirteen populations are again divided into two categories; those from colder mid-winter climates (the Aleut, Arikara, Chinese,

African and Caucasian Americans and the Spitalfields group) and those from year-round warmer climates (the Pachacama, Australians, Ibo, Sri Lankans, Khoisan and Egyptians). Like the femur, this table shows that the populations from warmer winter climates are also those with smaller proximal tibiae with one notable exception (Spitalfields).

Population	Centroid size	Mid-Winter Temps ^{0}C	Winter Climates
Andaman Islands	115.082	26.6	Warmer
Sri Lankan	117.992	25.0	Warmer
Khoisan	123.656	11.1	Warmer
Ibo	124.575	26.3	Warmer
Australian	125.532	14.4	Warmer
Spitalfields	125.893	5.5	Colder
Egyptian	127.575	14.5	Warmer
Pachacama	128.118	15.3	Warmer
Chinese	128.154	-12.2	Colder
Aleut	129.083	-7.9	Colder
Cauc. American	133.689	-1.5	Colder
Arikara	135.937	-5.2	Colder
African American	136.855	-1.5	Colder

Table 6.36: Populations sorted in ascending order of centroid size of the tibia in relation to mid-winter temperatures.

Like Table 6.32 for the femur, Table 6.36 emphasises that temperature and more specifically cold temperature, constitutes an important factor in influencing the size of the knee joint.

6.4.4a(iv) Tibia: Maximum length and robusticity of the shaft in relation to climate

Table 6.37 shows the correlation of maximum length and robusticity indices of the tibia against the three features of the climate. Results show that temperature affects size measurements to a greater degree than either rainfall or altitude and, like the femur, the robusticity of the tibial shaft appears to be more greatly influenced by temperature than its length. This is clearly seen in Table 6.38, which uses the two categories previously used for the analysis comparing centroid size and mid-winter temperatures.

As with the femur, although no clear pattern emerges in relation to maximum length, the populations with smaller robusticity indices are those from warmer mid-winter climates with, like the femur, the same exception of the Pachacama.

Measures	Mean Annual Temps. °C	Mid-Winter Temperature °C	Mid-Summer Temperature °C	Annual Rainfall in mm	Altitude in feet above sea level
M2	0.08	0.08	0.34	0.18	0.09
	0.09	**0.05**	**<0.0001**	**<0.0001**	**0.03**
RI	0.51	0.42	0.44	0.04	0.08
	<0.0001	**<0.0001**	**<0.0001**	0.39	**0.05**

Table 6.37: Maximum length and robusticity indices for the tibia correlated with the three features of the climate. Figures in black denote the correlation co-efficient; lower figures in red denote the associated *p* values. Bold figures indicate statistically significant correlations.

6.4.4b Ancestral history

Ancestral (or geographical) groupings and genetic affiliations are conspicuously difficult to determine, although scientists have continually striven to categorise and cluster different populations into allied groups on the basis of either similarity of morphology or similarity of genotypes. Using six traditional and broad groupings based on ancestry, the thirteen populations in this study have been placed into the categories shown in Table 6.39. Such categories will always be subject to much debate, with some populations fitting uneasily into any major grouping as, for example the Khoisan, Sri Lankan and Andaman Islanders. Admixture with other populations in the recent past will also affect how accurately a group can be placed into a particular category (see Chapter 2 section 2.1.2f; Weiss and Mann, 1989).

Population	M2 Length	Mid-Winter Temps ^{0}C	Winter Climates
Andaman Islands	322.68	26.6	Warmer
Aleut	329.24	-7.9	Colder
Pachacama	340.24	15.3	Warmer
Chinese	340.83	-12.2	Colder
Spitalfields	347.72	5.5	Colder
Sri Lankan	348.50	25.0	Warmer
Khoisan	357.83	11.1	Warmer
Arikara	361.85	-10.6	Colder
Cauc. American	364.88	-1.5	Colder
Ibo	375.00	26.3	Warmer
Egyptian	377.05	14.5	Warmer
Australian	378.11	14.4	Warmer
African American	388.19	-1.5	Colder

(a)

Population	RI	Mid-Winter Temps ^{0}C	Winter Climates
Egyptian	6.91	14.5	Warmer
Ibo	6.96	26.3	Warmer
Andaman Islands	7.00	26.6	Warmer
Khoisan	7.02	11.1	Warmer
Sri Lankan	7.07	25.0	Warmer
Australian	7.12	14.4	Warmer
Cauc. American	7.49	-1.5	Colder
African American	7.52	-1.5	Colder
Pachacama	7.53	15.3	Warmer
Arikara	7.67	-10.6	Colder
Chinese	7.76	-12.2	Colder
Spitalfields	7.90	5.5	Colder
Aleut	8.28	-7.9	Colder

(b)

Table 6.38: Inter-population variation in the tibia. Populations sorted in ascending order of size for (a) maximum length measurements and (b) robusticity indices of the diaphysis in relation to mid-winter temperatures.

Population	Ancestral Derivation	Region of Origin
Chinese	Northern Asian	Northern China
Aleut	Amerindian	Alaska, USA
Pachacama	Amerindian	Peru, S. America
Arikara	Amerindian	South Dakota, USA
African American	Sub-Saharan African	Western and Central Africa
Ibo	Sub-Saharan African	Nigeria
Khoisan	Sub-Saharan African	Southern and S.W. Africa
Australian	Australian Aborigine	Australia
Andaman Islanders	South East Asian	Andaman Islands, India
Sri Lankan	Indian Subcontinent	Sri Lanka
Egyptian	North African Caucasian	Egypt
Spitalfields	European Caucasian	Northern Europe
Caucasian American	European Caucasian	Northern Europe

Table 6.39: Categorisation of the thirteen populations into groups of ancestral affiliation.

6.4.4b(i) Femur: The form of the knee joint in relation to ancestry

Table 6.13, which is based upon the Mahalanobis' squared distances between groups, indicates relatively few correlations with evolutionary or genetic histories, although for the four associated North Asian (Chinese) and Amerindian populations, all allied samples are positioned within the first four positions relative to the primary sample (with the exception of the Aleut in two instances). Two of the three Sub-Saharan African samples, the Ibo and Khoisan are positioned relatively closely. The three Caucasian populations (Egyptians, Spitalfields and Caucasian Americans) are not conspicuously associated.

To test the association between knee joint shape and ancestral history further, a discriminant analysis is carried out using the same 387 specimens used in section 6.4.1a. In this analysis the thirteen population samples are grouped into the six ancestral groupings shown in Table 6.39. The data is analysed after GPA by subjecting the Procrustes fitted co-ordinates to PCA. Table 6.11 gives the proportional and accumulated variance for PCs 1 to 71, which represents the total

variance within the sample. The scores for each specimen on the resultant PCs are then subjected to canonical discriminant analysis to establish the relationships between ancestral groups based upon the Mahalanobis' squared distances between group means. For the femur, the best separation of ancestral groups is achieved using 100% of total variance. This assessment was reached after separate discriminant and cross-validation analyses were carried out using PCs accounting for between c.50% to 100% of total variance. Results are summarised in Figure 6.11.

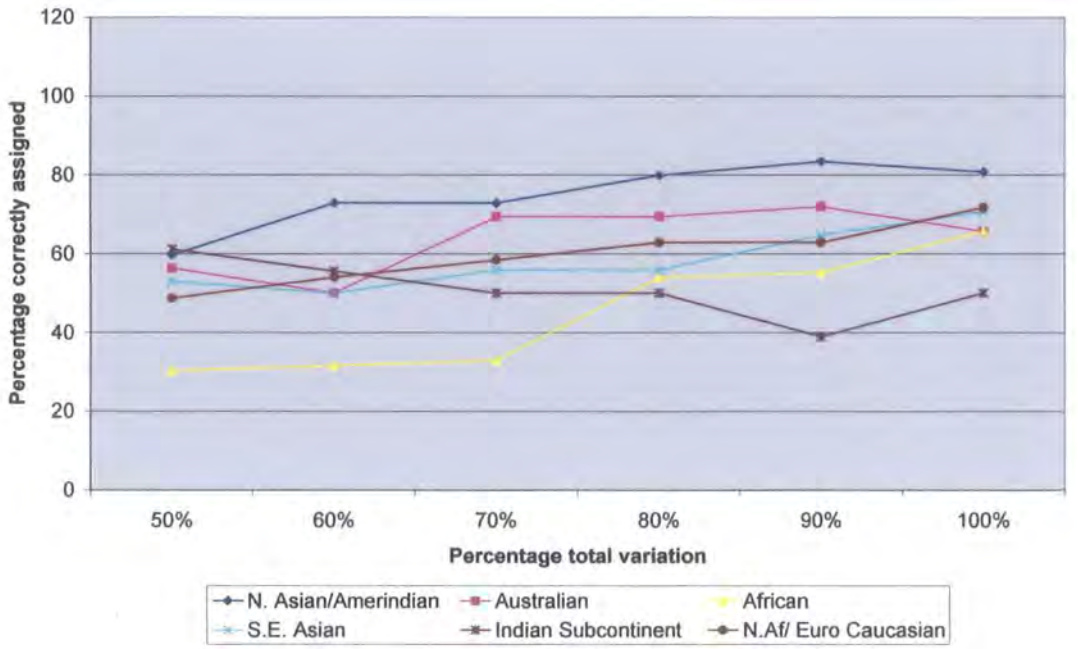

Figure 6.11: Separation of 13 populations for the femur based on ancestry. Summary of separate discriminant and cross-validation analyses using PCs accounting for c.50% (PCs 1-9), 60% (PCs 1-12), 70% (PCs 1-17), 80% (PCs 1-25), 90% (PCs 1-37) and 100% (PCs 1-71).

The Mahalanobis' squared distances between the six categories, generated by the discriminant analysis are shown in Table 6.40. Table 6.41 shows the results of cross-validation analysis with individuals assigned to the correct ancestral groups ranging from 50% for the Sri Lankan group to 80.70% for the Northern Chinese/Amerindian group. Therefore, cross-validation analysis indicates that there is a stronger tendency for populations of the same ancestral group to be associated on the basis of femoral knee joint shape than is apparent in Table 6.13.

Asian/Amerind.	0					
Australian	18.96	0				
African	16.05	16.53	0			
S.E. Asian	32.44	20.3	27.44	0		
Indian Sub.	15.26	21.49	14.54	34.55	0	
Caucasian	14.42	17.20	9.22	27.85	13.19	0
	Asian/ Amerind.	Australian	African	S.E. Asian	Indian Sub.	Caucasian

Table 6.40: Inter-population variation in the femur. Mahalanobis' squared distance between the 6 ancestral groups using canonical discriminant analysis, on the basis of 100% variance.

Number of Observations and Percent Classified into Group							
From Group	Asian/ Amerind	Austral.	African	S.E. Asian	Indian Sub.	Cauc.	Total
Asian/Amerind	92 80.7	3 2.63	6 5.26	0 0	6 5.26	7 6.14	114 100
Australian	3 9.38	21 65.63	2 6.25	3 9.38	1 3.13	2 6.25	32 100
African	6 7.89	2 2.63	50 65.79	2 2.63	4 5.26	12 15.79	76 100
S.E. Asian	0 0	4 11.76	2 5.88	24 70.59	3 8.82	1 2.94	34 100
Indian Sub.	2 11.11	1 5.56	2 11.11	0 0	9 50	4 22.22	18 100
Caucasian	4 3.54	9 7.96	14 12.39	0 0	5 4.42	81 71.68	113 100
Total	107 27.65	40 10.34	76 19.64	29 7.49	28 7.24	107 27.65	387 100

Table 6.41: Inter-population variation in the femur. Cross-validation of 6 ancestral groups based on 100% total variance. Upper figure denotes number of individuals; lower figure denotes percentage. Red figures denote number of individuals placed into their correct group.

Further exploration of the possible association between femoral knee joint shape and ancestry is carried out using the population means. Using the co-ordinates for PCs 1 to 8 (section 6.4.1a), Figures 6.12 to 6.15 give two-dimensional visual representations of the distances between the thirteen population means relative to each other along the four bivariate plots of PC1 with PC2, PC3 with PC4, PC5 with PC6 and PC7 with PC8. Together these eight PCs cumulatively account for 95.4% of total variance between means. They are repeated here with indicators giving the ancestry of each group (Table 6.33).

Despite few *clear* signs of association on the basis of genetic relatedness, some indications are apparent. For example, the four Chinese/Amerindian means are placed relatively closely on PCs 1 and 3. The Aleut, Arikara and Chinese are placed closely together on PC7, although the Pachacama lies at a considerable distance.

For the three Caucasian means, the Spitalfields and Caucasian American means are placed closely together on PC1 but distant from the Egyptian means. All three means lies are placed close together on PC3. The Spitalfields and Egyptian means are positioned together on PC7, distant from the Caucasian American mean.

For the three African means, the plots of PC1 with PC2 and PC3 with PC4 show the Ibo and Khoisan placed closely together. For PCs 5 and 6, all three African populations means lie in the positive quadrant, close together on PC7.

6.4.4b(ii) Tibia: The shape and size of the knee joint in relation to ancestry

Table 6.19, using the total sample and based upon the Mahalanobis' squared distances between groups, indicates that there are relatively few ancestral links between samples, although for the three Amerindian populations, the two remaining populations of the three are placed within the first three positions relative to the primary group. The North Asian sample (Chinese) is placed close to the Caucasian Americans (in position 1), although it includes the Arikara and Pachacama within the subsequent three positions. Some degree of affinity is also shown between the three the Sub-Saharan African populations, although the Ibo is positioned at considerable distance from the Khoisan (at position 11).

Figure 6.12:

Inter-population variation in the femur in 13 populations. Bivariate plot of PC1 with PC2, showing the separation of sample means of 13 populations. Each population is accompanied by its traditional ancestral derivation.

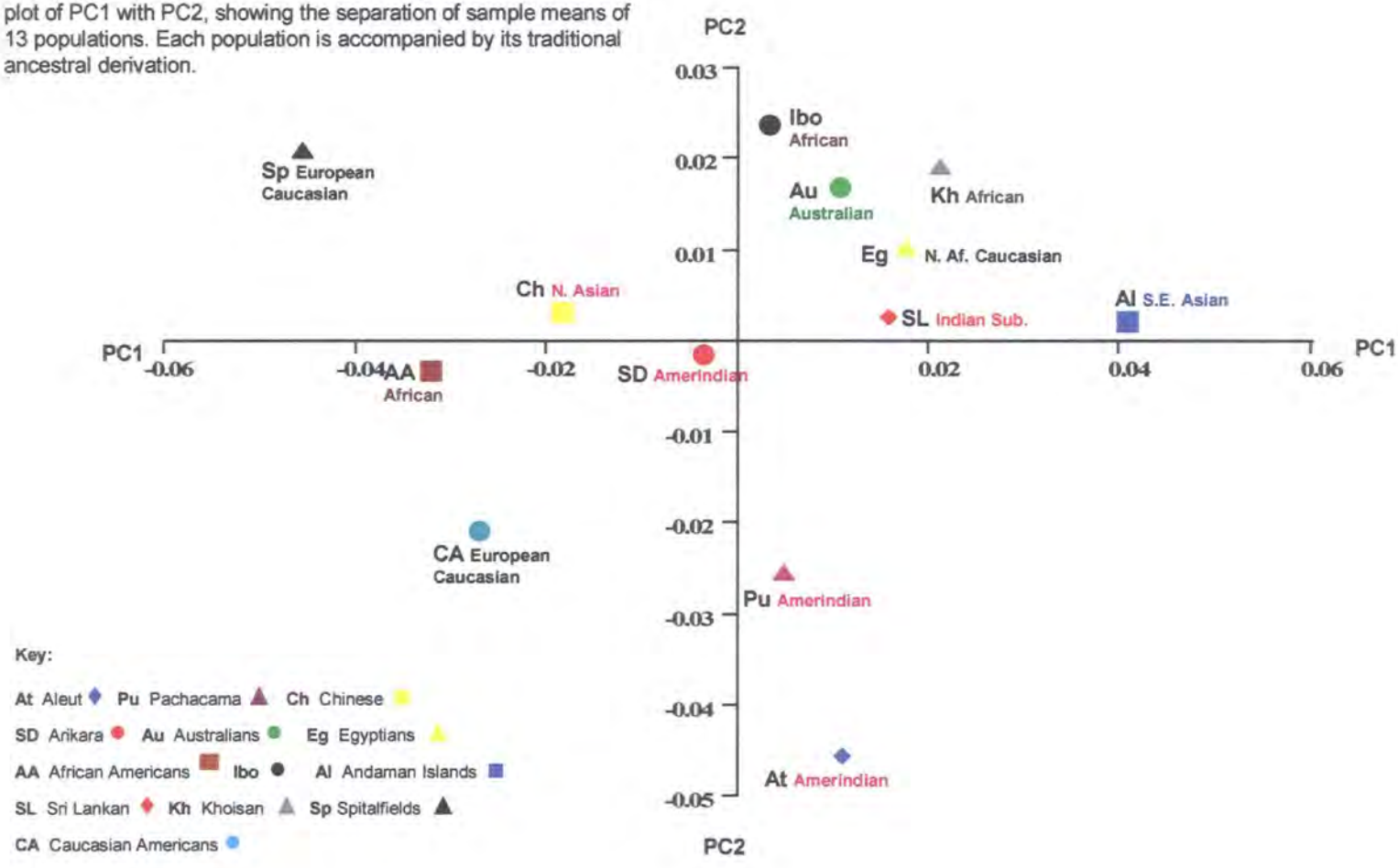

Figure 6.13:

Inter-population variation in the femur in 13 populations. Bivariate plot of PC3 with PC4, showing the separation of sample means of 13 populations. Each population is accompanied by its traditional ancestral derivation.

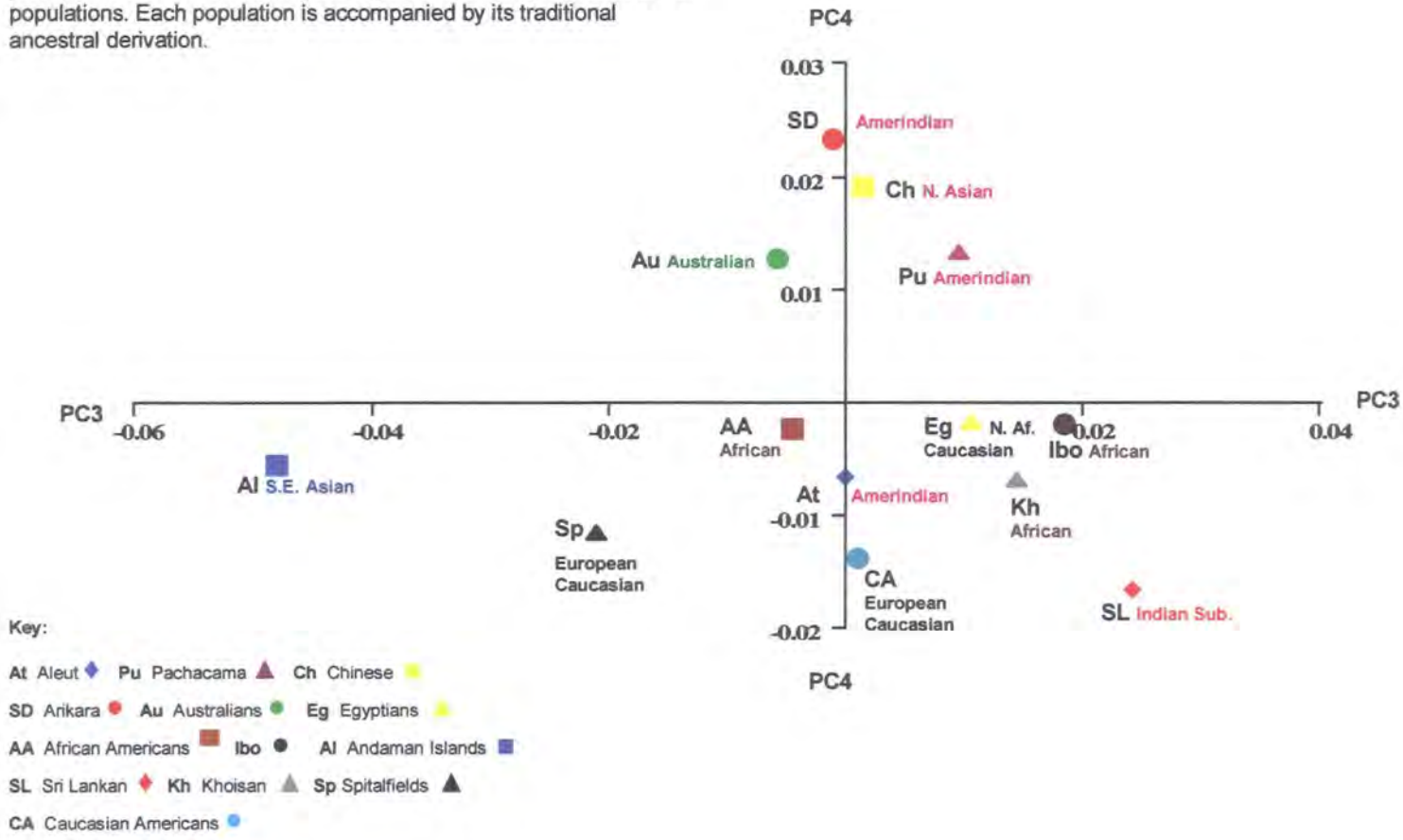

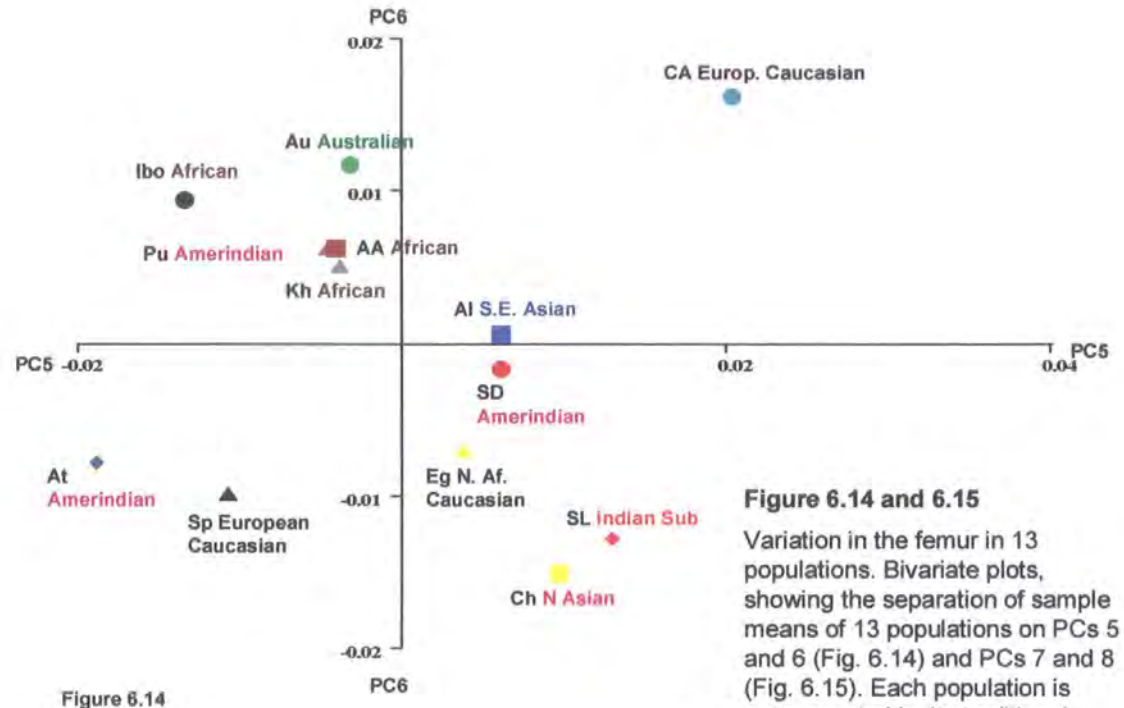

Figure 6.14

Figure 6.14 and 6.15

Variation in the femur in 13 populations. Bivariate plots, showing the separation of sample means of 13 populations on PCs 5 and 6 (Fig. 6.14) and PCs 7 and 8 (Fig. 6.15). Each population is accompanied by its traditional ancestral derivation.

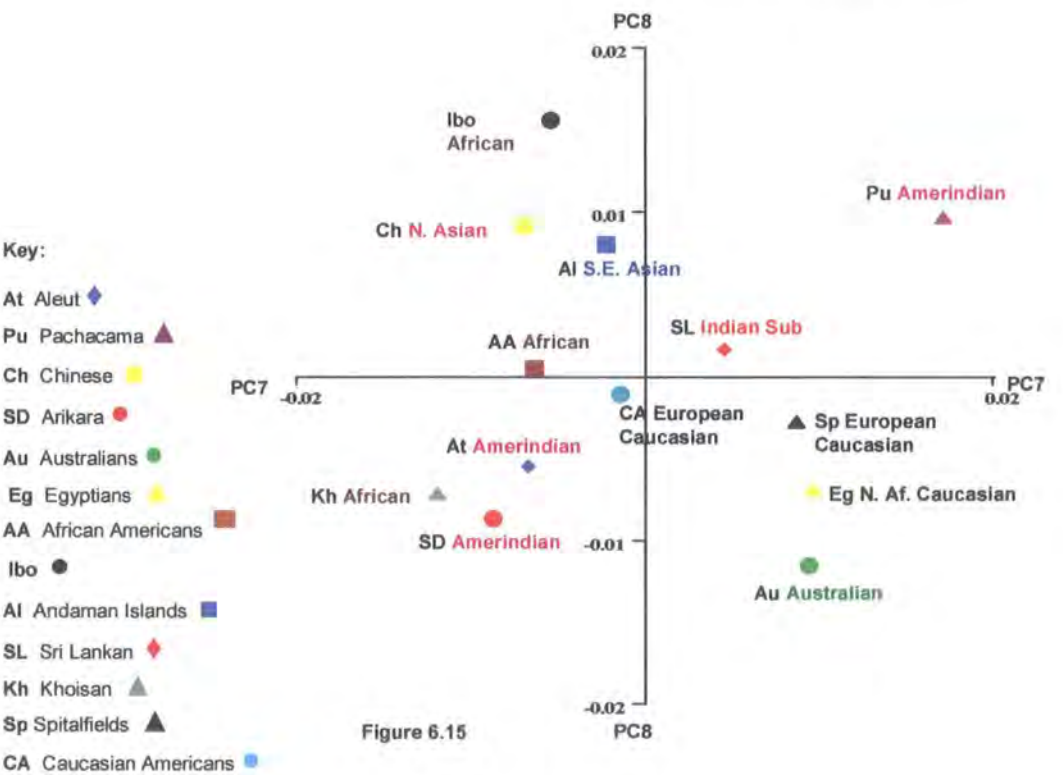

Figure 6.15

The association between the shape of the proximal tibia and ancestry is further tested by a discriminant analysis which is carried out using the same 370 specimens used in section 6.4.1a. The thirteen population samples are again grouped into the six ancestral categories shown in Table 6.39. The data is analysed after GPA by subjecting the Procrustes fitted co-ordinates to PCA. Table 6.18 gives the proportional and accumulated variance for PCs 1 to 56, which represents the total variance within the sample. The scores for each specimen on the resultant PCs are then subjected to canonical discriminant analysis to establish the relationships between ancestral groups based upon the Mahalanobis' squared distances between group means.

For the tibia, the best separation of ancestral groups is achieved using the total variance. This assessment was reached after separate discriminant and cross-validation analyses were carried out using PCs accounting for between c.50% to 100% of total variance. Results are summarised in Figure 6.16.

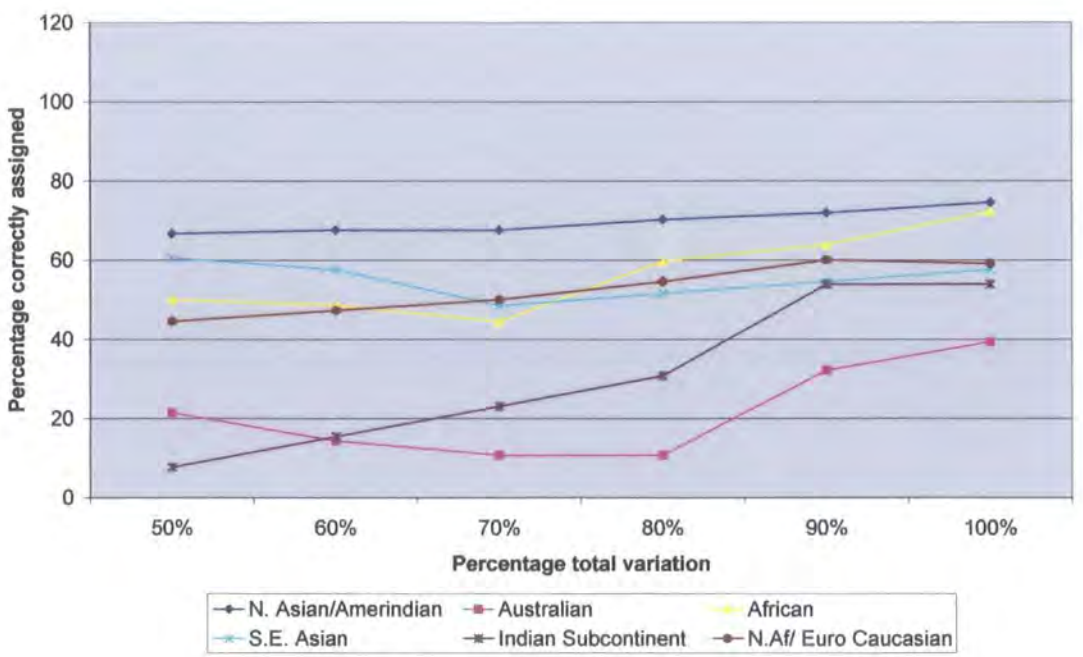

Figure 6.16: Separation of 13 Populations for the tibia based on ancestry. Summary of separate discriminant and cross-validation analyses using PCs accounting for c.50% (PCs 1-6), 60% (PCs 1-9), 70% (PCs 1-14), 80% (PCs 1-20), 90% (PCs 1-30) and 100% (PCs 1-56).

The Mahalanobis' squared distances between groups, generated by the discriminant analysis, are shown in Table 6.42. Table 6.43 shows the results of cross-validation analysis; individuals assigned to the correct ancestral groups ran from 39.29% for the Australians group to 72.22% and 74.56% for the African and Chinese/Amerindian samples, respectively. Cross-validation analysis therefore indicates that there is a tendency for populations of the same ancestral group to be associated on the basis of the shape of the proximal tibia than is apparent from Table 6.19, particularly for samples in the Chinese/Amerindian and African groups.

Further exploration of the possible association between the shape of the proximal tibia and ancestry is carried out using the population means. Using the means of the co-ordinates for PCs 1 to 6 (section 6.4.1a), Figures 6.17 to 6.19 give two-dimensional visual representations of the distances between the thirteen population means relative to each other on the three bivariate plots of PC1 with PC2, PC3 with PC4 and PC5 with PC6. Together, these six PCs account for 90.7% of total variance. They are shown here with indicators giving the ancestry of each population.

All of the Chinese and Amerindian group are positioned in close proximity on PC1, with the three Amerindian groups scoring in the same quadrant in the plot of PC3 with PC4. All four means are positioned close together on PC5.

In relation to the African group, the plot of PC1 with PC2 shows the African American and Ibo means scoring close together, with the African American and Khoisan closely positioned within the same quadrant for PC3 with PC4. The plot of PC5 with PC6 shows a close association of the Ibo with the Khoisan, away from the African American means.

The three Caucasian means are placed close together on PCs 2, 4 and 6 but are relatively distant from each other on PCs 1, 3 and 5.

Asian/Amerind.	0					
Australian	6.79	0				
African	10.63	10.74	0			
S.E.Asian	18.08	15.69	18.33	0		
Indian Sub.	16.46	16.73	15.27	21.35	0	
Caucasian	7.67	9.17	8.38	18.40	17.78	0
	Asian/ Amerind.	Australian	African	S.E. Asian	Indian Sub.	Caucasian

Table 6.42: Inter-population variation in the tibia. Mahalanobis' squared distance between the 6 ancestral groups using canonical discriminant analysis, on the basis of 100% variance.

Number of Observations and Percent Classified into Group							
From Group	Asian/ Amerind	Austral.	African	S.E. Asian	Indian Sub.	Cauc.	Total
Asian/Amerind	85 74.56	13 11.4	4 3.51	2 1.75	5 4.39	5 4.39	114 100
Australian	6 21.43	11 39.29	4 14.29	2 7.14	3 10.71	2 7.14	28 100
African	3 4.17	8 11.11	52 72.22	0 0	1 1.39	8 11.11	72 100
S.E.Asian	2 6.06	3 9.09	2 6.06	19 57.58	5 15.15	2 6.06	33 100
Indian Sub.	3 23.08	0 0	2 15.38	0 0	7 53.85	1 7.69	13 100
Caucasian	16 14.55	9 8.18	13 11.82	4 3.64	3 2.73	65 59.09	110 100
Total	115 31.08	44 11.89	77 20.81	27 7.3	24 6.49	83 22.43	370 100

Table 6.43: Inter-population variation in the tibia. Cross-validation of 6 ancestral groups based on 100% total variance. Upper figure denotes number of individuals; lower figure denotes percentage. Red figures denote number of individuals placed into their correct group.

Figure 6.17:

Inter-population variation in the tibia in 13 populations. Bivariate plot of PC1 with PC2, showing the separation of sample means of 13 populations. Each population is accompanied by its traditional ancestral derivation.

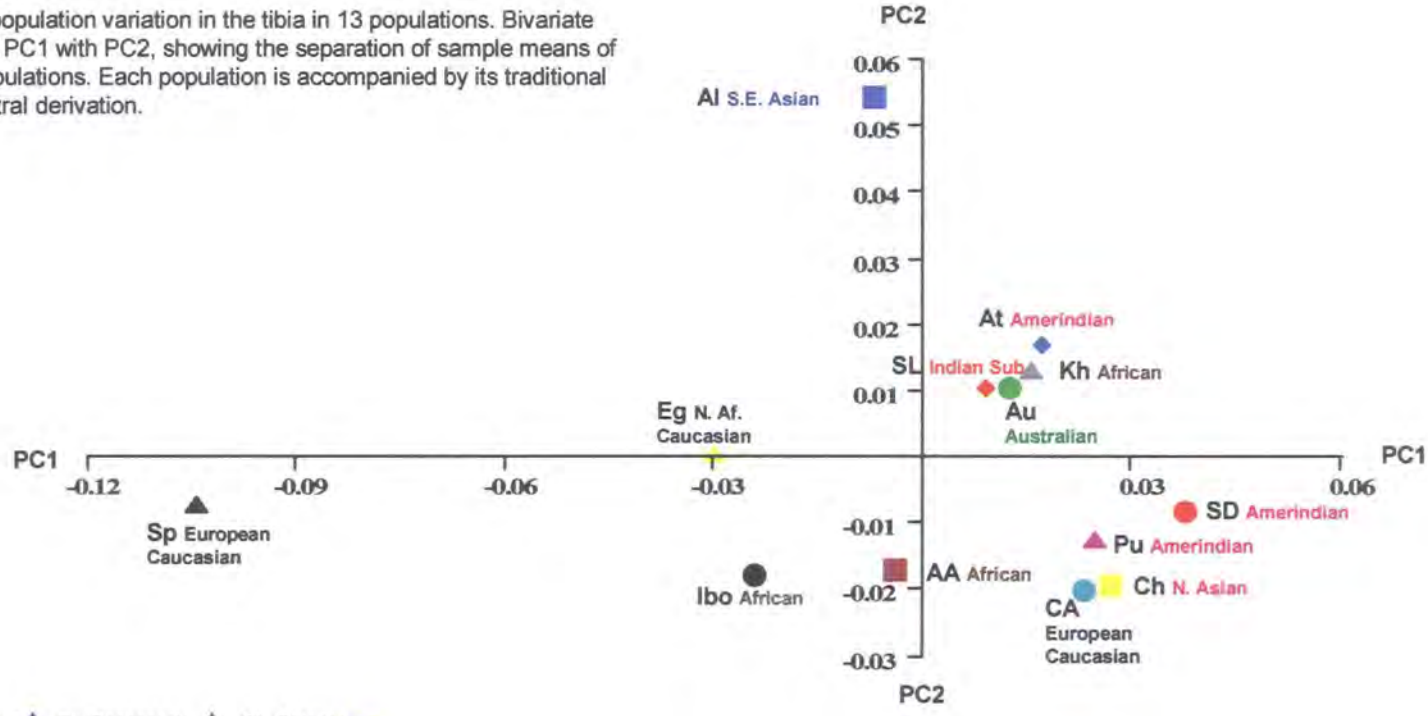

Key:

At Aleut Pu Pachacama Ch Chinese
SD Arikara Au Australians Eg Egyptians
AA African Americans Ibo Al Andaman Islands
SL Sri Lankan Kh Khoisan Sp Spitalfields
CA Caucasian Americans

Figure 6.18:

Inter-population variation in the tibia in 13 populations. Bivariate plot of PC3 with PC4, showing the separation of sample means of 13 populations. Each population is accompanied by its traditional ancestral derivation.

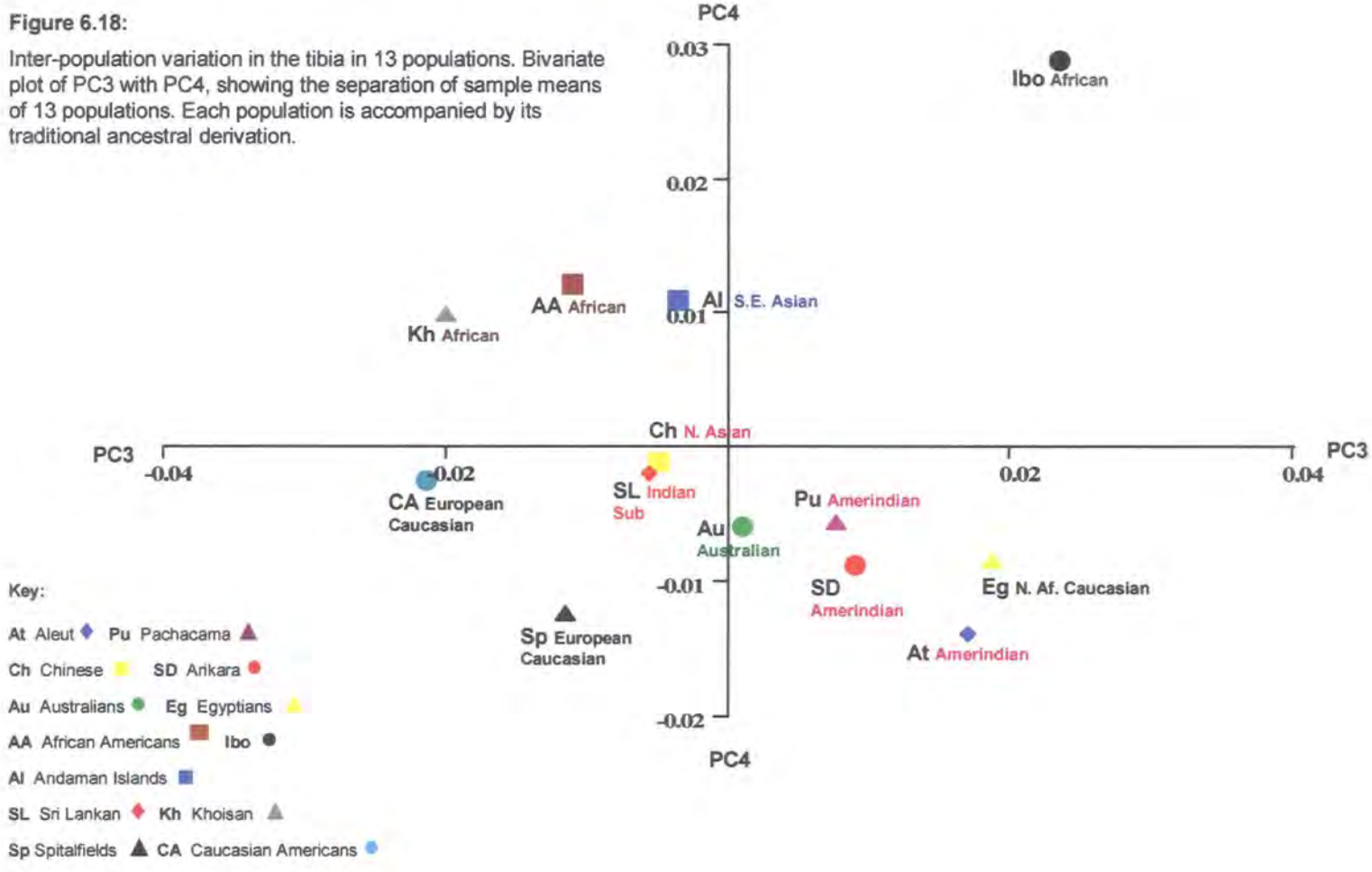

Figure 6.19:

Inter-population variation in the tibia in 13 populations. Bivariate plot of PC5 with PC6, showing the separation of sample means of 13 populations. Each population is accompanied by its traditional ancestral derivation.

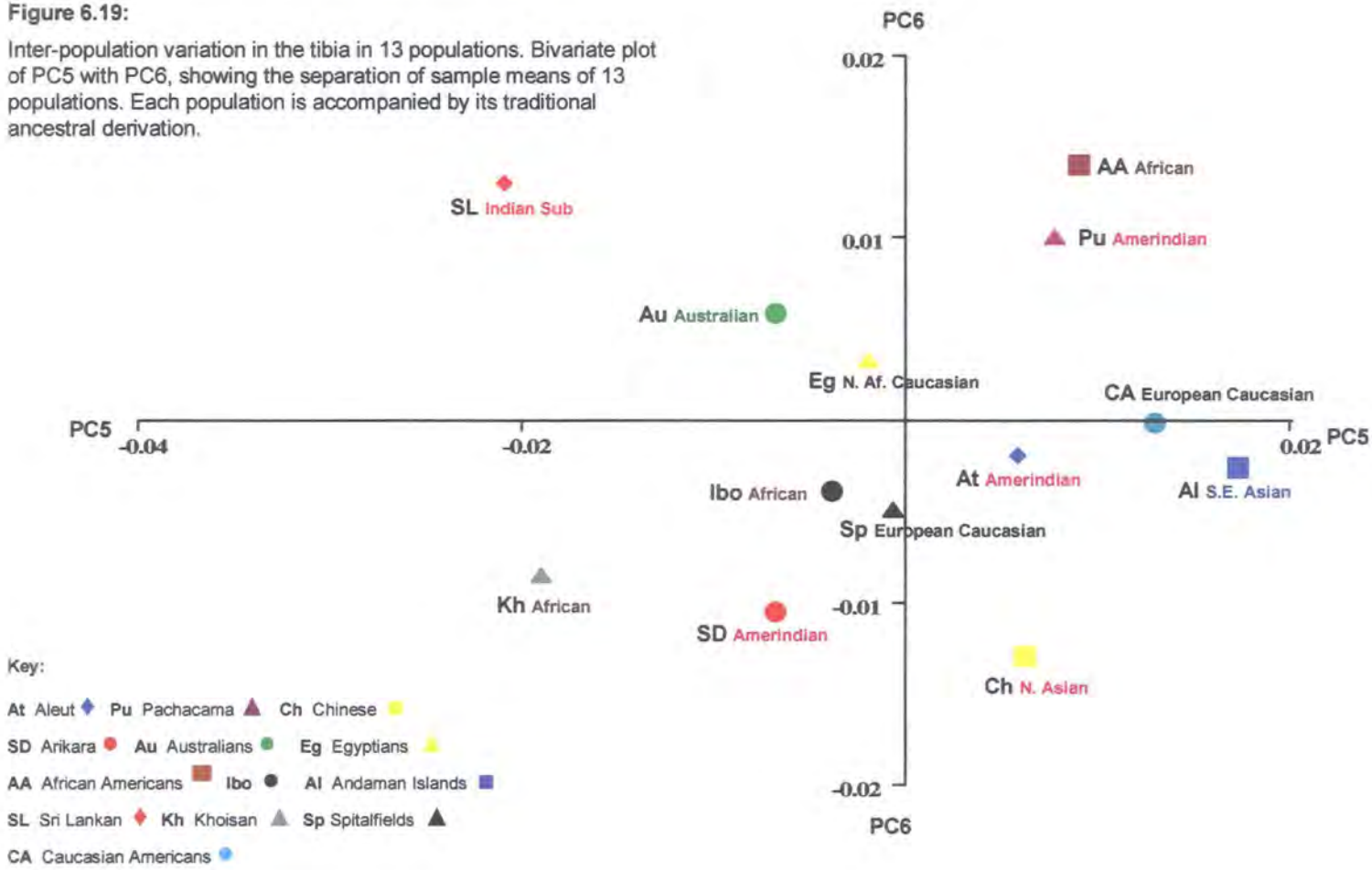

6.4.4c Differences in the habitual use of footwear and subsistence strategies

Table 6.44 shows the subsistence strategies practiced by the thirteen populations together with the use made of footwear on a habitual basis, if any. The histories of some groups may not be sufficient to provide a definitive answer although there will have been strong indications in the literature and reports accompanying the original archaeological excavations or museum collections for using the descriptions provided below.

Population	Footwear use	Footwear type	Traditional Subsistence Strategies
Aleut	Yes	Hard	Marine hunter-gatherers
Pachacama	Yes	Hard	Trade/ Agriculturalists
Arikara	Yes	Soft	Hunter-gatherer/ Farmers
Chinese	Yes	Hard	Agriculturalists? Urban workers?
Australian	No	None	Hunter-gatherers
African American	Yes	Hard	Urban workers
Ibo	No	None	Hunter-gatherers
Andaman Islanders	No	None	Hunter-gatherers
Sri Lankan	No	None	Hunter-gatherers
Khoisan	No	None	Hunter-gatherers
Egyptian	Yes	Soft	Trade/ Agriculturalists/ Admin
Spitalfields	Yes	Hard	Urban workers
Cauc. American	Yes	Hard	Urban workers

Table 6.44: Categorisation of the footwear and subsistence strategies used by the thirteen populations.

6.4.4c(i) Femur: The shape and size of the knee joint in relation to the habitual use of footwear

To test the association between femoral knee joint shape and the habitual use of footwear, a discriminant analysis is carried out using the 387 specimens used in section 6.4.1a. In this analysis, the thirteen population samples are grouped into the three categories shown in Table 6.44. The data is analysed after GPA by subjecting the Procrustes fitted co-ordinates to PCA. Table 6.11 gives the proportional and

accumulated variance for PCs 1 to 71, which represents the total variance within the sample. The scores for each specimen on the resultant PCs are then subjected to canonical discriminant analysis to establish the relationships between categories based upon the Mahalanobis' squared distances between group means.

For the femur, the best separation of groups based upon footwear types is achieved using 100% of total variance. This assessment was reached after separate discriminant and cross-validation analyses were carried out using PCs accounting for between c.50% to 100% of total variance. Results are summarised in Figure 6.20.

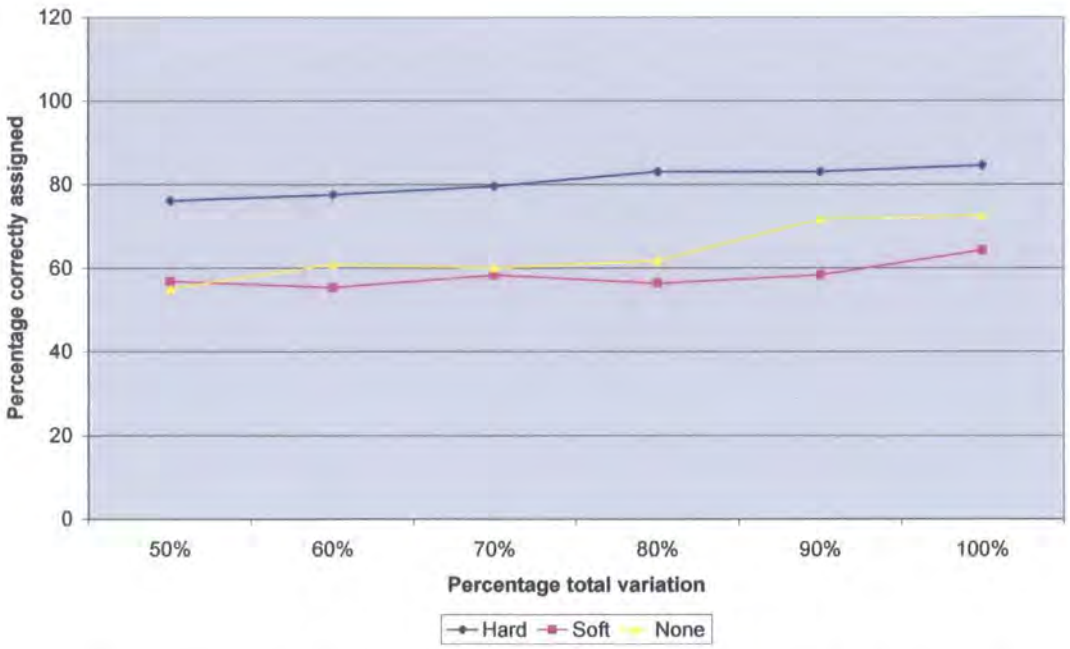

Figure 6.20: Separation of 13 populations for the femur based on footwear types. Summary of separate discriminant and cross-validation analyses using PCs accounting for c.50% (PCs 1-9), 60% (PCs 1-12), 70% (PCs 1-17), 80% (PCs 1-25), 90% (PCs 1-37) and 100% (PCs 1-71).

The Mahalanobis' squared distances between differently shod groups, generated by the discriminant analysis, are shown in Table 6.45. All distances between each type of footwear category are shown at a level of statistical significance. Table 6.46 shows the results of cross-validation analysis with individuals assigned to the correct footwear categories ranging from 64.18% for the group using soft footwear to 84.50% for the group using hard footwear. Cross-validation analysis therefore gives

a strong indication that there is similarity of shape of the distal femur in populations sharing the same footwear category.

Hard	0		
	1.0000		
Soft	9.44	0	
	0.0001	1.0000	
None	13.64	6.54	0
	0.0001	0.0001	1.0000
	Hard	Soft	None

Table 6.45: Inter-population variation in the femur. Mahalanobis' squared distance between groups based on footwear type, using canonical discriminant analysis using 100% total variance. Upper figure in red denotes distance between groups; lower value in black gives the Hotelling's t^2 *p*-value.

Number of Observations and Percent Classified into Group				
From Group	Hard	Soft	None	Total
Hard	169	22	9	200
	84.5	11	4.5	100
Soft	9	43	15	67
	13.43	64.18	22.39	100
None	11	22	87	120
	9.17	18.33	72.5	100
Total	189	87	111	387
	48.84	22.48	28.68	100

Table 6.46: Inter-population variation in the femur. Cross-validation of groups based on footwear type using 100% total variance. Upper figure denotes number of individuals; lower figure denotes percentage. Red figures denote number of individuals placed into their correct group.

6.4.4c(ii) Femur: The shape and size of the knee joint in relation to subsistence strategies

To test the association between the shape of the distal femur and the subsistence strategies undertaken, a discriminant analysis is carried out using the 387 specimens used in section 6.4.1a. In this analysis the thirteen populations are grouped into three

broad categories of 'Hunter-gatherers', 'Trade/Agriculturalists' and 'Industrial' workers, shown in Table 6.44. The data are analysed after GPA by subjecting the Procrustes fitted co-ordinates to PCA. Table 6.11 gives the proportional and accumulated variance for PCs 1 to 71, which represents the total variance within the sample. The scores for each specimen on the resultant PCs are then subjected to canonical discriminant analysis to establish the relationships between categories based upon the Mahalanobis' squared distances between group means.

For the femur, the best separation of groups based upon subsistence strategies is achieved using the total variance. This assessment was reached after separate discriminant and cross-validation analyses were carried out using PCs accounting for between c.50% to 100% of total variance. Results are summarised in Figure 6.21.

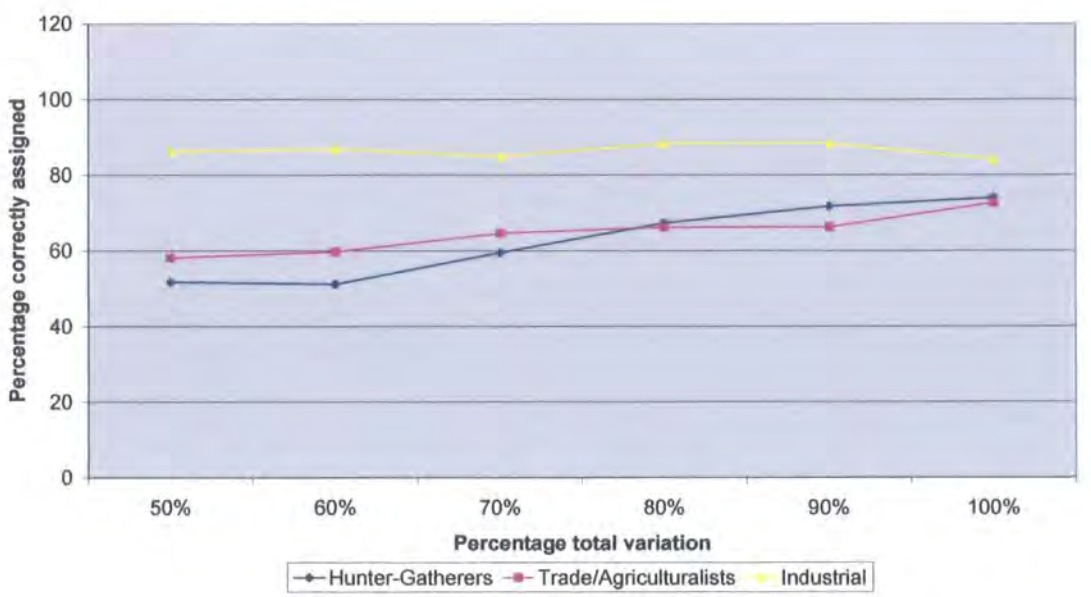

Figure 6.21: Separation of 13 populations for the femur based on subsistence strategies: Summary of separate discriminant and cross-validation analyses using PCs accounting for c.50% (PCs 1-9), 60% (PCs 1-12), 70% (PCs 1-17), 80% (PCs 1-25), 90% (PCs 1-37) and 100% (PCs 1-71).

The Mahalanobis' squared distances between categories, generated by the discriminant analysis are shown in Table 6.47.

Hunters	0		
	1.0000		
Trade/	6.42	0	
Agric.	0.0001	1.0000	
Industrial	13.20	16.17	0
	0.0001	0.0001	1.000
	Hunters	T/Agric	Indust.

Table 6.47: Inter-population variation in the femur. Mahalanobis' squared distance between groups based on subsistence strategies, using canonical discriminant analysis using 100% total variance. Upper figure in red denotes distance between groups; lower value in black gives the Hotelling's t^2 *p*-value.

All distances between each subsistence category are shown at a level of statistical significance. Table 6.48 shows the results of cross-validation analysis with individuals assigned to the correct subsistence categories, ranging from 72.58% for the Trade/Agriculturalists to 84.14% for the Industrial workers. Cross-validation analysis therefore gives a strong indication that there is similarity in femoral knee joint shape in populations carrying out similar subsistence strategies.

Number of Observations and Percent Classified into Group				
From Group	Hunters	T/Agric	Indust.	Total
Hunters	133 73.89	35 19.44	12 6.67	180 100
Trade/ Agric	14 22.58	45 72.58	3 4.84	62 100
Indust.	10 6.9	13 8.97	122 84.14	145 100
Total	157 40.57	93 24.03	137 35.4	387 100

Table 6.48: Inter-population variation in the femur. Cross-validation of groups based on subsistence strategies using 100% total variance. Upper figure denotes number of individuals; lower figure denotes percentage. Red figures denote number of individuals placed into their correct group.

6.4.4c(iii) Femur: Knee joint shape using population means in relation to footwear types and subsistence strategies

To explore the association of the shape of the distal femur with footwear type and subsistence categories further, Figure 6.22 shows the plot of PC1 with PC2 using sample means (accounting for nearly 50% of total variance). PC1 shows that all four industrial and heavily shod populations (Spitalfields, African and Caucasian American and Chinese) are placed on the negative side of the scale. All other means are seen to be placed close to zero and towards the positive extreme of PC1. All populations positioned towards the positive extreme are unshod or lightly shod and are hunter-gatherers or possibly occupied in light trade or agriculture. The exception to this group is the Aleut, which, whilst being hunters, were heavily shod. PC2 does not indicate a clear association of means based on either footwear or subsistence types.

The bivariate plot of PCs 3 and 4 (Figure 6.23) using sample means (accounting for a cumulative 24.99% of total variance) and of PCs 5 and 6 and PCs 7 and 8 (Figures 6.24 and 6.25) (accounting for a cumulative 18.20% of total variance), indicates no clear clustering of groups based on either the habitual use of footwear or similarity of subsistence strategy.

6.4.4c(iv) Tibia: The shape and size of the knee joint in relation to the habitual use of footwear

To test the association between the shape of the proximal tibia and the habitual use of footwear, a discriminant analysis is carried out using the 370 specimens used in section 6.4.1b. In this analysis, the thirteen population samples are grouped into the three categories shown in Table 6.44. The data are analysed after GPA by subjecting the Procrustes fitted co-ordinates to PCA. Table 6.18 gives the proportional and accumulated variance for PCs 1 to 56, which represents the total variance within the sample. The scores for each specimen on the resultant PCs are then subjected to canonical discriminant analysis to establish the relationships between categories based upon the Mahalanobis' squared distances between means.

Figure 6.22:

Inter-population variation in the femur in 13 populations. Bivariate plot of PC1 with PC2, showing the separation of sample means of 13 populations. Populations are distinguished by type of subsistence strategies and footwear worn when living. 5 of 6 population means inside circled area are hunter-gatherer, unshod populations from year-round warm climates.

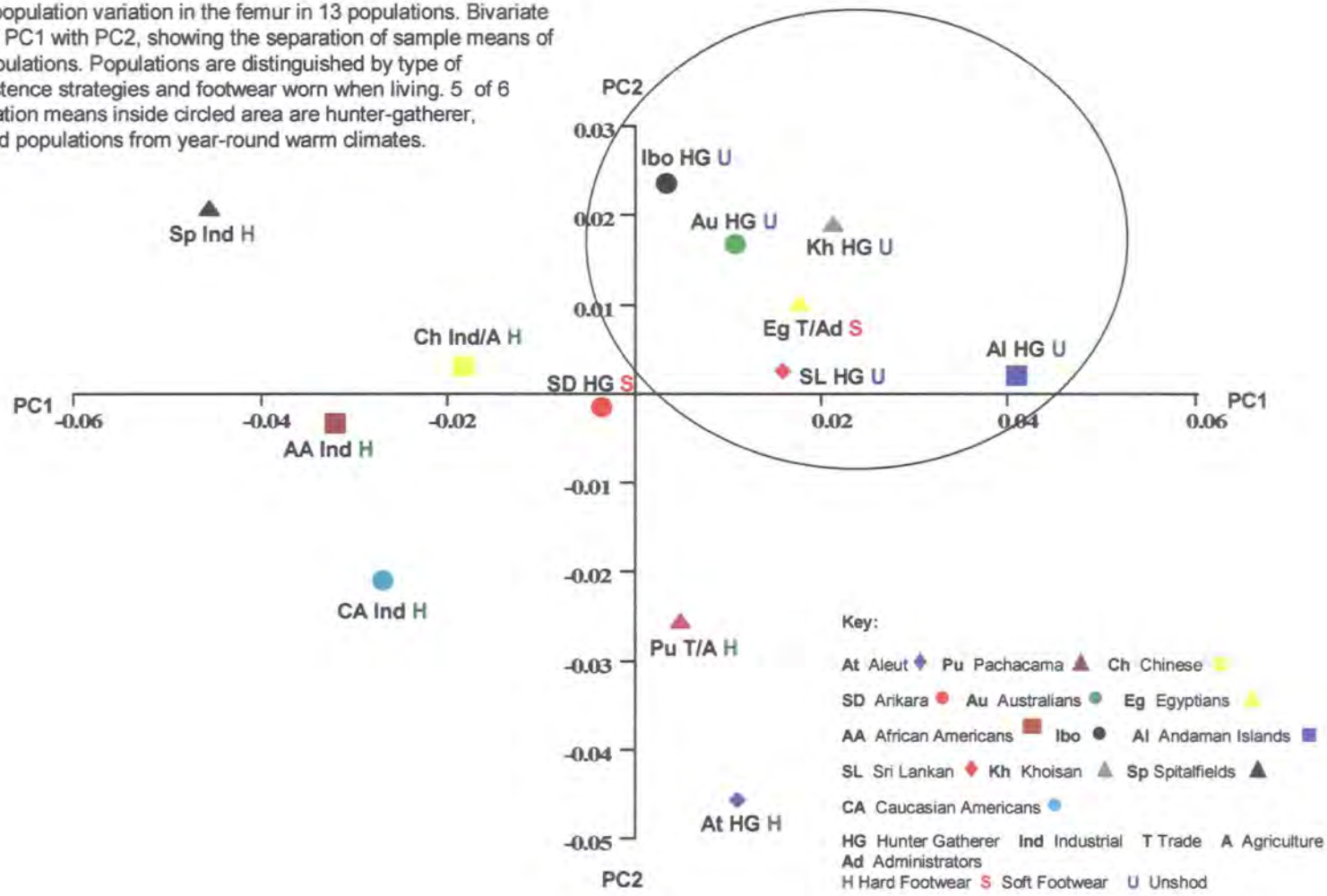

Figure 6.23:

Inter-population variation in the femur in 13 populations. Bivariate plot of PC3 with PC4, showing the separation of sample means of 13 populations. Populations are distinguished by type of subsistence strategies and footwear worn when living.

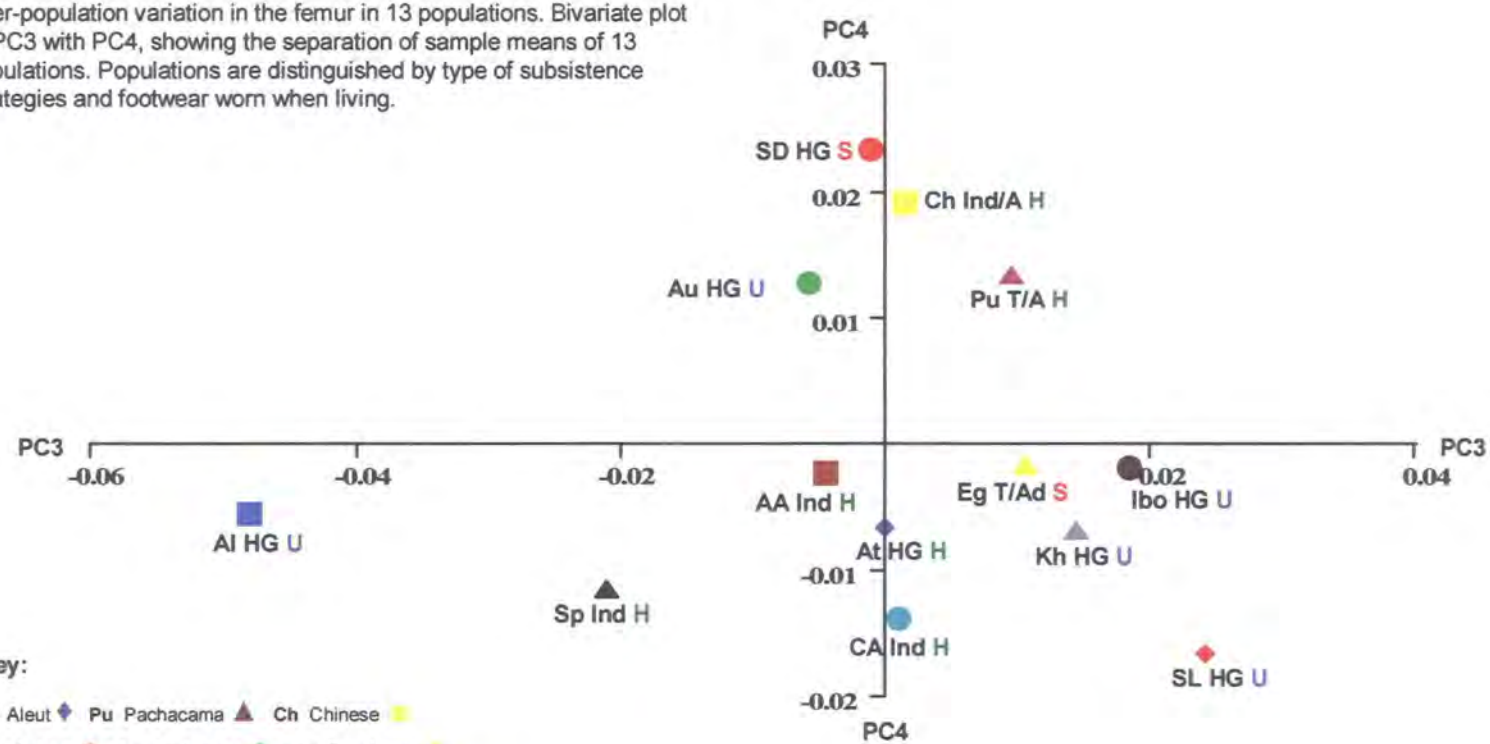

Key:

At Aleut **Pu** Pachacama **Ch** Chinese
SD Arikara **Au** Australians **Eg** Egyptians
AA African Americans **Ibo** **Al** Andaman Islands
SL Sri Lankan **Kh** Khoisan **Sp** Spitalfields
CA Caucasian Americans
HG Hunter Gatherer **Ind** Industrial **T** Trade **A** Agriculture **Ad** Administrators
H Hard Footwear S Soft Footwear U Unshod

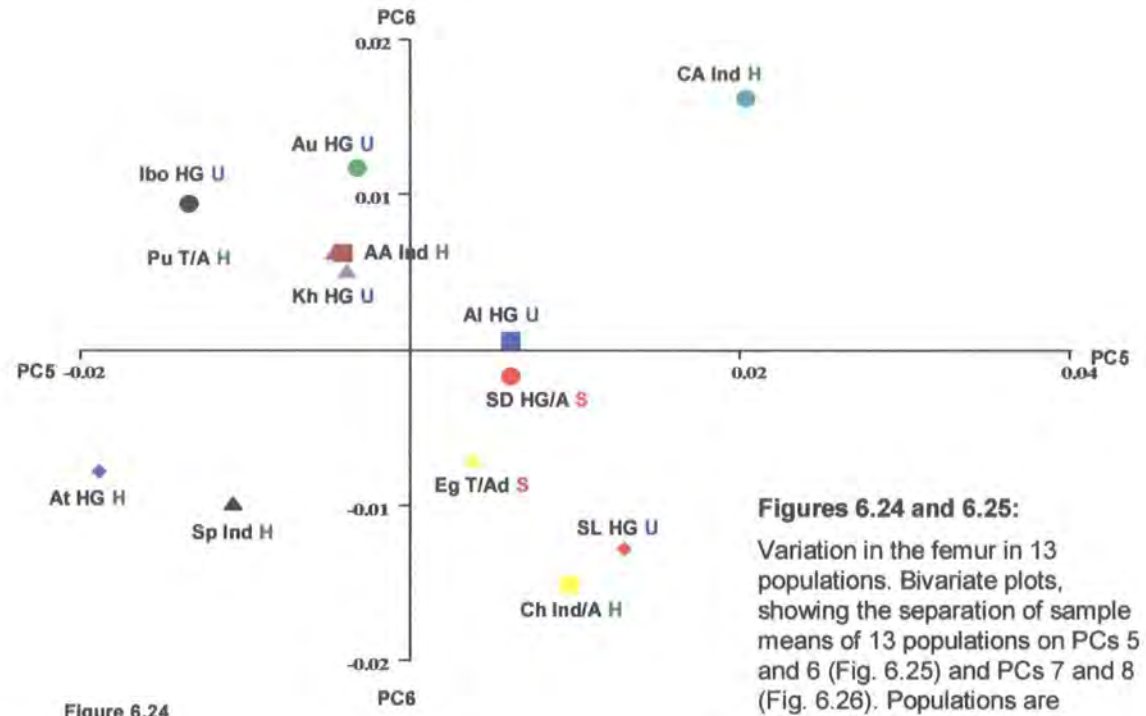

Figure 6.24

Figures 6.24 and 6.25:

Variation in the femur in 13 populations. Bivariate plots, showing the separation of sample means of 13 populations on PCs 5 and 6 (Fig. 6.25) and PCs 7 and 8 (Fig. 6.26). Populations are distinguished by type of subsistence strategies and footwear worn when living.

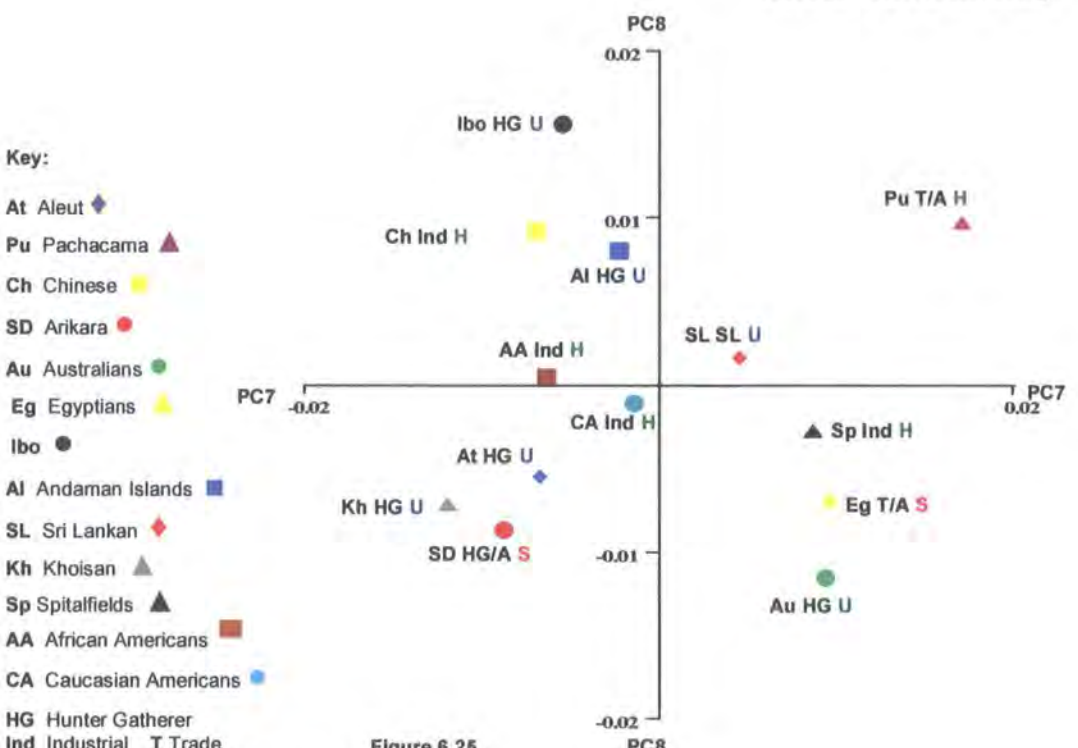

Figure 6.25

Key:

At Aleut
Pu Pachacama
Ch Chinese
SD Arikara
Au Australians
Eg Egyptians
Ibo
Al Andaman Islands
SL Sri Lankan
Kh Khoisan
Sp Spitalfields
AA African Americans
CA Caucasian Americans

HG Hunter Gatherer
Ind Industrial **T** Trade
A Agriculture **Ad** Administrators
H Hard Footwear **S** Soft Footwear
U Unshod

For the tibia, the best separation of groups based upon footwear types is achieved using 90% of total variance. This assessment was reached after separate discriminant and cross-validation analyses were carried out using PCs accounting for between c.50% to 100% of total variance. Results are summarised in Figure 6.26.

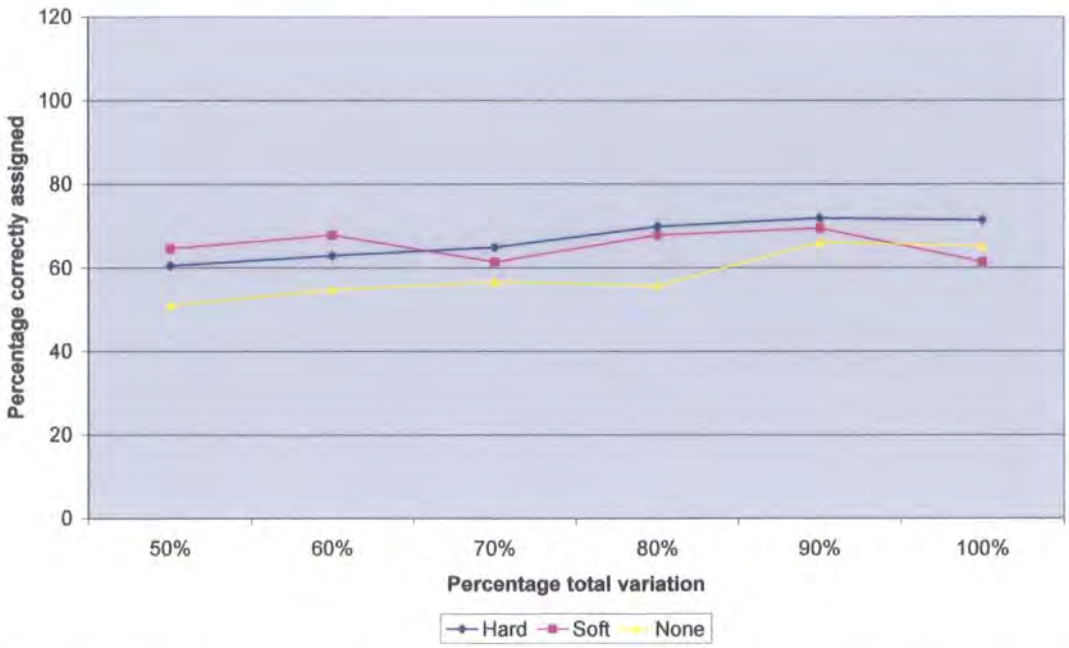

Figure 6.26: Separation of 13 populations for the tibia based on footwear types. Summary of separate discriminant and cross-validation analyses using PCs accounting for c.50% (PCs 1-6), 60% (PCs 1-9), 70% (PCs 1-14), 80% (PCs 1-20), 90% (PCs 1-30) and 100% (PCs 1-56).

The Mahalanobis' squared distances between differently shod groups, generated by the discriminant analysis, are shown in Table 6.49. All distances between each type of footwear category are statistically significant. Table 6.50 shows the results of cross-validation analysis with individuals assigned to the correct footwear categories, ranging from 66.05% for the unshod group to 71.78% for the group using hard footwear. Cross-validation analysis therefore gives an indication that there is similarity in tibial knee joint shape in populations sharing the same footwear category.

Hard	0		
	1.0000		
Soft	3.48	0	
	0.0001	1.0000	
None	3.81	3.84	0
	0.0001	0.0001	1.0000
	Hard	Soft	None

Table 6.49: Inter-population variation in the tibia. Mahalanobis' squared distance between using canonical discriminant analysis using 100% total variance. Upper figure in red denotes distance between groups; lower value in black gives the Hotelling's t^2 *p*-value.

Number of Observations and Percent Classified into Group				
From Group	Hard	Soft	None	Total
Hard	145	33	24	202
	71.78	16.34	11.88	100
Soft	9	43	10	62
	14.52	69.35	16.13	100
None	15	21	70	106
	14.15	19.81	66.04	100
Total	169	97	104	370
	45.68	26.22	28.11	100

Table 6.50: Inter-population variation in the tibia. Cross-validation of groups based on footwear type using 100% total variance. Upper figure denotes number of individuals; lower figure denotes percentage. Red figures denote number of individuals placed into their correct group.

6.4.4c(v) Tibia: The shape and size of the knee joint in relation to subsistence strategies

To test the association between knee joint shape and the subsistence strategies undertaken, a discriminant analysis is carried out using the 370 specimens used in section 6.4.1b. In this analysis the thirteen population samples are grouped into the three broad categories of subsistence shown in Table 6.44. The data is analysed after

GPA by subjecting the Procrustes fitted co-ordinates to PCA. The scores for each specimen on the resultant PCs are then subjected to canonical discriminant analysis to establish the relationships between categories based upon the Mahalanobis' squared distances between means.

For the tibia, the best separation of groups based upon subsistence strategies is achieved using 100% of total variance. This assessment was reached after separate discriminant and cross-validation analyses were carried out using PCs accounting for between c.50% to 100% of total variance. Results are summarised in Figure 6.27.

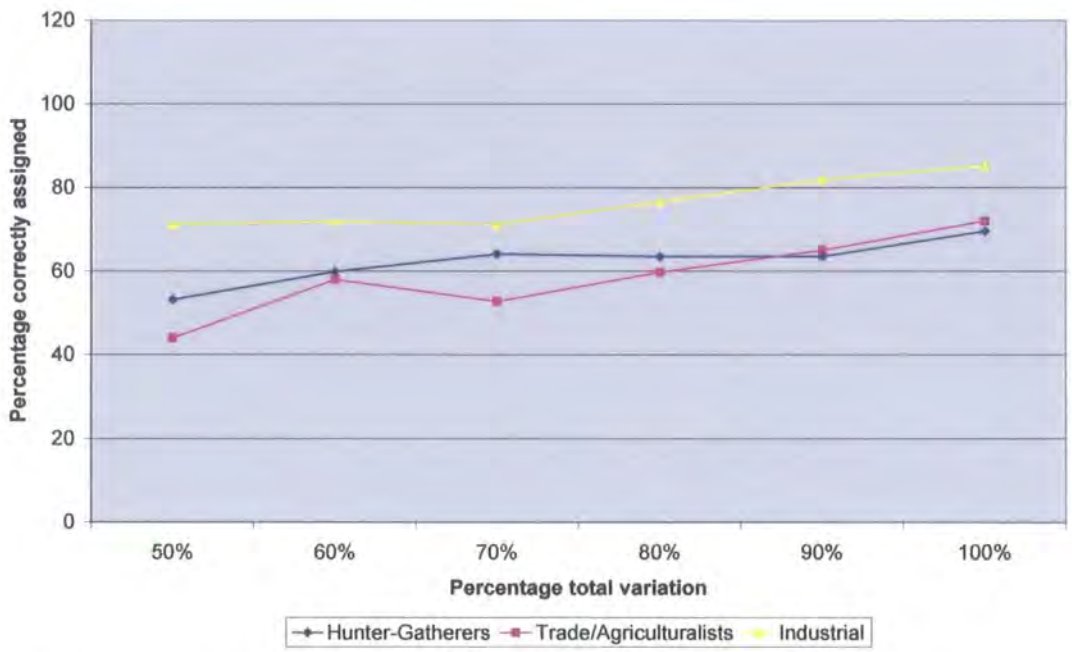

Figure 6.27: Separation of 13 Populations for the tibia based on subsistence strategies. Summary of separate discriminant and cross-validation analyses using PCs accounting for c.50% (PCs 1-6), 60% (PCs 1-9), 70% (PCs 1-14), 80% (PCs 1-20), 90% (PCs 1-30) and 100% (PCs 1-56).

The Mahalanobis' squared distances between categories, generated by the discriminant analysis are shown in Table 6.51. All distances between each subsistence category are statistically significant. Table 6.52 shows the results of cross-validation analysis with individuals assigned to the correct subsistence categories, ranging from 69.51% for the Hunter-gatherers to 85.23% for the Industrial workers. Cross-validation analysis therefore gives an indication that there

is similarity in the shape of the tibia in populations carrying out similar subsistence strategies.

Hunters	0		
	1.0000		
Trade/	5.30	0	
Agric.	0.0001	1.0000	
Industrial	9.05	10.97	0
	0.0001	0.0001	1.0000
	Hunters	T/Agric	Indust.

Table 6.51: Inter-population variation in the tibia. Mahalanobis' squared distance between groups based on subsistence strategies, using canonical discriminant analysis using 100% total variance. Upper figure in red denotes distance between groups; lower value in black gives the Hotelling's t^2 *p*-value.

Number of Observations and Percent Classified into Group				
From Group	Hunters	T/Agric	Indust.	Total
Hunters	114	30	20	164
	69.51	18.29	12.2	100
Trade/ Agric	12	41	4	57
	21.05	71.93	7.02	100
Indust.	13	9	127	149
	8.72	6.04	85.23	100
Total	139	80	151	370
	37.57	21.62	40.81	100

Table 6.52: Inter-population variation in the tibia. Cross-validation of groups based on subsistence strategies using 100% total variance. Upper figure denotes number of individuals; lower figure denotes percentage. Red figures denote number of individuals placed into their correct group.

6.4.4c(vi) Tibia: Knee joint shape using population means in relation to footwear types and subsistence strategies

To explore the association of tibial knee joint shape with footwear type and subsistence categories further, Figure 6.28 shows the plot of PC1 with PC2 using population means (accounting for 69.2% of total variance). Figure 6.28 indicates two

Figure 6.28:

Inter-population variation in the tibia in 13 populations. Bivariate plot of PC 1 with 2, showing the separation of sample means of 13 populations. Populations are distinguished by type of subsistence strategies and footwear worn when living.

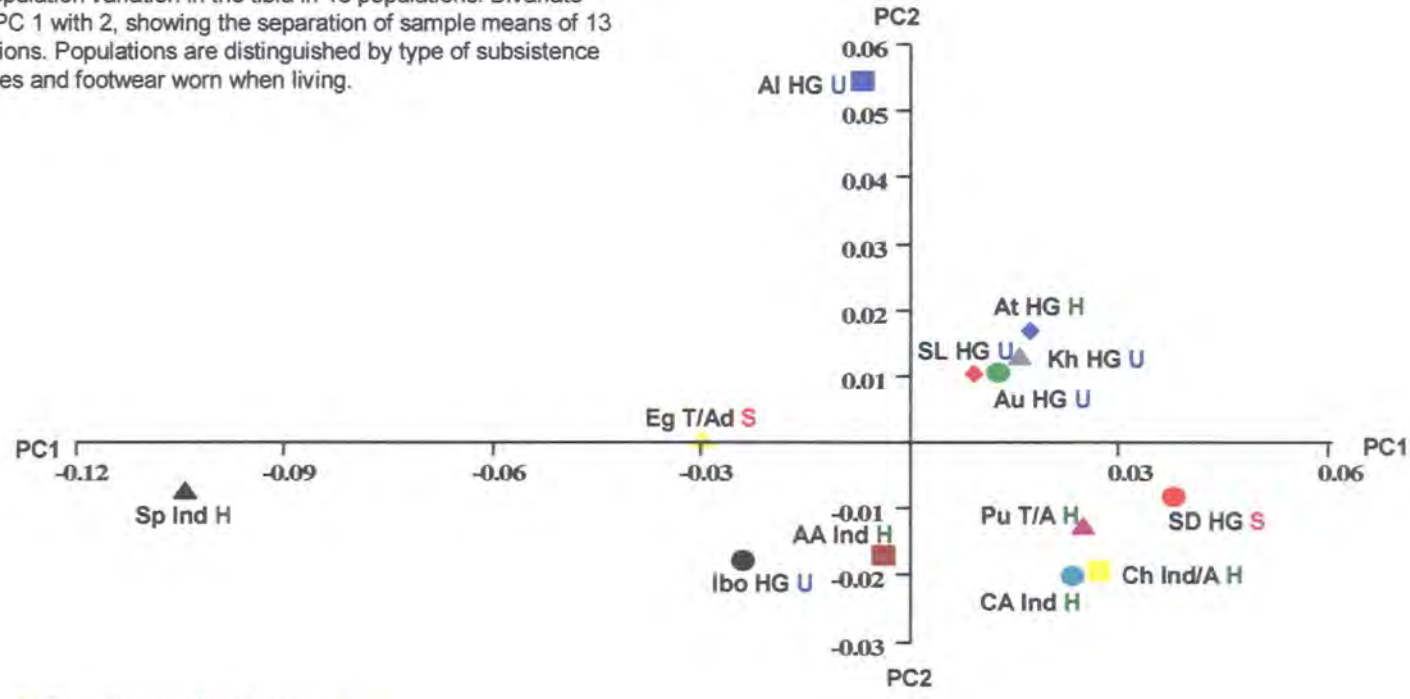

Key:

At Aleut **Pu** Pachacama **Ch** Chinese

SD Arikara **Au** Australians **Eg** Egyptians

AA African Americans **Ibo** **Al** Andaman Islands

SL Sri Lankan **Kh** Khoisan **Sp** Spitalfields

CA Caucasian Americans

HG Hunter Gatherer **Ind** Industrial **T** Trade **A** Agriculture
Ad Administrators
H Hard Footwear S Soft Footwear U Unshod

single outlying populations, the Spitalfields group and the Andaman Islanders, and three loose clusters the Aleut, Australians, Sri Lankans and Khoisan together, the Pachacama, Arikara, Chinese and Caucasian Americans together, and the African Americans, Ibo and Egyptians together. Only for the first cluster could any case be made for similarity of subsistence pattern, as all four are hunter-gatherer groups. This cluster, however, excludes the other hunter-gatherer population Andaman Islanders and includes different footwear types. Figures 6.29 and 6.30, the bivariate plots for PC3 with PC4 and PC5 with PC6, also provide little indication of grouping on the basis of either subsistence strategies or types of footwear. Any conclusions from these two two-dimensional representations are therefore less clear than results shown in Tables 6.47 and 6.48.

6.5 Discussion

6.5.1 The shape of the knee joint

H.6.1 There is no significant difference in the shape of the knee joint between the thirteen different populations of *Homo sapiens*.

The above analyses of knee joint shape show that all populations can be statistically separated on the basis of the morphology of the knee joint, using 100% of total variance. As shown in Tables 6.14 for the femur and 6.20 for the tibia, results from discriminant analysis with cross-validation show that between 85.71% and 100% of individuals are correctly assigned to groups for the femur and between 78.57% and 100% of individuals are correctly assigned for the tibia. The strength of differentiation in the shape of the knee joint therefore refutes the first hypothesis.

It appears that differences between populations for both femur and tibia predominantly lie with the angle of attachment of the diaphysis to the epiphysis and therefore, in relation to the femur, the changes in the intercondylar shelf angle. This changing angle of attachment, which explains much of the variation in the initial four PCs (using sample means) has been recognised in recent research by Craig (2000), who extended previous research by Baker et al. (1990).

Figure 6.29:

Inter-population variation in the tibia in 13 populations. Bivariate plot of PC3 with PC4, showing the separation of sample means of 13 populations. Populations are distinguished by type of subsistence strategies and footwear worn when living.

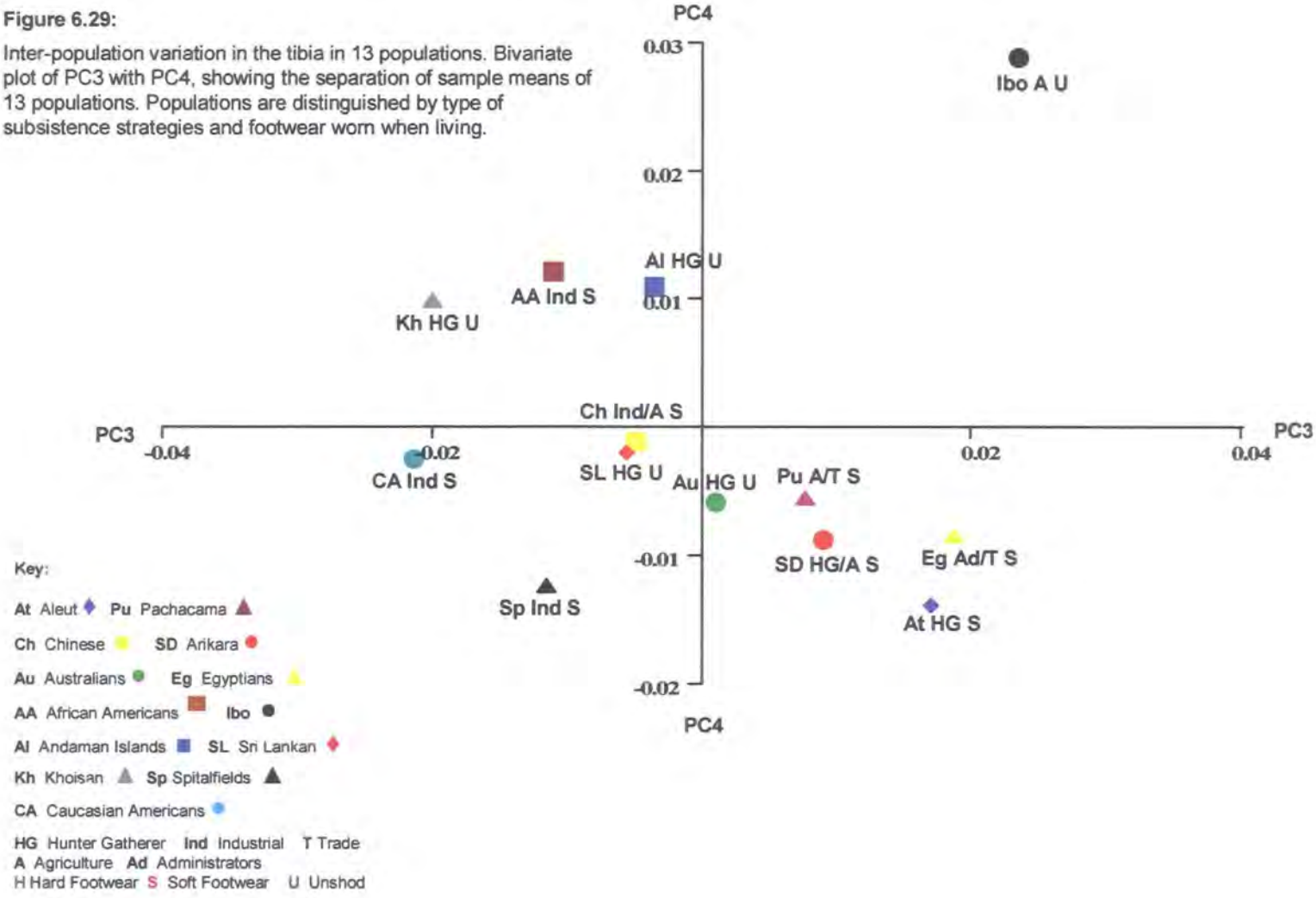

Figure 6.30:

Inter-population variation in the tibia in 13 populations. Bivariate plot of PC5 with PC6, showing the separation of sample means of 13 populations. Populations are distinguished by type of subsistence strategies and footwear worn when living.

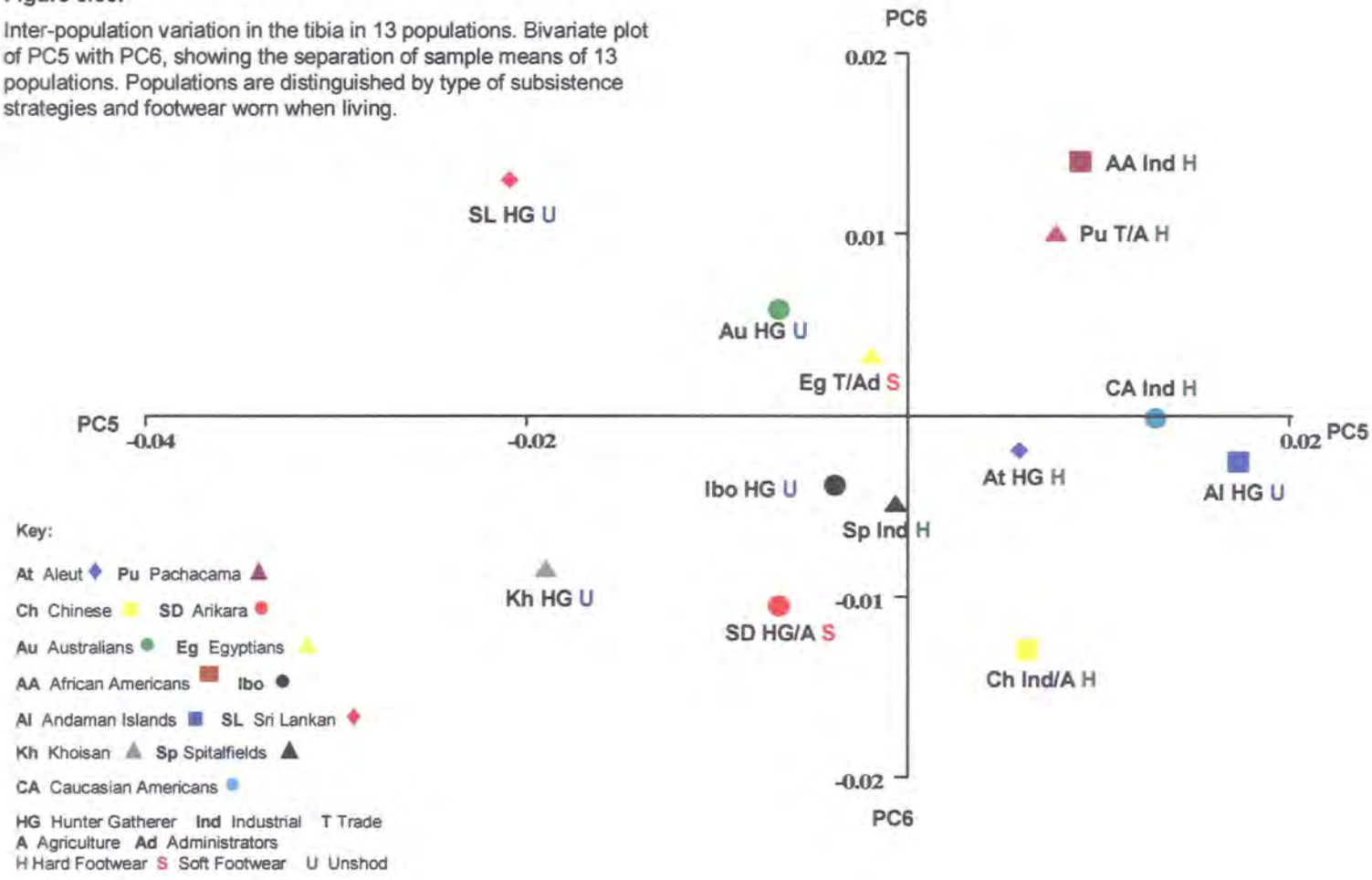

Whilst Baker et al. (1990) appreciated that the intercondylar notch height varied between two groups with different ancestral backgrounds (using African and Caucasian American samples), Craig proved that this difference in height changed the angle between the shaft and the joint along 'Blumensaat's Line', the line visible on a radiograph between the 'roof' of the intercondylar notch and the posterior shaft. Results showed that the more obtuse the angle, the more likely the individual to be Caucasian and conversely, the more acute angle the more likely the individual to be substantially African.

Tables 6.12 and 6.18 for both femur and tibia using the total sample, show the Spitalfields sample at a considerable distance from all others in terms of Mahalanobis' squared distances. Figures 6.2 and 6.7 for the femur and tibia, using population means, confirm this separation, showing the Spitalfields mean placed at a distance from all other means on the bivariate plots of PC1 with PC2. It was noted in section 6.4.1 that the angle between the diaphysis and epiphysis in both bones is greater in this sample than in any other and therefore the diaphysis is in a relatively more upright position relative to the joint. Figure 6.2 also explains the relatively greater degree of protrusion of the femoral medial condyle in the Andaman Islanders compared to other groups, with this population mean and the Spitalfields mean placed at opposite extremes of PC1. PC2 shows the varying width of the femoral posterior section of the joint, with the Aleut and Ibo placed at opposite extremes of the scale. For the femur, these four initial PCs explain nearly 75% of total variance (using population means) and are largely interpreted in terms of changes in the angle of attachment. For the tibia, the four initial PCs explain nearly 83% of total variance and, like the femur, predominantly explain this angle of attachment, together with differences in the shape of the tibial plateau (depending on the magnitude of the angle), and the length of the tibial tuberosity.

It is unclear if there is any functional utility to the differences in knee joint shape between populations and if so, what adaptive advantages may be conferred by such differences, or if shape changes arise largely as a consequence of differences in loading pressure or other environmental influences, without selective advantage.

Movement at the knee joint is complex and involves motion taking place in three planes; the coronal, transverse and sagittal planes. Movement in the sagittal plane is by far the greatest, taking the knee from full extension to full flexion (from 0^{o} to approximately 140^{o}). Safely accomplished movement involves various motions that are intrinsically unstable, for example, the femoral condyles are required to slide as well as roll over the articular surfaces of the tibia, the former being a relatively unstructured motion and one which comes into greater effect after 20^{o} flexion, i.e., for the majority of movement (Chapter 1 sections 1.6 and 1.7.2; Nordin and Frankel, 2001; Kingston, 2001).

The stability of the joint is largely controlled by the soft tissue within the joint capsule, relying on a complex arrangement and interaction of the cruciate and collateral ligaments with the menisci, which are obliged to actively distort on the tibial surface to accommodate the screwing mechanism of the femoral condyles. This spiralling motion of the tibia about the femur during extension and flexion is the result of the asymmetric configuration of the femoral condyles; the medial condyle extends more distally and is narrower and more protruding than the lateral condyle. At one stage during the process of extension, the medial condyle will be both sliding and rolling whilst the lateral condyle is still rolling. Any wear or damage to the menisci or ligaments causes some degree of mechanical 'play' in the joint with undue erosion of the cartilaginous surfaces and subsequent wear to the underlying bone surfaces. The less stable movements involved in the slide and slide-with-roll mechanisms are therefore put under even greater pressure (Palastanga e al., 1998; Kapandji, 2001; Kingston, 2001).

Basic differences in the anatomy of the sexes together with differences in loading pressures brought about by a sexual division of labour (Chapter 4), differences in the incidence and degree of osteoarthritis between the sexes and between different groups and populations (Chapter 5), and the effects of differing body-weight and obesity (Chapter1, section 1.8) alert us to the fact that different stresses and strains and differing levels of wear and tear can have far-reaching effects on the shape of joints over an entire sample. It is therefore understandable, given the complexity of movement within the knee joint, that this joint in particular will vary in shape between groups because of the multiplicity of external forces acting upon it and

regardless of intrinsic shape differences that may have arisen through genotype and evolutionary history.

6.5.2 The size of the knee joint

H.6.2 There is no significant difference in the centroid size of the knee joint between the thirteen populations of *Homo sapiens*.

H.6.3 The degree of difference in the shape of the knee joint between the thirteen populations is highly correlated with the degree of difference in centroid size.

Tables 6.23 (for the femur) and 6.26 (for the tibia) show that the centroid size of the knee joint varies between the thirteen samples and therefore refutes hypothesis H.6.2, that there is no difference in centroid size between the thirteen populations.

Differences in size appear to be smaller than differences in shape, with only 69.23% of pairwise comparisons for the femur and 53.85% of pairwise comparisons for the tibia reaching a statistically significant difference in size, compared to the 100% statistically significant difference (for both femur and tibia) in terms of shape. In addition, results from analyses of centroid size (based on the distances between the sample means for centroid size) compared to those of shape (based on Mahalanobis' squared distances between sample means), indicate that there is no statistically significant correlation between shape and size ($r = 0.06$, $p = 0.63$ for the femur and $r = 0.03$, $p = 0.79$ for the tibia).

These results therefore refute hypothesis H.6.3, that the degree of difference in the shape of the knee joint is highly correlated with the degree of difference in their centroid sizes. Populations with bigger knee joints are not hypermorphic versions of smaller ones and differences in the form of the knee joint are primarily based upon differences in shape, rather than differences in size.

6.5.3 Comparisons of sizes of the knee joint and the diaphyses

H.6.4 In a comparison of the femur with the tibia and within each bone separately, the three component size measurements (centroid size, maximum length and robusticity of the diaphyses) react to the various genetic and environmental forces influencing them to the same degree across different populations.

6.5.3a The three size elements of the femur and the three size elements of the tibia

In the light of previous research (e.g., Jacobs, 1985, Holliday and Ruff, 2000) that suggest that changing environmental conditions may affect the length of different parts of the anatomy at differing rates, this study compares size measurements between different parts of the same bone and between the two bones.

Tables 6.24 (for the femur) and 6.27 (for the tibia), using the total sample, show comparisons between the three size measurements for each bone. These tables indicate that the centroid size of the knee joint is correlated to a highly significant degree with both maximum length and robusticity indices of the diaphyses. For the femur, centroid size is correlated with maximum length ($r= 0.51$, $p<0.0001$) and with robusticity ($r= 0.31$, $p<0.0001$), as they are for the tibia ($r= 0.49$, $p=<0.0001$ and $r= 0.24$, $p<0.0001$, respectively).

The tables also show, however, that the degree of correlation between measurements within individual samples is not uniform. Five of the six populations show a statistically significant correlation between centroid size and maximum length for both femur and tibia, with the Spitalfields group showing a significant correlation for the femur only. Two of the four populations show the same high level of significant correlation for both the femur and tibia between centroid size and robusticity, while two further groups show a significant correlation for the femur only. Length is correlated with robusticity to a high level of statistical significance in the total sample and in all individual samples for both femur and tibia, with the notable exception of the Ibo tibia.

Therefore, the relative proportions of the three size elements appear to vary between the thirteen populations, despite the statistically significant correlations between the three size elements for the total sample. For example, the Andaman Islanders and the Sri Lankans have relatively short lower limbs, low centroid size at the knee joint and low robusticity indices of the shaft. The Australians are relatively gracile with long limbs and relatively small knee joints, and the Aleut have moderately large sized joints, moderately short stature, but high robusticity indices of the shaft.

This study has established a significant correlation between size and temperature; especially between size and cold temperature. For the femur, a significant correlation has been established between cold winter temperature and centroid size of the knee joint ($r= 0.49$, $p<0.0001$) (Table 6.31); and between robusticity and mean annual temperature ($r= 0.40$, $p<0.0001$) (Table 6.33). Whilst significant, the correlation is relatively weak between temperature and maximum length ($r= 0.11$, $p= 0.01$) although this improves when mean annual temperature is divided into mid-winter and mid-summer temperatures (Table 6.33). In relation to the tibia, again results show a highly significant and strong correlation between centroid size and mid-winter temperatures ($r= 0.43$, $p<0.0001$) (Table 6.35) and between robusticity and mean annual temperature ($r= 0.51$, $p<0.0001$) (Table 6.37). The correlation between mean annual temperature and maximum length is not significant ($r= 0.08$, $p= 0.09$), although when correlated with both mid-winter and mid-summer temperatures, it reaches a level of statistical significance.

These results therefore indicate that, whilst ambient temperature influences both the robusticity and length of bone, it has a greater influence on robusticity than on length. Length is therefore more likely to be influenced by additional factors. Thus, in using the previous examples, whilst the Australians from a year-round warm environment are relatively gracile, they are also relatively long limbed (Collier, 1989). In contrast, the Andaman Islanders and Sri Lankans, who are also from warm environments, are equally gracile but are of short stature, whilst the cold-adapted Aleut have moderately large knee joints with high robusticity indices but also have short limbs.

This variability between size elements within the same bone indicates that additional forces, such as the genetic history of a population, may be of greater significance than ambient temperature and other climatic considerations in determining leg length compared to external thickness (Formicola and Giannecchini, 1999), or of knee joint size. The increase in stature and lower limb length between first and subsequent generation migrants with increased quantity and quality of nutrition is also well documented and analysed (Martorell, 1988; Janz and Janz, 1999; De Mendonca, 2000; Loesch, 2000). In addition, whilst applying to both length and robusticity, previous research has noted that there is a considerable impact made on bone structure and bone mineral density in the lower limbs with changing activity patterns and particularly, with changing patterns of nutrition (e.g., Brock and Ruff, 1988; Bridges, 1989; Owsley and Jantz, 1994; Ruff, 1991, 1994; Ruff et al., 1984; Larsen, 1995, Jurmain, 2002).

6.5.3b The femur compared to the tibia

Predictably, results show a very strong and highly significant correlation between the centroid sizes of the distal femur with the proximal tibia, using the total sample ($r=0.93$, $p<0.0001$). Similarly, the correlations between the lengths and the robusticity of the two long bones are also highly significant and strong ($r= 0.88$, $p<0.0001$ and $r= 0.59$, $p<0.0001$, respectively).

Despite the strengths of these correlations between comparable elements of the femur and tibia for the total sample, however, the results of tibial size as a percentage of femoral size (Table 6.29), together with correlation statistics and associated probability values, indicate considerable variability between populations in the proportions of each bone relative to the other. Thus, whilst there is a limited range of difference in tibial centroid size of the knee joint relative to femoral size (2.97% across all samples), the range of difference in tibio-femoral indices across all samples is wider (6.13%) and for robusticity across all samples is wider still. For robusticity, there is a difference of 9.15% between the Chinese (with no significant correlation) and the Egyptians.

Results from this study therefore refute hypothesis H.6.4, (the three constituent size elements react to genetic and environmental forces influencing them to the same degree across different populations). It is shown that the various genetic and environmental forces acting upon the two bones are probably unique to each of the thirteen populations, which result in differing proportions between the three elements within each bone and between the two bones. Such a conclusion concurs with research that stresses the variability in shape and size (and bone density) of different elements of the postcranial skeleton under differing circumstances and environmental conditions and of relative variation in the proximal and distal limb segments, both within and between populations (Allen, 1877; Jacobs, 1985; Janz and Janz, 1999; Holliday and Ruff, 1997, 2001).

6.5.4 The relationships between populations: This study in relation to the research by Howells (1989) and Cavelli-Sforza et al. (1994)

H.6.5 Similarity in the shape of the knee joint between different populations is related to similarity of craniofacial shape or ancestral history or both.

Differences in results between the craniofacial morphology and molecular approaches centre on the affinity between Africans and other populations; either they are related to Australians and Andaman Islanders (Howells, 1989) or they are dissimilar to all other populations (Cavelli-Sforza et al., 1994). The results of analyses using these different approaches can be seen in Figure 6.31, taken from Howells (1989), and Figure 6.32, which has been derived from data by Cavelli Sforza et al. (1994). Howells (1973), Van Vark (1985), O'Rourke et al. (1985) and Cavelli-Sforza et al. (1994) largely attribute the differences in results to the influence of climate, although other factors may also be responsible (e.g., parallel evolution from earlier morphologies; Stringer, 1992).

The present study uses seven population samples from the 28 comparable to those used by Howells (1989) (Australians, Bushmen [Khoisan], Andaman Islanders, Egyptians, Peruvians [Pachacama], Arikara and Eskimo [Aleut]). In relation to these seven samples, Howells' results show the Andaman Islanders clustering closely to the San and relatively closely to the Australians on the initial bifurcation.

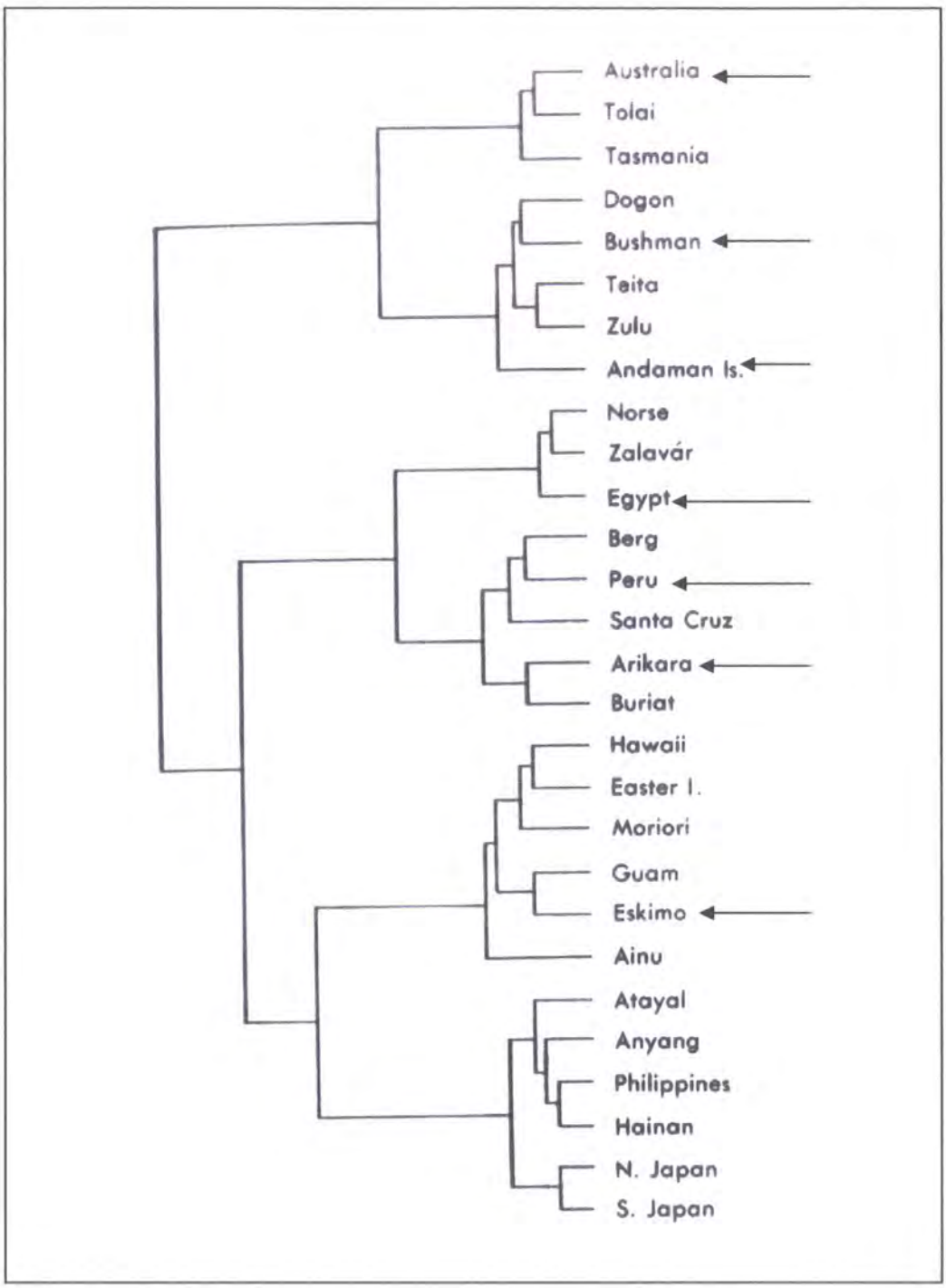

Figure 6.31: Dendogram of relationships between 28 male groups based on intergroup correlations calculated from cranial measurements. Dendogram reproduced from Howells (1989). Arrows highlight the populations comparable to those used in the present study.

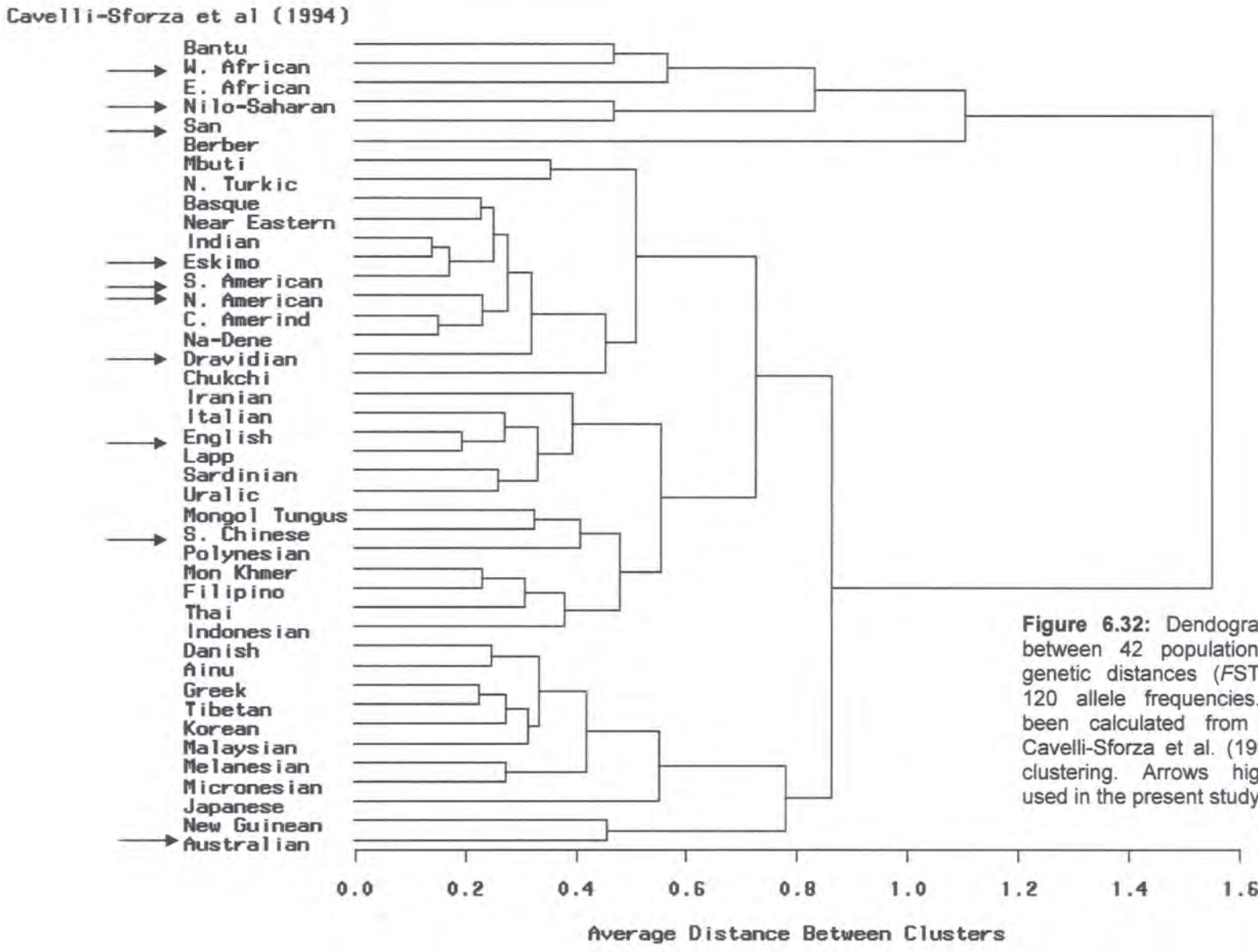

Figure 6.32: Dendogram of relationships between 42 populations based on their genetic distances (*F*ST), calculated from 120 allele frequencies. Dendogram has been calculated from data taken from Cavelli-Sforza et al. (1994), using UPGMA clustering. Arrows highlight populations used in the present study.

The Peruvian population clusters relatively closely to the Arikara, with the Eskimo clustering on a separate bifurcation away from the other two Amerindian groups and closer to Pacific and Asian populations. The Egyptians are shown clustering with northern European groups. There are ten population samples in this study comparable to those used by Cavelli-Sforza et al. (1994), (W. African [Ibo], Nilo-Saharan [Egyptian], San [Khoisan], English [Spitalfields], Dravidian [Sri Lankan], N. American [Arikara], S. American [Pachacama], Eskimo [Aleut], S. Chinese [Chinese] and Australian). The data of Cavelli-Sforza et al. (1994) produce results that show the South American Amerindians clustering more closely with the Eskimo than with the North American Amerindians and the Chinese clustering with Southeast Asian populations. The Australians and New Guineans are on a separate but closely linked branch to a mixed Asian and Caucasian group. The English are grouped with other European and non-European Caucasians. Six of the seven African populations, including the Caucasian Nilo-Saharan sample, are divided from all other populations on the first bifurcation. This latter group is seen in close proximity to the San; remaining closely linked to the East Africans and apart from the West Africans on a separate bifurcation.

In comparing the results of this study with those of Howells (1989) and Cavelli-Sforza et al. (1994), the Mahalanobis' squared distances in Tables 6.12 and 6.18 (and represented here in Figure 6.33 for the femur and Figure 6.34 for the tibia, generated from the distances), indicate relatively few similarities, apart from some degree of agreement between all three studies regarding the association of Amerindian groups. Although Figure 6.33 shows the Arikara are relatively distant from the Aleut and Pachacama for the femur, all three populations are closely linked for the tibia. For the femur, the Arikara is closely linked to the northern Asian (Chinese) population. Discriminant analysis with cross-validation (Tables 6.40 and 6.41) also emphasises the relatively close association between these four populations, by assigning 80.70% of individuals to the correct northern Asian/Amerindian group for the femur and 74.56% for the tibia. The results of Cavelli-Sforza et al. (1994) shows a similar pattern of a relatively close association between the Eskimo, North Americans and South Americans although Howell's (1989) results show the Eskimo positioned away from the more closely linked Arikaran and the Peruvian groups.

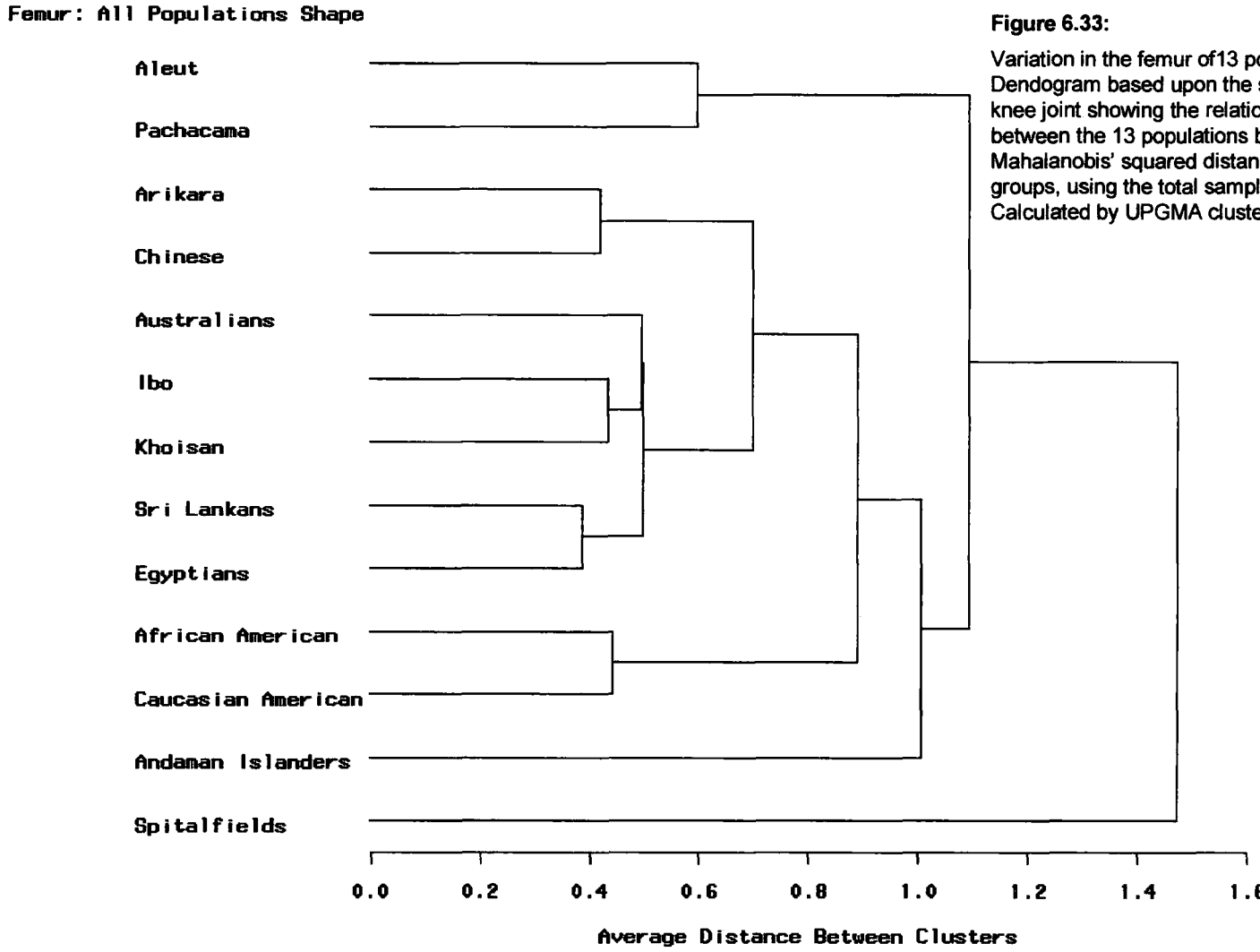

Figure 6.33:

Variation in the femur of13 populations. Dendogram based upon the shape of the knee joint showing the relationships between the 13 populations based on the Mahalanobis' squared distances between groups, using the total sample. Calculated by UPGMA clustering

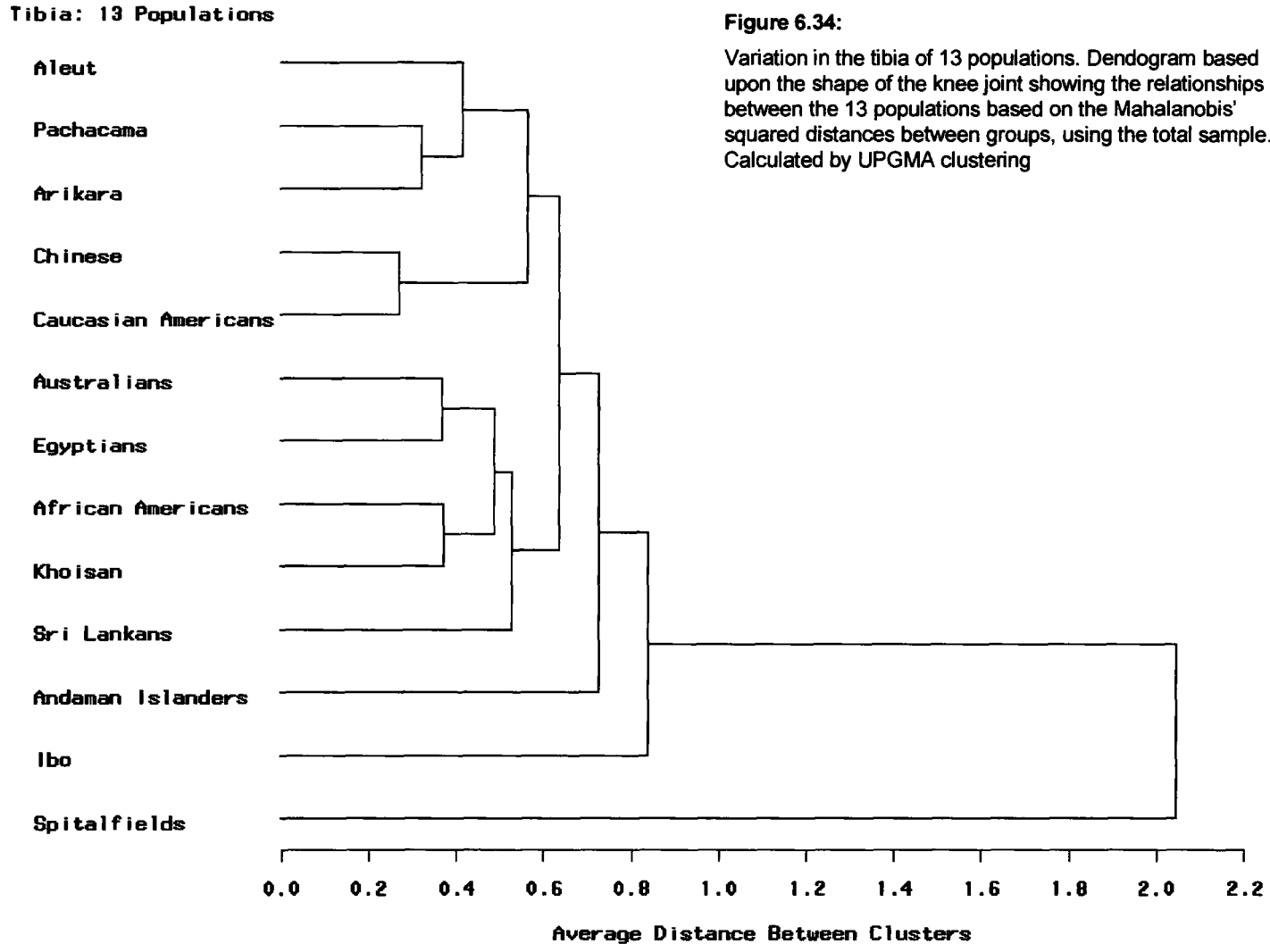

Figure 6.34:

Variation in the tibia of 13 populations. Dendogram based upon the shape of the knee joint showing the relationships between the 13 populations based on the Mahalanobis' squared distances between groups, using the total sample. Calculated by UPGMA clustering

In relation to the African populations, Howells' analysis shows three sub-Saharan populations clustering together, with the Egyptians remaining distinct. In the analysis by Cavelli-Sforza et al. (1994), the six African populations on the first bifurcation include the Nilo-Saharan sample. In the present study (using population means) Figure 6.33 for the femur, shows the Khoisan and Ibo closely linked with the third group of African derivation (the African Americans) remaining at a distance. For the tibia, Figure 6.34 shows the African Americans and Khoisan closely linked with the Ibo remaining distant on the second bifurcation. Although the Egyptians are positioned at a considerable distance from other African groups in the Howells' (1989) analysis, in this study they remain relatively close to the Khoisan and Ibo for the femur and to the Khoisan and African Americans for the tibia. Using the total sample, discriminant analysis with cross-validation (Tables 6.40 and 6.42) indicates a relatively high proportion of individuals from the three sub-Saharan African samples correctly assigned to group at 65.79% for the femur and 72.22% for the tibia. Although cross-validation indicates some degree of cohesion within this category, the strength of this association is, however, less clear from results in the dendograms using the total sample.

With respect to the three Caucasian groups of European and North African derivation, populations in this study show no close relationship (Figures 6.2 and 6.7 for the femur and tibia respectively). Discriminant analysis with cross-validation (Tables 6.40 and 6.42) correctly assigns 71.68% of individuals to group for the femur, but less than 60% of individuals are correctly assigned for the tibia.

In neither study by Howells (1989) nor Cavelli-Sforza et al. (1994) are individual populations seen as distinct outliers. This is in contrast to the present study (using population means), that shows the Spitalfields and Andaman Islanders at a considerable distance from all other populations for the femur (Figure 6.2) and the Andaman Islanders and Ibo and, particularly the Spitalfields group, at a considerable distance for the tibia (Figures 6.7); results that are confirmed in Tables 6.12 and 6.13 and Figure 6.33 for the femur and Tables 6.18 and 6.19 and Figure 6.34 for the tibia (using the total sample).

From the comparison with Howells' (1989) results, it appears that similarity of knee joint shape is unlikely to be based upon a population distinction in morphology that is carried throughout the cranial and postcranial skeleton. Therefore, similarity of cranial shape between populations is unlikely to be correlated with similarity of knee joint shape. Similarly, from the comparison of this study with the study by Cavelli-Sforza et al. (1994), similarity of knee joint shape does not appear to be solely or even predominately dependant on close genetic relatedness. Although a loose agreement can be made for the Amerindian populations between the three studies, in that the shape of the knee joint and of the cranium, together with the genotype of these groups may be seen as relatively distinct, there is little evidence to show that similarity in the shape of the knee joint between any of the other populations in the study is correlated with either craniofacial shape or ancestral history. As such, hypothesis H.6.5 must therefore be refuted.

6.5.5 Possible reasons for differences in the form of the knee joint between the thirteen populations

H.6.6 Similarity of form of the knee joint between different populations is highly correlated with similarity of their environmental background.

6.5.5a The influence of climate on the shape and size of the knee joint and the diaphyses

> "It seems logical to conclude that shape, and not only size, are strongly influenced by natural selection by climate"
> (Cavelli-Sforza et al., 1994, p72).

Results from this study indicate that climate may have a more powerful influence over the form of the knee joint than either genetic relatedness or other broad categories of environmental factors, in the majority of cases. Data for the femur using population means, indicate that the most obvious cluster of populations sharing similarity of knee joint shape are those sharing warmer year-round temperatures, including the Australians, Ibo, Sri Lankans, Egyptians, Khoisan and the Andamanese. Despite sharing the same warm summer temperatures as groups with

warm year-round climates, populations such as the Chinese, Arikara and African and Caucasian Americans, which experience severe winter temperatures, are less associated with this former group. Clustering of means based on climatic variables is less clear for the tibia (Figure 6.7) where the shapes of two outlying populations (the Spitalfields mean on PC1 and the Andamanese mean on PC2) are primarily driving the variation explained in the initial two PCs. As correlations between shape and temperature are much stronger with cold mid-winter temperatures (Tables 6.25 and 6.29), it is likely that it is this aspect of climate that more greatly affects shape than other climatic variables. Evidence to support the effect of cold upon morphology is provided by Hernandez et al. (1997) who concluded that the distinct cranial morphology of Tierra del Fuegians, which is mirrored by Eskimo groups, was in large part due to the cold, harsh climate they inhabited. Evidence from other mammals (rats) also supports these conclusions (Riesenfeld, 1973).

Results show that not only does temperature heavily influence shape, it also influences the size of the knee joint. For centroid size, mid-winter temperatures are shown to be far more influential than mid-summer temperatures, with a stronger correlation between bigger size and colder mid-winter temperature (the Spitalfields population being the one exception in relation to the tibia).

As predicted by Allen's and Bergman's Rules, climate also affects the length and the robusticity of long bones and the results of this study bear this out in relation to robusticity and, to a lesser extent, in relation to length (Tables 6.33 and 6.37). For the femur, results of correlations between temperature and maximum length reach a level of statistical significance for mean annual temperature, mid-winter and mid-summer temperatures. For the tibia, correlation is relatively weak for mid-winter temperature but stronger for mid-summer temperature. Robusticity of the long bones, however, is strongly correlated at high levels of statistical significance in both bones for mean annual temperature, mid-winter and mid-summer temperatures.

Tables 6.34 and 6.38 (for the femur and tibia, respectively) indicate the differing effects of temperature on length and robusticity, sorting the thirteen populations in terms of length, robusticity and mid-winter temperature. In this analysis, whilst length shows no discernable pattern between the two variables, levels of robusticity

are seen to be higher in populations with cold mid-winter temperatures. The exception to the pattern for both femur and tibia is the Pachacama, whose original location is unclear (see Chapter 2 section 2.1.2b).

Rainfall patterns also appear to have some influence over the determination of the morphology of the knee joint (Tables 6.25 and 6.29). It is likely, however, that rainfall levels are less crucial than temperature in determining shape as Figure 6.2 (for the femur, using population means), shows the Egyptians, (27mm of rainfall per annum), clustering with the Sri Lankans and Ibo (1,748mm and 1,866mm per annum respectively). A significant, albeit relatively weak, correlation is seen, however, between annual rainfall patterns and the length of the long bones. This finding concurs with research such as that by Ruff (1991), who pointed to the significant effects of rainfall and particularly humidity on body size. Robusticity appears to be less influenced by rainfall patterns for both femur and tibia.

This study indicates that altitude may not be of great significance in determining knee joint shape in the femur, although results show a greater degree of correlation between altitude and tibial shape (Table 6.35). There is no significant correlation between altitude and knee joint size. In addition, Tables 6.33 and 6.37 indicate that in relation to long bone length and robusticity, altitude may not be of great influence, with only weak correlations shown for the tibia ($r= 0.09$, $p= 0.03$ and $r= 0.08$, $p= 0.05$ respectively). As most populations in this study were living at lower altitudes, however, it is possible that the inclusion of a greater number of populations living at higher altitudes would have influenced results and produced more positive correlations for both femur and tibia.

Numerous pieces of research and most textbooks on human biology have stated that there is a causal link between climatic variables and body size and proportions, emphasising the importance of temperature, rainfall and humidity (Trinkaus, 1981; Kouchi, 1983; Weiss and Mann, 1989; Howells, 1989; Gugliemino-Matessi et al., 1979; Cavelli-Sforza et al., 1994; Holliday and Falsetti, 1995; Ruff, 1991, 1994; Holliday and Ruff, 1997; Hernandez et al., 1997; Pearson, 2000; Wells, 2000; Cavelli-Sforza, 2001; Jurmain, 2002; Angilletta et al., 2004). Correlations between altitude and body size and shape are less clear, with research tending to concentrate on physiological and genetic adaptations relating to the effects of cold temperature

and changing oxygen levels with increasing altitude (Harrison et al., 1964; Weiss and Mann, 1989; Jones et al., 1992; Rupert et al., 2003). The results of this study are supported by the previous research in demonstrating the association between temperature and rainfall in relation to centroid size and of the length and (more especially) the robusticity of the two long bones. Results of this study also demonstrate the association between knee joint shape and climatic variables, especially temperature. Any possible association between limb size and shape and altitude is less clear. Future research should be directed towards a better understanding of the effects of altitude on body length and robusticity and knee morphology. This would be achieved by extending the present dataset to include additional samples from higher altitudes.

6.5.5b Other factors influencing the shape of the knee joint

There is insufficient evidence from this study to determine how *great* an influence the type of footwear worn or the type of subsistence strategies undertaken has in determining the shape of the knee joint, although results show that both factors have some significant effect. Results of discriminant analysis with cross-validation (Tables 6.45 and 6.47 for the femur and 6.49 and 6.51 for the tibia) indicate that for both footwear types and subsistence strategies, a relatively high percentage of specimens are correctly assigned to group. This separation is also indicated in Figure 6.25 (femur) using population means, where for PC1 the four heavily shod and industrial populations (Spitalfields, African and Caucasian Americans and Chinese) are placed towards the negative extreme, with remaining groups placed more towards the positive extreme. No other PCs for the femur (or any for the tibia) show a clear separation of means based on either footwear or subsistence category.

Previous research, however, has indicated that the type of subsistence systems practised has an important influence over morphology, and that bone shape, size and robusticity are significantly affected by the type of activity and changing patterns of activity undertaken by populations (Owsley and Jantz, 1985, 1994; Gregg and Gregg, 1987; Brock and Ruff, 1988; Bridges, 1989; Collier, 1989; Hawkey and Merbs, 1995; Larsen, 1995; Churchill and Morris, 1998; Jurmain, 2002). Examples in the literature cite changes in the internal and external structure of the femoral diaphysis,

which is thought to become more rounded with changing bending stresses in the transition from hunting and gathering to agriculture (Ruff and Hayes, 1983; Ruff et al., 1984; Brock and Ruff, 1988). These adaptations in shape are frequently linked to the changing patterns of nutrition associated with a shift in subsistence strategies (Brock and Ruff, 1988; Bridges, 1989; Larsen, 1995; Owsley and Jantz, 1985, 1994; Collier, 1989; Jurmain, 2002). Results thus indicate a complex relationship between changing activity, activity levels and the type, quality, quantity and reliability of food supplies with changes in skeletal morphology. Research from these sources has been used previously in this study to help interpret differences in morphology between right and left limbs and between males and females from the same populations.

Lord et al. (2000) have outlined the forceful effect that the type of footwear worn can have on the bone structure of individuals, particularly with fashionable footwear with high heels, and the detrimental effects that can be produced on postural stability. This research is reinforced by Rossi (2005), who differentiates between 'normal' gait, which is unnatural through being forced to accommodate footwear, and the gait produced from bare feet, which is anatomically 'natural'. Both studies support earlier research by Lanyon et al. (1975), who found that, whilst running, the lower limb strain measurements in any individual can vary by 40%, depending whether one is shod or unshod. Undoubtedly, the use of certain types of shoes that change the biomechanics of the foot and ankle will have some impact on knee joint shape.

The powerful influences of the quality and quantity of good nutrition and the deleterious impact of disease (both the degenerative diseases of bone and joint wear and of infectious disease) must also have an important effect on bone shape. The effect of specific diseases directly attacking bone such as the arthritic and bone-wasting diseases obviously has a direct impact on the shape of bone. The effect of these diseases on knee joint shape has been examined in Chapter 5. From results in Chapter 5, it is clear that shape changes from such diseases are likely to be progressive over a long period, resulting in gradual change and frequently culminating in dramatic alterations to the external appearance of bone. Infections that do not initially attack bone but subsequently cause infection of bone (osteomyelitis), will therefore affect the skeleton and change its internal and external architecture. Bone, regardless of type or location, is a highly vascular organ and the many diseases

and infections that affect the degree and quality of the blood supply passing through will have an effect on its structure, particularly in the developing skeleton (Johnson, 2004; Chapter 1 section 1.3). Typical examples of the type of bacilli causing osteomyelitis are staphylococci, streptococci and pneumococci infections, influenza, typhoid and tuberculosis (Roberts and Manchester, 1997; Aufderheide and Rodriguez-Martin, 1998).

Relevant to this study, it is also acknowledged that of the joints, the knee is highly vulnerable to osteomyelitis and that the tibia has the highest rate of infection of all bones in the skeleton, particularly the anterior tibia (Dickel, 1984; Milner, 1991; Roberts and Manchester, 1997; Larsen, 1999). Larsen (1999) suggests that the reason for the vulnerability of the anterior tibia is its lack of a thick muscular covering and thus slightly cooler temperature leading to greater levels of bacterial colonisation, together with the generally poorer circulation of blood in the lower limbs due to gravity. In addition, bone structure damaged by infection also leads to an increased susceptibility to trauma.

Two infections that are also known to affect bone, particularly the tibia, include syphilis and malaria (Cronin et al., 1986; Miller, 2000). Syphilis is known to have seriously affected the Andaman Islander individuals used in this sample, and malaria (together with sickle-cell anaemia), to have been endemic in the Ibo homelands at the time this present sample were alive. Both secondary and tertiary syphilis produce systemic symptoms including bone pain and frequently form lesions on the tibia, as well as the skull, clavicles, ribs and sternum (Cronin et al., 1986; Larsen, 1999). Syphilis was commonplace in many communities, both rural and urban throughout the eighteenth and nineteenth centuries and beyond and 'medicines' containing arsenic, mercury and other compounds now regarded as seriously deleterious to skeletal health, were frequently administered. The Andaman Islanders in this sample had been treated for the disease in a sheltered hospice (see Chapter 2 section 2.1.2h). Malaria likewise, has serious implications for bone health; one of the side effects being enlargement of the marrow spaces (*parotic hyperostosis*). Resulting lesions are usually found in the skull bones prior to affecting the postcranial skeleton (Robertson, 2004). Although only lesion-free and apparently healthy long bones

were chosen for use in this study, both the Andaman Islanders and the Ibo have proved to be outlying samples in this study (see section 6.6.5 below).

Today, a high quality and well balanced diet is known to be necessary for the development and maintenance of the skeleton. In one extreme example of a poor and insufficient diet, *anorexia nervosa*, the disturbance in bone formation and remodelling capability is well known and largely understood. Osteoporosis is a well-known concomitant of *anorexia nervosa* (Zanker and Cooke, 2004). Also, numerous experiments on animals and observations on humans have attested to the effects of a deficiency or excess of various minerals and vitamins for bone health, particularly calcium. In humans, several reports have been conducted on the effects of an excess or deficiency in copper, zinc, selenium, phosphorus, fluoride and sodium, together with most vitamins (Turan, 1997; Klevay and Wildman, 2002). When using rats, Riond et al. (2000) found that an excess of magnesium in the diet reduced the strength of vertebrae and their load-bearing capability.

6.5.5c Summary

Although results in this study indicate that climatic variables constitute powerful influences over knee joint and long bone shape and size (perhaps the most powerful influence), they are therefore unlikely to be the only factors involved. The effects of activity patterns, types of footwear and of disease and nutrition must be considered important and additional variables that affect bone morphology in this part of the skeleton.

6.6 Implications of results

Results of Chapters 3, 4 and 5, analysing intra-population differences in knee joint morphology (using a restricted number of populations) and Chapter 6 analysing inter-population differences (using the full sample) have shown that a variety of influences create differences within and between populations. These influences have been analysed and assessed above. Results have also shown that *combinations* of factors appear to be highly influential in creating more extreme morphologies. In this study, the morphology of the Spitalfields knee joint is distinctive for both the femur

and, more especially for the tibia, relative to the other twelve populations. This is seen in the extreme distance between this sample and all others in Tables 6.12 and 6.18 (using the total sample) and in Figures 6.2 and 6.7, (using population means), together with results from previous analyses conducted in Chapters 3, 4 and 5. The possible causes for this distinctive shape require some explanation.

The following section will detail the implications of results in relation to the present Spitalfields sample and will indicate how future research could be directed, if supplementary data were used from additional specimens in the museum collection.

6.6.1 The Spitalfields sample

In relation to the other twelve populations, the English climate is relatively temperate with cool (but not cold) winters and mild summers. Although the climate for the Spitalfields population was considerably colder than today because of the 'Little Ice Age' of the period (Molleson and Cox, 1993), temperatures would have been well within the limits for other regions experiencing cold winter climates. Annual rainfall is below average for the thirteen populations tested here (752mm, compared to the mean for the thirteen populations of 996 mm per annum), and the altitude for London is relatively low (23 metres above sea level) compared to the other twelve groups (Table 6.30). The footwear worn by the population in the eighteenth and early nineteenth centuries was heavy but as many of the inhabitants were manual workers, the majority were unlikely to have worn fashionable shoes with high heels during their workaday lives, although some (notably the wealthier Huguenot class) may have worn more extravagant styles at least some of the time (Molleson and Cox, 1993; Cox, 1996).

It is therefore unlikely, that the distinctive shape of the Spitalfields knee joint can be attributed to the general broad categories of climate and footwear. Three explanations for the distinctive shape are therefore possible: firstly, the damage to the growing skeleton caused by repetitive strain in the silk weaving industry in a sizeable proportion of the population and the continuation of this damage into adult life, secondly, the damage to the skeleton caused by food and water pollution and thirdly, the effects of infectious diseases on the skeleton, especially the tibia.

In an attempt to determine the specific attributes of the Spitalfields population and the causes of the distinctive knee joint morphology, the following section will explore any differences in life histories between this sample compared to the other twelve populations. As far as can be inferred, none of the other twelve populations shared all three features that may have influenced the distinctive shape of the Spitalfields knee joint.

6.6.2 The shape of the Spitalfields joint

PC1 in Figures 6.2 and 6.3 for the femur and, especially, Figures 6.7 and 6.8 for the tibia (using population means) show Spitalfields as an outlying sample. For the femur, the first two PCs (49.2% of total variance, using sample means) predominantly explain differences in shape between populations in terms of the angle of retroversion of the diaphysis to the epiphysis, and a relative narrowing of the posterior proportions across the condyles. Thus, the Spitalfields epiphysis has a greater angle of retroversion relative to the diaphysis, with a narrower and more 'squared' appearance relative to those of other populations. For the tibia, PCs 1 and 2 (69.2% of total variance, using sample means), explain a greater angle of retroversion of the epiphysis relative to the shaft, relative to the other populations, together with a decreased anteroposterior length relative to mediolateral width (complimenting the greater angle and more squared appearance of the distal femur). The relative depth of the tibial tuberosity is also greater in this sample relative to the other twelve populations. There are no indications of excessive distortions in the epiphyses or pathologies that could be construed as 'damage' in either the distal femur or proximal tibia.

6.6.3 Extreme working practices

It is suggested that the physical stresses endured by a significant number of the Spitalfields community have effected sufficient change in the shape of the knee in the sample mean to create this extreme distance from the other populations. Many of the Spitalfields individuals are known to have worked in the silk weaving industry, estimated as approximately 20,000 journeymen at any time during the eighteenth and first half of the nineteenth centuries (Cox, 1996). At this time, the silk weaving

process used handlooms powered by treadles that were operated by the feet and legs (Bythell, 1969; Tummins, 1993). The knees in particular would have been in continual motion, involving repetitive movements repeated many thousands of times each day (Cox, 1996). It is suggested that the continual flexing and extending of the knee might have had repercussions for the shape of the joint, particularly if practised from childhood onwards (see Chapter 2, section 21.2l).

Whilst others in the remaining twelve populations (including the African and Caucasian Americans, the Aleut and the Chinese), would have been exposed to severe working conditions they were unlikely to have been exposed as *children* to the same potential skeletal damage that the Spitalfields people faced in the industrial workplace. By the early twentieth century in the USA, few children would have been involved in the heavy industrial processes endured by the African and Caucasian American adults. The male-only Chinese sample in this study were first-generation adult migrants working in Alaskan canning factories, although nothing is known of their early lives in Northern China. The Chinese specimens in the museum collection (whether used in this study or not) were, however, in relatively good condition with no visually obvious distinguishing marks of injury, deformity or growth disruption (Chapter 2, sections 2.1.2f and 2.1.2d).

The Aleut would have been used to an extremely arduous working life in extreme climatic conditions. Whilst ancient Thule Eskimos show many stress lesions in the postcranial skeleton, particularly in relation to damage to the clavicle ('kyaker's clavicle'), these are absent in Aleut skeletons (Hawkey and Merbs, 1995). Such lesions were avoided in the Aleut because of the preconditioning of young boys by physical training, to prevent muscle damage in adult life (Hawkey and Merbs, 1995). This preconditioning was undoubtedly absent in the Spitalfields sample, where children were used as weaving loom operators from an early age (Molleson and Cox, 1993).

The Arikara were one of the North American Indian populations severely affected by a rapidly changing and disrupted environment following contact with incoming Europeans. Whilst such disruption caused a deterioration in demography, health and nutrition (Owsley and Jantz, 1985; Palkovich, 1994; Stodder, 1994), and created new

types of stresses on the lower skeleton through the introduction of horses (Erikson, 2000), this Arikaran sample are thought to come from the pre-contact period and it is unlikely that the lower limbs would have been subjected to abnormal influences on morphology such as unaccustomed physical stresses (section 2.1.2c).
To test the suggestion that extreme working practices in sufficient numbers of the Spitalfields population might be affecting the shape of the Spitalfields mean relative to the other populations, the following analyses are applied. Only the proximal tibia is tested as there is insufficient information of occupations for the current distal femoral specimens.

Figure 6.35 shows the bivariate plot of PC1 and PC2 (using the total sample of 370 individuals from the thirteen populations, including 40 Spitalfields specimens). The Spitalfields population is highlighted at the negative extreme of PC1 (accounting for 21% of total variance, see Table 6.17). Individuals from other populations that overlap with the Spitalfields sample are also highlighted, and include specimens from seven other samples; indicating that no other single sample shares the Spitalfields morphology. Therefore, the Spitalfields sample is relatively distinct from the majority of other samples on PC1. There is considerable variability, however, within the Spitalfields sample on both PCs 1 and 2.

To explore further the possible association between distinctive morphology and occupation, Figure 6.36 shows the separation of twelve specimens whose occupations are known (from collection records held in the NHM). By convention, Spitalfields individuals are divided into four categories; master weavers, journeymen weavers, non-manual workers and manual workers from non-weaving occupations (personal communication from T. Molleson, NHM). For this analysis, only male specimens are used, as some females (particularly those from the non-manual category) would not have been employed outside the home.

For this analysis, PCs 1 and 2 account for a cumulative 50.4% of total variation. Figure 6.36 shows some degree of separation of non-manual workers on PC2, on the negative side of the scale. All other individuals are placed towards zero and the positive extreme. The mean configuration on PC2 shows wide variability in shape between the twelve specimens, with individuals at the positive extreme having

Figure 6.35:

Inter-population variation in the tibia in 13 populations. Bivariate plot of PC1 with PC2, highlighting the Spitalfields individuals relative to the other populations (using the total sample). The plot also highlights those individuals from other populations who overlap with the Spitalfields sample.

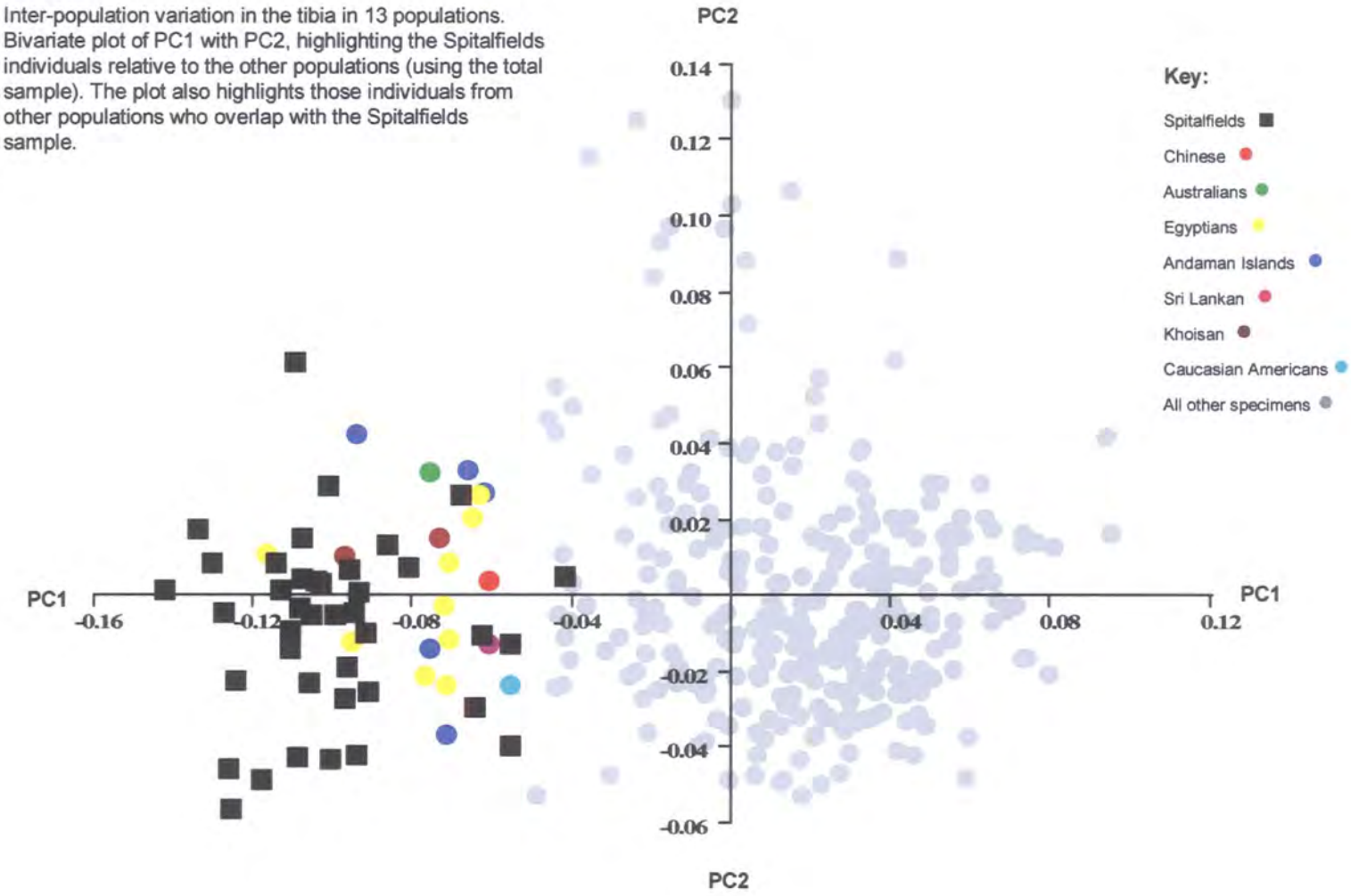

Figure 6.36:

Bivariate plot of PC1 with PC2, showing variation in the tibia in 12 known male workers in the Spitalfields population. Images represent the mean configuration if warped to the extremes of PC2 (at 0.10 and -0.10). Image at positive extreme of PC2 shows landmarks discussed in text (section 6.6.3).

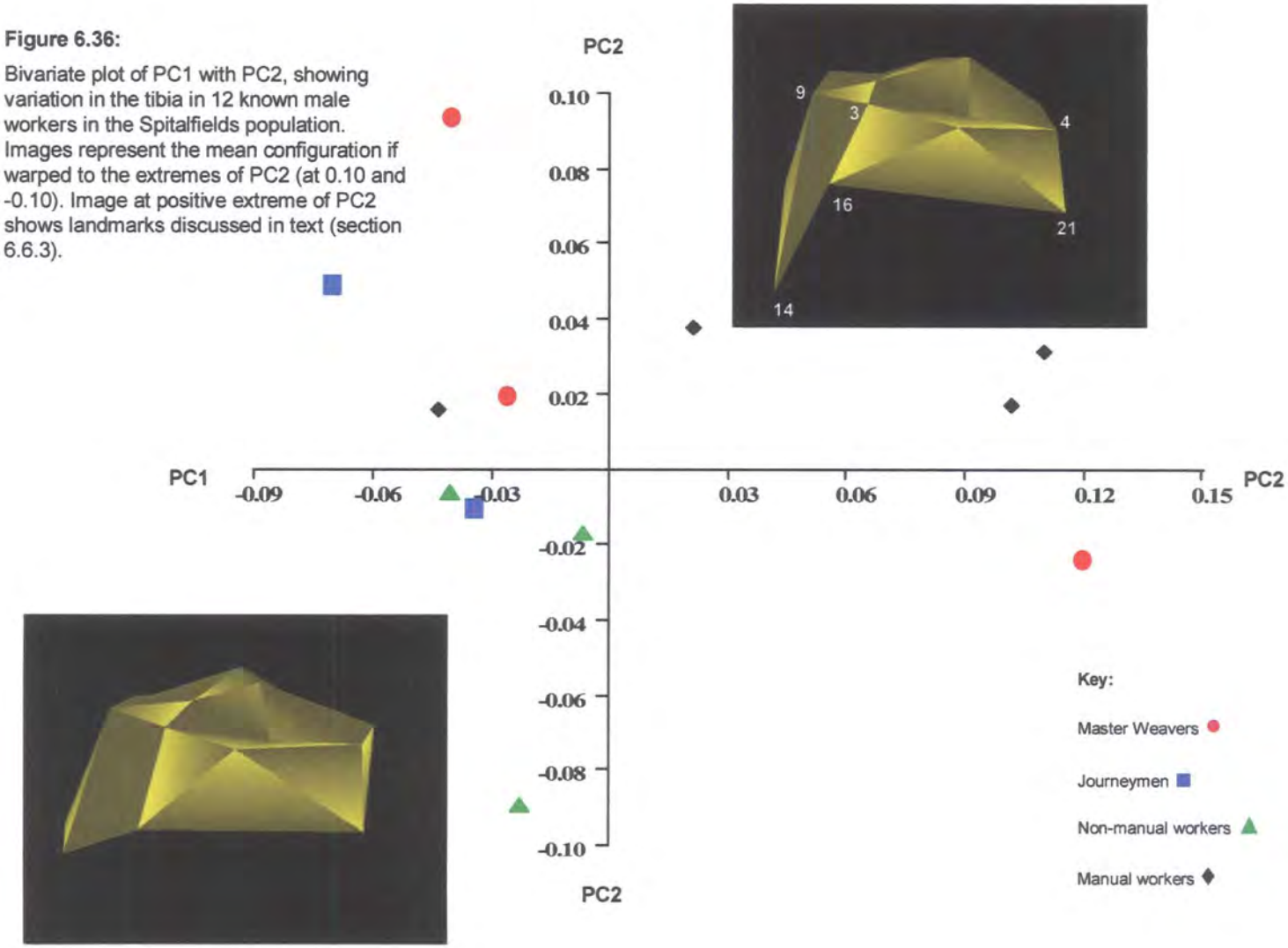

considerably greater length of the tibial tuberosity (from the edge of the tibial plateau (landmarks 3 and 9), relative to those at the negative extreme. The anterior region of bone is also more anteriorly projecting with decreased length in the tibial tuberosity, whilst at the same time, the posterior region appears less projecting posteriorly (seen in the difference in positions of landmarks 4 and 21). Results in Chapter 4 noted that in the African American population (and confirmed in five of the six populations when analysed jointly), that greater length of the anterior region is a masculine trait. Although all specimens in this present analysis are male, these results suggest the possibility that those in less physically stressful occupations present with a more feminised shape.

Results using a limited number of specimens imply an association between extreme physical loading caused by occupation and knee joint shape. Figure 6.35, however, indicates that the distinctive morphology is relatively general to all Spitalfields individuals. Therefore, a selected few highly stressed individuals do not appear to be skewing the distribution, thus creating extreme distance in the population mean. It is apparent, therefore, that factors other than (or at least in addition to) extreme working practices, are creating the distinctive Spitalfields morphology.

It is interesting to note that Grieve (1996) found no causal relationship between the incidence of osteoarthritis in weavers relative to non-weavers. This also implies that the cause of the atypical Spitalfields morphology is less likely to lie with the effects of occupational stress. Grieve also notes, however, that whilst journeymen proved to have the least percentage of arthritis overall of the four occupational categories, they also had the greatest degree of severe arthritis.

6.6.4 Harmful or inadequate nutrition

Although the Spitalfields population would have been sufficiently well-off to purchase adequate supplies of food, the quality of foodstuffs was severely compromised (section 6.5.5b). Foodstuffs were frequently and deliberately adulterated with contaminants including alum, chalk, lead, copper and sulphuric acid (see Chapter 2, section 2.1.2l). Copper pans used in middle-class households for cooking impregnated foodstuffs with traces of copper, and the use of lead water

pipes was probably instrumental in causing the high concentrations of lead found in the Spitalfields skeletons (see Chapter 2 section 2.1.2l; Cox, 1996). It is understood that an excess (or deficiency) of a wide range of chemicals can lead to skeletal abnormality (see section 6.5.5b). High concentrations of lead, for example, are known to "impair a child's development, resulting in learning disabilities or *stunted growth*" (St. Clare and Zaslow, 2005). Excessive concentrations of lead from water pipes, however, would also have been a problem for other urban populations tested here (e.g., the African and Caucasian Americans).

The water supplies were severely contaminated with raw sewage and carried various diseases such as cholera and typhoid. Regardless of social status, all Londoners were exposed to the most appalling insanitary conditions, particularly on the lower-sloping south side of the Thames around the Spitalfields area, where the incidence of water-borne diseases was three or four times greater than on the higher, northern side (Picard, 2005). The Victorian commentator and reformer, Henry Mayhew believed that the drinking water of his fellow Londoners of that period was a "solution of our own faeces" (Mayhew and Binney, 1862).

Of those other populations where sufficient information is available, not all would have experienced similar conditions. Undoubtedly, others in the twelve samples faced extreme poverty, and these are likely to have included the low-caste Sri Lankans (section 2.1.2i). The African and Caucasian Americans living in twentieth century St Louis, however, would have had access to a relatively clean water supply compared to eighteenth and nineteenth century London (albeit still contaminated by lead from the water pipes). Also, the availability of food may have been inadequate in terms of modern expectations; it is unlikely to have been as severely and purposefully contaminated as that of eighteenth and nineteenth century London. The ingestion or inhalation of now-recognised poisons or carcinogenic materials in the working environment would have been largely confined to adults in early twentieth century America.

Of the remaining populations, the Pachacama were recovered from a famous and richly endowed temple site, implying that they were unlikely to have been from the poorest labouring classes (section 2.1.2b). The Egyptians, likewise, were excavated

from cemeteries known to have contained royal remains (section 2.1.2k). The Aleut are thought to have been well supplied with a good variety of plant, marine fauna and bird-life, in a period when starvation was practically unknown (Taylor, 2000). The Arikara also lived in an area which was relatively fertile and supplies of food and other necessities would have been adequate, if not good (Taylor, 2002). It is not known whether the remaining samples of Australians, Ibo, Andaman Islanders and Khoisan had been exposed to harmful or severely inadequate nutrition during their lives (sections 2.1.2e, 2.1.2g, 2.1.2h and 2.1.2j respectively).

6.6.5 The effects of infectious disease

Even by the middle of the nineteenth century, by five years of age, 35 out of every 45 children had suffered one or more of tuberculosis, smallpox, measles, scarlet fever, diphtheria, whooping cough, typhus or enteric fever (Flanders, 2003). In addition, staphylococci, streptococci and pneumococci infections would have been an inevitable consequence of the insanitary conditions. The epithet 'convulsions' frequently described the cause of death and was likely to have been either tuberculosis or meningitis. Rickets was rife in London at that time, even amongst the middle-classes, and as many as 15% of children had deformed legs and pelves (Picard, 2005). In addition, illnesses were usually self-doctored with quack medicines made up from a variety of toxic substances including antimony, ammonia, opium and derivatives, creosote, arsenic and mercury (Picard, 2005).

With respect to tuberculosis, 90% of lesions involve a joint, with the bacilli usually becoming deposited in the trabecular bone of the metaphyses and epiphyses (rarely the cortical bone of the diaphyses) (Aufderheide and Rodriguez-Martin, 1998). Tuberculosis initially impedes the blood supply to the affected joints and leads to ulceration of the cartilage and exposure of the bone surfaces. The knee, spine and hip are the most frequently affected joints; the knee being most frequently affected in adults (Aufderheide and Rodriguez-Martin, 1998). In eighteenth and nineteenth century London, typhoid infections often proved rapidly fatal prior to developing osteomyelitis, although it is thought that up to 90% of sufferers recover the immediate effects of typhoid spontaneously (Aufderheide and Rodriguez-Martin, 1998). Of those that recover the immediate effects (until the advent of modern anti-

biotics) many went on to develop osteomyelitis, (primarily) affecting the tibia, ribs and lumbar vertebrae (Aufderheide and Rodriguez-Martin, 1998). In addition, although many of the Spitalfields skeletons in the total collection are deformed by visually apparent symptoms of degenerative bone diseases and were excluded from this sample, the results of Chapter 5 suggest that the earliest non-visual symptoms affect the structure of bone, both internally and externally. As noted above (Chapter 5 section 5.6), Maquet (1983) describes such changes in the proximal tibia as involving the formation of a dense triangle of bone under the medial condyle, with a reduction of bone beneath the lateral condyle.

In addition to the infections to which the Spitalfields sample were exposed, this study includes the Andaman Islanders who are known to have been exposed to syphilis and a third sample, the Ibo, who originated from a region of endemic malaria and anaemia. A fourth sample, the Sri Lankans, were recovered from a hospital morgue, although the causes of death of the individuals are not recorded. Like Spitalfields, both the Andaman and Ibo means lie at a distance from other means on PCs analysed in Chapter 6. The Andaman mean is at a distance in Figure 6.2 for PC2 and Figure 6.5 for PCs 3 and 4, for the femur and in Figure 6.7 for PCs 1 and 2 for the tibia. The Ibo mean lies at a distance from other means in Figure 6.10 for PCs 3 and 4 for the tibia. Results of this study also highlight anomalies in the shape of the Ibo tibiae relative to the other samples (see section 6.4.2d).

The Sri Lankan sample is not an outlier on any PCs for either femur or tibia (Figures 6.2 and 6.7) when using population means. The Procrustes distances between specimens in Tables 2.6 and 2.11, however, show this sample to separate into two distinct groups; a separation not thought to be based on either ethnicity or sexual dimorphism. This is also reflected in the high values for Procrustes distances seen in Tables 6.15 and 6.21 between the Sri Lankan mean and the other twelve population means (see section 6.4.1). The relative distance and separation between the two sections of the sample for Procrustes distances, however, is not reflected in the Mahalanobis' squared distances between this sample and the other eleven samples (excluding the Spitalfields sample), when using the total sample (Tables 6.12 and 6.18) The reasons for this internal separation within the sample is unclear. In the light of the three examples outlined above, in relation to the effects of disease on

skeletal morphology (Spitalfields, Andaman Islanders and Ibo), however, the internal division within the Sri Lankan sample may possibly reflect the effect of long term infections suffered by some of the hospital patients before death.

6.7 Future research

Extreme and abnormal usage of the limbs, particularly whilst the skeleton is developing, together with the ingestion of harmful materials over a long period and exposure to many infections and diseases (non-specific to bone but resulting in osteomyelitis) will, possibly, cause an alteration in skeletal morphology. Unfortunately, whilst it is unlikely that the effects of extreme working practices and the effects of harmful nutrition and disease can be incontrovertibly tested or measured (Cox, 1996), future research should be directed towards a more exhaustive examination of the causes of the distinctive Spitalfields knee joint morphology.

Results here imply that variation throughout the Spitalfields sample for the proximal tibia is wide (Figure 6.35 for both PCs 1 and 2), but there are no small clusters of individuals with atypical morphologies. The analysis of twelve male individuals (Figure 6.36), however, suggests that there is a degree of separation between non-manual workers and the three manual categories (including the master weavers, who were exposed to heavy loading stresses on the knee joint during adolescence). Therefore, it is *possible* that extreme occupational loading might be affecting knee joint shape. Additional research should investigate this aspect by selectively choosing more specimens whose occupations are known, at the initial stage of data collection. The lack of tight clusters of individuals with atypical morphologies within the total sample suggests, however, that the cause of the more distinct shape of the Spitalfields is relatively *general* throughout the population. In addition, it has been suggested that extreme loading pressures will affect the relative size of the joint, particularly of the lateral condyle in the tibia. Given a sufficient number of specimens of known occupation and the use of a subset of landmarks, it would also be appropriate to explore any relationship between the centroid size of the whole joint and of selected regions of the joint with occupation (see Chapter 3, section 3.6; Heberden Society, 1970). Grieve (1996), suggests a link between increased size of

the lateral condyle of the tibia and all male manual workers, and this should be examined further in relation to specific occupations.

Investigation into the possible effects of the quality of the water and food ingested and the high incidence of oseomyelitis suffered may provide insight into the atypical shape of the Spitalfields knee joint. As there is insufficient information accompanying the Spitalfields collection itself, initial research should be conducted on other populations with detailed life-histories and causes of death (e.g., the African and Caucasian American specimens in the Terry Collection, NMNH, Smithsonian Institution). Although results in this study do not show atypical morphologies in either population for the distal femur or proximal tibia, the shape of the knee joint in specimens with a history of infectious diseases over a period of time should be compared with those of non-infected individuals. This comparison might give insight into the shape of the knee joint of the Spitalfields population, where it is likely that the majority of individuals suffered from infections known to affect bone, as opposed to a selected few. Analyses comparing other parts of the Spitalfields skeleton with those of other populations may also give insight into the effects of adulterated and contaminated foodstuff and water and of infectious disease. It is suggested that bones such as the ribs (which are also severely affected by osteomyelitis) would be suitable for comparison in this context.

6.8 Summary and Conclusion

Results indicate that the shape and size of the knee joint are independently responsive to the various environmental forces acting upon them; so also is the shape and size of the constituent elements of the long bones and the femur relative to the tibia. It is problematic, however, to estimate the *magnitude* of influence each of the various modifying factors will have on bone morphology. Climatic factors are probably the most important of these environmental forces. Temperature (specifically cold temperature) and rainfall are undoubtedly important factors. Altitude may also be of significant influence (albeit to a lesser degree), and the degree of influence should be examined further in future research. The type of footwear worn and the economic activities of a population will have some significant effect; the type, quality and quantity of food and water is important and so also is the

health and medical history of the population. Results above bear out the significance of all of these environmental factors. In addition, an example is provided of the powerful influence high levels of exposure to disease and deleterious nutrition and possibly highly stressful types of activity *might* have on knee joint morphology, in relation to the distinctive shape of the Spitalfields joint. Whilst such environmental factors appear to be fundamental to the morphology of the knee joint and lower limbs, there is also some indication that ancestral history might have a limited influence in some population groups.

Hypothesis H.6.6 states that 'similarity of form of the knee joint between different populations is highly correlated with similarity of their environmental background'. It is unlikely, however, that any distinct population will share all environmental factors in common and that even similarity of climate and altitude will be overwhelmed by the individual factors of cultural practises, health and hygiene, and economic development, which are also of such evident importance. In this study, results indicate that *cold* temperature is more influential in determining shape than warm temperature. The highlighted cluster of population means (Figure 6.2, for the femur) which share a similarity of shape, however, also share year-round *warm* temperatures. It is therefore possible that cold temperature exaggerates the distinctive morphology of a group, rather than perpetuating a shared, more generalised morphology. Therefore, attempting to estimate the significance of each of the individual factors will be problematic. For example, climate, footwear and subsistence strategies are palpably linked, in that climate will largely dictate the type of footwear worn, although heavy industrial processes will require protective footwear even in warm climates. 'Hunter-gatherer' communities encompass such varied peoples as the heavily shod, arctic, marine-based Inuit and the barefoot Australian Aborigines. 'Farmers' undertake a multiplicity of tasks and include both the pastoralist Khoi and some Amerindian hoe agriculturalists whose ways of life were more arduous and physically demanding than the previous hunting-and-gathering lifeways (Bridges, 1989). In other words, trying to construct 'best-fit' activity-based scenarios to explain morphological variation in a highly stressed region of the skeleton may prove too challenging.

To state that '*similarity* of form of the knee joint between different populations is highly correlated with *similarity* of their environmental background' cannot be unconditionally proven and hypothesis H.6.6 must therefore be rejected. Results, however, have unquestionably established that the form of the knee joint and the geometric proportions of the bones in this region of the skeleton are determined by a multiplicity of environmental effects, for which there can be no single explanation (Jurmain, 2002).

Chapter 7

Summary and Conclusion

The aim of this study is to investigate variation in the form of the knee joint in *Homo sapiens* and to place this morphology within the context of the overall size and shape of the lower limbs. The knee joint is considered the most complex of all human joints, allowing both extension and flexion with rotation. This complexity and flexibility of movement is achieved at the cost of stability. The degree of complex movement is made possible through an imprecise articulation between the two major bony elements and a reliance on the soft tissue within and surrounding the joint to cushion and protect the surfaces and to constrain excess movement (Palastanga et al., 1998; Seeley et al., 1998; McGowan, 1999; Kapandji, 2001; Platzer, 2004). The knee joint is a major weight-bearing joint, intrinsic to efficient bipedalism and subject to high load-bearing during normal standing and locomotion. It is also vulnerable to additional and eccentrically applied loading placed upon it by any dysfunctions in the hip and ankle joints. With forces applied at up to 24 times body weight under normal physical activities (Palastanga et al., 1998), individuals will load the knee joint in a variety of different ways and frequencies, depending on personal choice or necessity. Therefore, with the expectation of variable loading patterns leading to considerable variation in knee joint form, this study examines morphological variation by looking at differences both within and between populations. In addition, the results generated from the three intra-population analyses determine the samples that can be used for each subsequent set of analyses and for the examination of inter-population differences.

It is found in Chapter 3 that the size of the knee joint and of diaphyseal length and robusticity between right and left sides are not sufficiently different to be statistically significant. There is a clear and statistically significant difference, however, in knee joint shape between right and left sides in all five samples examined. Joint shape asymmetry is principally manifest as a difference in the degree of orientation of the knee joint relative to the diaphysis, although both the pattern and degree of this orientation are

population specific. With few exceptions (primarily Spitalfields), the joint from each side is relatively more similar in morphology to that of the same side from other populations than the matching limb from its own population. In addition, both the African American femur and tibia show a statistically significant sexual difference in shape asymmetry. This observation is not repeated in the other populations. Therefore, the degree of difference in asymmetry between males and females of each population is, again, sample specific.

That the knee joint is asymmetric is predictable in the light of previous research on limb usage which has shown that *Homo sapiens* is both strongly handed and footed, with a distinct bias towards the right side (Coren and Porac, 1977). This limb preference is thought to be largely genetically controlled and determined at an early stage of foetal development (Ruff and Jones, 1981; McManus, 2003; Faurie and Raymond, 2004). This early predisposition towards handedness is enhanced by an activity-related bias during early childhood (Inglemark, 1974; McManus, 2003). It has also been found that individuals use one leg in a slightly different way to the other and therefore subject the limbs to asymmetric loading and remodelling (Sadeghi, 2000; Kettlekamp et al., 1970; Nordin and Frankel, 2001).

Previous research has used linear measurements from the distal femur and proximal tibia as useful tools for comparing and contrasting different populations (Craig, 1995; Gill, 2001). Assuming that the right and left sides are symmetric, such researchers have tended to use the best preserved side from each individual pair rather than preferentially selecting only right or left sided specimens. Results from this study demonstrate that the joint is directionally asymmetric and thus using conglomerated samples of right and left sides to infer sample specific morphologies will tend to introduce confounding and unnecessary variance, masking or diffusing any potential results. In the light of these findings, all subsequent analyses are carried out on right limbs only.

Analyses in Chapter 4 establish the presence of sexual dimorphism in size in both the knee joint and diaphyseal length and robusticity. It is also found that sexual dimorphism

of size in the knee joint (c.10%) is greater than dimorphism in both length and robusticity (c.6%). Therefore, the centroid size of the knee joint can be a population specific discriminator of sex in the postcranium.

Results also establish the presence of variable degrees of sexual dimorphism of shape in the knee joint within and between six populations of *Homo sapiens*. In both femur and tibia, the African and Caucasian Americans and Spitalfields show strong sexual dimorphism with distances between samples at a high level of statistical significance, when all six populations are analysed jointly. For the remaining three Native American populations, results are less clear, with non-significant distances between Pachacama males and females for the femur and between males and females from all three populations for the tibia, when the six populations are analysed jointly. Sexual dimorphism for the Aleut, Arikara and Pachacama therefore appears weaker relative to the other three populations, particularly for the tibia. Again, therefore, the degree of sexual dimorphism of the knee joint is specific to each population. Despite results indicating variable degrees of sexual dimorphism in knee joint morphology, they also show that males and females of the same population remain more similar in shape to each other than to any other population. Therefore, it is apparent that the population specific morphologies are more distinctive than those due to sexual dimorphism.

In the third set of intra-population analyses, Chapter 5 establishes the presence of progressive changes in shape at the knee joint with ageing between the youngest and oldest adults. Despite the statistically significant separation of the three age categories, however, such morphological changes are found to be subtle in nature. In addition, despite distances remaining at a statistically significant level (with one exception for the femur), when differences between males and females are analysed, changes in shape with ageing are small and difficult to interpret. It is apparent that differences due to sexual dimorphism are generally more pronounced than the subtle changes due to ageing, although neither suite of differences appears so strong as to totally mask the effects of the other. Results in Chapter 5 also show that changes in shape with ageing are population specific and that each age group from the three populations examined is more

similar in shape to the other two age groups from the same population than to any other sample, including those of the same age group but from a different population. Changes in shape with ageing are therefore too subtle to over-ride the specific morphologies of each population.

Conclusions drawn from results of the three intra-population examinations for subsequent analyses are first, that asymmetry in the knee joint is so great as to render invalid the use of both left and right specimens of distal femora and proximal tibiae within the same sample, second, it is valid to use pooled samples of males and females from the same population without compromising results in inter-population analyses and third, it is valid to pool ostensibly healthy specimens of all ages within any one sample in inter-population analyses.

Chapter 6 analyses differences in morphology at the knee joint and lower limbs between thirteen samples of recent *Homo sapiens* from a variety of ancestral, climatic, cultural and economic backgrounds. Despite the high degree of loading and the highly individualistic manner of loading to which each knee joint is subjected, results confirm that the morphology of the joint is highly population specific. This conclusion reaffirms results from the analyses in earlier chapters where examination of sexual dimorphism and changes due to ageing (using a more restricted number of samples) show intra-population differences to be of lesser significance relative to inter-population differences.

Various factors are discussed as potentially causing these population specific differences in knee joint shapes; these include a residual degree of genetic affiliation, the effects of climate, cultural factors and subsistence strategies, the incidence of disease and the quality and quantity of nutrition. Of these various forces, the most influential is found to be ambient temperature, particularly cold temperature. This conclusion is repeated in relation to knee joint size and long bone robusticity where there is a strong indication that cold temperature has a direct and significant effect. The influence of temperature on diaphyseal length is less critical, however, with results indicating that other factors, such as ancestral history and nutrition, have a more influential part to play. In addition, the

example of the Spitalfields population, which has a distinctive knee joint morphology, demonstrates the strong influence of specific cultural and historic factors on the shape of the knee joint. For Spitalfields, it is likely that a high incidence of infectious disease and the poor quality of nutrition, together with the possible influence of extreme working practices, are of crucial importance.

Both the distal femur and the proximal tibia are integral elements of the knee joint and results in Chapter 6 indicate a high degree of correlation in shape and size between the two bones. As the two articulating surfaces are protected from direct contact in healthy joints (within the limits of functionality), however, each element is able to adapt and remodel to a different degree in response to differing or changing environmental forces and loading pressures placed upon them. Intra-population analyses find that the distal femur shows a higher degree of sample specific variation in shape relative to the proximal tibia, particularly in relation to asymmetry and sexual dimorphism. Inter-population analyses, however, also show that, in certain circumstances the tibia appears to react to specific influences to a greater degree than the femur. Results of this study imply that a high incidence of infectious disease within a population may prove fundamental in creating distinctive shape differences, conclusions that are drawn from evidence of the distinctive shapes of the tibial knee joint in three populations in the dataset (Spitalfields, the Andaman Islanders and the Ibo), and further supported by the closer range of results between the femur and tibia relative to changes in shape with ageing. Such conclusions are also strongly supported by Dickel (1984), Milner (1991), Roberts and Manchester (1997), Larsen (1999) and Aufderheide and Rodriguez-Martin (1998), who highlight the great vulnerability of the tibia to bone infection.

The implications of results should take future research in several directions. First, the realisation of shape asymmetry at the knee joint in humans should be tested against the possible presence of shape asymmetry in non-human primates. Results from such research would provide greater insight into the innate lateralisation of the brain and the effects of bipedal locomotion on shape asymmetry. Second, results showing shape differences between the sexes in humans should be compared with results of future

research between male and female non-human primates. It is suggested that data from such species as the common chimpanzee (*Pan troglodytes*), that shares a similar body-weight ratio with humans at c.80% female-to-male body weight, and the Western lowland gorilla (*Gorilla gorilla*), with a ratio of approximately 42%, female-to-male body-weight, should be used as comparison groups. Results from such research would give greater insight into the primary causes of sexual dimorphism of shape differences at the knee joint in humans. Third, with respect to shape differences caused by ageing, it is suggested that future research should be directed towards a better understanding of the overall effects of BMC loss with ageing and the earliest effects of degenerative bone diseases on the epiphysis, and specifically, between males and females.

Finally, results from all analyses indicate that the Spitalfields knee joint morphology is atypical with respect to the other twelve populations studied here. Analyses in Chapter 6 indicate that several environmental and genetic factors influence the shape and size of the knee joint. It is apparent, however, that the atypical nature of the Spitalfields joint is caused by a combination of additional factors idiosyncratic to that population. Initial research indicates that, whilst specific occupational stresses might be of influence (using data from a limited number of specimens of known occupation), the causes of shape differences are likely to be general to all individuals in the sample rather than to a selected few. Influences that affect all individuals include the effects on the skeleton of harmful substances ingested in food and water, and of infectious diseases that cause osteomyelitis, especially in children and adolescents. Future research should determine the magnitude of these various influences by conducting analyses using additional specimens from the Spitalfields collection together with comparative data from another population, using specimens with known histories of infectious diseases relative to a control group. Comparisons of results using other populations might give insight into the effects of infection in the Spitalfields population where the majority was exposed to illnesses known to cause osteomyelitis, particularly in the tibia. It is also suggested that the comparison of other bones in the postcranial skeleton to determine shape differences between Spitalfields and other populations (such as the ribs), might provide additional insight into the causes of the atypical morphology found here in the knee joint.

BIBLIOGRAPHY

Abrahams, P.H. (Ed.) 2000. *McMinn's Colour Atlas of Human Anatomy* Hodder

Aiello L. and Dean C. 1999. *Evolutionary Human Anatomy.* Academic Press.

Allen, J.A. 1877. The influence of physical conditions in the genesis of the species. *Rad. Rev.* Vol 1 p108-140

Al-Turaiki, H.S. 1986 *The Human Knee.* King Saud University

Amithalingam, G. 2003. *Customs and Cultures of Sri Lanka.* A and S Books, London UK.

Anderson, J. and Trinkaus, E. 1998. Patterns of sexual, bilateral and interpopulational variation in human femoral neck-shaft angles. *Journal of Anatomy* Vol. 192 p279-285.

Angilletta, M.J., Niewiarowski, P.H., Dunham, A.E., Leache, A.D. and Porter W.P. 2004. Bergmann's clines in ectotherms: Illustrating a life history perspective with sceloporine lizards. *American Naturalist* Vol. 164 6 E168-E183. http:// wost.wok.minimas.ac.uk/CIW.cgi

Annett, M. 1985. *Left hand, right hand and brain; the right shift theory.* London: LEA Publishers.

Arking, R. 1998. *Biology of Ageing.* Sinauer Assoc. Inc. Publishers.

Arsenault, A.B. et al. 1986 Bilateralism of EMG profiles in human locomotion *American Journal of Physical Anthropology* Vol. 65 p1-16.

Asala, S.A., Bidmos, M.A. and Dayal, M.R. 2004. Discriminant function sexing of fragmentary femur of South African Blacks. *Forensic Science International* Vol. 145 1 p25-29.

Aufderheide, A.C. and Rodriguez-Martin, C. 1998. *The Cambridge Encyclopedia of Human Paleopathology.* Cambridge University Press.

Auffray, J-C. 1999. Shape Asymmetry and Developmental Stability in: *On Growth and Form: Spatio-temporal Pattern Formation in Biology.* (Eds.) Mark, A.J., Chaplain, G.D., Singh, J.C. and McLachlan, J.C. Wiley.

Australian Aborigines 2005 From: Wikipedia, the free encyclopedia http://en.wikipedia.org/wiki/Australian_Aborigine#The_20th_century

Baker, S.J., Gill, G.W. and Kieffer, D.A. 1990 Race and sex discrimination from the intercondylar notch of the distal femur In: *Skeletal attribution of race* (Eds). G.W. Gill and S. Rhine Alburquerque: Maxwell Museum of Anthropology p91-95

Bailey, D.A. 1986. *The Influence of Exercise, Physical Activity and Athletic Performance on the Dynamics of Human Growth Human Growth: A Comprehensive Treatise* (Eds.) Faulkner, F. and Tanner, J. New York Plenum.

Bass, W.M. 1995 *Human Osteology: A laboratory and field manual* Special Publication No. 2 of the Missouri Archaeological Society Fourth Edition

Beck, J.T. et al. 1992 Sex differences in geometry of the femoral neck with ageing: A structural analysis of bone mineral data *Calcif. Tissue Int.* Vol. 50 p24-29.

Black, L. 1983 Some problems in the interpretation of Aleut prehistory. *Arctic Anthropology* Vol. 20 No 1 p49-78.

Boaersma, P. and Weenik, D. 1999 University of Amsterdam http://www.resample.com/xlminer/help/PCA/pca_intro.htm

Bogin, B., Smith, P., Orden, A.B., Varela Siva, M.I. and Loucky, J. 2002 Rapid change in height and body proportions of Maya American Children *American Journal of Human Biology* Vol. 14 p753-761

Bookstein, F.L. 1984 A statistical method for biological shape comparisons *Journal of Theoretical Biology* Vol. 107 p475-520.

Bookstein, F.L. 1989 Principal warps: thin plate splines and the decomposition of deformations. *IEEE Transactions on Pattern Analysis and Machine Intelligence* Vol. 11: 567-585.

Bookstein, F.L. 1991 *Morphometric Tools for Landmark Data: Geometry and Biology.* Cambridge: Cambridge University Press

Brickley, M. 1999 Measurement of Changes in trabecular Bone Structure with Age in an Archaeological Population *Journal of Archaeological Science* Vol. 26 p151-157.

Bridges, P.S. 1985 *Changes in long bone structure with the transition to agriculture: Implications for prehistoric activities.* Ann Arbor: University of Michigan PhD thesis.

Bridges, P.S. 1989 Changes in activities with the shift to agriculture in the southeastern United States. *Current Anthropology* Vol. 30 p385-394.

Bridges, P.S. 1991 Degenerative joint disease in hunter-gatherers and agriculturalists from the south eastern United States. *American Journal of Physical Anthropology* Vol. 85 p379-391.

Bridges, P.S. 1992 Prehistoric arthritis in the Americas *Annual Review of Anthropology.* Vol. 21 p67-91.

Brock, S.L. 1985 *Changes in long bone structure with the transition to agriculture: Implications for prehistoric activities* PhD dissertation. University of Michegan Ann Arbor

Brock, S.L. Ruff, C.B. 1988 Diachronic patterns of change in structural properties of the femur in prehistoric American Southwest. *American Journal of Physical Anthropology* Vol. 75 p113-127.

Brothwell, D.R. 1981 *Digging Up Bones.* British Museum Natural History. Cornell University Press, Ithaca, New York.

Buikstra, J.E. and Ubelaker, D.H. (Eds.) 1994 *Standards for Data Collection* from Human Skeletal Remains: Proceedings of a Seminar at the Field Museum of Natural History Arkansas Archaeological Survey Research Series No 44.

Burr, D.B. et al. 1983 Sexual Dimorphism and Mechanics of the Human Hip: A Multivariate Assessment *American Journal of Physical Anthropology* Vol. 47 p273-278.

Bythell, D. 1969 *The Handloom Weavers* Cambridge University Press, London

Carey, D.P., Smith, G., Smith, D.T., Shepherd, J.W., Skriver, J., Ord, L and Rutland, A. 2001 Two-footedness in world soccer: A preliminary analysis of France '98. *Journal of Sports Sciences* Vol 19 p855-864

Cavelli-Sforza, L.L., Menozzi, P. and Piazza, A. 1994 *The History and Geography of Human Genes* Princeton, University Press.

Cavelli-Sforza, L.L. 2001 *Genes, Peoples and Languages* Penguin Books

Chaplin, G., Jablonski, N.G. and Cable, N.T.1994 Physiology, Thermoregulation and Bipedalism. *Journal of Human Evolution.* Vol. 27 p497-510.

Chapman, F.H. 1972 Vertebral osteophytosis in prehistoric populations of central and southern Mexico. *American Journal of Physical Anthropology.* Vol. 36 p31-37.

Cech, D. and Martin, C. 2002 *Functional Movement Development: Across the Life Span* W.B. Saunders Company

Chhibber, S.R. and Singh, I. 1970 Asymmetry in muscle weight and one-sided dominance in the human lower limbs *Journal of Anatomy* Vol. 106 3 p553-556

Chou, L.S. et al. 1995 Predicting the kinematics and kinetics of gait based on the optimum projectory of the swing limb *Journal of Biomechanics* Vol. 28 4 p377-85

Churchill, S. and Morris, A.G. 1998 Muscle Marking Morphology and Labour Intensity in Prehistoric Khoisan Foragers *International Journal of Osteoarchaeology* Vol. 8 p390-411

Cole, T.M. III and Richtsmeier, J.T. 1998 A simple method of visualization of influential landmarks when using Euclidean Distance Matrix Analysis *American Journal of Physical Anthropology* Vol. 107 p273-283

Collier, S. 1989 The influence of economic behaviour and environment upon robusticity of the post-cranial skeleton; a comparison of Australian Aborigines and other populations *Archaeol Oceania* Vol. 24 p17-30

Colombian Electronic Encyclopaedia 2004 http://infoplease.com/ce6/society/A0805377.html 6th edition Colombia University Press

Coran, S. and Porac, C. 1977 Fifty centuries of right handedness: The historical record *Science* Vol. 198 p631-632

Cordey, J. and Nolte L-P. 1998 Quantitative Computed Tomography Supports the Distinction between Osteoporosis Type I trabecular and Type II CorticalM.E. Muller-Institut fur Biomechanik, University of Bern http://www.utc.fr/esh/esb98/abs_htm/378.html

Corp, N. and Byrne, R.W. 2004 Sex Differences in Chimpanzee Handedness *American Journal of Physical Anthropology* Vol 123 No 1 p62-68

Cox, M. 2000 Assessment of Parturition In: *Human Osteology in Archaeology and Forensic Science* (Eds.) M Cox and S. Mays GMM

Cox, M. 1996 *Life and Death in Spitalfields 1700 to 1850* The British Library

Craig, EA. 1995 Intercondylar Shelf Angle: a new method to determine race from the distal femur *Journal of Forensic Science* Vol. 40 5 p777-782

Cronin, B.E. et al. 1986 Radionuclide imaging in syphilis http://www.med.harvard.edu/JPNM/BoneTF/Case11/WriteUp11.html

De Mendorca, M.C. 2000 Estimation of height and the length of long bones in an adult Portuguese population *American Journal of Physical Anthropology* Vol.112 p 39-48

DeVita P. et al. 1991 Effects of asymmetric load-carrying on the biomechanics of walking *Journal of Biomechanics* Vol. 24 p1119-1129

Dickel, D.N. et al. 1984 Central California prehistoric subsistence changes and health In: Palaeopathology at the Origins of Agriculature (Eds.) M.N.Cohen and G.J Armelagos Orlando Academic Press

Dittmar, M. 2002 Functional and postural lateral preference in humans; interrelations and life-span age differences *Human Biology* Vol. 74 4 p569-585

Dittrick, J. and Suchey, J.M. 1986 Sex Determination of Prehistoric Central Californian Skeletal Remains using Discriminant Analysis of the Femur and Humerus *American Journal of Physical Anthropology* Vol. 70 p3-9

Drusini, A.G. et al. 2000 Cortical bone dynamics and age-related osteopenia in a Longobard archaeological sample from three graveyards of the Veneto region Northeast Italy *Int. Journal of Osteoarchaeolgy* Vol. 10 p268-279

Dryden, I.L and Mardia, K.V.1998 Statistical Shape Analysis John Wiley and Sons

Du, R., Yuan, Y., Hwang, J., Mountain, J. and Cavelli-Sforza, L.L. 1992 Chinese Surnames and the Genetic Differences between North and South China *Journal of Chinese Linguistics* Monograph series number 5

Dvornyk, V., Liu, X-H., Shen, H., Lei, S-F., Zhao, L-J., Huang, Q-R., Qin, Y-H., Jiang, D-K., Long, J-R., Zhang, Y-Y., Gong, G., Recker, R.R. and Deng, H-W 2003 Differentiation of Caucasians and Chinese at bone mass candidate genes for ethnic difference of bone mass *Annals of Human Genetics* Vol 67 p216-227

Endicott, P., Thomas, M., Gilbert, P., Stringer, C., Lalueza-Fox, C., Willerrslev, E., Hansen, A.J. and Cooper, A. 2003 The Genetic Origins of the Andaman Islanders *American Journal of Human Genetics* Vol. 72(1) report no.178 http://www.andaman.org/book/chapter6/text6.htm

Eriksen, M.F. 1976 Cortical bone loss with age in three Native American populations *American Journal of Physical Anthropology* Vol. 45 p443-452

Eriksen, M.F. 1991 Histologic estimation of age at death using the anterior cortex of the femur *American Journal of Physical Anthropology* Vol. 84 p171-179

Erickson, J.D. 2000 Fourier Analysis of Acetabular Shape in Native American Arikara Populations Before and After Acquision of Horses *American Journal of Physical Anthropology* Vol. 113 p473-480

Eveleth P.B. and Tanner J.M. 1990 Worldwide Variation in Human Growth Cambridge University Press

Fagan, B. 1998 *Peoples of the Earth: An Introduction to World Prehistory* Longman

Fagan, B. 2000 *The Little Ice Age* Basic Books

Faurie C. and Raymond, M. 2004 Handedness, homicide and negative frequency-dependent selection *Proceedings of the Royal Society B* Online publication 04PB0598.1

Felson, D.T. 1988 Epidemiology of hip and knee osteoarthritis *Epidemiology Review* Vol. 10 p1-24

Flanders, J. 2003 *The Victorian House: Domestic life from childbirth to deathbed* Harper-Collins

Forde, D. and Jones, G.I. 1960 The Ibo and Ibibio-speaking peoples of South-eastern Nigeria In: *Ethnographic survey of Africa: Western Africa Part III* (Ed.) D.Forde

Formicola, V. and Giannecchini, M. 1999 Evolutionary trends of stature in Upper Palaeolithic and Mesolithic Europe *Journal of Human Evolution* Vol. 36 p319-333

Freeman, M.A.R. 2001 Locomotor Science: How the knee moves *Current Orthopaedics* Vol. 15 p444-450

Fresia, A.E., Ruff, C.B. and Larsen, C.S. 1990 Temporal decline in bilateral asymmetry of the upper limb on the Georgia Coast papers of the American Museum of Natural History Vol. 68 p121-150

Gallagher, J.A. 1991 Human Bone Remodeling *Encyclopaedia of Human Biology* Vol. 1 Academic Press

Giles, E. and Elliott, M.A. and O. 1962 Race identification from cranial measures *Journal of Forensic Science* Vol. 7 p147-157

Gill, G.W. 2001 Racial Variation in the proximal and distal femur: heritability and forensic utility *Journal of Forensic Science* Vol. 46 4 p791-799

Goodall, C. 1991 Procrustes methods in the statistical analysis of shape *Journal of the Royal Statistical Society B* Vol. 53 No 2 p285-339

Gregg, J.B. and Gregg, P.S. 1987 *Dry Bones: Dakota Territory Reflected* Sioux Printing Inc., South Dakota.

Grieve, A. 1996 A study on occupation as the primary etiological factor for osteoarthritis in a sample population from Spitalfields, London, 1739-1852 (Third year undergraduate project in Zoology) King's College, University of London.

Gugliemino-Matessi, C.R, Gluckman, P. and Cavelli-Sforza, L.L. 1979 Climate and the evolution of skull metrics in man *American Journal of Physical Anthropology* Vol. 50 p549-564

Hadler, N.M. 1977 Industrial Rheumatology: Clinical investigations into the influence and usage on the pattern of regional musculoskeletal disease *Arthritis and Rheumatism* Vol. 20 No 4 p1019-1025

Hall, B.K. 1988 The Embryonic Development of Bone *American Scientist* 762 p174-81

Hall, B.K. 1991 Bone, Embryonic Development *Encyclopaedia of Human Biology* Vol. 1 Academic Press

Handy, J.R. 1996 Osteoarthritis in Elderly Knees http://www.sma.org/smj/96nov1.htm

Hanihara, T. 1996 Comparison of craniofacial features of major human groups *American Journal of Physical Anthropology* Vol. 99 p389-412

Harrison, G.A., Weiner,G.A, Tanner,J.S. and Barnicot, N.A. 1964 Human Biology. Oxford at the Clarendon Press

Harvati, K. 2003 The Neanderthal taxonomic position: models of infra- and inter specific craniofacial variation. *Journal of Human Evolution* Vol. 44 Issue 1 p107-132

Hawkey, D.E. and Merbs, C.F. 1995 Activity-induced musculoskeletal stress markers and subsistence strategy changes amongst ancient Hudson-Bay Eskimos *Int. Journal of Osteoarchaeology* Vol. 5 p324-338

Hayes, W.C. et al. 1978 Axisymmetric Finite Element Analysis of the Lateral Tibial Plateau *Journal of Biomechanics* Vol. 11 p21-33

Hrdlička, A. 1914 Anthrolopolgical work in Peru in 1913, with Notes on the Pathology of the Ancient Peruvians City of Washington: *Smithsonian Institution Publications*

Heberden Society 1970 Clinical Meeting, June 1968. Osteoarthritis of the Knee Joint *Annals of Rheumatic Diseases* Vol. 29 p190

Hepper, P.G. et al. 1998 Laterized behaviour in first-trimester human fetuses *Neuropsychologia* Vol. 36 p531-4

Hernadez, M., Lalueza Fox, C. and Garcia-Moro C. 1977 Fueguian cranial morphology; The adaptation to a cold harsh environment *American Journal of Physical Anthropology* Vol. 103 p103-117

Hernborg, J.S. and Nillson, B.E. 1973 Age and sex incidence of osteophytes in the knee joint. *Acta Orthopaedica Scandinavica.* Vol. 44 p66-68

Holland, T.D. 1991 Sex assessment using the proximal tibia *American Journal of Physical Anthropology* Vol. 85 p221-227

Holliday, T.W. and Falsetti, A.B. 1995 Lower limb length of early European early modern humans in relation to mobility and climate *Journal of Human Evolution* Vol. 29 p141-153

Holliday, T.W. and Ruff, C.B. 1997 Ecogeographical patterning and stature predictions: Comments on M R Feldsman and R L Fountain, In: *American Journal of Physical Anthropology* 1996 100: 207-224 *American Journal of Physical Anthropology* Vol. 103 p137-140

Holliday, T.W. and Ruff, C.B. 2001 Relative variation in human proximal and distal limb segment lengths. *American Journal of Physical Anthropology* Vol. 116 26-33

Hopkins, W.D. 1996 Chimpanzee Handedness Revisited: 55 Years since Finch (1941) *Psychonomic Bulletin and Review* Vol 3(4) p449-457

Hopkins, W.D. et al. 2003 Comparative assessment of handedness for a co-ordinated bimanual task in chimpanzees (Pan troglodytes), gorillas (Gorilla gorilla) and Orangutans (Pongo Pygmaeus) *Journal of Comparative Psychology* Vol 117 (3) p302-308

Howells, W.W. 1973 Cranial variation in man: a study of multivariate analysis of patterns of difference among recent human populations. *Pap. Peabody Mus. Archaeol. Ethnol. Harv. Univ.* Vol. 67 p1-259

Howells, W.W. 1989 Skull shapes and the map: craniometric analyses in the dispersion of modern *Homo*. *Pap. Peabody Mus. Archaeol. Ethnol. Harv. Univ.* Vol. 79 p1-189

Huelster, L. 1953 The relationship between bilateral contour asymmetry in the Human Body in standing and walking *Res. Quarterly* p44-55

Inglemark, B.E. 1974 Asymmetries in the length of the extremities and their relation to right- and left-handedness *Upsala Laekarefoerening Forhandlingar* Vol 52 p17-82

Inman, V.T. and Ralston, H.J. 1981 *Human Walking* Williams and Wilkins

Irving, O., Rebeiz, J.J. and Tomlinson, B.E. 1974 The numbers of limb motor neurons in the individual segments of the human lumbo-sacral cord *Journal of Neurological Science* Vol 21 p203-212

Iscan, M.Y. and Miller-Shaivitz, P. 1984a Discriminant function sexing of the tibia. *Journal of Forensic Science* Vol. 29 p1087-1093

Iscan, M.Y. and Miller-Shaivitz, P. 1984b Determination of sex from the tibia. *American Journal of Physical Anthropology* Vol.64 p53-57

Iscan, M.Y. and Miller-Shaivitz, P. 1986 *Sexual dimorphism in the femur and tibia. In: Forensic Osteology: Advances in the detection of Human Remains.* (Ed.) K.J.Reichs Charles C. Thomas, Springfield II p102-111

Iscan, M.Y., Yoshino, M. and Kato, S. 1994 Sex determination from the tibia: standards from contemporary Japan. *Journal of Forensic Science* Vol. 39 p785-792

Iscan, M.Y. and Shihai, D. 1995 Sexual dimorphism in the Chinese femur. *Forensic Science International* Vol. 74 1-2 p79-87

Jacobs, K.H. 1985 Evolution in the postcranial skeleton of Late Glacial and early Postglacial European hominids. *Z. Morph. Anthrop.* Vol.. 75 3 p307-326

Janz, R.L. 1973 Microevolutionary change in Arikara crania: A multivariate analysis *American Journal of Physical Anthropology* Vol. 38 p15-26

Janz L.M. and Janz R.L. 1999 Secular change in the long bone length and proportion in the United States, 1800-1970 *American Journal of Physical Anthropology* Vol. 110 1 p5.7-67

Johnson, E.O. et al. 2004 Vascular anatomy and microcirculation of skeletal zones vulnerable to osteonecrosis: vascularization of the femoral head. *Orthopedic Clinics of North America* Vol. 35 Issue 3 p285

Johnson, F. et al. 1980 The distribution of load across the knee. *Journal of Bone and Joint Surgery* Vol. 62 B no. 3

Jones, S., Martin, R. and Pilbeam, D. (Eds.) 1992 *The Cambridge Encyclopaedia of Human Evolution.* Cambridge University Press

Joskeliene, V. et al. 1996 Prevelence and risk factors for asymmetric posture in preschool children aged 6-7 years. *International Journal of Epidemiology* Vol. 25 p1053-1059

Jurmain, R. 2002 *Stories from the Skeleton.* Gordon and Breach Publishers.

Kai, M.C., Anderson, M. and Lau, E.M.C. 2003 Exercise interventions, defusing the world's osteoporosis time bomb *Bull. World Health Organisation* Vol 81 no. 11 p827-830

Kannus, P. et al. 1994 The site-specific effects of lone term unilateral activity on bone mineral density and context. *Bone* Vol. 15 p279-284

Kapandji, I.A. 1985 *The Physiology of the Joints.* Churchill Livingstone

Kettlekamp, D.B. et al. 1970 An electrogoriometric study of knee motion in normal gait. *Journal of Joint Surgery* Vol. 52-A p775-790

Kendall, D.G. 1984 Shape manifolds, Procrustean metrics and complex projective spaces. *Bulletin of the London Mathematical Society* Vol. 16 p81-121

Kent, J.T. 1994 The complex Bingham distribution and shape analysis. *Journal of the Royal Statistical Society* Series B Vol. 59 p281-290

King C.A., Iscan, M.Y. and Loth S.R. 1998 Metric and Comparative Analysis of Sexual Dimorphism in the Thai Femur. *Journal of Forensic Science* Vol. 43 p954-958

Kingston, B. 2001 *Understanding Joints: a practical guide to their structure and function.* Nelson, Thornes Ltd.

Klevay, L.M. and Wildman, R.E.C. 2002 Meat diets and fragile bones: Inferences about osteoporosis. *Journal of Trace Elements in Medicine and Biology* Vol. 16 Issue 3 p149-154

Kouchi, M. 1983 *Geographic variation in modern Japanese somatometric data and its interpretation. Bulletin No. 22* The University Museum: The University of Tokyo http://www.um.utokyo.ac.jp/publish_db/Bulletin/no22/no22004.html

Krogman, W.M. and Iscan, M.Y. 1986 *The Human Skeleton in Forensic Medicine.* Charles C Thomas

Kyle, R.F. 1994 Fractures of the Proximal Part of the Femur. *Journal of Bone and Joint Surgery* 76 p924-950

Landau, P.S. and Kaspin, D. (Eds) 2002 *Images and Empires; Visuality in Colonial and Postcolonial Africa* University of California Press

Lanyon, L.E., Hamson, W.G.H. and Goodship, A.G. 1975 Bone deformation recorded in vivo from strain gauges attached to the human tibial shaft. *Acta Orthopaedica Scandinavica* Vol. 45 p256-258

Larsen, C.S. 1981 Functional implications of postcranial size reductions on the prehistoric Georgia coast, USA. *Journal of Human Evolution* Vol.10 p489-502

Larsen, C.S. 1982 The Anthropology of St. Catherine's Island: 3. Prehistoric Human Biological Adaptation. *Anthropological Papers of the American Museum of Natural History* Vol. 57 part 3

Larsen, C.S. 1995 Biological changes in human populations with agriculture. *Annual Review of Anthropology* Vol. 24 p185-213

Larsen, C.S. 1999 *Bioarchaeology: Interpreting behaviour from the human skeleton.* Cambridge University Press.

Larsen, C.S. 2000 Skeletons in Our Closet. *Princeton University Press*

Larsen, C.S. and Milner, G.R. (Eds.) 2000 *In the Wake of Contact.* Wiley-Liss

Latimer, H.B. and Lowrance, E.W. 1965 Bilateral asymmetry in weight and length of human bones. *Anat. Rec.* Vol. 152 p217-224

Layton, R. 1992 *Rock Art* Cambridge University Press.

Lele, S.R. 1991 Some comments on coordinate-free and scale invariant methods in morphometrics. *American Journal of Physical Anthropology* Vol. 85 p407-417

Lele, S.R. 1993 Euclidean distance matrix analysis: estimation of mean form and form difference. *Mathematical Geology* Vol. 25 p573-602

Lele, S.R. 1999 *Invariance and Morphometrics: A critical appraisal of statistical techniques for landmark data In: On Growth and Form: Spatio-temporal Pattern of Formation in Biology* (Eds.) Mark, A.J., Chaplain, G.D., Singh, J.C. and McLachlan, J.C. John Wiley and Sons Ltd.

Lele, S.R. and Richtsmeister, J.T. 1991 Euclidean distance matrix analysis: a coordinate free approach for comparing biological shapes using landmark data. *American Journal of Physical Anthropology* Vol. 86 p415-427

Lele, S.R. and Richtsmeister, J.T. 1992 On comparing biological shapes: Detection of Influential landmarks. *American Journal of Physical Anthropology* Vol. 87 p49-65

Lele, S.R. and Richtsmeister, J.T. 1995 Euclidean Distance Matrix Analysis: Confidence intervals for form and growth differences. *American Journal of Physical Anthropology* Vol. 98 p73-86

Lele, S.R. and Richtsmeister, J.T. 2001 *An Invariant Approach to Statistical Analysis of Shapes.* Chapman and Hall/C.R.C.

Lele, S.R. and McCulloch, C.E. 2002 Invariance, Identifiability and Morphometrics *Journal of American Statistical Association* Vol. 97 No 459 p796-806

Leonard, W.R. and Robertson, M.L. 1992 Energetic Efficiency of Human Bipedality. *American Journal of Physical Anthropology* Vol. 97 p335-338

Lieberman, D.E. 1996 How and why humans grow thin skulls: Experimental evidence for systemic cortical robusticity. *American Journal of Physical Anthropology* Vol. 101 p217-236

Lieberman, D.E. 1998 *Neanderthal and Early Modern Human Mobility Patterns: Comparing Archaeological and Anatomical Evidence.* Neanderthals and Modern Humans in Western Asia. eds Akazawa T. et al. Plenum Press New York.

Leiberman, D.E. et al. 2001 Articular area response to mechanical loading; effects of exercise, age and skeletal location. *American Journal of Physical Anthropology* Vol. 116 p266-277

Livshits, G. and Smouse, P.E.1993 Multivariate fluctuating asymmetry in Israeli adults. *Human Biology* Vol. 65 4 p547-578

Loesch, D.Z., Stokes, K. and Huggins, R.M. 2000 Secular trend in body height and weight of Australian children and adolescents. *American Journal of Physical Anthropology* Vol. 111 p545-556

Lowrance, E.W. and Latimer, H.B. 1957 Weights and linear measurements of 105 human skeletons from Asia. *American Journal of Anatomy* Vol. 101 p445-459

Lord, S.R., Sherrington, C. and Menz, H.B 2000 Falls in Older People. Cambridge University Press

Lovejoy, C.O. 1988 Evolution of Human Walking. *Scientific American* 259 p82-89

Macho, G.A. 1990 Is sexual dimorphism in the femur a "population-specific phenomenon"? *Z. Morph Anthrop* Vol. 78 2 ps 229-242

McManus, C. 2003 *Right Hand, Left Hand.* Phoenix

McManus, I.C. et al. 2004 Handedness and *situs inversus* in primary ciliary dyskinesia. *Proceedings of the Royal Society B* Online publication 04PB0174.1

Maquet, G.J. 1983 What predisposes for Osteoarthritis? Geometry? *Journal of Rheumatology* (Supplement) Vol 9 p27-28

Marcus, R. 1987 Normal and Abnormal Bone Remodeling in Man. *Annual Review of Medicine* Vol.. 38 p129-41

Marcus, L.F. et al. 1996 *Advances in Morphometrics.* New York: Plenum Press

Marras, S. and Mirka, G.A. 1989 Trunk strength during asymmetric trunk motion. *Human Factors* Vol. 31 6 p667-677

Martin, R. 1957 *Lehrbuch der Anthropologie 3 Stuttgart.* G. Fisher

Martin, R.B. and Atkinson, P.J. 1977 Age and sex-related changes in the structure and strength of the human femoral shaft. *Journal of Biomechanics* Vol. 10 p 223-321

Martin, R.B., Burr, D.B. and Sharkey, N.A. 1998 *Skeletal Tissue Mechanics* Springer.

Martorell, R. et al. 1988 Body Proportions in Three Ethnic Groups: Children and Youths 2-17 Years in NHANES II and HHANES. *Human Biology* Vol. 60 p 205-222

Marsk, A. 1958 Studies on Weight Distribution upon the Lower Extremities in Individuals Working in a Standing Position. *Acta Orthopaedica Scandinavica* Supp XXXI Vol. 27

Mays S., Steele, J. and Ford, M. 1999 Directional asymmetry in the human clavicle. *Int. Journal of Osteoarchaeology* Vol. 9 p18-28

McGowan, C. 1999 *A Practical Guide to Vertebrate Mechanics.* Cambridge University Press

McNeill Alexander, R. 2002 *Principles of Animal Locomotion* Princeton University Press

Mensforth,R.P. and Lovejoy, C.O. 1985 Anatomical, physiological and epidemiological correlates of the ageing process: a confirmation of the multifactorial determination of the Libben population. *American Journal of Physical Anthropology* Vol. 68 p87-106

Miller, H. 2000 *Secrets of the Dead* Channel 4 Books

Milner, G.R. 1991 Health and cultural change in the late prehistoric American Bottom, Illinois In *'What Mean These Bones?' Studies in Southeastern Bioarchaeology* (Eds.) M.L.Powell, P.S. Bridges and A.M. Mires University of Alabama

Molleson, T. 1994 The Eloquent Bones of Abu Hureya. *Scientific American* 271 2: 70-75

Molleson, T. and Cox, M. 1993 The Spitalfields Project. Vol. 2 The Anthropology: The Middling Sort. Research Report 86 York: *Council for British Archaeology.*

McGowan, C. 1999 *A Practical Guide to Vertebrate Mechanics.* Cambridge University Press.

Murdock, G.P. and Provost, C. 1973 factors in the division of labour by sex: a cross-cultural analysis. *Ethnology* Vol. 12 p203-225

Murray, M.P., Drought, A.B. and Kory, R.C. 1964 Walking patterns of normal men *Journal of Bone and Joint Surgery* Vol. 46A p335-360

Murray, M.P, Kory, R.C. and Sepic, S.B. 1970 Walking patterns of normal women. *Archives of Physical Medicine and Rehabilitation* Vol. 51 p637-650

Nei, M. and Roychoudhury, A.K. 1993 Evolutionary Relationships of Human Populations on a global scale. *Molecular Biology and Evolution* Vol. 105 927-943

Nei, M. and Takezaki, N. 1996 The Root of the Phylogenetic Tree of Human Populations. *Molecular Biology and Evolution* Vol. 131 170-177

Nissinenson, M.J. et al. 2000 Development of trunk asymmetry in a cohort of children ages 11 to 22 years. *Spine* Vol. 25 p570-574

Nordin, M. and Frankel, V.H.2001 *Basic Mechanics of the Musculoskeletal System.* Lippincott, Williams and Wilkins

O'Higgins, P. 2000 The study of morphological variation in the hominid fossil record: biology, landmarks and geometry *Journal of Anatomy* Vol. 197 p103-120

O'Higgins, P. 2000 Quantitative approaches to the study of craniofacial growth and evolution: advances in morphometric techniques In: *Development Growth and Evolution.*

O'Higgins, P. and Jones, N. 1998 Facial Growth in *Cerecocebus torquatus*: an application of three-dimensional geometric morphometric techniques to the study of morphological variation. *Journal of Anatomy* Vol.. 193 p251-272

O'Higgins, P. and Strand Viðarsdóttir, U. 2000 New approaches to the quantitative analysis of craniofacial growth and variation In: *Human Growth in the past: studies from bones and teeth* (Eds.) R.D. Hoppa and C.M. Fitzgerald Cambridge University Press

O'Higgins, P., Chadfield, P. and Jones, N. 2001 Facial growth and the ontogeny of morphological variation within and between the primates *Cebus apella* and *Cercocebus torquatus* *Journal of Zoology, London* Vol. 254 p337-357

Omer-Cooper, J.D. 1994 *History of Southern Africa* David Phillip James Currey Heinemann.

O'Rouke, D.H., Suarez, B.K. and Crouse, J.D. Genetic variation in North Amerindian populations: Covariance with climate *American Journal of Physical Anthropology* Vol.. 67 p241-250

Owsley, D.W. and Jantz, R.L. 1994 *Skeletal Biology in the Great Plains.* UK Monographs

Padez, C. 2002 Stature and stature distribution in Portuguese male adults 1904-1998: The role of environmental factors *American Journal of Human Biology* Vol. 14 p39-49

Palastanga, N., Field, D. and Soames, R. 1998 *Anatomy and Human Movement.* Butterworth and Heinemann

Palkovich, A.M. 1994 Historic Epidemics of the American Pueblos In: *In the Wake of Contact.* eds C.S. Larsen and G.R. Milner Wiley-Liss Publications.

Parfitt, M.A. 1991 Bone density and fragility, Age-related changes In *Encyclopedia of Human Biology* Vol. 1 Academic Press, Inc

Palmer, M. Updated 2005 *Ordination methods for ecologists* Oklahoma State University http://www.okstate.edu/artsci/botany/ordinate/PCA.htm

Parnell, R.J. 2001 Hand Preference for Food Processing in Wild Western Lowland Gorillas *Journal of Comparative Psychology* Vol 115 (4) p365-375

Pearson, O.M, 2000 Activity, climate and postcranial robusticity: Implications for modern human origins and scenarios of adaptive change. *Current Anthropology* Vol. 41 No. 4 p569-607

Perry, A.K. et al. 1988 Preferred Speeds in Terrestrial Vertebrates: Are They Equivalent? *Journal of Experimental Biology* 137 p207-219

Pfieffer, S. 1998 Variability in osteons size in recent human populations. *American Journal of Physical Anthropology* Vol. 106 p219-227

Plato, C.C., Wood, J.L. and Norris, A.H. 1980 Bilateral Asymmetry in Bone Measurements of the Hand and Lateral hand Dominance. *American Journal of Physical Anthropology* Vol. 31 p27-31

Plato, C.C. et al. 1985 Measures of lateral functional dominance: Hand dominance. *Human Biology* .Vol. 56 p259-275

Platzer, W. 2004 *Colour Atlas of Human Anatomy* Vol. 1 Locomotor System Thieme.

Plochocki, J.H. 2002 Directional bilateral asymmetry in human sacral morphology. *Int. Journal of Osteoarchaeology* Vol. 12 p349-355

Plochocki, J.H. 2004 Bilateral variation in limb articular surface dimensions. *American Journal of Human Biology* Vol. 16 p328-333

Porter, R. 1990 *English Society in the Eighteenth Century* Penguin Books Ltd., UK

Pribut, S.M. 2003 *Gait Biomechanics.* http:/www.drpribut.com/sports/spgait.html

Purkait, R. 2002 Sexual dimorphism in the femur: an Indian study *Forensic Science Communications* Vol. 4 Number 3 also http:/www.fbi.gov/hq/lab/fsc/backissu/july2002/purkait.htm

Purkait, R. and Chandra, H. 2004 A study of sexual variation in Indian femur. *Forensic Science International* Vol. 146 1 p25-33

Rafferty, K.L. and Ruff, C.B. 1994 Articular structure and function in Hylobates, Colobus and Papio. *American Journal of Physical Anthropology* Vol.. 94 p398-408

Relethford, J.H. 1994 Cranimetric variation among modern human populations *American Journal of Physical Anthropology* Vol. 95 p53-62

Rohlf, F.J. and Slice, D.E. 1990 Extensions of the Procrustes method for the optimal superimposition of landmarks *Systematic Zoology* Vol. 39 p40-59

Rohlf, F.J. and Marcus, L.F. 1993 A Revolution in Morphometrics. *Trends in Ecological Evolution TREE* Vol. 8 4 p129-132

Picard, L. 2005 *Victorian London* Weidenfeld and Nicholson, London

Riddle, J.M., Duncan, H., Pitchford, W.C., Ellis, B.I., Brennan, T.A. and Fisher, L.J. 1988 Anteroposterior radiographic view of the knee: An unreliable indicator of bone damage. *Clinical Rheumatology* Vol 7 (4) p504-513

Riesenfeld, A. 1973 The effect of extreme temperatures and starvation on the body proportions of the rat. *American Journal of Physical Anthropology* Vol. 39 p427-460

Riond, J.L. 2000 Long-term excessive magnesium supplementation is deleterious whereas suboptimal supply is beneficial for bones in rats *Magnesium Research* Vol. 13 Issue 4 p249-264

Rightmire, G.P. 1963 Bushman, Hottentot and South African Negro crania studied by distance and discrimination *American Journal of Physical Anthropology* Vol. 33 p169-196

Robling, A.G. and Stout, S.D. 2000 *Histomorphometry of human cortical bone: applications to age estimations In Biological Anthropology of the Human Skeleton* (Eds.) M.A. Katzenberg and S.R. Saunders Wiley-Liss

Roberts, C. and Manchester, K. 1997 *The Archaeology of Disease* Sutton Publishing Ltd.

Robertson, H. 2004 History of malaria http://www.museums.org.za/bio/apicomplexa/historyofmalaria.htm

Rodgers, J., Watt, I. and Dieppe, P. 1990 Comparisons of visual and radiographic defects of the bony changes at the knee joint *British Medical Journal* Vol 300 p 367-8

Rogucka, E. et al. 2001 Bone mineral status of Polish men in the course of normal ageing *Andrologia* Vol. 33 Issue 5 p287-292

Ross, M.H., Romrell, L.J. and Kaye, G.I. 1998 *Histology: A Text and Atlas.* Williams and Wilkins

Rossi, W.A. 2005 Why shoes make 'normal' gait impossible: How flaws in footwear affect this complex human function. http://www.unshod.org/pfbc /pfrossi2.htm

Rowe, N. 1999 *The Pictorial Guide to the Living Primates* Pogonius Press

Roy, T.A., Ruff, C.B. and Plato, C.C. 1994 Hand dominance and bilateral asymmetry in structure of the second metacarpal. *American Journal of Physical Anthropology* Vol. 94 p203-211

Ruff, C.B. 1987 Sexual dimorphism in human lower limb bone structure: relationship to subsistence strategy and sex. *Journal Human Evolution* Vol. 16 p391-416

Ruff, C.B. 1991 Climate and Body Shape in Hominid Evolution. *Journal of Human Evolution* Vol. 21 81-105

Ruff, C.B. 1994 Biomechanical Analysis of Northern and Southern Plains Femora: Behavioural Implications In: *Skeletal Biology in the Great Plains* (Eds.) Owsley, D.W. and Jantz R.L.

Ruff, C.B. 1994 Morphological Adaptation to Climate in Modern and Fossil Hominids. *Yearbook of Physical Anthropology* Vol..37 p65-107

Ruff, C.B. 1997 Structural analysis of long bones from La Florida: interpreting behaviour. *American Journal of Physical Anthropology* Supp. 24 p201

Ruff, C.B. 2000 Biomechanical Analyses of Archaeological Human Skeletons. *In Biological anthropology of the Human Skeleton* (Eds.) Katzenberg, M.A. and Saunders, S.R.

Ruff, C.B. and Jones, H.H. 1981 Bilateral asymmetry in cortical bone of the humerus and tibia- sex and age factors. *Human Biology* Vol.53 p69-83

Ruff, C.B. and Hayes, W.C. 1983 Cross-sectional geometry of Pecos Pueblos femora and tibia- a biomechanical investigation: II Sex, Age and Side differences. *American Journal of Physical Anthropology* Vol. 60 p383-400

Ruff, C.B., Larsen, C.S. and Hayes, W.C 1984 Structural changes in the femur with the transition to agriculture on the Georgia coast. *American Journal of Physical Anthropology* Vol. 64 p125-136

Ruff, C.B. and Hayes, W.C. 1984 Age changes in geometry and mineral content of the lower limbs. *Annals of Biomedical Engineering* Vol. 12 p573-584

Ruff, C.B. and Hayes, W.C 1988 Sex differences in age-related remodeling of the femur and tibia *Journal of Orthopaedic Research* Vol. 6 p886-896

Ruff, C.B., Walker, A. and Trinkaus, E. 1993 Postcranial Robusticity in Homo: 1 Temporal Trends and Mechanical Interpretation. *American Journal of Physical Anthropology* Vol.91 p21-53

Rupert, J.L., Kidd, K.K., Norman, L.E., Monsalve, M.V., Hochachka, P.W. and Devine, D.V. 2003 Genetic polymorphisms in the Rennin-Angiotensin System in high-altitude and low-altitude Native American populations. *Annals of Human Genetics* Vol. 67 p17-25

Sadeghi, H., Allard, P., Prince, F. and Labelle,H. 2000 Symmetry and limb dominance in able bodied gait: a review. *Gait and Posture* Vol.. 12 p34-45

Sakaue, K 1998 Bilateral asymmetry of the humerus in Jomon People and modern Japanese. *Anthropological Science* Vol. 105 4 p231-246

Saudek, C.E. 1985 The *Hip The Hip Orthopaedic and Sports Physical Therapy.* eds Gould J.A. and Davies G.G.

Scheuer, L. and Black, S. 2000 *Juvenile Developmental Osteology* Blackwell

Schnitzler, C.M. 1993 Bone quality: a determinant for certain risk factors for bone fragility. *Calcif. Tissue International* Vol. 53 supplementary 1 pS27-31

Schultz, A.H. 1937 Proportions, variability and asymmetries of the long bones of the limbs and clavicles in man and apes *Human Biology* Vol. 9 p281-328

Schmitt, A., Murail, P., Cuhna, E. and Rouge, D. 2002 Variability of the pattern of ageing on the human skeleton: evidence from bone indicators and implications on age at death. *Journal of Forensic Science* Vol. 47 6 p348-476

Seeley, R.R., Stephens, T.D. and Tate, P. 1998 *Anatomy and Physiology* McGraw-Hill

Seeman, E. 1995 The Dilemma of Osteoporosis in Men. *American Journal of Medicine* Vol. 98 2A Supplement p2A-76S to 2A-88S

Seeman, E. 2002 Pathogenesis of bone fragility in women and men. *Lancet* May Vol. 359 9320 p1841-1850

Shephard, R.J. 1991 *Body Composition in Biological Anthropology.* Cambridge University Press.

Shipman, P., Walker A. and Birchell, D. 1985 *The Human Skeleton* Harvard University Press.

Siegal, A.F. and Benson, R.H. 1982 A robust comparison of biological shapes *Biometrics* Vol. 38 p341-350

Singer S.S. and Schwibbe, M.H. 1999 Right or left, hand or mouth: Genera-specific preferences in marmosets and tamarinds *Behaviour* Vol 136 p119-145

Slice, D.E. 1996 A Glossary for Geometric Morphometrics. In: *Advances in Morphometrics* (Eds.) F.L. Marcus, Corti, M., Loy, A., Naylor, G.J.P. and Slice, D.

Smith, J.W. 1953 The act of standing *Acta Orthopaedica Scandinavica* Vol. 23 p159-168

Snodgrass, J.J. 2004 Sex differences and ageing of the vertebral column. *Journal of Forensic Science* Vol.. 49 3

Snow, C.M., Shaw, J.M., Winter, K.M. and Witzke, K.A. 2000 Long-term exercise using weighted vests prevents hip bone loss in postmenopausal women *The Journals of Gerontology Series A: Biological Sciences* Vol 55: M489-M491

Soloman, L. 1979 Bone density in ageing Caucasian and African populations. *Lancet* Vol. 2 p1326-1330

St. Clair, M.B. and Zaslow, S.A. *Water quality and waste management; Lead in drinking water* http://www.bae.ncsu.edu/programs/extension/publicat/wqwm/he395.html 12/11/2005

Steele, D.G. and Bramblett, C.A. 1988 *The Anatomy and Biology of the Human Skeleton* Texas AandM University Press

Steele, J. and Mays, S. 1995 Handedness and directional asymmetry in the long bones of the human upper limb. *Int. Journal of Osteoarchaeology* Vol. 5 p39-49

Steele, J. 2000 Handedness in past populations: skeletal markers. *Laterality* Vol. 5 3 p193-220

Stevens, A. and Lowe, J. 1998 *Human Histology.* Mosby

Steyn, M. and Iscan, M.Y. 1997 Sex determination from the femur and tibia in South African whites. *Forensic Science International* Vol. 90 p111-119

Stini, W.A. 1985 *Growth rates and Sexual Dimorphism in Evolutionary Perspective In: The Analysis of Prehistoric Diets.* (Eds.) R.I. Gilbert and J.H. Miekle Orlando Academic Press

Stirland, A.J. 1993 Asymmetry and activity-related change in the male humerus. *Int. Journal of Osteorchaeology* Vol. 3 p105-113

Stodder, A.L.W. 1994 Bioarchaeological Investigations of Protohistoric Pueblo Health and Demography In: *In the Wake of Contact.* (Eds.) C.S. Larsen and G.R. Milner Wiley-Liss Publications

Stone, R.J. and Stone, J.A. 2000 *Atlas of Skeletal Muscles* McGraw-Hill International Editions

Streudel, K. 1996 Limb Morphology, Bipedal Gait and the Energetics of Hominid Locomotion *American Journal of Physical Anthropology* Vol. 99 p345-355

Stringer, C.B. 1992 Reconstructing recent human evolution *Philosophical Transactions of the Royal Society of London*, B Vol. 33 p217-224

Tabachnick, B.G. and Fidell, L.S. 2001 *Using Multivariate Statistics* Fourth edition Allyn and Bacon

Tanaka, H. 1999 Numerical analysis of the proximal humeral outline: Bilateral shape differences. *American Journal of Human Biology* Vol. 11 3 p343-357

Taylor, C.F. 2002 *The American Indian* Salamander Books

Terry Collection *The Robert J. Terry Anatomical Skeletal Collection.* http://www.nmnh.si.edu/anthro/Collmgt/terry.htm.

Thomason, J.J. 1995 To What Extent can the Mechanical Environment of a Bone be Inferred from its Internal Architecture? *Functional Morphology in Vertebrate Palaeontology.* Thonason, J.J. (Ed.) ISBN 0521440955

Thompson, C.W. and Floyd, R.T. 1998 *Manual of Structural Kinesiology* McGraw-Hill International Editions.

Thompson, D. 2002a 3/19 *Stride Analysis.* http://moon.ouhsc.edu/dthompso/gait/knmatics/stride.htm

Thompson, D. 2002b 4/24 *Changes in the gait pattern across the lifespan.* http://moon.ouhsc.edu/dthompso/gait/matgait/matgait.htm

Thompson, D.A. 1917 *On Growth and Form* Cambridge: Cambridge University Press.

Timmins, G. 1993 *The Last Shift: The decline of handloom weaving in nineteenth century Lancashire* Manchester University Press

Trinkaus, E. 1981 Neanderthal limb proportions and cold adaptation In: *Aspects of Human Evolution* (Eds.) C.B. Stringer, Taylor and Francis: London

Trinkaus, E. 1993 Femoral neck-shaft angles of Qafzeh-Skhul early modern humans and activity patterns among immature Near Eastern Middle palaeolithic hominids. *Journal of Human Evolution* 1993 Vol.. 25, p393-416

Trinkaus, E. 2005 Anatomical evidence for the antiquity of human footwear use *Journal of Archaeological Science* Vol 32 (10) p1515-1526

Trinkaus, E., Churchill, S.E. and Ruff, C.B. 1994 Postcranial robusticity in Homo, II: Humeral bilateral asymmetry and bone plasticity. *American Journal of Physical Anthropology* Vol. 93 p1-34

Turan. B., Balcik, C. and Akkas, N. 1996 Effects of dietary selenium and vitamin E on the biomechanical properties of rabbit bones *Clinical Rheumatology* Vol. 16 5 p441-449

Uhle, M. 1903 Pachacamac: A reprint of the 1903 edition by Max Uhle and Pachacamac Archaeology: Retrospect and Prospect. *University Museum Monologue 62* Published 1991 by University of Pennsylvania.

Van Gerven, D.P. 1972 The contribution of size and shape variation to patterns of sexual dimorphism of the human femur. *American Journal of Physical Anthropology* Vol. 37 p49-60

Van Vark, G.N. 1985 The study of hominid skeletal remains by means of statistical methods In: *Biological Anthropology: The State of the Science* (Eds.) N.T. Boas and L.D. Wolfe

Vaughan, J. 1981 *The Physiology of Bone.* Clarendon Press. Oxford

Vellacott, J. and Side, S. 1998 Understanding Advanced Human Biology

Hodder Arnold

Viðarsdóttir, U. Strand 1999 Ph.D. Thesis Changes in the form of the facial skeleton during growth: A comparative geometric morphometric study of modern humans and Neanderthals. University College London

Viðarsdóttir, U. Strand, O'Higgins, P. and Stringer, C. 2002 A geometric morphometric study of regional differences in the ontogeny of the modern human facial skeleton *Journal of Anatomy* Vol. 201 p211-229

Waldron, T. 1992 Osteoarthritis in a Black Death cemetery in London. *Int. Journal of Osteoarchaeology* Vol. 2 p235-240

Walker, P.S. and Hajek, J.V. 1972 The load-bearing area of the knee joint *Journal of Biomechanics* Vol. 5 p581-589

Weber, G. 2004 The Lonely Islands: an on-line documentation on the Andamanese and other Negrito people and the earliest migrations of early modern humans http://www.andaman.org/index.htm

Wells, J.C.K. 2000 Environmental temperature and human growth in early life. *Journal of Theoretical Biology* Vol. 204 2 p299-305

White, T.D. 2000 *Human Osteology* Academic Press

Wilson, F.C. 1983 *The Musculoskeletal System*

Weiss M.L. and Mann, A.E. 1989 *Human Biology and Behaviour: An Anthropological Perspective* Scott, Foreman/Little, Brown Higher Education.

Wesley, M.J., Fernadez-Carriba, S., Hostetter, A., Pilcher, D., Poss, S. and Hoskins, W.D. 2002 Factor analysis of multiple measures of hand use in captive chimpanzees: An alternative approach to the assessment of handedness in nonhuman primate *International Journal of Primatology* Vol 23 (6) p1155-1168

Wilczak, C. 1998 Consideration of sexual dimorphism, age and asymmetry in quantitative measurements of muscle insertion sites *Int. Journal of Osteoarchaeology* Vol. 8 p311-325

WorldClimate.com 2003 http://worldclimate.com

Wood, C.G. and Lynch, J.M. 1996 Sexual dimorphism in the Craniofacial Skeleton of Modern Humans In: *Advances in Morphometrics* (Eds.) F.L. Marcus, Corti, M., Loy, A., Naylor, G.J.P. and Slice, D.

Wright, A. 2003 'Arthritis? But I'm only 24.' *The Daily Telegraph* May 2 2003 (Ed.) C. Doyle

Zanker, C. and Cooke, C.B. 2004 Energy balance, bone turnover and skeletal health in physically active individuals *The American College of Sports Medicine* August Vol. 36 8 p1372-1381